Treatment of NSCLC and Respiratory Diseases through Innovative Particle Engineering Approaches: Lipid Nanoparticles and Advanced Spray Drying Techniques

Submitted for the Degree of Doctor of Philosophy

School of Pharmacy

ARWA AL KHATIB

June 2024

Declaration of original authorship

I confirm that this is my own work and the use of all material from other sources has been properly and fully acknowledged.

Arwa Al Khatib 2024

Acknowledgements

Abstract

Background: NSCLC is the most common type of lung cancer, making up 85% of all lung cancer cases. One of the primary challenges is the difficulty in early detection, leading to low survival rates. Respiratory infections can damage cells, impair lung function, and hinder lung cells from destroying cancer cells. Such infections complicate 50-70% of cancer cases and cause immunosuppression, preventing the immune system from effectively combating cancer. Additionally, chronic lung tissue inflammation can progress into cancer. Lung cancer is often accompanied by secondary infections and inflammation related to the cancer itself.

Aim: To improve the therapeutic effectiveness of treatments for NSCLC and respiratory infections, addressing the primary challenge of limited drug targeting, suboptimal bioavailability, and systemic toxicity. Our focus was on investigating innovative strategies through particle engineering in pulmonary drug delivery to provide more tailored solutions for effective treatments.

Methods: This thesis investigated the development and evaluation of lipid nanoparticles produced using the microemulsion technique, subsequently transformed into powders through spray drying. Additionally, it explored the development of spray-dried microparticles utilizing the two and three fluid nozzle configurations, loaded with one or two repurposed drugs—pimozide, hydroxychloroquine, or rifaximin—to target NSCLC and related infections and inflammations. The thesis evaluated their physical stability, chemical integrity, functional performance, and in vitro efficacy.

Results & Conclusion: Pimozide-loaded nanostructured lipid carriers (NLCs) outperformed solid lipid nanoparticles (SLNs) and liquid lipid carriers (LLCs) with higher encapsulation efficiency, potential cytotoxicity against A549 lung cancer cells, and a biphasic drug release profile. NLCs with pimozide and hydroxychloroquine showed synergistic antiproliferative and anti-inflammatory effects. Microparticles made with the three-fluid nozzle method had better recovery percentages, customized release profiles, and enhanced activities compared to the two-fluid nozzle method. Microparticles with hydroxychloroquine and rifaximin, prepared using the three-fluid nozzle, exhibited

superior antiproliferative, anti-inflammatory, and antimicrobial effects against drug-resistant *A. baumannii*.

List of Publications

Al Khatib, A.O., El-Tanani, M., Al-Obaidi, H. Inhaled medicines for targeting non-small cell lung cancer. Pharmaceutics. 2023 Dec 14;15(12):2777.

Abu Elella, M.H.; **Al Khatib, A.O.**; Al-Obaidi, H. Spray-Dried Nanolipid Powders for Pulmonary Drug Delivery: A Comprehensive Mini Review. Pharmaceutics 2024, 16, 680. https://doi.org/10.3390/pharmaceutics16050680.

List of Conferences and Activities

Drug Delivery to the Lungs Conference (DDL), December 2023 – Poster Presentation

YES23 (Your Entrepreneurs Scheme)- Winner of Best sustainable agriculture business plan sponsored by Syngenta

Table of Contents

Abbreviation	Full Form
2FN	Two-fluid Nozzle
3FN	Three-fluid Nozzle
A549 cells	Human alveolar adenocarcinoma epithelial
ANOVA	Analysis of Variance
APIs	Active Pharmaceutical Ingredients
ARDS	Acute Respiratory Distress Syndrome
CI	Combination Index
COPD	Chronic Obstructive Pulmonary Disease
CUMS	Chronic Unpredictable Mild Stress
CYP1A1	Cytochrome P450 1A1
DLS	Dynamic Light Scattering
DMSO	Dimethyl Sulfoxide
DOE	Design of Experiments
DPI	Dry Powder Inhaler
DPIs	Dry Powder Inhalers
DVS	Dynamic Vapor Sorption
D.W	Distilled Water
EE	Encapsulation Efficiency
EE%	Encapsulation Efficiency Percentage
FDA	Food and Drug Administration
FTIR	Fourier Transform Infrared

	Spectroscopy
GIT	Gastrointestinal Tract
HIF 1α	Hypoxia Inducible Factor 1 α
HPLC	High Performance Liquid Chromatography
HQ	Hydroxychloroquine
HPMC-E5	Hydroxypropyl Methylcellulose E5
IFN	Interferons
ICU	Intensive Care Units
IL	Interleukins
IRAK1	Interleukin-1 receptor-associated kinase 1
LLC	Liquid Lipid Carriers
LLCPH	Liquid Lipid Carriers loaded with pimozide and hydroxychloroquine
LNPs	Lipid Nanoparticles
LPS	Lipopolysaccharide
MHA	Mueller Hinton agar
MIC	Minimum Inhibitory Concentration
MMP	Matrix Metalloproteinases
MDR	Multi-Drug Resistant
NHE	Na+/H+ exchangers
NLC	Nanostructured Lipid Carriers
NLCPH	Nanostructured Lipid Carriers loaded with pimozide and hydroxychloroquine
NSCLC	Non-Small Cell Lung Cancer

PBS	Phosphate Buffer Saline
PCNA	Proliferating Cell Nuclear Antigen
PDI	Polydispersity Index
PEG	Polyethylene Glycol
PIT	Phase Inversion Temperature
PMA	Phorbol 12 myristate 13 acetate
PMZ	Pimozide
PVP	Polyvinylpyrrolidone
RFX	Rifaximin
RSV	Respiratory Syncytial Virus
SEM	Scanning Electron Microscope
SLF	Simulated Lung Fluid
SLN	Solid Lipid Nanoparticles
SLNPH	Solid Lipid Nanoparticles loaded with pimozide and hydroxychloroquine
TLR	Toll-like receptors
TNF α	Tumor necrosis factor alpha
XDR	Extensive Drug Resistance
XRPD	X-Ray Powder Diffraction

Chapter 1

General Introduction

1. Introduction to particle engineering strategies in formulation development

Particle engineering is a pivotal aspect of pharmaceutical development, enabling targeted drug delivery and enhanced bioavailability. This section explores various facets of particle engineering, emphasizing its critical role in advancing drug delivery systems.

1.1 Overview of particle engineering and its significance in drug delivery systems

Particle engineering is a transformative approach in the formulation development of Active Pharmaceutical Ingredients (APIs). This field uses advanced approaches to modify particle characteristics, including size, shape, surface properties, and crystallinity, which are critical for optimizing drug performance and patient outcomes. The strategic alteration of these particle properties enhances the bioavailability, dissolution, and stability of APIs, addressing key challenges in pharmaceutical development [1]. Particle engineering in pharmaceuticals aims to enhance the effectiveness and delivery of medications. One approach involves decreasing particle size to the micro or nanoscale which can notably boost surface area and improve the solubility of drugs that are poorly soluble. Methods of transforming the size to the nano or micro level, and high energy ball milling are frequently utilized to produce these particles [2].

Beyond size reduction, particle engineering also involves modifying the crystal form of an API. Polymorphism, the ability of a solid material to exist in more than one form or crystal structure, can affect the physical and chemical properties of a drug, including its solubility and melting point. Selecting the optimal polymorphic form is therefore essential for maximizing the therapeutic efficiency of a formulation [3].

Surface engineering is another key area of particle technology in medicines. Modifying particle surface properties can improve medication targeting, minimize toxicity, and increase interaction with biological surroundings. Coating, surface functionalization, and the application of surfactants are used to alter the surface properties of APIs in order to achieve specific therapeutic goals [4].

Particle engineering also intersects with advanced drug delivery systems such as solid dispersions, liposomes, and nanoparticles. These systems utilize engineered particles to overcome the limitations of conventional dosage forms, offering controlled release profiles and targeted delivery that can significantly improve patient adherence and therapeutic outcomes [5, 6].

2. Non-small cell lung cancer (NSCLC) and related respiratory conditions

Non-small cell lung cancer (NSCLC) accounts for most lung cancer incidences globally and poses considerable treatment problems due to its complexity and resistance to traditional medicines. This section delves into NSCLC in depth, examining its biological properties, current therapeutic problems, and the critical need for novel drug delivery mechanisms. It also addresses linked respiratory disorders, such as bacterial lung infections, which complicate the treatment landscape and emphasize the necessity for integrated therapy methods.

2.1 Overview of non-small cell lung cancer NSCLC

Non-small cell lung cancer (NSCLC) makes up the majority, 85% of all lung cancer cases with smoking being the cause, in around 90% of these instances. However various other factors also contribute to the onset of lung cancer. Exposure to secondhand smoke, air pollution, radon and a family history of lung cancer are influencers. Genetic predispositions, like variations in the CYP1A1 gene can heighten vulnerability [7]. Additionally, exposure to substances such as asbestos, tar, soot, arsenic, chromium, and nickel have been identified as risk factors [8].

The examination of precursor lesions has gained importance in lung cancer screening efforts to emphasize detection. Currently acknowledged are three types of NSCLC; adenocarcinoma; squamous cell carcinoma; and large cell undifferentiated carcinoma as shown in **(Figure 1)** [9]. The risks linked with these lesions differ based on smoking intensity and duration [10]. Other conditions like fibrosis have also been linked to an increased likelihood of developing lung cancer. This underscores the interplay among factors, environmental influences, and lifestyle choices, in the development of NSCLC [11].

Adenocarcinoma
The most common type of lung cancer, often develops in the glands of the alveoli in the lung's outer regions and tends to grow slowly. It predominantly affects nonsmokers, young adults, and women.

Squamous cell carcinoma
The second most prevalent type of lung cancer and the most common among smokers, typically starts in the squamous cells within the bronchi at the center of the lung and generally grows slowly.

Large cell lung carcinoma
The least common type, originates in large cells predominantly located in the outer parts of the lung and is typically fast-growing.

Figure 1. Types of non-small cell lung cancer

2.2   Challenges and current treatment limitations

With the fact that there are many advances occurring when it comes to diagnosing and treating NSCLC, yet still, NSCLC which represents around 85% of lung cancer cases is an intimidating enemy as lung cancer is responsible for more than 1.6 million deaths in the world yearly [12]. Detection at an early stage, therapeutic resistance and failure to control the tumors' relapse and metastatic spread are examples of the detrimental obstacles which in turn limit the survival rates and disease-free patients. NSCLC, among other lung cancers, is recognized by not showing any visible symptoms at their development at the initial stages. Symptoms like breathing problems, chronically having headaches, back and chest pain, are usually noticed in later development of tumor stages. While diagnostic imaging is the tool of choice in tumors' detection. Computed low-dose tomography and computed contrast enhanced tomography are the number one choice of tools in utilizing radio diagnoses for the purpose of screening [13, 14]. There is so much clinical evidence suggesting the decreasing effects of chemotherapy with progressive number of cycles of treatment administered to the patients. NSCLC, among every other type of cancer, is much more likely to gain resistance even though there are many different

drug combinations being used. Every patient that receives treatment gains resistance after treatment cycles [15, 16].

2.3   Lung infections: Overview of bacterial infections affecting the lungs

Respiratory infections affecting the lungs can be caused by bacteria, viruses and fungi showing symptoms, like coughing, chest discomfort, difficulty breathing and fever. Certain groups like the elderly or individuals with existing health issues may face varying degrees of impact from discomfort to respiratory issues. Complications include lung abscesses, pleural effusions, or acute respiratory distress syndrome (ARDS) leading to lung function problems that may need medical care [17].

Pneumonia, a type of lung infection occurs when the air sacs in the lungs become inflamed and can be triggered by pathogens like *Streptococcus pneumoniae*, *Haemophilus influenzae*, and *Staphylococcus aureus* [18]. The seriousness of the condition varies depending on the agent and the overall health of the individual. While fungal pneumonia is less frequent it poses a threat to people with immune systems, such as those with HIV/AIDS or undergoing chemotherapy and is often caused by fungi such as *Pneumocystis jirovecii* [19]. Additionally, viruses like Respiratory Syncytial Virus (RSV) and influenza are common causes of pneumonia that especially impact individuals with compromised immune systems [20].

Multidrug-resistant bacterial strains complicate lung infection treatment and offer an increasing risk in hospital settings. *Acinetobacter baumannii* thrives in hospitals and is especially hazardous to persons with weaker immune systems because it is resistant to several therapies [21]. Similarly, *Klebsiella pneumoniae* causes severe hospital-acquired infections and has gained resistance to carbapenems, which are critical last-resort antibiotics, making treatment more difficult [22]. *Pseudomonas aeruginosa* is another challenging bacterium that affects cystic fibrosis sufferers and those who require mechanical ventilation. It is noted for its widespread antibiotic resistance, which complicates infection treatment [23].

3.   Advanced pulmonary drug delivery systems in treating NSCLC and respiratory infections

Non-small cell lung cancer (NSCLC) presents significant challenges due to its resistance to conventional chemotherapy and high metastatic potential. Advanced drug delivery systems, such as nanoparticle carriers and inhaled targeted therapies, offer promising solutions by delivering chemotherapeutics directly to tumor sites. These methods aim to enhance treatment efficacy, minimize side effects, and bypass some of the body's natural defense mechanisms that typically reduce drug effectiveness [24].

Respiratory infections, particularly those caused by multidrug-resistant bacteria, complicate the treatment situation for individuals with lung conditions, including NSCLC patients. These pathogens are notorious for their robust antibiotic resistance, especially in hospital settings, making infections difficult to manage with standard treatments [21-23]. Advanced pulmonary drug delivery systems are crucial in these scenarios for effectively targeting and treating infections, minimizing the impact of resistance, and improving patient outcomes.

Moreover, the history of lung infections may contribute to long-term lung health issues, including an increased risk of lung cancer. Conditions like chronic inflammation and cellular damage, along with impaired lung function and weakened immune responses, can heighten the susceptibility to lung cancer [25]. The interaction between these infections and other risk factors, such as smoking, suggests that lung infections could synergistically increase lung cancer risks, emphasizing the importance of comprehensive strategies in both treatment and prevention [26].

Responsive pulmonary drug delivery technologies that adapt to specific lung tissue conditions, such as variations in pH or the presence of enzymes, are being developed to address these healthcare challenges more effectively. By facilitating the localized and controlled release of medications, these innovative pulmonary delivery systems hold the potential to revolutionize the management of both NSCLC and severe respiratory infections, reducing disease burden and enhancing quality of life for affected individuals [27].

The integration of these advanced technologies into clinical practice is imperative for addressing the aggressive nature of NSCLC and the growing issue of antibiotic-

resistant respiratory infections. Ongoing research and development efforts are essential to refine these delivery mechanisms and ensure they meet the complex needs of these patient populations [28].

3.1 Overview of pulmonary delivery devices

Pulmonary delivery systems benefit from the respiratory tract's unique anatomical features, providing a direct route for pharmaceutical administration to the lungs. This is advantageous due to the vast surface area and significant vascularization, which promote rapid drug absorption [29]. These systems include nebulizers, metered-dose inhalers (MDIs), dry powder inhalers (DPIs), and soft mist inhalers, all of which are designed to suit varying drug characteristics and patient usability [30]. Effective medication deposition is critical and controlled by factors such as particle size and the patient's breathing pattern; aim for the appropriate particle size to ensure targeted delivery to lung tissues [31].

Recent technological advances include nanoparticle-based drug carriers and smart inhalers that enhance drug stability and patient compliance [32, 33]. Regulatory and safety considerations are crucial, as all devices must meet stringent standards to ensure consistent and safe drug delivery [34].

3.2 Advantages and challenges of pulmonary drug delivery systems

Inhaled drug products have been around for years, their ability of treating lung diseases is acknowledged as a first line therapy in many cases such as chronic obstructive pulmonary disease (COPD), and asthma. Furthermore, studies have explored the possibility of using inhaled therapy in chronic systemic illnesses such as diabetes mellitus [35, 36]. The following are significant benefits of inhaled medications that have demonstrated their effectiveness over time. These advantages include the ability to deliver high concentrations of the medication directly to the site of illness, thereby reducing the risk of systemic side effects.

Moreover, pulmonary drug delivery can achieve comparable or superior efficacy with much smaller doses compared to systemic administration. Additionally, it eliminates the need for invasive injection-based delivery systems. Inhalable medication offers

versatility for a variety of products, whether they are small molecules or large proteins [37, 38]. Another aspect that makes pulmonary delivery system desirable is the massive absorptive surface area and the highly porous membrane in the alveolar region [39, 40]. Low absorption rates are often found in large molecules, but when inhaled, they can be absorbed in notable amounts as slow mucociliary clearance in the lungs leads to extended residency time [41]. Furthermore, inhaled therapy's environment is enzymatically low which is entirely free of hepatic first-pass metabolism. The absorption kinetics are reproducible in the pulmonary delivery system, since in the field of pharmaceuticals, small alterations, in the size and site of deposition of aerosols are not expected to significantly affect how quickly small molecules are absorbed when inhaled. On the other hand, administering medications to parts of the gastrointestinal tract (GIT) can lead to changes in absorption rates because of notable differences in pH levels and surface areas, among those regions [38]. The biphasic release of the inhaled therapy proved the ability to provide a high concentration of the drug and maintain the concentration at a therapeutic level [42].

Moving forward to addressing the drawbacks in pulmonary drug delivery, mucociliary clearance stands out as a lung clearance mechanism responsible for removing drug particles that accumulate in the conducting airways. Goblet cells within the airway epithelium, along with secreted mucus from submucosal glands, form a dual-layer mucus blanket over the ciliated epithelium. This blanket comprises a low-viscosity sol layer beneath a high-viscosity gel layer. Consequently, insoluble particles are propelled towards the throat (pharynx) and subsequently into the gastrointestinal tract through upward movement facilitated by the metachronous beating of the cilia [43, 44]. In healthy lungs, the activity of mucus varies across different areas of the airways, as determined by the quantity and rhythm of beating of ciliated cells. To maintain effective mucociliary clearance, it is essential for cilia activity to be normal, airway epithelial cells to remain intact, and the structure of the cilia to be preserved [44].

Other factors influencing the effectiveness of inhalation therapy and its bioavailability in the lungs include the drug's aqueous solubility, its dissolution rate, and its elimination and clearance by alveolar macrophages. Notably, insoluble nanoparticles with an aerodynamic diameter of less than 6 μm are often eliminated through

mucociliary clearance. While nano-sized particles can more readily and rapidly reach the epithelial region and evade clearance mechanisms.

3.3 Advancements in particle engineering for optimized pulmonary drug delivery

Particle engineering is crucial in inhaled therapy, utilizing advanced techniques to tailor particles for specific therapeutic needs, including enhanced dispersibility and consistent particle size for reliable drug delivery to the lungs. It also aims to improve drug stability and bioavailability, essential for maintaining medication integrity [45]. Additionally, particle engineering develops extended-release formulations and precise targeting to treat chronic respiratory diseases, minimizing systemic side effects and improving therapeutic efficacy [46]. These efforts are vital as they can transform pulmonary disease treatment by overcoming current drug delivery challenges and catering to varied patient needs.

3.4 Selection of active pharmaceutical ingredients (APIs)

Drug development involves multiple stages to ensure safety, efficacy, and regulatory compliance. Clinical trials usually last six to seven years, with the entire approval process for a drug averaging 10.5 years and costing approximately $2.6 billion [47]. These hurdles have popularized "drug repurposing." Drug repurposing, also known as repositioning, seeks new uses for existing FDA-approved drugs [48]. This method is less risky and cheaper than traditional drug development because it builds on previous successful preclinical trials, thereby also speeding up the evaluation process [49]. Around 70% of Phase I and II trials for repurposed drugs are funded by academic institutions, which often collaborate with industry for Phase III studies. Nevertheless, a shift from industry to academia has weakened this collaboration, reducing drug repositioning research and funding for commercialization [50].

In the context of non-small cell lung cancer (NSCLC), the repurposing of existing drugs shows significant promise. These drugs, originally developed for other diseases, are now being explored for their ability to inhibit tumor growth, induce apoptosis, and enhance the effectiveness of existing cancer treatments. Their established safety profiles and mechanisms of action provide a crucial advance in

cancer drug development, potentially improving survival rates and enabling more personalized treatment approaches. As clinical trials verify these benefits, repurposed medications are becoming an increasingly vital component of NSCLC treatment strategies [51, 52].

The selection of drugs for inclusion in this thesis highlights the innovative use of repurposed medications for treating non-small cell lung cancer (NSCLC) via advanced delivery systems such as lipid nanoparticles (LNPs) and solid dispersions via spray drying. The clinical uses and physicochemical properties of all APIs used in this thesis are summarised in (**Table 1**).

Table 1. Clinical uses and physicochemical properties of pimozide, hydroxychloroquine, and rifaximin

Property	Pimozide (PMZ)	Hydroxychloroquine (HQ)	Rifaximin (RFX)
Clinical Use	Antipsychotic (treats schizophrenia)	Antimalarial, treats autoimmune disorders	Antibiotic, treats gastrointestinal infections
Aqueous Solubility [53]	0.01 mg/mL at 25°C	20.0 mg/mL at 25°C	0.20 mg/mL at 25°C
Dissolution Rate	Slow	Likely fast due to high solubility	Relatively slow
Melting Point	218°C	203°C	188°C
Partition Coefficient (Log P)	6.3	4.6	2.6
Chemical Stability	Stable under normal conditions	Stable under normal conditions, degrades in light	Sensitive to light and moisture
Molecular Weight	461.59 g/mol	434.95 g/mol	785.94 g/mol
Polarity	Relatively non-polar	Polar	Polar
pKa	8.6	8.3, 9.7	7.9
Crystal Form and Polymorphism	Crystalline solid	Crystalline solid	Crystalline solid

The first candidate is pimozide, originally an antipsychotic, which has demonstrated potential in inhibiting cancer cell proliferation by blocking STAT3 signaling pathways, commonly active in cancer progression [54, 55]. Its delivery through inhalation therapy directly targets lung tissue, potentially enhancing drug concentration at the tumor site, while reducing systemic side effects, thereby optimizing therapeutic efficacy against NSCLC [56]. Pimozide depicted in **Figure 2 (A)** with a molecular weight of 461.59 g/mol shows low solubility in water (approximately 0.03 mg/mL at 25°C) and low dissolution affecting how well it can be absorbed when taken orally. It has a level of lipophilicity shown by its Log P value of 6.3 making it easier for the compound to pass through cell membranes.

Pimozide's melting point is typically around 218°C indicating that it remains stable under heat. With a pKa of 8.6 pimozide can exist in both charged and uncharged states. Due to its high lipophilicity, indicated by a Log P value of 6.3, and a pKa of 8.6, pimozide can effectively cross the lipid-rich cell membranes in the lungs. At the typical pH of lung fluid, which ranges from 6.3 to 7.4, the drug mostly remains non-ionized, facilitating its movement across pulmonary barriers. This characteristic is beneficial for targeted drug delivery to the lungs. However, its high lipophilicity could also hinder its solubility in the aqueous lung environment, potentially limiting how well it is absorbed. To overcome this, solubilizing agents or advanced encapsulation technologies might be needed to enhance its water solubility and ensure effective distribution and activity within the lungs.

Hydroxychloroquine, traditionally used for malaria and autoimmune disorders, exhibits notable antitumor and antiviral properties. It interferes with autophagy, a survival mechanism in cancer cells, and its antiviral properties are advantageous in managing respiratory infections that can complicate NSCLC [57]. Hydroxychloroquine, shown in **Figure 2 (B)**, dissolves well in water, which contributes to its rapid dissolution rate in biological fluids and enhances its bioavailability. It melts at around 203°C and has a Log P value of about 4.6, indicating its lipophilicity and facilitating its movement across cell membranes. Hydroxychloroquine is chemically stable under typical conditions and has a molecular weight of 434.95 g/mol. With polar groups and multiple pKa values around 8.3 and 9.7, hydroxychloroquine can behave differently across various pH levels and interacts effectively with biological molecules.

Hydroxychloroquine, with its characteristic Log P value, exhibits strong lipophilicity, enabling it to effectively penetrate lipid-rich cell membranes, such as those in the lungs. At lung fluid's typical pH, the drug remains in its non-ionized state, facilitating efficient transport across pulmonary barriers that is a key advantage for pulmonary drug administration. However, its high lipophilicity might limit its solubility in the lungs' aqueous environment, potentially affecting its absorption. Thus, to target the lung, it may require a tailored delivery system such as encapsulation into LNPs or solid dispersions.

The synergistic effects of combining hydroxychloroquine with pimozide in particle engineering delivery systems may amplify their anticancer effects, offering a robust dual-drug strategy for NSCLC therapy.

Furthermore, rifaximin, primarily recognized for its antibacterial action, can target secondary bacterial infections in NSCLC patients, potentially improving their treatment outcomes and quality of life [58, 59]. Moreover, a previous study investigated the anticancer activity of rifaximin on Caco-2 cells, where the results revealed a significant reduction in cell viability with rifaximin treatment, accompanied by concentration-dependent decreases in cellular markers associated with proliferation, angiogenesis, and survival pathways [60]. These findings suggest that rifaximin's potential as a therapeutic agent for NSCLC could involve disrupting crucial signaling pathways involved in cancer cell viability.

Rifaximin, displayed in **Figure 2 (C**), exhibits several physicochemical properties critical for its pharmacological effectiveness. It is moderately soluble in methanol and ethanol but slightly soluble in water, with a water solubility of about 0.2 mg/mL, which influences its oral and intravenous formulation. The compound has a melting point around 188°C. With a Log P value of 2.6, rifaximin is lipophilic, enabling effective membrane permeation crucial for its antibacterial action. It also has a molecular weight of 785.94 g/mol and features various polar groups affecting its interactions in biological systems. The pKa of approximately 7.9 impacts its ionization and thus its behavior in biological fluids. Rifaximin, with a Log P value of 2.6 and a pKa of approximately 7.9, suggests effective pulmonary absorption and therapeutic potential. At the lung's pH, the compound exists in its non-ionized form, optimizing its membrane penetration and bioavailability. This balance between solubility and

permeability at lung pH levels makes it particularly suited for treating pulmonary conditions, ensuring that it remains effective across varying respiratory environments.

Integrating dual therapies as hydroxychloroquine with pimozide or with rifaximin in therapeutic regimens could provide a comprehensive approach to both bacterial and tumor challenges in NSCLC patients. This thesis highlights the strategic repurposing as well as the combination of these drugs, delivered through advanced systems, as a promising avenue to significantly improve therapeutic outcomes in NSCLC treatment and respiratory diseases.

A	B	C
Pimozide- (PMZ)	Hydroxychloroquine- (HQ)	Rifaximin- (RFX)
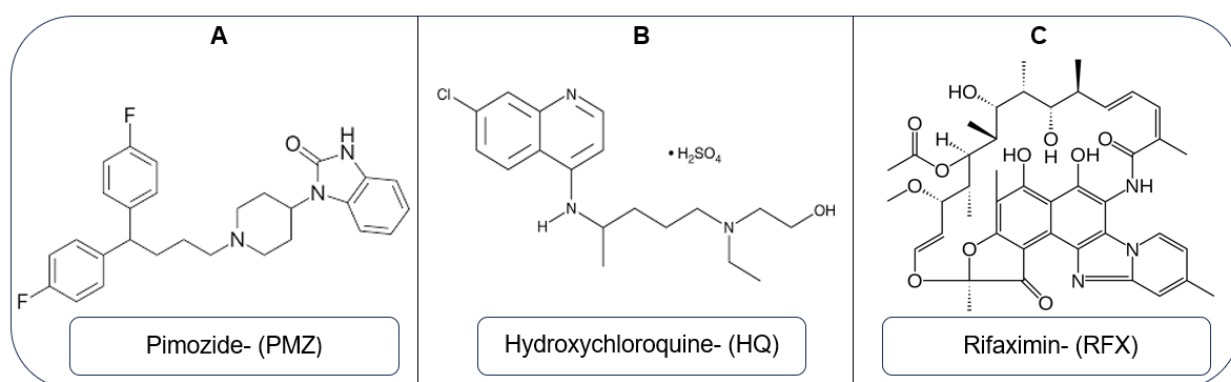
Figure 2. Chemical structures of different APIs used in this thesis

3.5   Selection of excipients

The appropriate choice of excipients for particle engineering is critical since a suitable excipient can improve medication stability, bioavailability, and patient compliance, hence optimizing therapeutic outcomes. Excipients play a diverse role in the formulation of inhalation products, influencing aspects from the aerodynamic behavior of particles to their hygroscopic properties. The selection process must consider factors such as the interaction between the drug and the excipient, the excipient's impact on the drug delivery mechanism, and its behavior under various physiological conditions. In this thesis, we utilized excipients such as stearic acid, oleic acid, poloxamer 407, PEG 400, PVP, HPMC-E5, trehalose, OraRez, and isomalt, which are among those currently employed in inhalation therapy. **Table 2**

lists a variety of excipients that have been utilized in inhalation therapies, reflecting their crucial roles and widespread application.

Table 2. Current excipients used in inhalation

Excipient	Reference(s)
L-leucine	[61-65]
Dileucine	[65]
Tri leucine	[66-69]
Lactose	[70]
Glucose	[71]
Sucrose	[65, 72]
Trehalose	[73]
Isomalt	[74-77]
Hypromellose	[78]
Hydroxypropyl Cellulose	[79, 80]
Hydroxypropyl Methylcellulose (HPMC-E5)	[81-84]
Sorbitol	[85, 86]
Mannitol	[87]
Ethanol	[88-92]
Menthol	[89, 93]
Alcohol	[89, 93]
Poly (vinyl alcohol) (PVA)	[65, 94-96]
Polyvinylpyrrolidone (PVP)	[97-100]
trometamol	[101]
Myo-inositol	[85, 86]
Thymol	[89]
Chloro-butanol	[89, 93]
Poly (lactic-co-glycolic acid) (PLGA)	[65, 96, 102]
Ethylenediaminetetraacetic acid (EDITA)	[103]
Hydrochloric Acid (HCl)	[101, 104]
Citric Acid	[78, 93, 101]

Oleic Acid	[89, 93, 105]
Sulfuric Acid	[67, 89, 93, 106]
Ascorbic Acid	[67, 93, 107]
Hydrochloric Acid	[89, 93]
Nitric Acid	[89, 93]
Oligo-lactic Acid	[89-92]
Stearic Acid	[108-110]
Propionic Acid	[68]
Poloxamer 407	[111-113]
Benzoic Acid	[68, 114]
Hyaluronic Acid	[65, 68, 96, 115]
Maleic Acid	[65]
Succinic Acid	[65, 116]
Poly (lactic acid) (PLA)	[117]
Pullulan	[118]
Chitosan	[119, 120]
Sorbitans	[101]
Propylparaben	[101]
Methylparaben	[101]
HFA 134a (1,1,1,2-tetrafluoroethane)	[101]
HFA 227 (heptafluoropropane)	[101]
Sorbitan Trioleate (SPAN 85)	[89, 93, 105]
Ovalbumin	[106, 121]
Dichlorodifluoromethane	[93]
Dichlorotetrafluoroethane	[93]
Acetylcysteine	[93]
Trichloromonofluoromethane	[93]
Tromethamine	[89, 104]
Stearyl Amine (SAM)	[108, 122]
Povidone K25	[78]
Apaflurane (HFA 227)	[78]
Norflurane (HFA 134a)	[93]
Soya Lecithin	[89, 93, 105]
Hydrogenated Soy Lecithin	[89, 93]

Gelatin	[78, 106, 121]
Glycine	[85, 89, 123]
Saccharin	[89, 93]
OraRez	[124, 125]
Saccharin Sodium	[89, 93]
Sodium Bisulfite	[103]
Sodium Chloride (NaCl)	[101]
Sodium Hydroxide (NaOH)	[101, 104]
Sodium Citrate	[85, 89, 106]
Acetone Sodium Bisulfate	[89, 93]
Edetate Sodium	[89, 93, 104]
Disodium Edetate	[78]
Sodium Maleate	[65]
Magnesium Stearate	[126]
Calcium Chloride	[89, 106]
Phosphates	[101]
Polysorbates	[127]
Polysorbate 80	[89, 104, 128]
Lysine Monohydrate	[89]
Alginate	[106, 121]
Phospholipids	[89]
Fatty Acid Soaps	[67-69]
Distearyolphosphatidylcholine (DSPC)	[78, 106]
DSPC[1]	[106]
DSPC[2]	[106]
1,2-Distearoyl-sn-glycero-3-phosphoglycerol (DSPG)	[78, 106, 129, 130]
Dipalmitoyl phosphatidylcholine (DPPC)	[94, 106, 129-131]
Carboxylic Acid Functionalized Methyl Polyethylene Glycol	[89-92]
1,2-Dipalmitoyl-sn-glycero-3-phosphoglycerol (DPPG)	[108]
Polyethylene Glycol (PEG 400)	[132]
Ammonia	[89, 93]

Polyethylene Glycol (PEG 6000)	[128]
Benzalkonium Chloride	[78, 89, 133]
Cetylpyridinium chloride (CPC)	[89, 93]
Fumaryl Diketopiperazine	[104, 134, 135]
Water	[78]

To provide further insight into some of the key excipients utilized in the different formulations throughout the whole work, **Table 3** outlines the physicochemical properties, of all the excipients utilized in this thesis which are critical to understanding their functionality and role in inhalation products.

Table 3. Physicochemical properties of excipients utilized in this thesis

Excipient	Molecular Weight (g/mol)	Physical State	Melting Point (°C)	Tg (°C)	Solubility in Water	Density (g/cm³)	Key Features
Stearic Acid	284.48	Solid	69.3	-	Insoluble	0.941	Low solubility in water, lubricant
Oleic Acid	282.46	Oily liquid	Liquid at room temperature	-	Insoluble	0.895	Low solubility in water, moisturizer
Poloxamer 407	12,000 - 14,000	White granular powder	Approx. 56	<25	Soluble	-	Thermo-reversible, surfactant
PEG 400	400	Clear viscous liquid	Liquid at room temperature	-	Miscible	1.125	High viscosity, solvent
PVP 40	40000	White powder	N/A	150-180	Highly soluble	-	Binder, stabilizer, Higher viscosity than HPMC-E5
HPMC-E5	1261.4	White to off-white powder	N/A	178-200	Soluble in cold water	-	Film formation, thermal gelation, low hygroscopicity, viscosity 3-6 mPas

Trehalose	342.3	White crystalline powder	97	120	Highly soluble	-	Stability, less hygroscopic
Isomalt	344.3	White crystalline	145-150	60	Moderately soluble	-	Stability, low-caloric sweetener
OraRez	-	White free-flowing powder	No defined melting point	-	Soluble	-	Bio-adhesive, soluble in water

Stearic acid is commonly used as a structural component in the formulation of lipid nanoparticles, where it forms a solid core that encapsulates the API, offering protection against degradation. This saturated fatty acid has a high melting point that contributes to a stable, rigid nanoparticle structure, ideal for sensitive molecules that degrade easily. Additionally, its role extends to functioning as a functional modifier by controlling the release rate of the encapsulated drug, thus facilitating sustained-release formulations [136].

Oleic acid, a monounsaturated fatty acid, is used in lipid nanoparticles to produce the lipid shell or matrix, providing fluidity and flexibility due to its cis-double bond, which causes a bend in the structure. Oleic acid's fluid nature at body temperature makes it ideal for encapsulating APIs, especially those that require a dynamic environment for stability. Oleic acid influences nanoparticle surface features such as charge and hydrophobicity, which impacts cellular absorption and circulation time in the body. Furthermore, oleic acid increases the bioavailability of hydrophobic pharmaceuticals by increasing their solubility and enabling the uptake of drug-loaded nanoparticles into cells, leveraging its affinity for biological membranes to boost drug absorption rates [137, 138].

Poloxamer 407 plays an essential role in drug delivery systems that use nanoparticles attributed to their unique amphiphilic properties. Acting as both a surfactant and stabilizer it helps reduce the surface tension between lipid nanoparticles and water thus enhancing their stability and preventing clumping. Its emulsifying qualities are key in creating and maintaining emulsions during nanoparticle production. Moreover, Poloxamer 407's ability to form a gel at body temperature (37°C) is beneficial for controlling the release of drugs over time. This

feature also enhances the wetting of nanoparticles improving their interaction with tissues and promoting their uptake by temporarily altering the cell membrane's permeability. Compared to distinct types of poloxamers, Poloxamer 407 stands out due to its molecular weight and well balanced hydrophilic hydrophobic group ratio making it ideal for developing more potent and efficient drug delivery formulations [111-113].

Polyethylene Glycol (PEG 400) enhances the stability, solubility, biocompatibility, and efficacy of lipid nanoparticles (LNPs). As a surfactant, it decreases surface tension at the oil-water interface, enhancing colloidal stability and avoiding nanoparticle aggregation [139]. This ensures that drugs are delivered consistently and effectively. Furthermore, PEG 400 improves the solubility of hydrophobic medicines within LNPs, increasing their total bioavailability [132]. Its role in PEGylation offers "stealth" qualities on LNPs. PEGylation, which involves attaching PEG molecules to the surface of nanoparticles, creates camouflage that allows the nanoparticles to avoid detection by the body's immune system. This decreases opsonization and phagocytosis, increasing the nanoparticles' circulation duration in the bloodstream. PEG 400 is also known for its biological compatibility and minimal harmful effects, which lowers possible immunogenic responses and boosts the safety characteristics of nanoparticle formulations. PEG 400's variety of features makes it a fundamental component in the fabrication of effective and safe nanoparticle-based drug delivery systems [132].

Hydroxypropyl Methylcellulose (HPMC-E5)'s contribution to LNPs is critical to improving the stability, efficacy, and safety of pulmonary drug delivery systems. As a stabilizing agent, it prevents particle aggregation in the respiratory system by establishing a hydrophilic barrier surrounding the nanoparticles and increasing the formulation's viscosity [83]. This viscosity alteration is especially useful since it allows for the controlled release of active substances straight into the lungs, which supports long-term therapeutic effects. Furthermore, HPMC-E5 boosts the mucoadhesive capabilities, allowing them to stick to respiratory tract mucosal surfaces more efficiently [82]. This extends the formulation's duration of action at the site of absorption, potentially boosting the drug's therapeutic efficacy [83].

On the other hand, HPMC-E5 enhances the spray drying procedure by acting as a stabilizer, binder, and film former, which ensures uniformity and stability in the feed solution and the final dried particles [81]. It improves the solubility and dissolution rates of spray-dried powders, essential for pharmaceuticals that require rapid absorption. As a protective agent, it shields sensitive active ingredients from thermal degradation during the drying process. Additionally, its capacity to form a controlled-release matrix supports the gradual release of drugs, enhancing therapeutic outcomes [84]. HPMC-E5 also increases the load capacity of spray-dried particles, allowing for higher concentrations of active ingredients.

In the spray drying of drugs intended for inhalation, Polyvinylpyrrolidone (PVP) serves multiple crucial roles due to its exceptional binding, stabilizing, and physicochemical properties. As a stabilizer, PVP the APIs from thermal and chemical degradation during the drying process, maintaining their efficacy [100]. It acts as a carrier, effectively encapsulating APIs to form stable, homogeneous particles with controlled sizes and morphologies suitable for optimal lung deposition [99]. PVP also enhances the solubility and dissolution rates of poorly soluble drugs, facilitating immediate release and absorption in the lungs [98]. Additionally, it can be formulated to provide controlled or sustained drug release, which is beneficial for chronic treatments, while protecting the drug from environmental factors like moisture during storage and use [97].

Trehalose plays a multifunctional role in the spray drying of inhaled therapies, primarily by stabilizing sensitive biological molecules such as proteins and peptides during the drying process [140, 141]. It protects these molecules from denaturation and degradation by forming a stable amorphous matrix that immobilizes them. This is due to its high glass transition temperature. As an excipient, trehalose enhances the flow properties and dispersibility of the dry powder, crucial for ideal lung delivery. It also controls hygroscopicity, preventing excessive moisture absorption that could compromise the powder's stability and aerodynamic performance. Additionally, trehalose acts as a bulking agent, evenly distributing active ingredients within the powder, and serves as a taste-masking agent, improving patient compliance by providing a slightly sweet flavor [142].

OraRez, a pharmaceutical-grade copolymer of methyl vinyl ether and maleic anhydride, significantly enhances the performance of inhaled delivery systems through its role as a film former. Its solubility in water and alcohols facilitates uniform mixing with APIs and other components, allowing it to form continuous films during the spray drying process. These films encapsulate APIs, providing a protective barrier that maintains stability against thermal and mechanical stress. This encapsulation is crucial for preserving the integrity of sensitive molecules and controlling drug release kinetics. The protective films also influence the physical properties of the resultant spray-dried particles, such as size, shape, and surface roughness, optimizing their aerodynamics for deeper lung penetration and effective deposition in the respiratory tract [125].

Moreover, OraRez's strong chelating properties enable it to form complexes with APIs, further enhancing stability and delivery efficiency. Its film-forming ability also serves to manage moisture sensitivity, preventing clumping and preserving the dispersibility and flow characteristics of dry powders. Additionally, OraRez increases the mucoadhesive properties of formulations, improving retention time within the respiratory tract, which benefits prolonged drug action [124].

Isomalt plays a critical role in the spray drying of pulmonary-delivered therapies due to its stability, inertness, and physical properties. As a carrier and bulking agent, it facilitates the formation of consistently sized particles optimal for lung deposition [74, 76]. Isomalt's thermal stability protects heat-sensitive APIs during spray drying, while its low hygroscopicity prevents moisture-related clumping, ensuring powders remain free-flowing for effective delivery through inhalation devices [75]. Additionally, isomalt is chemically inert, it is compatible with other excipients, allowing for complex formulations without adverse interactions. Its mildly sweet taste can also mask the bitter flavors of certain APIs, improving patient compliance [77].

4.   Design of experiments (DoE)

A structured factorial design approach and Design of Experiments (DoE) are employed to assess the influence of various formulations on drug stability, solubility, and other physical properties. DoE provides several advantages compared to the

traditional method. These advantages include the capability to both identify and predict interactions among multiple variables, enhancing the robustness and efficiency of our experimental analyses [143].

By employing DoE, the impact of multiple formulation variables (independent variables) is efficiently investigated on selected drug attributes (dependent variables). In this thesis, the dependent variables include key physical properties of the drug, such as stability under various storage conditions and encapsulation efficiency in different formulations. The independent variables are the components of the drug formulation itself, such as the variety of excipients, or lipid utilized, and the type of nozzle used during spray drying. These were chosen based on preliminary literature reviews, which indicated their likely impact on the drug's physical properties.

To analyze the data obtained from these experiments, one-way Analysis of Variance (ANOVA) is utilized. This statistical method allows us to determine whether there are statistically significant differences between the means of three or more independent (unrelated) groups. By applying one-way ANOVA, the impact of each formulation variable on the drug properties is effectively assessed. This analysis helps in identifying which factors significantly influence the outcome, providing a statistical basis for selecting the optimal drug formulation.

5. Particle engineering techniques employed in this thesis

In this thesis, key particle engineering techniques are discussed, including the encapsulation of APIs into lipid nanoparticles for enhanced delivery and protection, and spray drying, to control particle size and stability, improving solubility and handling.

5.1 Lipid-Based Nanoparticle delivery systems (LNPs)

Lipid nanoparticles, known as (LNPs) have made progress in the field of nanomedicine by providing solutions for drug delivery systems especially for RNA, DNA, proteins and small molecule medications [144]. These particles are made up of a core composed of the lipid matrix encapsulating APIs and surrounded by a

protective layer comprising surfactants. This design not only shields the substances inside from enzymatic breakdown in the bloodstream but also improves their effectiveness in reaching target cells. Such a setup is particularly advantageous for maintaining the stability and uptake of molecules like mRNA and siRNA. Those are naturally fragile, making them essential for gene therapy applications [145].

In gene therapy, LNPs have improved how genes are delivered, making the process more efficient and stable. This technology played a role, in the creation of mRNA-based vaccines like those developed for COVID 19 [146]. LNPs played a role in stabilizing the mRNA helping it enter host cells effectively to prompt the desired response. Apart from fighting diseases researchers are looking into using LNPs for developing vaccines, against cancer. In this area LNPs are used to encapsulate antigens and adjuvants to enhance response and ensure delivery [147].

Moreover, LNPs play a role in cancer treatment by targeting tumor cells thereby reducing the adverse effects linked to traditional chemotherapy. Customizing LNPs to react to triggers like the environment within tumors or enzymes unique to tumors allows these particles to transport medication straight, to the tumor location enhancing treatment effectiveness and minimizing overall bodily harm [148].
LNPs are leading the way in transforming therapy for difficult conditions like non-small cell lung cancer (NSCLC) which is the most common type of lung cancer. LNPs are perfectly designed to tackle the challenges of NSCLC treatment by providing drug delivery methods that play a role in improving treatment effectiveness and reducing side effects linked to traditional therapies [149].

The development of LNPs, for treating NSCLC is centered around their ability to transport substances directly to cancer cells avoiding harm to tissues. This customized approach depends on the characteristics of tumor environments such as proteins found on cancer cell surfaces or the acidic nature within tumors, which prompt the release of the contained medications [150]. For instance, LNPs can be modified to contain molecules that bind to receptors, on NSCLC cell surfaces ensuring that the therapeutic cargo reaches the cancer cells precisely.

Moreover, researchers are investigating LNPs for their ability to deliver drugs together. In the case of NSCLC this might involve mixing chemotherapy medications,

with targeted therapies or immune system regulators in a nanoparticle. These combinations could target pathways related to tumor development and resistance potentially enhancing treatment effectiveness and addressing the issue of drug resistance frequently encountered in NSCLC treatment [151].

5.2   Amorphous solid dispersions

Amorphous solid dispersions represent a breakthrough in science, especially in enhancing the solubility, bioavailability, and dissolution rate of poorly soluble medications. During this formulation process APIs are dispersed within a carrier matrix which is usually a polymer. This technique plays an essential role in enhancing drug delivery systems by transforming poorly soluble medications into more soluble forms.

 Solid dispersions are a pharmaceutical technique used to increase medication solubility, primarily by converting APIs from crystalline to amorphous states. This transition is significant because the amorphous form is less stable than the crystalline form, but it is more soluble. While the stability decrease may appear to be a drawback, it allows for a faster dissolving rate when the drug is put into biological fluids, resulting in increased drug absorption into the body. This transformation procedure is particularly important because many freshly created chemical compounds have low solubility issues throughout the drug discovery phase.

Polymers are frequently used as carriers inside solid dispersions to sustain the amorphous state and improve formulation stability. These polymers help to stabilize the medication's amorphous shape, protecting it from returning to its original less soluble crystalline form. The stability provided by polymers is vital for preserving the drug's solubility during its shelf life. It should be noted that the choice of polymer, as well as the exact manufacturing technique utilized to form the dispersion and the drug-to-carrier ratio, are all major elements that impact the final pharmaceutical product's effectiveness [152].

Spray drying, melt extrusion, and solvent evaporation are some of the production techniques that can be used to produce solid dispersions. Each of these techniques

has specific advantages in terms of scalability, drug loading capability, and compatibility with distinct types of APIs [153].

Solid dispersions can be characterized as the API's dispersion of a solid state in an inert carrier that is prepared by dissolution, melting or melting-dissolution [154]. To develop an amorphous solid dispersion composition successfully, three main aspects must be monitored including the characteristics of the API, stabilizing polymer, and the technology used in processing, for example melt extrusion and spray drying [155]. Amorphous products could be classified into pure amorphous drugs, and solid dispersions. The composition of the molecularly pure consists solely of the drug and performed by the using the evaporation of the rotary evaporator, freeze-drying or spray-drying [156]. Crystal structures are prevented from forming by quick solvent removal; hence, this results in the formation of random amorphous materials [157].

Amorphous solid dispersions are mixtures of low water solubility drugs with hydrophilic carriers, accountable for the drug release profile modulation, and indicated by the size reduction of the drug particle to a molecular level co-dissolving or solubilizing the drug in soluble carriers. In general, they offer better dispersibility and wettability as the supersaturation state of the drug is enforced by solubilization in hydrophilic carriers [156, 158, 159]. Interestingly, solid amorphous dispersions are used as a method of elevating the bioavailability of drugs of low solubility by enhancing their dissolution extent and rate[154]. The solid dispersion's physical state will rely on physicochemical characteristics of the drug and the carrier, the interactions between the drug and the carrier and the method of preparation [160].

5.2.1 Advantages and limitations of co-amorphous systems

Co-amorphous solid dispersions represent another approach in which the stabilization of the amorphous drug is performed through strong intermolecular interactions with another low molecular weight co-former. It applies stability and solubility enhancements over the crystalline and amorphous drugs. Co-amorphization prevents recrystallization in the case of contacting biological fluids or while in storage, through molecular interactions [161]. One amorphous drug stabilizing technique is to hinder the molecular dynamics through the creation of binary mixtures with sugars, polymers, etc.[162]. These mixtures are named co-amorphous systems

and are indicated by enhanced drugs stability in glassy state in addition to improved dissolution rate and solubility [163].

Co amorphous forms are receiving attention in the pharmaceutical industry due, to their ability to improve the solubility and stability of soluble medications. This method involves turning forms of APIs into non crystalline states by thoroughly blending them with small molecules or other APIs without the need for polymers commonly used in amorphous solid dispersions [164]. The primary goal of utilizing such forms in pharmaceuticals is to boost the solubility and dissolution rates of drugs which are significant challenges for many new chemical compounds. By mixing the API with a co former, like another drug or a pharmaceutical additive, the molecular interactions between these components prevent the drug from re-crystallizing thus preserving its co-amorphous state and enhancing its absorption into the body [161].

Preserving the crystalline state of the medication helps ensure its efficacy and safety until it reaches the patient, thus extending its lifespan. Co-amorphous systems are instrumental in developing combination medications. By combining two APIs within an amorphous system, synergistic therapeutic benefit can be achieved, improving patient compliance by reducing the necessity for multiple prescriptions and potentially minimizing undesired side effects through dosage adjustments, for each component [165]. However, developing co-amorphous forms poses several challenges. It is critical to choose a suitable co-former that is both API compatible with and successful at stabilizing the amorphous form. Furthermore, the manufacturing process must be closely monitored to ensure a uniform mixture and avoid separation during scale-up and production.

6.   Solid state variability and its impact on pharmaceutical development

Various physical states, like crystalline and amorphous structures, can impact how well a drug dissolves, its stability and its distribution in the body. These differences can influence the effectiveness and safety of a drug requiring research and monitoring, throughout the drug development process.

6.1 Comparative analysis of crystalline and amorphous solids

Solid substances can exist in either crystalline or amorphous forms **(Figure 3)**. In a crystalline state, molecules arrange themselves in a lattice pattern, with long range organization resulting in a low energy structure. This stability impacts physical properties like melting point and solubility which vary based on the type of bonds present within the crystal structure. On the other hand, amorphous solids lack this long-range order seen in crystals and exhibit short range interactions between molecules. The absence of a defined structure in amorphous solids places them in a higher energy state making them more soluble and prone to faster dissolution rates than their crystalline counterparts [166]. However, it's important to note that amorphous solids are not as stable as crystals and may transform into crystalline forms over time requiring stabilization when used in pharmaceutical applications, for optimal effectiveness.
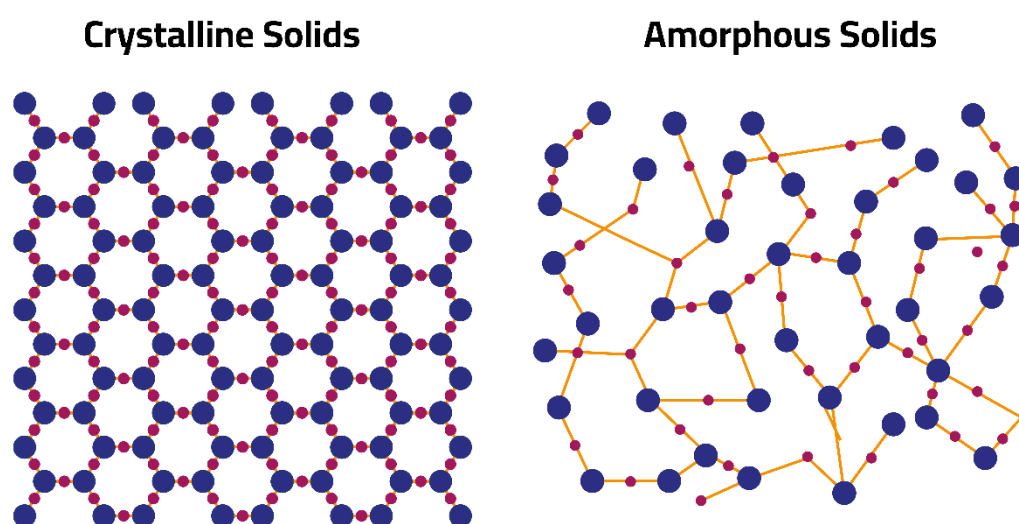

Figure 3. Crystalline and amorphous solids

6.2 Understanding polymorphism in APIs: Stability, solubility, and screening processes

The API molecule can exist in a variety of crystalline forms known as polymorphs, each having a different molecular packing inside three dimensions. Because their crystal structures differ, these polymorphs have diverse physical properties. A metastable polymorph is less stable than the most stable form, with a lower melting point and higher solubility. These metastable polymorphs, like amorphous solids, eventually return to their most stable crystalline form. This shift is frequently facilitated by a solvent-mediated process during dissolution, in which the API recrystallizes into a more stable form with reduced solubility as it approaches equilibrium [167]. Given the potential for any API to exhibit polymorphism, a comprehensive screening is essential to identify all polymorphs and the specific conditions that promote their formation.

6.3 Impact of polymorphism on drug deposition and effectiveness

The polymorphism of materials is affected by the conditions of operating, the solvent mixture [168], and additives[169], in the process of spray-drying. Polymorphism could take part in hydrogen bonding, conformational exchanges as well as ionization[170]. The polymorphism of the API shows an essential aspect that might change the energy of the surface, flow crystal shape, aerosolization, and mechanical characteristics of the adhesive mixture [171]. The Fine Particle Fraction (FPF) of inhalable dry powders is influenced by many factors, such as morphology, size, and polymorphism, thus when combined affect the performance of the aerosol [172].

Powder compositions must include the drug in the required aerodynamic size distribution to deposit in the target area at the flow rate which they are supposed to be inhaled [70]. Functional requirements necessitate good flow characteristics of the composition and managing of the inter-particulate forces in the powder. To accomplish these needs several kinds of compositions, with or without excipients, and specific engineering of the particles could be applied [70]. Size of the particle is a sensitive aspect that affects the performance of the aerosol, it can impact lung deposition and retention in several airway regions. It is shown as the aerodynamic diameter (Da) reflecting the diameter of the unit density sphere with the same settling velocity as the particle. Therefore, using aerodynamic diameters facilitates the comparison of particles with varied sizes, shapes, and densities in terms of their settling behavior in an airflow stream. The aerodynamic diameter is the parameter of

choice that distinguishes the powder's aerosol performance. Particles with 1 to 5 µm Da value are usually stated to be preferred for lung deposition and distribution [173-175]. If the powder has a large median particle size, the FPF, (the mass % of fine particles in the aerosol < 5 µm) is low. Particles with a higher than 5 µm Da value are most likely to be deposited in the oropharynx and the upper respiratory tract regions. While in particles of Da value less than 0.5 µm are likely to be exhaled out.

The shape of the particle is another property that may affect the aerodynamic diameter directly because it affects how a particle interacts with air. Non-spherical particles, such as elongated or irregular forms, have higher air resistance and settling velocities than spherical particles. This is due to differences in drag, effective density, and particle orientation as it passes through the air. These elements combine to affect how rapidly and efficiently a particle can travel and settle in an airflow, influencing aerodynamic diameter predictions [176, 177].

7. Preparation of lipid nanoparticles and solid dispersions

7.1 Detailed description of different lipid nanoparticles: SLN, NLC, LLC

Particle engineering is utilized to develop APIs via lipid nanoparticles (LNPs) to improve drug delivery, stability, and bioavailability by enclosing ingredients, in lipid-based carriers. Lipid nanoparticles (LNPs) are becoming increasingly popular as carriers for drug delivery because of their characteristics and benefits. LNPs consist of formulations, such as nanostructured lipid carriers (NLCs), solid lipid nanoparticles (SLNs), hybrid lipid nanoparticles, and liposomes. These nanoparticles have features that make them well suited for drug delivery systems. Initially they demonstrate biocompatibility and biodegradability.

LNPs can be made up of lipids like phospholipids, cholesterol and other lipid derivatives that closely resemble the bilayers in cell membranes [177]. This structural resemblance enhances their compatibility with systems. Reduces the chances of toxicity. Additionally, LNPs have a capability to encapsulate both hydrophilic and hydrophobic drugs in their core or lipid layers. This flexibility allows for the delivery of many therapeutic agents, including small molecules, proteins, nucleic acids, and gene-based treatments. By enclosing drugs in the core and hydrophilic drugs in the

aqueous layer of LNPs controlled release is facilitated leading to enhanced bioavailability [178]. LNPs can protect encapsulated drugs from degradation, metabolism, and elimination in the body, thereby extending their circulation time and enhancing their therapeutic efficacy.

 Moreover, LNPs can improve drug solubility, enabling the delivery of poorly water-soluble drugs that would otherwise exhibit limited bioavailability [179]. LNPs also can overcome biological barriers, such as the blood-brain barrier, by utilizing specific targeting ligands, which can enhance drug accumulation in desired tissues or cells while minimizing off-target effects [180]. Formulation and manufacturing of LNPs can be achieved by different production methods such as hot or cold high-pressure homogenization or micro-emulsion techniques [181].

In this thesis, the utilized techniques are classified into three categories: Solid Lipid Nanoparticles (SLN), Nanostructured Lipid Carriers (NLC), and Liquid Lipid Carriers (LLC) **(Figure 4)**. All LNPs are prepared by the microemulsion formation technique [182]. This method uses oil, water, and surfactants to stabilize small droplets within another liquid. To prepare SLN, NLC, and LLC, the components comprising the lipid, water, and surfactant were heated beyond the Phase Inversion Temperature (PIT) with intensive agitation to create microemulsions. Specifically, the hydrophobic drug was dissolved at 85°C in a lipid phase, which was made of stearic acid for SLN, oleic acid for LLC, or a combination of both for NLC formulations.

Solid Lipid Nanoparticles (SLN) are composed of solid lipids, providing a strong framework for encapsulating hydrophobic drugs. This encapsulation reduces drug leakage and degradation, enhancing stability and allowing for controlled release [183]. SLNs are particularly effective for improving the bioavailability of soluble drugs and ensuring sustained release within targeted delivery systems. By preserving active compounds until they reach their intended site of action, SLNs represent a leading nanotechnology-based delivery method that optimizes therapeutic efficacy and stability.

Nanostructured Lipid Carriers (NLC) advance beyond SLN by combining solid and liquid lipids to form a structured matrix that increases drug loading capacity and reduces potential drug expulsion [184]. This blend allows NLCs to accommodate

both hydrophilic and hydrophobic medications, addressing SLN limitations such as drug loading and expulsion [185]. Additionally, the unique composition of NLCs enhances carrier stability and offers adjustable drug release patterns, making them an effective solution for controlled drug delivery.

Liquid Lipid Carriers (LLCs) use liquid lipids that remain fluid at both ambient and physiological temperatures, which provides considerable benefits for drug delivery [186]. One major advantage of LLCs is their capacity to dissolve and stabilize high quantities of liquid-soluble pharmaceuticals, hence increasing the solubility of poorly water-soluble treatments. These carriers enable the quick release of active substances, which is critical for illnesses needing urgent therapeutic benefits [186]. Furthermore, LLCs are biocompatible, and their affinity for biological membranes promotes effective drug absorption. Despite its benefits, the fluid nature of LLCs can provide obstacles such as potential leakage and stability issues, which must be managed carefully through formulation and storage procedures.
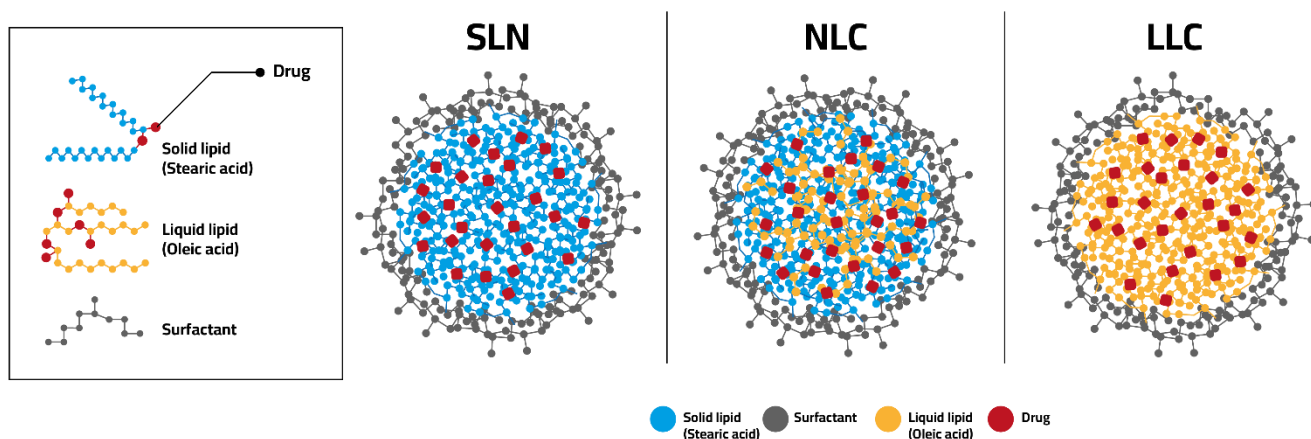

Figure 4. Lipid nano particles prepared in this thesis including, SLN, NLC, and LLC.

7.1.1 Limitations of lipid nanoparticles LNPs

One of the main constraints of LNPs is their stability. Lipid nanoparticles can be susceptible to temperature, pH, and ionic strength variations in their surroundings, affecting their structural integrity and, as a result, the efficacy of the encapsulated medicine. This instability might result in premature drug release or nanoparticle

disintegration, posing substantial storage and distribution issues, especially in areas lacking advanced healthcare infrastructure [187].

Another issue to consider is the chance of immunogenicity. Although LNPs are commonly viewed as safe and compatible with the body there is a risk that they might elicit reactions, in some people [188]. This could lead to inflammation or other negative outcomes impacting the efficacy of the drug delivery method and safety worries for patients.

Additionally, the ability to increase production poses a challenge. The processes involved in LNP production are complex and demand a level of accuracy, making scaling up operations both challenging and costly. This limitation could hinder the large-scale production needed for use especially for treatments that necessitate global distribution, like vaccines [189]. Moreover, the precision of targeting with LNPs is still restricted. While LNPs can be customized to target tissues or cells, achieving the precision required for certain medical purposes remains a challenge. The characteristics of the lipid components and the changing nature of systems can impact targeting effectiveness by modifying how LNPs interact with target cells [190].

Furthermore, the encapsulation efficiency of certain medications, particularly those with strong hydrophilicity, can be low. This inefficiency may necessitate higher doses to produce therapeutic effects, thus raising treatment costs and complexity.

7.2   Overview of spray drying in particle engineering

Spray drying is a pivotal technology in particle engineering, offering extensive control over particle characteristics and playing an essential role in optimizing drug delivery and efficacy. The technique's adaptability, efficiency, and scalability make it a cornerstone in pharmaceutical manufacturing. Spray drying is an advanced technique widely used in particle engineering, particularly in the pharmaceutical sector, to enhance the physical properties of drug particles. This process transforms a liquid solution, suspension, or emulsion into a dry powder by atomizing the liquid into a hot drying chamber where the solvent evaporates rapidly [191]. The ability to control particle size, morphology, and composition makes spray drying invaluable for producing consistent, high-quality pharmaceutical products [192].

The spray drying process begins with atomization, where the liquid feed is dispersed into fine droplets using an atomizer, which significantly increases the surface area of the liquid and facilitates rapid heat and mass transfer. As these droplets encounter hot air, the solvent quickly evaporates, leading to the formation of solid particles. Finally, the dried particles are collected; larger particles settle under gravity, while finer particles are removed using cyclone separators [193]. This efficient sequence ensures effective drying and particle recovery.

The spray drying process is carefully designed to accommodate various properties of the feed solution, which significantly influence the choice of equipment and operational parameters. Atomization, where the liquid feed is dispersed into fine droplets using an atomizer, is a critical step that depends on the viscosity of the feed. This property determines how smoothly the feed will flow through the system and impacts decisions regarding atomization techniques to ensure optimal cleaning and maintenance. The atomizer type used affects droplet size and distribution, crucial for determining the final particle size and morphology [194].

Feed solutions with unique characteristics such as high pH, flammability, hygroscopic nature, abrasiveness, and thermoplastic properties pose additional challenges [195]. For instance, feeds with a high pH can corrode equipment walls, while flammable feeds necessitate stringent safety measures during the drying process. Hygroscopic products may become sticky, affecting their interaction with equipment surfaces, and abrasive materials can wear down vital components like piping systems and pumps. Thermoplastic materials with lower glass transition temperatures add complexity to the spray drying process, as they can become tacky when exposed to heat, leading to material sticking to equipment and forming clumps [196].

The process parameters like inlet and outlet temperatures are closely monitored to control the drying rate and temperature of the drying gas, which directly impacts the solvent evaporation rate and ensures the integrity of thermally sensitive feeds. Inlet temperature is important to quickly dry the solvent from the liquid feed solution while the outlet temperature indicates how much moisture has been removed. The aspirator processing at full capacity is essential for the efficient generation of airflow, transport of droplets, transfer and control of heat, collection of products, and

prevention of particle aggregation. Nitrogen gas is used to avoid oxidation or explosion. Additionally, the residence time in the drying chamber is optimized to ensure complete drying without degrading the product. Each of these parameters is adapted based on the specific properties of the feed to achieve efficient drying while maintaining product quality and ensuring the longevity and safety of the drying equipment [197, 198].

The Péclet number is a crucial dimensionless metric in spray drying, expressing the relationship between the solvent evaporation rate and solute diffusion within a droplet. A low Péclet number indicates that solute diffusion is comparable to or exceeds the rate of solvent evaporation, typically resulting in denser particles with minimal void spaces [199]. Conversely, a high Péclet number suggests that evaporation outpaces diffusion, leading to solute accumulation at the droplet surface, which often forms a shell and results in hollow particles after drying. This relationship highlights the impact of the Péclet number on particle morphology during the spray drying process. The Péclet number can be raised by altering the feedstock's viscosity, either by adding polymer excipients or by increasing the solute concentration [200, 201]. This adjustment decreases the diffusion movement of molecules within the solvent, influencing particle morphology. A thorough understanding of solute kinetics within the droplet is essential for producing particles with distinct morphologies. By modifying the composition of the feedstock and the drying conditions, composite particles with varying proportions of API and excipients at the core and surface have been successfully developed [200, 201].

7.2.1 Applications of spray drying

Spray drying offers several significant benefits in pharmaceutical applications and manufacturing processes. It enhances the bioavailability of poorly soluble drugs by converting them into highly bioavailable particles, and through microencapsulation, it allows for controlled drug release, which improves therapeutic effects and minimizes side effects [202]. Additionally, it is capable of producing inhalable medications, creating powders with optimal particle sizes for effective pulmonary delivery [203]. The advantages of spray drying extend to its versatility in handling various formulations such as solutions, suspensions, and emulsions [204]. It is an efficient process that quickly dries materials, preventing thermal degradation of heat-sensitive

substances [192]. Moreover, it allows for the customization of particle shapes like porous or hollow structures, which can impact how quickly drugs dissolve and their availability, in the body [205].

Spray drying is crucial in the pharmaceutical industry, not only for its direct applications in drug formulation but also for its role in advancing drug delivery technologies like dry powder inhalers (DPIs). The method allows for precise control over particle characteristics, crucial for ensuring the effectiveness, safety, and stability of pharmaceutical products [201].

7.2.2 Advanced spray drying strategies

Advanced spray drying strategies have significantly enhanced the ability to engineer particle properties for specialized pharmaceutical applications. Among these strategies, the implementation of two-fluid and three-fluid nozzles **(Figure 5)** provides sophisticated tools for tailoring particle characteristics such as size, distribution, and morphology.

The two-fluid nozzle (2FN) is the cornerstone of spray drying, combining two streams: a liquid holding the medicine and excipients and a compressed gas. This structure allows the gas to shear the liquid into fine droplets, which quickly dry when they encounter the drying chamber's heated air. The fundamental advantage of the 2FN is its simple design and ability to generate small particles with exact control over their size and distribution [206]. This feature is useful for creating particles suitable for specific routes of administration, such as inhalation.

On the other hand, the three fluid nozzle (3FN) enhances flexibility by incorporating another feed solution into the atomization procedure [207]. This additional fluid enables the creation of particle structures like core shell configurations with the core holding the medication and the shell acting as a barrier to regulate release timing. This capability proves valuable in crafting controlled or sustained release drugs, where precise control, over drug release timing and speed significantly influences effectiveness.

The 3FN has a distinguished, multiple-layered concentric structure that is made from inner and outer nozzles for liquid, and an outermost nozzle for gas [208]. Hence, this nozzle configuration has the ability of spraying two different solvents simultaneously, solving conventional two fluid nozzles' obstacles which is only able of spraying one solvent at a time, in which the drug and the coating agent are suspended or dissolved. This suggests that conventional 2FN spray drying might not be effective for microencapsulation when there is a notable contrast between the materials forming the core and shell of the microcapsules. This difference, such as variations in solubility or miscibility, could necessitate a substantial amount of coating agent to ensure proper encapsulation [209].

The 3FN allows dissolving the drug and carrier in separate solvents, which spares the need of a common solvent. Application of this nozzle in the stage of atomization of spray drying permits gel formation, ionic complexation, and cross-linking, and hence the formed complexes/gels may be dried into particulates instantly [210]. In this method, the feeds of the two liquids are separately pumped and only mixed when reaching the nozzle's tip where they meet. The feeds of the two feed solutions may be made from immiscible materials which permits single core microcapsule formation [211]. Aggregation of incompatible particles is avoided when using 3FN which may take place in the case of using traditional 2FN since it only has a single feed channel and nozzle [212].
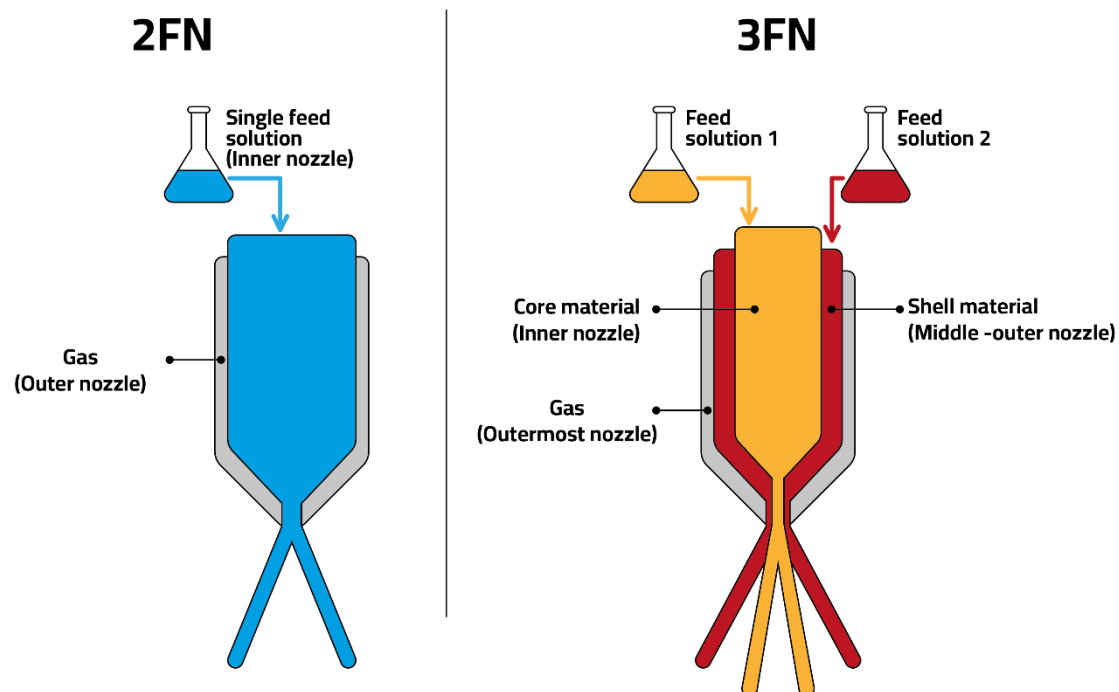
Figure 5. Schematic illustration of two different nozzle types: two-fluid nozzle (2FN) and three-fluid nozzle (3FN).

7.2.3 Limitations of spray drying in pharmaceutical formulations

Spray drying is known for its energy usage, which can be a downside. It involves a large amount of heat and air flow leading to increased expenses and energy consumption. This can make spray drying less cost effective for large scale operations. Additionally, the elevated temperatures during the process can harm heat substances such as proteins, enzymes, and certain pharmaceutical compounds by causing them to deteriorate or lose their effectiveness. Another limitation is the potential for product loss. During spray drying, small particles can be carried away with the exhaust gases, which not only reduces the yield but can also lead to inconsistencies in product quality [213]. This loss can be particularly significant when processing high-value products or when strict dosage accuracy is required.

Handling extremely viscous liquids or suspensions can also be difficult. Spray drying equipment is normally efficient at handling particular viscosity ranges; however, solutions that are very viscous may clog the nozzles, disturbing the process continuity and harming the uniformity and quality of the finished product. Adjusting

these qualities frequently necessitates additional processing stages, which adds complexity and significant costs to the manufacturing process.

Moreover, the control over particle size and morphology in spray drying can sometimes be limited. While the technique is excellent for creating powders with a uniform size distribution, achieving precise control over particle shape and exact size can be difficult. This limitation can affect applications that require highly specific particle geometries for proper function, such as certain drug delivery systems.

Lastly, the scale-up of spray drying processes from laboratory to industrial scale can introduce unexpected challenges. Parameters optimized on a small scale may not translate directly to larger systems due to differences in drying kinetics and spray dynamics. This issue requires careful re-optimization and control, which can delay development timelines and increase costs.

8. Physicochemical characterization techniques

In the development of advanced particle engineering for pulmonary drug delivery systems, rigorous physicochemical characterization is essential to ensure the physical stability, chemical integrity, and functional performance of the formulated solid dispersions. This section delves into the most critical characterization techniques that directly impact the performance and therapeutic outcomes of inhalable therapies.

8.1 Spectroscopic methods

Dynamic light scattering (DLS) is used for analyzing particle size and zeta potential in LNPs and spray-dried solid dispersions, applicable whether these systems encapsulate one or multiple APIs. In the context of LNPs, DLS helps determine the size distribution and stability of the nanoparticles, which are crucial for ensuring consistent drug delivery, effective tissue targeting, and reduced clearance by the body's immune system [214]. The zeta potential measurement provided by DLS assesses the surface charge of nanoparticles, which influences their colloidal stability and interaction with biological membranes [215]. It indicates the electrostatic stability

of the nanoparticles in physiological conditions, which is crucial for their interaction with cell membranes and subsequent drug release and absorption.

Similarly, for spray-dried solid dispersions, DLS is instrumental in determining the uniformity of particle sizes resulting from the spray drying process. This uniformity is essential for achieving predictable dissolution rates and bioavailability in pharmaceutical formulations. Zeta potential measurements can help in assessing the surface charge of the particles, which influences their stability in suspension and their ability to avoid premature aggregation, ensuring consistent delivery and efficacy, also can guide the optimization of surface properties to enhance the stability and dispersibility of the particles in biological fluids.

Fourier Transform Infrared Spectroscopy (FTIR) spectroscopy is essential for analyzing bonding characteristics in crystalline and amorphous states, examining molecular absorption across the infrared spectrum. This absorption is due to molecular vibrations, such as stretching and bending, occurring at frequencies that are specific to different functional groups and their dipole moments. The resulting absorption patterns and frequencies provide insights into the chemical structure of molecules, helping identify functional groups and their roles in intermolecular bonding. FTIR is particularly valuable in understanding the chemical dynamics of drug encapsulation in nanoparticle and solid dispersion formulations.

In the context of spray-dried LNP and solid dispersion systems, FTIR analysis elucidates chemical interactions and encapsulation efficiencies. For single-drug LNP formulations, distinct peaks characterize individual compounds, indicating successful encapsulation within lipid matrices. Broadening of bands above 3000 cm^{-1} suggests the formation of intermolecular hydrogen bonds between drugs and lipids, enhancing molecular cohesion [216]. Significant changes in aromatic and carbonyl stretches suggest additional hydrogen bonding [217], while the decrease in peak intensity may reflect conformational changes due to encapsulation [218].

In dual-drug LNP formulations, spectral shifts and peak broadening indicate interactions within lipid matrices that affect encapsulation efficiency and stability. Comparisons between 2FN and 3FN systems show enhanced molecular interactions and homogeneity in 2FN systems, indicative of the formation of drug microspheres. Further, analysis of dual-drug solid dispersions highlights the impact of delivery methods on integration, with inner nozzle delivery yielding superior peak intensities and interactions compared to single-feed systems, and external nozzle delivery showing the least effectiveness in optimal dispersion and integration within the matrix.

X-Ray Powder Diffraction (XRPD) employs Bragg's Law, which correlates the angles and wavelengths of diffracted X-rays to the spacing of crystal planes, making it highly effective for analyzing crystalline structures. XRPD identifies different crystalline phases within a sample; each crystalline substance produces a distinct set of diffraction peaks, similar to a fingerprint [219]. The patterns indicated in the formulation are compared to the pure drug diffractogram to identify the substance. Additionally, XRPD determines the degree of crystallinity, distinguishing between fully crystalline, semi-crystalline, and amorphous materials based on their unique diffraction patterns [220].

The technique is vital in evaluating spray-dried solid dispersions. XRPD assesses the crystalline or amorphous nature of APIs, influencing the physical stability and dissolution behavior of the drug. Moreover, it determines crystallinity within the lipid or polymer matrix, impacting encapsulation efficiency and drug release kinetics, ensuring APIs maintain their desired physical state for effective delivery.

8.2   Drug release method

The encapsulation efficiency indicates the quality of the drug delivery mechanism while also influencing the formulation approach for optimal therapeutic effects. It is used to evaluate the efficacy of drug delivery systems, such as LNPs and spray-dried solid dispersions, regardless of whether they include one or more active medicinal components.

Encapsulation efficiency (EE%) in LNPs defines how well the lipid-based nanoparticles encapsulate and preserve the APIs from degradation, resulting in targeted distribution and controlled release. In the case of spray-dried solid dispersions, this technique assesses the spray drying process's capacity to evenly distribute and embed the API inside the polymeric or inert matrix, which is crucial for achieving optimal solubility and release profiles. When numerous APIs are involved, encapsulation efficiency becomes even more important since it assesses the delivery system's ability to manage different drugs at the same time without compromising their stability or overall formulation efficacy. The encapsulation efficiency percentage for the LNPs was calculated using equation (1) [221]:

$$EE\,(\%) \; = \frac{Total\;Drug - Free\;Drug}{Total\;Drug} \; x100\%$$

(Equation 1)

To estimate the in vivo performance of inhalable therapies, drug release studies are conducted utilizing dialysis bag measurements and a simulated lung fluid (SLF) as the dissolving medium to accurately imitate the lung's unique environment.
SLF is formulated to reflect the ionic composition and pH of lung fluids, providing a realistic setting for evaluating how the drug will behave once inhaled. When testing formulations intended for pulmonary delivery, the dialysis bag is filled with the drug formulation and then submerged in SLF. This setup allows for the assessment of how quickly and effectively the drug is released from particles small enough to be carried deep into the lung tissues.

For spray-dried solid dispersions, this method determines how the physicochemical properties of the formulation influence the dissolution rate in the lung environment. Factors such as the solubility of the matrix, particle size, and the presence of hygroscopic or mucoadhesive excipients can significantly affect the release profile. Similarly, for LNPs, studying drug release in SLF can provide insights into how the encapsulation within lipid-based nanoparticles protects the drug during inhalation and

facilitates its release at the target site. The ability to release the drug in a controlled manner is evaluated for the formulations through this method.

8.3   Thermal analysis methods

Dynamic Vapor Sorption (DVS) is a critical technique for analyzing moisture interaction properties of spray-dried solid dispersions. It measures the absorption and release of moisture under controlled humidity conditions, essential for creating sorption isotherms that demonstrate the relationship between moisture content and relative humidity. These isotherms provide vital insights into a material's hygroscopicity and moisture stability [222]. For spray-dried solid dispersions, monitoring moisture uptake is crucial as excessive moisture can degrade APIs, affecting drug efficacy and shelf life. DVS plays a key role in determining the stability of these dispersions across various humidity conditions, helping to maintain structural integrity and ensure controlled release of encapsulated APIs [223].

8.4   Surface and particle analysis

Scanning Electron Microscopy (SEM) generates high-resolution images by focusing an electron beam on sample surfaces, revealing shape and surface properties of spray-dried solid dispersions. SEM analysis involves exposing samples to a high-energy electron beam, producing signals from backscattered and secondary electrons that indicate the atomic number of surface atoms and sample topography, respectively. Coating with a thin gold layer enhances image quality by ensuring uniform surface conductivity [224]. SEM provides crucial visual data on particle size, shape, and distribution, key for assessing the quality and consistency of drug formulations. It also detects size increases possibly due to nanoparticle aggregation during spray drying [225, 226], and investigates the degree of aggregation impacting solubility and dissolution rates of APIs.

SEM assesses surface texture, differentiating between smooth and wrinkled particles, with implications for their physical behaviour. Smooth surfaces improve particle flowability by reducing inter-particle friction, whereas wrinkled surfaces hinder

close packing, reducing aggregation likelihood and potentially enhancing dissolution rates due to increased surface area [227, 228].

9. Biological Assays

9.1 Importance of biological assays in evaluating drug efficacy

In the attempt to advance pulmonary drug delivery systems for the treatment of NSCLC and respiratory infections, biological assays play a pivotal role in assessing the therapeutic efficacy and safety of novel formulations. Throughout this thesis, an array of biological tests, including cell culture, MTT cell viability assays, anti-inflammatory assays, and antimicrobial activity assessments are used, to evaluate the interaction of APIs within spray-dried LNP and solid dispersion systems.

Cell culture and MTT cell viability assay utilizing the A549 cell line, derived from human lung carcinoma, provide a relevant biological context to evaluate inhalation therapies, reflecting the cellular environment of human alveolar basal epithelial cells. The MTT assay offers quantitative insights into the cytotoxicity and biological compatibility of these formulations, measuring cell viability through mitochondrial activity. This is crucial for understanding the impact of single and dual drug-loaded systems on lung cancer cells, particularly when investigating the synergistic effects of drugs like pimozide and hydroxychloroquine.

On the other hand, the anti-inflammatory assays are integral for testing how spray-dried LNPs and solid dispersions modulate inflammation, a significant concern in respiratory infections and cancer [229]. By evaluating cytokine levels and gene expression related to inflammation, such as IRAK1, through PCR techniques, the anti-inflammatory potential of our formulations can be assessed. This helps in understanding whether the formulations can effectively reduce inflammation markers compared to controls, providing insights into their potential therapeutic benefits.

Furthermore, given the dual challenges of NSCLC and respiratory infections, assessing the antimicrobial efficacy of formulations containing drugs like rifaximin and hydroxychloroquine is critical. Using methods such as disc diffusion and

Minimum Inhibitory Concentration (MIC) tests, the activity of these drugs against pathogens, including multidrug-resistant strains was evaluated. These assays are essential for confirming that our engineered particles can effectively target and inhibit bacterial growth, which is vital for treating respiratory infections alongside cancer.

By integrating these biological assays into our research, we aim to comprehensively evaluate the efficacy of our drug delivery systems, ensuring they meet the therapeutic needs for treating NSCLC and respiratory infections.

9.2   Cell culture and viability assays

Cell culture, MTT, and cell viability assay are used to determine the cytotoxicity, therapeutic effectiveness, and interaction of APIs within the spray-dried LNPs and solid dispersions delivery systems. Cell culture using A549 cells, derived from human lung carcinoma, is a fundamental method in pulmonary drug delivery research, allowing for the assessment of therapeutic agents designed for respiratory conditions. These cells serve as a model for human alveolar basal epithelial cells, making them particularly suitable for evaluating inhalation therapies such as spray-dried solid dispersions and LNPs [230]. The A549 cell line provides a relevant biological environment to test the interaction of these particles with lung tissue, especially important when these formulations are intended to be delivered directly to the lungs.

The MTT cell viability assay, utilized alongside A549 cell culture, is used for measuring the cytotoxicity and biological compatibility of pharmaceutical formulations. This assay involves the conversion of the MTT reagent, a yellow tetrazole, into an insoluble purple formazan product by active mitochondrial enzymes present only in living cells. The amount of formazan produced is directly proportional to the number of viable cells, thus providing a quantitative measure of cell viability [231].

When formulations contain two different APIs, understanding their combined effect on cells is crucial. This is where the Combination Index (CI) becomes essential. The CI is calculated using the results from the MTT assay to evaluate the type of interaction between the APIs at various concentrations. A synergistic interaction (CI < 1) suggests that the combined effect of the APIs is greater than their individual effects,

potentially allowing for dose reduction without compromising therapeutic efficacy. An additive effect (CI = 1) indicates that the APIs work independently without enhancing or reducing each other's activity. An antagonistic effect (CI > 1) implies that one API may interfere with the activity of the other, which could diminish the formulation's overall therapeutic value [232].

9.3 Anti-inflammatory Assays

Anti-inflammatory tests are used to evaluate how well spray dried LNPs, and solid dispersions can reduce inflammation. These tests analyze cytokines, like IL 1β, IL 6, IL 8 and TNF α to understand the effectiveness of drug formulations. Cytokines play a role in indicating inflammation levels and the body's response to it.

The anti-inflammatory test method involves using the THP 1 cell line, which is transformed into macrophages through Phorbol 12-myristate 13-acetate (PMA) treatment. These macrophages are then triggered with lipopolysaccharide (LPS) to induce a reaction. After stimulation, the cells are exposed to test substances. RNA is extracted for analysis. The expression of IRAK1 RNA, a gene related to inflammation, is measured using PCR (qPCR). This process involves converting RNA into cDNA that is amplified in a PCR cycle. The relative IRAK1 expression is calculated using the 2−ΔΔCT method with 18S rRNA, as the reference gene.

This approach accurately assesses the ability of substances to reduce inflammation by monitoring changes in genes related to inflammation following treatment. This analysis aids in determining whether the formulation can effectively decrease the production of these molecules compared to a control group indicating the therapeutic value of the formulation. Additionally, when multiple active pharmaceutical ingredients are present in formulations it is essential to evaluate not only the anti-inflammatory properties of each ingredient, but also how they collectively impact inflammation. This assessment can indicate additive or conflicting interactions, among the ingredients.

9.4 Antimicrobial activity

The antimicrobial activity of spray-dried formulations containing two APIs against clinical isolates is evaluated using two primary methods: the disc diffusion method

and the Minimum Inhibitory Concentration (MIC) test, both conducted according to CLSI guidelines (CLSI M100, 2023).

For the disc diffusion test, blank discs impregnated with the formulations were placed on Mueller-Hinton agar plates inoculated with a standard bacterial suspension of Acinetobacter baumannii, including strains with Multi-Drug Resistant (MDR) and Extensively Drug-Resistant (XDR) phenotypes. After incubating overnight at 37°C, the diameter of the inhibition zones around the discs is measured, indicating the effectiveness of the antimicrobial agents against these challenging bacterial profiles.

In parallel, the MIC is determined by adding the formulations to broth microdilutions with a standardized bacterial culture, including MDR and XDR strains, and then incubating these mixtures to identify the lowest concentration of the formulation that prevented visible bacterial growth.

10. Applications of particle engineering for pulmonary drug delivery

Particle engineering for pulmonary drug delivery refers to a variety of strategies for increasing the efficacy and safety of drugs used to treat respiratory disorders. This technique improves medication solubility, bioavailability, and targeted specificity by adjusting particle size, shape, and surface features [1]. It can be used to treat respiratory disorders like infections, and lung cancer by allowing medications to be delivered directly to the lungs more efficiently. Particle engineering also helps to develop pulmonary vaccination, immunotherapy, gene delivery, and diagnostic imaging, all of which provide promise revolutionary options for respiratory healthcare.

10.1 How LNPs and spray drying contribute to pulmonary drug delivery

LNP delivery system has numerous uses in pulmonary medication delivery, addressing issues in treating respiratory disorders such as asthma, COPD, infections, and non-small cell lung cancer **(Figure 6).** LNPs successfully encapsulate hydrophobic medicines, increasing their solubility and bioavailability, which are critical for effective treatment. Tailored surface alterations allow for targeted distribution, decreasing off-target effects, while regulated release mechanisms extend therapeutic

effects. LNPs also play a vital role in lung vaccination, immunotherapy, and gene delivery, triggering strong immune responses and permitting the safe transfer of nucleic acids for gene therapy, including NSCLC treatment [233, 234].
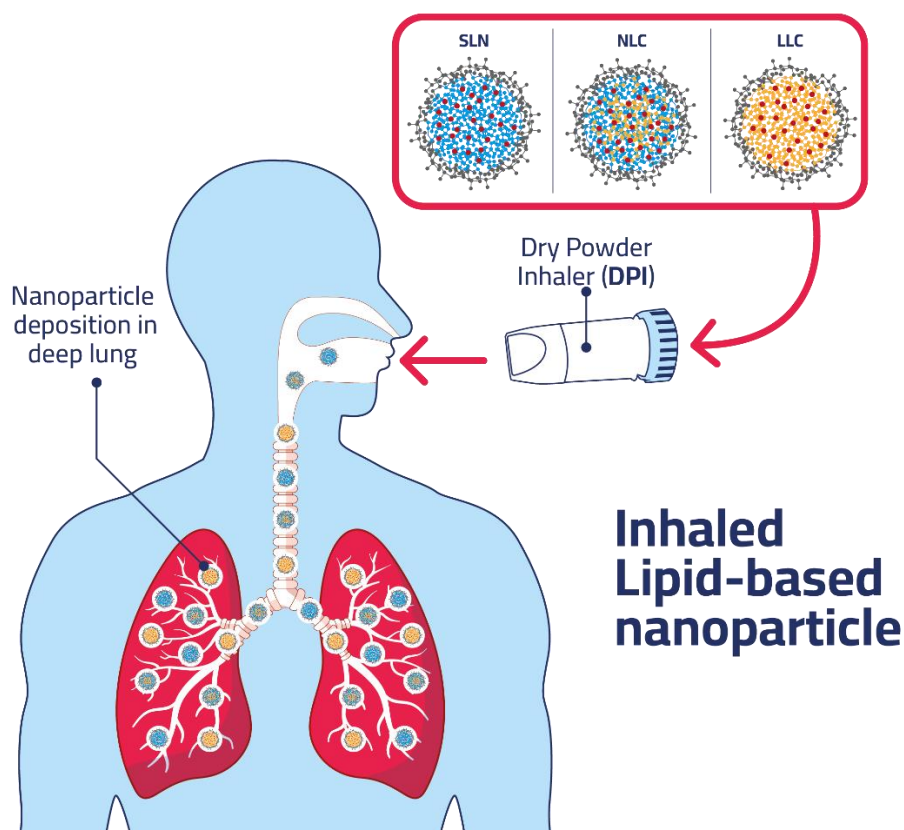

Figure 6. A schematic view of the delivery of therapeutics through lipid-based nanoparticles via a dry powder inhaler**.**

Furthermore, LNPs act as carriers for imaging probes, facilitating non-invasive diagnostic imaging of lung diseases [235]. These achievements demonstrate LNPs' potential to alter pulmonary medicine by enhancing therapeutic efficacy, safety, and patient outcomes in a variety of respiratory diseases, including NSCLC.

On the other hand, spray drying is important in pulmonary medication delivery because it allows for a wide range of applications that improve therapeutic effects.

Spray drying allows for the creation of inhalable powders with the best aerodynamic qualities for lung deposition by precisely controlling particle size and morphological characteristics [236]. This approach improves drug stability by eliminating moisture and forming a protective matrix, ensuring an extended shelf life. It also makes it

easier to develop controlled release systems, which allow for more consistent medication release kinetics and better patient compliance. Spray drying facilitates the development of combination therapies by allowing numerous medications to be co-encapsulated in a single particle. Furthermore, it is used in the manufacturing of dry powder vaccines, which provide better durability and immunological response than liquid formulations [237].

10.2 Potential impact on treating NSCLC and other respiratory diseases

Pulmonary drug delivery systems provide targeted treatment for lung cancer and other respiratory illnesses, maximizing therapeutic efficacy while minimizing systemic adverse effects. They allow for direct administration of drugs to the lungs, which provides fast relief and improves treatment outcomes.

It has been proven that inhaled anticancer medications are effective in treating lung cancers [238-244]. Inhaled anticancer drugs can modify the bio-distribution of the medications and elevate the accumulation of a bigger proportion in the lungs in comparison to intravenous administration [245-249] . Moreover, the systemic distribution is limited in the case of inhaled anticancer medications which also limits the correlated toxicity [238, 243]. Common side effects of inhaled anticancer drugs are usually localized, mild and treatable such as glossitis. Few cases have reported difficulties relating to respiration, like hypoxia and forced expiratory volume. Most of the side effects after treatment with inhaled anticancer drugs are caused by the drug type, dose, and duration of treatment [238, 240-244]. Nevertheless, these side effects could be not related directly to inhaled anticancer drugs or the disease state of progression [241, 243].

Earlier research demonstrated that a certain quantity of inhaled medications was detected in the lymph nodes. Tatsumura et al. conducted a study where they used 5-fluorouracil in the treatment of lung cancer and 5-fluorouracil was present in elevated levels in the regional lymph nodes, which lead to the assumption of the drug being absorbed in the bronchial tree into the lymphatic path [242]. Furthermore, absorbed medications into the lymphatic circulation could be redistributed in the peripheral airways, which could allow accessing hardly parts of the lungs [44, 250]. Therefore, in cases where cancer metastasizes to the lungs, which are typically located distally

from the major airways but receive blood from pulmonary veins and arteries, inhaled anticancer medications may offer significant benefits [251-253].

Contagious illnesses that are caused by bacterial pathogens play a leading role in human mortality and morbidity which makes them a vital threat to human health worldwide [254, 255]. While many of the currently available inhaled products are corticosteroids and bronchodilators that are used in the treatment of asthma and COPD [256], the inhalation of antibiotics is still limited in comparison with bronchodilators, not opposing intense pre-clinical and clinical studies and implications concerned with the emergence of resistances of bacterial antibiotics[256].

Nevertheless, there is a wide use of inhaled antibiotics in intensive care units (ICU) in the treatment of particularly severely ill patients [257]. ICU patients are significantly at risk of nosocomial infections, and almost 40% of severely diseased patients are at risk of developing ventilator-associated pneumonia, which in turn could cause a longer stay in the ICU and may increase the rate of mortality [258].
Most of these infections are treated with antibiotics intravenously, and to date, there is no routine use of inhaled antibiotics. ICU patients can be subjected to extensively drug-resistant microorganisms and multidrug resistant microorganisms' emergence. Hence, it is called for novel approaches and new treatments that cope with the pandemic to abolish infections caused by significant resistant bacteria [259, 260].

Among the advantages of administering antibiotics through the pulmonary route, the most noticeable would be the direct delivery of high antibiotic doses to the lung directly, as the concentrations of the antibiotic locally are much greater when compared to the pathogen's inhibitory concentration [261]. A recent double-blind placebo trial studied the emergence of bacterial resistance following the inhalation of antibiotics in severely diseased patients following mechanical ventilation. When compared to the placebo group, the group which received the inhaled antibiotics succeeded in abolishing multidrug resistant pathogens and intercepted the emergence resistant strains [262].

Recently, a trial confirmed those previous studies assuring minimum bacterial resistance in patients that are undergoing treatment via nebulized antibiotics [263].

Due to the low systemic bioavailability, inhaled therapy of colistin and aminoglycosides significantly limited nephrotoxicity [264, 265], and this benefit may overcome possible respiratory adverse effects. Intravenous colistin was compared to aerosolized colistin in a recent study in patients with ventilator-associated pneumonia that occurred due to multidrug-resistant Gram-negative bacteria. The results of this study showed lower incidence of renal complications in the group which received colistin via inhalation [266]. As mentioned above, pulmonary administration of antibiotics can reduce harmful outcomes of systemic antibiotics. As it may decrease the potential diarrhoea risk of *Clostridioides difficile* due to the antibiotic being disposed in the lungs only.

11. Aims and objectives

Effective drug delivery for non-small cell lung cancer (NSCLC) and respiratory infections remains a critical challenge due to several factors, including inadequate targeting of drugs to the affected lung tissues, limited bioavailability of therapeutic agents, and the risk of systemic toxicity from drugs that affect non-target areas. Despite existing advances in drug delivery, these issues persist and impact treatment outcomes. This thesis addresses these gaps by developing and evaluating novel pulmonary drug delivery systems that incorporate advanced particle engineering techniques. Specifically, the work focuses on improving drug targeting precision, enhancing bioavailability within the lung, and minimizing systemic side effects, thus bridging significant knowledge gaps in the design and implementation of more effective pulmonary drug delivery strategies. The structure of this thesis is outlined in **Figure (7)**.

The specific objectives are as follows:

1.   Investigate the literature on advanced inhalation therapies for NSCLC and respiratory infections, emphasizing the potential of sophisticated targeting mechanisms and repurposed drugs formulated through particle engineering methods.
2.   Develop and optimize spray-dried lipid nanoparticle (LNP) formulations loaded with repurposed drugs, particularly pimozide (PMZ), for inhalation delivery.

3.   Evaluate the efficacy of dual drug-loaded spray-dried LNP formulations, focusing on the synergistic effects of PMZ and hydroxychloroquine (HQ) in inhibiting the growth of A549 lung cancer cells and their anti-inflammatory properties.

4.   Compare the therapeutic potential of PMZ and HQ combination therapy using advanced spray drying techniques, such as two-fluid and three-fluid nozzle spray drying, to optimize particle characteristics, drug release profiles, and therapeutic effects.

5.   Assess the antimicrobial effects of spray-dried rifaximin (RFX) and HQ loaded particles using advanced spray drying techniques, aiming to develop a combination therapy for NSCLC and respiratory infections targeting both bacterial infections and antitumor activity.

By achieving these objectives, the thesis seeks to contribute to the advancement of pulmonary drug delivery systems, offering tailored solutions for the effective treatment of NSCLC and respiratory diseases through innovative particle engineering approaches.
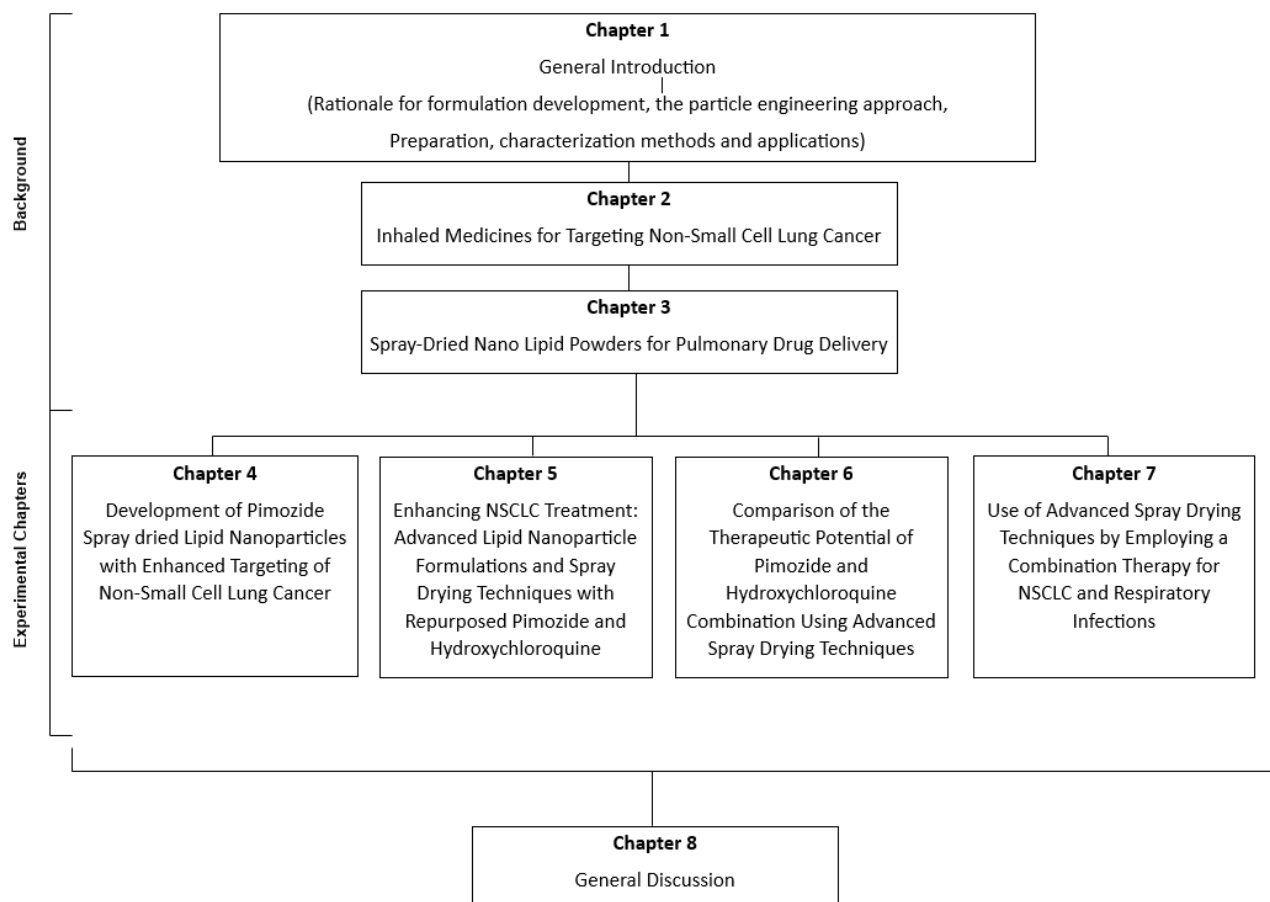
Background

Chapter 1

General Introduction

(Rationale for formulation development, the particle engineering approach,

Preparation, characterization methods and applications)

Chapter 2

Inhaled Medicines for Targeting Non-Small Cell Lung Cancer

Chapter 3

Spray-Dried Nano Lipid Powders for Pulmonary Drug Delivery

Experimental Chapters

Chapter 4

Development of Pimozide Spray dried Lipid Nanoparticles with Enhanced Targeting of Non-Small Cell Lung Cancer

Chapter 5

Enhancing NSCLC Treatment: Advanced Lipid Nanoparticle Formulations and Spray Drying Techniques with Repurposed Pimozide and Hydroxychloroquine

Chapter 6

Comparison of the Therapeutic Potential of Pimozide and Hydroxychloroquine Combination Using Advanced Spray Drying Techniques

Chapter 7

Use of Advanced Spray Drying Techniques by Employing a Combination Therapy for NSCLC and Respiratory Infections

Chapter 8

General Discussion

Figure 7. Diagram illustrating the framework of this PhD Thesis

References:

[1]   D. Cun, C. Zhang, H. Bera, and M. Yang, "Particle engineering principles and technologies for pharmaceutical biologics," *Advanced Drug Delivery Reviews,* vol. 174, pp. 140-167, 2021.

[2]   M. Chogale, S. Gite, and V. Patravale, "Comparison of media milling and microfluidization methods for engineering of nanocrystals: a case study," *Drug development and industrial pharmacy,* vol. 46, no. 11, pp. 1763-1775, 2020.

[3]   W.-R. Ke, R. Y. K. Chang, and H.-K. Chan, "Engineering the right formulation for enhanced drug delivery," *Advanced Drug Delivery Reviews,* vol. 191, p. 114561, 2022.

[4]   R. Scherließ, S. Bock, N. Bungert, A. Neustock, and L. Valentin, "Particle engineering in dry powders for inhalation," *European Journal of Pharmaceutical Sciences,* vol. 172, p. 106158, 2022.

[5]   Y. Duan *et al.*, "A brief review on solid lipid nanoparticles: Part and parcel of contemporary drug delivery systems," *RSC advances,* vol. 10, no. 45, pp. 26777-26791, 2020.

[6]   A. L. Onugwu, A. A. Attama, P. O. Nnamani, S. O. Onugwu, E. B. Onuigbo, and V. V. Khutoryanskiy, "Development and optimization of solid lipid nanoparticles coated with chitosan and poly (2-ethyl-2-oxazoline) for ocular drug delivery of ciprofloxacin," *Journal of Drug Delivery Science and Technology,* vol. 74, p. 103527, 2022.

[7]   A. L. Marshall and D. C. Christiani, "Genetic susceptibility to lung cancer--light at the end of the tunnel?," *Carcinogenesis,* vol. 34, no. 3, pp. 487-502, Mar 2013, doi: 10.1093/carcin/bgt016.

[8]   R. N. Jones, J. M. Hughes, and H. Weill, "Asbestos exposure, asbestosis, and asbestos-attributable lung cancer," *Thorax,* vol. 51 Suppl 2, pp. S9-15, Aug 1996, doi: 10.1136/thx.51.suppl_2.s9.

[9]   S. Rahimian, H. Najafi, B. Afzali, and M. Doroudian, "Extracellular Vesicles and Exosomes: Novel Insights and Perspectives on Lung Cancer from Early Detection to Targeted Treatment," *Biomedicines,* vol. 12, no. 1, p. 123, 2024.

[10]   A. J. Alberg and J. M. Samet, "Epidemiology of lung cancer," *Chest,* vol. 123, no. 1 Suppl, pp. 21S-49S, Jan 2003, doi: 10.1378/chest.123.1_suppl.21s.

[11]   R. Hubbard, A. Venn, S. Lewis, and J. Britton, "Lung cancer and cryptogenic fibrosing alveolitis. A population-based cohort study," *Am J Respir Crit Care Med,* vol. 161, no. 1, pp. 5-8, Jan 2000, doi: 10.1164/ajrccm.161.1.9906062.

[12]   D. Das, J. Wang, and J. Hong, "Next-Generation Kinase Inhibitors Targeting Specific Biomarkers in Non-Small Cell Lung Cancer (NSCLC): A Recent Overview," *ChemMedChem,* vol. 16, no. 16, pp. 2459-2479, 2021.

[13]   A. El-Baz, A. Elnakib, M. Abou El-Ghar, G. Gimel'farb, R. Falk, and A. Farag, "Automatic Detection of 2D and 3D Lung Nodules in Chest Spiral CT Scans," *Int J Biomed Imaging,* vol. 2013, p. 517632, 2013, doi: 10.1155/2013/517632.

[14]   M. Kumar and A. Sarkar, "Current Therapeutic Strategies and Challenges in Nsclc Treatment: A Comprehensive Review," *Exp Oncol,* vol. 44, no. 1, pp. 7-16, May 2022, doi: 10.32471/exp-oncology.2312-8852.vol-44-no-1.17411.

[15]   A. Chang, "Chemotherapy, chemoresistance and the changing treatment landscape for NSCLC," *Lung Cancer,* vol. 71, no. 1, pp. 3-10, Jan 2011, doi: 10.1016/j.lungcan.2010.08.022.

[16]   P. Seve and C. Dumontet, "Chemoresistance in non-small cell lung cancer," *Curr Med Chem Anticancer Agents,* vol. 5, no. 1, pp. 73-88, Jan 2005, doi: 10.2174/1568011053352604.

[17]   F. R. Prabhu, K. Hobart, I. Sulapas, and A. Sikes, "Pulmonary infections," in *Family Medicine: Principles and Practice*: Springer, 2022, pp. 1183-1202.

[18]   T. J. Marrie, "Community-acquired pneumonia," *Clinical infectious diseases,* vol. 18, no. 4, pp. 501-513, 1994.

[19]   J. E. Connolly Jr, H. P. McAdams, J. J. Erasmus, and M. L. Rosado-de-Christenson, "Opportunistic fungal pneumonia," *Journal of thoracic imaging,* vol. 14, no. 1, pp. 51-62, 1999.

[20]   O. Ruuskanen, E. Lahti, L. C. Jennings, and D. R. Murdoch, "Viral pneumonia," *The Lancet,* vol. 377, no. 9773, pp. 1264-1275, 2011.

[21]   A. Y. Peleg, H. Seifert, and D. L. Paterson, "Acinetobacter baumannii: emergence of a successful pathogen," *Clinical microbiology reviews,* vol. 21, no. 3, pp. 538-582, 2008.

[22]   R. M. Martin *et al.*, "Identification of pathogenicity-associated loci in Klebsiella pneumoniae from hospitalized patients," *Msystems,* vol. 3, no. 3, pp. 10.1128/msystems. 00015-18, 2018.

[23]   P. D. Lister, D. J. Wolter, and N. D. Hanson, "Antibacterial-resistant Pseudomonas aeruginosa: clinical impact and complex regulation of chromosomally encoded resistance mechanisms," *Clinical microbiology reviews,* vol. 22, no. 4, pp. 582-610, 2009.

[24]   A. Florczak, I. Grzechowiak, T. Deptuch, K. Kucharczyk, A. Kaminska, and H. Dams-Kozlowska, "Silk particles as carriers of therapeutic molecules for cancer treatment," *Materials,* vol. 13, no. 21, p. 4946, 2020.

[25]   E. A. Engels, "Inflammation in the development of lung cancer: epidemiological evidence," *Expert review of anticancer therapy,* vol. 8, no. 4, pp. 605-615, 2008.

[26]   M. B. Schabath and M. L. Cote, "Cancer progress and priorities: lung cancer," *Cancer epidemiology, biomarkers & prevention,* vol. 28, no. 10, pp. 1563-1579, 2019.

[27]   W. Zhao, Y. Zhao, Q. Wang, T. Liu, J. Sun, and R. Zhang, "Remote light-responsive nanocarriers for controlled drug delivery: advances and perspectives," *Small,* vol. 15, no. 45, p. 1903060, 2019.

[28]   E. Carrasco-Esteban *et al.*, "Current role of nanoparticles in the treatment of lung cancer," *Journal of Clinical and Translational Research,* vol. 7, no. 2, p. 140, 2021.

[29]   N. A. Gujarathi *et al.*, "Pulmonary Drug Delivery System," in *Topical and Transdermal Drug Delivery Systems*: Apple Academic Press, 2023, pp. 205-234.

[30]   J. G. Jang, J. H. Chung, K.-C. Shin, H. J. Jin, K. H. Lee, and J. H. Ahn, "Comparative study of inhaler device handling technique and risk factors for critical inhaler errors in Korean COPD patients," *International Journal of Chronic Obstructive Pulmonary Disease,* pp. 1051-1059, 2021.

[31]   H. Gangurde, M. Chordiya, N. Baste, S. Tamizharasi, and C. Upasani, "Approaches and devices used in pulmonary drug delivery system: a review," *Asian Journal of Pharmaceutical Research and Health Care,* vol. 4, no. 1, pp. 11-27, 2012.

[32]   L. K. Al-Halaseh *et al.*, "Revolutionized drug delivery by using pulmonary nanotechnology: A review," *Research Journal of Pharmacy and Technology,* vol. 16, no. 9, pp. 4462-4468, 2023.

[33]   M. Cazzola, F. Cavalli, O. S. Usmani, and P. Rogliani, "Advances in pulmonary drug delivery devices for the treatment of chronic obstructive pulmonary disease," *Expert opinion on drug delivery,* vol. 17, no. 5, pp. 635-646, 2020.

[34]   H.-G. Lee, D.-W. Kim, and C.-W. Park, "Dry powder inhaler for pulmonary drug delivery: human respiratory system, approved products and therapeutic equivalence guideline," *Journal of Pharmaceutical Investigation,* vol. 48, pp. 603-616, 2018.

[35]   M. Dolovich, "New propellant-free technologies under investigation," (in eng), *J Aerosol Med,* vol. 12 Suppl 1, pp. S9-17, 1999, doi: 10.1089/jam.1999.12.suppl_1.s-9.

[36]   N. R. Labiris and M. B. Dolovich, "Pulmonary drug delivery. Part I: physiological factors affecting therapeutic effectiveness of aerosolized medications," *British journal of clinical pharmacology,* vol. 56, no. 6, pp. 588-599, 2003.

[37]   R. Wolff, "Safety of inhaled proteins for therapeutic use," *Journal of aerosol medicine,* vol. 11, no. 4, pp. 197-219, 1998.

[38]   P. R. Byron and J. S. PATTON, "Drug delivery via the respiratory tract," *Journal of Aerosol medicine,* vol. 7, no. 1, pp. 49-75, 1994.

[39]   R. Cole and A. Mackay, "Concepts of pulmonary physiology," *Essentials of respiratory disease, New York, Churchill Livingstone,* vol. 3, pp. 49-60, 1990.

[40]   J. S. Patton, "Mechanisms of macromolecule absorption by the lungs," *Advanced drug delivery reviews,* vol. 19, no. 1, pp. 3-36, 1996.

[41]   P. Barnes, "Drug-induced asthma: In Barnes PJ, Grunstein MM, Leff AR et al.: Asthma," ed: Philadelphia, Lippincott-Raven, 1997.

[42]   M. Mohseni, K. Gilani, and S. A. Mortazavi, "Preparation and characterization of rifampin loaded mesoporous silica nanoparticles as a potential system for pulmonary drug delivery," *Iranian journal of pharmaceutical research: IJPR,* vol. 14, no. 1, p. 27, 2015.

[43]   E. Houtmeyers, R. Gosselink, G. Gayan-Ramirez, and M. Decramer, "Regulation of mucociliary clearance in health and disease," *Eur Respir J,* vol. 13, no. 5, pp. 1177-88, May 1999, doi: 10.1034/j.1399-3003.1999.13e39.x.

[44]   P. Zarogoulidis *et al.*, "Inhaled chemotherapy in lung cancer: future concept of nanomedicine," *Int J Nanomedicine,* vol. 7, pp. 1551-72, 2012, doi: 10.2147/IJN.S29997.

[45]   A. H. Chow, H. H. Tong, P. Chattopadhyay, and B. Y. Shekunov, "Particle engineering for pulmonary drug delivery," *Pharmaceutical research,* vol. 24, pp. 411-437, 2007.

[46]   K. Koushik and U. Kompella, "Particle and device engineering for inhalation drug delivery," *Drug Deliv. Technol,* vol. 4, pp. 40-50, 2004.

[47]   V. Prasad and S. Mailankody, "Research and development spending to bring a single cancer drug to market and revenues after approval," *JAMA internal medicine,* vol. 177, no. 11, pp. 1569-1575, 2017.

[48]   N. Krishnamurthy, A. A. Grimshaw, S. A. Axson, S. H. Choe, and J. E. Miller, "Drug repurposing: a systematic review on root causes, barriers and facilitators," *BMC health services research,* vol. 22, no. 1, p. 970, 2022.

[49]   M. Rudrapal, S. J. Khairnar, and A. G. Jadhav, "Drug repurposing (DR): an emerging approach in drug discovery," *Drug repurposing-hypothesis, molecular aspects and therapeutic applications,* vol. 1, no. 1, 2020.

[50]   P. Polamreddy and N. Gattu, "The drug repurposing landscape from 2012 to 2017: evolution, challenges, and possible solutions," *Drug Discovery Today,* vol. 24, no. 3, pp. 789-795, 2019.

[51]   Z. Zhang *et al.*, "Overcoming cancer therapeutic bottleneck by drug repurposing," *Signal Transduction and Targeted Therapy,* vol. 5, no. 1, p. 113, 2020/07/02 2020, doi: 10.1038/s41392-020-00213-8.

[52]   A. Kirtonia *et al.*, "Repurposing of drugs: An attractive pharmacological strategy for cancer therapeutics," in *Seminars in cancer biology*, 2021, vol. 68: Elsevier, pp. 258-278.

[53]   B. P. Commission. "British Pharmacopoeia 2024." The Stationery Office. https://www.pharmacopoeia.com (accessed August 5, 2024.

[54]   J. M. Gonçalves, C. A. B. Silva, E. R. C. Rivero, and M. M. R. Cordeiro, "Inhibition of cancer stem cells promoted by Pimozide," *Clinical and Experimental Pharmacology and Physiology,* vol. 46, no. 2, pp. 116-125, 2019.

[55]   V. Shaw, S. Srivastava, and S. K. Srivastava, "Repurposing antipsychotics of the diphenylbutylpiperidine class for cancer therapy," in *Seminars in cancer biology*, 2021, vol. 68: Elsevier, pp. 75-83.

[56]   P. Kumbhar *et al.*, "Inhalation delivery of repurposed drugs for lung cancer: approaches, benefits and challenges," *Journal of Controlled Release,* vol. 341, pp. 1-15, 2022.

[57]   W. Zhou, H. Wang, Y. Yang, Z.-S. Chen, C. Zou, and J. Zhang, "Chloroquine against malaria, cancers and viral diseases," *Drug Discovery Today,* vol. 25, no. 11, pp. 2012-2022, 2020.

[58]   T. Berghmans, J.-P. Sculier, and J. Klastersky, "A prospective study of infections in lung cancer patients admitted to the hospital," *Chest,* vol. 124, no. 1, pp. 114-120, 2003.

[59]   K. Akinosoglou, K. Karkoulias, and M. Marangos, "Infectious complications in patients with lung cancer," *European Review for Medical & Pharmacological Sciences,* vol. 17, no. 1, 2013.

[60]   G. Esposito *et al.*, "Rifaximin, a non-absorbable antibiotic, inhibits the release of pro-angiogenic mediators in colon cancer cells through a pregnane X receptor-dependent pathway," *International Journal of Oncology,* vol. 49, no. 2, pp. 639-645, 2016.

[61]   P. Lu *et al.*, "Physicochemical and pharmacokinetic evaluation of spray-dried coformulation of Salvia miltiorrhiza polyphenolic acid and L-Leucine with improved bioavailability," *Journal of aerosol medicine and pulmonary drug delivery,* vol. 33, no. 2, pp. 73-82, 2020.

[62] M. A. Momin, B. Rangnekar, S. Sinha, C.-Y. Cheung, G. M. Cook, and S. C. Das, "Inhalable dry powder of bedaquiline for pulmonary tuberculosis: In vitro physicochemical characterization, antimicrobial activity and safety studies," *Pharmaceutics,* vol. 11, no. 10, p. 502, 2019.

[63] M. A. Momin, S. Sinha, I. G. Tucker, and S. C. Das, "Carrier-free combination dry powder inhaler formulation of ethionamide and moxifloxacin for treating drug-resistant tuberculosis," *Drug Development and Industrial Pharmacy,* vol. 45, no. 8, pp. 1321-1331, 2019.

[64] I. E. Stewart *et al.*, "Development and characterization of a dry powder formulation for anti-tuberculosis drug spectinamide 1599," *Pharmaceutical research,* vol. 36, no. 9, pp. 1-13, 2019.

[65] F. Ungaro, G. De Rosa, A. Miro, F. Quaglia, and M. I. La Rotonda, "Cyclodextrins in the production of large porous particles: development of dry powders for the sustained release of insulin to the lungs," *European Journal of Pharmaceutical Sciences,* vol. 28, no. 5, pp. 423-432, 2006.

[66] M. Gomez *et al.*, "Development of a formulation platform for a spray-dried, inhalable tuberculosis vaccine candidate," *International Journal of Pharmaceutics,* vol. 593, p. 120121, 2021.

[67] T. Tarara *et al.*, "Formulation of Dry Powders for Inhalation Comprising High Doses of a Poorly Soluble Hydrophobic Drug. Front," *Drug. Deliv,* vol. 2, p. 862336, 2022.

[68] J. G. Weers and D. P. Miller, "Formulation design of dry powders for inhalation," *Journal of pharmaceutical sciences,* vol. 104, no. 10, pp. 3259-3288, 2015.

[69] L. Chen, T. Okuda, X.-Y. Lu, and H.-K. Chan, "Amorphous powders for inhalation drug delivery," *Advanced drug delivery reviews,* vol. 100, pp. 102-115, 2016.

[70] M. Hoppentocht, P. Hagedoorn, H. Frijlink, and A. De Boer, "Technological and practical challenges of dry powder inhalers and formulations," *Advanced drug delivery reviews,* vol. 75, pp. 18-31, 2014.

[71] S. Aziz, R. Scherlieβ, and H. Steckel, "Development of High Dose Oseltamivir Phosphate Dry Powder for Inhalation Therapy in Viral Pneumonia," *Pharmaceutics,* vol. 12, no. 12, p. 1154, 2020.

[72] N. Shetty, H. Park, D. Zemlyanov, S. Mangal, S. Bhujbal, and Q. T. Zhou, "Influence of excipients on physical and aerosolization stability of spray dried high-dose powder formulations for inhalation," *International journal of pharmaceutics,* vol. 544, no. 1, pp. 222-234, 2018.

[73] A. Nieto-Orellana *et al.*, "Targeted PEG-poly (glutamic acid) complexes for inhalation protein delivery to the lung," *Journal of controlled release,* vol. 316, pp. 250-262, 2019.

[74] M. Auerbach and A. k. Dedman, "Bulking Agents–Multi-Functional Ingredients," *Sweeteners and sugar alternatives in food technology,* pp. 433-470, 2012.

[75] A.-K. Koskinen *et al.*, "Physical stability of freeze-dried isomalt diastereomer mixtures," *Pharmaceutical Research,* vol. 33, pp. 1752-1768, 2016.

[76] E. Matta, M. J. Tavera-Quiroz, and N. Bertola, "Isomalt-plasticized methylcellulose-based films as carriers of ascorbic acid," *Food and Bioprocess Technology,* vol. 13, pp. 2186-2199, 2020.

[77] A. Sentko and I. Willibald-Ettle, "Isomalt," *Sweeteners and sugar alternatives in food technology,* pp. 243-274, 2012.

[78] D. Ž. Kusonić *et al.*, "Excipients of inhaled medications with potential to cause adverse reactions," *Hospital Pharmacology-International Multidisciplinary Journal,* vol. 8, no. 3, pp. 1109-1117, 2021.

[79] N. R. Labiris and M. B. Dolovich, "Pulmonary drug delivery. Part II: the role of inhalant delivery devices and drug formulations in therapeutic effectiveness of aerosolized medications," *British journal of clinical pharmacology,* vol. 56, no. 6, pp. 600-612, 2003.

[80] D. Daniher *et al.*, "Protective effects of aerosolized pulmonary surfactant powder in a model of ventilator-induced lung injury," *International Journal of Pharmaceutics,* vol. 583, p. 119359, 2020.

[81] S. N. Deshmukh *et al.*, "Novel film forming spray from tea tree leaves with special emphasis on development, formulation and evaluation," *Journal of Positive School Psychology,* pp. 5179–5184-5179–5184, 2022.

[82]   E. Ilan *et al.*, "Improved oral delivery of desmopressin via a novel vehicle: mucoadhesive submicron emulsion," *Pharmaceutical research,* vol. 13, pp. 1083-1087, 1996.

[83]   M. B. Schulz and R. Daniels, "Hydroxypropylmethylcellulose (HPMC) as emulsifier for submicron emulsions: influence of molecular weight and substitution type on the droplet size after high-pressure homogenization," *European Journal of Pharmaceutics and Biopharmaceutics,* vol. 49, no. 3, pp. 231-236, 2000.

[84]   J. Zheng, B. Wang, J. Xiang, and Z. Yu, "Controlled release of curcumin from HPMC (hydroxypropyl methyl cellulose) co-spray-dried materials," *Bioinorganic chemistry and applications,* vol. 2021, 2021.

[85]   S. Agarkhedkar *et al.*, "Safety and immunogenicity of dry powder measles vaccine administered by inhalation: a randomized controlled Phase I clinical trial," *Vaccine,* vol. 32, no. 50, pp. 6791-6797, 2014.

[86]   S. P. Cape, J. A. Villa, E. T. Huang, T.-H. Yang, J. F. Carpenter, and R. E. Sievers, "Preparation of active proteins, vaccines and pharmaceuticals as fine powders using supercritical or near-critical fluids," *Pharmaceutical Research,* vol. 25, no. 9, pp. 1967-1990, 2008.

[87]   T. Sou *et al.*, "Designing a multi-component spray-dried formulation platform for pulmonary delivery of biopharmaceuticals: the use of polyol, disaccharide, polysaccharide and synthetic polymer to modify solid-state properties for glassy stabilisation," *Powder technology,* vol. 287, pp. 248-255, 2016.

[88]   P. Salvatori, "The rationale of ethanol inhalation for disinfection of the respiratory tract in SARS-CoV-2-positive asymptomatic subjects," *The Pan African Medical Journal,* vol. 40, 2021.

[89]   P. B. Myrdal, P. Sheth, and S. W. Stein, "Advances in metered dose inhaler technology: formulation development," *Aaps Pharmscitech,* vol. 15, no. 2, pp. 434-455, 2014.

[90]   R. Scherrer, J. Stefely, and S. Stein, "inventors; 3M Innovative Properties Company, assignee," *Medicinal aerosol formulations comprising ion pair complexes. World Intellectual Property Organization patent WO,* vol. 59316, p. 24, 2003.

[91]   J. Stefely, D. C. Duan, P. B. Myrdal, D. Ross, D. Schultz, and C. Leach, "Design and utility of a novel class of biocompatible excipients for HFA-based MDIs," in *Respiratory Drug Delivery*, 2000, vol. 7, pp. 83-90.

[92]   S. Stein, B. Forsyth, J. Stefely, J. Christensen, T. Alband, and P. Jinks, "Expanding the dosing range of metered dose inhalers through formulation and hardware optimization," *Respir Drug Deliv,* vol. 1, pp. 125-34, 2004.

[93]   C. W. Park, H. M. Mansour, and D. Hayes, "Pulmonary inhalation aerosols for targeted antibiotics drug delivery," 2011.

[94]   A. A. Matthews, P. L. R. Ee, and R. Ge, "Developing inhaled protein therapeutics for lung diseases," *Molecular biomedicine,* vol. 1, no. 1, pp. 1-14, 2020.

[95]   K. Ganguly *et al.*, "Computational modeling of lung deposition of inhaled particles in chronic obstructive pulmonary disease (COPD) patients: identification of gaps in knowledge and data," *Critical reviews in toxicology,* vol. 49, no. 2, pp. 160-173, 2019.

[96]   J. G. Weers, N. Rao, D. Huang, D. Miller, and T. E. Tarara, "Dry powder formulations of particles that contain two or more active ingredients for treating obstructive or inflammatory airways diseases," ed: Google Patents, 2015.

[97]   N. Al-Zoubi, G. Al-Obaidi, B. Tashtoush, and S. Malamataris, "Sustained release of diltiazem HCl tableted after co-spray drying and physical mixing with PVAc and PVP," *Drug development and industrial pharmacy,* vol. 42, no. 2, pp. 270-279, 2016.

[98]   J. H. Lee *et al.*, "Enhanced dissolution rate of celecoxib using PVP and/or HPMC-based solid dispersions prepared by spray drying method," *Journal of Pharmaceutical Investigation,* vol. 43, pp. 205-213, 2013.

[99]   T. Sou, M. P. McIntosh, L. M. Kaminskas, R. J. Prankerd, and D. A. Morton, "Designing a multicomponent spray-dried formulation platform for pulmonary delivery of biomacromolecules: the effect of polymers on the formation of an amorphous matrix for glassy state stabilization of biomacromolecules," *Drying technology,* vol. 31, no. 13-14, pp. 1451-1458, 2013.

[100] F. Tewes, L. Tajber, O. I. Corrigan, C. Ehrhardt, and A.-M. Healy, "Development and characterisation of soluble polymeric particles for pulmonary peptide delivery," *European Journal of Pharmaceutical Sciences,* vol. 41, no. 2, pp. 337-352, 2010.

[101] G. Pilcer and K. Amighi, "Formulation strategy and use of excipients in pulmonary drug delivery," *International journal of pharmaceutics,* vol. 392, no. 1-2, pp. 1-19, 2010.

[102] H. Sato *et al.*, "Design and characterizations of inhalable poly (lactic-co-glycolic acid) microspheres prepared by the fine droplet drying process for a sustained effect of salmon calcitonin," *Molecules,* vol. 25, no. 6, p. 1311, 2020.

[103] W. H. Nikolaizik, V. Jenni-Galović, and M. H. Schöni, "Bronchial constriction after nebulized tobramycin preparations and saline in patients with cystic fibrosis," *European journal of pediatrics,* vol. 155, no. 7, pp. 608-611, 1996.

[104] S. Hou, J. Wu, X. Li, and H. Shu, "Practical, regulatory and clinical considerations for development of inhalation drug products," *Asian journal of pharmaceutical sciences,* vol. 10, no. 6, pp. 490-500, 2015.

[105] S. P. Newman, "Principles of metered-dose inhaler design," *Respiratory care,* vol. 50, no. 9, pp. 1177-1190, 2005.

[106] Y. Ye, Y. Ma, and J. Zhu, "The future of dry powder inhaled therapy: Promising or Discouraging for systemic disorders?," *International journal of pharmaceutics,* p. 121457, 2022.

[107] W. Wang *et al.*, "Effects of surface composition on the aerosolisation and dissolution of inhaled antibiotic combination powders consisting of colistin and rifampicin," *The AAPS journal,* vol. 18, no. 2, pp. 372-384, 2016.

[108] N. Shetty *et al.*, "Effect of lipidic excipients on the particle properties and aerosol performance of high drug load spray dried particles for inhalation," *Journal of Pharmaceutical Sciences,* vol. 111, no. 4, pp. 1152-1163, 2022.

[109] E. Benke, Á. Farkas, I. Balásházy, P. Szabó-Révész, and R. Ambrus, "Stability test of novel combined formulated dry powder inhalation system containing antibiotic: physical characterization and in vitro–in silico lung deposition results," *Drug Development and Industrial Pharmacy,* vol. 45, no. 8, pp. 1369-1378, 2019.

[110] C. Parlati *et al.*, "Pulmonary spray dried powders of tobramycin containing sodium stearate to improve aerosolization efficiency," *Pharmaceutical research,* vol. 26, no. 5, pp. 1084-1092, 2009.

[111] A. M. Bodratti and P. Alexandridis, "Amphiphilic block copolymers in drug delivery: Advances in formulation structure and performance," *Expert opinion on drug delivery,* vol. 15, no. 11, pp. 1085-1104, 2018.

[112] L. Djekic, B. Čalija, and Đ. Medarević, "Gelation behavior, drug solubilization capacity and release kinetics of poloxamer 407 aqueous solutions: The combined effect of copolymer, cosolvent and hydrophobic drug," *Journal of Molecular Liquids,* vol. 303, p. 112639, 2020.

[113] G. Dumortier, J. L. Grossiord, F. Agnely, and J. C. Chaumeil, "A review of poloxamer 407 pharmaceutical and pharmacological characteristics," *Pharmaceutical research,* vol. 23, pp. 2709-2728, 2006.

[114] W. M. Kolling, "Handbook of pharmaceutical excipients," *American Journal of Pharmaceutical Education,* vol. 68, no. 1-5, p. BF1, 2004.

[115] D. Nikjoo, I. van der Zwaan, M. Brülls, U. Tehler, and G. Frenning, "Hyaluronic Acid Hydrogels for Controlled Pulmonary Drug Delivery—A Particle Engineering Approach," *Pharmaceutics,* vol. 13, no. 11, p. 1878, 2021.

[116] Q. Liao and J. K. Lam, "Inhaled antifungal agents for the treatment and prophylaxis of pulmonary mycoses," *Current Pharmaceutical Design,* vol. 27, no. 12, pp. 1453-1468, 2021.

[117] M. Hoppentocht, P. Hagedoorn, H. W. Frijlink, and A. H. de Boer, "Developments and strategies for inhaled antibiotic drugs in tuberculosis therapy: a critical evaluation," *European Journal of Pharmaceutics and Biopharmaceutics,* vol. 86, no. 1, pp. 23-30, 2014.

[118] N. Teekamp *et al.*, "Addition of pullulan to trehalose glasses improves the stability of β-galactosidase at high moisture conditions," *Carbohydrate polymers,* vol. 176, pp. 374-380, 2017.

[119] N. Changsan and C. Sinsuebpol, "Dry powder inhalation formulation of chitosan nanoparticles for co-administration of isoniazid and pyrazinamide," *Pharmaceutical Development and Technology,* vol. 26, no. 2, pp. 181-192, 2021.

[120] M. Mukhtar *et al.*, "Aerodynamic properties and in silico deposition of isoniazid loaded chitosan/thiolated chitosan and hyaluronic acid hybrid nanoplex DPIs as a potential TB treatment," *International Journal of Biological Macromolecules,* vol. 165, pp. 3007-3019, 2020.

[121] M. Z. R. Sabuj, T. R. Dargaville, L. Nissen, and N. Islam, "Inhaled ciprofloxacin-loaded poly (2-ethyl-2-oxazoline) nanoparticles from dry powder inhaler formulation for the potential treatment of lower respiratory tract infections," *Plos one,* vol. 16, no. 12, p. e0261720, 2021.

[122] A. Patil-Gadhe and V. Pokharkar, "Single step spray drying method to develop proliposomes for inhalation: a systematic study based on quality by design approach," *Pulmonary Pharmacology & Therapeutics,* vol. 27, no. 2, pp. 197-207, 2014.

[123] M. Babenko, R. G. Alany, G. Calabrese, W. Kaialy, and A. ElShaer, "Development of drug alone and carrier-based GLP-1 dry powder inhaler formulations," *International Journal of Pharmaceutics,* vol. 617, p. 121601, 2022.

[124] O. Ivaniuk, T. Yarnykh, and I. Kovalevska, "Determination of the bioadhesion indicators of vaginal gel with resveratrol and hyaluronic acid," 2019.

[125] Y. S. Maslii, O. Ruban, Y. V. Levachkova, and T. Y. Kolisnyk, "Choice of mucosal adhesive in the composition of a new dental gel," 2020.

[126] M. A. Rashid *et al.*, "Inhaled Edoxaban dry powder inhaler formulations: Development, characterization and their effects on the coagulopathy associated with COVID-19 infection," *International journal of pharmaceutics,* vol. 608, p. 121122, 2021.

[127] C. Kriegel, M. Festag, R. S. Kishore, D. Roethlisberger, and G. Schmitt, "Pediatric safety of polysorbates in drug formulations," *Children,* vol. 7, no. 1, p. 1, 2019.

[128] L. Ely, W. Roa, W. H. Finlay, and R. Löbenberg, "Effervescent dry powder for respiratory drug delivery," *European Journal of Pharmaceutics and Biopharmaceutics,* vol. 65, no. 3, pp. 346-353, 2007.

[129] A. Castoldi *et al.*, "Calcifediol-loaded liposomes for local treatment of pulmonary bacterial infections," *European Journal of Pharmaceutics and Biopharmaceutics,* vol. 118, pp. 62-67, 2017.

[130] B. B. Eedara, I. G. Tucker, and S. C. Das, "Phospholipid-based pyrazinamide spray-dried inhalable powders for treating tuberculosis," *International Journal of Pharmaceutics,* vol. 506, no. 1-2, pp. 174-183, 2016.

[131] J. O. Morales, J. I. Peters, and R. O. Williams, "Surfactants: their critical role in enhancing drug delivery to the lungs," *Therapeutic delivery,* vol. 2, no. 5, pp. 623-641, 2011.

[132] A. A. D'souza and R. Shegokar, "Polyethylene glycol (PEG): a versatile polymer for pharmaceutical applications," *Expert opinion on drug delivery,* vol. 13, no. 9, pp. 1257-1275, 2016.

[133] Y. Zhang, W. Wright, W. Tam, T. Nguyen-Dang, C. Salome, and A. Woolcock, "Effect of inhaled preservatives on asthmatic subjects: II. benzalkonium chloride," *American Review of Respiratory Disease,* vol. 141, no. 6, pp. 1405-1408, 1990.

[134] J. A. Champion, Y. K. Katare, and S. Mitragotri, "Particle shape: a new design parameter for micro-and nanoscale drug delivery carriers," *Journal of controlled release,* vol. 121, no. 1-2, pp. 3-9, 2007.

[135] J. C. Sung, B. L. Pulliam, and D. A. Edwards, "Nanoparticles for drug delivery to the lungs," *Trends in biotechnology,* vol. 25, no. 12, pp. 563-570, 2007.

[136] L. Xu, X. Wang, Y. Liu, G. Yang, R. J. Falconer, and C.-X. Zhao, "Lipid nanoparticles for drug delivery," *Advanced NanoBiomed Research,* vol. 2, no. 2, p. 2100109, 2022.

[137] M. Bloemen, W. Brullot, T. T. Luong, N. Geukens, A. Gils, and T. Verbiest, "Improved functionalization of oleic acid-coated iron oxide nanoparticles for biomedical applications," *Journal of Nanoparticle Research,* vol. 14, pp. 1-10, 2012.

[138] A. D'Souza and R. Shegokar, "Nanostructured lipid carriers (NLCs) for drug delivery: Role of liquid lipid (oil)," *Current Drug Delivery,* vol. 18, no. 3, pp. 249-270, 2021.

[139]   K. Okuda *et al.*, "On the size-regulation of RNA-loaded lipid nanoparticles synthesized by microfluidic device," *Journal of controlled release,* vol. 348, pp. 648-659, 2022.

[140]   A. Teo, Y. Lam, S. J. Lee, and K. K. Goh, "Spray drying of whey protein stabilized nanoemulsions containing different wall materials–maltodextrin or trehalose," *LWT,* vol. 136, p. 110344, 2021.

[141]   M. A. Haque, J. Chen, P. Aldred, and B. Adhikari, "Denaturation and physical characteristics of spray-dried whey protein isolate powders produced in the presence and absence of lactose, trehalose, and polysorbate-80," *Drying technology,* vol. 33, no. 10, pp. 1243-1254, 2015.

[142]   S. Ohtake and Y. J. Wang, "Trehalose: Current Use and Future Applications," *Journal of Pharmaceutical Sciences,* vol. 100, no. 6, pp. 2020-2053, 2011/06/01/ 2011, doi: https://doi.org/10.1002/jps.22458.

[143]   M. J. Anderson and P. J. Whitcomb, "Design of experiments," *Kirk-Othmer Encyclopedia of Chemical Technology,* pp. 1-22, 2000.

[144]   L. M. Ickenstein and P. Garidel, "Lipid-based nanoparticle formulations for small molecules and RNA drugs," *Expert opinion on drug delivery,* vol. 16, no. 11, pp. 1205-1226, 2019.

[145]   M. Puccetti, M. Pariano, A. Schoubben, S. Giovagnoli, and M. Ricci, "Biologics, Theranostics, and Personalized Medicine in Drug Delivery Systems," *Pharmacological Research,* p. 107086, 2024.

[146]   L. Schoenmaker *et al.*, "mRNA-lipid nanoparticle COVID-19 vaccines: Structure and stability," *International journal of pharmaceutics,* vol. 601, p. 120586, 2021.

[147]   D. Chatzikleanthous, D. T. O'Hagan, and R. Adamo, "Lipid-based nanoparticles for delivery of vaccine adjuvants and antigens: toward multicomponent vaccines," *Molecular pharmaceutics,* vol. 18, no. 8, pp. 2867-2888, 2021.

[148]   R. A. Paun, S. Jurchuk, and M. Tabrizian, "A landscape of recent advances in lipid nanoparticles and their translational potential for the treatment of solid tumors," *Bioengineering & Translational Medicine,* vol. 9, no. 2, p. e10601, 2024.

[149]   A. Gencer, C. Duraloglu, S. Ozbay, T. T. Ciftci, S. Yabanoglu-Ciftci, and B. Arica, "Recent advances in treatment of lung cancer: nanoparticle-based drug and siRNA delivery systems," *Current drug delivery,* vol. 18, no. 2, pp. 103-120, 2021.

[150]   R. Alzhrani *et al.*, "Improving the therapeutic efficiency of noncoding RNAs in cancers using targeted drug delivery systems," *Drug discovery today,* vol. 25, no. 4, pp. 718-730, 2020.

[151]   F. Gorachinov *et al.*, "Nanotechnology–a robust tool for fighting the challenges of drug resistance in non-small cell lung cancer," *Beilstein journal of nanotechnology,* vol. 14, no. 1, pp. 240-261, 2023.

[152]   A. Singh and G. Van den Mooter, "Spray drying formulation of amorphous solid dispersions," *Advanced Drug Delivery Reviews,* vol. 100, pp. 27-50, 2016/05/01/ 2016, doi: https://doi.org/10.1016/j.addr.2015.12.010.

[153]   R. Tiwari, G. Tiwari, B. Srivastava, and A. K. Rai, "Solid dispersions: an overview to modify bioavailability of poorly water soluble drugs," *International Journal of PharmTech Research,* vol. 1, no. 4, pp. 1338-1349, 2009.

[154]   G. Van den Mooter, "The use of amorphous solid dispersions: A formulation strategy to overcome poor solubility and dissolution rate," *Drug Discovery Today: Technologies,* vol. 9, no. 2, pp. e79-e85, 2012.

[155]   H. Sandhu, N. Shah, H. Chokshi, and A. W. Malick, "Overview of Amorphous Solid Dispersion Technologies," in *Amorphous Solid Dispersions: Theory and Practice*, N. Shah, H. Sandhu, D. S. Choi, H. Chokshi, and A. W. Malick Eds. New York, NY: Springer New York, 2014, pp. 91-122.

[156]   T. Vasconcelos, S. Marques, J. das Neves, and B. Sarmento, "Amorphous solid dispersions: Rational selection of a manufacturing process," *Advanced drug delivery reviews,* vol. 100, pp. 85-101, 2016.

[157]   E. H. Lee, "A practical guide to pharmaceutical polymorph screening & selection," *asian journal of pharmaceutical sciences,* vol. 9, no. 4, pp. 163-175, 2014.

[158]   F. Damian *et al.*, "Physicochemical characterization of solid dispersions of the antiviral agent UC-781 with polyethylene glycol 6000 and Gelucire 44/14," *European Journal of Pharmaceutical Sciences,* vol. 10, no. 4, pp. 311-322, 2000.

[159] T. Vasconcelos, B. Sarmento, and P. Costa, "Solid dispersions as strategy to improve oral bioavailability of poor water soluble drugs," *Drug discovery today,* vol. 12, no. 23-24, pp. 1068-1075, 2007.

[160] S. Janssens and G. Van den Mooter, "Physical chemistry of solid dispersions," *Journal of Pharmacy and Pharmacology,* vol. 61, no. 12, pp. 1571-1586, 2009.

[161] A. Karagianni, K. Kachrimanis, and I. Nikolakakis, "Co-amorphous solid dispersions for solubility and absorption improvement of drugs: Composition, preparation, characterization and formulations for oral delivery," *Pharmaceutics,* vol. 10, no. 3, p. 98, 2018.

[162] J. Pacułt, M. Rams-Baron, B. Chrząszcz, R. Jachowicz, and M. Paluch, "Effect of polymer chain length on the physical stability of amorphous drug–polymer blends at ambient pressure," *Molecular Pharmaceutics,* vol. 15, no. 7, pp. 2807-2815, 2018.

[163] K. Lehmkemper, S. O. Kyeremateng, M. Bartels, M. Degenhardt, and G. Sadowski, "Physical stability of API/polymer-blend amorphous solid dispersions," *European Journal of Pharmaceutics and Biopharmaceutics,* vol. 124, pp. 147-157, 2018.

[164] A. Ainurofiq, D. S. Putro, D. A. Ramadhani, G. M. Putra, and L. D. C. D. E. Santo, "A review on solubility enhancement methods for poorly water-soluble drugs," *Journal of Reports in Pharmaceutical Sciences,* vol. 10, no. 1, pp. 137-147, 2021.

[165] H. Wang, P. Zhao, R. Ma, J. Jia, and Q. Fu, "Drug–drug co-amorphous systems: An emerging formulation strategy for poorly water-soluble drugs," *Drug Discovery Today,* p. 103883, 2024.

[166] D. E. Alonzo, G. G. Zhang, D. Zhou, Y. Gao, and L. S. Taylor, "Understanding the behavior of amorphous pharmaceutical systems during dissolution," *Pharmaceutical research,* vol. 27, pp. 608-618, 2010.

[167] A. Bhatia, S. Chopra, K. Nagpal, P. K. Deb, M. Tekade, and R. K. Tekade, "Polymorphism and its implications in pharmaceutical product development," in *Dosage Form Design Parameters*: Elsevier, 2018, pp. 31-65.

[168] R. Sarrate *et al.*, "Modification of the morphology and particle size of pharmaceutical excipients by spray drying technique," *Powder Technology,* vol. 270, pp. 244-255, 2015.

[169] A. B. D. Nandiyanto and K. Okuyama, "Progress in developing spray-drying methods for the production of controlled morphology particles: From the nanometer to submicrometer size ranges," *Advanced powder technology,* vol. 22, no. 1, pp. 1-19, 2011.

[170] S. Q. Henwood*, W. Liebenberg, L. R. Tiedt, A. P. Lötter, and M. M. De Villiers, "Characterization of the solubility and dissolution properties of several new rifampicin polymorphs, solvates, and hydrates," *Drug development and industrial pharmacy,* vol. 27, no. 10, pp. 1017-1030, 2001.

[171] J. K. Guillory, "Generation of polymorphs, hydrates, solvates, and amorphous solids," *Drugs and the pharmaceutical sciences,* vol. 95, pp. 183-226, 1999.

[172] F. Lyu, J. J. Liu, Y. Zhang, and X. Z. Wang, "Combined control of morphology and polymorph in spray drying of mannitol for dry powder inhalation," *Journal of Crystal Growth,* vol. 467, pp. 155-161, 2017.

[173] P. Mack, K. Horvath, A. Garcia, J. Tully, and B. Maynor, "Particle engineering for inhalation formulation and delivery of biotherapeutics," *Inhalation,* vol. 6, no. 4, pp. 16-20, 2012.

[174] R. J. Malcolmson and J. K. Embleton, "Dry powder formulations for pulmonary delivery," *Pharmaceutical Science & Technology Today,* vol. 1, no. 9, pp. 394-398, 1998.

[175] S. P. Newman and S. W. Clarke, "Therapeutic aerosols 1--physical and practical considerations," *Thorax,* vol. 38, no. 12, p. 881, 1983.

[176] W. C. Hinds, *Aerosol Technology: Properties, Behavior, and Measurement of Airborne Particles*. Wiley, 1982.

[177] J. Auclair and A. Rathore, "Analysis of Lipid Nanoparticles," *LCGC North America,* vol. 41, no. 06, pp. 216–219-216–219, 2023.

[178] R. H. Müller, M. Radtke, and S. A. Wissing, "Solid lipid nanoparticles (SLN) and nanostructured lipid carriers (NLC) in cosmetic and dermatological preparations," *Advanced drug delivery reviews,* vol. 54, pp. S131-S155, 2002.

[179] C. Desfrançois, R. Auzély, and I. Texier, "Lipid nanoparticles and their hydrogel composites for drug delivery: a review," *Pharmaceuticals,* vol. 11, no. 4, p. 118, 2018.

[180]   R. Shankar, M. Joshi, and K. Pathak, "Lipid nanoparticles: a novel approach for brain targeting," *Pharmaceutical nanotechnology,* vol. 6, no. 2, pp. 81-93, 2018.

[181]   R. Kumar, D. S. Dkhar, R. Kumari, S. Mahapatra, V. K. Dubey, and P. Chandra, "Lipid based nanocarriers: Production techniques, concepts, and commercialization aspect," *Journal of Drug Delivery Science and Technology,* vol. 74, p. 103526, 2022.

[182]   P. Ghasemiyeh and S. Mohammadi-Samani, "Solid lipid nanoparticles and nanostructured lipid carriers as novel drug delivery systems: applications, advantages and disadvantages," *Research in pharmaceutical sciences,* vol. 13, no. 4, pp. 288-303, 2018.

[183]   E. Subroto, R. Andoyo, and R. Indiarto, "Solid lipid nanoparticles: Review of the current research on encapsulation and delivery systems for active and antioxidant compounds," *Antioxidants,* vol. 12, no. 3, p. 633, 2023.

[184]   G. I. Sakellari, I. Zafeiri, H. Batchelor, and F. Spyropoulos, "Formulation design, production and characterisation of solid lipid nanoparticles (SLN) and nanostructured lipid carriers (NLC) for the encapsulation of a model hydrophobic active," *Food hydrocolloids for health,* vol. 1, p. 100024, 2021.

[185]   I. Chauhan, M. Yasir, M. Verma, and A. P. Singh, "Nanostructured lipid carriers: A groundbreaking approach for transdermal drug delivery," *Advanced pharmaceutical bulletin,* vol. 10, no. 2, p. 150, 2020.

[186]   N. Aditya *et al.*, "Development and evaluation of lipid nanocarriers for quercetin delivery: A comparative study of solid lipid nanoparticles (SLN), nanostructured lipid carriers (NLC), and lipid nanoemulsions (LNE)," *LWT-Food Science and Technology,* vol. 59, no. 1, pp. 115-121, 2014.

[187]   A. Deshpande, M. Mohamed, S. B. Daftardar, M. Patel, S. H. Boddu, and J. Nesamony, "Solid lipid nanoparticles in drug delivery: Opportunities and challenges," *Emerging nanotechnologies for diagnostics, drug delivery and medical devices,* pp. 291-330, 2017.

[188]   Y. Lee, M. Jeong, J. Park, H. Jung, and H. Lee, "Immunogenicity of lipid nanoparticles and its impact on the efficacy of mRNA vaccines and therapeutics," *Experimental & Molecular Medicine,* vol. 55, no. 10, pp. 2085-2096, 2023.

[189]   M. Mehta, T. A. Bui, X. Yang, Y. Aksoy, E. M. Goldys, and W. Deng, "Lipid-based nanoparticles for drug/gene delivery: an overview of the production techniques and difficulties encountered in their industrial development," *ACS Materials Au,* vol. 3, no. 6, pp. 600-619, 2023.

[190]   X. Cheng and R. J. Lee, "The role of helper lipids in lipid nanoparticles (LNPs) designed for oligonucleotide delivery," *Advanced drug delivery reviews,* vol. 99, pp. 129-137, 2016.

[191]   C. Aundhia *et al.*, "Spray Drying in the pharmaceuticaul Industry-A Review," *Journal of Pharmaceutical Research,* vol. 2, pp. 63-65, 2011.

[192]   S. Keshani, W. R. W. Daud, M. Nourouzi, F. Namvar, and M. Ghasemi, "Spray drying: An overview on wall deposition, process and modeling," *Journal of Food Engineering,* vol. 146, pp. 152-162, 2015.

[193]   D. Santos, A. C. Maurício, V. Sencadas, J. D. Santos, M. H. Fernandes, and P. S. Gomes, "Spray drying: an overview," *Biomaterials-Physics and Chemistry-New Edition,* pp. 9-35, 2018.

[194]   J. P. Szczap and I. C. Jacobs, "Chapter 6 - Atomization and spray drying processes," in *Microencapsulation in the Food Industry (Second Edition)*, R. Sobel Ed.: Academic Press, 2023, pp. 59-71.

[195]   T. Furuta and T. L. Neoh, "Microencapsulation of food bioactive components by spray drying: A review," *Drying Technology,* vol. 39, no. 12, pp. 1800-1831, 2021.

[196]   L. E. Kurozawa, K. J. Park, and M. D. Hubinger, "Effect of maltodextrin and gum arabic on water sorption and glass transition temperature of spray dried chicken meat hydrolysate protein," *Journal of Food Engineering,* vol. 91, no. 2, pp. 287-296, 2009.

[197]   I. Schmitz-Schug, U. Kulozik, and P. Foerst, "Modeling spray drying of dairy products–Impact of drying kinetics, reaction kinetics and spray drying conditions on lysine loss," *Chemical Engineering Science,* vol. 141, pp. 315-329, 2016.

[198]   H. M. Lisboa, M. E. Duarte, and M. E. Cavalcanti-Mata, "Modeling of food drying processes in industrial spray dryers," *Food and Bioproducts Processing,* vol. 107, pp. 49-60, 2018.

[199]   J. Vicente, J. Pinto, J. Menezes, and F. Gaspar, "Fundamental analysis of particle formation in spray drying," *Powder technology,* vol. 247, pp. 1-7, 2013.

[200]   J. Archer, J. S. Walker, F. K. Gregson, D. A. Hardy, and J. P. Reid, "Drying kinetics and particle formation from dilute colloidal suspensions in aerosol droplets," *Langmuir,* vol. 36, no. 42, pp. 12481-12493, 2020.

[201]   A. Lechanteur and B. Evrard, "Influence of composition and spray-drying process parameters on carrier-free DPI properties and behaviors in the lung: A review," *Pharmaceutics,* vol. 12, no. 1, p. 55, 2020.

[202]   C.-W. Park *et al.*, "Advanced spray-dried design, physicochemical characterization, and aerosol dispersion performance of vancomycin and clarithromycin multifunctional controlled release particles for targeted respiratory delivery as dry powder inhalation aerosols," *International journal of pharmaceutics,* vol. 455, no. 1-2, pp. 374-392, 2013.

[203]   M. Beck-Broichsitter, C. Schweiger, T. Schmehl, T. Gessler, W. Seeger, and T. Kissel, "Characterization of novel spray-dried polymeric particles for controlled pulmonary drug delivery," *Journal of controlled release,* vol. 158, no. 2, pp. 329-335, 2012.

[204]   R. Deshmukh, P. Wagh, and J. Naik, "Solvent evaporation and spray drying technique for micro-and nanospheres/particles preparation: A review," *Drying technology,* vol. 34, no. 15, pp. 1758-1772, 2016.

[205]   J. Leng *et al.*, "Advances in nanostructures fabricated via spray pyrolysis and their applications in energy storage and conversion," *Chemical Society Reviews,* vol. 48, no. 11, pp. 3015-3072, 2019.

[206]   N. Marasini *et al.*, "Development of excipients free inhalable co-spray-dried tobramycin and diclofenac formulations for cystic fibrosis using two and three fluid nozzles," *International Journal of Pharmaceutics,* vol. 624, p. 121989, 2022.

[207]   X. Wang *et al.*, "Advances in controlled-release fertilizer encapsulated by organic-inorganic composite membranes," *Particuology,* 2023.

[208]   T. T. Nguyen, T. Hirano, R. N. Chamida, E. L. Septiani, N. T. Nguyen, and T. Ogi, "Porous pectin particle formation utilizing spray drying with a three-fluid nozzle," *Powder Technology,* p. 119782, 2024.

[209]   K. Kondo, T. Niwa, and K. Danjo, "Preparation of sustained-release coated particles by novel microencapsulation method using three-fluid nozzle spray drying technique," *European Journal of Pharmaceutical Sciences,* vol. 51, pp. 11-19, 2014.

[210]   H. Jiang, M. Zhang, S. McKnight, and B. Adhikari, "Microencapsulation of α-amylase by carrying out complex coacervation and drying in a single step using a novel three-fluid nozzle spray drying," *Drying Technology,* vol. 31, no. 16, pp. 1901-1910, 2013.

[211]   X. Shi and Y. Lee, "Encapsulation of tributyrin with whey protein isolate (WPI) by spray-drying with a three-fluid nozzle," *Journal of Food Engineering,* vol. 281, p. 109992, 2020.

[212]   D.-L. Yang *et al.*, "A general strategy for efficiently constructing multifunctional cluster fillers using a three-fluid nozzle spray drying technique for dental restoration," *Engineering,* vol. 8, pp. 138-147, 2022.

[213]   B. R. Bhandari, K. C. Patel, and X. D. Chen, "Spray drying of food materials-process and product characteristics," *Drying technologies in food processing,* vol. 4, pp. 113-157, 2008.

[214]   Y. Wu *et al.*, "Macrophage cell membrane-based nanoparticles: a new promising biomimetic platform for targeted delivery and treatment," *Journal of nanobiotechnology,* vol. 20, no. 1, p. 542, 2022.

[215]   H. Ragelle, F. Danhier, V. Préat, R. Langer, and D. G. Anderson, "Nanoparticle-based drug delivery systems: a commercial and regulatory outlook as the field matures," *Expert opinion on drug delivery,* vol. 14, no. 7, pp. 851-864, 2017.

[216]   F. M. Pelissari, M. V. E. Grossmann, F. Yamashita, and E. A. G. Pineda, "Antimicrobial, Mechanical, and Barrier Properties of Cassava Starch–Chitosan Films Incorporated with Oregano Essential Oil," *Journal of Agricultural and Food Chemistry,* vol. 57, no. 16, pp. 7499-7504, 2009/08/26 2009, doi: 10.1021/jf9002363.

[217] Y. Song, Y. Cong, B. Wang, and N. Zhang, "Applications of Fourier transform infrared spectroscopy to pharmaceutical preparations," (in eng), *Expert Opin Drug Deliv,* vol. 17, no. 4, pp. 551-571, Apr 2020, doi: 10.1080/17425247.2020.1737671.

[218] I. Hasni, P. Bourassa, S. Hamdani, G. Samson, R. Carpentier, and H.-A. Tajmir-Riahi, "Interaction of milk α- and β-caseins with tea polyphenols," *Food Chemistry,* vol. 126, no. 2, pp. 630-639, 2011/05/15/ 2011, doi: https://doi.org/10.1016/j.foodchem.2010.11.087.

[219] H. G. Brittain, "X-Ray Diffraction of Pharmaceutical Materials," in *Profiles of Drug Substances, Excipients and Related Methodology*, vol. 30, H. G. Brittain Ed.: Academic Press, 2003, pp. 271-319.

[220] P. Riello, "Quantitative Analysis of Amorphous Fraction in the Study of the Microstructure of Semi-crystalline Materials," in *Diffraction Analysis of the Microstructure of Materials*, E. J. Mittemeijer and P. Scardi Eds. Berlin, Heidelberg: Springer Berlin Heidelberg, 2004, pp. 167-184.

[221] P. Kaur, V. Mishra, T. Shunmugaperumal, A. K. Goyal, G. Ghosh, and G. Rath, "Inhalable spray dried lipidnanoparticles for the co-delivery of paclitaxel and doxorubicin in lung cancer," *Journal of Drug Delivery Science and Technology,* vol. 56, p. 101502, 2020.

[222] P. T. Mah *et al.*, "The use of hydrophobic amino acids in protecting spray dried trehalose formulations against moisture-induced changes," *European Journal of Pharmaceutics and Biopharmaceutics,* vol. 144, pp. 139-153, 2019.

[223] Y. Jiang *et al.*, "Highly transparent, UV-shielding, and water-resistant lignocellulose nanopaper from agro-industrial waste for green optoelectronics," *ACS Sustainable Chemistry & Engineering,* vol. 8, no. 47, pp. 17508-17519, 2020.

[224] D. Mahl, J. Diendorf, W. Meyer-Zaika, and M. Epple, "Possibilities and limitations of different analytical methods for the size determination of a bimodal dispersion of metallic nanoparticles," *Colloids and Surfaces A: Physicochemical and Engineering Aspects,* vol. 377, no. 1, pp. 386-392, 2011/03/05/ 2011, doi: https://doi.org/10.1016/j.colsurfa.2011.01.031.

[225] P. Tewa-Tagne, S. Briançon, and H. Fessi, "Preparation of redispersible dry nanocapsules by means of spray-drying: development and characterisation," *European Journal of Pharmaceutical Sciences,* vol. 30, no. 2, pp. 124-135, 2007.

[226] C. Yue-Xing *et al.*, "The effect of l-leucine on the stabilization and inhalability of spray-dried solid lipid nanoparticles for pulmonary drug delivery," *Journal of Drug Delivery Science and Technology,* vol. 46, pp. 474-481, 2018.

[227] L. Acosta-Domínguez, H. Hernández-Sánchez, G. F. Gutiérrez-López, L. Alamilla-Beltrán, and E. Azuara, "Modification of the soy protein isolate surface at nanometric scale and its effect on physicochemical properties," *Journal of Food Engineering,* vol. 168, pp. 105-112, 2016/01/01/ 2016, doi: https://doi.org/10.1016/j.jfoodeng.2015.07.031.

[228] A. Baldelli and R. Vehring, "Analysis of cohesion forces between monodisperse microparticles with rough surfaces," *Colloids and Surfaces A: Physicochemical and Engineering Aspects,* vol. 506, pp. 179-189, 2016/10/05/ 2016, doi: https://doi.org/10.1016/j.colsurfa.2016.06.009.

[229] N. Singh, D. Baby, J. P. Rajguru, P. B. Patil, S. S. Thakkannavar, and V. B. Pujari, "Inflammation and cancer," *Annals of African medicine,* vol. 18, no. 3, pp. 121-126, 2019.

[230] N. Yaqub, G. Wayne, M. Birchall, and W. Song, "Recent advances in human respiratory epithelium models for drug discovery," *Biotechnology Advances,* vol. 54, p. 107832, 2022/01/01/ 2022, doi: https://doi.org/10.1016/j.biotechadv.2021.107832.

[231] K. Eslin Ustun, C. Cagla Eren, and A. Ayla Melisa, "Colorimetric Cytotoxicity Assays," in *Cytotoxicity*, S. Anil and M. Mahmoud Ahmed Eds. Rijeka: IntechOpen, 2022, p. Ch. 3.

[232] E. Potuckova *et al.*, "Quantitative analysis of the anti-proliferative activity of combinations of selected iron-chelating agents and clinically used anti-neoplastic drugs," *PloS one,* vol. 9, no. 2, p. e88754, 2014.

[233] H. Wang, L. Qin, X. Zhang, J. Guan, and S. Mao, "Mechanisms and challenges of nanocarriers as non-viral vectors of therapeutic genes for enhanced pulmonary delivery," *Journal of Controlled Release,* vol. 352, pp. 970-993, 2022/12/01/ 2022, doi: https://doi.org/10.1016/j.jconrel.2022.10.061.

[234] T. Huang *et al.*, "Lipid nanoparticle-based mRNA vaccines in cancers: Current advances and future prospects," (in eng), *Front Immunol,* vol. 13, p. 922301, 2022, doi: 10.3389/fimmu.2022.922301.

[235] X. Gao, L. Guo, J. Li, H. E. Thu, and Z. Hussain, "Nanomedicines guided nanoimaging probes and nanotherapeutics for early detection of lung cancer and abolishing pulmonary metastasis: Critical appraisal of newer developments and challenges to clinical transition," *Journal of Controlled Release,* vol. 292, pp. 29-57, 2018/12/28/ 2018, doi: https://doi.org/10.1016/j.jconrel.2018.10.024.

[236] B. Chaurasiya and Y.-Y. Zhao, "Dry Powder for Pulmonary Delivery: A Comprehensive Review," *Pharmaceutics*, vol. 13, no. 1*,* p. E31doi: 10.3390/pharmaceutics13010031.

[237] P. B. Fourie, W. A. Germishuizen, Y. L. Wong, and D. A. Edwards, "Spray drying TB vaccines for pulmonary administration," *Expert Opinion on Biological Therapy,* vol. 8, no. 7, pp. 857-863, 2008/07/01 2008, doi: 10.1517/14712598.8.7.857.

[238] E. Lemarie *et al.*, "Aerosolized gemcitabine in patients with carcinoma of the lung: feasibility and safety study," *J Aerosol Med Pulm Drug Deliv,* vol. 24, no. 6, pp. 261-70, Dec 2011, doi: 10.1089/jamp.2010.0872.

[239] S. Mangal, W. Gao, T. Li, and Q. Zhou, "Pulmonary delivery of nanoparticle chemotherapy for the treatment of lung cancers: challenges and opportunities," *Acta Pharmacologica Sinica,* vol. 38, no. 6, pp. 782-797, 2017/06/01 2017, doi: 10.1038/aps.2017.34.

[240] G. A. Otterson *et al.*, "Phase I/II study of inhaled doxorubicin combined with platinum-based therapy for advanced non-small cell lung cancer," *Clin Cancer Res,* vol. 16, no. 8, pp. 2466-73, Apr 15 2010, doi: 10.1158/1078-0432.CCR-09-3015.

[241] G. A. Otterson *et al.*, "Phase I study of inhaled Doxorubicin for patients with metastatic tumors to the lungs," *Clin Cancer Res,* vol. 13, no. 4, pp. 1246-52, Feb 15 2007, doi: 10.1158/1078-0432.CCR-06-1096.

[242] T. Tatsumura, S. Koyama, M. Tsujimoto, M. Kitagawa, and S. Kagamimori, "Further study of nebulisation chemotherapy, a new chemotherapeutic method in the treatment of lung carcinomas: fundamental and clinical," *Br J Cancer,* vol. 68, no. 6, pp. 1146-9, Dec 1993, doi: 10.1038/bjc.1993.495.

[243] P. Zarogoulidis *et al.*, "Feasibility and effectiveness of inhaled carboplatin in NSCLC patients," *Invest New Drugs,* vol. 30, no. 4, pp. 1628-40, Aug 2012, doi: 10.1007/s10637-011-9714-5.

[244] T. Tatsumura, K. Yamamoto, A. Murakami, M. Tsuda, and S. Sugiyama, "[New chemotherapeutic method for the treatment of tracheal and bronchial cancers--nebulization chemotherapy]," *Gan No Rinsho,* vol. 29, no. 7, pp. 765-70, Jun 1983. [Online]. Available: https://www.ncbi.nlm.nih.gov/pubmed/6308308.

[245] F. Gagnadoux *et al.*, "Aerosolized chemotherapy," *J Aerosol Med Pulm Drug Deliv,* vol. 21, no. 1, pp. 61-70, Mar 2008, doi: 10.1089/jamp.2007.0656.

[246] A. E. Hershey *et al.*, "Inhalation chemotherapy for macroscopic primary or metastatic lung tumors: proof of principle using dogs with spontaneously occurring tumors as a model," *Clin Cancer Res,* vol. 5, no. 9, pp. 2653-9, Sep 1999. [Online]. Available: https://www.ncbi.nlm.nih.gov/pubmed/10499645.

[247] N. V. Koshkina, J. C. Waldrep, L. E. Roberts, E. Golunski, S. Melton, and V. Knight, "Paclitaxel liposome aerosol treatment induces inhibition of pulmonary metastases in murine renal carcinoma model," *Clin Cancer Res,* vol. 7, no. 10, pp. 3258-62, Oct 2001. [Online]. Available: https://www.ncbi.nlm.nih.gov/pubmed/11595722.

[248] N. R. Labiris and M. B. Dolovich, "Pulmonary drug delivery. Part I: physiological factors affecting therapeutic effectiveness of aerosolized medications," *Br J Clin Pharmacol,* vol. 56, no. 6, pp. 588-99, Dec 2003, doi: 10.1046/j.1365-2125.2003.01892.x.

[249] S. Sharma, D. White, A. R. Imondi, M. E. Placke, D. M. Vail, and M. G. Kris, "Development of inhalational agents for oncologic use," *J Clin Oncol,* vol. 19, no. 6, pp. 1839-47, Mar 15 2001, doi: 10.1200/JCO.2001.19.6.1839.

[250] M. E. Deffebach, N. B. Charan, S. Lakshminarayan, and J. Butler, "The bronchial circulation. Small, but a vital attribute of the lung," *Am Rev Respir Dis,* vol. 135, no. 2, pp. 463-81, Feb 1987, doi: 10.1164/arrd.1987.135.2.463.

[251] R. L. Keith *et al.*, "Angiogenic squamous dysplasia in bronchi of individuals at high risk for lung cancer," *Clin Cancer Res,* vol. 6, no. 5, pp. 1616-25, May 2000. [Online]. Available: https://www.ncbi.nlm.nih.gov/pubmed/10815878.

[252] B. J. Miller and A. S. Rosenbaum, "The vascular supply to metastatic tumors of the lung," *Surg Gynecol Obstet,* vol. 125, no. 5, pp. 1009-12, Nov 1967. [Online]. Available: https://www.ncbi.nlm.nih.gov/pubmed/6075076.

[253] E. N. Milne, C. D. Noonan, A. R. Margulis, and J. A. Stoughton, "Vascular supply of pulmonary metastases. Experimental study in rats," *Invest Radiol,* vol. 4, no. 4, pp. 215-29, Jul-Aug 1969. [Online]. Available: https://www.ncbi.nlm.nih.gov/pubmed/5351389.

[254] S. H. Lee, J. Teo, D. Heng, W. K. Ng, H. K. Chan, and R. B. Tan, "Synergistic combination dry powders for inhaled antimicrobial therapy: formulation, characterization and in vitro evaluation," *Eur J Pharm Biopharm,* vol. 83, no. 2, pp. 275-84, Feb 2013, doi: 10.1016/j.ejpb.2012.09.002.

[255] R. W. Pinner *et al.*, "Trends in infectious diseases mortality in the United States," *JAMA,* vol. 275, no. 3, pp. 189-93, Jan 17 1996. [Online]. Available: https://www.ncbi.nlm.nih.gov/pubmed/8604170.

[256] P. Szychowiak, M. Desgrouas, and S. Ehrmann, "Inhaled antibiotics in critical care: State of the art and future perspectives," *Infect Dis Now,* vol. 52, no. 6, pp. 327-333, Sep 2022, doi: 10.1016/j.idnow.2022.05.003.

[257] J. Alves *et al.*, "Nebulization of antimicrobial agents in mechanically ventilated adults in 2017: an international cross-sectional survey," *Eur J Clin Microbiol Infect Dis,* vol. 37, no. 4, pp. 785-794, Apr 2018, doi: 10.1007/s10096-017-3175-5.

[258] L. Papazian, M. Klompas, and C. E. Luyt, "Ventilator-associated pneumonia in adults: a narrative review," *Intensive Care Med,* vol. 46, no. 5, pp. 888-906, May 2020, doi: 10.1007/s00134-020-05980-0.

[259] A. C. Kalil *et al.*, "Management of Adults With Hospital-acquired and Ventilator-associated Pneumonia: 2016 Clinical Practice Guidelines by the Infectious Diseases Society of America and the American Thoracic Society," *Clin Infect Dis,* vol. 63, no. 5, pp. e61-e111, Sep 1 2016, doi: 10.1093/cid/ciw353.

[260] C. E. Luyt, G. Hekimian, D. Koulenti, and J. Chastre, "Microbial cause of ICU-acquired pneumonia: hospital-acquired pneumonia versus ventilator-associated pneumonia," *Curr Opin Crit Care,* vol. 24, no. 5, pp. 332-338, Oct 2018, doi: 10.1097/MCC.0000000000000526.

[261] S. I. Rennard *et al.*, "Estimation of volume of epithelial lining fluid recovered by lavage using urea as marker of dilution," *J Appl Physiol (1985),* vol. 60, no. 2, pp. 532-8, Feb 1986, doi: 10.1152/jappl.1986.60.2.532.

[262] L. B. Palmer and G. C. Smaldone, "Reduction of bacterial resistance with inhaled antibiotics in the intensive care unit," *Am J Respir Crit Care Med,* vol. 189, no. 10, pp. 1225-33, May 15 2014, doi: 10.1164/rccm.201312-2161OC.

[263] M. H. Kollef *et al.*, "A Randomized Trial of the Amikacin Fosfomycin Inhalation System for the Adjunctive Therapy of Gram-Negative Ventilator-Associated Pneumonia: IASIS Trial," *Chest,* vol. 151, no. 6, pp. 1239-1246, Jun 2017, doi: 10.1016/j.chest.2016.11.026.

[264] J. F. Oliveira, C. A. Silva, C. D. Barbieri, G. M. Oliveira, D. M. Zanetta, and E. A. Burdmann, "Prevalence and risk factors for aminoglycoside nephrotoxicity in intensive care units," *Antimicrob Agents Chemother,* vol. 53, no. 7, pp. 2887-91, Jul 2009, doi: 10.1128/AAC.01430-08.

[265] L. Sorli *et al.*, "Trough colistin plasma level is an independent risk factor for nephrotoxicity: a prospective observational cohort study," *BMC Infect Dis,* vol. 13, p. 380, Aug 19 2013, doi: 10.1186/1471-2334-13-380.

[266] S. Abdellatif, A. Trifi, F. Daly, K. Mahjoub, R. Nasri, and S. Ben Lakhal, "Efficacy and toxicity of aerosolised colistin in ventilator-associated pneumonia: a prospective, randomised trial," *Ann Intensive Care,* vol. 6, no. 1, p. 26, Dec 2016, doi: 10.1186/s13613-016-0127-7.

Chapter 2

Inhaled Medicines for Targeting Non-Small Cell Lung Cancer

Publication Details:

Al Khatib, A.O., El-Tanani, M., Al-Obaidi, H. Inhaled medicines for targeting non-small cell lung cancer. Pharmaceutics. 2023 Dec 14;15(12):2777.

Chapter Summary:

In this chapter, current literature regarding methods for delivering drugs directly to the lungs is reviewed, highlighting the progress and challenges in this field. The focus is on lung cancer treatment, particularly non-small-cell lung cancer (NSCLC). Traditional administration routes like oral and parenteral are compared with direct lung delivery, which offers reduced side effects and enhanced targeting precision. The chapter explores active and passive targeting strategies, emphasizing advanced tools such as nanoparticles and lipid carriers. Additionally, it discusses the potential benefits of combining inhalation therapy with chemotherapy and immunotherapy to improve therapeutic outcomes and patient well-being.

Review
Inhaled Medicines for Targeting Non-Small Cell Lung Cancer

Arwa Omar Al Khatib [1,2] , Mohamed El-Tanani [2,3] and Hisham Al-Obaidi [1,*]

1 School of Pharmacy, University of Reading, Reading RG6 6AD, UK
2 Faculty of Pharmacy, Al Ahliyya Amman University, Amman 19111, Jordan
3 College of Pharmacy, RAK Medical and Health Sciences University,
  Ras Al Khaimah P.O. Box 11172, United Arab Emirates
* Correspondence: h.al-obaidi@reading.ac.uk

Abstract: Throughout the years, considerable progress has been made in methods for delivering drugs directly to the lungs, which offers enhanced precision in targeting specific lung regions. Currently, for treatment of lung cancer, the prevalent routes for drug administration are oral and parenteral. These methods, while effective, often come with side effects including hair loss, nausea, vomiting, susceptibility to infections, and bleeding. Direct drug delivery to the lungs presents a range of advantages. Notably, it can significantly reduce or even eliminate these side effects and provide more accurate targeting of malignancies. This approach is especially beneficial for treating conditions like lung cancer and various respiratory diseases. However, the journey towards perfecting inhaled drug delivery systems has not been without its challenges, primarily due to the complex structure and functions of the respiratory tract. This comprehensive review will investigate delivery strategies that target lung cancer, specifically focusing on non-small-cell lung cancer (NSCLC)—a predominant variant of lung cancer. Within the scope of this review, active and passive targeting techniques are covered which highlight the roles of advanced tools like nanoparticles and lipid carriers. Furthermore, this review will shed light on the potential synergies of combining inhalation therapy with other treatment approaches, such as chemotherapy and immunotherapy. The goal is to determine how these combinations might amplify therapeutic results, optimizing patient outcomes and overall well-being.

Keywords: NSCLC; passive and active targeting; nanoparticles; immunotherapy; liposomes; inhalers

1. Introduction

The respiratory tract has three major physiological functions: ventilation, diffusion, and perfusion. Ventilation is the process of breathing in which air enters the lungs due to the mechanical movement of the diaphragm. This process also involves air movement from the blood into the bronchial trees and alveolar space. Diffusion is the molecular mechanism that encompasses carbon dioxide transport, which ultimately affects the pH of the blood. Perfusion is critical for ventilation and diffusion as it maintains efficient blood circulation in order to match the high rate of gas exchange in the lungs [1].

The passage of air and the amount of energy required for ventilation is influenced by several physical factors [2]. These factors include alveolar surface tension, lung compliance, and airway resistance, which are vital for maintaining optimal respiratory function. One of the most important of these factors is alveolar surface tension, which refers to the tendency of the surface of the alveoli to resist expansion. This is reduced by lung surfactant, which coats the alveolar surface and decreases surface tension. By doing so, the surfactant helps keep the alveoli open during exhalation and promotes easier breathing during inhalation. Without surfactants, the airways would collapse after exhalation, making re-inflation during inhalation harder and less efficient.

Lung compliance is another crucial factor and refers to the ability of the lungs to expand when the air volume is increased. It is expressed as the volume change per unit of pressure change (mL/cm H_2O or L/cm H_2O) and depends on two essential factors:

elasticity and surface tension. Elasticity refers to the tendency of the lung tissue to return to its original shape after being stretched, while surface tension refers to the tendency of the liquid lining the alveoli to resist expansion. Decreased surface tension and increased elasticity of the lung tissues enhance pulmonary compliance, allowing the lungs to rebound after being stretched during inhalation. This, in turn, increases the upstream pressure, which promotes better ventilation. Finally, airway resistance refers to the force that resists air flow through the airways. It is influenced by several factors, including the diameter and length of the airways, as well as the viscosity of the air. Higher airway resistance makes it harder for the air to move through the airways, leading to breathing difficulties. Understanding these physical factors is vital to maintaining healthy respiratory function and can help to identify and treat any underlying respiratory conditions.

2. Lung Cancer, Etiology, and Current Practice

Lung cancer remains a predominant cause of cancer-induced fatalities across the globe, representing nearly one-fourth of these tragic deaths [3]. Cancer is complex and therefore requires treatments that are dependent on several factors, such as the stage of the disease, its specific location within the body, the patient's overall health and age, and other underlying medical conditions. Predominantly, localized cancers that have not spread beyond their point of origin are treated with surgical interventions, followed by chemotherapy sessions [4]. Non-small-cell lung cancer (NSCLC) encompasses a variety of lung cancer types, including adenocarcinoma, squamous cell, and large-cell undifferentiated carcinoma. Adenocarcinoma is the most prevalent, constituting about 40–50% of NSCLC cases [5], with bronchiolo-alveolar carcinoma accounting for 10–15% of these cases [6]. While squamous cell cancer typically originates at the central regions of the lung, large-cell undifferentiated carcinoma is characterized by its rapid proliferation and its ability to manifest anywhere within the lung [7]. Collectively, NSCLC represents roughly 85% of all diagnosed lung cancer cases, with a significant majority of patients being elderly. The average age of diagnosis is around 70 years [8].

Tobacco smoking remains the main cause of NSCLC, being responsible for nearly 90% of all cases, yet there are other contributors like exposure to second-hand smoke, the presence of radon, environmental pollution, genetic predispositions towards lung cancer, and certain genetic markers like the *CYP1A1* gene variant [9]. External factors, such as exposure to harmful substances like asbestos, tar, and specific metals, also play a pivotal role [10]. The probability of developing lung cancer is intrinsically tied to the frequency and longevity of smoking habits [11]. Interestingly, individuals with HIV present heightened risks of lung cancer as compared to the broader population [12], and a noticeable association has been established between pulmonary fibrosis and increased lung cancer susceptibility [13].

For NSCLC, the range of therapeutic alternatives includes surgery, radiation, chemotherapy, and specialized medical interventions. Chemotherapy typically involves a combination of a platinum-based compound with other therapeutic agents. First-line treatments usually encompass a platinum-based compound, synergized with a third-generation cytotoxic drug [14]. There are FDA-sanctioned treatments for NSCLCs exhibiting EGFR mutations, including compounds like gefitinib, erlotinib, and others [15]. Moreover, Bevacizumab, a compound targeting VEGF, has been approved for the first-line treatment of non-squamous NSCLC, especially when paired with chemotherapy [6]. Lung carcinoid tumors, although rare, are categorized as either typical or atypical carcinoids, both originating from neuroendocrine cells. Central carcinoids emerge within the central regions of the lungs, while peripheral carcinoids evolve toward the lungs' extremities.

For patients with metastatic lung carcinoids, a variety of treatments is available, which range from surgical procedures to chemotherapy. Subcutaneous administrations of drugs like octreotide are commonly the go-to treatments, while targeted drugs like everolimus also show efficacy. To treat stage III atypical carcinoids, a mix of cisplatin and etoposide is typically used and is occasionally augmented with radiation sessions.

The European Neuroendocrine Tumor Society has approved adjuvant therapy for atypical carcinoids with lymph node involvement, but such interventions are not recommended for typical carcinoids [16]. As medical research progresses, newer therapeutic strategies continue to emerge, offering hope and improved outcomes for patients globally. It is crucial to understand that each patient's treatment plan is tailored based on their unique medical history and the specific nature of their cancer. Collaborations between oncologists, radiologists, and other medical professionals ensure the best care and outcome for each individual. In the area of cancer therapy, especially NSCLC, the development of drug delivery systems containing naturally occurring compounds has attracted attention. Recent research has described the anticancer effects of the natural cAMP-activating drug forskolin in NSCLC cells. It was shown that forskolin can inhibit both proliferation and migration in NSCLC cells. Interestingly, forskolin-mediated synergistic effects against Paclitaxel-induced cytotoxicity were also observed [17]. In a different study, the sustained release and intracellular accumulation of forskolin was found to prevent outer hair cells apoptosis [18].

3. Advantages of Direct Delivery to the Lungs to Target Lung Cancer

The administration of drugs to the lungs, or pulmonary delivery, has emerged as a highly promising option for drug delivery due to its numerous advantages. The lungs have a high surface area, which allows for the rapid and efficient absorption of drugs [19,20]. As a result, the respiratory tissues have the ability to absorb large quantities of drugs, making them an ideal route for drug delivery. Compared to the oral route, pulmonary drug delivery offers a faster onset of action, higher bioavailability, and better patient compliance, all while being non-invasive in nature [21–24]. Moreover, inhaled medication does not undergo first-pass metabolism, leading to lower drug degradation. This method also promotes the direct effect of the drug on the lungs, resulting in better selectivity and reduced circulation into the body's system, which in turn leads to fewer side effects and better therapeutic outcomes.

Studies have demonstrated that inhaling anticancer agents can effectively combat micro metastasis and distant metastasis by targeting the lymphatic drainage of the alveoli [25]. The interstitial space is crucial in delivering drugs directly to the lungs, which is vital for suppressing lung cancer metastasis [19]. Upon being excreted from the lungs, these drugs can accumulate in the interstitium, the peripheral airways, and the pulmonary lymphatic system, enabling them to interact with cancer cells beyond the alveolar space and to restrict the invasiveness and metastasis of cancer [19]. Pulmonary drug delivery also limits systemic exposure to drugs [26]. Intravenous treatments are impeded by poor selectivity, systemic toxicity (including nausea, vomiting, nephrotoxicity, neurotoxicity, and anaemia), and the development of multidrug-resistant pumps [26–28], as well as the necessity for optimising drug dosing [29].

4. Lung Surfactants and Impact on Drug Deposition

Lung surfactants, also known as endogenous surfactants, are a combination of lipids and proteins found in the lung's alveolar lining. Their main role is to decrease surface tension by forming a single layer at the alveolar air-liquid boundary [30]. Lung surfactants facilitate the efficient spreading of drugs delivered to the lungs across mucus surfaces and improve the aerosol transport between lung areas, resulting in more consistent drug dosing within the deeper lung regions.

Exogenous surfactants are employed when there is a surfactant deficiency, serving as a substitute treatment for respiratory distress syndromes [31]. These can be either natural or artificially produced. Natural surfactants primarily contain phospholipids, mainly dipalmitoylphosphatidylcholine (DPPC), neutral fats (chiefly cholesterol), and proteins. Frequently used natural surfactants come from sources like humans, animals, cows, and pigs. On the other hand, synthetic exogenous lung surfactants like colfosceril and lucinactant are entirely synthesized, often based on DPPC.

The surfactant layer plays a crucial role in drug deposition within the lungs [32]. Inhaled drugs must first navigate this layer to access the underlying tissue. The presence of lung surfactants influences drug deposition in multiple ways, such as:

- Diffusion limitation: The surfactant layer might act as a barrier, hindering drugs from reaching deeper tissues. This can lead to reduced drug concentrations in the lungs and diminished treatment effectiveness.
- Extended residence time: The surfactant layer can prolong the duration of time that the drugs linger in the lungs. This is beneficial for drugs that are rapidly expelled, as it allows for extended exposure to lung tissue, which enhances their potency.
- Drug particle dimensions: The size of the drug particles affects their deposition depth in the lungs. Larger particles might be trapped atop the surfactant layer, which limits their penetration, while smaller particles might navigate past the layer to access the deeper lung regions.

In essence, lung surfactants can enhance deposition by ensuring even alveolar expansion during inhalation and enhancing alveolar resistance to collapse upon exhalation [33]. Additionally, lung surfactants quickly adhere and redistribute effectively at the air–water boundary, facilitating the even spread of inhaled drugs across the mucus-covered lung surfaces, optimizing drug deposition [30]. Thus, the surfactant quantity present can considerably influence the drug amounts deposited in the lungs.

5. Mucociliary Clearance and Mucoadhesion, Getting the Balance Right

Mucociliary clearance (MCC) represents the mechanism by which the respiratory system expels foreign entities, such as medications, via the synchronized efforts of cilia and mucus. It is an essential protective function that safeguards the lungs from inhaled invaders like allergens, harmful substances, and microbes [34]. This protective action propels the mucus, along with any dissolved or adhered substances, from the lung's tracheobronchial region to the GIT. Conversely, the alveolo-bronchiolar clearance process shifts solutes, lining fluid, and/or macrophages from the alveoli towards the MCC area [35]. An extended clearance phase, lasting several days to several weeks, is characterized as the peripheral and alveolar removal of particles via the macrophages. There is a notable correlation between how long particles stay in the airways and their physical dimension. MCC quickly expels larger particles from the airways, while tinier particles remain longer [36]. It has been suggested, however, that the MCC's efficiency diminishes in the deeper sections of the respiratory system [35].

Multiple factors can modulate the MCC, including those influencing the mucus or cilia. Factors like augmented mucus secretion, reduced mucus thickness, and elevated ciliary motion can enhance the MCC's speed. In contrast, altering the unique properties of mucus or disrupting its structure can decelerate the MCC. Ambient conditions, such as temperatures around 23 °C, can induce a moderate decline in MCC rates [37]. Additionally, smoking can hinder the MCC by reducing ciliary abundance, thereby altering mucus dynamics. Moreover, various upper respiratory ailments can affect the MCC due to their effects on ciliary motion and/or mucus behavior; these include conditions like asthma, rhinitis, and chronic sinusitis [37]. Accelerated MCC is seen as a limitation for inhaled treatments as it limits the time that drugs remain at the deposition locale, thereby lowering the drug bioavailability [36,38]. To counter this challenge, there is a need to enhance mucoadhesion, which signifies a drug's capability to bind to the mucus layer and ensure prolonged residence in the lungs [37]. Utilizing innovative mucoadhesive drug delivery systems capable of adhering to the pulmonary mucosa [39] will extend the retention period at the action site [40,41] and enhance the interaction between the pulmonary mucosa and the medication, ensuring a broader drug spread. This mucoadhesive approach elevates drug concentrations at the deposition site and increases drug uptake, thereby elevating drug bioavailability and enhancing its absorption [42,43]. In essence, both mucociliary clearance and mucoadhesion are essential determinants that influence drug transport within the respiratory system. Achieving the right equilibrium between these elements is paramount for ideal respiratory

drug delivery. While it is crucial to reduce the MCC to boost the performance of drugs delivered to the lungs via mucoadhesive techniques, this adjustment should be performed carefully, as the MCC acts as a native defense strategy of the lower respiratory tract against potential infections, and overly aggressive mucoadhesive actions could jeopardize this defense [44]. Overall, the MCC can positively affect the efficacy of inhaled anticancer therapies because the MCC is crucial for removing inhaled particles including anticancer therapeutic agents, which prevents drug accumulation and reduces toxicity. The MCC can also affect the distribution of drugs across the respiratory tract. Thus, understanding the MCC is essential for designing inhalable drug formulations that can target lung cancer effectively. On the other hand, The MCC poses additional challenges because the rapid clearance of inhaled anticancer therapies can limit the time that a therapeutic agent spends in target tissue, especially within the lungs. Therefore, optimizing drug formulations for effective penetration is crucial for balancing the contact time with the mucosal surface absorption risk, as diseases affecting mucociliary clearance vary.

6. Methods and Devices for Inhalation

Inhalation devices are commonly utilized for administering medications in the form of finely-ground particles, suspensions, or solutions. The efficacy of drug delivery to the lower respiratory tract is influenced by a multitude of factors, including the type of inhaler used, the internal resistance of dry powder inhalers, the drug formulation, the size of the particle, the velocity of the produced aerosol of pressurized metered-dose inhalers, and the ease of use [45]. It should be noted that each inhalation device has its own unique set of advantages and disadvantages, which can affect the way that medication is delivered to the lungs. Consequently, it is essential to carefully consider the characteristics of each inhaler before selecting an appropriate device for drug administration [46].

The most commonly used devices for inhalation include pressurized metered-dose inhalers (PMDIs), which are inhalers that use a metering system to correctly dispense the desired propellant volume; PMDIs with spacers or valves holding chambers that serve as aerosol reservoirs and are linked to a pressurized metered-dose inhaler. These devices are especially beneficial for small children because they require less coordination between inhaling and dispensing medication. Additionally, there are the breath-actuated pressurized metered-dose inhalers that are activated by the patient's inhalation, removing the requirement for hand-to-breath coordination [47]. One of the most essential advantages of these inhalers is their ability to administer several doses of medication. The dry powder inhalers (DPIs) also spread medication as a powdered substance of respirable-sized micronised particles. Moreover, there are nebulisers which generate aerosol particles by either using a high-velocity gas jet of oxygen or air (jet nebuliser) or a rapidly vibrating piezoelectric crystal (ultrasonic nebuliser) [47]. Soft mist inhalers are types of nebulizers that are designed to convert liquid medicine into inhalable droplets, similar to handheld nebulizers and multi-dose devices like metered-dose inhalers and dry powder inhalers [47].

7. Assessment of Drug Deposition, Current Methods, and Accuracy for Assessment of Deposition of Anticancer Agents

Accurately assessing the distribution of drugs throughout the lungs is crucial when evaluating their efficacy in treating lung cancer via inhaled chemotherapy [48]. Administering the appropriate chemotherapeutic agents at the correct doses, intervals, and disease locations can lead to better outcomes for patients [49]. Factors such as particle size, density, shape, velocity, charge, hygroscopicity, and surface properties [50], as well as the patient's breathing pattern and respiratory system condition, are all vital factors for efficiently depositing the particles in the lungs [51]. Various methods, including lung imaging techniques, pharmacokinetic analysis, and direct drug concentration assay in lung tissue, can be used to assess the deposition of anticancer agents [52]. However, the accuracy of these methods depends on the types of anticancer agent, delivery system, and target

tissue. The process of determining the rate of the absorption of inhaled drugs is crucial for determining their effectiveness [53].

When it comes to assessing the absorption and disposition of inhaled medications meant for systemic administration, there are different methods that can be used. These methods include in vivo, in vitro, and ex vivo models. The Andersen cascade impactor is a commonly used method for determining lung deposition. The next generation impactor (NGI) is another method that calculates various aerosolization performance parameters such as mass median aerodynamic diameter (MMAD), geometric standard deviation (GSD), fine particle fraction (FPF), emitted fraction percent (EF%), and residual fraction percent (RF%) based on the drug deposition percentage at each step [54]. On the other hand, the isolated perfused lung (IPL) is an ex vivo technique that involves removing the lungs from an animal, such as a rodent or guinea pig, and placing them in a synthetic environment.

The advancement of inhaled therapeutics and the exploration of aerosol dynamics have significantly benefited from in silico techniques, which robust mechanisms for anticipating deposition within respiratory tracts [55]. Numerous computational strategies, intricate airway designs, and diverse suppositions related to flow and aerosol mechanics have been employed in past numerical examinations. An array of in silico techniques exists for forecasting the aerosol accumulation in the upper respiratory tracts, encompassing medical imaging-derived airway designs from techniques like computed tomography (CT) and magnetic resonance imaging (MRI), airflow designs such as Reynolds-averaged Navier-Stokes (RANS), large eddy simulation (LES), and direct numerical simulation (DNS), alongside aerosol movement and accumulation models like Lagrangian or Eulerian methodologies [56].

The in vivo-in vitro correlation (IVIVC) procedure plays a crucial role in pharmaceutical advancement, linking the deposition of medicines in human lungs to estimates derived from in vitro physical respiratory designs and in silico computational models. This correlation offers insightful projections concerning a drug's final destination post-administration through diverse inhalation aerosol mechanisms. The process of labelling is integral in this context, necessitating validation to ascertain the radiotracer's accuracy as a drug marker prior to the radioactive aerosol's inhalation by the patient or participant. This entails quantifying the dosage and particle size distribution of the aerosolized medication and radiotracer and comparing these findings with the unlabelled drug [57].

Gamma scintigraphy is a widely used method for evaluating lung deposition accuracy and is often used to quantify whole-lung deposition and oropharyngeal deposition. However, despite its effectiveness, single-photon emission computed tomography (SPECT) and positron emission tomography (PET) have a stronger theoretical basis for quantification [58]. The multi-planar information provided by SPECT and PET enables a precise and in-depth evaluation of the deposited dosage in various lung regions [59]. Overall, the accuracy of these methods can vary depending on various factors, including the sensitivity and specificity of the imaging technique, the timing and duration of drug administration, and the variability in patient anatomy and breathing patterns.

8. Effect of Particle Size and Shape on Their Lung Deposition

As the inhaled particles travel through the respiratory tract, their physical characteristics including size, shape, and density influence their inertia and, consequently, their deposition [50,60,61]. This behaviour is largely defined by the particles' aerodynamic diameters, which correspond to the diameter of a unit-density sphere that achieves the same velocity in the airstream as the particle in question. Techniques such as light scattering, laser diffraction, or image analysis can be employed to measure the geometric diameter of these particles, which can then be translated into their aerodynamic diameters [62].

The deposition of these inhaled particles in the airways occurs primarily through three mechanisms: inertial impaction, gravitational sedimentation, and diffusion [63,64]. Particles larger than 5 μm generally cannot alter their path within the airflow and tend to impact and deposit in the upper airways through inertial impaction [65–67]. Particles

between 1 and 5 µm usually settle in the lower airways (bronchioles and alveoli) through gravitational sedimentation [68]. Meanwhile, particles smaller than 1 µm often stay suspended in the airstream and are likely to be exhaled without depositing, with diffusion being their main deposition mechanism [68,69]. Notably, particles smaller than about 500 nm may show increased lung deposition [70–72].

For inhaled chemotherapeutic agents, particles within the aerodynamic diameter range of 1–5 µm are preferred [73]. The effectiveness of these inhaled formulations is frequently assessed based on the fine particle fraction (FPF) or fine particle dose (FPD), which refers to the portion or dose of particles within this size range. Another important metric is the mass median aerodynamic diameter (MMAD), the diameter below which 50% of the particles fall, which serves as an indicator of the aerosol characteristics of these formulations [60]. Also, the clearance of the inhaled particles is highly dependent on their size and occurs through three primary mechanisms: mucociliary clearance, phagocytosis, and systemic uptake [74].

Mucociliary clearance is the most prominent mechanism in the upper airways [75]. Here, mucus secreted by the ciliated columnar epithelium traps particles, which are then moved upward by cilia and eventually coughed out or swallowed This method is particularly effective for particles larger than 5 µm [76]. In contrast, smaller particles, which reach the deeper parts of the lungs, remain there longer as mucociliary clearance is less dominant in these regions [77,78]. While macrophages are present in the upper airways, their role in phagocytosis is less pronounced [79].

In the deeper lungs, the clearance mechanisms are more complex and largely depend on the particles' dissolution characteristics. Slowly dissolving or insoluble particles can be cleared through a combination of mucociliary clearance, phagocytosis by alveolar macrophages, and endocytosis [80–82]. Alveolar macrophages predominantly handle the clearance in the deep lungs, dealing mainly with particles sized between 1 and 5 µm [83]. These macrophages engulf the particles, which are then either digested lysosomally or expelled through the lymphatic system or via mucociliary clearance [83]. Particles smaller than 200 nm often evade detection by macrophages due to their size. They can be quickly taken up by the epithelial cells or translocate to the systemic circulation through protein/receptor-mediated mechanisms or by endocytosis via alveolar caveolae [84].

Another important aspect affecting the lung drug delivery of inhaled chemotherapy is the shape of the inhaled agents. The larger the contact areas, such as elongated shapes, the less effective inhalation is for lung targeting. This is because their shape leads to stronger van der Waals forces, resulting in a higher tendency for the particles to clump together or aggregate [85]. This was investigated by a study that compared particles that had similar sizes but different shapes, including spheres, cubes, plates, needles, and pollen-like forms. This study aimed to explore how particle shape affects the particles' movements, aerosolization, and ability to deposit in the lungs. It was found that particles resembling pollen were most advantageous for inhalation drug delivery. Compared to the other shapes, these pollen-like particles demonstrated superior aerosolization, flowability, and deposition qualities, making them more suitable for this application [86].

The efficacy and safety of inhaled anti-lung cancer treatments depend on the drug deposition in the lungs. Several factors determine the success of these therapies. The site of action is critical because the medication targets tumor cells inside the lungs. Therefore, it is crucial for drug particles to deposit at the target site for therapeutic efficacy. The size and dispersion of the medication particles determine their deposition in the respiratory tract. Ideally, the particles should be small enough to reach the deeper areas of the lungs where cancer cells reside. The aerodynamic properties of the particles significantly impact their penetration and deposition. Additionally, individual differences in lung function and physiology can influence inhaled drug deposition patterns. Factors such as respiratory rate, tidal volume, and airway geometry can alter drug deposition. The appropriate device selection should be based on the drug and patient's specific properties and the formulation of the anti-cancer agent, which influences its deposition in the lungs. Finally, the drug's

distribution in the tumor microenvironment is critical and can be affected by factors such as blood flow, tumor vascularization, and interstitial pressure.

9. Challenges for the Delivery of Inhaled Chemotherapy

Inhaled therapy is a popular method for treating respiratory disorders like asthma, chronic obstructive pulmonary disease (COPD), and cystic fibrosis. This method delivers medication straight to the lungs through inhalation. Nevertheless, various challenges come with inhaled chemotherapy that can affect its safety and effectiveness.

9.1. Uniform Drug Deposition

It is difficult to achieve the homogenous deposition of the chemotherapeutic medication in the lungs. Inhaled medications may not be distributed equally throughout the respiratory system, resulting in drug concentration differences at distinct lung areas.

9.2. Patient Variability

Variability in patient anatomy, respiratory rates, and inhalation patterns can all have an impact on inhaled chemotherapeutic deposition. It is difficult to provide consistent and effective drug distribution across a heterogeneous patient group.

9.3. Device Design and Performance

Inhalation device design and function are critical for medicine delivery. Issues such as device blockage, poor aerosolization, or insufficient patient breathing techniques can all have an impact on inhaled anti-lung-cancer agents' delivery efficiency.

9.4. Disease-Specific Challenges

Inhaled chemotherapy may bring distinct complications for certain lung conditions. Conditions such as chronic obstructive pulmonary disease (COPD) or cystic fibrosis, for example, may change lung physiology, which in turn impacts drug deposition and effectiveness.

9.5. Toxicity and Side Effects

Chemotherapy inhalation may induce local irritation or systemic side effects. The continuous difficulty of designing inhaled chemotherapy formulations involves balancing therapeutic efficacy with minimizing side effects.

9.6. Drug Stability

Some chemotherapy medications could be affected by environmental conditions such as temperature and humidity. It is critical to ensure a drug's stability during storage and inhalation in order to preserve its effectiveness.

10. Formulation of Anticancer Agents Using Carrier Free Technology

Carrier-free technology is an innovative approach to drug delivery and involves the direct transportation of the drug to the desired target without the need for any auxiliary carrier particles. This method has gathered significant attention due to its inherent ability to enhance therapeutic results while simultaneously reducing potential side effects [87]. In the area of nanotechnology, there has been a surge of comprehensive research that focuses on the delivery of anti-cancer drugs. The primary objective of these studies is to strengthen therapeutic effectiveness while limiting associated toxicities [88–90]. As the medical field continues to advance, there has been a notable evolution in the formulation of carrier-free nanodrugs. These nano-drugs are self-assembled using prodrugs, unmodified drugs, or amphiphilic drug-drug conjugates [91]. Their unique attributes, such as enhanced pharmacodynamics/pharmacokinetics, diminished toxicity, and superior drug-loading capabilities, have made carrier-free nanodrugs a focal point for oncological treatments. An essential area of exploration is the design and application of multi-functional carrier-free nanodrugs, especially those with potent anti-cancer properties suitable for clinical administration. In

comparison to nanodrugs that utilize inorganic or organic carriers, carrier-free nanodrugs offer a plethora of advantages. Among those advantages is their impressive drug-carrying capacities combined with their reduced side effects [92–94]. Their engineered structures enhance accumulation within tumors [95,96]. Furthermore, the synthesis process of these carrier-free nanodrugs is both simple and environmentally friendly [95], often avoiding the use of harmful reagents like organic solvents. These nanodrugs also demonstrate prolonged retention in the bloodstream as compared to standard anti-cancer drugs [93,94]. This extended retention facilitates the build-up of anti-cancer agents within tumor tissues, leading to increased absorption by tumor cells [93]. Carrier-free technology stands out as a groundbreaking advancement in drug delivery, offering a multitude of benefits that are not present in the traditional carrier-based systems [97].

A variety of techniques have been innovatively developed for the synthesis of carrier-free nanodrugs. These include methods such as nanoprecipitation, template-assisted nanoprecipitation, thin-film hydration, the spray-drying approach, the supercritical fluid (SCF) method, and wet media grinding [98]. These techniques have catalyzed the latest breakthroughs in the domain of carrier-free nanodrugs tailored for oncological interventions. Broadly, these advancements can be segmented into three distinct categories:

1. Self-assembly of a singular anti-cancer drug.
2. Self-assembly of multiple anti-cancer drugs.
3. Self-assembly of anti-cancer drugs in conjunction with other therapeutic agents, including photosensitizers, photothermal agents, immune reagents, and genetic materials [99,100].

The formulation of carrier-free nanodrugs often involves the strategic coupling of two drug entities or the conjugation of functional organic compounds—such as fatty acids, vitamins, proteins, and photosensitizers—to drug molecules. This is achieved through the establishment of covalent bonds and/or physical interactions. Such an intricate design enhances the stability, targeting precision, and therapeutic potency of anti-cancer medications [101]. In a research study, a unique carrier-free multidrug nanocrystal was employed for combination chemotherapy. This involved the assembly of three primary water-insoluble drugs into nanorods, which were subsequently conjugated with PEG to bolster their environmental stability [96]. Both the in vivo and in vitro assessments revealed that these multidrug nanocrystals exhibited a therapeutic efficacy that was up to three times superior to that of the unbound drugs, even when administered in equivalent dosages. Furthermore, they effectively overcame the phenomenon of multidrug resistance. In another study, distinct formulations of pure nanodrugs were prepared with curcumin and 10-hydroxycamptothecin, using a variety of solvents and anti-solvents [102]. As per the documented findings, the synthesis of the nanoparticles from agents like doxorubicin, ionidamine, and triphenylphosphine had the potential to diminish metabolic energy by specifically targeting the mitochondria [103]. Notably, these prepared nanoparticles succeeded in extending the half-life of doxorubicin in the circulatory system to a commendable 3 h [94].

A recent research study has made a significant breakthrough in creating lactose-free dry powder formulations of two important medicines, fluticasone propionate and salmeterol xinafoate FP/SX, by utilizing advanced organic solutions and a spray-drying particle engineering design. These formulations also feature mannitol as an excipient, which helps in molecular combination. The resultant spray-dried powders exhibit crucial properties that are essential for the effective administration of the inhaled medication [104].

Two other studies have reported on the development of carrier-free chemo-photodynamic nanodrugs. In one study, chlorine e6 and doxorubicin molecules self-assembled into nanoparticles through electrostatic π-π stacking and hydrophobic interactions [95]. The other study created a carrier-free nanodrug by using curcumin with a donor-acceptor pair composed of perylene and 5,10,15,20-tetro(4-pyridyl)porphyrin (H2TPyP) as photosensitizers [105]. This allowed for photodynamic therapy and curcumin inhibited cancer cell growth. The fluorescence state of the curcumin was only activated when it was released

from the nano-platform, allowing for the self-monitoring of the drug release [94]. Combining more than two different drug types is often necessary to achieve a more effective therapeutic impact. Optimising the ratios of various chemotherapy drugs in nanodrugs will increase their efficiency while reducing the likelihood of additional side effects. Recently, different targeting ligands, such as antibodies, peptides, and specific cell membranes with a high affinity for cancer cells, have been developed to improve the targeting capability of carrier-free nanodrugs. To increase the stability and therapeutic effectiveness of carrier-free nanodrugs, which are somewhat unstable and prone to precipitation and aggregation, it is essential to incorporate amphiphilic protein, peptide, and nucleic acid preparations with therapeutic functions as stabilisers. Coating the carrier-free nanodrugs with different cell membranes is another promising approach for endowing the unprotected nanodrugs with excellent biocompatibility and biological stabilisation [106].

Two research studies have investigated the formulation of carrier-free chemo-photodynamic nanodrugs. The first study explored the self-assembly of chlorine e6 and doxorubicin molecules into nanoparticles. This assembly was facilitated by the intricate interplay of electrostatic π-π stacking and hydrophobic forces [95]. In a parallel study, a distinctive carrier-free nanodrug was prepared by combining curcumin with a donor-acceptor, specifically perylene and 5,10,15,20-tetro(4-pyridyl)porphyrin (H2TPyP), which acted as photosensitizers [105]. This innovative combination not only enabled photodynamic therapy but also effectively reduced the proliferation of the cancer cells. Interestingly, the fluorescence state of the curcumin was exclusively activated upon its release from the nano-platform, offering a unique mechanism for the real-time monitoring of the drug dispersion [94]. In cancer therapy, the combination of multiple drug variants is often imperative for achieving an enhanced therapeutic outcome. By optimising the proportions of diverse chemotherapy agents within nanodrugs, one can potentially increase their efficacy while simultaneously diminishing the risk of supplementary adverse reactions. In recent times, a plethora of targeting ligands, encompassing antibodies, peptides, and specific cell membranes with a pronounced affinity for malignant cells, have been innovatively designed. These advancements aim to augment the targeting precision of carrier-free nanodrugs. However, it is crucial to acknowledge that carrier-free nanodrugs, in their native states, exhibit certain limitations such as instability and tendencies for precipitation and aggregation. To counteract these challenges and improve the stability and therapeutic efficacy of these nanodrugs, the integration of amphiphilic proteins, peptides, and nucleic acid formulations with therapeutic attributes has been deemed essential. These components act as stabilizers, ensuring the robustness of the nanodrugs. Furthermore, enveloping the carrier-free nanodrugs with diverse cell membranes has emerged as a promising strategy. This encapsulation not only confers the nanodrugs with superior biocompatibility but also ensures their biological stabilisation, leading to enhanced therapeutic outcomes [106].

11. Strategies for Drug Targeting of NSCLC

Although various treatment options are available for NSCLC, the survival rate remains relatively low; therefore, there is a need for new treatment strategies. Figure 1 shows some examples of the current strategies for targeting NSCLC while Table 1 shows examples of the current pulmonary-delivered medicines that have been investigated for lung cancer.
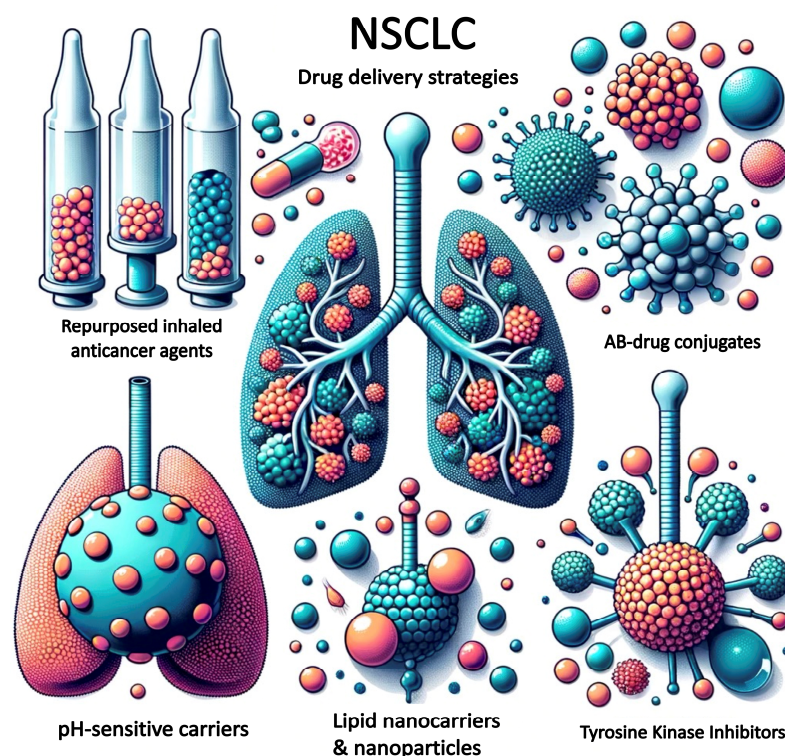
Figure 1. Examples of current drug delivery strategies for the treatment of NSCLC.

11.1. Active Targeting for NSCLC in Inhaled Therapies

Active targeting is a therapeutic strategy that uses monoclonal antibodies or small-molecule inhibitors to specifically target the proteins or signaling pathways that are dysregulated in cancer cells. This technique involves the use of ligands or antibodies to selectively deliver therapeutic agents to the tumor site. One of the most commonly used approaches of active targeting is the targeting of overexpressed receptors on cancer cells, such as the epidermal growth factor receptor (EGFR) or the human epidermal growth factor receptor 2 (HER2). This method has been found to be effective in several cancer types, including non-small-cell lung cancer (NSCLC).

In NSCLC, targeted therapies have been developed that specifically target these receptors, including tyrosine kinase inhibitors (TKIs) and monoclonal antibodies (mAbs). For instance, osimertinib, a third-generation EGFR-TKI, has shown efficacy for treating NSCLC patients with EGFR mutations [107]. This drug has been found to be particularly effective in patients who have developed resistance to other EGFR-TKIs. Similarly, Trastuzumab, a mAb that targets HER2, has shown efficacy in NSCLC patients with HER2 overexpression [108]. Other examples of active targeting strategies for NSCLC include the use of ligands that target tumor-specific antigens, such as folate or transferrin receptors, or the use of nanoparticles that can selectively deliver therapeutic agents to the tumor site. These strategies are still in experimental phases and require further research and development. Active targeting is a promising therapeutic strategy for the treatment of NSCLC and other cancers. By selectively delivering therapeutic agents to the tumor site, this technique can minimize the side effects associated with traditional chemotherapy and improve patient outcomes.

11.1.1. Immune Checkpoint Inhibitors (ICIs)

Immunotherapy has emerged as an effective treatment option for cancer patients. Immune checkpoint inhibitors (ICIs) are a type of immunotherapy that work by blocking specific pathways in the immune system. These pathways, known as immune checkpoints, are responsible for regulating the immune system's response against cancer cells.

One of the most important immune checkpoint pathways is the programmed death 1 (PD-1)/programmed death ligand 1 (PD-L1) pathway. Cancer cells can activate this pathway to evade detection by the immune system. ICIs such as pembrolizumab, nivolumab, and atezolizumab target the PD-1/PD-L1 pathway, preventing cancer cells from evading the immune system [109]. Another important immune checkpoint pathway is the cytotoxic T-lymphocyte-associated protein 4 (CTLA-4) pathway. This pathway regulates the activity of T cells, which play a crucial role in the immune response against cancer cells. ICIs such as ipilimumab target the CTLA-4 pathway, enhancing the activity of T cells against cancer cells. Non-small-cell lung cancer (NSCLC) is one type of cancer that can be treated with ICIs. These treatments have been shown to be effective in improving the survival rates and the quality of life for patients with NSCLC. Ongoing research aims to identify new ICIs and optimize their use in order to further improve outcomes for cancer patients.

11.1.2. Tyrosine Kinase Inhibitors (TKIs)

Non-small-cell lung cancer (NSCLC) is often associated with mutations in receptor tyrosine kinases, such as EGFR and ALK. Tyrosine kinase inhibitors (TKIs) are a class of drug that have been developed to specifically target these mutations in the tyrosine kinase domain of these receptors. TKIs work by obstructing the downstream signaling pathways that are triggered by these mutations. By doing so, they prevent the cancer cells from proliferating and cause them to undergo apoptosis, or programmed cell death. This mechanism makes TKIs a promising treatment option for NSCLC. Several TKIs have been approved for the treatment of NSCLC, including erlotinib, afatinib, and crizotinib [110]. These drugs have shown significant efficacy in improving the overall survival and the quality of life of NSCLC patients. However, the choice of TKI may depend on the specific genetic profile of the tumor and the patient's overall health condition. Overall, TKIs are a targeted therapy that offers a promising treatment option for NSCLC patients with mutations in their receptor tyrosine kinases. With the availability of several approved TKIs and ongoing research in this field, the future of NSCLC treatment looks more hopeful than ever before.

11.1.3. Antibody-Drug Conjugates (ADCs)

Antibody-drug conjugates (ADCs) are a type of targeted cancer therapy that combines an antibody with a cytotoxic medication. The antibody is designed to specifically recognize and bind to a particular antigen on the surface of the cancer cells. Once the antibody attaches to the cancer cells, the cytotoxic medicine is released and delivered directly to the cancer cells, sparing the healthy cells from damage. This targeted approach can potentially enhance the efficacy of the chemotherapy while reducing its side effects. Rovalpituzumab tesirine and sacituzumab govitecan are some of the ADCs that are currently being studied for non-small-cell lung cancer (NSCLC) and have shown promising results in clinical trials [111].

11.1.4. Personalized Inhaled Medicine Approaches

Individualizing inhaled medicines based on the genetic and molecular profiles of NSCLC tumors can improve treatment outcomes. Identifying specific mutations or indicators that can be targeted with personalized medicine formulations could be part of this approach.

11.2. Passive Targeting for NSCLC in Inhaled Therapies

Passive targeting is a method of delivering medicines to a tumor site by taking advantage of the increased permeability and retention (EPR) effect, which occurs due to the abnormal blood vessels in the tumor. This approach allows for a higher concentration of medicine to accumulate in the tumor tissues than in healthy tissues. Some examples of passive targeting strategies for NSCLC (Non-small-cell lung cancer) are listed below.

11.2.1. Use of Amorphous Solid Dispersions

Solid dispersions refer to a formulation technique that involves dispersing a drug in a solid matrix. In this technique, the drug is mixed with an inert carrier molecule, which helps to reduce the loss of the drug within the inhalation device and minimize the deposition of the drug in the oropharyngeal area [112].

11.2.2. Use of Nanoparticle Delivery Systems

Non-small-cell lung cancer (NSCLC) is a challenging disease to treat due to its complex molecular heterogeneity and resistance to conventional therapies. However, nanoparticle-based drug delivery systems have emerged as promising approaches for combatting NSCLC. These tiny particles offer numerous advantages, including the ability to selectively target cancer cells, enhance drug efficacy, and reduce toxicity. Inhalable self-assembled albumin nanoparticles conjugated with doxorubicin and octyl aldehyde and adsorbed with the apoptotic TRAIL protein represent a novel inhalation-based combination therapy method for the treatment of resistant lung cancer [113]. A study reported that inhaling mesoporous silica nanoparticles (MSNs) resulted in the preferential concentration of nanoparticles in mouse lungs, preventing the MSNs' escape into the systemic circulation and limiting their accumulation in other organs. The experimental data showed that the proposed DDS meets the key requirements for effective non-small-cell lung cancer treatment [114].

11.2.3. Lipid-Based Nanoparticle Delivery Systems (LNPs)

Lipid-drug conjugate nanoparticles are a type of drug delivery system that shows great potential for the targeted delivery of drugs to cancer cells, including NSCLC. These nanoparticles are composed of a core of drug molecules that are covalently attached to lipid molecules, forming a protective shell around the drug core. The lipid shells of these nanoparticles can be designed to be either hydrophilic or hydrophobic, enabling them to interact with different types of cells and tissues in the body and providing a platform for efficient drug delivery. The covalent linkage of drugs to lipid molecules allows them to self-assemble into nanoparticles, which can provideenhanced stability and circulation times as compared to other lipid nanoparticle formulations. The conjugation of the drugs to lipids also offers improved biocompatibility, making these nanoparticles safe and effective drug carriers.

A study found that the NLC was highly effective for the tumor-targeted inhaled delivery of anticancer drugs (doxorubicin or paclitaxel) and the delivery of siRNA mixtures specifically to lung cancer cells, resulting in efficient tumor growth suppression and the prevention of adverse side effects on healthy organs [115]. This technology has the potential to revolutionize cancer treatment by enabling targeted drug delivery and improving treatment outcomes.

11.2.4. Liposomes

Liposomes are small, spherical structures made up of a double layer of phospholipids that can hold hydrophobic drugs within their core. They consist of one or more layers of lipid bilayer that encircle an aqueous pocket. Liposomes have been found to accumulate in non-small-cell lung cancer (NSCLC) tumors and can enhance the effectiveness of chemotherapy drugs in this type of cancer [116]. Several studies have demonstrated that liposomal formulations of chemotherapy drugs, such as the inhalable liposomal curcumin formulation, represent a promising pulmonary medicine for the treatment of lung cancer [117]. Another study showed that liposomal nanoparticles loaded with paclitaxel showed superior antitumor activity against NSCLC in vitro and in vivo as compared to free paclitaxel [118].

11.2.5. Solid Lipid Nanoparticles (SLNs)

Solid lipid nanoparticles (SLNs) are tiny particles made up of solid lipids that are dispersed in an aqueous solution. They are smaller than liposomes and are known for their

high stability and biocompatibility. SLNs have shown immense drug delivery potential for the treatment of non-small-cell lung cancer (NSCLC) due to their ability to improve drug efficacy and reduce toxicity. Studies have reported that different types of SLNs have been successful in enhancing the anti-tumor efficacy of drugs used to treat NSCLC. For instance, paclitaxel-loaded solid lipid nanoparticles (PTX-SLNs) were found to be effective in improving the anti-tumor efficacy of paclitaxel in lung cancer cells both in vitro and in a mouse model of NSCLC [119]. Similarly, another study reported the creation of an erlotinib-loaded solid lipid nanoparticle (ERL-SLNs)-based dry powder inhaler formulation. The synthesized ETB-SLNs exhibited high anticancer activity in lung cancer cells [120]. In a different study, findings confirmed that in a mouse inhalation model, the repeated inhalation exposure to SLN at concentrations lower than a 200-μg deposit dosage was safe [121]. Dry powder formulations using chitosan-derivative-coated solid lipid nanoparticles for inhalation have contributed to increased anti-cancer action in folate receptor-positive lung tumors [122]. According to a different study, epirubicin solid lipid nanoparticles (EPI-SLNs) could be used as an inhalable delivery strategy for lung cancer treatment [123].Finally, another study has reported that SLNs are a promising pulmonary delivery mechanism for enhancing the bioavailability of medicines that are weakly water soluble, such as naringeninin NSCLC [124].

11.2.6. Nanostructured Lipid Carriers (NLCs)

Nanostructured lipid carriers (NLCs) are a drug delivery system similar to solid lipid nanoparticles (SLNs) but which have the added benefit of containing a mixture of solid and liquid lipids. Because of this, NLCs can encapsulate multiple drugs with different physicochemical properties, making them more versatile for accommodating a wider range of drugs. NLCs have been shown to improve the solubility and bioavailability of drugs and enhance their targeting ability. Docetaxel-loaded poloxamer-coated poly (lactic-co-glycolic acid) (PLGA) NPs were developed for the treatment of NSCLC via the pulmonary route. When compared to free DTX, these nanoparticles demonstrated greater cytotoxicity and regulated drug release, indicating improved treatment efficacy [125]. In vivo investigations demonstrated that the optimised formulation of nano-lipid carriers (NLCs) containing Paclitaxel (PTX) and Doxorubicin (DOX) exhibited improved retention and drug accumulation in the lungs with no evidence of tissue abnormalities and helped to reduce harmful effects in non-target tissues. Furthermore, both the cell line and in vivo results revealed that low-medication doses could be effective in achieving targeted therapeutic outcomes. These findings support the hypothesis that the pulmonary delivery of chemotherapeutics via an adequate inhalable nano-lipid carrier could be a promising chemotherapeutic method for lung cancer [126].

11.2.7. Lipid-Polymer Hybrid Nanoparticles (LPHN)

Hybrid nanoparticles are a combination of lipids and polymers that have the potential to improve a drug's loading and release properties. They can overcome biological barriers and increase therapeutic effectiveness, making them attractive platforms for drug delivery. These nanoparticles are designed to target non-small-cell lung cancer (NSCLC) by incorporating tumor-targeting ligands or antibodies onto their surfaces. This allows them to selectively bind to tumor cells and deliver drugs directly to the cancerous tissue.

Studies have shown that inhalable hybrid lipid protein nanoparticles nanocomposites that are dual-targeted can deliver genistein and all-trans retinoic acid for lung cancer therapy [127]. Aptamer-decorated lipid-polymer hybrid nanoparticles (ALPNPs) have also been found to have high drug loading capacities and good stability and are efficiently taken up by lung cancer cells in vitro. Co-delivery of docetaxel prodrug and cisplatin in the ALPNPs resulted in synergistic cytotoxicity against lung cancer cells compared to either drug alone. Another study reported that inhalation formulations based on silibinin-loaded chitosan-coated PLGA/PCL nanoparticles improved cytotoxicity and bioavailability in lung cancer patients [128].

11.2.8. Polymeric Nanoparticle Delivery Systems

Polymeric nanoparticles are synthesized using biodegradable polymers such as poly (lactic-co-glycolic acid) (PLGA) and polyethylene glycol (PEG). These nanoparticles are capable of encapsulating drugs for targeted delivery, and they can release the drugs in a controlled and sustained manner. This feature of polymeric nanoparticles makes them an attractive option for drug delivery in the treatment of lung cancer, especially non-small-cell lung cancer (NSCLC).

According to a recent study on A549 cells, the afatinib-loaded PLGA nanoparticles dry powder inhaler had improved penetration and a stronger cytotoxic capability at a lower IC50 value than the plain afatinib dimaleate solution [129].

11.2.9. Gold Nanoparticle Delivery Systems

Gold nanoparticles are tiny biocompatible particles that can be functionalized with targeting ligands in order to selectively target cancer cells. They have been used as a passive targeting strategy for non-small-cell lung cancer (NSCLC), as they can accumulate in tumors through the EPR effect and can be imaged using computed tomography (CT) scans [130]. Researchers have developed gold nanocages coated with hyaluronic acid (HA) for the targeted delivery of docetaxel to the NSCLC cells that overexpress CD44, a receptor for HA. These nanocages were shown to selectively accumulate in CD44-positive NSCLC cells and enhance the cytotoxicity of docetaxel. In addition, a multifunctional AuNP-based nanoplatform was developed for the targeted co-delivery of cisplatin and siRNA to NSCLC cells. According to the most recent research, inhalation is the best route for delivering gold nanoparticles to the lung, with high deposition efficiency, good distribution, tissue integrity preservation, and no evidence of caused inflammation [131].

11.2.10. Use of pH-Sensitive Drug Delivery Systems

A recent study demonstrated that the pulmonary co-delivery of doxorubicin and siRNA via pH-Sensitive nanoparticles has an improved antitumor activity as compared to the single delivery method [132]. According to one study, nanoparticles of pH-responsive PEG-Doxorubicin conjugates were rapidly released at acidic pH. They spread easily in propellant-based metered-dose inhalers [133].

Overall, pH-sensitive drug delivery systems offer a promising approach for targeted drug delivery to tumors, including NSCLC. These systems can be tailored to respond to the unique properties of a tumor's microenvironment, such as its acidic pH, and can deliver drugs with increased efficacy and reduced toxicity.

Table 1. Examples of current pulmonary-delivered medicines and repurposed medicines investigated for lung cancer.

API Type	Formulation Type	Delivery Method	Reference
Azacitidine	Solution	Aerosol, Nebulizer	[134]
Azacitidine	Solution/Dry powder	Aerosol, Nebulizer/Dry powder, nose-only inhalation	[135]
Bevacizumab	Dry powder	Aerosol, nasal inhalation	[136]
2-ME 2-methoxyestradiol	Nanocomposites and nanoaggregates	Intratrchial insufflation	[137]
5-Fluorouracil	Lipid coated nanoparticles	Inhalation Aerosol, Nebulizer	[138,139]
Epirubicin	Solid Lipid Nanoparticles (SLNs)	Inhalation Aerosol, Nebulizer	[123]
9-Nitrocampthotecin	Liposome	Inhalation Aerosol, Nebulizer	[140–142]

Table 1. *Cont.*

API Type	Formulation Type	Delivery Method	Reference
Afatinib & paclitaxel	Lipid-based nanocarriers	In vitro: Turbospin (single dose powder inhaler device). In vivo: Dry powder insufflator—Lipid-based nanocarriers	[129,143]
Camptothecin	Aerosolized liposomal Camptothecin	Inhalation Aerosol, Nebulizer	[144]
Carboplatin	Solution	Inhalation Aerosol, Nebulizer	[145]
Doxorubicin Celecoxib	Liposomes, EGF-modified gelatine nanoparticles, PLGA microparticles, drug conjugates	Inhalation, Aerosol, pMDI	[114,146–151]
	Lipid-based nanocarriers	Inexpose™ nebulizer Nanolipidcarriers	[152]
Celecoxib & Docetaxel	Solution	Inhalation Aerosol, MDI	[153,154]
Cisplatin	SLIT: Lipid vesicles	Inhalation Aerosol, nebulizer	[155]
Cisplatin loaded EGF-modified GP	Gelatin nanoparticle	Endotrachial installation	[156]
CpG & Poly I:C	Liposomal formulations	Intratracheal instillation	[157]
Curcumin	Nanocomposites and nanoaggregates	In vitro: Aerosol using cascade impactors	[158]
	Liposomal formulations	Intratracheal instillation	[159]
	Liposomal formulations	IntratrachialInsufflator	[117]
Curcuminoids	Lipid-based nanocarriers	Aerosol, Side stream jet nebulizer	[160]
Methotroxate	HFA-based Microparticles	Aerosol, Metered Dose Inhaler	[161]
Docetaxel	Liposomal formulations	Intratracheal administration	[116]
Docetaxel	Lipid-based nanoemulsion	OMRON MicroAIR nebulize	[162]
Docetaxel	Nanoparticles	DPI	[125]
Docetaxel and Curcumin	Nanoemulsion	In vitro: Aerosol, Anderson cascade impactor	[163]
Doxorubicin	Poly(butyl cyanoacrylate) nanoparticles	Aerosol, DPI	[164]
	Effervescent nanoparticles	Intratrachial insufflator	[165]
	Highly porus large PLGA microparticles	Inhalation	[28,133,144,166–170]
	Liposomal formulations	Intratracheal administration using microsprayer	[171]
	Solution (0.4 to 9.4 mg/m^2)	Aerosol, Nebulizer	[172]
	Liposomal formulations	Aerosol, One-jet Collison nebulizer	[173]
Doxorubicin & ASO, or siRNA	LHRH receptor-targeted mesoporous silica nanoparticles	Inhalation	[114,132]
Doxorubicin and paclitaxel	Lipid-based nanocarriers	Collision nebulizer connected to nose-only exposure chamber	[115,126]
Epirubicin	Solid lipid nanoparticles	Aerosol, nebulizer	[123]
Erlotinib	Microparticles	Aerosol, DPI	[120]

<p align="center">**Table 1.** *Cont.*</p>

API Type	Formulation Type	Delivery Method	Reference
Gefitinib	Lipid-based nanocarriers	Intratracheal installation	[174]
Cisplatin	EGF-modified Gelatin Nanoparticles (LNPs)	Aerosol, nebulizer	[27]
Gemcitabine & cisplatin	Niosomes	Aerosol, nebulizer	[175]
Gemcitabine	Solution	Aerosol, nebulizer	[176–178]
Retinoic acid and and genistein	Nanoparticles	DPI	[127]
Gemcitabine-HCl	Liposomal formulations	Intratracheal/Insufflator (Aerosol)	[179]
HC & 5-Amino levulinic acid	Cationic Liposomal nanoparticles	Endotrachial installation	[180]
Hyaluronan (HA)-cisplatin conjugates	Drug conjugates	Endotrachial installation	[181]
IL-2	Liposomes	Aerosol, nebulizer	[181]
Doxorubicin	Solution	Aerosol, nebulizer	[113]
Cyclosporin A and paclitaxel	Liposomes	Aerosol nebulizer	[182]
Doxorubicin	Self-assembled albumin nanoparticles	Aerosol, nebulizer	[113]
Anti-carbonic anhydrase IX (CA IX) antibody, conjugated to the surface of triptolide (TPL)	Liposomes	Aerosol	[118]
9-Bromo-noscapine	Lipid-based nanocarriers	Inhalation by indigenously developed apparatus	[183]
Myricetin	Nanoencapsulated Phospholipid Complex	In vitro: Aerosol using Aerolizer connected to Anderson Cascade Impigner	[184]
Silibinin	Nanoparticles	Inhalation, DPI	[128]
Nitro-camptothecin	Liposomes	Aerosol, nebulizer	[185–187]
Oridonin	DLPC liposome	Aerosol jet nebulizer	[188]
Paclitaxel	Liposomes	Aerosol, nebulizer	[168]
	Lung surfactant mimetic and pH-responsive lipid nanovesicles	Inhalation	[139]
	Chitosan-coated folate-PEG nanoparticles	Endotracheal administration, Micro Sprayer Aerosolizer IA-1C	[119]
	Lipid-based nanocarriers	DP insufflator	[189]
	Lipid-based nanocarriers	Aerosol, Collison nebulizer	[190]
	SLN- solid lipid nanoparticle	DPI- dry powder inhaler	[122]
Phospho-sulindac	Liposome	Aerosol, nebulizer	[191]
Quercetin	Lipid-based nanocarriers	OMRON MicroAIR nebulizer	[192–194]
Naringenin	SLN	Intratracheal instillation	[124]
Resveratrol	Nanocomposites and nanoaggregates	Inhalation	[195]
siRNA	DOTAP-modified PLGA nanoparticles	In vitro: aerosol generated by small scale powder disperser	[196]
Sorafenib Tosylate	Liposomal formulations	In vitro: DPI, Revolizer device	[197]

Table 1. *Cont.*

API Type	Formulation Type	Delivery Method	Reference
TAS-103	PLGA Nanocomposites and nanoaggregates	DPI, insufflator	[198]
Temozolomide	Liposomal formulations	Intratracheal administration using Microsprayer IA-1C system	[199]
	Nanocomposites and nanoaggregates	In vitro: DPI, Axahaler™	[200]
	Liposomal formulations	Micro sprayer Aerosolizer Pulmonary Aerosol Kit for Mouse Model PAK-MSA	[201]
Amodiaquine	Nanoparticles	Inhalation, aerosol	[202]
Pioglitazone	Powder	Inhalation, aerosol	[203]
Telmisartan	Nanoparticles	Intratumoral distribution	[204]
Amodiaquine	Inhalable nanoparticulate system	Inhalation, nebulizer	[202]
Bexarotene (Targretin) & budesonide	Powders	Inhalation, aerosol, turbuhaler	[205–207]
Itraconazole	Dry powder for inhalation	In vitro: Cyclohaler™ Dry Powder Inhaler, twin stage impigner apparatus.	[208]
	Dry powder for inhalation	Inhalation Aerosol, DPI	[209]
	Solid dispersion	Inhalation Aerosol, DPI	[210]
Fisetin	Dry powder	Aerosol, DPI	[211]
Isotretinoin	Powder	Aerosol	[212]
Metformin	Sterosomes	Aerosol, nebulizer	[213]
Pirfenidone	Liposome	Microsprayer® Aerosolizer Pulmonary Aerosol-Kit for Mouse	[214]

The pioneering work by Cory et al. in exploring the various delivery systems for 5-fluorouracil (5-FU) has significantly contributed to lung cancer therapy. Their investigation into liposomes, microspheres, and lipid-coated nanoparticles (LNPs) has provided crucial insights. In particular, the varying release times, with liposomes releasing 5-FU within 4–10 h and microspheres composed of poly-(lactide-co-glycolide) (PLGA) and poly-(lactide-co-caprolactone) (PLCL), showed slower release rates and demonstrated the potential for customizable delivery durations. This is crucial for tailoring treatments to specific patient needs [138].

Building on this context, another study by Cory et al. examined the inhalation delivery of 5-FU in LNPs using a hamster model. The research highlighted the distribution and concentration of 5-FU in different tissues post-inhalation, revealing initial high concentrations in the trachea, larynx, and esophagus, and comparatively lower levels in the lung. This distribution pattern underlines the feasibility of LNPs for lung cancer chemotherapy through inhalation [139].

Bart et al.'s study on aerosolized SLIT cisplatin in lung carcinoma patients further supports this potential. The treatment was well-received, showing minimal systemic toxicity and manageable side effects, which were predominantly gastrointestinal and respiratory. The pharmacokinetic analysis revealed low plasma platinum levels, which were indicative of effective local delivery, bolstering the case for aerosolized SLIT cisplatin as a viable lung cancer treatment [155].

Similarly, Zhang et al.'s investigation into liposomal gefitinib dry powder inhalers (LGDs) for non-small-cell lung cancer (NSCLC) treatment aligns with these findings. The LDGs' rapid absorption from the lung, their higher concentration and retention as compared to oral administration, and their reduced inflammatory response and potential for lung injury, all point to the superiority of this method for NSCLC treatment [174].

In a parallel vein, Kim et al. focus on doxorubicin-loaded PLGA microparticles (Dox PLGA MPs), revealing their high encapsulation efficiency and effective aerosolization characteristics. After pulmonary administration, these MPs demonstrated prolonged lung retention and significant in vitro cytotoxicity against melanoma cells. The resulting smaller tumor sizes in a melanoma metastasis mouse model illustrate the potential of Dox PLGA MPs for long-term inhalation therapy in lung cancer [147].

In the area of in vivo activity, Koshkina and Kleinerman investigated the efficacy of aerosolized gemcitabine for treating osteosarcoma lung metastases. Aerosol GCB's superiority over intraperitoneal administration in inhibiting lung metastases growth, coupled with its non-toxic profile, showcases its potential as an effective treatment modality [176]. The authors in other studies evaluated the aerosolized paclitaxel (PTX) in liposomal formulations, which similarly demonstrated a significant reduction in lung tumour burdens and enhanced survival rates in a murine model of renal carcinoma with pulmonary metastases [168]. Shepard et al. contributed to this growing body of research by developing a dry powder pulmonary formulation of bevacizumab, a monoclonal antibody used in NSCLC treatment. This formulation's suitability for deep lung delivery, coupled with the maintenance of bevacizumab's anti-VEGF bioactivity and its efficacy at lower doses than intravenous controls in a rat NSCLC model, underscores the potential of such innovative formulations [136].

The development of an inhalable, stable dry powder formulation of 5-azacytidine (5AZA), an epigenetic therapy drug by Kuehl et al., further exemplifies this trend. The formulation's superior pharmacokinetics and its effectiveness in reducing the tumour burden in an orthotopic rat lung cancer model, demonstrates its ability to reprogram the cancer genome and marks a significant advancement in lung cancer treatment [135].

The study on phospho-sulindac, a derivative of sulindac with anticancer activity, addresses the challenges of metabolic stability that limit its use in systemic therapy. The aerosolized form of phospho-sulindac, developed to overcome first-pass metabolism, showed high levels of the intact drug in the lungs and significantly inhibited lung tumorigenesis. This method not only improved the survival of mice bearing orthotopic A549 xenografts but also minimized hydrolysis to less active metabolites [191].

Based on combination therapy, a study by Koshkina et al. examined the co-delivery of cyclosporine A paclitaxel via liposomal aerosol in a Renca-lung-metastases mouse model. The combination yielded favorable effects on tumor growth, although weight loss in the treated mice suggested potential toxicity in need of management. However, no significant toxicity was observed histopathologically [182].

In the clinical setting, Zarogoulidis et al. explored inhaled chemotherapy as an alternative for NSCLC treatment. Patients receiving a combination of intravenous and inhaled carboplatin showed a significant increase in survival rates, suggesting the efficacy of inhaled carboplatin as an alternative pulmonary drug delivery method [145].

12. Use of Repurposed Inhaled Anticancer Agents for Targeting NSCLC

Over the past few years, there has been a growing interest in repurposing inhaled anticancer agents for the treatment of non-small-cell lung cancer (NSCLC). Several inhaled anticancer agents have shown promise in targeting NSCLC, as indicated in Table 1. For instance, paclitaxel, a drug that stabilizes microtubules and inhibits cell division, has been found to be effective when inhaled using a nebulizer in the preclinical models of NSCLC [215]. In a phase II clinical trial, the combination of paclitaxel and carboplatin was linked with significant survival rates and moderate toxicity in fit, older patients with advanced NSCLC [216]. Another potential candidate for being repurposed as an anti-cancer

therapy is amodiaquine, a drug that is commonly used to treat malaria. In pre-clinical studies, amodiaquine was shown to have anti-cancer properties, especially for NSCLC [202]. The drug has been found to inhibit the growth of cancer cells and induce cell death in vitro. Further studies are needed to evaluate its efficacy in treating NSCLC in vivo. Liposomal cisplatin is another inhaled anticancer agent that has shown promise for treating NSCLC. Cisplatin is a chemotherapy drug that can effectively kill cancer cells, but its use is limited due to its toxic side effects. Liposomal cisplatin is a reformulated version of cisplatin, which is encapsulated in a liposomal carrier to reduce its toxicity.

Several examples of repurposed drugs that are used to target NSCLC are listed in Table 1. These drugs have been approved for other indications and are being repurposed for NSCLC treatment based on their potential anticancer properties. Repurposing these drugs can provide a faster and more cost-effective approach to drug development, as these drugs have already undergone safety and efficacy testing for their original indications. The pulmonary route appears to be a viable strategy for reducing the significant systemic toxicity associated with chemotherapy. In phase I, Ib/IIa, and II clinical trials, inhaled chemotherapy was shown to be both practical and safe. Inhalation permits strong therapeutic doses to be delivered directly to lung tumours without prior distribution in the body. As a result, any severe systemic toxicities are decreased [217]. A recent review showed that as a local treatment, inhaled cytotoxic chemotherapy is a potential therapy for bridging the gap between local and broad systemic treatments. It could concentrate the dose in the lungs and gradually disperse it into the blood and lymph systems, which are the primary pathways for cancer invasion [218].

With the introduction of repurposed and targeted medications that offer greater therapeutic alternatives, non-small-cell lung cancer (NSCLC) treatment has witnessed tremendous breakthroughs. It can be seen from previous research that several medications have been tested for their anticancer activities such as, but not limited to, amodiaquine inhalable nanoparticles, which were successfully formulated and optimised by employing a systematic strategy of experiment design via a scalable high-pressure homogenization (HPH) approach [202]. Another study claimed that pioglitazone aerosol could be a beneficial drug for regional lung cancer prevention, and may even be used with other medicines to create a combination chemoprevention (e.g., retinoids, biguanides such as metformin, etc.) [203]. Since 1968, the inhalation of cytotoxic chemotherapy has been the focus of various research studies, although only a few clinical trials have been conducted so far [142,145,155,172,178,219–221] (Table 2). These trials have revealed that inhalation can result in lower or minimal systemic side effects, offering an improved pharmacokinetic profile. However, a major challenge in these trials is the exclusive use of nebulizers, including jet, ultrasonic wave, and vibrating mesh types, to administer the chemotherapy. Typically delivered via intravenous perfusion, these nebulizers aim to convert the chemotherapy solution into fine droplets smaller than 5 µm for direct lung inhalation. However, a significant portion of the aerosol is lost during the nebulization, affecting the effectiveness of this delivery method [222–224].

Cytotoxic chemotherapy comprises hazardous drugs, necessitating extensive protective measures for healthcare personnel to minimize the exposure risks [225]. Achieving effective lung deposition might require large drug doses administered over extended periods through nebulization, which raises health concerns [155]. Additionally, the infusion of certain cytotoxic drugs, which make up about 10–30% of lung cancer chemotherapies, can cause pulmonary toxicities, leading to clinician hesitancy in using this treatment approach [226].

Technological and pharmaceutical advancements offer new possibilities for inhaled cytotoxic chemotherapy, contingent upon addressing key clinical and technological factors. The administration time for aerosolized drugs varies based on dose and concentration, and the efficiency of nebulizers in depositing the drug in the lungs also differs. For example, a jet-nebulizer delivered only 10–15% of a radiolabelled CIS dose to the lungs, whereas a vibrating mesh nebulizer achieved 43% lung deposition with a radiolabelled

gemcitabine solution. This low efficiency imposes a critical limitation on delivering effective treatment [178,219]. Additionally, the pressure generated by the nebulizer, which influences the rate of nebulization (up to 0.3 mL/min), also impacts how quickly and efficiently the drug is delivered to the patient's lungs and plays a significant role in the overall success of the therapy [155].

Table 2. Clinical studies investigating the safety and efficacy of inhaled chemotherapy for NSCLC.

Drug	Phase	Device, Formulation	Patient Status (*n*)	Deposition in the Lung	Local Dose Limiting Toxicity	Severe Systemic Toxicity	Disease Response (*n*)	Reference
Azacitidine	Phase 1/2	Aerosol, Nebulizer/Dry powder, nose-only inhalation	Local and metastatic lung cancer	Direct deposition into the bronchi and lung	No pulmonary toxicity	Pale skin, shortness of breath, fast heartbeat, chest pain, cough, unusual bruising or bleeding	(29%) of patients had stable disease with one partial, and one complete response	[134,135]
5-FU	Pilot	Wave nebulizer, iv solution	Lung cancer [222], lung metastasis [223]	5–15 times more concentrated in tumor compared to lung tissues	None	None	Complete response [142], Partial response [219], progressive disease [219]	[172]
9-nitro-camptothecin	I	Jet nebulizer, liposome dispersion	Lung cancer and lung metastases [70]	4–10 time more concentrated in the bronchoalveolar lavage compared to serum	Grade 2: cough, bronchial irritation Grade 3: Chemical pharyngitis	Grade 2: nausea, vomiting, anaemia, neutropenia	Partial response [155], stable disease [155]	[142]
Cisplatin	I	Jet nebulizer, liposome dispersion	Advanced NSCLC [61], SCLC [172]	10–15% (radiolabelled solution)	Grade 3: Bronchitis, dyspnea, decreased lung function	Grade 3: Fatigue Grade 4: thrombosis	Stable disease [225], progressive disease [219]	[155]
	Ib/IIa		Osteosarcoma with lung metastases [64]	N/A	Grade 2: Hoarseness	Grade 3: Nausea, vomiting	Partial response [172], stable disease [178], progressive disease [145]	[219]
Doxorubicin	I	Jet nebulizer, solution	Lung metastases: [221] sarcoma [64], Osteosarcoma [219], NSCLC [61], colorectal [221], thyroid [155], Miscellaneous [221]	Correct deposition in the lung (radiolabelled solution)	Grade 2: Cough, wheezing, dyspnea Grade 3: Hypoxia Grade 4: Respiratory distress, dyspnea	No Grade 3/4 toxicity observed	Partial response [172], stable disease [145], progressive disease [142]	[221]
Doxorubicin (inhaled) + cisplatin (iv) and docetaxel (iv)	I/II	Jet nebulizer, solution	Advanced NSCLC [227]	N/A	Grade 3–4: Cough, decrease in pulmonary function test	Grade 3–4: Constipation, hyponatremia, neutropenia	No significant improve in survival, most patients had stable disease	[221]
Gemcitabine	I	Mesh nebulizer, iv solution	NSCLC [224]	42 ± 16% (homogenous deposition)	Grade 2–3: Cough Grade 4: bronchospasm	Grade 3: Fatigue, vomiting	Minor response [172], stable disease [219], progressive disease [219]	[178]

Table 2. *Cont.*

Drug	Phase	Device, Formulation	Patient Status (*n*)	Deposition in the Lung	Local Dose Limiting Toxicity	Severe Systemic Toxicity	Disease Response (*n*)	Reference
Carboplatin	I/II	Jet nebulizer, solution	NSCLC [145]	Deposition in lung parenchyma (radiola-belled solution)	Grade 2–3 Cough Grade 3: Dyspnea, hoarseness	Grade 3: Fatigue, alopecia, rash, anorexia, anemia, neutropenia, pharyngitis, mucositis Grade 4: anorexia, neutropenia	No significant improve in survival, most patients had progressive disease	[145]

13. Conclusions

This review provides an in-depth analysis of the different drug delivery systems for the lungs that have been developed to address non-small cell lung cancer (NSCLC). It begins by explaining the anatomy and physiology of the respiratory system, highlighting the essential roles of both the upper and lower tracts in facilitating efficient drug delivery. This article also discusses various inhalation devices ranging from pressurized petered-dose inhalers, dry powder inhalers, nebulizers, and soft mist inhalers, underscoring the range of options available and their unique advantages in delivering therapeutic agents to specific lung regions. The success of each treatment is determined by several factors such as the inhalation technique, the disease state, and the adherence to prescribed regimens. The article also explores the use of carrier-free nanodrugs, which offer a green and straightforward synthesis technique that holds promise for longer drug retention and reduced side effects. Targeting strategies for NSCLC have also advanced significantly in recent years, including active targeting techniques that leverage monoclonal antibodies or small molecule inhibitors that promise enhanced specificity. Passive targeting mechanisms, such as gold nanoparticles, have potential for tumor accumulation and imaging capabilities and also hold promise for NSCLC treatment. Collectively, these diverse innovations, when harmoniously integrated, have the potential to dramatically transform the therapeutic landscape for NSCLC, heralding a future with more effective, tailored, and patient-centric treatments.

Institutional Review Board Statement: Not applicable.

Informed Consent Statement: Not applicable.

Data Availability Statement: Not applicable.

Conflicts of Interest: The authors declare no conflict of interest.

References

1. Person, A.; Mintz, M.L. Anatomy and Physiology of the Respiratory Tract. In *Disorders of the Respiratory Tract: Common Challenges in Primary Care*; Mintz, M.L., Ed.; Humana Press: Totowa, NJ, USA, 2006; pp. 11–15.
2. Kenney, W.L.; Wilmore, J.H.; Costill, D.L. *Physiology of Sport and Exercise*; Human Kinetics: Champaign, IL, USA, 2021.
3. Rocco, D.; Della Gravara, L.; Ragone, A.; Sapio, L.; Naviglio, S.; Gridelli, C. Prognostic Factors in Advanced Non-Small Cell Lung Cancer Patients Treated with Immunotherapy. *Cancers* **2023**, *15*, 4684. [CrossRef] [PubMed]
4. Rocco, D.; Sapio, L.; Della Gravara, L.; Naviglio, S.; Gridelli, C. Treatment of Advanced Non-Small Cell Lung Cancer with RET Fusions: Reality and Hopes. *Int. J. Mol. Sci.* **2023**, *24*, 2433. [CrossRef] [PubMed]
5. Lopez-Olivo, M.A.; Minnix, J.A.; Fox, J.G.; Nishi, S.P.E.; Lowenstein, L.M.; Maki, K.G.; Leal, V.B.; Tina Shih, Y.C.; Cinciripini, P.M.; Volk, R.J. Smoking cessation and shared decision-making practices about lung cancer screening among primary care providers. *Cancer Med.* **2021**, *10*, 1357–1365. [CrossRef] [PubMed]
6. Huang, C.-Y.; Ju, D.-T.; Chang, C.-F.; Reddy, P.M.; Velmurugan, B.K. A review on the effects of current chemotherapy drugs and natural agents in treating non–small cell lung cancer. *Biomedicine* **2017**, *7*, 23. [CrossRef] [PubMed]

7. Herbst, R.S.; Morgensztern, D.; Boshoff, C. The biology and management of non-small cell lung cancer. *Nature* **2018**, *553*, 446–454. [CrossRef] [PubMed]

8. Janssen-Heijnen, M.L.; Houterman, S.; Lemmens, V.E.; Louwman, M.W.; Maas, H.A.; Coebergh, J.W. Prognostic impact of increasing age and co-morbidity in cancer patients: A population-based approach. *Crit. Rev. Oncol. Hematol.* **2005**, *55*, 231–240. [CrossRef] [PubMed]

9. Marshall, A.L.; Christiani, D.C. Genetic susceptibility to lung cancer--light at the end of the tunnel? *Carcinogenesis* **2013**, *34*, 487–502. [CrossRef]

10. Jones, R.N.; Hughes, J.M.; Weill, H. Asbestos exposure, asbestosis, and asbestos-attributable lung cancer. *Thorax* **1996**, *51* (Suppl. S2), S9–S15. [CrossRef]

11. Alberg, A.J.; Samet, J.M. Epidemiology of lung cancer. *Chest* **2003**, *123*, 21S–49S. [CrossRef]

12. Kirk, G.D.; Merlo, C.; O'Driscoll, P.; Mehta, S.H.; Galai, N.; Vlahov, D.; Samet, J.; Engels, E.A. HIV infection is associated with an increased risk for lung cancer, independent of smoking. *Clin. Infect. Dis.* **2007**, *45*, 103–110. [CrossRef]

13. Hubbard, R.; Venn, A.; Lewis, S.; Britton, J. Lung cancer and cryptogenic fibrosing alveolitis. A population-based cohort study. *Am. J. Respir. Crit. Care Med.* **2000**, *161*, 5–8. [CrossRef] [PubMed]

14. Zappa, C.; Mousa, S.A. Non-small cell lung cancer: Current treatment and future advances. *Transl. Lung Cancer Res.* **2016**, *5*, 288. [CrossRef] [PubMed]

15. Lavacchi, D.; Mazzoni, F.; Giaccone, G. Clinical evaluation of dacomitinib for the treatment of metastatic non-small cell lung cancer (NSCLC): Current perspectives. *Drug Des. Dev. Ther.* **2019**, *13*, 3187–3198. [CrossRef]

16. Robelin, P.; Hadoux, J.; Forestier, J.; Planchard, D.; Hervieu, V.; Berdelou, A.; Scoazec, J.-Y.; Valette, P.-J.; Leboulleux, S.; Ducreux, M. Characterization, prognosis, and treatment of patients with metastatic lung carcinoid tumors. *J. Thorac. Oncol.* **2019**, *14*, 993–1002. [CrossRef] [PubMed]

17. Salzillo, A.; Ragone, A.; Spina, A.; Naviglio, S.; Sapio, L. Forskolin affects proliferation, migration and Paclitaxel-mediated cytotoxicity in non-small-cell lung cancer cell lines via adenylyl cyclase/cAMP axis. *Eur. J. Cell Biol.* **2023**, *102*, 151292. [CrossRef] [PubMed]

18. An, X.; Wang, R.; Chen, E.; Yang, Y.; Fan, B.; Li, Y.; Han, B.; Li, Q.; Liu, Z.; Han, Y.; et al. A forskolin-loaded nanodelivery system prevents noise-induced hearing loss. *J. Control. Release* **2022**, *348*, 148–157. [CrossRef] [PubMed]

19. Mahmud, A.; Discher, D.E. Lung vascular targeting through inhalation delivery: Insight from filamentous viruses and other shapes. *IUBMB Life* **2011**, *63*, 607–612. [CrossRef]

20. Sung, J.C.; Pulliam, B.L.; Edwards, D.A. Nanoparticles for drug delivery to the lungs. *Trends Biotechnol.* **2007**, *25*, 563–570. [CrossRef]

21. Patton, J.S.; Byron, P.R. Inhaling medicines: Delivering drugs to the body through the lungs. *Nat. Rev. Drug Discov.* **2007**, *6*, 67–74. [CrossRef]

22. Kaialy, W.; Nokhodchi, A. Particle engineering for improved pulmonary drug delivery through dry powder inhalers. In *Pulmonary Drug Delivery: Advances and Challenges*; John Wiley & Sons, Ltd.: Hoboken, NJ, USA, 2015; pp. 171–198.

23. Liu, W.K.; Liu, Q.; Chen, D.H.; Liang, H.X.; Chen, X.K.; Chen, M.X.; Qiu, S.Y.; Yang, Z.Y.; Zhou, R. Epidemiology of acute respiratory infections in children in Guangzhou: A three-year study. *PLoS ONE* **2014**, *9*, e96674. [CrossRef]

24. Pilcer, G.; Amighi, K. Formulation strategy and use of excipients in pulmonary drug delivery. *Int. J. Pharm.* **2010**, *392*, 1–19. [CrossRef] [PubMed]

25. Zarogoulidis, P.; Darwiche, K.; Krauss, L.; Huang, H.; Zachariadis, G.A.; Katsavou, A.; Hohenforst-Schmidt, W.; Papaiwannou, A.; Vogl, T.J.; Freitag, L.; et al. Inhaled cisplatin deposition and distribution in lymph nodes in stage II lung cancer patients. *Future Oncol.* **2013**, *9*, 1307–1313. [CrossRef]

26. Jinturkar, K.A.; Anish, C.; Kumar, M.K.; Bagchi, T.; Panda, A.K.; Misra, A.R. Liposomal formulations of Etoposide and Docetaxel for p53 mediated enhanced cytotoxicity in lung cancer cell lines. *Biomaterials* **2012**, *33*, 2492–2507. [CrossRef] [PubMed]

27. Tseng, C.-L.; Su, W.-Y.; Yen, K.-C.; Yang, K.-C.; Lin, F.-H. The use of biotinylated-EGF-modified gelatin nanoparticle carrier to enhance cisplatin accumulation in cancerous lungs via inhalation. *Biomaterials* **2009**, *30*, 3476–3485. [CrossRef] [PubMed]

28. Videira, M.; Almeida, A.J.; Fabra, À. Preclinical evaluation of a pulmonary delivered paclitaxel-loaded lipid nanocarrier antitumor effect. *Nanomed. Nanotechnol. Biol. Med.* **2012**, *8*, 1208–1215. [CrossRef] [PubMed]

29. Kandala, B.; Hochhaus, G. Pharmacometrics in pulmonary diseases. In *Applied Pharmacometrics*; Springer: New York, NY, USA, 2014; pp. 349–382.

30. Zasadzinski, J.A.; Ding, J.; Warriner, H.E.; Bringezu, F.; Waring, A.J. The physics and physiology of lung surfactants. *Curr. Opin. Colloid Interface Sci.* **2001**, *6*, 506–513. [CrossRef]

31. Tanaka, Y.; Takei, T.; Aiba, T.; Masuda, K.; Kiuchi, A.; Fujiwara, T. Development of synthetic lung surfactants. *J. Lipid Res.* **1988**, *27*, 475–485. [CrossRef]

32. Hickey, A.J. Lung deposition and clearance of pharmaceutical aerosols: What can be learned from inhalation toxicology and industrial hygiene? *Aerosol Sci. Technol.* **1993**, *18*, 290–304. [CrossRef]

33. Wnek, G.; Bowlin, G. Lung Surfactants. In *Encyclopedia of Biomaterials and Biomedical Engineering*; Notter, R.H., Wang, Z., Eds.; CRC Press: Boca Raton, FL, USA, 2008; pp. 1715–1726.

34. Pardeshi, C.V.; Kulkarni, A.D.; Sonawane, R.O.; Belgamwar, V.S.; Chaudhari, P.J.; Surana, S.J. Mucoadhesive nanoparticles: A roadmap to encounter the challenge of rapid nasal mucociliary clearance. *Indian J. Pharm. Educ. Res.* **2019**, *53*, S17–S27. [CrossRef]

35. Sakagami, M.; Sakon, K.; Kinoshita, W.; Makino, Y. Enhanced pulmonary absorption following aerosol administration of mucoadhesive powder microspheres. *J. Control. Release* **2001**, *77*, 117–129. [CrossRef]

36. Henning, A.; Schneider, M.; Nafee, N.; Muijs, L.; Rytting, E.; Wang, X.; Kissel, T.; Grafahrend, D.; Klee, D.; Lehr, C.-M. Influence of particle size and material properties on mucociliary clearance from the airways. *J. Aerosol Med. Pulm. Drug Deliv.* **2010**, *23*, 233–241. [CrossRef] [PubMed]

37. Ugwoke, M.I.; Verbeke, N.; Kinget, R. The biopharmaceutical aspects of nasal mucoadhesive drug delivery. *J. Pharm. Pharmacol.* **2001**, *53*, 3–22. [CrossRef] [PubMed]

38. Prasher, P.; Sharma, M.; Singh, S.K.; Gulati, M.; Jha, N.K.; Gupta, P.K.; Gupta, G.; Chellappan, D.K.; Zacconi, F.; Pinto, T.d.J.A. Targeting mucus barrier in respiratory diseases by chemically modified advanced delivery systems. *Chem. Biol. Interact.* **2022**, *365*, 110048. [CrossRef] [PubMed]

39. Gatti, T.H.H.; Eloy, J.O.; Ferreira, L.M.B.; Silva, I.C.D.; Pavan, F.R.; Gremião, M.P.D.; Chorilli, M. Insulin-loaded polymeric mucoadhesive nanoparticles: Development, characterization and cytotoxicity evaluation. *Braz. J. Pharm. Sci.* **2018**, *54*. [CrossRef]

40. Zaki, N.M.; Awad, G.A.; Mortada, N.D.; Abd ElHady, S.S. Enhanced bioavailability of metoclopramide HCl by intranasal administration of a mucoadhesive in situ gel with modulated rheological and mucociliary transport properties. *Eur. J. Pharm. Sci.* **2007**, *32*, 296–307. [CrossRef] [PubMed]

41. Puri, V.; Kaur, V.P.; Singh, A.; Singh, C. Recent advances on drug delivery applications of mucopenetrative/mucoadhesive particles: A review. *J. Drug Deliv. Sci. Technol.* **2022**, *75*, 103712. [CrossRef]

42. Marttin, E.; Schipper, N.G.; Verhoef, J.C.; Merkus, F.W. Nasal mucociliary clearance as a factor in nasal drug delivery. *Adv. Drug Deliv. Rev.* **1998**, *29*, 13–38. [CrossRef] [PubMed]

43. Bhise, S.B.; Yadav, A.V.; Avachat, A.M.; Malayandi, R. Bioavailability of intranasal drug delivery system. *Asian J. Pharm. (AJP)* **2008**, *2*, 201. [CrossRef]

44. Carvalho, F.C.; Barbi, M.S.; Sarmento, V.H.V.; Chiavacci, L.A.; Netto, F.M.; Gremião, M.P. Surfactant systems for nasal zidovudine delivery: Structural, rheological and mucoadhesive properties. *J. Pharm. Pharmacol.* **2010**, *62*, 430–439. [CrossRef]

45. Nelson, H.S. Inhalation devices, delivery systems, and patient technique. *Ann. Allergy Asthma Immunol.* **2016**, *117*, 606–612. [CrossRef]

46. Scichilone, N.; Benfante, A.; Bocchino, M.; Braido, F.; Paggiaro, P.; Papi, A.; Santus, P.; Sanduzzi, A. Which factors affect the choice of the inhaler in chronic obstructive respiratory diseases? *Pulm. Pharmacol. Ther.* **2015**, *31*, 63–67. [CrossRef] [PubMed]

47. Lavorini, F. The challenge of delivering therapeutic aerosols to asthma patients. *Int. Sch. Res. Not.* **2013**, *2013*, 102418. [CrossRef] [PubMed]

48. Scheuch, G.; Bennett, W.; Borgström, L.; Clark, A.; Dalby, R.; Dolovich, M.; Fleming, J.; Gehr, P.; Gonda, I.; O'Callaghan, C. Deposition, imaging, and clearance: What remains to be done? *J. Aerosol Med. Pulm. Drug Deliv.* **2010**, *23*, S-39–S-57. [CrossRef] [PubMed]

49. Carvalho, T.C.; Carvalho, S.R.; McConville, J.T. Formulations for pulmonary administration of anticancer agents to treat lung malignancies. *J. Aerosol Med. Pulm. Drug Deliv.* **2011**, *24*, 61–80. [CrossRef] [PubMed]

50. Heyder, J. Deposition of inhaled particles in the human respiratory tract and consequences for regional targeting in respiratory drug delivery. *Proc. Am. Thorac. Soc.* **2004**, *1*, 315–320. [CrossRef]

51. Gonda, I. Systemic delivery of drugs to humans via inhalation. *J. Aerosol Med.* **2006**, *19*, 47–53. [CrossRef]

52. Snell, N.J.C.; Ganderton, D. Assessing lung deposition of inhaled medications. Consensus statement from a workshop of the British Association for Lung Research, held at the Institute of Biology, London, UK on 17 April 1998. eds. *Respir. Med.* **1999**, *93*, 123–133. *Erratum in Respir. Med.* **2000**, *94*, 918–919. [CrossRef]

53. Sakagami, M. In vivo, in vitro and ex vivo models to assess pulmonary absorption and disposition of inhaled therapeutics for systemic delivery. *Adv. Drug Deliv. Rev.* **2006**, *58*, 1030–1060. [CrossRef]

54. Kabil, M.F.; Nasr, M.; Ibrahim, I.T.; Hassan, Y.A.; El-Sherbiny, I.M. New repurposed rolapitant in nanovesicular systems for lung cancer treatment: Development, in-vitro assessment and in-vivo biodistribution study. *Eur. J. Pharm. Sci.* **2022**, *171*, 106119. [CrossRef]

55. Koullapis, P.; Kassinos, S.C.; Muela, J.; Perez-Segarra, C.; Rigola, J.; Lehmkuhl, O.; Cui, Y.; Sommerfeld, M.; Elcner, J.; Jicha, M. Regional aerosol deposition in the human airways: The SimInhale benchmark case and a critical assessment of in silico methods. *Eur. J. Pharm. Sci.* **2018**, *113*, 77–94. [CrossRef]

56. Kleinstreuer, C.; Zhang, Z. Airflow and Particle Transport in the Human Respiratory System. *Annu. Rev. Fluid Mech.* **2010**, *42*, 301–334. [CrossRef]

57. Pitcairn, G.; Newman, S. Radiolabelling of dry powder formulations. In *Respiratory Drug Delivery VI*; Interpharm Press: Buffalo Grove, IL, USA, 1998; Volume 397399.

58. Newman, S.P.; Chan, H.-K. In vitro-in vivo correlations (IVIVCs) of deposition for drugs given by oral inhalation. *Adv. Drug Deliv. Rev.* **2020**, *167*, 135–147. [CrossRef] [PubMed]

59. Dolovich, M.; Nahmias, C.; Coates, G. Unleashing the PET: 3D imaging of the lung. In *Respiratory Drug Delivery VII Niological, Pharmaceutical, Clinical and Regulatory Issues Relating to Optimized Drug Delivery by Aerosol*; Serentec Press, Inc.: Raleigh, NC, USA, 2000; pp. 215–230.

60. Yeh, H.; Phalen, R.; Raabe, O. Factors influencing the deposition of inhaled particles. *Environ. Health Perspect.* **1976**, *15*, 147–156. [CrossRef] [PubMed]

61. Lin, Y.-W.; Wong, J.; Qu, L.; Chan, H.-K.; Zhou, Q.T. Powder production and particle engineering for dry powder inhaler formulations. *Curr. Pharm. Des.* **2015**, *21*, 3902–3916. [CrossRef] [PubMed]
62. Telko, M.J.; Hickey, A.J. Dry powder inhaler formulation. *Respir. Care* **2005**, *50*, 1209–1227. [PubMed]
63. Davies, C.; Muir, D. Deposition of inhaled particles in human lungs. *Nature* **1966**, *211*, 90–91. [CrossRef] [PubMed]
64. Martonen, T.B.; Katz, I.M. Deposition patterns of aerosolized drugs within human lungs: Effects of ventilatory parameters. *Pharm. Res.* **1993**, *10*, 871–878. [CrossRef]
65. Sturm, R.; Hofmann, W. A theoretical approach to the deposition and clearance of fibers with variable size in the human respiratory tract. *J. Hazard. Mater.* **2009**, *170*, 210–218. [CrossRef]
66. Yeh, H.-C.; Schum, G. Models of human lung airways and their application to inhaled particle deposition. *Bull. Math. Biol.* **1980**, *42*, 461–480. [CrossRef]
67. Stahlhofen, W.; Gebhart, J.; Heyder, J. Biological variability of regional deposition of aerosol particles in the human respiratory tract. *Am. Ind. Hyg. Assoc. J.* **1981**, *42*, 348–352. [CrossRef]
68. Heyder, J.; Gebhart, J.; Rudolf, G.; Schiller, C.F.; Stahlhofen, W. Deposition of particles in the human respiratory tract in the size range 0.005–15 μm. *J. Aerosol Sci.* **1986**, *17*, 811–825. [CrossRef]
69. Heyder, J.; Rudolf, G. Mathematical models of particle deposition in the human respiratory tract. *J. Aerosol Sci.* **1984**, *15*, 697–707. [CrossRef]
70. Chalupa, D.C.; Morrow, P.E.; Oberdörster, G.; Utell, M.J.; Frampton, M.W. Ultrafine particle deposition in subjects with asthma. *Environ. Health Perspect.* **2004**, *112*, 879–882. [CrossRef] [PubMed]
71. Jaques, P.A.; Kim, C.S. Measurement of total lung deposition of inhaled ultrafine particles in healthy men and women. *Inhal. Toxicol.* **2000**, *12*, 715–731. [PubMed]
72. Byron, P.R. Prediction of drug residence times in regions of the human respiratory tract following aerosol inhalation. *J. Pharm. Sci.* **1986**, *75*, 433–438. [CrossRef] [PubMed]
73. Sardeli, C.; Zarogoulidis, P.; Kosmidis, C.; Amaniti, A.; Katsaounis, A.; Giannakidis, D.; Koulouris, C.; Hohenforst-Schmidt, W.; Huang, H.; Bai, C. Inhaled chemotherapy adverse effects: Mechanisms and protection methods. *Lung Cancer Manag.* **2019**, *8*, LMT19. [CrossRef] [PubMed]
74. Martins, V.; Minguillón, M.C.; Moreno, T.; Querol, X.; de Miguel, E.; Capdevila, M.; Centelles, S.; Lazaridis, M. Deposition of aerosol particles from a subway microenvironment in the human respiratory tract. *J. Aerosol Sci.* **2015**, *90*, 103–113. [CrossRef]
75. Moller, W.; Haussinger, K.; Winkler-Heil, R.; Stahlhofen, W.; Meyer, T.; Hofmann, W.; Heyder, J. Mucociliary and long-term particle clearance in the airways of healthy nonsmoker subjects. *J. Appl. Physiol.* **2004**, *97*, 2200–2206. [CrossRef]
76. Kreyling, W.G.; Semmler-Behnke, M.; Möller, W. Ultrafine particle–lung interactions: Does size matter? *J. Aerosol Med.* **2006**, *19*, 74–83. [CrossRef]
77. Moller, W.; Felten, K.; Sommerer, K.; Scheuch, G.; Meyer, G.; Meyer, P.; Haussinger, K.; Kreyling, W.G. Deposition, retention, and translocation of ultrafine particles from the central airways and lung periphery. *Am. J. Respir. Crit. Care Med.* **2008**, *177*, 426–432. [CrossRef]
78. Schmid, O.; Möller, W.; Semmler-Behnke, M.; Ferron, G.A.; Karg, E.; Lipka, J.; Schulz, H.; Kreyling, W.; Stöger, T. Dosimetry and toxicology of inhaled ultrafine particles. *Biomarkers* **2009**, *14*, 67–73. [CrossRef] [PubMed]
79. Bur, M.; Henning, A.; Hein, S.; Schneider, M.; Lehr, C.-M. Inhalative nanomedicine—Opportunities and challenges. *Inhal. Toxicol.* **2009**, *21*, 137–143. [CrossRef] [PubMed]
80. Geiser, M.; Schurch, S.; Gehr, P. Influence of surface chemistry and topography of particles on their immersion into the lung's surface-lining layer. *J. Appl. Physiol.* **2003**, *94*, 1793–1801. [CrossRef] [PubMed]
81. Arredouani, M.; Yang, Z.; Ning, Y.; Qin, G.; Soininen, R.; Tryggvason, K.; Kobzik, L. The scavenger receptor MARCO is required for lung defense against pneumococcal pneumonia and inhaled particles. *J. Exp. Med.* **2004**, *200*, 267–272. [CrossRef] [PubMed]
82. Gumbleton, M. Caveolae as potential macromolecule trafficking compartments within alveolar epithelium. *Adv. Drug Deliv. Rev.* **2001**, *49*, 281–300. [CrossRef] [PubMed]
83. Palecanda, A.; Kobzik, L. Receptors for unopsonized particles: The role of alveolar macrophage scavenger receptors. *Curr. Mol. Med.* **2001**, *1*, 589–595. [CrossRef] [PubMed]
84. Madl, A.K.; Pinkerton, K.E. Health effects of inhaled engineered and incidental nanoparticles. *Crit. Rev. Toxicol.* **2009**, *39*, 629–658. [CrossRef]
85. Wang, X.; Wan, W.; Lu, J.; Quan, G.; Pan, X.; Liu, P. Effects of L-leucine on the properties of spray-dried swellable microparticles with wrinkled surfaces for inhalation therapy of pulmonary fibrosis. *Int. J. Pharm.* **2021**, *610*, 121223. [CrossRef]
86. Hassan, M.S.; Lau, R.W.M. Effect of particle shape on dry particle inhalation: Study of flowability, aerosolization, and deposition properties. *Aaps Pharmscitech* **2009**, *10*, 1252–1262. [CrossRef]
87. Shi, J.; Li, J.; Xu, Z.; Chen, L.; Luo, R.; Zhang, C.; Gao, F.; Zhang, J.; Fu, C. Celastrol: A review of useful strategies overcoming its limitation in anticancer application. *Front. Pharmacol.* **2020**, *11*, 558741. [CrossRef]
88. Zhou, Q.; Dong, C.; Fan, W.; Jiang, H.; Xiang, J.; Qiu, N.; Piao, Y.; Xie, T.; Luo, Y.; Li, Z. Tumor extravasation and infiltration as barriers of nanomedicine for high efficacy: The current status and transcytosis strategy. *Biomaterials* **2020**, *240*, 119902. [CrossRef]
89. Zhou, J.; Kroll, A.V.; Holay, M.; Fang, R.H.; Zhang, L. Biomimetic nanotechnology toward personalized vaccines. *Adv. Mater.* **2020**, *32*, 1901255. [CrossRef] [PubMed]

90. Yu, D.; Peng, P.; Dharap, S.S.; Wang, Y.; Mehlig, M.; Chandna, P.; Zhao, H.; Filpula, D.; Yang, K.; Borowski, V. Antitumor activity of poly (ethylene glycol)–camptothecin conjugate: The inhibition of tumor growth in vivo. *J. Control. Release* **2005**, *110*, 90–102. [CrossRef]

91. Mei, H.; Cai, S.; Huang, D.; Gao, H.; Cao, J.; He, B. Carrier-free nanodrugs with efficient drug delivery and release for cancer therapy: From intrinsic physicochemical properties to external modification. *Bioact. Mater.* **2022**, *8*, 220–240. [CrossRef] [PubMed]

92. Fan, L.; Zhang, B.; Xu, A.; Shen, Z.; Guo, Y.; Zhao, R.; Yao, H.; Shao, J.-W. Carrier-free, pure nanodrug formed by the self-assembly of an anticancer drug for cancer immune therapy. *Mol. Pharm.* **2018**, *15*, 2466–2478. [CrossRef] [PubMed]

93. Qin, S.-Y.; Zhang, A.-Q.; Cheng, S.-X.; Rong, L.; Zhang, X.-Z. Drug self-delivery systems for cancer therapy. *Biomaterials* **2017**, *112*, 234–247. [CrossRef] [PubMed]

94. Karaosmanoglu, S.; Zhou, M.; Shi, B.; Zhang, X.; Williams, G.R.; Chen, X. Carrier-free nanodrugs for safe and effective cancer treatment. *J. Control. Release* **2021**, *329*, 805–832. [CrossRef]

95. Zhang, R.; Xing, R.; Jiao, T.; Ma, K.; Chen, C.; Ma, G.; Yan, X. Carrier-free, chemophotodynamic dual nanodrugs via self-assembly for synergistic antitumor therapy. *ACS Appl. Mater. Interfaces* **2016**, *8*, 13262–13269. [CrossRef] [PubMed]

96. Zhou, M.; Zhang, X.; Yang, Y.; Liu, Z.; Tian, B.; Jie, J.; Zhang, X. Carrier-free functionalized multidrug nanorods for synergistic cancer therapy. *Biomaterials* **2013**, *34*, 8960–8967. [CrossRef]

97. Shim, M.K.; Park, J.; Yoon, H.Y.; Lee, S.; Um, W.; Kim, J.-H.; Kang, S.-W.; Seo, J.-W.; Hyun, S.-W.; Park, J.H. Carrier-free nanoparticles of cathepsin B-cleavable peptide-conjugated doxorubicin prodrug for cancer targeting therapy. *J. Control. Release* **2019**, *294*, 376–389. [CrossRef]

98. Cho, K.; Wang, X.; Nie, S.; Chen, Z.; Shin, D.M. Therapeutic nanoparticles for drug delivery in cancer. *Clin. Cancer Res.* **2008**, *14*, 1310–1316. [CrossRef] [PubMed]

99. Yang, M.-Y.; Zhao, R.-R.; Fang, Y.-F.; Jiang, J.-L.; Yuan, X.-T.; Shao, J.-W. Carrier-free nanodrug: A novel strategy of cancer diagnosis and synergistic therapy. *Int. J. Pharm.* **2019**, *570*, 118663. [CrossRef] [PubMed]

100. Ferrari, M. Cancer nanotechnology: Opportunities and challenges. *Nat. Rev. Cancer* **2005**, *5*, 161–171. [CrossRef] [PubMed]

101. Ramalho, M.J.; Andrade, S.; Loureiro, J.A.; do Carmo Pereira, M. Nanotechnology to improve the Alzheimer's disease therapy with natural compounds. *Drug Deliv. Transl. Res.* **2020**, *10*, 380–402. [CrossRef] [PubMed]

102. Zhang, J.; Li, S.; An, F.-F.; Liu, J.; Jin, S.; Zhang, J.-C.; Wang, P.C.; Zhang, X.; Lee, C.-S.; Liang, X.-J. Self-carried curcumin nanoparticles for in vitro and in vivo cancer therapy with real-time monitoring of drug release. *Nanoscale* **2015**, *7*, 13503–13510. [CrossRef] [PubMed]

103. Liu, Y.; Zhang, X.; Zhou, M.; Nan, X.; Chen, X.; Zhang, X. Mitochondrial-targeting lonidamine-doxorubicin nanoparticles for synergistic chemotherapy to conquer drug resistance. *ACS Appl. Mater. Interfaces* **2017**, *9*, 43498–43507. [CrossRef]

104. Muralidharan, P.; Mallory, E.K.; Malapit, M.; Phan, H.; Ledford, J.G.; Hayes, D.; Mansour, H.M. Advanced design and development of nanoparticle/microparticle dual-drug combination lactose carrier-free dry powder inhalation aerosols. *RSC Adv.* **2020**, *10*, 41846–41856. [CrossRef]

105. Zhang, J.; Liang, Y.-C.; Lin, X.; Zhu, X.; Yan, L.; Li, S.; Yang, X.; Zhu, G.; Rogach, A.L.; Yu, P.K. Self-monitoring and self-delivery of photosensitizer-doped nanoparticles for highly effective combination cancer therapy in vitro and in vivo. *ACS Nano* **2015**, *9*, 9741–9756. [CrossRef]

106. Wei, W.; Zhang, X.; Chen, X.; Zhou, M.; Xu, R.; Zhang, X. Smart surface coating of drug nanoparticles with cross-linkable polyethylene glycol for bio-responsive and highly efficient drug delivery. *Nanoscale* **2016**, *8*, 8118–8125. [CrossRef]

107. Ramalingam, S.S.; Yang, J.C.; Lee, C.K.; Kurata, T.; Kim, D.W.; John, T.; Nogami, N.; Ohe, Y.; Mann, H.; Rukazenkov, Y.; et al. Osimertinib As First-Line Treatment of EGFR Mutation-Positive Advanced Non-Small-Cell Lung Cancer. *J. Clin. Oncol.* **2018**, *36*, 841–849. [CrossRef]

108. Hirsch, F.R.; Scagliotti, G.V.; Mulshine, J.L.; Kwon, R.; Curran, W.J., Jr.; Wu, Y.L.; Paz-Ares, L. Lung cancer: Current therapies and new targeted treatments. *Lancet* **2017**, *389*, 299–311. [CrossRef] [PubMed]

109. Reck, M.; Rodríguez-Abreu, D.; Robinson, A.G.; Hui, R.; Csőszi, T.; Fülöp, A.; Gottfried, M.; Peled, N.; Tafreshi, A.; Cuffe, S.; et al. Pembrolizumab versus Chemotherapy for PD-L1-Positive Non-Small-Cell Lung Cancer. *N. Engl. J. Med.* **2016**, *375*, 1823–1833. [CrossRef]

110. Wu, Y.-L.; Cheng, Y.; Zhou, X.; Lee, K.H.; Nakagawa, K.; Niho, S.; Tsuji, F.; Linke, R.; Rosell, R.; Corral, J.; et al. Dacomitinib versus gefitinib as first-line treatment for patients with EGFR-mutation-positive non-small-cell lung cancer (ARCHER 1050): A randomised, open-label, phase 3 trial. *Lancet Oncol.* **2017**, *18*, 1454–1466. [CrossRef] [PubMed]

111. Rudin, C.M.; Pietanza, M.C.; Bauer, T.M.; Ready, N.; Morgensztern, D.; Glisson, B.S.; Byers, L.A.; Johnson, M.L.; Burris, H.A., 3rd; Robert, F.; et al. Rovalpituzumab tesirine, a DLL3-targeted antibody-drug conjugate, in recurrent small-cell lung cancer: A first-in-human, first-in-class, open-label, phase 1 study. *Lancet Oncol.* **2017**, *18*, 42–51. [CrossRef] [PubMed]

112. Al-Obaidi, H.; Granger, A.; Hibbard, T.; Opesanwo, S. Pulmonary Drug Delivery of Antimicrobials and Anticancer Drugs Using Solid Dispersions. *Pharmaceutics* **2021**, *13*, 1056. [CrossRef] [PubMed]

113. Choi, S.H.; Byeon, H.J.; Choi, J.S.; Thao, L.; Kim, I.; Lee, E.S.; Shin, B.S.; Lee, K.C.; Youn, Y.S. Inhalable self-assembled albumin nanoparticles for treating drug-resistant lung cancer. *J. Control. Release* **2015**, *197*, 199–207. [CrossRef] [PubMed]

114. Taratula, O.; Garbuzenko, O.B.; Chen, A.M.; Minko, T. Innovative strategy for treatment of lung cancer: Targeted nanotechnology-based inhalation co-delivery of anticancer drugs and siRNA. *J. Drug Target.* **2011**, *19*, 900–914. [CrossRef]

115. Taratula, O.; Kuzmov, A.; Shah, M.; Garbuzenko, O.B.; Minko, T. Nanostructured lipid carriers as multifunctional nanomedicine platform for pulmonary co-delivery of anticancer drugs and siRNA. *J. Control. Release* **2013**, *171*, 349–357. [CrossRef]

116. Zhu, X.; Kong, Y.; Liu, Q.; Lu, Y.; Xing, H.; Lu, X.; Yang, Y.; Xu, J.; Li, N.; Zhao, D.; et al. Inhalable dry powder prepared from folic acid-conjugated docetaxel liposomes alters pharmacodynamic and pharmacokinetic properties relevant to lung cancer chemotherapy. *Pulm. Pharmacol. Ther.* **2019**, *55*, 50–61. [CrossRef]

117. Zhang, T.; Chen, Y.; Ge, Y.; Hu, Y.; Li, M.; Jin, Y. Inhalation treatment of primary lung cancer using liposomal curcumin dry powder inhalers. *Acta Pharm. Sin. B* **2018**, *8*, 440–448. [CrossRef]

118. Lin, C.; Wong, B.C.K.; Chen, H.; Bian, Z.; Zhang, G.; Zhang, X.; Kashif Riaz, M.; Tyagi, D.; Lin, G.; Zhang, Y.; et al. Pulmonary delivery of triptolide-loaded liposomes decorated with anti-carbonic anhydrase IX antibody for lung cancer therapy. *Sci. Rep.* **2017**, *7*, 1097. [CrossRef]

119. Rosière, R.; Van Woensel, M.; Gelbcke, M.; Mathieu, V.; Hecq, J.; Mathivet, T.; Vermeersch, M.; Van Antwerpen, P.; Amighi, K.; Wauthoz, N. New Folate-Grafted Chitosan Derivative To Improve Delivery of Paclitaxel-Loaded Solid Lipid Nanoparticles for Lung Tumor Therapy by Inhalation. *Mol. Pharm.* **2018**, *15*, 899–910. [CrossRef] [PubMed]

120. Bakhtiary, Z.; Barar, J.; Aghanejad, A.; Saei, A.A.; Nemati, E.; Ezzati Nazhad Dolatabadi, J.; Omidi, Y. Microparticles containing erlotinib-loaded solid lipid nanoparticles for treatment of non-small cell lung cancer. *Drug Dev. Ind. Pharm.* **2017**, *43*, 1244–1253. [CrossRef] [PubMed]

121. Nassimi, M.; Schleh, C.; Lauenstein, H.D.; Hussein, R.; Hoymann, H.-G.; Koch, W.; Pohlmann, G.; Krug, N.; Sewald, K.; Rittinghausen, S. A toxicological evaluation of inhaled solid lipid nanoparticles used as a potential drug delivery system for the lung. *Eur. J. Pharm. Biopharm.* **2010**, *75*, 107–116. [CrossRef] [PubMed]

122. Rosière, R.; Amighi, K.; Wauthoz, N.; Dalby, R.; Byron, P.R.; Peart, J. New dry powders for inhalation containing chitosan derivative-coated solid lipid nanoparticles for targeted delivery to lung cancer cells. *RDD Eur.* **2015**, *2015*, 447–452.

123. Hu, L.; Jia, Y. Preparation and characterization of solid lipid nanoparticles loaded with epirubicin for pulmonary delivery. *Die Pharmazie Int. J. Pharm. Sci.* **2010**, *65*, 585–587.

124. Ji, P.; Yu, T.; Liu, Y.; Jiang, J.; Xu, J.; Zhao, Y.; Hao, Y.; Qiu, Y.; Zhao, W.; Wu, C. Naringenin-loaded solid lipid nanoparticles: Preparation, controlled delivery, cellular uptake, and pulmonary pharmacokinetics. *Drug Des. Dev. Ther.* **2016**, *10*, 911–925. [CrossRef]

125. Chishti, N.; Jagwani, S.; Dhamecha, D.; Jalalpure, S.; Dehghan, M.H. Preparation, optimization, and in vivo evaluation of nanoparticle-based formulation for pulmonary delivery of anticancer drug. *Medicina* **2019**, *55*, 294. [CrossRef]

126. Kaur, P.; Mishra, V.; Shunmugaperumal, T.; Goyal, A.K.; Ghosh, G.; Rath, G. Inhalable spray dried lipidnanoparticles for the co-delivery of paclitaxel and doxorubicin in lung cancer. *J. Drug Deliv. Sci. Technol.* **2020**, *56*, 101502. [CrossRef]

127. Kamel, N.M.; Helmy, M.W.; Abdelfattah, E.Z.; Khattab, S.N.; Ragab, D.; Samaha, M.W.; Fang, J.Y.; Elzoghby, A.O. Inhalable Dual-Targeted Hybrid Lipid Nanocore-Protein Shell Composites for Combined Delivery of Genistein and All-Trans Retinoic Acid to Lung Cancer Cells. *ACS Biomater. Sci. Eng.* **2020**, *6*, 71–87. [CrossRef]

128. Raval, M.; Patel, P.; Airao, V.; Bhatt, V.; Sheth, N. Novel Silibinin Loaded Chitosan-Coated PLGA/PCL Nanoparticles Based Inhalation Formulations with Improved Cytotoxicity and Bioavailability for Lung Cancer. *BioNanoScience* **2021**, *11*, 67–83. [CrossRef]

129. Vanza, J.D.; Lalani, J.R.; Patel, R.B.; Patel, M.R. DOE supported optimization of biodegradable polymeric nanoparticles based dry powder inhaler for targeted delivery of afatinib in non-small cell lung cancer. *J. Drug Deliv. Sci. Technol.* **2023**, *84*, 104554. [CrossRef]

130. Madamsetty, V.S.; Mukherjee, A.; Paul Manash, K. Chapter 9—Bioinspired nanoparticles-based drug delivery systems for cancer theranostics. In *Biogenic Nanoparticles for Cancer Theranostics*; Patra, C., Ahmad, I., Ayaz, M., Khalil, A.T., Mukherjee, S., Ovais, M., Eds.; Elsevier: Amsterdam, The Netherlands, 2021; pp. 189–228.

131. Guinart, A.; Perry, H.L.; Wilton-Ely, J.; Tetley, T.D. Gold nanomaterials in the management of lung cancer. *Emerg. Top. Life Sci.* **2020**, *4*, 627–643. [CrossRef] [PubMed]

132. Xu, C.; Wang, P.; Zhang, J.; Tian, H.; Park, K.; Chen, X. Pulmonary codelivery of doxorubicin and siRNA by pH-sensitive nanoparticles for therapy of metastatic lung cancer. *Small* **2015**, *11*, 4321–4333. [CrossRef] [PubMed]

133. Rao, K.K.; Zhong, Q.; Bielski, E.R.; da Rocha, S.R. Nanoparticles of pH-responsive, PEG–doxorubicin conjugates: Interaction with an in vitro model of lung adenocarcinoma and their direct formulation in propellant-based portable inhalers. *Mol. Pharm.* **2017**, *14*, 3866–3878. [CrossRef] [PubMed]

134. Cheng, H.; Zou, Y.; Shah, C.D.; Fan, N.; Bhagat, T.D.; Gucalp, R.; Kim, M.; Verma, A.; Piperdi, B.; Spivack, S.D. First-in-human study of inhaled Azacitidine in patients with advanced non-small cell lung cancer. *Lung Cancer* **2021**, *154*, 99–104. [CrossRef] [PubMed]

135. Kuehl, P.J.; Tellez, C.S.; Grimes, M.J.; March, T.H.; Tessema, M.; Revelli, D.A.; Mallis, L.M.; Dye, W.W.; Sniegowski, T.; Badenoch, A. 5-Azacytidine inhaled dry powder formulation profoundly improves pharmacokinetics and efficacy for lung cancer therapy through genome reprogramming. *Br. J. Cancer* **2020**, *122*, 1194–1204. [CrossRef] [PubMed]

136. Shepard, K.B.; Vodak, D.T.; Kuehl, P.J.; Revelli, D.; Zhou, Y.; Pluntze, A.M.; Adam, M.S.; Oddo, J.C.; Switala, L.; Cape, J.L. Local treatment of non-small cell lung cancer with a spray-dried bevacizumab formulation. *AAPS PharmSciTech* **2021**, *22*, 230. [CrossRef]

137. Guo, X.; Zhang, X.; Ye, L.; Zhang, Y.; Ding, R.; Hao, Y.; Zhao, Y.; Zhang, Z.; Zhang, Y. Inhalable microspheres embedding chitosan-coated PLGA nanoparticles for 2-methoxyestradiol. *J. Drug Target.* **2014**, *22*, 421–427. [CrossRef]

138. Hitzman, C.J.; Elmquist, W.F.; Wattenberg, L.W.; Wiedmann, T.S. Development of a Respirable, Sustained Release Microcarrier for 5-Fluorouracil I: In Vitro Assessment of Liposomes, Microspheres, and Lipid Coated Nanoparticles. *J. Pharm. Sci.* **2006**, *95*, 1114–1126. [CrossRef]

139. Hitzman, C.J.; Wattenberg, L.W.; Wiedmann, T.S. Pharmacokinetics of 5-fluorouracil in the hamster following inhalation delivery of lipid-coated nanoparticles. *J. Pharm. Sci.* **2006**, *95*, 1196–1211. [CrossRef] [PubMed]

140. Knight, V.; Kleinerman, E.S.; Waldrep, J.C.; Giovanella, B.C.; Gilbert, B.E.; Koshkina, N.V. 9-Nitrocamptothecin liposome aerosol treatment of human cancer subcutaneous xenografts and pulmonary cancer metastases in mice. *Ann. N. Y. Acad. Sci.* **2000**, *922*, 151–163. [CrossRef] [PubMed]

141. Koshkina, N.V.; Kleinerman, E.S.; Waldrep, C.; Jia, S.-F.; Worth, L.L.; Gilbert, B.E.; Knight, V. 9-Nitrocamptothecin liposome aerosol treatment of melanoma and osteosarcoma lung metastases in mice. *Clin. Cancer Res.* **2000**, *6*, 2876–2880. [PubMed]

142. Verschraegen, C.F.; Gilbert, B.E.; Loyer, E.; Huaringa, A.; Walsh, G.; Newman, R.A.; Knight, V. Clinical evaluation of the delivery and safety of aerosolized liposomal 9-nitro-20(s)-camptothecin in patients with advanced pulmonary malignancies. *Clin. Cancer Res.* **2004**, *10*, 2319–2326. [CrossRef] [PubMed]

143. Yang, Y.; Huang, Z.; Li, J.; Mo, Z.; Huang, Y.; Ma, C.; Wang, W.; Pan, X.; Wu, C. PLGA Porous Microspheres Dry Powders for Codelivery of Afatinib-Loaded Solid Lipid Nanoparticles and Paclitaxel: Novel Therapy for EGFR Tyrosine Kinase Inhibitors Resistant Nonsmall Cell Lung Cancer. *Adv. Healthc. Mater.* **2019**, *8*, e1900965. [CrossRef]

144. Koshkina, N.V.; Knight, V.; Gilbert, B.E.; Golunski, E.; Roberts, L.; Waldrep, J.C. Improved respiratory delivery of the anticancer drugs, camptothecin and paclitaxel, with 5% CO2-enriched air: Pharmacokinetic studies. *Cancer Chemother. Pharmacol.* **2001**, *47*, 451–456. [CrossRef]

145. Zarogoulidis, P.; Eleftheriadou, E.; Sapardanis, I.; Zarogoulidou, V.; Lithoxopoulou, H.; Kontakiotis, T.; Karamanos, N.; Zachariadis, G.; Mabroudi, M.; Zisimopoulos, A.; et al. Feasibility and effectiveness of inhaled carboplatin in NSCLC patients. *Investig. New Drugs* **2012**, *30*, 1628–1640. [CrossRef]

146. Anabousi, S.; Bakowsky, U.; Schneider, M.; Huwer, H.; Lehr, C.-M.; Ehrhardt, C. In vitro assessment of transferrin-conjugated liposomes as drug delivery systems for inhalation therapy of lung cancer. *Eur. J. Pharm. Sci.* **2006**, *29*, 367–374. [CrossRef]

147. Kim, I.; Byeon, H.J.; Kim, T.H.; Lee, E.S.; Oh, K.T.; Shin, B.S.; Lee, K.C.; Youn, Y.S. Doxorubicin-loaded highly porous large PLGA microparticles as a sustained-release inhalation system for the treatment of metastatic lung cancer. *Biomaterials* **2012**, *33*, 5574–5583. [CrossRef]

148. Long, J.-T.; Cheang, T.-y.; Zhuo, S.-Y.; Zeng, R.-F.; Dai, Q.-S.; Li, H.-P.; Fang, S. Anticancer drug-loaded multifunctional nanoparticles to enhance the chemotherapeutic efficacy in lung cancer metastasis. *J. Nanobiotechnol.* **2014**, *12*, 1–11. [CrossRef]

149. Tagami, T.; Ando, Y.; Ozeki, T. Fabrication of liposomal doxorubicin exhibiting ultrasensitivity against phospholipase A2 for efficient pulmonary drug delivery to lung cancers. *Int. J. Pharm.* **2017**, *517*, 35–41. [CrossRef] [PubMed]

150. Zhong, Q.; da Rocha, S.R. Poly (amidoamine) dendrimer–doxorubicin conjugates: In vitro characteristics and pseudosolution formulation in pressurized metered-dose inhalers. *Mol. Pharm.* **2016**, *13*, 1058–1072. [CrossRef] [PubMed]

151. Garbuzenko, O.B.; Mainelis, G.; Taratula, O.; Minko, T. Inhalation treatment of lung cancer: The influence of composition, size and shape of nanocarriers on their lung accumulation and retention. *Cancer Biol. Med.* **2014**, *11*, 44.

152. Patel, A.R.; Chougule, M.B.; Townley, I.; Patlolla, R.; Wang, G.; Singh, M. Efficacy of aerosolized celecoxib encapsulated nanostructured lipid carrier in non-small cell lung cancer in combination with docetaxel. *Pharm. Res.* **2013**, *30*, 1435–1446. [CrossRef] [PubMed]

153. Fulzele, S.V.; Shaik, M.S.; Chatterjee, A.; Singh, M. Anti-cancer effect of celecoxib and aerosolized docetaxel against human non-small cell lung cancer cell line, A549. *J. Pharm. Pharmacol.* **2006**, *58*, 327–336. [CrossRef]

154. Fulzele, S.V.; Chatterjee, A.; Shaik, M.S.; Jackson, T.; Singh, M. Inhalation delivery and anti-tumor activity of celecoxib in human orthotopic non-small cell lung cancer xenograft model. *Pharm. Res.* **2006**, *23*, 2094–2106. [CrossRef]

155. Wittgen, B.P.; Kunst, P.W.; Van Der Born, K.; Van Wijk, A.W.; Perkins, W.; Pilkiewicz, F.G.; Perez-Soler, R.; Nicholson, S.; Peters, G.J.; Postmus, P.E. Phase I study of aerosolized SLIT cisplatin in the treatment of patients with carcinoma of the lung. *Clin. Cancer Res.* **2007**, *13*, 2414–2421. [CrossRef]

156. Xie, Y.; Aillon, K.L.; Cai, S.; Christian, J.M.; Davies, N.M.; Berkland, C.J.; Forrest, M.L. Pulmonary delivery of cisplatin–hyaluronan conjugates via endotracheal instillation for the treatment of lung cancer. *Int. J. Pharm.* **2010**, *392*, 156–163. [CrossRef]

157. Loira-Pastoriza, C.; Vanvarenberg, K.; Ucakar, B.; Machado Franco, M.; Staub, A.; Lemaire, M.; Renauld, J.-C.; Vanbever, R. Encapsulation of a CpG oligonucleotide in cationic liposomes enhances its local antitumor activity following pulmonary delivery in a murine model of metastatic lung cancer. *Int. J. Pharm.* **2021**, *600*, 120504. [CrossRef]

158. Taki, M.; Tagami, T.; Fukushige, K.; Ozeki, T. Fabrication of nanocomposite particles using a two-solution mixing-type spray nozzle for use in an inhaled curcumin formulation. *Int. J. Pharm.* **2016**, *511*, 104–110. [CrossRef]

159. Adel, I.M.; ElMeligy, M.F.; Abdelrahim, M.E.A.; Maged, A.; Abdelkhalek, A.A.; Abdelmoteleb, A.M.M.; Elkasabgy, N.A. Design and Characterization of Spray-Dried Proliposomes for the Pulmonary Delivery of Curcumin. *Int. J. Nanomed.* **2021**, *16*, 2667–2687. [CrossRef] [PubMed]

160. Al Ayoub, Y.; Gopalan, R.C.; Najafzadeh, M.; Mohammad, M.A.; Anderson, D.; Paradkar, A.; Assi, K.H. Development and evaluation of nanoemulsion and microsuspension formulations of curcuminoids for lung delivery with a novel approach to understanding the aerosol performance of nanoparticles. *Int. J. Pharm.* **2019**, *557*, 254–263. [CrossRef] [PubMed]

161. Shaik, M.S.; Haynes, A.; McSween, J.; Ikediobi, O.; Kanikkannan, N.; Singh, M. Inhalation delivery of anticancer agents via HFA-based metered dose inhaler using methotrexate as a model drug. *J. Aerosol Med.* **2002**, *15*, 261–270. [CrossRef] [PubMed]

162. Asmawi, A.A.; Salim, N.; Ngan, C.L.; Ahmad, H.; Abdulmalek, E.; Masarudin, M.J.; Abdul Rahman, M.B. Excipient selection and aerodynamic characterization of nebulized lipid-based nanoemulsion loaded with docetaxel for lung cancer treatment. *Drug Deliv. Transl. Res.* **2019**, *9*, 543–554. [CrossRef] [PubMed]

163. Asmawi, A.A.; Salim, N.; Abdulmalek, E.; Abdul Rahman, M.B. Modeling the Effect of Composition on Formation of Aerosolized Nanoemulsion System Encapsulating Docetaxel and Curcumin Using D-Optimal Mixture Experimental Design. *Int. J. Mol. Sci.* **2020**, *21*, 4357. [CrossRef]

164. Azarmi, S.; Tao, X.; Chen, H.; Wang, Z.; Finlay, W.H.; Löbenberg, R.; Roa, W.H. Formulation and cytotoxicity of doxorubicin nanoparticles carried by dry powder aerosol particles. *Int. J. Pharm.* **2006**, *319*, 155–161. [CrossRef]

165. Al-Hallak, M.K.; Sarfraz, M.K.; Azarmi, S.; Roa, W.H.; Finlay, W.H.; Rouleau, C.; Löbenberg, R. Distribution of effervescent inhalable nanoparticles after pulmonary delivery: An in vivo study. *Ther. Deliv.* **2012**, *3*, 725–734. [CrossRef]

166. Hershey, A.E.; Kurzman, I.D.; Forrest, L.J.; Bohling, C.A.; Stonerook, M.; Placke, M.E.; Imondi, A.R.; Vail, D.M. Inhalation chemotherapy for macroscopic primary or metastatic lung tumors: Proof of principle using dogs with spontaneously occurring tumors as a model. *Clin. Cancer Res.* **1999**, *5*, 2653–2659.

167. Alipour, S.; Montaseri, H.; Tafaghodi, M. Inhalable, large porous PLGA microparticles loaded with paclitaxel: Preparation, in vitro and in vivo characterization. *J. Microencapsul.* **2015**, *32*, 661–668. [CrossRef]

168. Koshkina, N.V.; Waldrep, J.C.; Roberts, L.E.; Golunski, E.; Melton, S.; Knight, V. Paclitaxel liposome aerosol treatment induces inhibition of pulmonary metastases in murine renal carcinoma model. *Clin. Cancer Res.* **2001**, *7*, 3258–3262.

169. Gill, K.K.; Nazzal, S.; Kaddoumi, A. Paclitaxel loaded PEG5000–DSPE micelles as pulmonary delivery platform: Formulation characterization, tissue distribution, plasma pharmacokinetics, and toxicological evaluation. *Eur. J. Pharm. Biopharm.* **2011**, *79*, 276–284. [CrossRef] [PubMed]

170. Meenach, S.A.; Anderson, K.W.; Hilt, J.Z.; McGarry, R.C.; Mansour, H.M. Characterization and aerosol dispersion performance of advanced spray-dried chemotherapeutic PEGylated phospholipid particles for dry powder inhalation delivery in lung cancer. *Eur. J. Pharm. Sci.* **2013**, *49*, 699–711. [CrossRef] [PubMed]

171. Tagami, T.; Kubota, M.; Ozeki, T. Effective Remote Loading of Doxorubicin into DPPC/Poloxamer 188 Hybrid Liposome to Retain Thermosensitive Property and the Assessment of Carrier-Based Acute Cytotoxicity for Pulmonary Administration. *J. Pharm. Sci.* **2015**, *104*, 3824–3832. [CrossRef] [PubMed]

172. Tatsumura, T.; Koyama, S.; Tsujimoto, M.; Kitagawa, M.; Kagamimori, S. Further study of nebulisation chemotherapy, a new chemotherapeutic method in the treatment of lung carcinomas: Fundamental and clinical. *Br. J. Cancer* **1993**, *68*, 1146–1149. [CrossRef]

173. Mainelis, G.; Seshadri, S.; Garbuzenko, O.B.; Han, T.; Wang, Z.; Minko, T. Characterization and application of a nose-only exposure chamber for inhalation delivery of liposomal drugs and nucleic acids to mice. *J. Aerosol. Med. Pulm. Drug Deliv.* **2013**, *26*, 345–354. [CrossRef] [PubMed]

174. Zhang, T.; Wang, R.; Li, M.; Bao, J.; Chen, Y.; Ge, Y.; Jin, Y. Comparative study of intratracheal and oral gefitinib for the treatment of primary lung cancer. *Eur. J. Pharm. Sci.* **2020**, *149*, 105352. [CrossRef] [PubMed]

175. Mohamad Saimi, N.I.; Salim, N.; Ahmad, N.; Abdulmalek, E.; Abdul Rahman, M.B. Aerosolized Niosome Formulation Containing Gemcitabine and Cisplatin for Lung Cancer Treatment: Optimization, Characterization and In Vitro Evaluation. *Pharmaceutics* **2021**, *13*, 59. [CrossRef]

176. Koshkina, N.V.; Kleinerman, E.S. Aerosol gemcitabine inhibits the growth of primary osteosarcoma and osteosarcoma lung metastases. *Int. J. Cancer* **2005**, *116*, 458–463. [CrossRef]

177. Gordon, N.; Koshkina, N.V.; Jia, S.-F.; Khanna, C.; Mendoza, A.; Worth, L.L.; Kleinerman, E.S. Corruption of the Fas pathway delays the pulmonary clearance of murine osteosarcoma cells, enhances their metastatic potential, and reduces the effect of aerosol gemcitabine. *Clin. Cancer Res.* **2007**, *13*, 4503–4510. [CrossRef]

178. Lemarie, E.; Vecellio, L.; Hureaux, J.; Prunier, C.; Valat, C.; Grimbert, D.; Boidron-Celle, M.; Giraudeau, B.; le Pape, A.; Pichon, E. Aerosolized gemcitabine in patients with carcinoma of the lung: Feasibility and safety study. *J. Aerosol Med. Pulm. Drug Deliv.* **2011**, *24*, 261–270. [CrossRef]

179. Gandhi, M.; Pandya, T.; Gandhi, R.; Patel, S.; Mashru, R.; Misra, A.; Tandel, H. Inhalable liposomal dry powder of gemcitabine-HCl: Formulation, in vitro characterization and in vivo studies. *Int. J. Pharm.* **2015**, *496*, 886–895. [CrossRef] [PubMed]

180. Xiao, Z.; Zhuang, B.; Zhang, G.; Li, M.; Jin, Y. Pulmonary delivery of cationic liposomal hydroxycamptothecin and 5-aminolevulinic acid for chemo-sonodynamic therapy of metastatic lung cancer. *Int. J. Pharm.* **2021**, *601*, 120572. [CrossRef] [PubMed]

181. Skubitz, K.M.; Anderson, P.M. Inhalational interleukin-2 liposomes for pulmonary metastases: A phase I clinical trial. *Anti-Cancer Drugs* **2000**, *11*, 555–563. [CrossRef]

182. Koshkina, N.V.; Golunski, E.; Roberts, L.E.; Gilbert, B.E.; Knight, V. Cyclosporin A aerosol improves the anticancer effect of paclitaxel aerosol in mice. *J. Aerosol Med.* **2004**, *17*, 7–14. [CrossRef] [PubMed]

183. Jyoti, K.; Kaur, K.; Pandey, R.S.; Jain, U.K.; Chandra, R.; Madan, J. Inhalable nanostructured lipid particles of 9-bromo-noscapine, a tubulin-binding cytotoxic agent: In vitro and in vivo studies. *J. Colloid Interface Sci.* **2015**, *445*, 219–230. [CrossRef]

184. Nafee, N.; Gaber, D.M.; Elzoghby, A.O.; Helmy, M.W.; Abdallah, O.Y. Promoted Antitumor Activity of Myricetin against Lung Carcinoma Via Nanoencapsulated Phospholipid Complex in Respirable Microparticles. *Pharm. Res.* **2020**, *37*, 82. [CrossRef]

185. Boehle, A.; Kurdow, R.; Boenicke, L.; Schniewind, B.; Faendrich, F.; Dohrmann, P.; Kalthoff, H. Wortmannin inhibits growth of human non-small-cell lung cancer in vitro and in vivo. *Langenbecks Arch. Surg.* **2002**, *387*, 234–239. [CrossRef]

186. Hemström, T.H.; Sandström, M.; Zhivotovsky, B. Inhibitors of the PI3-kinase/Akt pathway induce mitotic catastrophe in non-small cell lung cancer cells. *Int. J. Cancer* **2006**, *119*, 1028–1038. [CrossRef]

187. Zhang, T.; Cui, G.-B.; Zhang, J.; Zhang, F.; Zhou, Y.-A.; Jiang, T.; Li, X.-F. Inhibition of PI3 kinases enhances the sensitivity of non-small cell lung cancer cells to ionizing radiation. *Oncol. Rep.* **2010**, *24*, 1683–1689.

188. Zhu, L.; Li, M.; Liu, X.; Du, L.; Jin, Y. Inhalable oridonin-loaded poly(lactic-co-glycolic)acid large porous microparticles for in situ treatment of primary non-small cell lung cancer. *Acta Pharm. Sin. B* **2017**, *7*, 80–90. [CrossRef]

189. Kaur, P.; Garg, T.; Rath, G.; Murthy, R.S.; Goyal, A.K. Development, optimization and evaluation of surfactant-based pulmonary nanolipid carrier system of paclitaxel for the management of drug resistance lung cancer using Box-Behnken design. *Drug Deliv.* **2016**, *23*, 1912–1925. [CrossRef] [PubMed]

190. Garbuzenko, O.B.; Kuzmov, A.; Taratula, O.; Pine, S.R.; Minko, T. Strategy to enhance lung cancer treatment by five essential elements: Inhalation delivery, nanotechnology, tumor-receptor targeting, chemo- and gene therapy. *Theranostics* **2019**, *9*, 8362–8376. [CrossRef] [PubMed]

191. Cheng, K.W.; Wong, C.C.; Alston, N.; Mackenzie, G.G.; Huang, L.; Ouyang, N.; Xie, G.; Wiedmann, T.; Rigas, B. Aerosol administration of phospho-sulindac inhibits lung tumorigenesis. *Mol. Cancer Ther.* **2013**, *12*, 1417–1428. [CrossRef] [PubMed]

192. Riaz, M.K.; Zhang, X.; Wong, K.H.; Chen, H.; Liu, Q.; Chen, X.; Zhang, G.; Lu, A.; Yang, Z. Pulmonary delivery of transferrin receptors targeting peptide surface-functionalized liposomes augments the chemotherapeutic effect of quercetin in lung cancer therapy. *Int. J. Nanomed.* **2019**, *14*, 2879–2902. [CrossRef] [PubMed]

193. Arbain, N.H.; Basri, M.; Salim, N.; Wui, W.T.; Abdul Rahman, M.B. Development and Characterization of Aerosol Nanoemulsion System Encapsulating Low Water Soluble Quercetin for Lung Cancer Treatment. *Mater. Today Proc.* **2018**, *5*, S137–S142. [CrossRef]

194. Arbain, N.H.; Salim, N.; Masoumi, H.R.F.; Wong, T.W.; Basri, M.; Abdul Rahman, M.B. In vitro evaluation of the inhalable quercetin loaded nanoemulsion for pulmonary delivery. *Drug Deliv. Transl. Res.* **2019**, *9*, 497–507. [CrossRef]

195. Karthikeyan, S.; Prasad, N.R.; Ganamani, A.; Balamurugan, E. Anticancer activity of resveratrol-loaded gelatin nanoparticles on NCI-H460 non-small cell lung cancer cells. *Biomed. Prev. Nutr.* **2013**, *3*, 64–73. [CrossRef]

196. Jensen, D.K.; Jensen, L.B.; Koocheki, S.; Bengtson, L.; Cun, D.; Nielsen, H.M.; Foged, C. Design of an inhalable dry powder formulation of DOTAP-modified PLGA nanoparticles loaded with siRNA. *J. Control. Release* **2012**, *157*, 141–148. [CrossRef]

197. Patel, K.; Bothiraja, C.; Mali, A.; Kamble, R. Investigation of sorafenib tosylate loaded liposomal dry powder inhaler for the treatment of non-small cell lung cancer. *Part. Sci. Technol.* **2021**, *39*, 990–999. [CrossRef]

198. Tomoda, K.; Ohkoshi, T.; Hirota, K.; Sonavane, G.S.; Nakajima, T.; Terada, H.; Komuro, M.; Kitazato, K.; Makino, K. Preparation and properties of inhalable nanocomposite particles for treatment of lung cancer. *Colloids Surf. B Biointerfaces* **2009**, *71*, 177–182. [CrossRef]

199. Hamzawy, M.A.; Abo-Youssef, A.M.; Salem, H.F.; Mohammed, S.A. Antitumor activity of intratracheal inhalation of temozolomide (TMZ) loaded into gold nanoparticles and/or liposomes against urethane-induced lung cancer in BALB/c mice. *Drug Deliv.* **2017**, *24*, 599–607. [CrossRef]

200. Wauthoz, N.; Deleuze, P.; Saumet, A.; Duret, C.; Kiss, R.; Amighi, K. Temozolomide-based dry powder formulations for lung tumor-related inhalation treatment. *Pharm Res* **2011**, *28*, 762–775. [CrossRef] [PubMed]

201. Lin, C.; Zhang, X.; Chen, H.; Bian, Z.; Zhang, G.; Riaz, M.K.; Tyagi, D.; Lin, G.; Zhang, Y.; Wang, J.; et al. Dual-ligand modified liposomes provide effective local targeted delivery of lung-cancer drug by antibody and tumor lineage-homing cell-penetrating peptide. *Drug Deliv.* **2018**, *25*, 256–266. [CrossRef] [PubMed]

202. Parvathaneni, V.; Kulkarni, N.S.; Chauhan, G.; Shukla, S.K.; Elbatanony, R.; Patel, B.; Kunda, N.K.; Muth, A.; Gupta, V. Development of pharmaceutically scalable inhaled anti-cancer nanotherapy—Repurposing amodiaquine for non-small cell lung cancer (NSCLC). *Mater. Sci. Eng. C* **2020**, *115*, 111139. [CrossRef] [PubMed]

203. Seabloom, D.E.; Galbraith, A.R.; Haynes, A.M.; Antonides, J.D.; Wuertz, B.R.; Miller, W.A.; Miller, K.A.; Steele, V.E.; Suen, C.S.; O'Sullivan, M.G.; et al. Safety and Preclinical Efficacy of Aerosol Pioglitazone on Lung Adenoma Prevention in A/J Mice. *Cancer Prev. Res.* **2017**, *10*, 124–132. [CrossRef] [PubMed]

204. Godugu, C.; Patel, A.R.; Doddapaneni, R.; Marepally, S.; Jackson, T.; Singh, M. Inhalation delivery of Telmisartan enhances intratumoral distribution of nanoparticles in lung cancer models. *J. Control. Release* **2013**, *172*, 86–95. [CrossRef] [PubMed]

205. Wang, Y.; Wen, W.; Yi, Y.; Zhang, Z.; Lubet, R.A.; You, M. Preventive Effects of Bexarotene and Budesonide in a Genetically Engineered Mouse Model of Small Cell Lung CancerBexarotene Inhibits Small Cell Lung Carcinoma in Mice. *Cancer Prev. Res.* **2009**, *2*, 1059–1064. [CrossRef] [PubMed]

206. Balansky, R.; Ganchev, G.; Iltcheva, M.; Steele, V.E.; De Flora, S. Prevention of cigarette smoke–induced lung tumors in mice by budesonide, phenethyl isothiocyanate, and N-acetylcysteine. *Int. J. Cancer* **2010**, *126*, 1047–1054. [CrossRef] [PubMed]

207. Lam, S.; LeRiche, J.C.; McWilliams, A.; MacAulay, C.; Dyachkova, Y.; Szabo, E.; Mayo, J.; Schellenberg, R.; Coldman, A.; Hawk, E. A randomized phase IIb trial of pulmicort turbuhaler (budesonide) in people with dysplasia of the bronchial epithelium. *Clin. Cancer Res.* **2004**, *10*, 6502–6511. [CrossRef]

208. Jafarinejad, S.; Gilani, K.; Moazeni, E.; Ghazi-Khansari, M.; Najafabadi, A.R.; Mohajel, N. Development of chitosan-based nanoparticles for pulmonary delivery of itraconazole as dry powder formulation. *Powder Technol.* **2012**, *222*, 65–70. [CrossRef]

209. Lin, L.; Quan, G.; Peng, T.; Huang, Z.; Singh, V.; Lu, M.; Wu, C. Development of fine solid-crystal suspension with enhanced solubility, stability, and aerosolization performance for dry powder inhalation. *Int. J. Pharm.* **2017**, *533*, 84–92. [CrossRef] [PubMed]

210. Duret, C.; Wauthoz, N.; Sebti, T.; Vanderbist, F.; Amighi, K. Solid dispersions of itraconazole for inhalation with enhanced dissolution, solubility and dispersion properties. *Int. J. Pharm.* **2012**, *428*, 103–113. [CrossRef] [PubMed]

211. Mohtar, N.; Taylor, K.M.; Sheikh, K.; Somavarapu, S. Design and development of dry powder sulfobutylether-β-cyclodextrin complex for pulmonary delivery of fisetin. *Eur. J. Pharm. Biopharm.* **2017**, *113*, 1–10. [CrossRef] [PubMed]

212. Dahl, A.R.; Grossi, I.M.; Houchens, D.P.; Scovell, L.J.; Placke, M.E.; Imondi, A.R.; Stoner, G.D.; De Luca, L.M.; Wang, D.; Mulshine, J.L. Inhaled isotretinoin (13-cis retinoic acid) is an effective lung cancer chemopreventive agent in A/J mice at low doses: A pilot study. *Clin. Cancer Res.* **2000**, *6*, 3015–3024.

213. Osama, H.; Sayed, O.M.; Hussein, R.R.S.; Abdelrahim, M.; Elberry, A.A. Design, optimization, characterization, and in vivo evaluation of sterosomes as a carrier of metformin for treatment of lung cancer. *J. Liposome Res.* **2020**, *30*, 150–162. [CrossRef]

214. Parvathaneni, V.; Kulkarni, N.S.; Shukla, S.K.; Farrales, P.T.; Kunda, N.K.; Muth, A.; Gupta, V. Systematic Development and Optimization of Inhalable Pirfenidone Liposomes for Non-Small Cell Lung Cancer Treatment. *Pharmaceutics* **2020**, *12*, 206. [CrossRef]

215. Verco, J.; Johnston, W.; Frost, M.; Baltezor, M.; Kuehl, P.J.; Lopez, A.; Gigliotti, A.; Belinsky, S.A.; Wolff, R.; diZerega, G. Inhaled submicron particle paclitaxel (NanoPac) induces tumor regression and immune cell infiltration in an orthotopic athymic nude rat model of non-small cell lung cancer. *J. Aerosol Med. Pulm. Drug Deliv.* **2019**, *32*, 266–277. [CrossRef]

216. Borghaei, H.; Langer, C.J.; Millenson, M.; Ruth, K.J.; Litwin, S.; Tuttle, H.; Seldomridge, J.S.; Rovito, M.; Mintzer, D.; Cohen, R. Phase II study of paclitaxel, carboplatin, and cetuximab as first line treatment, for patients with advanced non-small cell lung cancer (NSCLC): Results of OPN-017. *J. Thorac. Oncol.* **2008**, *3*, 1286–1292. [CrossRef]

217. Rosière, R.; Berghmans, T.; De Vuyst, P.; Amighi, K.; Wauthoz, N. The position of inhaled chemotherapy in the care of patients with lung tumors: Clinical feasibility and indications according to recent pharmaceutical progresses. *Cancers* **2019**, *11*, 329. [CrossRef]

218. Wauthoz, N.; Rosière, R.; Amighi, K. Inhaled cytotoxic chemotherapy: Clinical challenges, recent developments, and future prospects. *Expert Opin. Drug Deliv.* **2021**, *18*, 333–354. [CrossRef]

219. Chou, A.J.; Gupta, R.; Bell, M.D.; Riewe, K.O.D.; Meyers, P.A.; Gorlick, R. Inhaled lipid cisplatin (ILC) in the treatment of patients with relapsed/progressive osteosarcoma metastatic to the lung. *Pediatr. Blood Cancer* **2013**, *60*, 580–586. [CrossRef]

220. Otterson, G.A.; Villalona-Calero, M.A.; Sharma, S.; Kris, M.G.; Imondi, A.; Gerber, M.; White, D.A.; Ratain, M.J.; Schiller, J.H.; Sandler, A. Phase I study of inhaled Doxorubicin for patients with metastatic tumors to the lungs. *Clin. Cancer Res.* **2007**, *13*, 1246–1252. [CrossRef]

221. Otterson, G.A.; Villalona-Calero, M.A.; Hicks, W.; Pan, X.; Ellerton, J.A.; Gettinger, S.N.; Murren, J.R. Phase I/II Study of inhaled doxorubicin combined with platinum-based therapy for advanced non–small cell lung cancer. *Clin. Cancer Res.* **2010**, *16*, 2466–2473. [CrossRef] [PubMed]

222. Lavorini, F.; Buttini, F.; Usmani, O.S. 100 years of drug delivery to the lungs. In *Concepts and Principles of Pharmacology: 100 Years of the Handbook of Experimental Pharmacology*; Springer: Cham, Switzerland, 2019; pp. 143–159.

223. Gagnadoux, F.; Hureaux, J.; Vecellio, L.; Urban, T.; Le Pape, A.; Valo, I.; Montharu, J.; Leblond, V.; Boisdron-Celle, M.; Lerondel, S.J. Aerosolized chemotherapy. *J. Aerosol Med. Pulm. Drug Deliv.* **2008**, *21*, 61. [CrossRef] [PubMed]

224. Darwiche, K.; Zarogoulidis, P.; Karamanos, N.K.; Domvri, K.; Chatzaki, E.; Constantinidis, T.C.; Kakolyris, S.; Zarogoulidis, K. Efficacy versus safety concerns for aerosol chemotherapy in non-small-cell lung cancer: A future dilemma for micro-oncology. *Future Oncol.* **2013**, *9*, 505–525. [CrossRef] [PubMed]

225. Bernabeu-Martínez, M.A.; Ramos Merino, M.; Santos Gago, J.M.; Álvarez Sabucedo, L.M.; Wanden-Berghe, C.; Sanz-Valero, J. Guidelines for safe handling of hazardous drugs: A systematic review. *PLoS ONE* **2018**, *13*, e0197172. [CrossRef]

226. Charpidou, A.G.; Gkiozos, I.; Tsimpoukis, S.; Apostolaki, D.; Dilana, K.D.; Karapanagiotou, E.M.; Syrigos, K.N. Therapy-induced toxicity of the lungs: An overview. *Anticancer Res.* **2009**, *29*, 631–639. [PubMed]

227. Lippmann, M.; Yeates, D.; Albert, R. Deposition, retention, and clearance of inhaled particles. *Occup. Environ. Med.* **1980**, *37*, 337–362. [CrossRef]

Chapter 3

Spray-Dried Nano lipid Powders for Pulmonary Drug Delivery: A Comprehensive Mini Review

Publication Details:

Chapter Summary:

In this chapter, the current literature on pulmonary drug delivery for treating lung diseases is reviewed. Pulmonary delivery offers benefits over traditional methods, such as non-invasive administration, localized delivery, low enzymatic activity, reduced drug degradation, higher patient compliance, and avoidance of first-pass metabolism. The focus is on inhalable nanocarrier powders, particularly lipid nanoparticle formulations like solid-lipid and nanostructured-lipid carriers, which offer deep lung deposition and controlled drug release. Spray drying is highlighted as a viable technique for producing these powders. Additionally, the chapter discusses dry powder inhalers (DPIs) for pulmonary delivery and the applications of SLN and NLC powders in treating chronic lung conditions.

Review

Spray-Dried Nanolipid Powders for Pulmonary Drug Delivery: A Comprehensive Mini Review

Mahmoud H. Abu Elella [1], Arwa Omar Al Khatib [1,2] and Hisham Al-Obaidi [1,*]

[1] School of Pharmacy, University of Reading, Reading RG6 6UR, UK;
m.h.e.abuelella@reading.ac.uk (M.H.A.E.); a.al-khatib@pgr.reading.ac.uk (A.O.A.K.)

[2] Faculty of Pharmacy, Al Ahliyya Amman University, Amman 19111, Jordan

* Correspondence: h.al-obaidi@reading.ac.uk

Abstract: Lung diseases have received great attention in the past years because they contribute approximately one-third of the total global mortality. Pulmonary drug delivery is regarded as one of the most appealing routes to treat lung diseases. It addresses numerous drawbacks linked to traditional dosage forms. It presents notable features, such as, for example, a non-invasive route, localized lung drug delivery, low enzymatic activity, low drug degradation, higher patient compliance, and avoiding first-pass metabolism. Therefore, the pulmonary route is commonly explored for delivering drugs both locally and systemically. Inhalable nanocarrier powders, especially, lipid nanoparticle formulations, including solid-lipid and nanostructured-lipid nanocarriers, are attracting considerable interest in addressing respiratory diseases thanks to their significant advantages, including deep lung deposition, biocompatibility, biodegradability, mucoadhesion, and controlled drug released. Spray drying is a scalable, fast, and commercially viable technique to produce nanolipid powders. This review highlights the ideal criteria for inhalable spray-dried SLN and NLC powders for the pulmonary administration route. Additionally, the most promising inhalation devices, known as dry powder inhalers (DPIs) for the pulmonary delivery of nanolipid powder-based medications, and pulmonary applications of SLN and NLC powders for treating chronic lung conditions, are considered.

Keywords: lung diseases; pulmonary drug route; inhalable lipid nanoparticles; spray drying technique; dry powder inhaler

1. Introduction

The lung is an attractive target for drug delivery due to its large surface area, which is about 75–140 m², and a relatively low enzymatic controlled environment for systemic absorption of medications [1]. The lungs, located in the thoracic cavity, consist of major structures, such as bronchi, bronchioles, alveoli, and blood vessels (Figure 1). The airway passages serve to transport air in and out of the lungs while exchanging both O_2 and CO_2 with the bloodstream, which is the main responsibility of the alveoli. Additionally, understanding their anatomy is vital in comprehending respiratory functions, diseases, and treatments [2,3].

The lungs have evolved protection mechanisms to prevent the invasion of unwanted airborne particles from invading the body, as they are a major port of entry. Despite their protective mechanisms, the lungs are consistently exposed to a range of stress factors, including chemical, microbial, and physical influences throughout life. Inhalation of various harmful toxins and microorganisms leads to the development of lung diseases. Lung diseases, including lung cancer, asthma, mycobacterium-based tuberculosis, COPD, and cystic fibrosis, are diseases that target the various regions of the lungs, particularly the airways [4–6]. Chronic inflammation typically elevates the susceptibility to debilitating lung conditions.

They pose significant public health challenges and burden healthcare systems considerably. Morbidity rates for these conditions have seen a sharp increase. As per the reported list by the WHO regarding the top ten reasons for mortality globally, four of them are attributed to lung diseases: lower respiratory conditions, COPD, lung cancer, and TB. They accounted for approximately one-third (31.35%) of the total global deaths [7]. Additionally, chronic lung diseases in the United Kingdom contribute to 24% of mortality cases [8]. A 2017 Global Burden of Disease Study identified that 545 million people suffer from chronic respiratory conditions globally [9].

COPD and asthma, among all inflammatory diseases, collectively impact millions of individuals globally. Chronic inflammatory ailments result from prolonged inflammatory processes caused by numerous heightened expressed genes associated with inflammation [4]. While a range of pharmacotherapeutic strategies, including antibiotics, peptides, and genetic therapy, such as siRNA and DNA, are utilized for treating lung diseases, these approaches provide relief from symptoms rather than achieving full disease eradication [10].

This review focuses on the development of inhalable lipid nanoparticle powders, which are fabricated using a spray dryer for pulmonary administration by using the most promising powder-medication-based inhalation device, known as dry powder inhalers (DPIs). Furthermore, it presents recent progress made in the pulmonary applications of SLN and NLC powders for the treatment of chronic lung diseases.
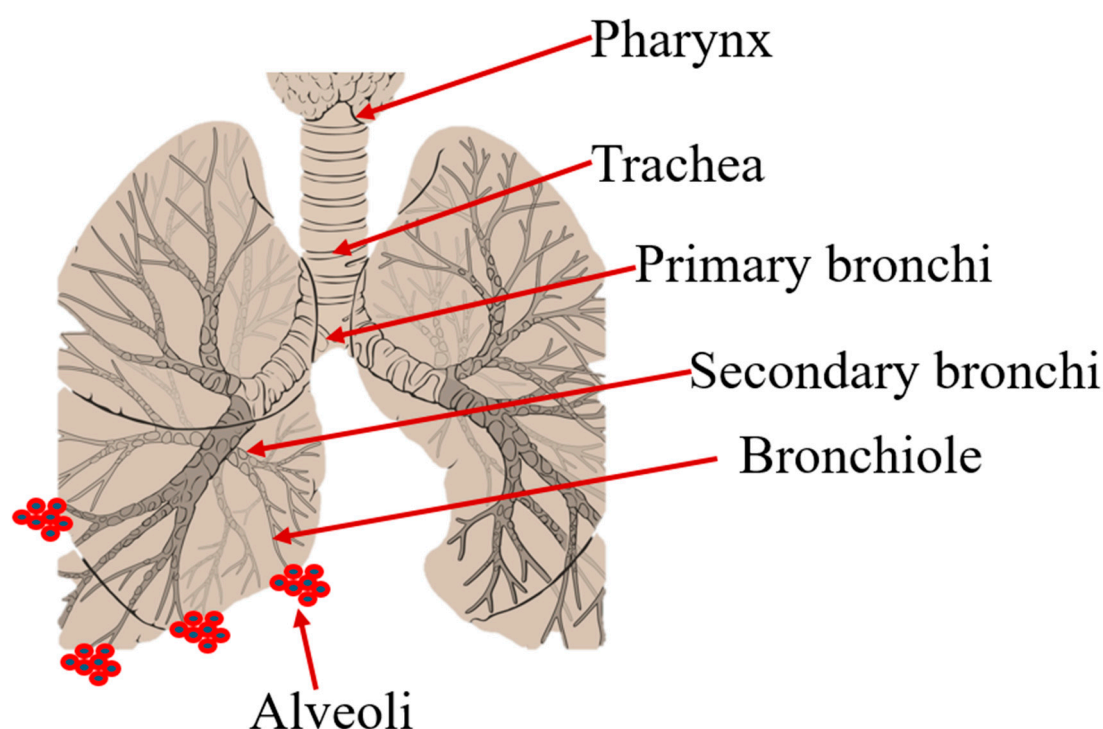
Figure 1. Schematic illustration of the respiratory system.

2. Pulmonary Drug Delivery and Use of Nanocarriers

The pulmonary drug administration route, involving direct inhalation of drugs into the lungs, is highly effective for drug delivery, particularly for treating lung diseases. It rapidly concentrates medication at the target site while minimizing systemic drug levels. Compared to traditional delivery methods, it offers distinct advantages (Figure 2), such as the lungs' large surface area, a non-invasive route, high epithelial permeability, targeted drug delivery, reduced enzymatic activity, minimal degradation, improved patient compliance, and bypassing first-pass metabolism, resulting in an immediate therapeutic response [11,12].

In addition to the extensive surface area of the lung, the alveolar region also benefits from a robust blood supply and a permeable membrane (0.2–0.7 µm), facilitating quick absorption. This strategy guarantees the swift and successful delivery of drugs to their intended site of action [11,13].

As a result, pulmonary delivery is gaining traction not only for treating airway diseases locally but also for administering drugs systemically, particularly for poorly water-soluble medications with limited bioavailability through alternative routes, such as oral administration [14].

For the localized management of airway diseases, pulmonary administration distinguishes itself by directly reaching the lung epithelium. This results in a swift onset of action and reduces the required dosage compared to traditional administration methods, like oral delivery [15,16].

To optimize the efficiency of respiratory delivery, it is essential to employ a well-suited drug formulation possessing suitable physicochemical properties. Nanotechnology is attracting considerable interest in addressing respiratory conditions. The development and application of nanocarriers hold great potential for enhancing the human quality of life. Nanomedicine entails the pharmaceutical application of nanotechnology to enhance patient healthcare [17]. Nanocarriers for pulmonary application have garnered significant attention over the past two decades because they must meet several criteria, including biocompatibility and biodegradability, adequate drug capacity, shielding the degradation of the drug, and good aerosolized stability.
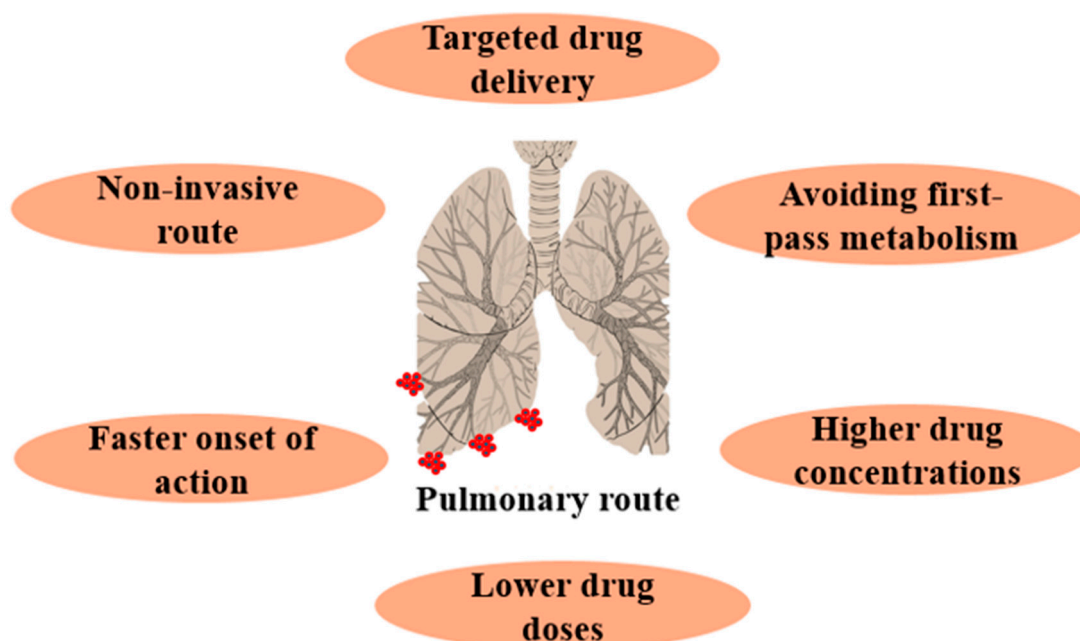
Figure 2. Benefits of the pulmonary drug delivery route.

Various nanocarriers, including SLNs, SLMs, liposomes, pro liposomes, polymeric NPs, polymeric MPs, and polymeric-coated NPs, have been explored in recent decades. Emerging therapies encompass inhalable nanocarriers designed to target inflammatory receptors at the early stages of infection. This approach holds promise as an ideal strategy for preventing disease progression and tissue damage. Recent research indicates that lipid NPs can meet these requirements, revealing their availability for the pulmonary administration route.

Interest in SLN and NLC as substitutes for other nanocarriers, such as liposomes, nanoemulsions, and polymeric-based nanoparticles, is growing, not only for pulmonary administration but also for other drug administration routes, including ocular, oral,

dermal, and parenteral routes [18–22]. This has included, for instance, the approval of PulmoSphere™ technology used in products like Pulmozyme® and TOBI® Podhaler™, which utilize liposomal formulations for pulmonary delivery to treat conditions like cystic fibrosis. These products demonstrate the clinical viability and effectiveness of nanoparticle-based inhalation therapies in enhancing drug delivery to the lungs, thus improving patient compliance and reducing systemic side effects.

Furthermore, the successful application of liposomal amikacin (Arikayce®) for the treatment of lung infections associated with cystic fibrosis and non-tuberculous mycobacterial infections further underscores the potential of lipid-based nanoparticles in pulmonary applications. These examples showcase their prospective transformative impact on pulmonary drug delivery systems.

3. Lung Surfactant and Impact on Pulmonary Drug Delivery

Lung surfactant is composed of a blend of lipids and proteins situated in the alveolar lining of the lungs. Its function involves reducing surface tension by creating a singular layer at the interface between alveolar air and the liquid. Additionally, lung surfactant plays a crucial role in enhancing the effective dispersion of inhaled drugs delivered to the lung throughout the mucus surface, and it improves the transport of aerosol among different lung regions, leading to more uniform drug distribution across the deeper lung areas [23].

Interestingly, inhaled drugs must initially penetrate the lung surfactant layer to reach the underlying tissue. Therefore, the presence of the surfactant layer affects drug deposition within the lungs in several ways, including diffusion limitation, drug particle size, and extended residence time [24]. In the former, the surfactant layer may serve as a barrier, impeding drugs from accessing the deeper tissues. Consequently, this could result in decreased drug concentrations in the lungs and reduced treatment efficacy. In the case of the drug particle size factor, notably, the size of drug particles influences how deeply they are deposited within the lungs. For example, large particle sizes could get trapped on the surface of the surfactant layer, thus restricting their penetration; conversely, small particles may bypass the layer and reach deeper regions of the lungs. In the latter case, the surfactant layer can extend the duration of drugs within the lungs. This is advantageous for drugs that are quickly expelled, as it enables prolonged exposure to the lung tissue, thereby increasing their effectiveness.

4. Inhalation of Nanolipid Powders for Pulmonary Drug Delivery

4.1. Lipid Nanoparticles

Lipid-based nanoparticles are vehicles for small molecule delivery, and, in the context of this review, they are used for pulmonary drug delivery. They are spherical-shaped vesicles comprised of ionizable lipids. These lipids, at low pH, carry a positive charge, whereas at physiological pH, they remain neutral, which helps to reduce potential toxic side effects. Due to their small, spherical size, these nanoparticles can deliver drugs into cells via endocytosis and release the cargo into the cytoplasm [25]. Lipid-based drug delivery is a growing area of interest due to its ability to overcome barriers faced by present conventional formulations. They are seen as a suitable replacement for other polymer NPs due to the biocompatible nature of lipids in the body [26].

The initial drug dosage integrating lipid-soluble drugs into droplet-based lipids emerged in the 1960s as the parenteral fat emulsion. Today, this formulation is extensively utilized for the parenteral administration of poorly water-soluble drugs, such as propofol or diazepam [27]. During the 1990s, three research teams, namely, Müller [28], Gasco [29], and Westesen et al. [30], pioneered the first generation of lipid nanoparticles, known as SLNs.

The solid lipid nanoparticle (abbreviated to SLN) category is the first generation of nanolipid carriers. Also referred to as colloidal carriers, SLNs have been developed as an alternative nanocarrier group to preexisting others, such as, for instance, emulsion-, liposome-, and polymer-based NPs. SLNs are essentially lipid-based emulsions in the range

of the submicron. The oil is substituted with solid lipids, resulting in a solid lipid matrix at ambient and physiological temperatures [26].

In SLNs (Figure 3), the oil component of the fat emulsion is substituted with a solid lipid or a mixture of solid lipids, resulting in a solid lipid matrix for SLNs at both room and body temperatures. SLNs typically consist of 0.1–30 wt.% dispersed lipid in an aqueous phase composed of surfactant (around 0.5–5 wt.%) as a stabilizer. The average diameter of SLNs typically falls within the range of 40–1000 nanometers [31,32].

SLNs typically offer a combination of advantages, merging the favorable characteristics of fluid-like, lipid-based colloidal particles (such as ingredient biocompatibility) with the straightforward production methods of solid matrix polymeric nanoparticles. This feature facilitates the local and systematic administration of hydrophobic therapeutic agents [33]. In contrast to polymeric nanoparticles, SLNs offer greater safety potential due to several factors: it is a green method without solvent, and it allows for the utilization of biocompatible and biodegradable ingredients (GRAS) [34]. However, there are a few limitations to SLN, such as, for example, its low loaded-drug capacity, due to the change from low lipid modification to a highly ordered, crystallized, firm structure during storage. To address these barriers, a second-generation nanolipid formulation was fabricated [35].

The second generation is called nanostructured lipid carriers (abbreviated as NLCs). These carriers contain a solid lipid matrix at both room and body temperatures, similarly to SLNs, but the difference here is that the matrix comprises a blend of a solid lipid as well as a liquid lipid (Figure 3), such as, for example, oleic acid, miglyol oil, or castor oil. The combination of both lipids creates a low-ordered lipid matrix allowing for high rooming for therapeutic agents. This can be accomplished through different development approaches, such as, for instance, hot or cold high-pressure homogenization, micro-emulsion, emulsification/solvent evaporation, or diffusion techniques [17,36].
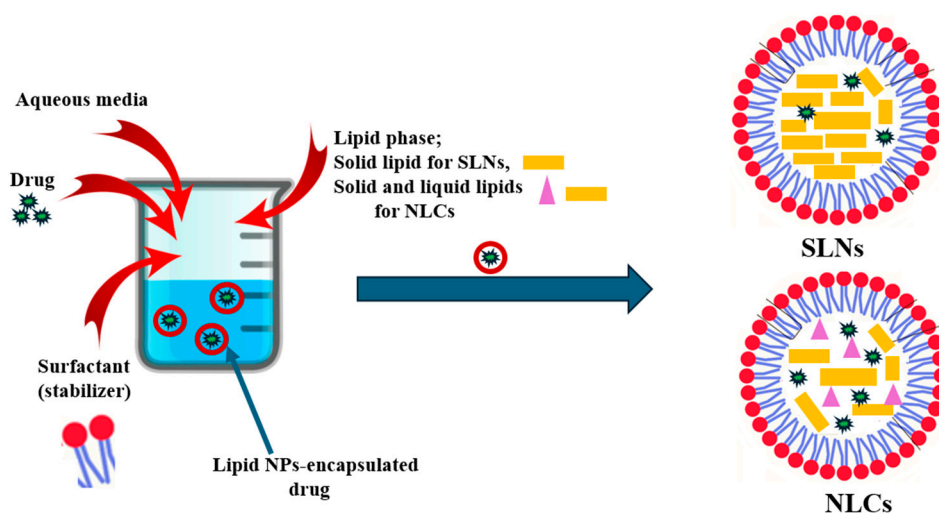
Figure 3. Schematic preparation of two lipid nanoparticle formulations (SLNs and NLCs).

For the pulmonary administration route, lipid nanoparticles offer several advantages (Figure 4a). Both SLNs and NLCs are sub-micron-sized, and this feature is beneficial for pulmonary delivery. This property enables nanoparticles to be readily entrapped within particles or aerosolized into droplets, which enables the active compound to be deposited far into the lung. Their size also allows for a longer period of adhesion to the mucosal surface in comparison to larger particles, which allows for longer drug action [17]. This adhesion factor, as well as the accumulation, retention, and prolonged release features of both SLNs and NLCs in the lungs, offer improved and sustained therapeutic outcomes, thereby promoting good patient compliance. It is important to link this back to the chronic indications this could potentially be used for, as many existing treatments require a minimum twice-daily dose thanks to their short lifetime in the lungs [37].
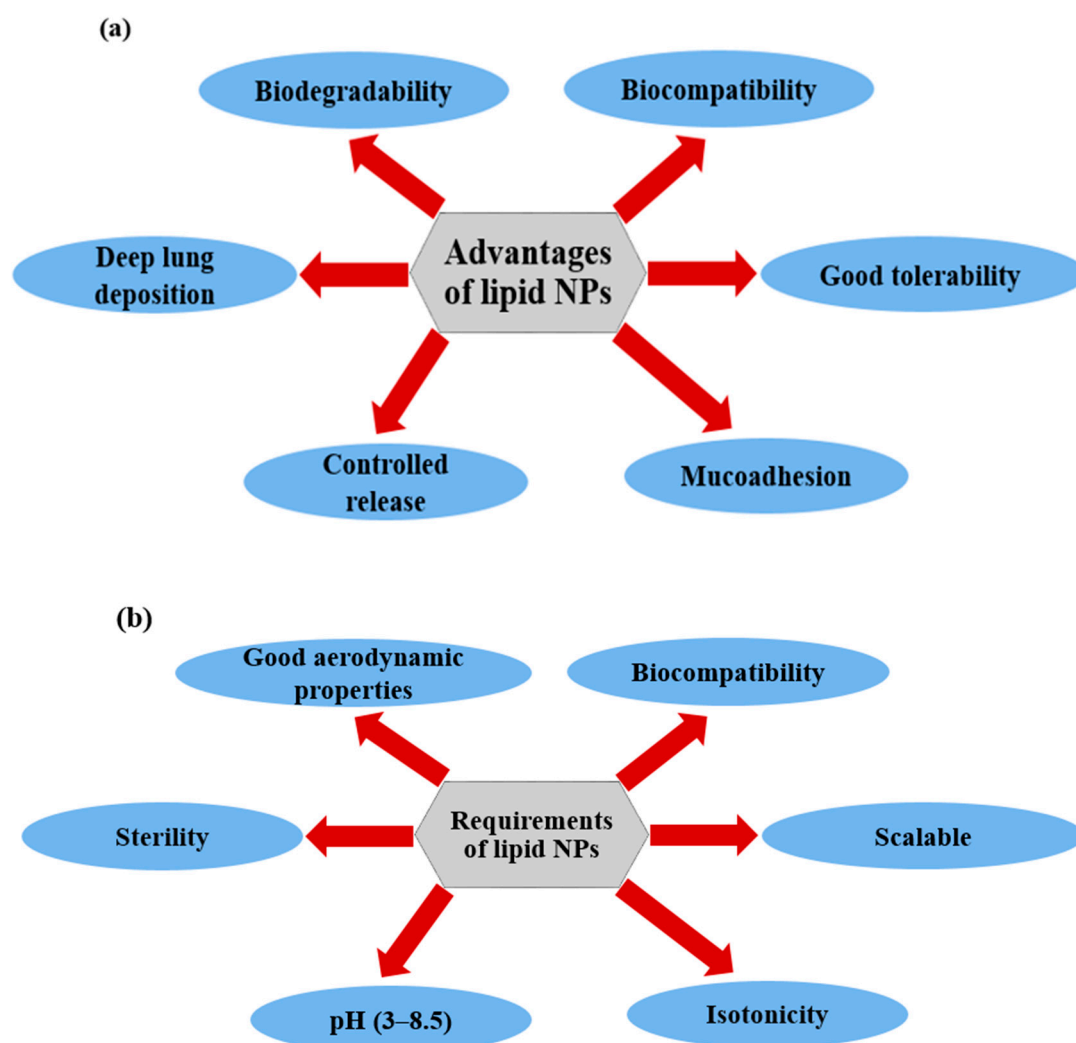
Figure 4. (**a**) Features of SLCs and NLCs for lung drug route, and (**b**) ideal criteria for SLCs and NLCs for pulmonary applications.

This feature can be particularly significant in curing chronic conditions, as many current inhalation formulations require administration twice daily because of their relatively short duration in the lung. Moreover, because both SLN and NLC are made of biocompatible lipids, this ensures good tolerability in the airways. Additionally, using the biodegradable lipid results in avoiding any toxic degradation products, thereby decreasing the risk of toxic effects and further increasing compliance [38].

4.2. Ideal Criteria for Lipid NPs Intended for Pulmonary Applications

To effectively address various lung diseases, the medication needs to primarily target and exert its effects within the lungs. This requirement contrasts conventional approaches to drug and dosage form design, which typically prioritize enhanced absorption and bioavailability throughout the body. However, when a medication designed to cure lung infections is taken up and distributed to other body organs, it can lead to diminished concentrations at the desired location and potentially cause significant adverse effects affecting the gastrointestinal, cardiovascular, and central nervous systems. Hence, for drug administration aimed at targeting lung diseases, both SLNs and NLCs must adhere to specific requirements for ideal pulmonary drug delivery systems, as illustrated in Figure 4b, including biocompatibility, good tolerability, isotonicity, sterility, and a neutral pH value. This is crucial, as the lungs possess limited buffering capacity [39].

To ensure biocompatibility, it is advisable to employ biodegradable and well-tolerated ingredients, including lipids and surfactants. Neutral isotonic carbohydrates are preferable to more highly ionic isotonic salts, like sodium chloride, to mitigate undesired effects. Formulations including an isotonicity around 300 mosmol/kg and a pH range between 3 and 8.5 are desirable [17].

Lipid NPs can be administered in pulmonary applications either as suspensions [40] or converted to inhaled dry powder [41]. These scenarios result in aerosols generated from suspended or dry powder formulations that exhibit a favorable, aerodynamic size to ensure adequate deposition in targeted airway parts. Consequently, the inhaled lipid NP formulations must possess ideal aerodynamic properties, including particle/droplet size and density, mass median aerodynamic diameter (MMAD), and fine particle fraction (FPF). Typically, the aerodynamic aerosol distribution falls between 0.5 μm and 10.0 μm. On the other hand, the ideal aerodynamic size is determined by the intended site of deposition, which varies according to the therapeutic approach. For suspension and powder formulations, the aerodynamic diameters of the inhaled formulations should ideally be below 5 μm to facilitate deep deposition within the lungs [42,43].

Each inhalable formulation requires sterilization utilizing suitable methods, such as sterilized steam, irradiated γ-rays, or a sterilized filtration membrane. Two key considerations must be addressed before the sterilization of lipid NPs. The impact of the sterilization procedure on lipid NPs' formulation stability, as well as the selection of the optimal sterilization procedure, should consider both the physical and chemical stability of the formulation during the sterilization process [17].

It is not possible to provide a general answer regarding how sterilized steam or gamma-ray irradiation affects the stability of the nanolipid. With γ-ray irradiation, there is a risk of the generation of free radicals from chemically modified drugs due to the formation of free radicals. Additionally, the sterilized filtration membrane is only viable if its size is less than 200 nm. Furthermore, during autoclaving, melting of lipids can occur, followed by recrystallization upon cooling, thus potentially altering the drug release pattern. Additionally, there is a possibility of lipid droplets coalescing before reforming into lipid NPs, resulting in large particles. As a result, autoclaving mainly presents physical–stability challenges, including increased size or aggregation. Cavalli [29], Heiati [44], and Nayak [45] have demonstrated successfully autoclaved SLN and NLC.

4.3. Biosafety and Pharmacokinetics of Inhalable Drug-Loaded Lipid Nanoparticle Delivery System

When drugs are provided without proper protection, they are vulnerable to degradation, which can limit their effectiveness. However, utilizing drug carrier systems, such as lipid nanoparticles (LNPs), in inhalation therapy can alleviate these risks. The pulmonary route is a popular method for drug delivery, as it helps to avoid drug loss due to gastrointestinal degradation and first-pass metabolism in the liver. However, the pulmonary tract also contains numerous xenobiotic metabolizing enzymes that are capable of modifying the integrity and pharmacokinetics of inhaled therapeutics. This can be a challenge for drug developers who need to ensure that their therapeutics are deliveredefficiently. Delivering drugs through the pulmonary route requires the drugs to withstand the shear forces experienced during the aerosolization process. Encasing inhaled therapeutics within lipid nanoparticles enhances their protection and helps delay degradation. This also improves the bioavailability of intact compounds and pharmacokinetic profiles. LNPs are a promising drug carrier system for inhalation therapy because they can protect the drug from degradation and modification while also allowing for efficient delivery to the lungs [46–49].

Moreover, it has been observed that inhalable drug-loaded lipid nanoparticles (LNPs) offer a promising strategy for mitigating the likelihood of inducing an immune response compared to administering drugs without protection. This is because LNPs provide a protective shield for the payload, thereby reducing its recognition as a foreign substance by the immune system. In addition, LNPs decrease phagocytic clearance by

alveolar macrophages, leading to a prolonged circulation time and higher drug bioavailability. As a result, patients can benefit from a faster clinical response and require less frequent dosing, thus reducing the risk of severe side effects. This could ultimately contribute to improved patient compliance and better treatment outcomes [50].

5. Spray-Dried Nanolipid Powder Formulation for the Pulmonary Route

5.1. Spray Drying Technique

Spray drying is the common method used to produce the inhalable powder. The spray-dried inhaled particle's size significantly impacts local drug deposition in the lungs. Particle sizes smaller than 5 μm have been noted to exhibit a strong correlation with whole-lung deposition. Spray drying is a commonly employed drying approach in pharmaceutical cosmetics and food applications for the development of various controlled particle sizes with good properties. The combination of formulation and spray drying conditions enables the creation of agglomerated powders possessing cohesive characteristics, like flowable particles, reconstitution behavior, bulky density, and mechanical stability [51].

One significant application of spray drying is the formation of lipid nanoparticle powders. Spray drying is a scalable and commercially viable technique to produce nanolipid powders. It can handle large volumes of feed solutions, making it suitable for industrial-scale manufacturing. Nanolipid powders have gained considerable attention due to their potential in various fields, including drug delivery, nutraceuticals, and the encapsulation of bioactive compounds. Moreover, the spray drying process is relatively fast and cost-effective compared to other techniques, such as microfluidics or solvent evaporation methods. It can be used with a wide range of lipid-based materials that are compatible with various excipients, surfactants, and active ingredients, allowing flexibility in the formulation design of nanolipid powders [52–55].

Spray drying has been extensively used to encapsulate various active ingredients, including drugs and functional lipids. Lipid nanoparticle powders are designed to encapsulate hydrophobic or lipophilic compounds. They are typically composed of lipids and surfactants, which self-assemble to form nanoparticles with a lipid core and a stabilizing shell. They offer numerous advantages, such as biocompatibility, controlled release, protection of encapsulated compounds, and the ability to target specific tissues [56].

The spray drying technique is composed of different parts, including a feed solution, a pump, an atomizer nozzle, a drying chamber, and a cyclone (Figure 5). The spray dryer operates through a series of four stages. First, the liquid forced for drying is atomized into a powder form, followed by the interaction between the hot gas and the nebulized liquid. Then, the solvent evaporates, and, finally, the dried product is separated in the cyclone [54,57]. The process revolves around atomizing a liquid within the drying chamber while hot gas circulates, thus rapidly drying the liquid as the nebulized droplets are exposed to a significant surface area.

The preparation of spray-dried nanolipid powders involves several steps. The lipid components, along with the active ingredient, are dissolved or dispersed in an appropriate solvent to form a feed solution. The selection of lipid components and surfactants is crucial in determining the characteristics and stability of the resulting nanolipid powders. The feed solution is atomized into fine droplets using various techniques, such as pressure nozzles or rotary atomizers [54,58]. The droplet size is a critical parameter that affects the final particle size and encapsulation efficiency. The droplets are exposed to a stream of hot air, leading to the rapid evaporation of the solvent. As the solvent evaporates, the lipid components self-assemble to form nanoparticles. The solidified particles are collected using a cyclone or a filter system. Further processing, such as milling or sieving, may be required to achieve the desired particle size distribution [59]
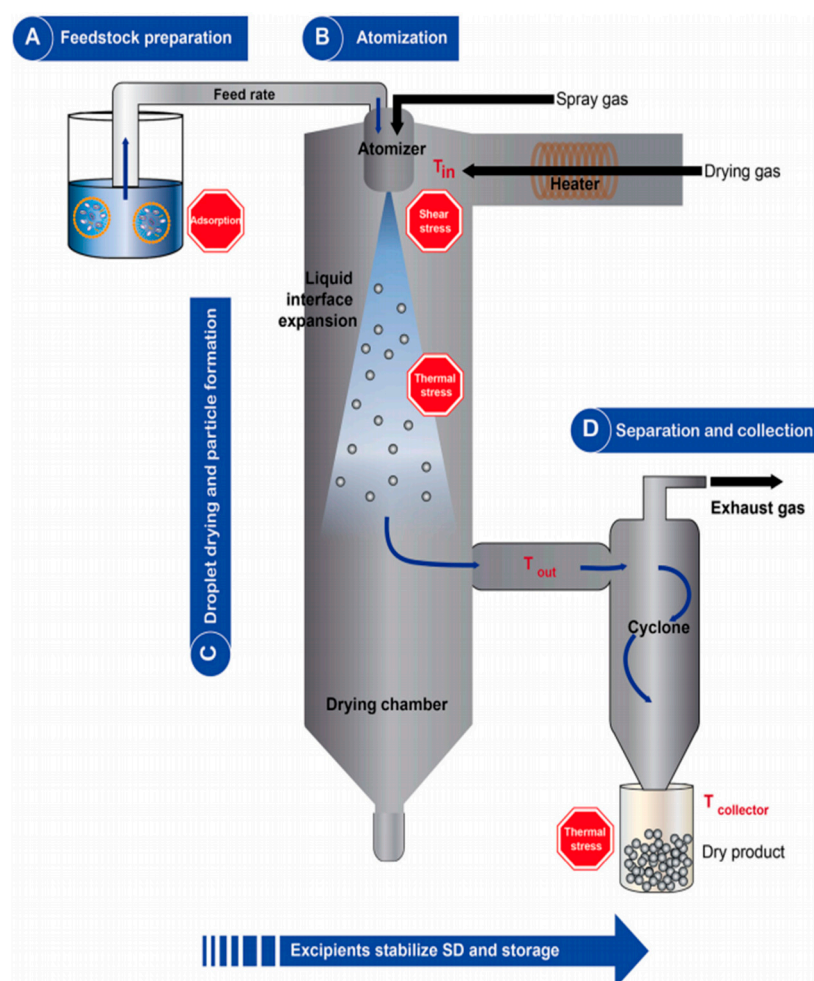
Figure 5. Schematic illustration of spray drying technique. Reproduced with permission from Friis, K.P., Journal of Controlled Release, published by Elsevier, 2023 [57].

Spray drying has a significant impact on the properties of nanolipid powders, including particle size, morphology, encapsulation efficiency, and stability. By manipulating the spray drying parameters, like the feed concentration and its flow rate, as well as the drying conditions, the particle size of nanolipid powders can be controlled within the desired range [60]. Smaller particle sizes generally lead to increased surface area and improved bioavailability. The loading capacity of nanolipid powders is based on the selection of lipids and surfactants and the properties of the active ingredient. Proper selection of drying conditions is crucial to maintain the integrity of lipid structures and prevent the degradation of encapsulated compounds. Additionally, spray drying provides a high surface-to-volume ratio, facilitating efficient encapsulation of hydrophobic compounds within the lipid powder that has improved solubility and bioavailability, thus enhancing therapeutic efficacy. In food applications, spray-dried nanolipid powders can be used to encapsulate bioactive compounds, such as vitamins, for improved stability and controlled release, resulting in enhanced functional food products [61].

Furthermore, the spray drying technique helps in maintaining nanolipid powders' stability within the drying condition. The rapid evaporation of the solvent promotes the self-assembly of lipids into nanoparticles, thus preserving the integrity of the lipid structures. Additionally, the conversion of the liquid feed into solid particles reduces the chances of chemical degradation or physical changes in the encapsulated compounds [53], resulting in enhanced stability. The atomization process generates fine droplets with a large surface area, thus providing efficient encapsulation of active ingredients within the

lipid core of the nanolipid powders and resulting in an improvement of the solubility and bioavailability of encapsulated compounds [62].

5.2. Inhalation Devices for Delivery of Spray-Dried Nanolipid Powders

The dry powder inhaler (DPI) is growing in popularity as a method for administering medication to the lungs, providing a convenient and effective option for both local and systemic treatment (Figure 6). These portable devices deliver medication in the form of microscale solid powder, either alone or in the presence of capsules as carriers. DPIs are applied by specially engineered devices that allow patients to inhale drugs directly to their lungs. Conversely, DPI formulations tend to be highly chemically stable compared to liquid formulations, and their development can present significant challenges [63,64].

Figure 6. Illustration of various types of capsule-based dry powder inhalers Adapted from MDPI, 2021 [64].

Their benefits are apparent in the increasing adoption of inhaled treatments for managing obstructive airway conditions in the last decades. While oral bioavailability of fluticasone propionate typically remains below 1%, inhaled forms of fluticasone offer a tenfold increase in bioavailability, with minimal side effects [65]. The effectiveness of a DPI relies on both designed inhalation devices and formulations of powder. DPI designers aim to strike a balance between inhaler resistance and flow rate, as a stronger airflow allows for more consistent and thorough dispersion of the medication, resulting in higher

fine particle fractions. However, if the airflow is too rapid, the medication may be deposited in the oropharynx, resulting in lowering the delivered dose of the drug to the lungs [66].

DPI devices exhibit a wide range of designs, and they are categorized into the single-unit type and the multiple-unit type. In the former one, powder is commonly placed into a single-use compartment. This classification can be further divided into three subgroups depending on the technique employed to open the capsule shell and   release the powder [64].

Numerous top–down and bottom–up approaches widely utilized to create inhalable powder depend on different costing and compatibility with APIs as well as powder stability. Top–down ones include reducing the particle size to a micro- or nanometer scale, often meeting only basic quality standards, such as jet milling. However, these methods require high energy input, are inefficient, and can present challenges in achieving more demanding performance criteria [67,68]. On the other hand, bottom–up approaches, such as the spray dryer, the spray-freeze dryer, the super critically fluid technique, and the non-wetting template, entail the assembly of the molecular constituent. Consequently, they offer remarkable powder quality, enabling the attainment of more intricate structural designs [68,69].

6. Applications of Spray-Dried Nanolipid Powders for Treatment of Lung Diseases via Pulmonary Drug Delivery

Pulmonary drug delivery, as previously mentioned, offers several advantages, making it particularly suitable for delivering drug-loaded nanolipid powders to treat various lung-related diseases. This section outlines the applications of and recent advancements in spray-dried lipid nanoparticle powders (SLNs, and NLCs) for pulmonary drug delivery tailored to treatment-specific lung diseases, such as lung cancer and TB.

6.1. Spray-Dried Lipid Nanoparticle Powders for Treatment of Lung Cancer

Lung cancer stands out as a substantial global health issue, holding the position as one of the most common cancers in pharmacokinetics worldwide. The prolonged utilization of traditional anticancer medications has resulted in a notable degree of resistance to lung cancer treatment [70,71]. Consequently, diverse strategies have arisen to combat this resistance, encompassing photothermal methodologies [72], immunotherapy [73], and the simultaneous delivery of chemotherapeutic agents [74]. Nevertheless, the photothermal approach is constrained by several limitations, including the emergence of robust antioxidant systems within cancer cells, challenges in delivering adequate levels of H_2O_2, and a low rate of free radical production [72]. Conversely, limitations associated with immunotherapy stem from its adverse effects on the immune system and its restricted efficacy against superficial cancer cells [73]. Intriguingly, the delivery of anticancer drugs amplifies cytotoxicity toward cancer cells with lower dosages, thereby reducing normal toxicity [74].

Tailoring the materials used in SLNs and NLCs can yield significant therapeutic advantages. They have a natural affinity for the lymphatic system, which aids in effectively eliminating hidden cancer cells. In addition, various lipid receptors are often found in abundance on the surface of cancer cells, enabling targeted delivery of anticancer agents [75–77]. For example, Jyoti et al. [78] investigated the effectiveness of using spray-dried SLN powders made of stearic acid and egg phosphatidylcholine to release 9-Bromonoscapine (9-Br-NOS) for lung cancer treatment. The researchers utilized the nanoemulsion technique and incorporated spray-dried lactose to modify the drug release properties. The results showed that the 9-Br-NOS-SLNs had an average particle size of 13.4 nm, an aerodynamic size of 2.3 μm, and a negative charge of −9.54 mV. The study also found that the SLNs had excellent apoptotic effects, were non-toxic, and had efficient cellular uptake in A549 lung cancer cells. Pharmacokinetic and distribution analyses demonstrated a 1.12- and 1.75-fold improvement in the half-life of the drug powder, leading to rapid dispersion, significant dissolution, and deep lung deposition of SLC powders following inhalation administration.

In the same vein, Bakhtiary et al. [79] engaged in the development of a DPI containing SLN powders composed of compritol and poloxamer 407 for the delivery of erlotinib to treat lung cancer. The nanolipid powder formulation achieved a high drug encapsulation efficacy of approximately 78.21%, resulting in enhanced cytotoxicity. This was confirmed by using the MTT method on A549 cells. The powders had an optimal flow (FPF of 30.98%) and an aerodynamic size of about 3.9 μm with the use of mannitol, allowing for deep lung inhalation and effective cancer treatment.

In a related study, Kaur et al. investigated the use of spray-dried NLC powders for delivering paclitaxel (PTX) via inhalation to combat drug-resistant lung cancer. The powders were formulated with glyceryl monostearate, oleic acid, and mannitol to enhance the flow properties, resulting in powders with the ideal aerodynamic size of 3.5 μm. In vitro analysis showed drug release levels of 64.9%, 62.3%, and 59.7% for NLCs loaded with Tween 80, Tween 20, and Tween 60, respectively, over 72 h. In vivo experiments using a DPI device on Wistar rats revealed significant improvement in drug localization within the lungs, effectively treating drug-resistant lung cancer by inhibiting P-glycoprotein inhibitors' efflux through the use of surfactant-based pulmonary delivery systems [80].

In a concurrent study, Nafee and colleagues incorporated myricetin into spray-dried SLN-based phospholipid Lipoid-S100. The resulting powders, which measured 2.7 μm, exhibited excellent flow characteristics, with a fine particle fraction (FPF) of approximately 81.23%. Additionally, more than 80% of the drug was released within 8 hours, and the encapsulation efficiency was approximately 93%, indicating a deep deposition in the bronchial region. It is noteworthy that cytotoxicity was increased, possibly due to enhanced cellular uptake, which was confirmed through confocal imaging and dual fluorescence sensing and resulted in a doubled fluorescence signal [81].

In a different study focused on researching the aerosolization of co-delivered PTX and DOX for treating lung cancer by using inhalable spray-dried NLC powders made of soya lecithin and oleic acid, by employing the cremophor EL surfactant, the research showed an improvement in the drugs' antitumor efficacy. Furthermore, an in vivo drug distribution analysis of inhalable NLCs/DPI on Wistar rats demonstrated increased drug distribution within the lungs compared to administering the drugs alone [82].

Recently, the pioneering work of Satari N. and his co-workers [83] has investigated diverse pulmonary delivery systems based on inhalable nanolipid powders for anticancer drugs for lung cancer therapy. They have reported the development of a DPI formulation containing gefitinib-loaded stearic acid SLNs targeted with glucosamine to deliver anticancer-agent-like gefitinib directly to lung tumors. The findings displayed enhanced anticancer efficacy compared to free gefitinib, with the enhanced uptake of targeted SLNs in A549 cells compared to non-targeted SLNs. Additionally, the developed mannitol-based microparticles exhibited favorable aerodynamic characteristics, with an acceptable MMAD of 4.48 μm and an FPF of 44.41%.

6.2. Spray-Dried Lipid Nanoparticle Powders for Treatment of Tuberculosis

Tuberculosis is considered a significant global public health challenge despite the significant progress achieved in the field. It continues to be one of the leading lung-infectious causes of death and illness worldwide, claiming the lives of nearly 2 million individuals annually. Mycobacterium tuberculosis is the pathogen responsible for causing tuberculosis, an infectious disease. Commonly prescribed drugs for treating tuberculosis consist of rifampicin, pyrazinamide, isoniazid, and ethambutol [84,85].

Traditional methods of drug delivery encompass oral and intravenous administration; nevertheless, these approaches may encounter dose restrictions and undergo first-pass effects in the liver, leading to inadequate drug levels in the lungs. Consequently, this can lead to the emergence of drug resistance and treatment inefficacy. Extended treatment durations and invasive procedures often result in poor patient adherence to the treatment regimen [86,87]. Therefore, pulmonary inhalation for drug delivery presents a promising avenue to tackle these challenges owing to its effective treatment and diagnosis of lung

infections. It offers a safe, convenient, and non-invasive diagnostic method [88]. Recently, lipid nanoparticle powders have garnered great attention for delivering anti-TB drugs to the lung via the pulmonary route because of the remarkable above-mentioned properties.

As an example, Gaspar D. and his team fabricated SLN powders composed of glyceryl dibehenate and glyceryl tristearate as a hybrid platform antibiotic drug carrier for the treatment of TB disease via the pulmonary route [89]. The microencapsulated rifabutin (RFB)-loaded SLN powders used FDA-approved excipients, such as mannitol and trehalose, via the spray drying method. An in vivo biodistribution study of inhalable DPI of RFB-loaded powders using BALB/c mice revealed that the antibiotic reached the tested organs via pulmonary administration after 15 and 30 min. Furthermore, the antimycobacterial activity was assessed in a murine infected with TB strain H37Rv, showing improved efficacy against TB infection compared to healthy animals.

In the same context, Nemati et al. [90] explored the pulmonary drug administration route for TB therapy using a DPI containing ethambutol drug-loaded Compritol SLN powders prepared via a hot homogenization/ultrasonication-assisted spray drying technique. Through MTT assay, the DPI formulations demonstrated excellent compatibility and non-toxicity. The resulting spray-dried powders exhibited notable flowability and inhalable characteristics, with an MMAD value of 4.148 μm and an FPF of 30.9%. Table 1 shows the different spray-dried nanolipid powders for pulmonary drug delivery via DPI for lung cancer and TB treatment.

Table 1. Different DPI formulations based on spray-dried nanolipid powders targeting both lung cancer and tuberculosis (TB) treatment via the pulmonary route.

Lipid Formulation	Lipid Composition	Active Ingredients	Lung Disease	Spray Drying Conditions		References
SLN	Stearic acid	9-Bromo-noscapine	Lung cancer	-	Spray-dried lactose carrier	[78]
NLC	Glyceryl monostearate and oleic acid	Paclitaxel (PTX)	Lung cancer	- - -	Mannose and leucine as carriers Inlet temp. is 80 °C Outlet temp. is 40 °C	[80]
NLC	Soya lecithin and oleic acid	PTX and doxorubicin (DOX)	Lung cancer	- - - -	Lactose and leucine (carrier) Inlet temp. is 80 °C Outlet temp. is 40–55 °C Flow rate of 830 L/h	[82]
SLN	Compritol	Erlotinib	Lung cancer	- - - - -	Mannitol (carrier) Inlet temp. is 110 °C Outlet temp. is 65 °C Feed rate of 10 mL/min Aspiration rate of 70%	[79]
SLN	Stearic acid and PEG/glucosamine	Gefitinib	Lung cancer	- - - - -	Mannitol and lactose (carriers) Inlet temp. is 160 °C Outlet temp. is 65 °C Feed rate of 1.5 mL/min Aspiration rate of 90%	[83]
SLN	Compritol	Ethambutol	Tuberculosis	- - - - -	Mannitol (carrier) Inlet temp. is 110 °C Outlet is 65 °C Feed rate of 10 mL/min Aspiration rate of 70%	[90]
SLN	Glyceryl dibehenate and glyceryl tristearate	Rifabutin	Tuberculosis	- - -	Mannitol and trehalose (carriers) Inlet temp. is 103 °C Feed rate of 8.5 mL/min Aspiration rate of 100%	[86]

7. Conclusions and Future Prospectives

Lipid nanoparticle powders stand out from other nanocarriers due to their numerous advantages, including excellent tolerability, as they consist of biodegradable ingredients, biocompatibility, facile production without the need for organic solvents, cost-effectiveness, good mucoadhesion, stability, and controlled release properties.

Moreover, this review pointed to the specific requirements of SLN and NLC powders for an ideal pulmonary drug delivery system aimed at targeting lung diseases. For instance, these include biocompatibility, good tolerability, isotonicity, sterility, a neutral pH value, adequate drug loading, protection of the drug from degradation, stability during aerosolization, and good aerodynamic properties.

This review also listed the advantages of the DPI-based spray dryer technique for the delivery of lipid nanoparticle powders through the pulmonary route, such as its portable design, the breath-activated mechanism that eliminates the need for patient hand–mouth coordination, and no propellant necessary.

The preceding studies discussed in this review showcase that pulmonary drug delivery enables the administration of various chemotherapy agents and anti-tuberculosis drugs via spray-dried nanolipid powders, effectively addressing both lung cancer and tuberculosis (TB), respectively. Furthermore, numerous studies have demonstrated the low toxicological potential of lipid nanoparticle powders administered via the pulmonary route.

The field of pulmonary drug delivery is constantly evolving, with new developments and advancements in technology. However, to enhance the effectiveness of such delivery systems, it is imperative to consider the long-term effects of repeated pulmonary administration of lipid nanoparticles. Currently, there is a lack of research in this area, and future studies should prioritize identifying biocompatible excipients to enhance the stability, absorption, and aerosol performance of inhaled biologics. Moreover, particle size and the presence of excipients play a crucial role in enhancing the therapeutic effects and achieving superior targeting of the drug. Therefore, it is essential to consider these parameters while designing inhalation devices for effective drug delivery. While dry powders as inhalable nanoparticles present unique advantages for targeted drug delivery, they also pose potential challenges, particularly in developing device-based dosage forms for pulmonary drug delivery. Currently, there is no perfect device that can undertake pulmonary drug delivery with ease. Hence, it is crucial to design pulmonary drug delivery devices that are small and simple to ensure patient compliance and ease of use. It should be noted that despite the potential benefits of these devices, their absorption, distribution, and protective capabilities are still in the research phase. Therefore, additional safety testing is required before their clinical application. The potential risk of regional toxicity with prolonged usage remains unknown, emphasizing the need for further research in this area. Overall, the pairing of nanotechnology with the design of inhalation devices holds promising potential for the advancement of pulmonary drug delivery systems.

References

1. Labiris, N.R.; Dolovich, M.B. Pulmonary drug delivery. Part I: Physiological factors affecting therapeutic effectiveness of aerosolized medications. *Br. J. Clin. Pharmacol.* **2003**, *56*, 588–599. https://doi.org/10.1046/j.1365-2125.2003.01892.x.
2. Ugalde, P.; Camargo, J.d.J.; Deslauriers, J. Lobes, fissures, and bronchopulmonary segments. *Thorac. Surg. Clin.* **2007**, *17*, 587–599. https://doi.org/10.1016/j.thorsurg.2006.12.008.
3. Castranova, V.; Rabovsky, J.; Tucker, J.; Miles, P. The alveolar type II epithelial cell: A multifunctional pneumocyte. *Toxicol. Appl. Pharmacol.* **1988**, *93*, 472–483. https://doi.org/10.1016/0041-008x(88)90051-8.
4. Gulati, N.; Chellappan, D.K.; MacLoughlin, R.; Dua, K.; Dureja, H. Inhaled nano-based therapeutics for inflammatory lung diseases: Recent advances and future prospects. *Life Sci.* **2021**, *285*, 119969. https://doi.org/10.1016/j.lfs.2021.119969.
5. Gould, G.S.; Hurst, J.R.; Trofor, A.; Alison, J.A.; Fox, G.; Kulkarni, M.M.; Wheelock, C.E.; Clarke, M.; Kumar, R. Recognising the importance of chronic lung disease: A consensus statement from the Global Alliance for Chronic Diseases (Lung Diseases group). *Respir. Res.* **2023**, *24*, 15. https://doi.org/10.1186/s12931-022-02297-y.
6. Ahmad, S.; Manzoor, S.; Siddiqui, S.; Mariappan, N.; Zafar, I.; Ahmad, A.; Ahmad, A. Epigenetic underpinnings of inflammation: Connecting the dots between pulmonary diseases, lung cancer and COVID-19. In *Seminars in Cancer Biology*; Elsevier: Amsterdam, The Netherlands, 2022.
7. Patil, T.S.; Deshpande, A.S. Nanostructured lipid carriers-based drug delivery for treating various lung diseases: A State-of-the-Art Review. *Int. J. Pharm.* **2018**, *547*, 209–225.
8. Naser, A.Y.; Mansour, M.M.; Alanazi, A.F.R.; Sabha, O.; Alwafi, H.; Jalal, Z.; Paudyal, V.; Dairi, M.S.; Salawati, E.M.; Alqahtan, J.S.; et al. Hospital admission trends due to respiratory diseases in England and Wales between 1999 and 2019: An ecologic study. *BMC Pulm. Med.* **2021**, *21*, 356. https://doi.org/10.1186/s12890-021-01736-8.
9. Soriano, J.B.; Kendrick, P.J.; Paulson, K.R.; Gupta, V.; Abrams, E.M.; Adedoyin, R.A.; Adhikari, T.B.; Advani, S.M.; Agrawal, A.; Ahmadian, E.; et al. Prevalence and attributable health burden of chronic respiratory diseases, 1990–2017: A systematic analysis for the Global Burden of Disease Study 2017. *Lancet Respir. Med.* **2020**, *8*, 585–596.
10. Da Silva, A.L.; Cruz, F.F.; Rocco, P.R.M.; Morales, M.M. New perspectives in nanotherapeutics for chronic respiratory diseases. *Biophys. Rev.* **2017**, *9*, 793–803.
11. Nongkhlaw, R.; Patra, P.; Chavrasiya, A.; Jayabalan, N.; Dubey, S. Biologics: Delivery options and formulation strategies. In *Drug Delivery Aspects*; Elsevier: Amsterdam, The Netherlands, 2020; pp. 115–155.
12. Das, S.C.; Khadka, P.; Shah, R.; McGill, S.; Smyth, H.D.C. Nanomedicine in pulmonary delivery. In *Theory and Applications of Nonparenteral Nanomedicines*; Elsevier: Amsterdam, The Netherlands, 2021; pp. 319–354.
13. Mishra, B.; Singh, J. Novel drug delivery systems and significance in respiratory diseases. In *Targeting Chronic Inflammatory Lung Diseases Using Advanced Drug Delivery Systems*; Elsevier: Amsterdam, The Netherlands, 2020; pp. 57–95.
14. Patton, J.S.; Fishburn, C.S.; Weers, J.G. The lungs as a portal of entry for systemic drug delivery. *Proc. Am. Thorac. Soc.* **2004**, *1*, 338–344.
15. Beck-Broichsitter, M.; Schmehl, T.; Seeger, W.; Gessler, T. Evaluating the controlled release properties of inhaled nanoparticles using isolated, perfused, and ventilated lung models. *J. Nanomater.* **2011**, *2011*, 163791. https://doi.org/10.1155/2011/163791.
16. Fei, Q.; Bentley, I.; Ghadiali, S.N.; Englert, J.A. Pulmonary drug delivery for acute respiratory distress syndrome. *Pulm. Pharmacol. Ther.* **2023**, *79*, 102196. https://doi.org/10.1016/j.pupt.2023.102196.
17. Weber, S.; Zimmer, A.; Pardeike, J. Solid Lipid Nanoparticles (SLN) and Nanostructured Lipid Carriers (NLC) for pulmonary application: A review of the state of the art. *Eur. J. Pharm. Biopharm.* **2014**, *86*, 7–22. https://doi.org/10.1016/j.ejpb.2013.08.013.
18. Nafee, N.; Makled, S.; Boraie, N. Nanostructured lipid carriers versus solid lipid nanoparticles for the potential treatment of pulmonary hypertension via nebulization. *Eur. J. Pharm. Sci.* **2018**, *125*, 151–162.
19. Nguyen, V.H.; Thuy, V.N.; Van, T.V.; Dao, A.H.; Lee, B.-J. Nanostructured lipid carriers and their potential applications for versatile drug delivery via oral administration. *OpenNano* **2022**, *8*, 100064. https://doi.org/10.1016/j.onano.2022.100064.
20. Garcês, A.; Amaral, M.; Lobo, J.S.; Silva, A. Formulations based on solid lipid nanoparticles (SLN) and nanostructured lipid carriers (NLC) for cutaneous use: A review. *Eur. J. Pharm. Sci.* **2018**, *112*, 159–167. https://doi.org/10.1016/j.ejps.2017.11.023.
21. Lakhani, P.; Patil, A.; Wu, K.-W.; Sweeney, C.; Tripathi, S.; Avula, B.; Taskar, P.; Khan, S.; Majumdar, S. Optimization, stabilization, and characterization of amphotericin B loaded nanostructured lipid carriers for ocular drug delivery. *Int. J. Pharm.* **2019**, *572*, 118771. https://doi.org/10.1016/j.ijpharm.2019.118771.
22. Kumar, M.; Tiwari, A.; Asdaq, S.M.B.; Nair, A.B.; Bhatt, S.; Shinu, P.; Al Mouslem, A.K.; Jacob, S.; Alamri, A.S.; Alsanie, W.F.; et al. Itraconazole loaded nano-structured lipid carrier for topical ocular delivery: Optimization and evaluation. *Saudi J. Biol. Sci.* **2022**, *29*, 1–10. https://doi.org/10.1016/j.sjbs.2021.11.006.
23. Zasadzinski, J.; Ding, J.; Warriner, H.; Bringezu, F.; Waring, A.J. The physics and physiology of lung surfactants. *Curr. Opin. Colloid Interface Sci.* **2001**, *6*, 506–513. https://doi.org/10.1016/s1359-0294(01)00124-8.
24. Hickey, A.J. Lung deposition and clearance of pharmaceutical aerosols: What can be learned from inhalation toxicology and industrial hygiene? *Aerosol Sci. Technol.* **1993**, *18*, 290–304.
25. Editorial. Let's talk about lipid nanoparticles. *Nat. Rev. Mater.* **2021**, *6*, 99. https://doi.org/10.1038/s41578-021-00281-4.
26. Ghasemiyeh, P.; Mohammadi-Samani, S. Solid lipid nanoparticles and nanostructured lipid carriers as novel drug delivery systems: Applications, advantages and disadvantages. *Res. Pharm. Sci.* **2018**, *13*, 288–303. https://doi.org/10.4103/1735-5362.235156.
27. Wretlind, A. Development of fat emulsions. JPEN *J. Parenter. Enter. Nutr.* **1981**, *5*, 230–235.

28. Schwarz, C.; Mehnert, W.; Lucks, J.; Müller, R. Solid lipid nanoparticles (SLN) for controlled drug delivery. I. Production, characterization and sterilization. *J. Control. Release* **1994**, *30*, 83–96. https://doi.org/10.1016/0168-3659(94)90047-7.

29. Cavalli, R.; Caputo, O.; Carlotti, M.E.; Trotta, M.; Scarnecchia, C.; Gasco, M.R. Sterilization and freeze-drying of drug-free and drug-loaded solid lipid nanoparticles. *Int. J. Pharm.* **1997**, *148*, 47–54. https://doi.org/10.1016/s0378-5173(96)04822-3.

30. Siekmann, B.; Westesen, K. P234 solid lipid nanoparticles stabilized by tyloxapol. *Eur. J. Pharm. Sci.* **1994**, *2*, 177. https://doi.org/10.1016/0928-0987(94)90407-3.

31. Pardeike, J.; Hommoss, A.; Müller, R.H. Lipid nanoparticles (SLN, NLC) in cosmetic and pharmaceutical dermal products. *Int. J. Pharm.* **2009**, *366*, 170–184. https://doi.org/10.1016/j.ijpharm.2008.10.003.

32. Müller, R.; Runge, S.; Ravelli, V.; Mehnert, W.; Thünemann, A.; Souto, E. Oral bioavailability of cyclosporine: Solid lipid nanoparticles (SLN®) versus drug nanocrystals. *Int. J. Pharm.* **2006**, *317*, 82–89. https://doi.org/10.1016/j.ijpharm.2006.02.045.

33. Bunjes, H. Lipid nanoparticles for the delivery of poorly water-soluble drugs. *J. Pharm. Pharmacol.* **2010**, *62*, 1637–1645. https://doi.org/10.1111/j.2042-7158.2010.01024.x.

34. Bhalekar, M.R.; Pokharkar, V.; Madgulkar, A.; Patil, N.; Patil, N. Preparation and evaluation of miconazole nitrate-loaded solid lipid nanoparticles for topical delivery. *AAPS PharmSciTech* **2009**, *10*, 289–296. https://doi.org/10.1208/s12249-009-9199-0.

35. Mäder, K. Solid lipid nanoparticles. In *Handbook of Materials for Nanomedicine*; Jenny Stanford Publishing: Singapore, 2020; pp. 173–206.

36. Yang, Y.; Corona, A.; Schubert, B.; Reeder, R.; Henson, M.A. The effect of oil type on the aggregation stability of nanostructured lipid carriers. *J. Colloid Interface Sci.* **2014**, *418*, 261–272. https://doi.org/10.1016/j.jcis.2013.12.024.

37. Patlolla, R.R.; Chougule, M.; Patel, A.R.; Jackson, T.; Tata, P.N.; Singh, M. Formulation, characterization and pulmonary deposition of nebulized celecoxib encapsulated nanostructured lipid carriers. *J. Control. Release* **2010**, *144*, 233–241. https://doi.org/10.1016/j.jconrel.2010.02.006.

38. Pilcer, G.; Amighi, K. Formulation strategy and use of excipients in pulmonary drug delivery. *Int. J. Pharm.* **2010**, *392*, 1–19. https://doi.org/10.1016/j.ijpharm.2010.03.017.

39. Russell, V. Four challenges for pulmonary drug delivery. *Pharm. Technol.* **2017**, *2017*, s16–s18.

40. Hu, L.; Jia, Y.; Ding, W. Preparation and characterization of solid lipid nanoparticles loaded with epirubicin for pulmonary delivery. *Pharm. Int. J. Pharm. Sci.* **2010**, *65*, 585–587.

41. Li, Y.-Z.; Sun, X.; Gong, T.; Liu, J.; Zuo, J.; Zhang, Z.-R. Inhalable Microparticles as Carriers for Pulmonary Delivery of Thymopentin-Loaded Solid Lipid Nanoparticles. *Pharm. Res.* **2010**, *27*, 1977–1986. https://doi.org/10.1007/s11095-010-0201-z.

42. Muralidharan, P.; Malapit, M.; Mallory, E.; Hayes, D.; Mansour, H.M. Inhalable nanoparticulate powders for respiratory delivery. *Nanomed. Nanotechnol. Biol. Med.* **2015**, *11*, 1189–1199. https://doi.org/10.1016/j.nano.2015.01.007.

43. Capstick, T.G.; Clifton, I.J. Inhaler technique and training in people with chronic obstructive pulmonary disease and asthma. *Expert Rev. Respir. Med.* **2012**, *6*, 91–103. https://doi.org/10.1586/ers.11.89.

44. Heiati, H.; Tawashi, R.; Phillips, N.C. Drug retention and stability of solid lipid nanoparticles containing azidothymidine palmitate after autoclaving, storage and lyophilization. *J. Microencapsul.* **1998**, *15*, 173–184. https://doi.org/10.3109/02652049809006847.

45. Nayak, A.P.; Tiyaboonchai, W.; Patankar, S.; Madhusudhan, B.; Souto, E.B. Curcuminoids-loaded lipid nanoparticles: Novel approach towards malaria treatment. *Colloids Surfaces B Biointerfaces* **2010**, *81*, 263–273. https://doi.org/10.1016/j.colsurfb.2010.07.020.

46. Chen, D.; Liu, J.; Wu, J.; Suk, J.S. Enhancing nanoparticle penetration through airway mucus to improve drug delivery efficacy in the lung. *Expert Opin. Drug Deliv.* **2021**, *18*, 595–606. https://doi.org/10.1080/17425247.2021.1854222.

47. Enlo-Scott, Z.; Backstrom, E.; Mudway, I.; Forbes, B. Drug metabolism in the lungs: Opportunities for optimising inhaled medicines. *Expert Opin. Drug Metab. Toxicol.* **2021**, *17*, 611–625. https://doi.org/10.1080/17425255.2021.1908262.

48. Matthews, A.A.; Ee, P.L.R.; Ge, R. Developing inhaled protein therapeutics for lung diseases. *Mol. Biomed.* **2020**, *1*, 11. https://doi.org/10.1186/s43556-020-00014-z.

49. Abdelaziz, H.M.; Gaber, M.; Abd-Elwakil, M.M.; Mabrouk, M.T.; Elgohary, M.M.; Kamel, N.M.; Kabary, D.M.; Freag, M.S.; Samaha, M.W.; Mortada, S.M.; et al. Inhalable particulate drug delivery systems for lung cancer therapy: Nanoparticles, microparticles, nanocomposites and nanoaggregates. *J. Control. Release* **2018**, *269*, 374–392. https://doi.org/10.1016/j.jconrel.2017.11.036.

50. Leong, E.W.X.; Ge, R. Lipid nanoparticles as delivery vehicles for inhaled therapeutics. *Biomedicines* **2022**, *10*, 2179. https://doi.org/10.3390/biomedicines10092179.

51. Eijkelboom, N.M.; van Boven, A.P.; Siemons, I.; Wilms, P.F.; Boom, R.M.; Kohlus, R.; Schutyser, M.A. Particle structure development during spray drying from a single droplet to pilot-scale perspective. *J. Food Eng.* **2023**, *337*, 111222. https://doi.org/10.1016/j.jfoodeng.2022.111222.

52. Haggag, Y.A.; Faheem, A.M. Evaluation of nano spray drying as a method for drying and formulation of therapeutic peptides and proteins. *Front. Pharmacol.* **2015**, *6*, 146438. https://doi.org/10.3389/fphar.2015.00140.

53. Sosnik, A.; Seremeta, K.P. Advantages and challenges of the spray-drying technology for the production of pure drug particles and drug-loaded polymeric carriers. *Adv. Colloid Interface Sci.* **2015**, *223*, 40–54. https://doi.org/10.1016/j.cis.2015.05.003.

54. Shishir, M.R.I.; Chen, W. Trends of spray drying: A critical review on drying of fruit and vegetable juices. *Trends Food Sci. Technol.* **2017**, *65*, 49–67. https://doi.org/10.1016/j.tifs.2017.05.006.

55. Xu, L.; Wang, X.; Liu, Y.; Yang, G.; Falconer, R.J.; Zhao, C.X. Lipid nanoparticles for drug delivery. *Adv. NanoBiomed Res.* **2022**, *2*, 2100109.

56. Albertsen, C.H.; Kulkarni, J.A.; Witzigmann, D.; Lind, M.; Petersson, K.; Simonsen, J.B. The role of lipid components in lipid nanoparticles for vaccines and gene therapy. *Adv. Drug Deliv. Rev.* **2022**, *188*, 114416. https://doi.org/10.1016/j.addr.2022.114416.

57. Friis, K.P.; Gracin, S.; Oag, S.; Leijon, A.; Sand, E.; Lindberg, B.; Lázaro-Ibáñez, E.; Lindqvist, J.; Whitehead, K.A.; Bak, A. Spray dried lipid nanoparticle formulations enable intratracheal delivery of mRNA. *J. Control. Release* **2023**, *363*, 389–401. https://doi.org/10.1016/j.jconrel.2023.09.031.

58. Samborska, K.; Sarabandi, K.; Tonon, R.; Topuz, A.; Eroğlu, E.; Kaymak-Ertekin, F.; Malekjani, N.; Jafari, S.M. Recent progress in the stickiness reduction of sugar-rich foods during spray drying. *Dry. Technol.* **2023**, *41*, 2566–2585. https://doi.org/10.1080/07373937.2023.2229916.

59. Dormenval, C.; Lokras, A.; Cano-Garcia, G.; Wadhwa, A.; Thanki, K.; Rose, F.; Thakur, A.; Franzyk, H.; Foged, C. Identification of Factors of Importance for Spray Drying of Small Interfering RNA-Loaded Lipidoid-Polymer Hybrid Nanoparticles for Inhalation. *Pharm. Res.* **2019**, *36*, 142. https://doi.org/10.1007/s11095-019-2663-y.

60. LeClair, D.A.; Cranston, E.D.; Xing, Z.; Thompson, M.R. Optimization of Spray Drying Conditions for Yield, Particle Size and Biological Activity of Thermally Stable Viral Vectors. *Pharm. Res.* **2016**, *33*, 2763–2776. https://doi.org/10.1007/s11095-016-2003-4.

61. Binesh, N.; Babaloo, H.; Farhadian, N. Microencapsulation: Spray drying. In *Principles of Biomaterials Encapsulation: Volume One*; Elsevier: Amsterdam, The Netherlands, 2023; pp. 271–296.

62. Davis, M.; Walker, G. Recent strategies in spray drying for the enhanced bioavailability of poorly water-soluble drugs. *J. Control. Release* **2018**, *269*, 110–127. https://doi.org/10.1016/j.jconrel.2017.11.005.

63. Sanchis, J.; Corrigan, C.; Levy, M.L.; Viejo, J.L. Inhaler devices–from theory to practice. *Respir. Med.* **2013**, *107*, 495–502.

64. Buttini, F.; Quarta, E.; Allegrini, C.; Lavorini, F. Understanding the Importance of Capsules in Dry Powder Inhalers. *Pharmaceutics* **2021**, *13*, 1936. https://doi.org/10.3390/pharmaceutics13111936.

65. Falcoz, C.; Oliver, R.; McDowall, J.E.; Ventresca, P.; Bye, A.; Daley-Yates, P.T. Bioavailability of Orally Administered Micronised Fluticasone Propionate. *Clin. Pharmacokinet.* **2000**, *39*, 9–15. https://doi.org/10.2165/00003088-200039001-00002.

66. Islam, N.; Cleary, M.J. Developing an efficient and reliable dry powder inhaler for pulmonary drug delivery—A review for multidisciplinary researchers. *Med. Eng. Phys.* **2012**, *34*, 409–427. https://doi.org/10.1016/j.medengphy.2011.12.025.

67. Shegokar, R.; Müller, R.H. Nanocrystals: Industrially feasible multifunctional formulation technology for poorly soluble actives. *Int. J. Pharm.* **2010**, *399*, 129–139. https://doi.org/10.1016/j.ijpharm.2010.07.044.

68. Xu, Y.; Thakur, A.; Zhang, Y.; Foged, C. Inhaled RNA Therapeutics for Obstructive Airway Diseases: Recent Advances and Future Prospects. *Pharmaceutics* **2021**, *13*, 177. https://doi.org/10.3390/pharmaceutics13020177.

69. Chan, H.-K.; Kwok, P.C.L. Production methods for nanodrug particles using the bottom-up approach. *Adv. Drug Deliv. Rev.* **2011**, *63*, 406–416. https://doi.org/10.1016/j.addr.2011.03.011.

70. Deng, Y.; Zhao, P.; Zhou, L.; Xiang, D.; Hu, J.; Liu, Y.; Ruan, J.; Ye, X.; Zheng, Y.; Yao, J.; et al. Epidemiological trends of tracheal, bronchus, and lung cancer at the global, regional, and national levels: A population-based study. *J. Hematol. Oncol.* **2020**, *13*, 98. https://doi.org/10.1186/s13045-020-00915-0.

71. Shanker, M.; Willcutts, D.; Roth, J.A.; Ramesh, R. Drug resistance in lung cancer. *Lung Cancer Targets Ther.* **2010**, *1*, 23–36.

72. Huang, J.; Deng, G.; Wang, S.; Zhao, T.; Chen, Q.; Yang, Y.; Yang, Y.; Zhang, J.; Nan, Y.; Liu, Z.; et al. A NIR-II Photoactivatable "ROS Bomb" with High-Density Cu_2O-Supported MoS_2 Nanoflowers for Anticancer Therapy. *Adv. Sci.* **2023**, *10*, 2302208.

73. Yang, Y.; Huang, J.; Liu, M.; Qiu, Y.; Chen, Q.; Zhao, T.; Xiao, Z.; Yang, Y.; Jiang, Y.; Huang, Q.; et al. Emerging Sonodynamic Therapy-Based Nanomedicines for Cancer Immunotherapy. *Adv. Sci.* **2023**, *10*, 2204365.

74. Gong, J.; Shi, T.; Liu, J.; Pei, Z.; Liu, J.; Ren, X.; Li, F.; Qiu, F. Dual-drug codelivery nanosystems: An emerging approach for overcoming cancer multidrug resistance. *Biomed. Pharmacother.* **2023**, *161*, 114505. https://doi.org/10.1016/j.biopha.2023.114505.

75. Elzayat, E.M.; Sherif, A.Y.; Nasr, F.A.; Attwa, M.W.; Alshora, D.H.; Ahmad, S.F.; Alqahtani, A.S. Enhanced Codelivery of Gefitinib and Azacitidine for Treatment of Metastatic-Resistant Lung Cancer Using Biodegradable Lipid Nanoparticles. *Materials* **2023**, *16*, 5364. https://doi.org/10.3390/ma16155364.

76. Harisa, G.I.; Sherif, A.Y.; Alanazi, F.K. Hybrid Lymphatic Drug Delivery Vehicles as a New Avenue for Targeted Therapy: Lymphatic Trafficking, Applications, Challenges, and Future Horizons. *J. Membr. Biol.* **2023**, *256*, 199–222. https://doi.org/10.1007/s00232-023-00280-2.

77. Butler, L.M.; Perone, Y.; Dehairs, J.; Lupien, L.E.; de Laat, V.; Talebi, A.; Loda, M.; Kinlaw, W.B.; Swinnen, J.V. Lipids and cancer: Emerging roles in pathogenesis, diagnosis and therapeutic intervention. *Adv. Drug Deliv. Rev.* **2020**, *159*, 245–293. https://doi.org/10.1016/j.addr.2020.07.013.

78. Jyoti, K.; Kaur, K.; Pandey, R.S.; Jain, U.K.; Chandra, R.; Madan, J. Inhalable nanostructured lipid particles of 9-bromo-noscapine, a tubulin-binding cytotoxic agent: In vitro and in vivo studies. *J. Colloid Interface Sci.* **2015**, *445*, 219–230. https://doi.org/10.1016/j.jcis.2014.12.092.

79. Bakhtiary, Z.; Barar, J.; Aghanejad, A.; Saei, A.A.; Nemati, E.; Dolatabadi, J.E.N.; Omidi, Y. Microparticles containing erlotinib-loaded solid lipid nanoparticles for treatment of non-small cell lung cancer. *Drug Dev. Ind. Pharm.* **2017**, *43*, 1244–1253. https://doi.org/10.1080/03639045.2017.1310223.

80. Kaur, P.; Garg, T.; Rath, G.; Murthy, R.S.R.; Goyal, A.K. Development, optimization and evaluation of surfactant-based pulmonary nanolipid carrier system of paclitaxel for the management of drug resistance lung cancer using Box-Behnken design. *Drug Deliv.* **2014**, *23*, 1912–1925. https://doi.org/10.3109/10717544.2014.993486.

81. Nafee, N.; Gaber, D.M.; Elzoghby, A.O.; Helmy, M.W.; Abdallah, O.Y. Promoted antitumor activity of myricetin against lung carcinoma via nanoencapsulated phospholipid complex in respirable microparticles. *Pharm. Res.* **2020**, *37*, 82. https://doi.org/10.1007/s11095-020-02794-z.

82. Kaur, P.; Mishra, V.; Shunmugaperumal, T.; Goyal, A.K.; Ghosh, G.; Rath, G. Inhalable spray dried lipidnanoparticles for the co-delivery of paclitaxel and doxorubicin in lung cancer. *J. Drug Deliv. Sci. Technol.* **2020**, *56*, 101502. https://doi.org/10.1016/j.jddst.2020.101502.

83. Satari, N.; Taymouri, S.; Varshosaz, J.; Rostami, M.; Mirian, M. Preparation and evaluation of inhalable dry powder containing glucosamine-conjugated gefitinib SLNs for lung cancer therapy. *Drug Dev. Ind. Pharm.* **2020**, *46*, 1265–1277. https://doi.org/10.1080/03639045.2020.1788063.

84. Millet, J.-P.; Moreno, A.; Fina, L.; del Baño, L.; Orcau, A.; de Olalla, P.G.; Caylà, J.A. Factors that influence current tuberculosis epidemiology. *Eur. Spine J.* **2012**, *22*, 539–548. https://doi.org/10.1007/s00586-012-2334-8.

85. Pham, D.-D.; Fattal, E.; Tsapis, N. Pulmonary drug delivery systems for tuberculosis treatment. *Int. J. Pharm.* **2014**, *478*, 517–529. https://doi.org/10.1016/j.ijpharm.2014.12.009.

86. Conte, J.E., Jr.; Golden, J.A.; McQuitty, M.; Kipps, J.; Duncan, S.; McKenna, E.; Zurlinden, E. Effects of gender, AIDS, and acetylator status on intrapulmonary concentrations of isoniazid. *Antimicrob. Agents Chemother.* **2002**, *46*, 2358–2364.

87. Prabakaran, D.; Singh, P.; Jaganathan, K.; Vyas, S.P. Osmotically regulated asymmetric capsular systems for simultaneous sustained delivery of anti-tubercular drugs. *J. Control. Release* **2004**, *95*, 239–248. https://doi.org/10.1016/j.jconrel.2003.11.013.

88. Wang, B.; Wang, L.; Yang, Q.; Zhang, Y.; Qinglai, T.; Yang, X.; Xiao, Z.; Lei, L.; Li, S. Pulmonary inhalation for disease treatment: Basic research and clinical translations. *Mater. Today Bio* **2024**, *25*, 100966. https://doi.org/10.1016/j.mtbio.2024.100966.

89. Gaspar, D.P.; Gaspar, M.M.; Eleutério, C.V.; Grenha, A.; Blanco, M.; Gonçalves, L.M.D.; Taboada, P.; Almeida, A.J.; Remuñán-López, C. Microencapsulated Solid Lipid Nanoparticles as a Hybrid Platform for Pulmonary Antibiotic Delivery. *Mol. Pharm.* **2017**, *14*, 2977–2990. https://doi.org/10.1021/acs.molpharmaceut.7b00169.

90. Nemati, E.; Mokhtarzadeh, A.; Panahi-Azar, V.; Mohammadi, A.; Hamishehkar, H.; Mesgari-Abbasi, M.; Dolatabadi, J.E.N.; de la Guardia, M. Ethambutol-loaded solid lipid nanoparticles as dry powder inhalable formulation for tuberculosis therapy. *AAPS PharmSciTech* **2019**, *20*, 120. https://doi.org/10.1208/s12249-019-1334-y.

Chapter 4

Development of Pimozide Spray- dried Lipid Nanoparticles with Enhanced Targeting of Non-small cell Lung Cancer

Arwa Omar Al Khatib[a,b], Mohamed El-Tanani[b], Hisham Al-Obaidi[a*]

[a] School of Pharmacy, University of Reading, Reading RG6 6AD, UK
[b] Faculty of Pharmacy, Al Ahliyya Amman University, Amman 19111, Jordan

Chapter Summary:

In this chapter, the development and evaluation of pimozide-loaded lipid nanoparticles (LNPs) for treating non-small cell lung cancer (NSCLC) are discussed. Using the microemulsion technique, three LNP types—SLN, NLC, and LLC—were synthesized and optimized into fine powders via spray drying. NLCs exhibited the highest encapsulation efficiency, while SLNs had the lowest. NLCs and LLCs demonstrated superior anti-proliferative activity and sustained drug release, highlighting their potential for effective NSCLC treatment.

4.1 Introduction:

Lung cancer continues to pose a health challenge contributing to a substantial number of cancer related deaths. Non-small cell lung cancer (NSCLC) a type, within the spectrum of lung cancers accounts for around 85% of all cases [1]. The complexity of this subtype becomes apparent in advanced stages of diagnosis. Traditional treatment methods like surgery, chemotherapy and radiation therapy often show effectiveness during these stages. With treatments facing constraints there is a growing emphasis on exploring therapeutic approaches. This shift is primarily motivated by the pursuit of less harmful treatment alternatives. Among the emerging strategies gaining attention is drug repurposing, which offers benefits such as quicker and cost effective pathways to clinical implementation due, to the extensive safety and efficacy testing these drugs have already undergone in their original applications [2].

In this context, the use of the antipsychotic drug pimozide (PMZ) has been identified as an option, for repurposing. Recent studies in the field of cancer research have revealed its abilities to combat NSCLC, particularly [3]. The idea that PMZ could be effective in fighting lung cancer cells provides an approach to treatment, which could potentially enhance outcomes for patients dealing with this illness. The shift of PMZ from a medication to a treatment for NSCLC calls for a reconsideration of how it is administered. Originally designed for conditions repurposing pimozide for oncology underscores the importance of drug delivery, especially vital when treating complex diseases like NSCLC. The main obstacle lies in ensuring that PMZ reaches the tumour location effectively maximizing its impact on cancer cells while minimizing side effects commonly linked with widespread distribution of drugs throughout the body. This accomplishment is significant due, to the precision needed to target cancer cells and navigate the environment within tumour sites.

In addressing this challenge, the use of lipid nanoparticles (LNPs) as a delivery mechanism is of a great importance. LNPs offer several advantages, such as enhancing drug solubility, stability, and bioavailability [4]. They provide a protective encapsulation for the drug, preventing against premature degradation and facilitating a more controlled release at the target site [5]. This targeted delivery is especially essential in cancer

treatment to minimize systemic exposure to potent medications, thereby reducing side effects [6]. The consideration of different types of LNPs presents a tailored approach to optimize pimozide's delivery.

Solid Lipid Nanoparticles (SLN) consist of solid lipids and create a stable matrix, conducive for a controlled drug release. Their solid state at body temperature aids in maintaining the integrity of PMZ, ensuring sustained effectiveness. Nanostructured Lipid Carriers (NLC), on the other hand, blend both solid and liquid lipids. This combination yields a more complex matrix, potentially allowing for a higher drug load and a more customized release profile [7], which could be vital for efficiently targeting NSCLC cells. Lastly, we have explored the single use of liquid lipids in nanoparticle formulation referred to as Liquid Lipid Carriers (LLC). This strategy which is primarily composed of liquid lipids, could offer distinct characteristics such as improved drug solubility and potentially quicker release rates. This could be advantageous for rapidly achieving therapeutic concentrations of PMZ at the tumour site. Such level of customization in drug delivery could therefore aid   in advancing the treatment of NSCLC.

Spray drying is widely used for formulating powders of fine particle sizes that are essential for effective lung deposition [8]. When dealing with respiratory diseases like NSCLC, ensuring that the drug reaches the deeper regions of the lungs is necessary for effective treatment [9]. This is where Dry Powder Inhalers (DPIs) become important. DPIs are increasingly favoured in pulmonary drug delivery due to their efficiency in delivering medication directly to the lungs [10]. Using spray drying, PMZ -loaded lipid nanoparticles can be transformed into a fine powder suitable for DPIs. This powder must have the right particle size distribution to ensure deep lung penetration, optimizing the drug's therapeutic effect on lung cancer cells.

The control over particle size, density, and morphology during spray drying is critical [11], as it directly impacts the drug's deposition in the lungs. In the case of PMZ formulations for NSCLC, the use of lipid matrices, such as stearic and oleic acids, and surfactants like Poloxamer 407 and PEG 400, provide the foundational stability [12]. These components help maintain the integrity of the particles and ensure consistent drug release. Additionally, this study introduces the use of stabilizers, such as conventional sugars like

isomalt and trehalose which have been traditionally used as stabilizers, and protectants [13].

4.2 Materials and methods:

4.2.1 Materials

Pimozide, stearic acid, oleic acid, poloxamer 407, PEG 400, and trehalose used in this study were purchased from Sigma-Aldrich- USA. While the methocel E5 (HPMC E5) was obtained from DuPont, Netherlands. Isomalt was purchased from BENEO GmbH, Germany, and OraRez PVM/MA copolymer, an alternating copolymer of methyl vinyl ether and maleic anhydride was obtained from HARKE Pharma GmbH, Germany. Finally, the MTT reagent was purchased from ThermoFisher Scientific, USA, and Dimethyl sulfoxide (DMSO) was obtained from Fisher Bioreagents, USA.

4.2.2 Preparation of lipid nanoparticles with different types of lipids

The microemulsion method was employed to create all lipid nanoparticles using different kinds of lipids. The optimized quantities of all ingredients including PMZ, stearic acid, oleic acid, polymer, and surfactants are indicated in Table 1. Excipients were incorporated at approximately a 5% ratio to serve as stabilizers and protectants [14].

This method combines oil, water, and surfactants, utilizing them to stabilize tiny droplets within another liquid. To prepare Lipid Nano Particles (LNPs), 50 mg pimozide was dissolved in the lipid phase—200 mg stearic acid for Solid Lipid Nanoparticles (SLNs), 100 µL oleic acid for Liquid Lipid Carriers (LLCs), or a combination of 100 mg stearic acid and 100 µL oleic acid for Nanostructured Lipid Carriers (NLCs)—at 85°C. The lipid phase volume was 1 mL. The aqueous phase consisted of 200 mg Poloxamer 407 and 100 µL PEG 400 dissolved in 50 mL water, with the aqueous phase volume being 50 mL. Both phases were heated to 85°C, above their Phase Inversion Temperature (PIT), facilitating the transformation from a microemulsion to a stable nanoparticle dispersion. The phases were then vigorously mixed at this temperature. After cooling, 300 mg HPMC-E5 and 60 mg of one of the excipients (trehalose, OraRez, or isomalt) were added with continuous stirring. The final nanoparticle suspension volume was 50 mL. The concentration of

pimozide in the final feed solution was 1 mg/mL. The resulting nanoparticle dispersion was then spray-dried to obtain the final powder formulation.

4.2.3 Preparation of spray- dried powders

A Büchi mini spray dryer B-290, from Büchi Labortechnik AG in Falwil, Switzerland, was used to transform SLN, NLC, and LLC nanosuspensions into fine dry powders. The process involved feeding the solution into a two-fluid nozzle for spray drying under specific conditions: a nitrogen gas flow of 50 mL/min, an inlet temperature of 120 °C (± 2 °C), an outlet temperature of 70 °C (± 2 °C), a feed flow rate of 2.4 mL/min, and the aspirator blower operating at full capacity.

Table 1: Composition of spray- dried pimozide- loaded lipid microparticles' formulations

	PMZ (mg)	Stearic acid (mg)	Oleic acid (µL)	Poloxamer 407 (mg)	PEG 400 (µL)	HPMC-E5 (mg)	Yield%	Excipients (mg)		
								Trehalose	OraRez	Isomalt
SLN 4	50	200	-	200	100	300	71.3	60	-	-
SLN 5	50	200	-	200	100	300	70.1	-	60	-
SLN 6	50	200	-	200	100	300	69.5	-	-	60
NLC 4	50	100	100	200	100	300	88.8	60	-	-
NLC 5	50	100	100	200	100	300	91.1	-	60	-
NLC 6	50	100	100	200	100	300	88.5	-	-	60
LLC 4	50	-	100	200	100	300	88.5	60	-	-
LLC 5	50	-	100	200	100	300	89.4	-	60	-
LLC 6	50	-	100	200	100	300	87.9	-	-	60

4.2.4 Encapsulation Efficiency (EE%)

To evaluate how well the PMZ was trapped, the LNPs containing PMZ were separated from the LNPs suspension through centrifugation, at 25,000 rpm for half an hour. Following this, 10 mL of the supernatant was mixed with 10 mL of methanol. A 1 mL sample of this mixture was then taken, and the amount of PMZ in this solution was measured using HPLC.

For the spray dried PMZ loaded LNPs, we first dissolved 10 mg of each powder in 10 mL of methanol. Then spun it at 13,000 rpm, for half an hour. After that we filtered the supernatant through 0.22 µm filters. Analysed the PMZ content using HPLC. The analysis was done using a C18 column that was 15 cm long with detection at a wavelength of 270 nm. Our mobile phase for HPLC consisted of 45% acetonitrile, and 55% water with pH adjusted to, around 2.5 using an amount of phosphoric acid. We used an isocratic elution method, with a flow rate of 1mL/min, injection volume of 20 µL, and run time of 10 minutes. Calculated the pimozide concentration based on the Area Under the Curve (AUC) derived from our HPLC data through a calibration curve created by linear regression. The percentage of encapsulation efficiency (EE%) was calculated using a specific formula:[15]

$$EE\% = \frac{Total_{PMZ} - Supernatant_{PMZ}}{Total_{PMZ}} \times 100\%$$

(Equation 2)

4.2.5 Particle size and zeta potential measurements

In this study, the average particle size of the prepared PMZ- loaded LNPs' nanosuspensions and spray- dried powders were determined using the dynamic light scattering (DLS) (a Zetasizer Nano ZS, (Malvern Instruments, UK). For determining zeta potential, the Malvern Zetasizer instrument used in our study employs laser Doppler electrophoresis. This technique analyses the motion of particles under an electric field to determine their surface charge. Briefly, 100-fold dilution of LNP nanosuspensions was prepared using distilled water.

For the preliminary assessments and the stability analysis following a two-month storage period at room temperature (20°C to 25°C) in a desiccator, 5 mg of each spray-dried LNP powder was first re-dispersed in 5 mL of distilled water. A 10 µL sample from this dispersion was further diluted to a final volume of 1000 µL with distilled water. The resulting dispersions were then placed into a glass cuvette and subjected to measurements under controlled conditions, which included a temperature set at 25 °C, a refractive index fixed at 1.33, and a measurement duration of 60 seconds. Average particle size, and zeta potential were performed in triplicate.

4.2.6 Dynamic Vapor Sorption (DVS) measurements

The moisture interaction and physical stability of the pimozide-loaded lipid nanoparticles (LNPs) were investigated using Dynamic Vapor Sorption (DVS) analysis. The DVS experiments were conducted on a Discovery Sorption Analyzer (Discovery SA) system (TA Instruments, USA), equipped with a vertical nulling microbalance. This setup allows for precise control over temperature and humidity conditions, essential for assessing the hygroscopic properties of the LNPs.

The DVS procedure was designed to evaluate the moisture sorption and desorption behaviour of the LNPs under controlled conditions. Initially, the system was equilibrated at 25 °C with a humidity setting of 0 %RH. To ensure the capture of significant moisture interactions, the experiment was programmed to abort the next segment if the percentage weight change was less than 0.01% for a duration of 10.0 minutes.
Following the equilibration, the sample underwent an isothermal hold for 1440.0 minutes (24 hours) to stabilize under the initial conditions. The humidity was then incrementally increased in steps of 10 %RH every 1440.0 minutes, progressing from 0 %RH to 90%RH.

Each humidity step was subjected to the same abort condition if the percentage weight change was less than 0.01% for 10 minutes, ensuring that the measurements reflected meaningful moisture uptake or release. The experiment also included a desorption phase, where the humidity was stepwise decreased from 90 %RH back to 0 %RH under the same

conditions and abort criteria, allowing for a comprehensive analysis of the LNPs' moisture interaction characteristics.

4.2.7 Fourier Transform Infrared spectroscopy (FTIR)

Fourier transform infrared (FTIR) spectra measurements were collected for all spray-dried samples using a Perkin-Elmer Spectrum 100 (Waltham, MA, USA) spectrophotometer, over a scan range of 650–4200 cm^{-1} with an average of 16 scans.

4.2.8 Raman spectroscopic analysis

Separate measurements of the various components constituting the spray-dried LNPs' powders were collected by simply placing a few grains of each sample on a microscope slide and scanned using LabRAM Soleil™ confocal Raman microscope (Horiba Scientific, Kyoto, Japan). The powders were found in the microscope using a low magnification lens and then after switching to a 50X objective a representative location was selected from a full focus ViewSharp™ image.

Spectra were acquired with the 532nm laser, 600 g/mm grating, 50X long working distance lens, 67 mW laser power at the sample and 10 second acquisition time. Measurements were taken at multiple locations to ensure that a representative spectrum was used for each sample. The only exceptions to this were the pimozide sample that was damaged by this high laser power so 17mW was used for a total of 20 seconds to give a comparable signal level. Similarly, the OraRez sample exhibited some fluorescence so a 20 second acquisition was used after illuminating the sample with laser light for 60 seconds to quench the fluorescence. An alternative laser could have been used but the 532 nm was selected to allow direct comparison with the map data.

A ViewSharp™ image was taken and the topography information used to rapidly autofocus at every point on the map. This allowed the system to be used in moderate confocality mode (100 μm pinhole) without any significant variation in signal level. Each map covered a 100 μm by 90 μm area with 1 μm step size. To analyse the maps, multivariate CLS (classical least squares) algorithm was used. The spectra of the

applicable constituents were used as loadings and the fitting coefficients were plotted as maps to show the location of each component.

4.2.9 X- ray powder diffraction (XRPD)

X-ray powder diffraction analysis was carried out using Bruker D8 Advance flat plate powder diffractometer (Bruker AXS GmbH, Germany). The samples were irradiated with copper source radiation (1.54A° angstroms). The data collection was carried from 5.0° to 90.0134° 2theta, 0.27646647° step size at 1.2 seconds per step.

4.2.10 Scanning Electron Microscopy (SEM)

The shape, surface, morphology, and microstructure of the particles were examined using SEM (Scanning Electron Microscopy) (Microscope: FEI Quanta 600 FEG SEM) (FEI Co. Inc., Hillsboro, Oregon). The produced microparticle samples were mounted on aluminium stubs with double-sided adhesive carbon tabs (Leit Adhesive Carbon Tabs 12mm Dia (Pack of 100)-Code: SP12-Supplier: EM Resolutions) (Pin stub 12.5mm (Aluminium) with groove (8mm pin) (pack of 100)-Code: SP12-Supplier: EM Resolutions)-Supplier: Agar Scientific-Code: AGG3347N). Carbon fibre was applied to all samples twice. To gold coat the samples for photos taken under high vacuum, an Edwards Sputter Coater S150B was used. All specimens were then photographed at different magnifications ranging from 100X to 10000X using an accelerating voltage of 20 kV.

4.2.11 Cell culture work and MTT cell viability assay

4.2.11.1 Cell culture

The A549 cancer cell model was used during the course of this study. Those cells were cultured and maintained in a Roswell Park Memorial Institute (RPMI) growth media (Euroclone, Italy) supplemented with 10% Fetal Bovine Serum (FBS) and 1% penicillin/streptomycin (Gibco). The cells were maintained at 37°C and 5% CO_2 in a humidified incubator.

4.2.11.2 MTT cell viability assay

Cell viability was evaluated using the MTT assay. Briefly, A549 lung cancer cells were seeded at a density of 5×10^3 cells per well in a 96-well plate which was subsequently incubated overnight to allow cell adhesion. Next day, cells were treated with various concentrations of PMZ, ranging from 0.3125-200 μM, or equivalent concentrations of each formulation, specifically the formulations that have exhibited a potential antiproliferative activity post the preliminary screening of all formulations, namely NLC4, NLC5, and LLC5, or blank excipients for a duration of 72 hours.

At the designated time point, each well was treated with 0.5 mg/mL of MTT reagent, and the plate was incubated for an additional 3 hours to facilitate the formation of formazan crystals. Subsequently, 100 µL of DMSO was added to each well to dissolve the formazan crystals. Finally, the absorbance was measured at 570 nm using a BioTek Cytation 5 multi-mode plate reader (USA). The results of cell viability were expressed as a percentage relative to the untreated control group.

4.2.12   Drug release study

Three formulations, in particular these having potential IC50 values, were evaluated to assess the PMZ release: NLC4, NLC5, and LLC5. Briefly, 10 mg of each spray-dried formulation was resuspended in 5 mL of simulated lung fluid (SLF) which is composed of (100 mM NaCl, 5 mM KCl, 2 mM CaCl2, 25 mM NaHCO3, 5 mM Na2HPO4, 1 mM NaH2PO4, 1 mM MgCl2 hexahydrate, pH = 7.4).

This suspension was immediately enclosed within a dialysis bag, which was subsequently immersed in a vial containing 20 mL of SLF under constant stirring at 800 rpm at 37°C. To monitor the PMZ release, 1 mL of the SLF containing the released PMZ was extracted from the vial at regular time intervals. Simultaneously, to ensure sink conditions, an equivalent volume of fresh SLF was added back into the system. These collected samples were then analyzed using HPLC utilizing a 5 cm C18 column with detection at 270 nm and an isocratic method comprising a 45:55 acetonitrile: water mobile phase and the cumulative drug release from each formulation was calculated. The release kinetic of free pimozide was also monitored and used as a control.

4.2.13 Statistical analysis

In order to compare the variations, between formulations we used a one-way analysis of variance (ANOVA) with Pythons SciPy library. All statistical analyses were carried out with significance levels set at $*p < 0.05$, $**p < 0.01$, and $***p < 0.001$, with a minimum sample size of $n = 3$.

4.3 Results and discussion

In this study, three types of PMZ-loaded lipid nanoparticles were developed: solid lipid nanoparticles (SLN), nanostructured lipid carriers (NLC), and a unique formulation that only uses liquid lipids, named as liquid lipid carriers (LLC). Spray drying transformed these lipid nanoparticles into a powdered form, causing them to shift from nanoscale to microparticle size. Following this transition, thorough physicochemical analyses of the spray-dried microparticles were conducted.

4.3.1 Encapsulation efficiency of spray dried particles

Figure 1(A) presents the encapsulation efficiency percentages (EE%) of nine spray-dried LNP formulations, highlighting the impact of formulation composition on EE%. Notably, NLC5 achieves the highest EE% at approximately 96%± 1.1%, likely due to the addition of oleic acid, which disrupts the solid lipid's crystalline structure and enhances the lipid matrix's drug entrapment capacity [16]. The incorporation of liquid lipid also aids in preventing drug expulsion, significantly improving EE% compared to SLNs [17]. This improvement is further supported by the reduced particle size in NLC formulations as discussed in Section 3.2, which provides a greater surface area relative to volume, enhancing drug-lipid interactions and stabilization within the formulations.

Conversely, SLN6 shows the lowest EE% at just over 70%± 3.4%, attributed to the rigid and crystalline nature of its solid lipid component, stearic acid, which tends to expel the drug during the cooling phase, thereby reducing EE% [17]. This expulsion of the drug is a common issue in highly ordered crystal lattices, which diminishes encapsulation efficiency [18]. Despite this, other NLC and LLC formulations exhibit significantly higher EE%, emphasizing the crucial role of lipid matrix composition in drug encapsulation. Table 1

indicates that variations within individual formulations (e.g., SLN4, SLN5, SLN6) are mainly due to different excipients used, accounting for only about 5% by weight of the overall formulation, showing a consistent EE% across groups.

The encapsulation efficiency (EE%) data shows that the mean EE% values for SLNs, NLCs, and LLCs are 74.0%, 94.2%, and 93.3%, respectively. This indicates that for SLNs, about 74.0% of the drug is encapsulated within the lipid nanoparticles, while for NLCs and LLCs, the encapsulation efficiency is significantly higher, with 94.2% and 93.3% of the drug being entrapped. High encapsulation efficiency is crucial as it enhances drug stability and protects it from degradation, ensuring sustained release and improved bioavailability. The relatively small percentage of free drug (26.0% for SLNs, 5.8% for NLCs, and 6.8% for LLCs) suggests efficient encapsulation, which minimizes the risk of rapid degradation or premature release, maintaining therapeutic drug levels over an extended period. Thus, achieving high EE% is essential for optimizing the formulation's effectiveness and ensuring the drug's stability and controlled release profile.

Figure 1(B) further compares EE% across different formulations. NLCs show a mean EE% of 94.2%± 2.10%, closely followed by LLCs at 93.3%± 1.00%. An ANOVA test confirms no statistically significant difference between these groups (p-value > 0.05). However, a comparison of SLNs against NLC and LLC groups reveals a notable statistical difference, with SLNs exhibiting a significantly lower mean EE% of 74.0%± 2.50%, underscoring the superior drug encapsulation capabilities of NLC and LLC formulations due to their lipid matrix properties. This finding is supported by previous research [19, 20], showing that incorporating liquid lipid into the matrix, as evidenced by XRPD data in Section 3.5, introduces imperfections into the crystalline structure, thereby increasing the space available for drug encapsulation [16] and preventing drug expulsion.

All types of LNPs experienced a reduction in EE% following spray drying. For SLNs, EE% decreased from 78.0% ± 1.80% to 74.1% ± 2.50%, indicating moderate vulnerability to the thermal and mechanical stresses of the drying process. Similarly, NLCs and LLCs exhibited slight decreases in EE%, with the drying process impacting their EE% minimally. These decreases can be attributed to the rapid evaporation of solvent during drying, altering the solubility and distribution of lipids, often leading to LNPs' aggregation or fusion

and resulting in larger particle sizes with a greater surface area to volume ratio [21]. Additionally, the high temperatures involved in spray drying can alter the lipid composition and induce changes in the crystallinity of lipid components, further compromising the physical stability and integrity of the nanoparticles [22].
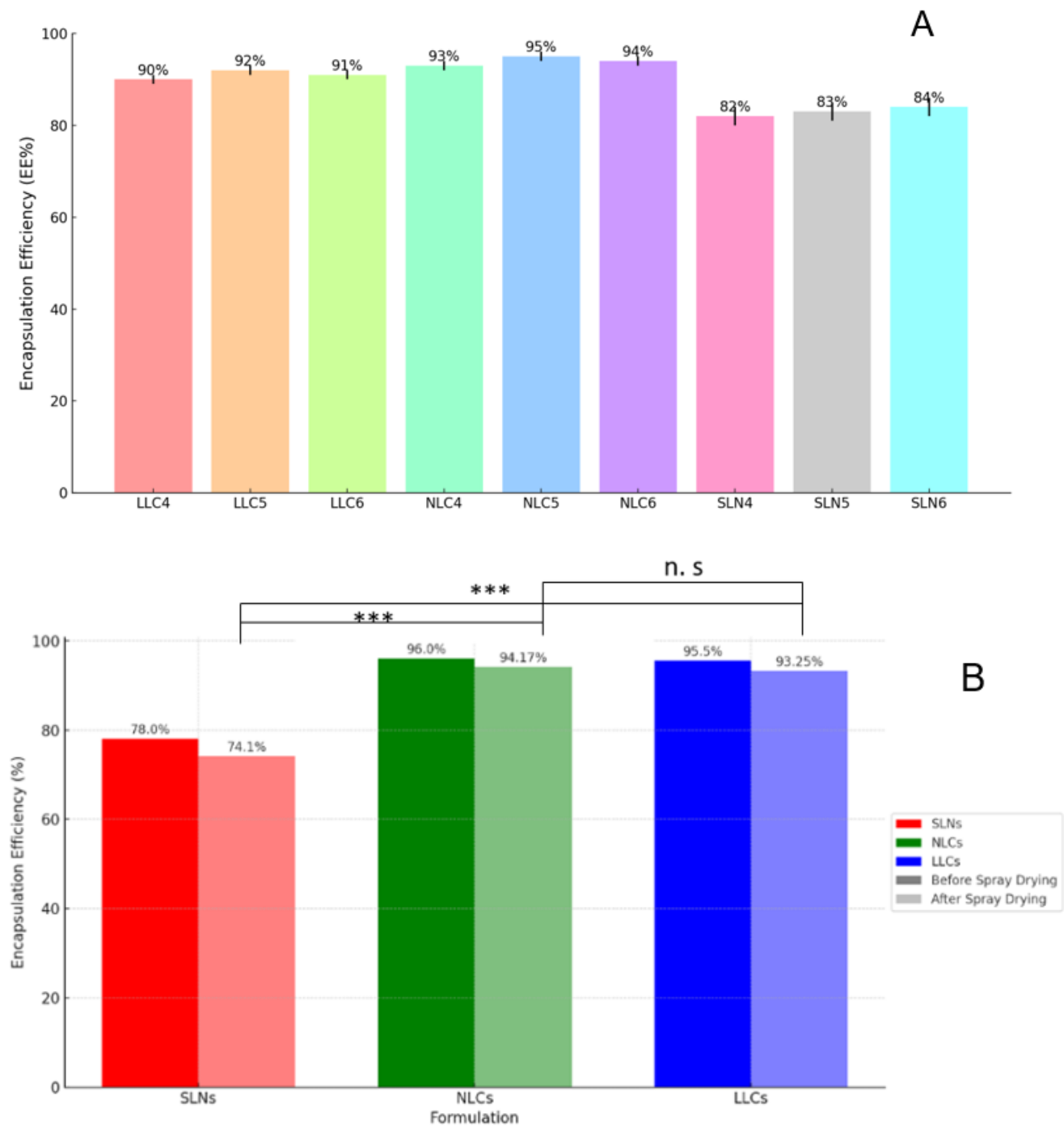
Figure 1. (A) Encapsulation Efficiency (EE%) of nine spray dried lipid nanoparticles (LNPs) with error bars showing the deviation (± SD). **(B)** EE% of three types of LNPs. Solid Lipid Nanoparticles (SLNs) Nanostructured Lipid Carriers (NLCs) and Liquid Lipid Carriers (LLCs). Before and, after spray drying. In the graph SLN formulations are depicted in red, NLC formulations in green, and LLC formulations in blue. Different shades indicate results before and after drying. Statistical significance comparing the encapsulation efficiency between SLN, NLC, and LLC is indicated by one way ANOVA; *$p < 0.05$ **$p < 0.01$ ***$p < 0.001$; "n.s" denotes statistically significant results with a *p* value, above 0.05 and a minimum sample size of n = 3.

4.3.2 Particle size and zeta potential

The impact of spray drying on the particle size of nine PMZ-loaded lipid nanoparticles, classified as SLN, NLC, and LLC, was investigated, with a detailed measurement and analysis of particle sizes before and after spray drying. **Figure 2(A)** reveals notable differences in particle sizes across SLN, NLC, and LLC formulations, largely attributable to the unique lipid characteristics of each. In SLNs, the rigid, crystalline nature of stearic acid may hinder efficient drug encapsulation, resulting in larger or more variably sized particles.

Conversely, NLC formulations, blending stearic and oleic acids, disrupt the crystalline structure, leading to a less perfect lattice that better incorporates PMZ and yields smaller particles. However, spray-dried LLC formulations, due to their pure liquid lipid systems, exhibited larger particles than NLCs. This could be due to lower viscosity, which might promote the coalescence of droplets leading to larger particle sizes. This effect is compounded by the surfactant stabilization possibly being less effective in the uniform liquid lipid phase of LLCs, failing to prevent the growth of larger particles. The absence of solid lipids in LLCs delays nucleation and solidification, allowing more time for particles to grow or coalesce, resulting in the observed larger particle sizes [23].

A significant increase in particle sizes across all formulations post-spray drying is indicated in **Figure 2(A, B)**, where a transition from nano to micro-scale was evident.

Initially, LNPs were within the nano-sized range, represented by minimal red bars, but post-spray drying, depicted by blue bars, there was a pronounced shift to the microparticle range. This increase primarily results from heating-induced phase transitions and aggregation due to particle interactions, indicating a high likelihood of particle aggregation or fusion during drying, influenced by factors such as drying temperature, shear stress, or the physicochemical properties of the lipids and drug [21, 24].

 PMZ-loaded SLNs, predominantly composed of stearic acid, are notably affected during spray drying. The properties of stearic acid, with its higher melting point and rigid structure, lead to significant aggregation and fusion due to melting and recrystallization under spray drying conditions [25].

This effect is particularly pronounced in formulations relying solely on solid lipids. In contrast, PMZ-loaded NLCs, which blend solid stearic acid and liquid oleic acid, experience less particle aggregation and fusion, benefiting from the fluidity of oleic acid. This blend results in a less organized lipid matrix, more effectively encapsulating the drug and limiting particle size growth. Similarly, PMZ-loaded LLCs, solely containing liquid oleic acid, show smaller size increases post-drying due to the highly flexible matrix that better withstands drying.
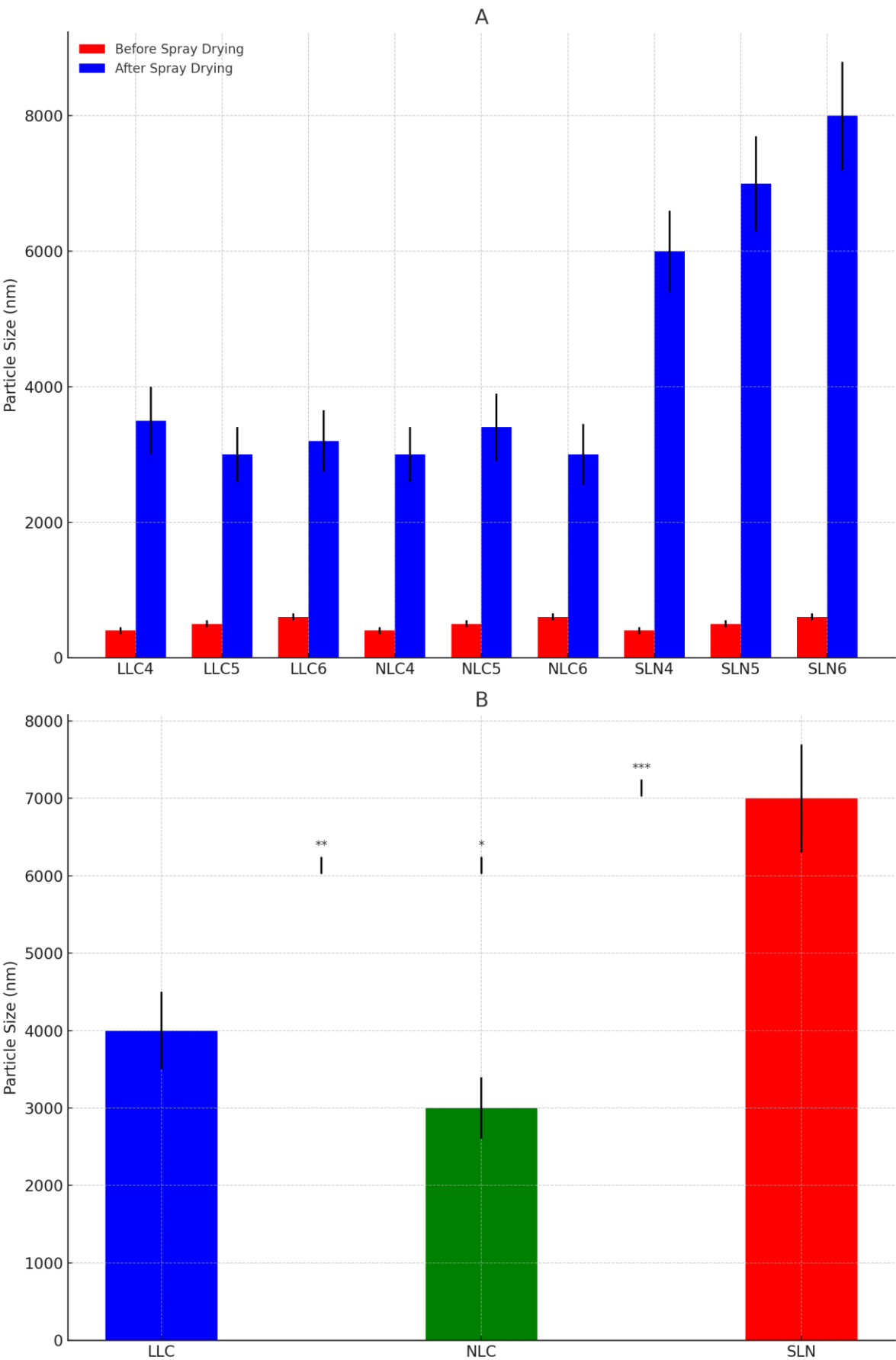
Figure 2. (A) Particle size measurements for nine spray-dried LNPs before and after spray drying, in this visualization, sizes of nanosuspensions are depicted in red, and after spray drying in blue. **(B)** Comparative analysis of particle sizes within three categories of spray-dried LNPs loaded, SLN, NLC, and LLC, along with their mean values and respective significance levels, *$p < 0.05$, **$p < 0.01$, ***$p < 0.001$, with a minimum sample size of n = 3. In the visualizations (B), SLN formulations are represented by red bars, NLC formulations are shown in green, and LLC formulations are highlighted in blue.

The zeta potential of all lipid nanoparticle formulations was found to be negative, influenced by the incorporation of negatively charged stearic acid in the SLN and NLC formulations [26] , and further amplified by the addition of oleic acid in the NLC and LLC formulations [27]. This negative charge is advantageous, especially for targeted therapy in NSCLC, as it can potentially enhance evasion from immune detection, reduce clearance rates, and prolong circulation time in the bloodstream [28].

Figure 3 (A) revealed a statistically significant change in zeta potential across all lipid nanoparticle types of post-spray drying, showing a general decrease in their negative charge. This trend was observed in various formulations, including NLC4, NLC5, NLC6, LLC4, LLC5, LLC6, and SLN4, SLN5, SLN6, indicating that spray drying alters the surface charge characteristics of nanoparticles. The decrease in negative charge could be due to reduced adsorption or degradation of non-ionic surfactant steric excipients at higher temperatures encountered during spray drying, which might result in less effective repulsion between particles [29].

Further analysis, as shown in **Figure 3 (B)**, revealed the post-spray drying zeta potential values for various formulations. SLN formulations had an average zeta potential of -22.0 mV ±8.3 mV, indicating moderate stability but nearing the threshold where particle aggregation might occur due to insufficient electrostatic repulsion. In contrast, NLC formulations exhibited greater stability with an average zeta potential of -33.0 mV ±2.9 mV, reflecting stronger repulsive forces and higher stability. LLC formulations displayed the least negative zeta potential at -14.1 mV ±1.4 mV, suggesting lower stability and a higher propensity for aggregation.
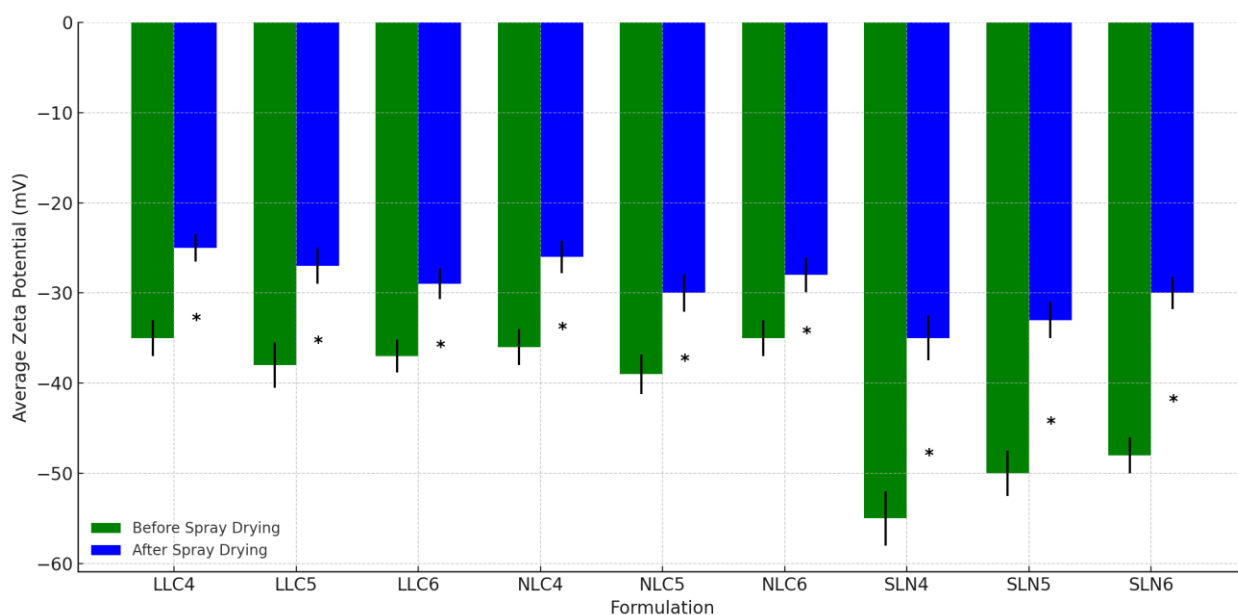
Figure 3. Average zeta potential before and after spray drying nine spray-dried LNPs, *p*-values indicate significant changes in zeta potential due to spray drying. In these visualizations, average zeta potential values before spray drying are depicted in green, and after spray drying in blue.

Stability studies of PMZ-loaded LNPs were conducted by assessing the average particle size and zeta potential after storage at room temperature (20°C to 25°C) in a desiccator for 2 months. The results, displayed in **Figure 4 (A)**, show a trend of maintained or slightly increased particle size, indicating moderate size stability or minor aggregation over time. Specifically, LLC formulations (LLC4, LLC5, LLC6) demonstrated a modest increase in average size, remaining within the standard deviation of initial measurements, suggesting stable nano-systems with slight aggregation.

In contrast, NLC formulations (NLC4, NLC5, NLC6) showed more consistent size stability, attributed to their inhibition of the recrystallization process in solid lipids, maintaining size consistency over the storage period [30]. However, SLN formulations (SLN4, SLN5, SLN6) exhibited a more pronounced size increase, indicating a greater tendency towards aggregation or particle growth, possibly due to lipid crystallization within the SLN structure leading to drug expulsion and increased particle size [31].

Figure 4 (B) presents zeta potential changes post-storage, revealing a notable decrease for LLC formulations (LLC4, LLC5, LLC6), suggesting less stability, likely exacerbated by moisture sensitivity as confirmed by DVS results in Section 3.3. This reduction in zeta potential may also be influenced by the Ostwald ripening effect, where smaller particles dissolve and redeposit onto larger ones, altering particle size distribution and decreasing zeta potential [32]. Conversely, NLC formulations showed minimal changes in zeta potential, maintaining more negative charges and indicating enhanced stability. SLN formulations (SLN4, SLN6), however, saw significant declines in their zeta potential, likely due to particle aggregation affecting the density of surface charge and lowering the negative zeta potential [33].
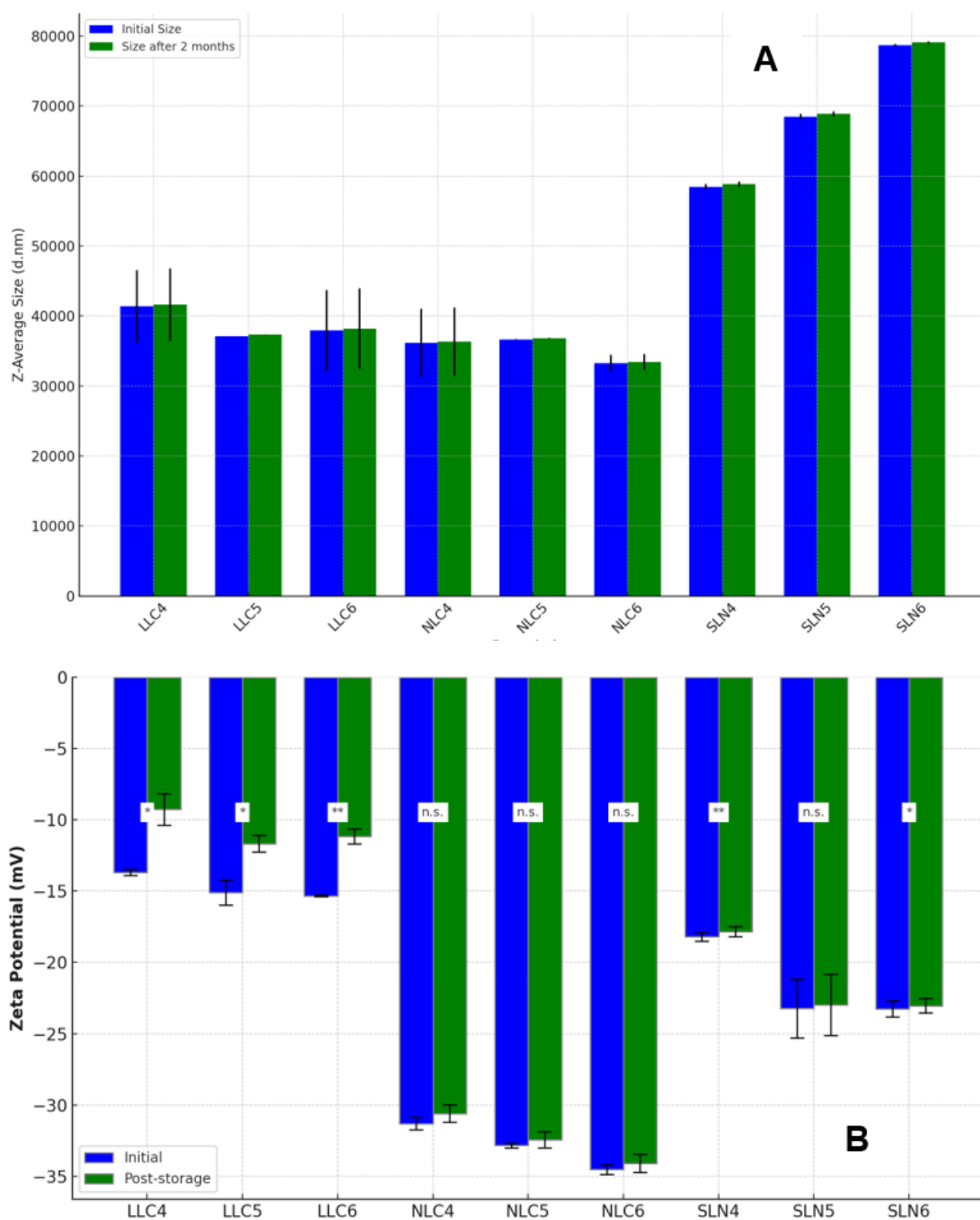
Figure 4. (A) The average size stability of SLN, NLC and LLC formulations before and after storage. Initial sizes are in blue post storage sizes are in green**. (B)** Zeta values

before and after storage. Statistical significance is indicated by $*p < 0.05$ $**p < 0.01$ $***p < 0.001$; "n.s" denotes results without significance ($p > 0.05$). The minimum sample size, for this analysis was n = 3.

4.3.3 Analysis of moisture sorption using Dynamic Vapour Sorption (DVS)

The study investigated the sorption behavior of relative humidity (RH%) across three representative LNP formulations: one solid lipid nanoparticle (SLN), one nanostructured lipid carrier (NLC), and one liquid lipid carrier (LLC). Despite similar encapsulation efficiencies, the sorption trends varied significantly among these formulations due to differences in their lipid compositions. **Figure 5 (A)** details SLN4's gradual and controlled moisture interaction, with a peak weight increase of 35% at high RH levels, indicating diffusion through a denser or less porous matrix. Interestingly, a decrease in sorption during a second cycle at 70% RH suggests potential crystallization within the matrix.

In contrast, NLC5 exhibited a more dynamic response to humidity as depicted in **Figure 5 (B)**. Initially, when RH% increased from 0% to about 80%, NLC5's weight quickly rose, peaking at 12%. This rapid weight gain doubled beyond 80% RH, reaching 25%, reflecting a highly porous internal structure capable of swift moisture adaptation.

LLC5's response, shown in **Figure 5 (C)**, was the most variable, with significant weight fluctuations up to 42% at similar RH levels, indicating a high sorption capacity. This was likely due to its liquid lipid composition, primarily oleic acid, which allows for more mobile and substantial moisture interactions. The pronounced fluctuations during the desorption phase, not mirrored in subsequent cycles, suggest an irregular pore distribution within LLC5, leading to differential rates of moisture absorption and release. This highlights the complex interaction between LLC5's unique composition and environmental moisture, underscoring the distinct sorption characteristics of each LNP type under varying humidity conditions.

The distinct moisture interaction behaviours observed among SLN4, NLC5, and LLC5 formulations can be attributed to their specific lipid compositions and stabilizers. SLN4, comprising only solid stearic acid lipid and trehalose, exhibits a gradual and controlled

moisture interaction, peaking at a 35% weight increase at high RH levels. This suggests diffusion through a denser or less porous matrix, with a decrease in sorption during a second cycle at 70% RH indicating potential crystallization within the matrix. NLC5, which includes a combination of solid stearic acid lipid, liquid oleic acid, and OraRez, shows a more dynamic response to humidity. Its weight rises quickly, peaking at 12% at about 80% RH, and then doubles to 25% beyond 80% RH, reflecting a highly porous internal structure capable of swift moisture adaptation. LLC5, composed of oleic acid liquid lipid and OraRez, exhibits significant weight fluctuations with sorption and desorption being asymmetric, peaking up to 42% at similar RH levels. This high sorption capacity is due to its liquid lipid composition, primarily oleic acid, allowing for substantial moisture interactions. The pronounced fluctuations during the desorption phase suggest an irregular pore distribution within LLC5, leading to differential rates of moisture absorption and release. Therefore, the differences in moisture interaction among the formulations are influenced by both the types of lipids and the stabilizers used, highlighting the complex interplay between these components in determining the overall moisture sorption characteristics.

SLN4: Weight Change and Relative Humidity

NLC5: Weight Change and Relative Humidity
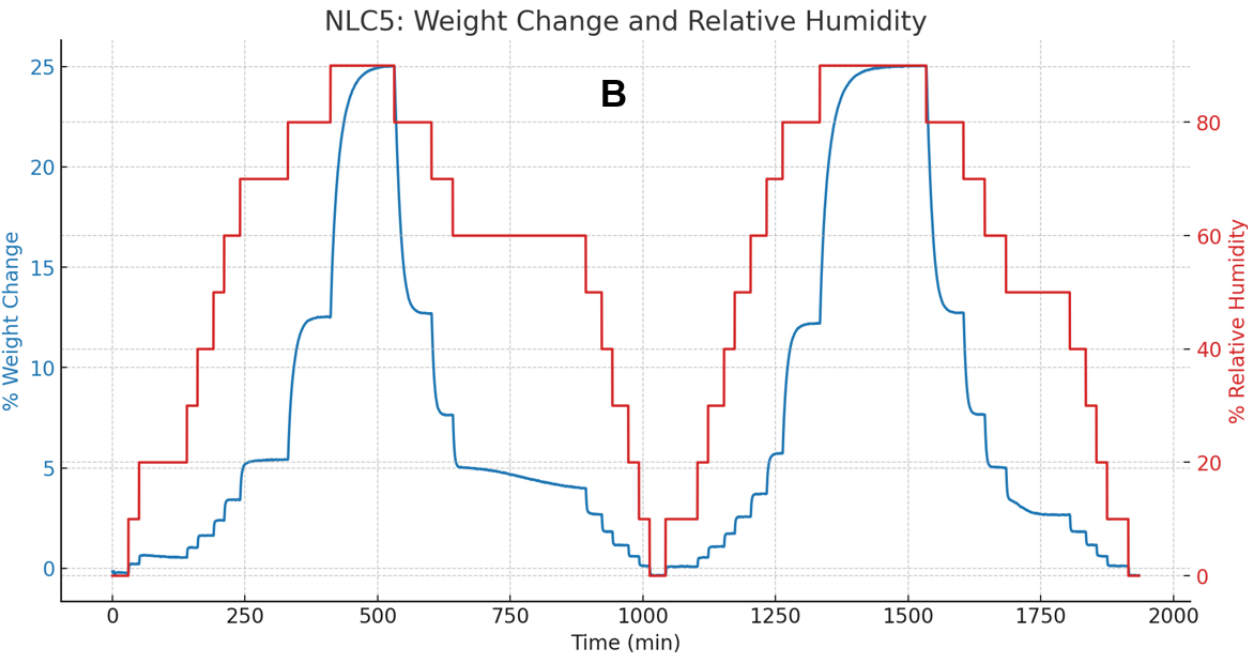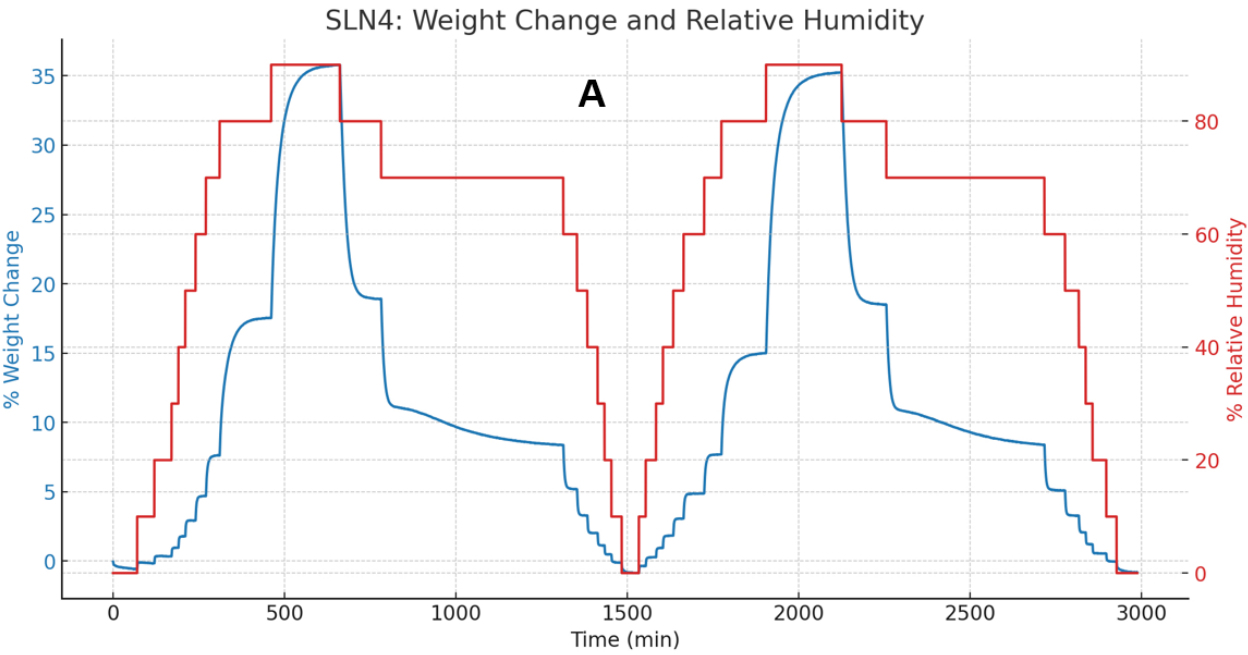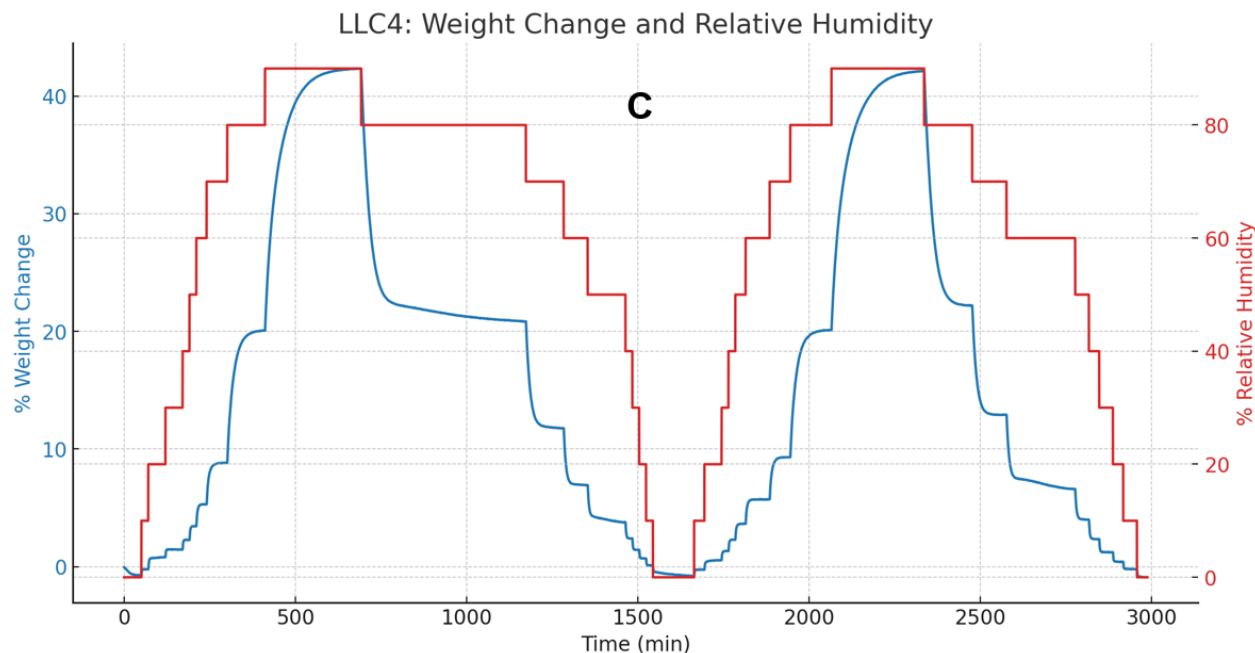
Figure 5. Dynamic Vapor Sorption profiles of various spray-dried LNP formulations, displaying characteristic moisture uptake and release over time for **(A)** SLN4**, (B)** NLC5, and **(C)** LLC4**.** The blue lines represent weight change percentage, and the red lines indicate relative humidity percentage over time.

4.3.4   Fourier Transform Infrared Spectroscopy (FTIR)

The FTIR spectroscopic analysis was performed to identify changes in chemical bonds and verify the encapsulation of PMZ within the spray-dried LNP formulations, revealing characteristic peaks for each compound. For PMZ, sharp peaks at 1697 cm^{-1} indicated C=O stretching, and bands between 1200 and 800 cm^{-1} suggested aromatic ring vibrations, characteristic of the PMZ fingerprint region [34]. Stearic acid's spectrum displayed a carbonyl stretch at about 1695 cm^{-1} and peaks at 2915 cm^{-1} and 2848 cm^{-1} due to aliphatic C-H stretching, representing methylene groups [35]. Oleic acid exhibited a strong carbonyl stretch near 1705 cm^{-1} and aliphatic C-H stretches in the 2850-2950 cm^{-1} range [36]. HPMC-E5 showed a peak at 1052 cm^{-1}, signifying C-O stretching of methoxy groups [37].

In **Figures 6 (A, B, and C)**, all spray-dried SLN, NLC, and LLC formulations demonstrated broadening of bands above 3000 cm^{-1}, suggesting hydrogen bond formation between

PMZ and lipid constituents. Specifically, **Figure 6 (A)** revealed significant changes in PMZ's aromatic C=C stretch at 1480 cm^{-1} and the C-H bending frequencies between 1225-1370 cm^{-1} in SLNs, displaying pronounced broadening and decreased peak intensities. The carbonyl group's C=O stretch at 1697 cm^{-1} also broadened. Stearic acid's characteristic carbonyl stretch shifted from 1690 cm^{-1} to 1700 cm^{-1} in SLNs, showing a decrease in intensity and more diffuse aliphatic C-H stretches. Methylene group vibrations also broadened, indicating potential crystallization or hydrogen bonding effects.

In HPMC-E5 within SLN formulations, a shift in the C-O stretching vibration at 1052 cm^{-1} suggested a disruption in the molecular environment due to hydrogen bonding, further indicated by changes in the C=O stretching environment in **Figure 6 (A)** [38]. This was observed across SLN4, SLN5, and SLN6, pointing to modifications in the electronic environment around PMZ, consistent with an amorphization process and suggesting successful encapsulation by the lipid matrix.

Figure 6 (B) displayed subtle modifications in the carbonyl (C=O) group around 1700 cm-1 and the aromatic C-H bonds at 2958 cm-1 in NLC formulations, indicating changes due to drug interactions with lipid components or reorganization within the NLC structure.

Likewise, **Figure 6 (C)** highlighted changes in LLC formulations, with variations in the intensity and position of the C=O stretching vibration around 1700 cm^{-1} and minor shifts in the aromatic C-C stretching area around 1585 cm^{-1}, suggesting interaction between PMZ molecules and the lipid or polymer matrix, impacting the compound's stability and bioavailability. The interaction between PMZ molecules and the lipid or polymer matrix can significantly enhance the compound's stability by improving its oxidative and hydrolytic stability. Lipid matrices can shield PMZ from oxidative degradation, thereby extending its shelf life and maintaining therapeutic efficacy, while polymers act as barriers against moisture, reducing the risk of hydrolysis and preserving the compound's integrity in aqueous environments. Additionally, the bioavailability of PMZ is enhanced through improved solubility and controlled release mechanisms provided by the lipid or polymer matrices. These matrices can increase the solubility of PMZ, making it more readily available for absorption in biological systems. Moreover, they can enable a sustained

release of PMZ, maintaining steady plasma levels and prolonging therapeutic effects, thus preventing possible toxicity associated with conventional dosing.
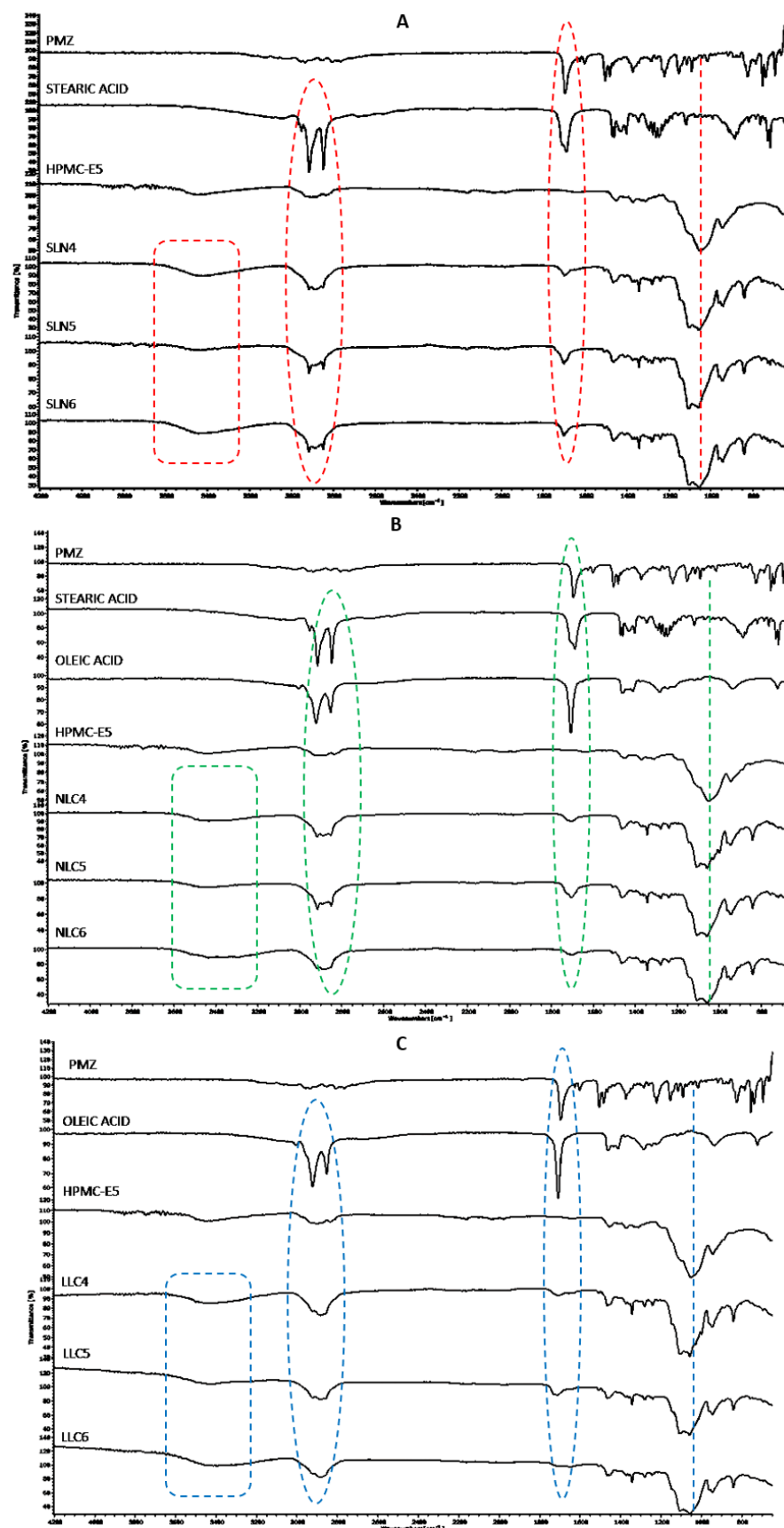
Figure 6. Fourier-transform infrared spectroscopy (FTIR) for three groups: **(A)** SLN4, SLN5, SLN6**, (B)** NLC4, NLC5, NLC6, and **(C)** LLC4, LLC5, LLC6. The graph employs circles and lines to denote variations and frequencies within specific spectral bands, with SLNs spectra highlighted in red, NLCs spectra in green, and LLCs spectra in blue.

4.3.5 Raman spectroscopic analysis

Figure 7 shows different spectra of components used to prepare the formulations. The aim was to use each as a reference to map the surface of the formed particles using Raman confocal microscopy. This analysis provides insight on how different components are distributed and how can they affect dissolution and stability.
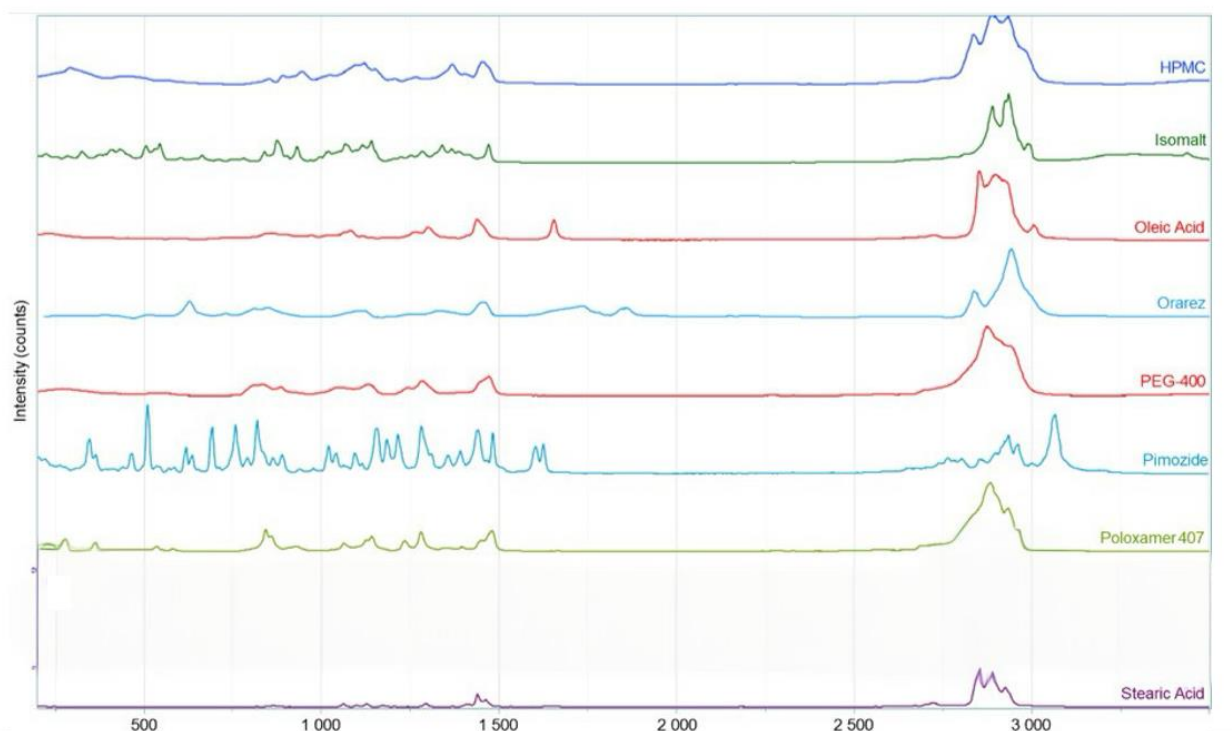
Figure7. Raman spectra for the various components of spray-dried LNPs.

Figure 8 shows that in the specific areas of NLC sample, no pimozide, oleic acid, PEG-400 or OraRez were observed which may indicate that those components did not appear

on the surface. The spatial distribution for the other components is shown below along with the ViewSharp™ white light image at the bottom right. It will be noted that the poloxamer 407 and stearic acid appear to be mainly co-located, suggesting potential interaction.
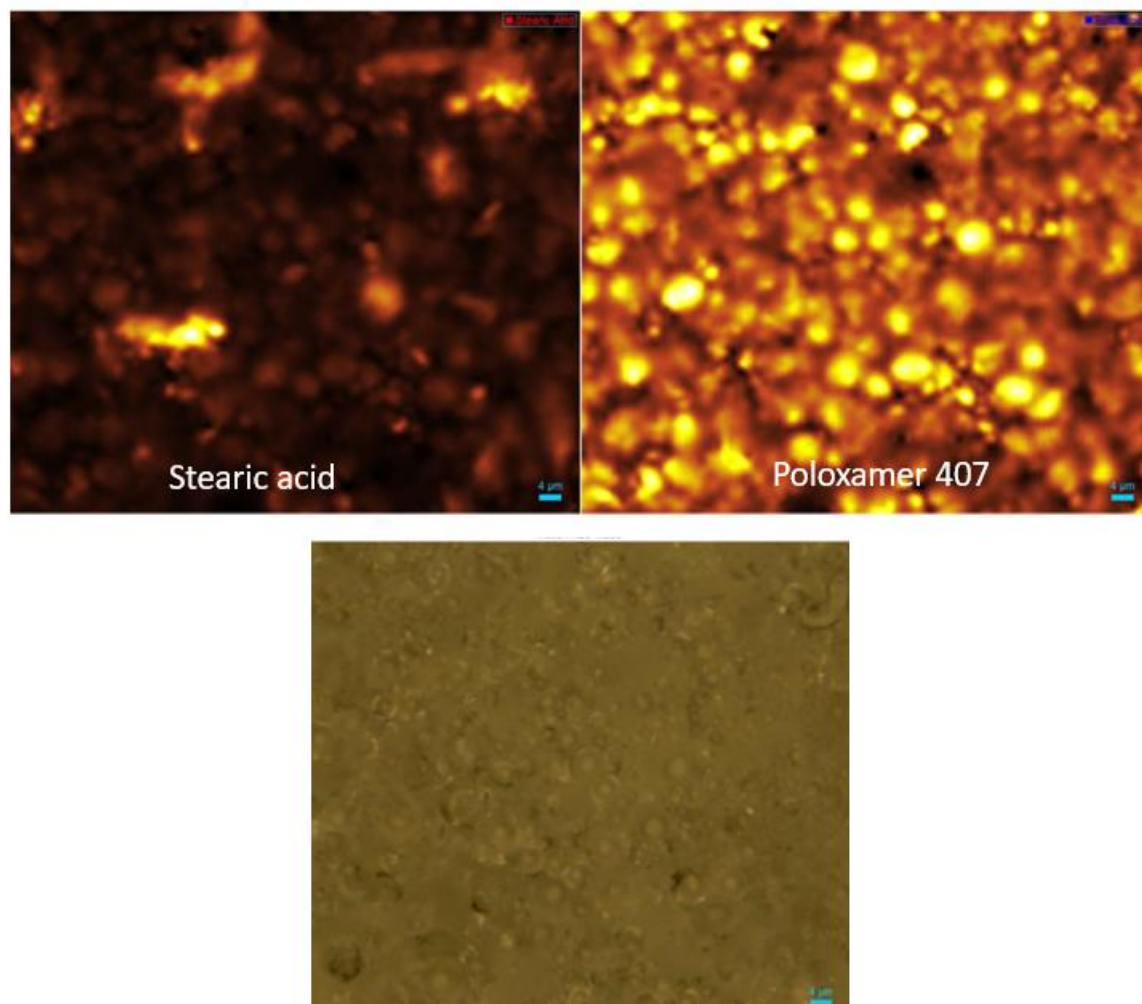
Figure 8. Raman maps illustrating the distribution of stearic acid and poloxamer 407 within the sample. The left image shows the spatial distribution of stearic acid, highlighted by its characteristic Raman signal. The middle image displays the distribution of poloxamer 407, similarly identified by its distinct Raman signature. The bright areas in both Raman maps indicate regions with a higher concentration of the respective substances. The bottom image is a full-focus white light image of the same sample region, providing a visual reference for the overall morphology and aiding in correlating the Raman mapping data

with the physical structure of the sample. Scale bars represent 4 µm for the Raman maps and 5 µm for the white light image.

To form an overall impression of the chemical distribution of the NLC sample, a false colour map (combining all constituents (each constituent is allocated a colour) has been generated **(Figure 9)**. The majority of the grains show as cyan indicating again that the poloxamer (green) and the polymer (blue) are co-located. Individual grains of stearic acid (red) are clearly visible.
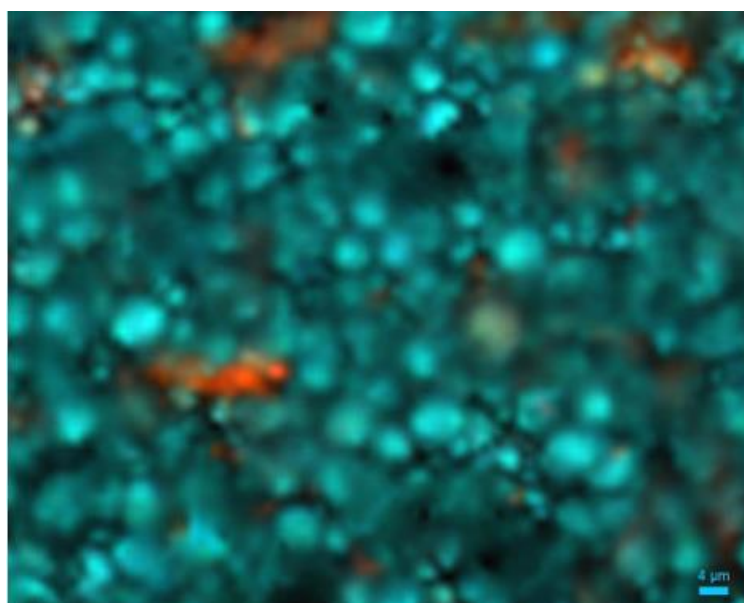
Figure 9. Chemical map illustrating the distribution of constituents in a spray-dried nanostructured lipid carrier (NLC) sample. The map is colour-coded to show the spatial distribution of different components: poloxamer (green) and polymer (blue) are co-located, resulting in most grains appearing cyan. Individual grains of stearic acid (red) are clearly visible, indicating areas where this constituent is concentrated. The scale bar represents 4 µm, providing a reference for the size of the particles.

A comparison was made with an LLC sample to understand the impact of excluding the solid lipid (stearic acid) as can be seen in **Figure 10**. Individual maps of the locations of

the various constituents are shown. The individual grains can be clearly seen. There is evidence that the oleic acid and PEG-400 are co located.
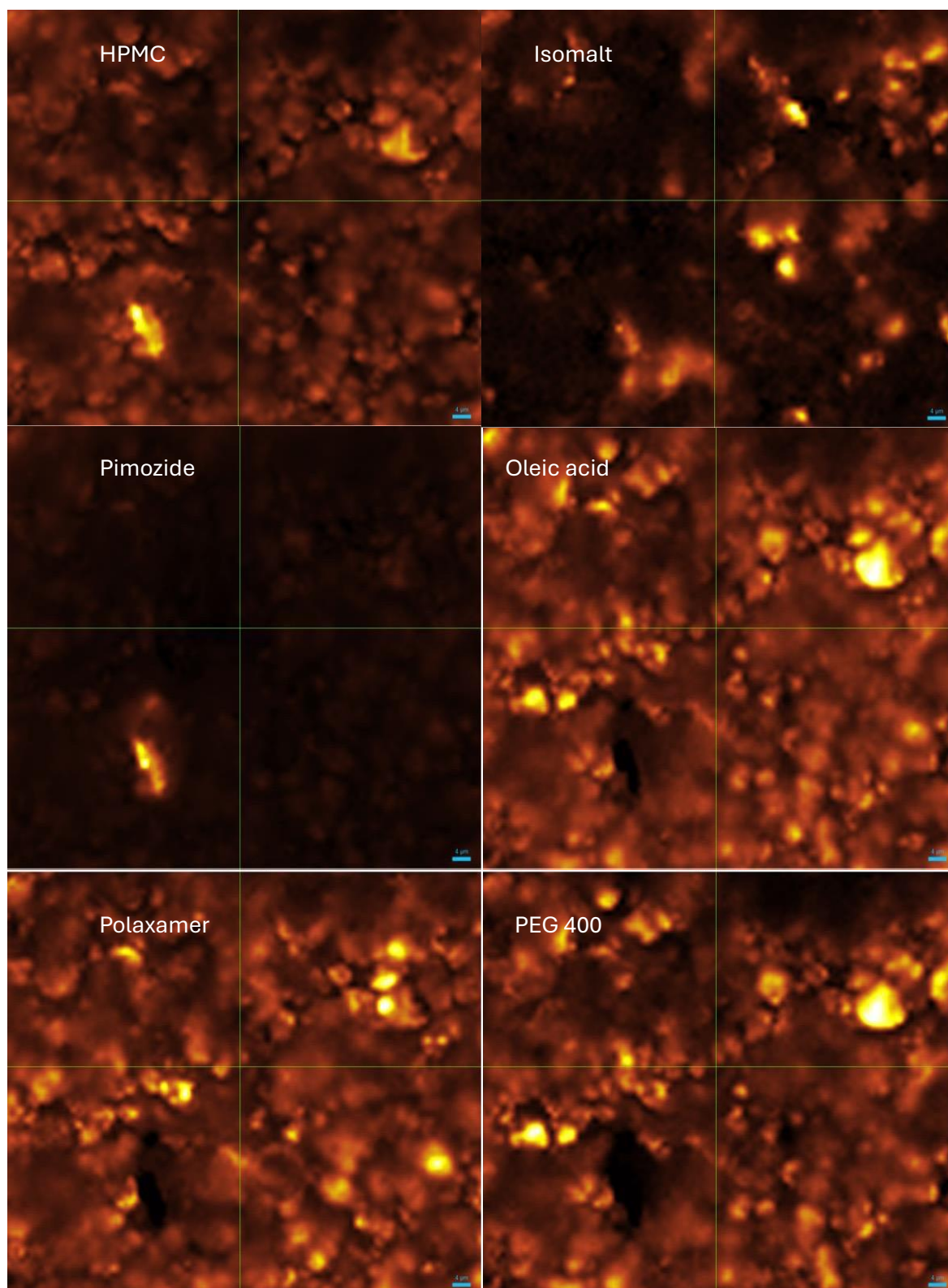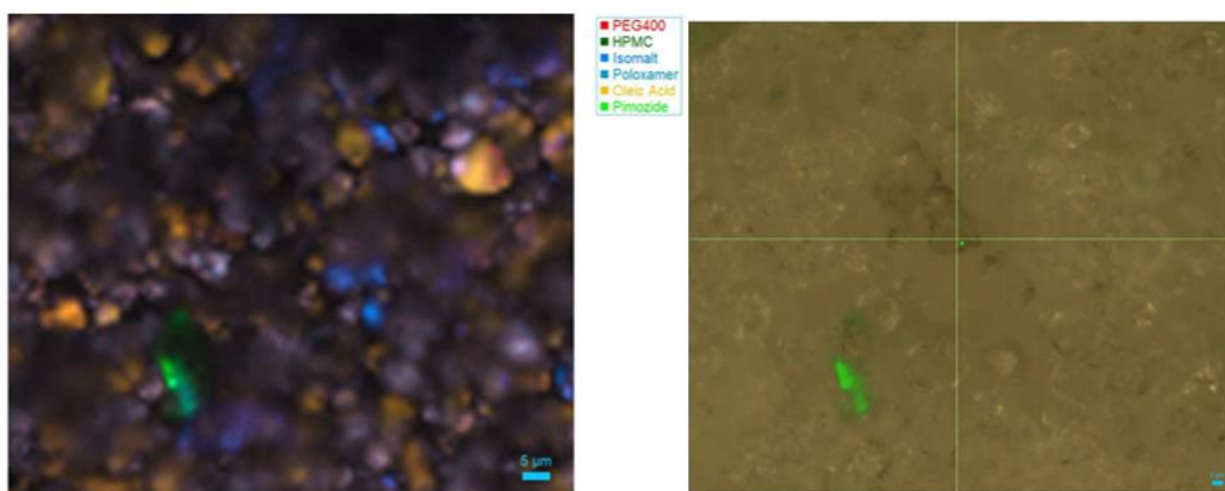
Figure 10. False colour maps illustrating the spatial distribution of various constituents in a spray-dried lipid liquid crystalline (LLC) sample. The images show the distribution of HPMC, isomalt, pimozide, oleic acid, poloxamer 407, and PEG 400. Each map highlights the specific location and concentration of these components within the sample. Bright areas in each map represent regions with a higher concentration of the respective constituent. The scale bar in each image represents 4 µm, providing a reference for the size of the observed features. These maps help visualize the co-localization and distribution patterns of the different compounds within the spray-dried matrix.

To get an overall impression of the chemical distribution, a false colour map (combining all constituents (each constituent is allocated a colour) has been generated as shown in **Figure 11**. It is also possible to overlay the false colour map of one or all constituents on the white light image. **Figure 11** shows the location of the pimozide relative to the white light image. The power of Raman spectroscopy is highlighted by the lack of obvious correlation with the white light image. The white light image cannot be used alone to identify the location of the drug particles.

Figure 11. False colour chemical map and overlay illustrating the distribution of various constituents within a spray-dried lipid liquid crystalline (LLC) sample. The left image presents a false colour map where different colours represent distinct constituents: PEG 400 (red), HPMC (purple), isomalt (blue), poloxamer (cyan), oleic acid (yellow), and

pimozide (green). This map visualizes the spatial distribution and co-localization of these components within the sample. The right image shows an overlay of the location of pimozide (green) relative to the white light image of the same region, providing a visual correlation between the chemical map and the sample's physical structure. The scale bar represents 5 µm.

Overall, the distribution of all the constituents was clearly observed. The silicon measurement showed that the background in the zoomed region is due to photoluminescence within the silicon, not a measurement artefact. To avoid any confusion, the data presented has not been baselined, smoothed, or subjected to any other form of data processing.

In this study, Raman spectroscopy was utilized to analyze both the structural and chemical properties of spray-dried LNPs, focusing on how oleic acid disrupts the lipid matrix to enhance EE%, supported by XRPD results documented in Section 3.6. This technique generated detailed false-color chemical maps that depicted the spatial co-localization of oleic acid and PEG-400, crucial for boosting drug loading capabilities. Furthermore, Raman maps pinpointed the presence of poloxamer 407, HPMC, and pimozide, demonstrating the method's exceptional capacity to reveal molecular arrangements not visible through traditional white light imaging.

Additionally, consistent with the changes noted in the FTIR analysis from Section 3.4, which showed interactions between the drug PMZ and various components of the lipid or polymer matrix, Raman spectroscopy provided detailed chemical maps. These maps clearly displayed how oleic acid and PEG-400 are co-located. The maps, using false-colours, outlined how PMZ, oleic acid, poloxamer 407, PEG-400, HPMC, and isomalt are distributed. They confirmed the presence of PMZ and all other ingredients in the spray-dried LNP sample, demonstrating that oleic acid was deliberately added to modify the lipid matrix, thus enhancing the drug's loading capacity and stability.

Moreover, the Raman maps for the NLC sample showed substantial co-localization of poloxamer and the polymer, suggesting possible molecular interactions that were not detectable on the surface, as evidenced by the absence of PMZ, oleic acid, PEG-400, and

OraRez in specific areas. The analysis of the LLC sample further reinforced the concept of increased molecular interactions within the more amorphous structures, as indicated by the XRPD data, through the observed co-location of oleic acid and PEG-400.
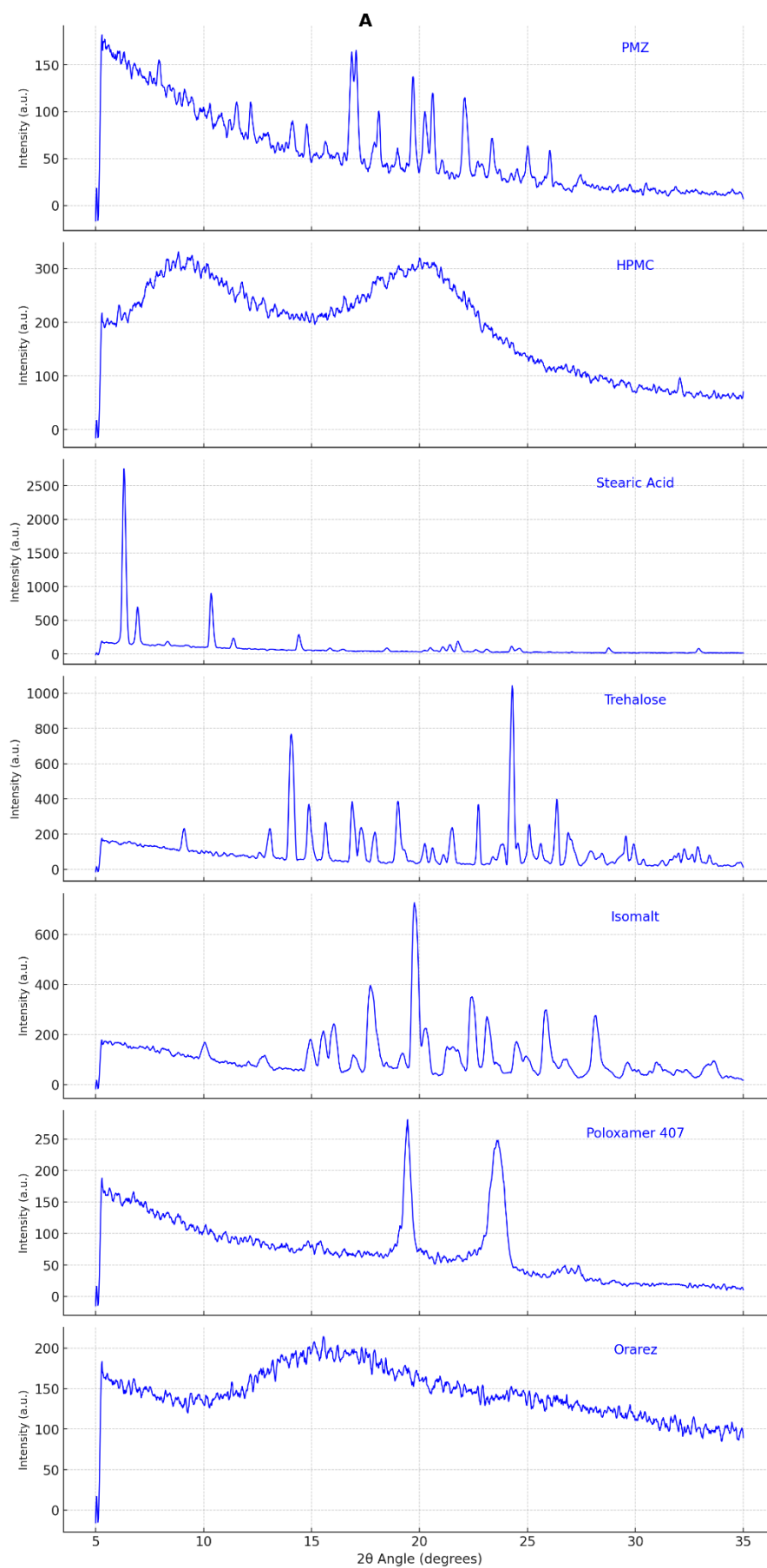
4.3.6 X-ray powder diffraction (XRPD)

XRPD analysis were conducted to assess how various components, affect the structural arrangement of nine spray-dried lipid nano formulations. The diffraction patterns of these formulations, which utilized stearic and oleic acids as solid and liquid lipids, respectively, are displayed in **Figure 12**. The analysis of pimozide's crystalline structure, as revealed through X-ray diffraction patterns, highlighted several prominent peaks that underscore its distinct molecular arrangement. Notably, a prominent peak at 2-theta value around 5˚ exhibited an intensity of 196. Additional peaks of equal intensity 187 were observed at 2-theta positions ranging between, 5˚ and 6˚. Furthermore, the analysis identified other important peaks located at 2-theta values of 16˚, 17˚, 19˚, and 20˚. In the diffraction patterns of stearic acid, major peaks at 2-theta values of around 6˚ and 10˚ were identified as characteristic of stearic acid.

Additionally, the observation of two peaks at 2-theta values of 19˚ and 23˚ suggested the presence of poloxamer 407, possibly located on the surface of all SLN, NLC, and LLC samples. The XRPD patterns presented in **Figure 12** revealed varying degrees of amorphization across the different spray-dried LNPs, with the order being LLC>NLC>SLN in terms of amorphous content. SLNs had sharper, more intense peaks, indicating increased crystallinity due to enhanced molecular ordering within the lipid matrix [39]. **Figure 12 (A)** revealed the highest degree of crystallinity in the structures of SLN formulations. Where they kept the crystal pattern of PMZ and poloxamer- 407, with many peaks, showing that PMZ's crystal structure was mostly present within the spray-dried SLN samples.

NLCs displayed a trend towards more amorphous structures, possibly as a result of the mixed lipid matrix interfering with crystal lattice and causing structural defects from nano-sizing, and crucial lipid matrix interactions [40]. **Figure 12 (B)** showed that NLC

formulations appeared to undergo more significant transformations, potentially leading to a mix of crystalline and amorphous structures.

In contrast, the LLC nanoparticles exhibited decrease in peak intensity and a pronounced shift towards amorphous structures, attributed to a more disrupted lipid matrix, potentially due to the sole use of oleic acid. **Figure 12 (C)** revealed that PMZ and its LLC formulations showed broader peaks with much reduced intensities, suggesting a decrease in crystallinity due to PMZ dispersion.
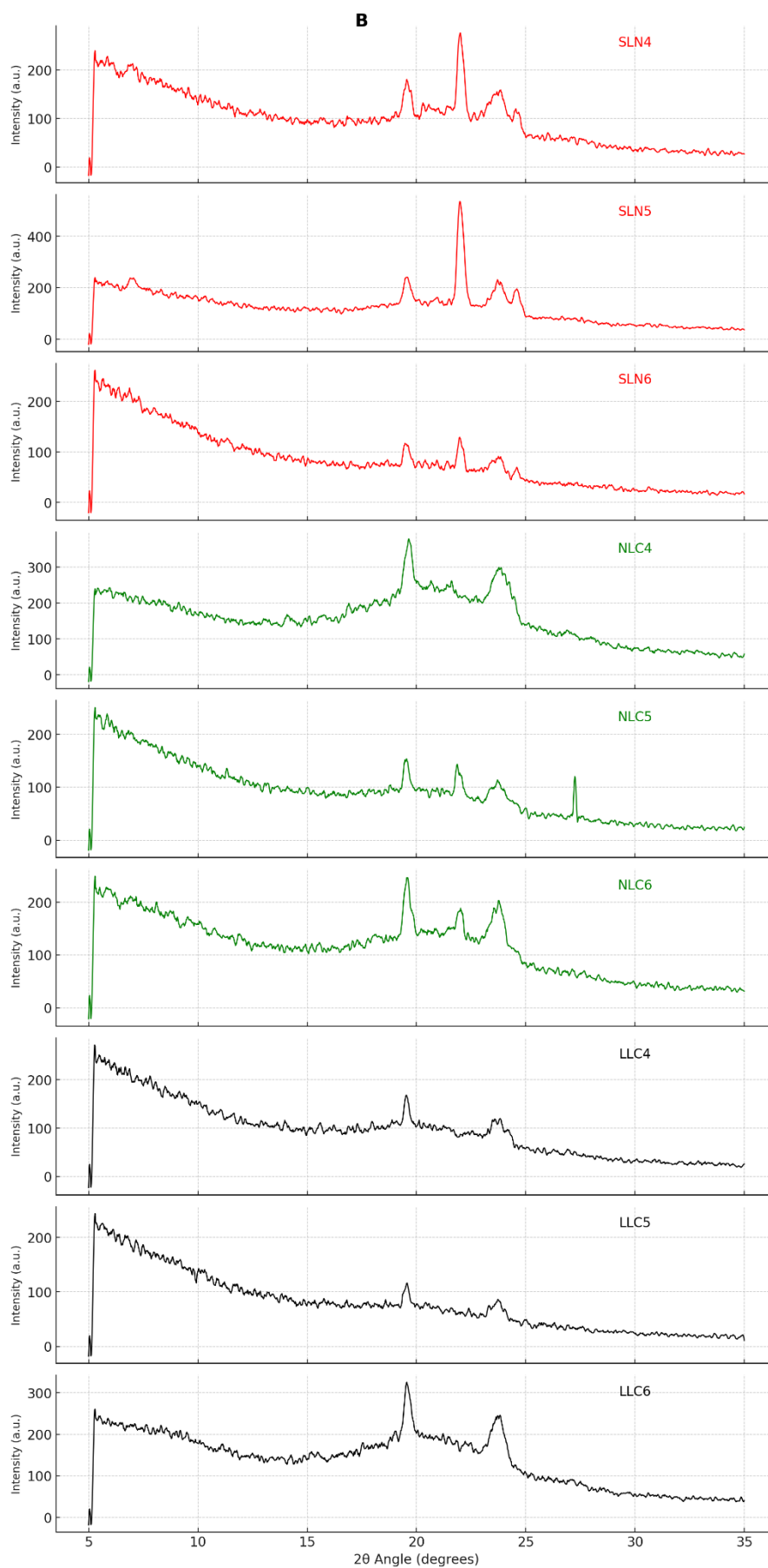
Figure 12. X-ray powder diffraction (XRPD) patterns of **(A)** pimozide (PMZ), HPMC-E5, stearic acid, trehalose, isomalt, and poloxamer 407, OraRez. **(B)** Spray-dried LNPs, including Solid lipid nanoparticles (SLNs) in red, Nanostructured lipid carriers (NLCs) in green, Liquid lipid carriers (LLCs) in black.

4.3.7 Surface morphology

A key finding from the SEM images, as depicted in **Figure 13 (A, B, and C)**, is that each formulation experienced size growth after spray drying, transforming from nanoparticles to microparticles. This increase in size might have resulted from the nanoparticles aggregating or fusion during the spray drying process [21, 24].

SEM images of SLN4 showed a mix of spherical particles and large lipid aggregates, while NLC5 displayed clusters that could be attributed to either shrinkage from drying or the concentration of the dispersion medium. **Figure 13 (A)** showed nanoparticles with a predominantly rounded morphology and a relatively smooth surface, with minor wrinkles and indentations [41, 42]. Notably, the smoother surface texture of SLN4, compared to NLC5 and LLC4, along with the presence of micro-wrinkles, could diminish particle cohesion, thus improving dispersibility. The incorporation of trehalose in SLN4 is believed to provide a glassy surface to the particles, further reducing stickiness and enhancing flowability [43].

NLC5 particles in **Figure 13 (B**) were distinguished by a mix of large, flake-like structures and smaller, rounded particles with irregular sizes and collapsed sides, a characteristic of spray-dried particles. Such variations in shape are suggested to result from the interaction dynamics between stearic and oleic acids during spray-drying. The surface roughness observed in NLC5 could potentially lower effective density and improve air suspension, crucial for consistent dose delivery.

SEM images of LLC4 in **Figure 13 (C)** revealed a non-spherical shape with a wrinkled, rough texture. The rough surface could reduce particle cohesion, essential for preventing aggregation and ensuring uniform particle dispersion during aerosolization and deep lung

delivery [44]. The aggregation tendency observed could impact aerosolization efficiency and respiratory tract deposition. However, the inclusion of trehalose was expected to stabilize the particles and aid in de-aggregation upon inhalation, enhancing dispersibility and deep lung penetration [43].

The observed morphologies in the SEM images can be attributed to the lipid composition, stabilizers, and the spray-drying process. For SLN4, the solid lipid crystallizes upon cooling, forming a relatively uniform and crystalline structure, with trehalose acting as a stabilizer that provides a glassy surface, reducing stickiness and enhancing flowability. In NLC5, the combination of solid and liquid lipids disrupts the crystalline lattice, leading to heterogeneous and less ordered structures with phase separation features. The OraRez stabilizer contributes to surface roughness, which can lower effective density and improve air suspension. For LLC4, the exclusive use of liquid lipids results in a highly irregular and amorphous structure due to the absence of crystallization, with trehalose helping to stabilize the particles and prevent aggregation. These variations in lipid composition and the role of stabilizers during the spray-drying process are key to understanding the distinct particle morphologies observed in the SEM images.
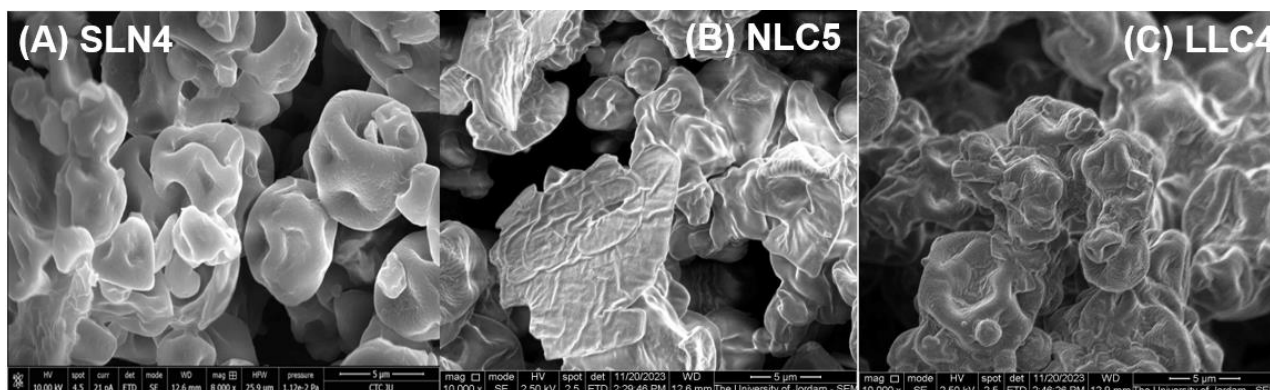

Figure 13. SEM images of SLN4, NLC5, and LLC4 spray-dried LNPs

4.3.8 Evaluating the anti-proliferative activity of pimozide loaded lipid nanoparticles against A549 cells

After conducting experiments, on nanoparticles containing PMZ and observing their impact on halting the growth of lung cancer cells, we utilized the MTT assay to assess

their ability to inhibit cell proliferation. NLC 4 NLC 5 and LLC 5 emerged as promising candidates among the tested formulations due to their effectiveness in impacting cell growth. The results of the MTT assay indicated that these spray dried LNP formulations were more successful than PMZ in impeding cell line growth. Specifically, NLC 4 showed an IC50 value of 8.00 µM (±0.94 µM) NLC 5 had a value of 7.52 µM (±1.20 µM). LLC 5 had a value of 9.39 µM (±1.16 µM) compared to PMZs IC50 value of 13.27 µM (±0.41 µM) as illustrated in Figure 14. These results align with studies conducted by Li et al. (2020) Wiklund et al. (2010). Dakir et al. (2018) that reported IC50 values, for PMZ [3, 45, 46].

To verify that the slowdown, in cell growth caused by the formulations stemmed from PMZ alone and not from the components we examined how the excipients impacted cell growth. Our experiments revealed that at a concentration of 1 mg/mL the excipients did not hinder the growth of cells in a lab setting. This observation backs the notion that it's indeed the PMZ content, rather than the excipients that is responsible, for the anti-proliferative effect of the formulation.

Statistical analysis of IC50 values indicated that the difference between the spray-dried LNP formulations and free PMZ was statistically significant as elucidated in **Figure 15**. The superior anti-proliferative performance of PMZ when formulated into nanoparticles as opposed to its free form could be attributed to improved cellular penetration and solubility [47]. The challenge of poor water solubility and limited bioavailability, common to many anticancer drugs including PMZ, often negatively impact their therapeutic efficacy [48]. The strategy of nanoparticle encapsulation not only seeks to increase solubility but also to enhance the drug's anti-proliferative effect.

An example of such enhancement in solubility and bioavailability through nanoparticle technology is Doxil®, a liposomal formulation of doxorubicin, which ensures effective drug delivery to tumor sites while reducing cardiotoxicity [49]. Furthermore, nanoparticles may increase the penetration of drugs into cancer cells, facilitating the release of the encapsulated drug to intracellular targets and thus enhancing its therapeutic effect. This concept is supported by findings from Swidan et al. (2016), who noted an increase in tumor cell penetration and cytotoxicity of paclitaxel when formulated into NLC [27]. However, these attributes need to be further investigated.
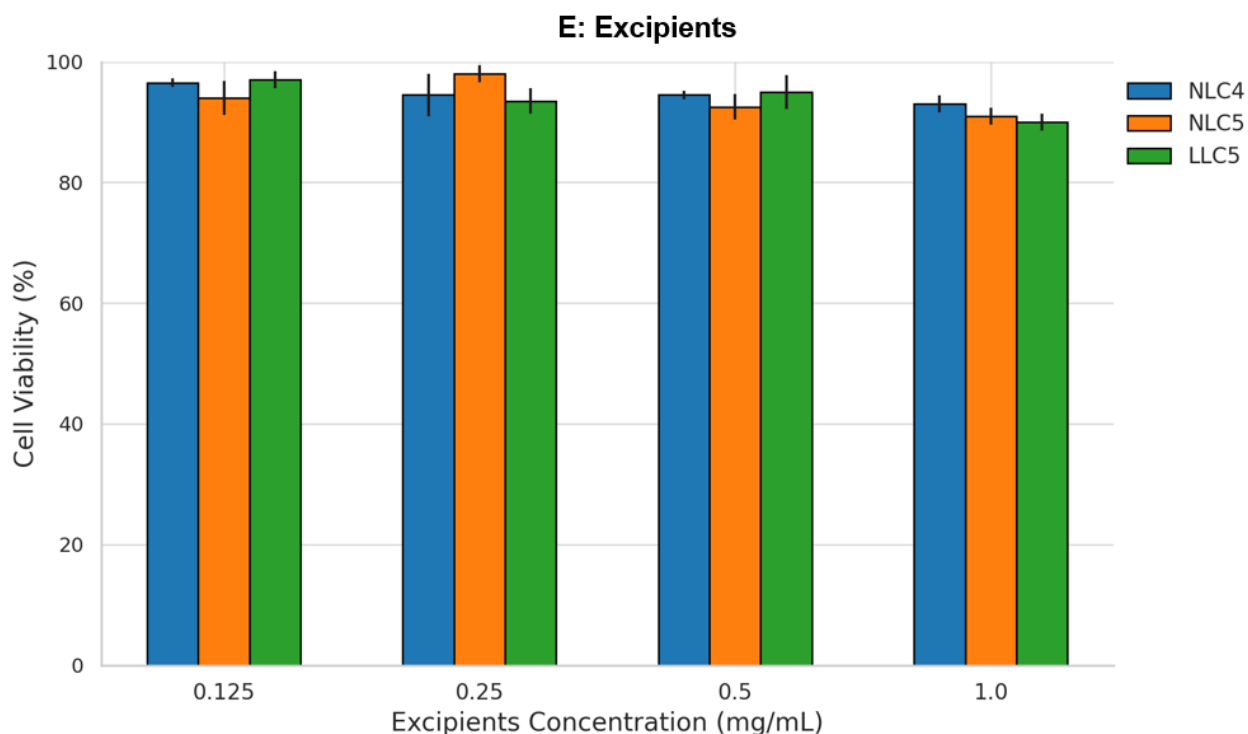
A: Free Pimozide

IC50: 13.27 µM

B: NLC4

IC50: 8.0 µM

C: NLC5

IC50: 7.52 µM

D: LLC5

IC50: 9.39 µM
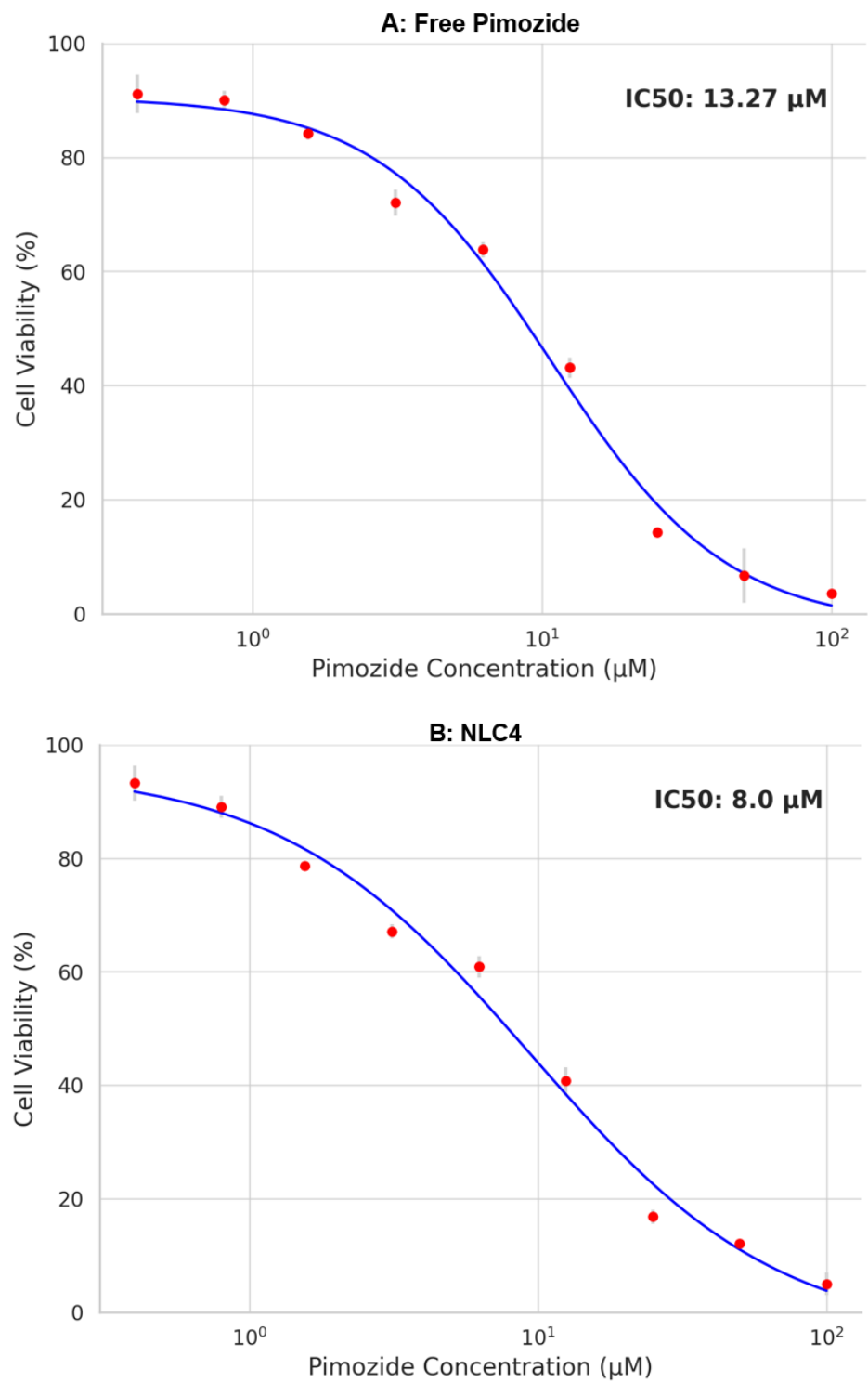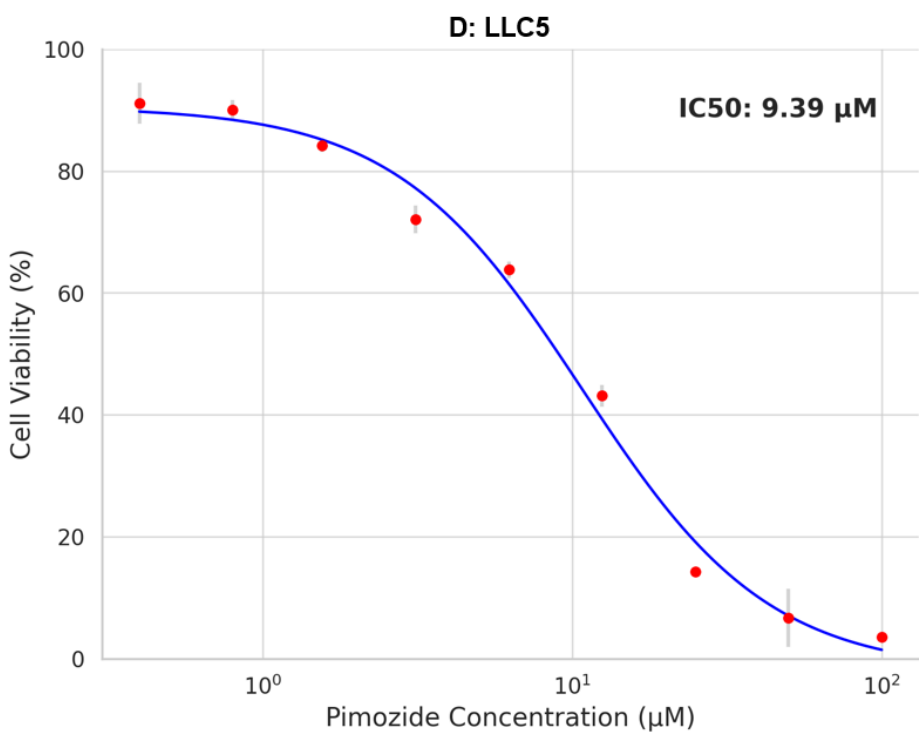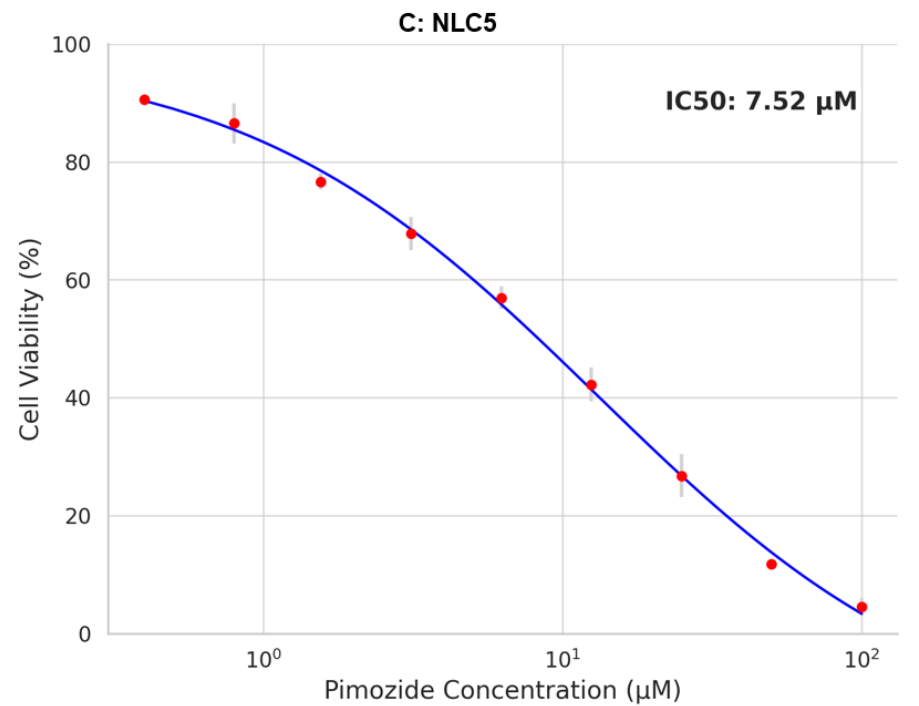
Figure 14. Anti-proliferative effect of **(A)** free pimozide, and its spray-dried lipid nano formulations **(B)** NLC4, **(C)** NLC5, and **(D)** LLC5, and **(E)** blank excipients against A549 cell line mode following 72 hours of treatment. Graphs are presented as percentage viability relative to the untreated control. Data represent the mean ± S.D.
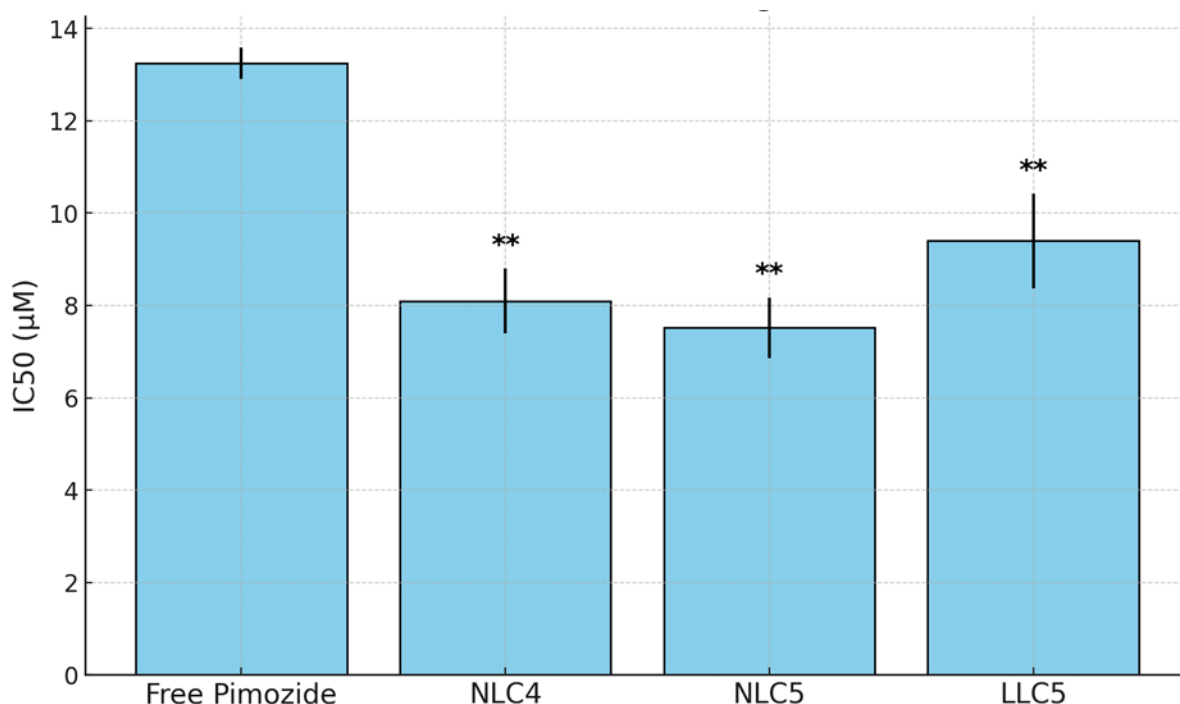
Figure 15. Bar graph showing the IC_{50} values for four different groups: Free pimozide, NLC 4, NLC 5, and LLC 5. ** *p* < 0.01 was calculated using one-way ANOVA. Data presented as mean ± SD. Comparisons were conducted between the formulation and the free drug.

4.3.9 Drug release studies

Following the identification of the promising anti-proliferative capabilities of NLC4, NLC5, and LLC5, their drug release profiles were carefully evaluated to determine how PMZ is delivered over time. Additionally, the release kinetic of free pimozide was evaluated. In the evaluation of the PMZ release profile from the formulations, a biphasic release pattern was observed followed by a sustained release phase. The release of PMZ as illustrated in **Figure 16** followed a biphasic manner with a mean of 18.9% ±2.07% after 2 hours. The release rate then reached 51.8% ±4.21% by 8 hours. This phase continued over the 72-hour period, peaking in a mean release of 89.2% ±3.08.

Similarly, PMZ release from NLC5 was biphasic, with a little lower first burst, yielding a mean release of 17.1% ±2.51% at 2 hours. At 72 hours, this formulation had a slightly

greater mean release of 92.0% ±2.61%, indicating a more consistent sustained phase. LLC5 had the slowest initial burst among the three formulations, exhibiting a biphasic PMZ release pattern with a mean release of 15.9% ±3.28% after 2 hours. The chemical was consistently released over the trial duration, reaching a mean of 89.8% ±2.37% by 72 hours, comparable to NLC4.

Free pimozide showed a markedly higher release 62.5 ± 2.50% compared to the lipid-based nanoparticles at the 2-hour mark. This trend of free pimozide leading the release continued at the 4-hour time point, reaching 94.2 ± 3.48% indicating an almost complete release. The biphasic release pattern characterized by an initial rapid release followed by a more gradual, sustained phase, corroborating previous studies [50-52]. The initial burst of drug release is thought to arise from drug molecules that are loosely bound to the surfaces of the nanoparticles, allowing for their quick dissemination into the target area [52]. This dual-phase release mechanism of the formulations may offer considerable advantages for inhalation therapy in NSCLC treatment by ensuring prolonged drug presence in the lung tissue, which could lead to sustained anti-cancer effects [53]. This may enhance the overall therapeutic efficacy, allowing for reduced dosing frequencies, thereby improving patient which could significantly impact the clinical management of NSCLC, potentially enhancing patient outcomes.

The initial burst release is primarily driven by the presence of free or loosely bound drug on the surface of the nanoparticles. This unencapsulated drug is readily available for dissolution and diffusion upon exposure to the release medium. In this study, free pimozide exhibits a rapid release, with approximately 60-64% of the drug released within the first two hours, reaching up to 98% by eight hours. This significant initial burst suggests that a considerable portion of the drug is present either as free drug or is poorly encapsulated, residing near or on the surface of the nanoparticles. This phase represents the unencapsulated drug fraction, which is immediately available to dissolve and diffuse out.

Following the initial burst, the formulations enter a more controlled and sustained release phase. This phase is governed by the release of the drug encapsulated within the nanoparticle matrix. The release kinetics during this phase are typically controlled by diffusion through the nanoparticle material, degradation or erosion of the nanoparticle

matrix, or a combination of both processes. For instance, LLC 5 continues to release up to 92% of the drug over 72 hours, while NLC 5 and NLC 4 demonstrate a gradual increase in release up to around 94% and 92%, respectively. This sustained release phase indicates the controlled release of the drug from within the nanoparticle, where the matrix acts as a barrier to drug diffusion and degradation.

The nanoparticle phase plays a crucial role in determining the release kinetics of the encapsulated drug. In NLC and LLC formulations, the lipid composition whether solid, and liquid, or only liquid significantly affects the release behavior. Solid lipids generally provide a more rigid structure, which limits the diffusion of the encapsulated drug, thereby offering a slower and more controlled release. In contrast, liquid lipids may allow for faster diffusion, contributing to a more rapid release profile. The observed release characteristics of LLC 5, NLC 5, and NLC 4 suggest that these formulations likely contain a mixture of solid and liquid lipids, typical of NLCs, or possibly entirely liquid lipids for LLCs, which contributes to the observed release kinetics.
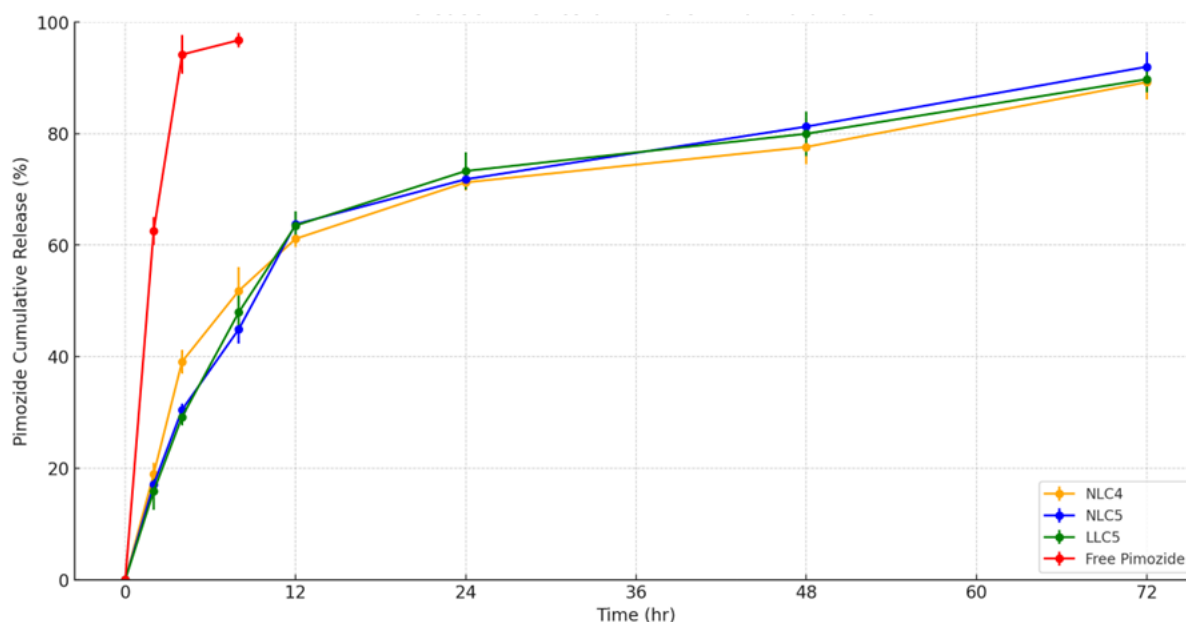
Figure 16. Time-dependent release kinetics of pimozide from three distinct spray-dried lipid nano formulations: NLC4, NLC5, and LLC5 compared to the free pimozide. Each panel represents the percentage of pimozide released over a 72-hour period, highlighting the biphasic release pattern characterized by an initial burst followed by a sustained release phase. Free drugs were used as control. Values are means ± SD.

4.4 Conclusion

In conclusion, this comprehensive study demonstrated the potential of pimozide-loaded LNPs as a promising strategy for the targeted treatment of NSCLC. The employment of the microemulsion technique to synthesize and optimize SLN, NLC, and LLC formulations has led to significant advancements in drug delivery technologies, as evidenced by the detailed characterization of each formulation's physicochemical properties, encapsulation efficiencies, and therapeutic effectiveness.

Notably, the incorporation of oleic acid into NLCs significantly enhanced drug encapsulation efficiency, while the diverse morphological properties underscored the complexity and potential of LNPs in achieving sustained drug delivery. The findings from FTIR, Raman spectroscopy, and XRPD analyses provided a deeper understanding of the drug-lipid interactions and the structural integrity of the formulations, further supporting their use in clinical applications. The demonstrated anti-proliferative efficacy against A549 lung cancer cells, combined with a favourable drug release profile, positions these LNPs as a possible alternative to traditional chemotherapy formulations. Future studies focusing on *in vivo* efficacy, safety profiles, and mechanisms of action will be pivotal in translating these formulations from bench to bedside, potentially revolutionizing NSCLC therapy.

Reference:

[1]   N. Duma, R. Santana-Davila, and J. R. Molina, "Non–small cell lung cancer: epidemiology, screening, diagnosis, and treatment," in *Mayo Clinic Proceedings*, 2019, vol. 94, no. 8: Elsevier, pp. 1623-1640.

[2]   S. Pushpakom *et al.*, "Drug repurposing: progress, challenges and recommendations," *Nature reviews Drug discovery,* vol. 18, no. 1, pp. 41-58, 2019.

[3]   B. Li *et al.*, "A novel drug repurposing approach for non-small cell lung cancer using deep learning," *PLoS One,* vol. 15, no. 6, p. e0233112, 2020.

[4]   P. Ghasemiyeh and S. Mohammadi-Samani, "Solid lipid nanoparticles and nanostructured lipid carriers as novel drug delivery systems: Applications, advantages and disadvantages," *Research in pharmaceutical sciences,* vol. 13, no. 4, pp. 288-303, 2018.

[5]   X.-Y. Ying, Y.-Z. Du, W.-W. Chen, H. Yuan, and F.-Q. Hu, "Preparation and characterization of modified lipid nanoparticles for doxorubicin controlled release," *Die Pharmazie-An International Journal of Pharmaceutical Sciences,* vol. 63, no. 12, pp. 878-882, 2008.

[6]   E. W. Leong and R. Ge, "Lipid nanoparticles as delivery vehicles for inhaled therapeutics," *Biomedicines,* vol. 10, no. 9, p. 2179, 2022.

[7]   A. Saedi, K. Rostamizadeh, M. Parsa, N. Dalali, and N. Ahmadi, "Preparation and characterization of nanostructured lipid carriers as drug delivery system: Influence of liquid lipid types on loading and cytotoxicity," *Chemistry and physics of lipids,* vol. 216, pp. 65-72, 2018.

[8]   K. Šimková, B. Joost, and G. Imanidis, "Production of fast-dissolving low-density powders for improved lung deposition by spray drying of a nanosuspension," *European Journal of Pharmaceutics and Biopharmaceutics,* vol. 146, pp. 19-31, 2020.

[9]   H. I. Pass, "Lung cancer surveillance: new technologies and novel strategies," *Annals of Surgical Oncology,* vol. 7, no. 3, p. 171, 2000.

[10]   N. R. Labiris and M. B. Dolovich, "Pulmonary drug delivery. Part II: the role of inhalant delivery devices and drug formulations in therapeutic effectiveness of aerosolized medications," *British journal of clinical pharmacology,* vol. 56, no. 6, pp. 600-612, 2003.

[11]   F. Iskandar, L. Gradon, and K. Okuyama, "Control of the morphology of nanostructured particles prepared by the spray drying of a nanoparticle sol," *Journal of Colloid and interface Science,* vol. 265, no. 2, pp. 296-303, 2003.

[12]   S. Javed, B. Mangla, Y. Almoshari, M. H. Sultan, and W. Ahsan, "Nanostructured lipid carrier system: A compendium of their formulation development approaches, optimization strategies by quality by design, and recent applications in drug delivery," *Nanotechnology Reviews,* vol. 11, no. 1, pp. 1744-1777, 2022.

[13]   A.-K. Tuderman, C. J. Strachan, and A. M. Juppo, "Isomalt and its diastereomer mixtures as stabilizing excipients with freeze-dried lactate dehydrogenase," *International Journal of Pharmaceutics,* vol. 538, no. 1-2, pp. 287-295, 2018.

[14]   N. Aditya *et al.*, "Development and evaluation of lipid nanocarriers for quercetin delivery: A comparative study of solid lipid nanoparticles (SLN), nanostructured lipid carriers (NLC), and lipid nanoemulsions (LNE)," *LWT-Food Science and Technology,* vol. 59, no. 1, pp. 115-121, 2014.

[15]   P. Kaur, V. Mishra, T. Shunmugaperumal, A. K. Goyal, G. Ghosh, and G. Rath, "Inhalable spray dried lipidnanoparticles for the co-delivery of paclitaxel and doxorubicin in lung cancer," *Journal of Drug Delivery Science and Technology,* vol. 56, p. 101502, 2020.

[16]   H. Nsairat *et al.*, "Lipid nanostructures for targeting brain cancer," *Heliyon,* vol. 7, no. 9, 2021.

[17]   S. Das and A. Chaudhury, "Recent advances in lipid nanoparticle formulations with solid matrix for oral drug delivery," *Aaps Pharmscitech,* vol. 12, pp. 62-76, 2011.

[18]   P. Mura, F. Maestrelli, M. D'Ambrosio, C. Luceri, and M. Cirri, "Evaluation and Comparison of Solid Lipid Nanoparticles (SLNs) and Nanostructured Lipid Carriers (NLCs) as Vectors to Develop Hydrochlorothiazide Effective and Safe Pediatric Oral Liquid Formulations," *Pharmaceutics*, vol. 13, no. 4*,* doi: 10.3390/pharmaceutics13040437.

[19]   M. Elmowafy and M. M. Al-Sanea, "Nanostructured lipid carriers (NLCs) as drug delivery platform: Advances in formulation and delivery strategies," *Saudi Pharmaceutical Journal,* vol. 29, no. 9, pp. 999-1012, 2021/09/01/ 2021, doi: https://doi.org/10.1016/j.jsps.2021.07.015.

[20]   S. Martins, I. Tho, D. Ferreira, E. Souto, and M. Brandl, "Physicochemical properties of lipid nanoparticles: effect of lipid and surfactant composition," *Drug development and industrial pharmacy,* vol. 37, no. 7, pp. 815-824, 2011.

[21]   P. Tewa-Tagne, S. Briançon, and H. Fessi, "Preparation of redispersible dry nanocapsules by means of spray-drying: development and characterisation," *European Journal of Pharmaceutical Sciences,* vol. 30, no. 2, pp. 124-135, 2007.

[22]   A. P. B. Ribeiro *et al.*, "Crystallization modifiers in lipid systems," *Journal of food science and technology,* vol. 52, pp. 3925-3946, 2015.

[23]   A. Gordillo-Galeano and C. E. Mora-Huertas, "Solid lipid nanoparticles and nanostructured lipid carriers: A review emphasizing on particle structure and drug release," *European Journal of Pharmaceutics and Biopharmaceutics,* vol. 133, pp. 285-308, 2018.

[24]   C. Yue-Xing *et al.*, "The effect of l-leucine on the stabilization and inhalability of spray-dried solid lipid nanoparticles for pulmonary drug delivery," *Journal of Drug Delivery Science and Technology,* vol. 46, pp. 474-481, 2018.

[25]   C. Freitas and R. H. Müller, "Spray-drying of solid lipid nanoparticles (SLNTM)," *European Journal of Pharmaceutics and Biopharmaceutics,* vol. 46, no. 2, pp. 145-151, 1998.

[26]   S. F. Taveira, L. M. de Campos Araújo, D. C. de Santana, A. Nomizo, L. A. P. de Freitas, and R. F. Lopez, "Development of Cationic Solid Lipid Nanoparticles with Factorial Design-Based Studies for Topical Administration of Doxorubicin," 2012.

[27]   S. A. Swidan, H. M. Ghonaim, A. M. Samy, and M. M. Ghorab, "Efficacy and in vitro cytotoxicity of nanostructured lipid carriers for paclitaxel delivery," *Journal of Applied Pharmaceutical Science,* vol. 6, no. 9, pp. 018-026, 2016.

[28]   I. V. Zelepukin *et al.*, "Fast processes of nanoparticle blood clearance: Comprehensive study," *Journal of controlled release,* vol. 326, pp. 181-191, 2020.

[29]   P. Kumar *et al.*, "Promises of a biocompatible nanocarrier in improved brain delivery of quercetin: Biochemical, pharmacokinetic and biodistribution evidences," *International journal of pharmaceutics,* vol. 515, no. 1-2, pp. 307-314, 2016.

[30]   J. Pardeike, A. Hommoss, and R. H. Müller, "Lipid nanoparticles (SLN, NLC) in cosmetic and pharmaceutical dermal products," *International journal of pharmaceutics,* vol. 366, no. 1-2, pp. 170-184, 2009.

[31]   K. Westesen, H. Bunjes, and M. Koch, "Physicochemical characterization of lipid nanoparticles and evaluation of their drug loading capacity and sustained release potential," *Journal of controlled release,* vol. 48, no. 2-3, pp. 223-236, 1997.

[32]   T. Delmas *et al.*, "How to prepare and stabilize very small nanoemulsions," *Langmuir,* vol. 27, no. 5, pp. 1683-1692, 2011.

[33]   Y.-C. Kuo and I.-C. Chen, "Evaluation of surface charge density and surface potential by electrophoretic mobility for solid lipid nanoparticles and human brain– microvascular endothelial cells," *The Journal of Physical Chemistry B,* vol. 111, no. 38, pp. 11228-11236, 2007.

[34]   H. Bera *et al.*, "Novel pimozide-β-cyclodextrin-polyvinylpyrrolidone inclusion complexes for Tourette syndrome treatment," *Journal of Molecular Liquids,* vol. 215, pp. 135-143, 2016/03/01/ 2016, doi: https://doi.org/10.1016/j.molliq.2015.12.054.

[35]   P. Sawunyama, L. Jiang, A. Fujishima, and K. Hashimoto, "Photodecomposition of a Langmuir– Blodgett film of stearic acid on TiO2 film observed by in situ atomic force microscopy and FT-IR," *The Journal of Physical Chemistry B,* vol. 101, no. 51, pp. 11000-11003, 1997.

[36]   J. Ibarra *et al.*, "Synthesis and characterization of magnetite/PLGA/chitosan nanoparticles," *Materials Research Express,* vol. 2, pp. 1-17, 09/11 2015, doi: 10.1088/2053-1591/2/9/095010.

[37]   Z. Song *et al.*, "Improving Breviscapine Oral Bioavailability by Preparing Nanosuspensions, Liposomes and Phospholipid Complexes," *Pharmaceutics,* vol. 13, p. 132, 01/20 2021, doi: 10.3390/pharmaceutics13020132.

[38]   A. Bhanderi, F. Bari, and H. Al-Obaidi, "Evaluation of the impact of surfactants on miscibility of griseofulvin in spray dried amorphous solid dispersions," *Journal of Drug Delivery Science and Technology,* vol. 64, p. 102606, 2021.

[39]   W. Mehnert and K. Mäder, "Solid lipid nanoparticles: Production, characterization and applications," *Advanced Drug Delivery Reviews,* vol. 64, pp. 83-101, 2012/12/01/ 2012, doi: https://doi.org/10.1016/j.addr.2012.09.021.

[40]   R. Shah *et al.*, "Production techniques," *Lipid Nanoparticles: Production, Characterization and Stability,* pp. 23-43, 2015.

[41]   V. Paramita, K. Iida, H. Yoshii, and T. Furuta, "Effect of additives on the morphology of spray-dried powder," *Drying Technology,* vol. 28, no. 3, pp. 323-329, 2010.

[42]   R. V. Tonon, C. R. Grosso, and M. D. Hubinger, "Influence of emulsion composition and inlet air temperature on the microencapsulation of flaxseed oil by spray drying," *Food Research International,* vol. 44, no. 1, pp. 282-289, 2011.

[43]   S. Aziz, "Trehalose physicochemical characteristics as a potential dry powder inhalation carrier for optimized aerosol generation," Christian-Albrechts Universität Kiel, 2015.

[44]   A. Baldelli and R. Vehring, "Analysis of cohesion forces between monodisperse microparticles with rough surfaces," *Colloids and Surfaces A: Physicochemical and Engineering Aspects,* vol. 506, pp. 179-189, 2016.

[45]   E. D. Wiklund *et al.*, "Cytotoxic effects of antipsychotic drugs implicate cholesterol homeostasis as a novel chemotherapeutic target," *International journal of cancer,* vol. 126, no. 1, pp. 28-40, 2010.

[46]   E.-H. Dakir *et al.*, "The anti-psychotic drug pimozide is a novel chemotherapeutic for breast cancer," *Oncotarget,* vol. 9, no. 79, p. 34889, 2018.

[47]   A. M. Faheem, A. A. Elkordy, and N. Uddin, "Fabrication and physicochemical characterisation of novel pimozide loaded PLGA nanoparticles," *British Journal of Pharmacy,* vol. 4, no. 1, 2019.

[48]   A. Ulldemolins Iglesias *et al.*, "Perspectives of nano-carrier drug delivery systems to overcome cancer drug resistance in the clinics," 2021.

[49]   J. Lee, M.-K. Choi, and I.-S. Song, "Recent Advances in Doxorubicin Formulation to Enhance Pharmacokinetics and Tumor Targeting," *Pharmaceuticals,* vol. 16, no. 6, p. 802, 2023.

[50]   A. Khan, S. Khan, M. A. Khan, Z. Qamar, and M. Waqas, "The uptake and bioaccumulation of heavy metals by food plants, their effects on plants nutrients, and associated health risk: a review," *Environmental science and pollution research,* vol. 22, pp. 13772-13799, 2015.

[51]   A. Khosa, S. Reddi, and R. N. Saha, "Nanostructured lipid carriers for site-specific drug delivery," *Biomedicine & Pharmacotherapy,* vol. 103, pp. 598-613, 2018.

[52]   A. M. Price-Whelan *et al.*, "The Astropy Project: sustaining and growing a community-oriented open-source project and the latest major release (v5. 0) of the core package," *The Astrophysical Journal,* vol. 935, no. 2, p. 167, 2022.

[53]   I. M. Abdulbaqi *et al.*, "Pulmonary delivery of anticancer drugs via lipid-based nanocarriers for the treatment of lung cancer: An update," *Pharmaceuticals,* vol. 14, no. 8, p. 725, 2021.

Chapter 5

Enhancing NSCLC Treatment: Advanced Lipid Nanoparticle Formulations and Spray Drying Techniques with Repurposed Pimozide and Hydroxychloroquine

Arwa Omar Al Khatib[a,b], Mohamed El-Tanani[b], Hisham Al-Obaidi[a]*

[a] School of Pharmacy, University of Reading, Reading RG6 6AD, UK
[b] Faculty of Pharmacy, Al Ahliyya Amman University, Amman 19111, Jordan

Chapter Summary:

In this chapter, the development and evaluation of pimozide (PMZ) and hydroxychloroquine (HQ) loaded lipid nanoparticles (LNPs) for NSCLC treatment are discussed. Three LNP types—SLNPH, NLCPH, and LLCPH—were prepared and spray-dried. NLCPH showed the highest encapsulation efficiencies for PMZ and HQ, better colloidal stability, and enhanced storage stability. Besides, NLCPH and LLCPH reduced A549 lung cancer cell viability and exhibited anti-inflammatory effects. NLCPH also demonstrated a sustained drug release profile.

5.1 Introduction:

Lung cancer, particularly non-small cell lung cancer (NSCLC), continues to pose a significant global health challenge, especially in advanced stages where treatment becomes more difficult [1]. Traditional therapies often have limitations, prompting the exploration of alternative strategies such as drug repurposing. This approach leverages existing drugs for new therapeutic purposes, offering quicker and cost-effective pathways to clinical implementation.

Among the drugs being repurposed, pimozide (PMZ), an antipsychotic, has shown promise in combating NSCLC. Recent research highlights its potential anti-cancer properties [2]. Similarly, hydroxychloroquine (HQ), traditionally used for malaria and autoimmune diseases, is being investigated not only for its ability to inhibit autophagy but also for its anti-inflammatory properties. Chronic inflammation is a known factor in cancer progression and can complicate treatment and reduce survival rates. Therefore, HQ's potential to address cancer-related inflammation makes it a valuable candidate for repurposing in NSCLC treatment [3-7].

The effective delivery of PMZ and HQ to tumor sites is crucial. Lipid nanoparticles (LNPs) present an innovative solution for this challenge. This study focuses on three types of LNPs: solid lipid nanoparticles (SLN), nanostructured lipid carriers (NLC), and liquid lipid carriers (LLC). Each type offers unique lipid compositions that optimize drug delivery and release characteristics, enhancing the bioavailability and therapeutic efficacy of PMZ and HQ [8, 9]. To ensure these drugs reach the deep lung regions, spray drying is employed to produce fine particles suitable for dry powder inhalers (DPIs). DPIs are essential for delivering medication directly to the lungs, crucial for treating respiratory diseases like NSCLC [10].

The stability of these particles during spray drying and storage is maintained using lipid matrices, including stearic and oleic acids, surfactants such as Poloxamer 407 and PEG 400, and stabilizers like isomalt and trehalose [11, 12].

This study aims to revolutionize NSCLC treatment by combining PMZ and HQ in LNP formulations, utilizing spray drying for effective lung delivery. By addressing both cancer and cancer-related inflammation, this research seeks to improve therapeutic outcomes and potentially enhance survival rates, representing a comprehensive approach to NSCLC therapy.

5.2 Materials and methods:

5.2.1 Materials

Pimozide, hydroxychloroquine stearic acid, oleic acid, poloxamer 407, PEG 400, and trehalose were acquired from Sigma-Aldrich, US. DuPont in the Netherlands supplied the methocel E5 (HPMC E5). Isomalt was purchased from BENEO GmbH, Germany, and OraRez PVM/MA copolymer, an alternating copolymer of methyl vinyl ether and maleic anhydride was obtained from HARKE Pharma GmbH, Germany. The MTT reagent was purchased from ThermoFisher Scientific, US, and the dimethyl sulfoxide (DMSO) was obtained from Fisher Bioreagents, US.

5.2.2 Preparation of LNP formulations

The microemulsion method was utilized to generate all PMZ- HQ-loaded LNP formulations including, SLNPH, NLCPH, and LLCPH, where the amounts of all components including the drugs, lipids, surfactants, bio-adhesive polymer, and excipients were optimized as listed in **Table 1**. Excipients were added at approximately a 5% ratio to serve as protectants [13].

This method uses oil, water, and surfactants to stabilize small droplets within another liquid. To prepare Lipid Nano Particles (LNPs), 50 mg pimozide was dissolved in the lipid phase, 200 mg stearic acid for Solid Lipid Nanoparticles (SLNs), 100 µL oleic acid for Liquid Lipid Carriers (LLCs), or a combination of 100 mg stearic acid and 100 µL oleic acid for Nanostructured Lipid Carriers (NLCs) at 85°C. The lipid phase volume was 1 mL.

The aqueous phase contained 200 mg Poloxamer 407 and 100 µL PEG 400, with 50 mg hydroxychloroquine dissolved in 50 mL water. Both phases were heated to 85°C, which was above their Phase Inversion Temperature (PIT), facilitating the transformation from a microemulsion to a stable nanoparticle dispersion. The phases were then vigorously mixed at this temperature. After cooling, 300 mg HPMC-E5 and 60 mg of one of the excipients (trehalose, OraRez, or isomalt) were added with continuous stirring. The final nanoparticle suspension volume was 50 mL. The concentration of pimozide in the final feed solution was 1 mg/mL, and the concentration of hydroxychloroquine in the final feed solution was also 1 mg/mL. The resulting nanoparticle dispersion was then spray-dried to obtain the final powder formulation.

Table 1: Composition of spray- dried pimozide- hydroxychloroquine loaded LNP formulations

	PMZ (mg)	HQ (mg)	Stearic acid (mg)	Oleic acid (µL)	Poloxamer 407 (mg)	PEG 400 (µL)	HPMC-E5 (mg)	Yield%	Excipients (mg)		
									Trehalose	OraRez	Isomalt
SLN 4PH	50	50	200	-	200	100	300	64.5	60	-	-
SLN 5PH	50	50	200	-	200	100	300	37.7	-	60	-
SLN 6PH	50	50	200	-	200	100	300	51.9	-	-	60
NLC 4PH	50	50	100	100	200	100	300	80.5	60	-	-
NLC 5PH	50	50	100	100	200	100	300	91.4	-	60	-
NLC 6PH	50	50	100	100	200	100	300	71.5	-	-	60
LLC 4PH	50	50	-	100	200	100	300	61.9	60	-	-
LLC 5PH	50	50	-	100	200	100	300	55.2	-	60	-
LLC 6PH	50	50	-	100	200	100	300	49.3	-	-	60

5.2.3 EE% Encapsulation Efficiency

For the assessment of the entrapment efficiency in all spray-dried PMZ- HQ- loaded LNPs. 10 mg of each powder was dissolved in 10 mL of methanol and then centrifuged at 13,000 rpm for 30 minutes. Subsequently, the supernatant was filtered using 0.22 µm filters and the amount of PMZ and HQ was determined using High-Performance Liquid Chromatography (HPLC). This analysis utilized a 15 cm C18 column, with a monitoring

wavelength set at 270 nm, and used an isocratic elution technique with a mobile phase consisting of 45% acetonitrile and 55% of acidified water (pH was adjusted to 2.5 ± 0.5 by using 0.1% v/v phosphoric acid), with a flow rate of 1mL/min, injection volume of 20 µL, and run time of 10 minutes. The drug concentration was calculated from the Area Under the Curve (AUC) from the HPLC readings, based on a calibration curve that was linearly fit for each drug. Lastly, the encapsulation efficiency percentage (EE%) was derived using the following equation [14]

$$EE\,(\%) \;=\; \frac{Total\;Drug - Free\;Drug}{Total\;Drug} \; x100\%$$

(Equation 3)

5.3 Results and discussion

In this study, three types of PMZ-HQ loaded into lipid nanoparticles were developed: solid lipid nanoparticles (SLNPH), nanostructured lipid carriers (NLCPH), and a novel formulation exclusively using liquid lipids, denoted as liquid lipid carriers (LLCPH). These lipid nanoparticles underwent transformation into a powdered state via spray drying, leading to their shift from the nanometer scale to becoming microparticles. After this transformation, the research progressed to a comprehensive physicochemical characterization of the spray-dried microparticles.

5.3.1 Encapsulation efficiency of spray- dried LNP powders

The bar graph shown in **Figure 1 (A)** illustrates the EE% across different LNP powder formulations, where the SLNPH formulations, namely SLN4PH, SLN5PH, and SLN6PH, exhibited varying encapsulation efficiencies for both drugs. These specific formulations, noted for their solid lipid matrix, generally showed lower EE% for PMZ (54%) and HQ (52%) in comparison to other LNPs. Such a trend suggests an underlying restriction of the solid matrix to adequately accommodate and stabilize the drug molecules within the

formulations. With regards to PMZ, this problem is caused by the solid lipid, composed solely of stearic acid, which forms a highly structured and crystalline matrix. Such configuration significantly restricts the amount of PMZ that can be dissolved or encapsulated, leading to a potential expulsion of PMZ from the lipid matrix during the cooling process [15]. Consequently, this phenomenon results in a diminished entrapment capacity and a decrease in encapsulation efficiency, confirming the challenge posed by the crystalline nature of the solid lipid in drug encapsulation processes that was reported in previous studies [16, 17].

On the other hand, the low EE% of HQ in SLNPH formulations can be due to a combination of limited drug compatibility with the solid lipid matrix and phase separation during cooling. Amphiphilic drugs like HQ, which can interact with both lipid and aqueous phases, find the solid lipid matrix of SLNs less than ideal due to its solid state at room temperature. The matrix's high crystallinity and tightly packed lipid molecules leave limited space for the encapsulation of HQ, particularly since it is not fitting well into the lipid's crystalline lattice. Furthermore, during SLN preparation, the cooling process required to solidify the lipid matrix may cause phase separation. This phenomenon can result in the expulsion of HQ from the lipid matrix, especially because HQ tends to locate preferentially at the interface. Such phase separation during solidification can significantly impact the drug's encapsulation efficiency, leading to lower EE% for HQ in SLNs.

In contrast, the NLC formulations, which include NLC4PH, NLC5PH, and NLC6PH, were found to be the most superior among the formulations, exhibiting the highest EE% for both drugs PMZ around 95% and HQ around 75%. This superior performance can be attributed to the unique structure of NLCs, which incorporate both solid and liquid lipid components, offering enhanced flexibility for drug encapsulation. Since it resulted in a lipid matrix that is less ordered and possessed more imperfections and voids compared to the highly crystalline structure of SLNs [17]. This structural characteristic facilitates improved drug compatibility, enabling easier accommodation and better dispersion of both PMZ and HQ within the carrier, thereby addressing the challenges posed by their distinct solubility profiles. Besides, the integration of liquid lipids serves to reduce phase separation by

acting as solvents for the PMZ and HQ during the cooling process, thereby maintaining drugs' solubility and preventing their expulsion [17]. This feature ensures a more stable encapsulation of PMZ and HQ, enhancing their EE%.

Moreover, this tailored combination of oleic acid and stearic acid, optimizes drug-lipid interactions. The interaction between HQ and stearic acid is characterized by hydrophobic interactions between the lipophilic parts of HQ and stearic acid's long hydrocarbon chain, although the solid and rigid structure of stearic acid may not efficiently dissolve or disperse amphiphilic molecules like HQ. In contrast, the interaction with the liquid oleic acid, is more favorable due to both hydrophobic interactions and potential hydrogen bonding, facilitated by oleic acid's *cis* double bond and its slightly polar nature. This increased fluidity and reduced packing order in oleic acid significantly enhance HQ's compatibility and incorporation into the lipid matrix, making oleic acid a superior choice for stabilizing amphiphilic drugs. Consequently, oleic acid is especially conducive to improving the encapsulation efficiency and stability of HQ in NLCPH formulations.

Furthermore, the addition of the hydrophilic polymer HPMC-E5 can further increase HQ solubility within the lipid matrix. NLCs also offer increased load capacity, particularly advantageous for accommodating higher quantities of challenging drugs like HQ without compromising particle stability. This increased capacity is important for drugs with varied solubility profiles such as PMZ and HQ, demonstrating the adaptability of NLCs to diverse pharmaceutical needs. Additionally, spray-dried NLCPH formulations could have encapsulated a higher proportion of PMZ and HQ owing to their reduced particle size compared to SLNPH and LLCPH formulations as shown in (section 3.2), leading to a greater surface area in relation to volume. This might have improved the interaction between the two drugs and the lipid matrix, aiding in their more efficient incorporation and stabilization within the formulations. This data combined with the controlled release profile in (section 3.9), highlights the potential of NLCPH formulations to enhance the delivery and effectiveness of both PMZ and HQ. This emphasizes their significance in the development of advanced drug delivery systems.

The LLC category, comprising LLC4PH, LLC5PH, and LLC6PH, displayed intermediate EE% values for PMZ (62%) and HQ (54%). This group's performance showed the potential advantages of their liquid lipid architecture in facilitating effective drug encapsulation, though not to the extent observed with NLC formulations. However, this could be attributed to the fluidity of the lipid matrix resulting from the sole use of oleic acid which could have led to the leakage of the encapsulated drugs.

Statistical analysis in **Figure 1 (B)** further refined our understanding of these observations. Specifically, for PMZ, there is a significant difference in EE% between SLNs and NLCs. For HQ, significant differences are observed between SLNs and NLCs, as well as between NLCs and LLCs. No significant differences are noted between other groups, such as NLCs vs LLCs for PMZ and SLNs vs LLCs for both PMZ and HQ.
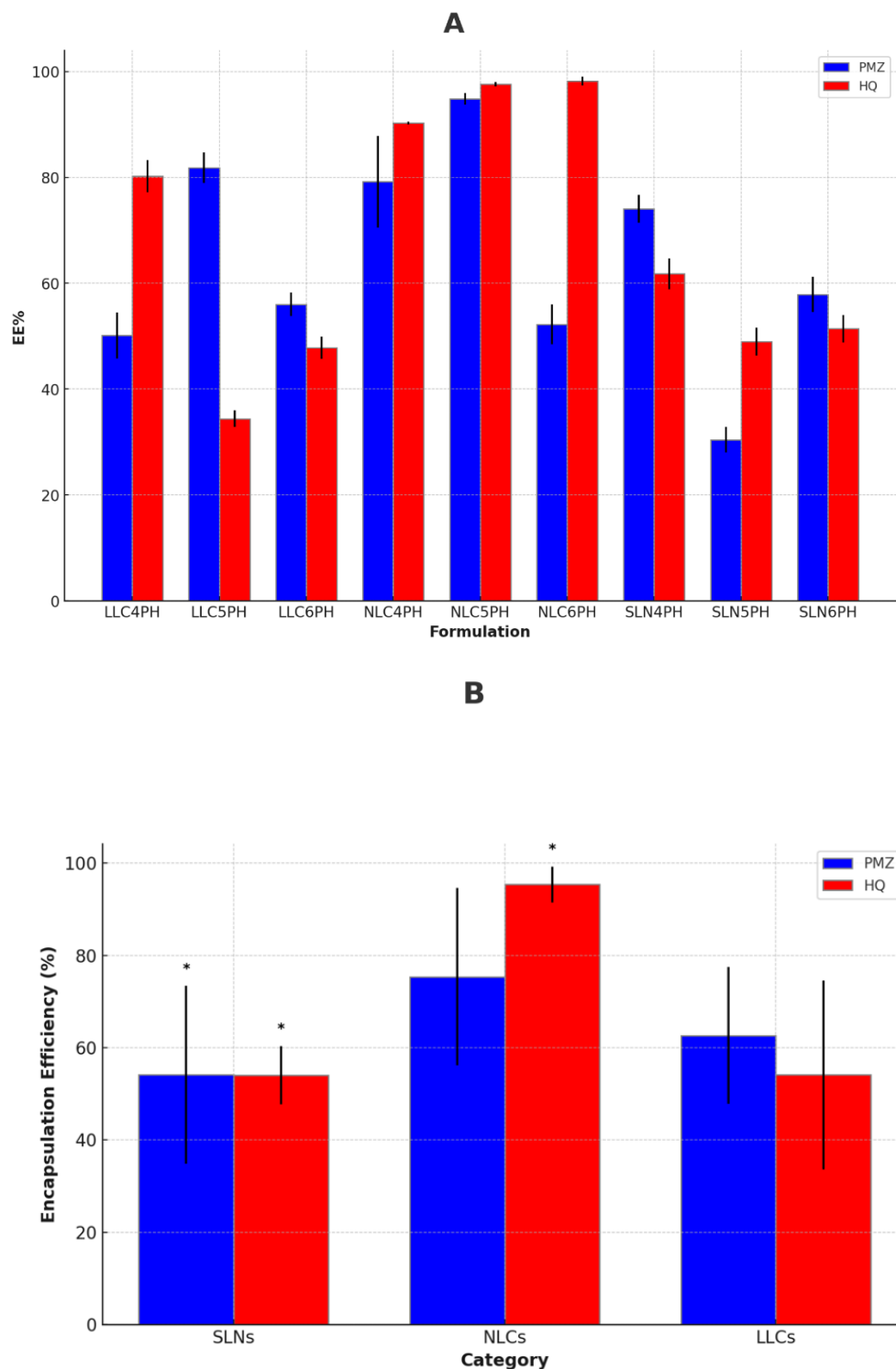
Figure 1. (A) EE% of PMZ and HQ within distinct spray-dried LNP powder formulations. **(B)** EE% and statistical significance (*p*-values) for PMZ and HQ across three different types of LNPs.

5.3.2 Particle size, PDI, and zeta potential

The particle size, PDI, and zeta potential of the LNP nanosuspensions and spray-dried samples are demonstrated in **Figures (2- 4)**. The analysis of nine different spray-dried PMZ-HQ-loaded LNPs, including SLNPH, NLCPH, and LLCPH, revealed trends depicted in **Figure 2**. Results showed a significant increase in average particle size post-spray drying across all formulations **Figure 2 (A)**, transitioning from nano- to micro-scale. This might be attributed to the spray drying process subjecting the particles to high temperatures and shear forces, which causes the lipids to aggregate, resulting in a noticeable rise in the overall size of the particles [18, 19].

Furthermore, after spray drying, LNPs tend to increase in size, due to the heating-induced phase transition and the aggregation initiated by particle-particle interactions [20]. SLN4PH exhibited the smallest particle size among SLN formulations, attributed to trehalose's higher solubility compared to isomalt and OraRez in SLN5PH and SLN6PH respectively [21, 22]. NLCPH formulations showed smaller and more uniform particle sizes, potentially because oleic acid disrupted the crystalline structure of the solid lipid. This disruption could result in a reduced packing density within the lipid matrix [23]. Additionally, the inclusion of solid lipid in NLCPH formulations aids in faster nucleation and solidification within the mixed lipid matrix. This process restricts the growth of particles, thereby promoting the development of smaller particles. **Figure 2 (B)** [24].

LLCPH formulations produced larger droplets because they lacked the solid matrix and had lower viscosity and slower cooling rates compared to NLCPH, which could promote the coalescence of droplets and lead to larger particle sizes **Figure 2 (B)**. Conversely, SLNPH formulations exhibited the largest particle sizes, which could be attributed to the crystallization of the solid lipid in the dispersed phase of the SLN upon cooling. This crystallization process might cause the expulsion of the drug, leading to an increase in particle size **(Figure 2C)** [25].
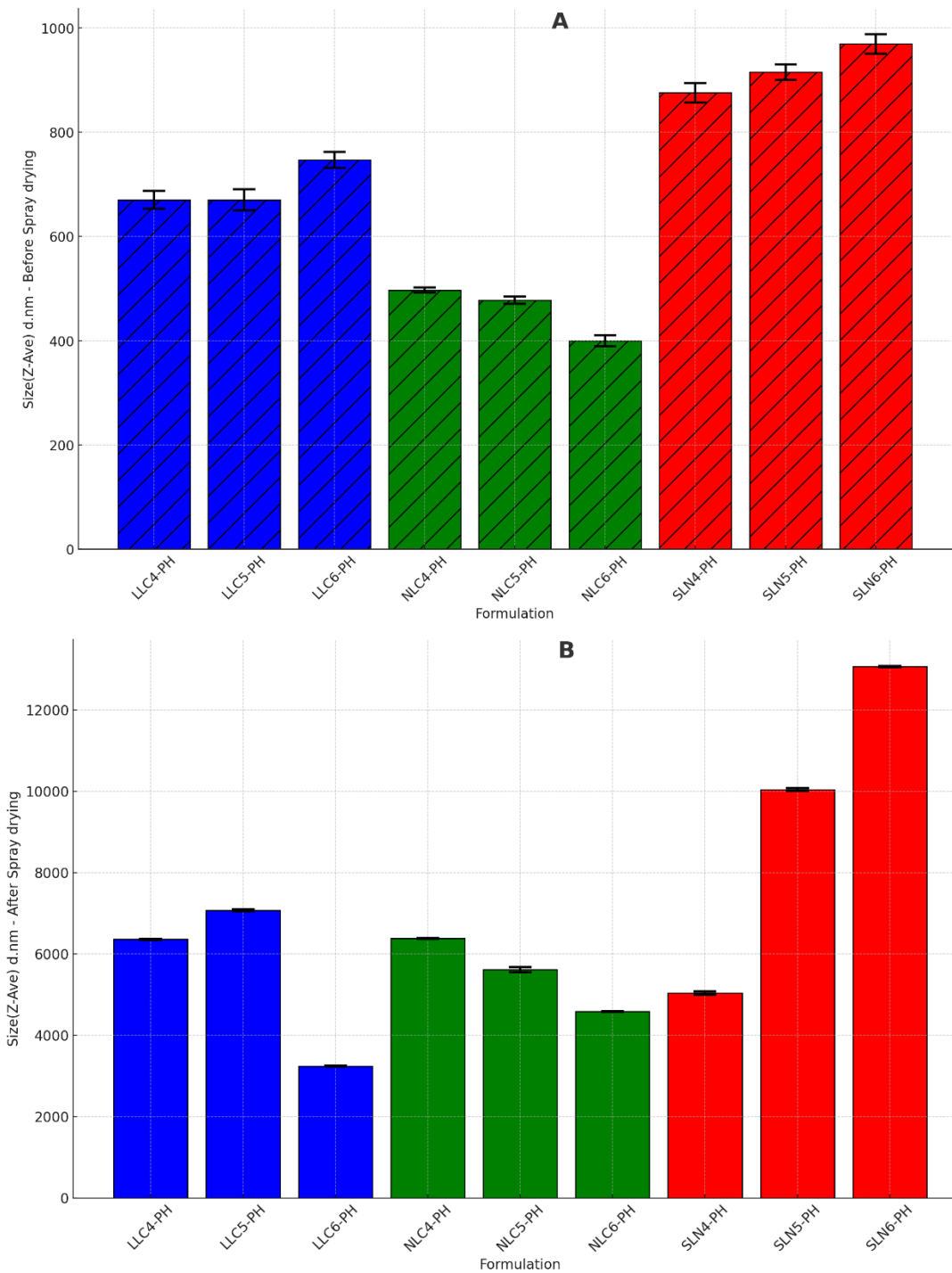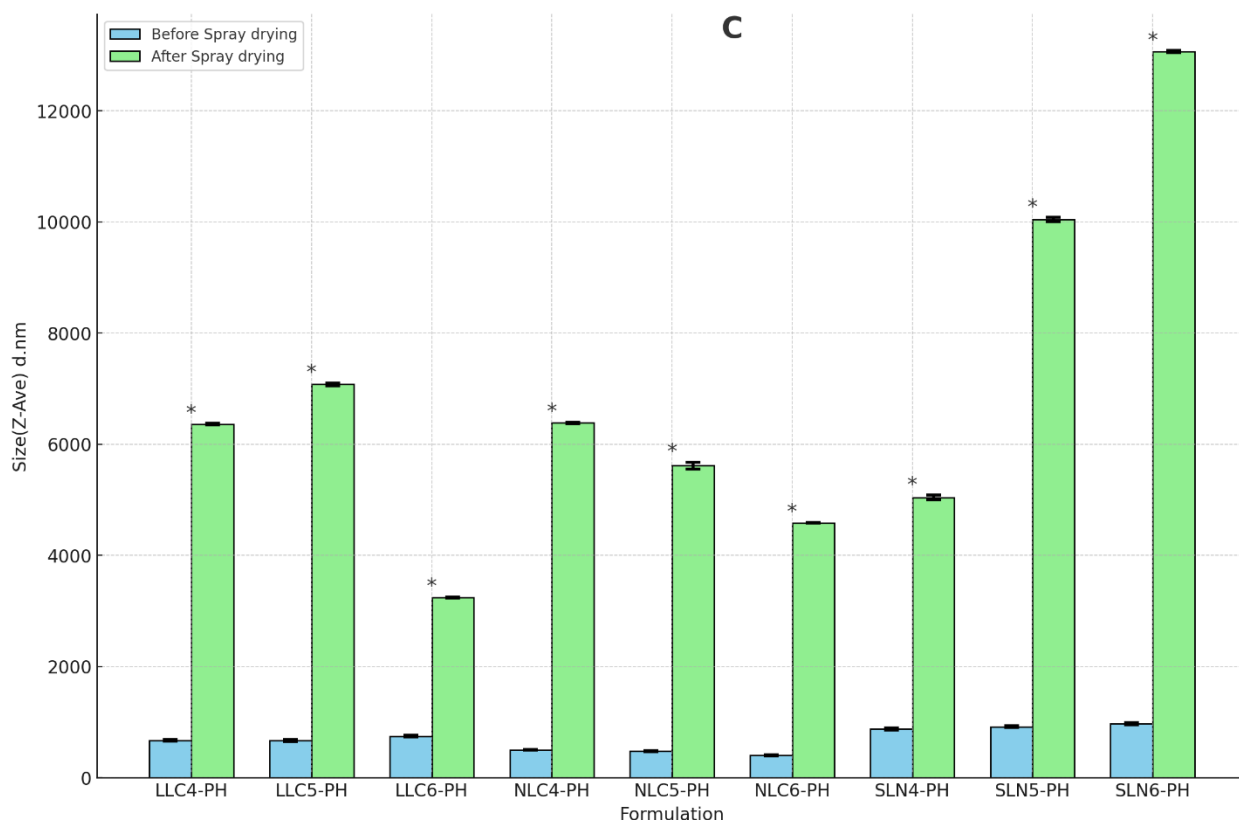
Figure 2. Particle size measurements for PMZ-HQ-loaded LNPs **(A)** before spray drying **(B)** after spray drying**.** In the visualizations (A) and (B), formulations of SLNPH are represented by red bars, formulations of NLCPH are shown in green, and formulations of LLCPH are highlighted in blue. **(C)** Comparative bar graph of particle size measurements before and after spray drying with respective significance levels (*p*-values).

The PDI analysis revealed significant differences among SLNPH, NLCPH, and LLCPH formulations, with distinct *p*-values reflecting variations within each group. SLNPH formulations exhibited higher PDI values due to the rigid, crystalline nature of stearic acid hindering uniform drug encapsulation, resulting in heterogeneous particle sizes and elevated PDIs around 0.8 [26]. In contrast, NLCPH formulations, incorporating oleic acid, showed more flexible lipid matrices, disrupting crystalline structure, facilitating consistent drug encapsulation, and achieving ideal PDIs around 0.2, indicating uniform particle size distribution [17].

LLCPH formulations, composed solely of oleic acid, demonstrated moderate PDIs, suggesting stable size distribution although slightly less uniform than NLCPH. The use of oleic acid in LLCPH provided fluidity crucial for generating uniformly sized particles, evidenced by a PDI of approximately 0.3. The significant difference between SLNPH and NLCPH formulations highlights the critical role of lipid composition in nanoparticle properties, with NLCPH achieving optimal particle distribution. Incorporating oleic acid, either partially as in NLCPH or entirely as in LLCPH, enhanced flexibility and control over nanoparticle formation, resulting in more uniform size distribution and lower PDIs.
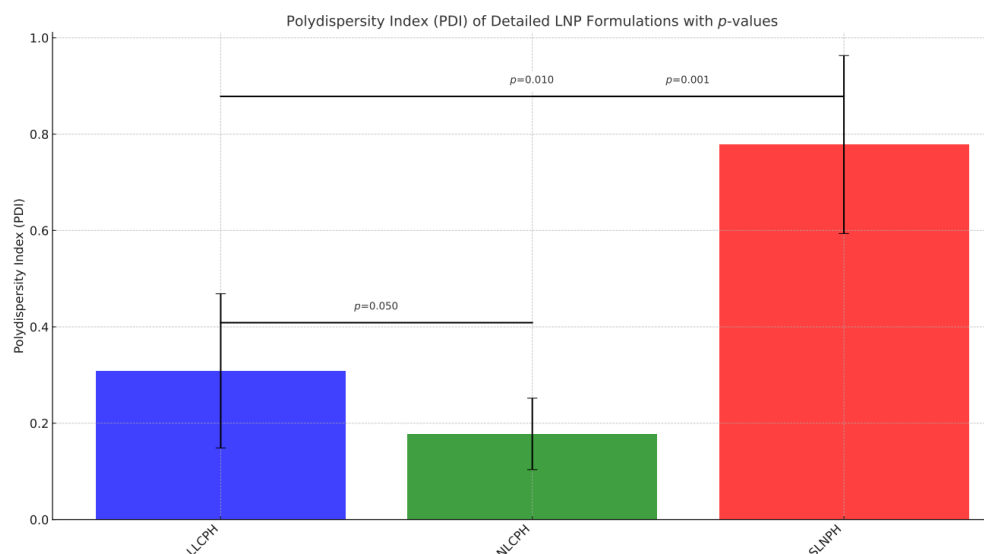

Figure 3. Comparison of the Polydispersity Index (PDI) across three groups of spray-dried LNPs loaded with PMZ and HQ, specifically in SLNPH, NLCPH, and LLCPH, including their statistical significance (*p*-values). SLNPH are indicated in red, NLCPH in green, and LLCPH in blue.

The integration of particle size and zeta potential data illustrates the delicate balance between physical stability and intended application of formulations. Analysis of zeta potentials across different LNPs revealed distinct ranges within LLCPH, NLCPH, and SLNPH groups. The reduction in negative zeta potential values, particularly pronounced in NLCPH and LLCPH, can be attributed to HQ's protonation, increasing surface charge. Significant variations in mean zeta potentials among formulations underscored the impact

of incorporating oleic acid and using mixed solid-liquid lipids versus purely liquid lipid. NLCPH formulations exhibited the highest negative zeta potential values, indicating potential colloidal stability, while SLNPH formulations showed slightly lower zeta potential, and LLCPH formulations recorded the least negative values, potentially reducing particle stability. These parameter variations emphasize the importance of careful formulation optimization and process control, particularly considering their biological impact on distribution, cellular uptake, and drug release profiles.
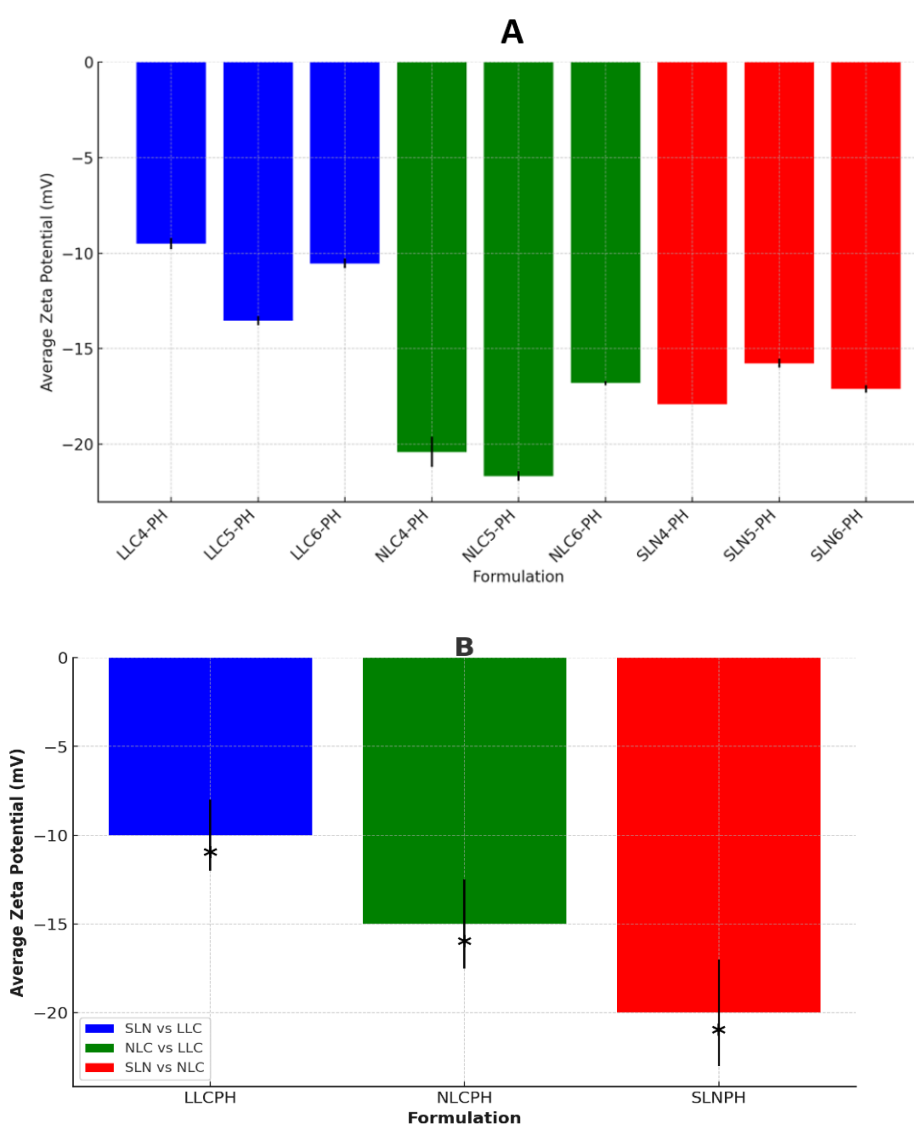

Figure 4. (A) Zeta potential values for the spray-dried PMZ-HQ-loaded LNP powders. **(B)** Comparison of zeta potential values across SLNPH, NLCPH, and LLCPH, along with their

respective significance levels (*p*-values). In these comparisons, SLNPH are depicted in red, NLCPH in green, and LLCPH in blue.

The stability of all nine spray-dried PMZ-HQ-loaded LNPs was assessed after two months of storage at room temperature (20°C to 25°C), revealing notable differences in particle size changes among the formulations. Results in **Figure 5(A)** showed a statistically significant increase in average particle size for all formulations. SLNPH formulations, particularly SLN4PH, SLN5PH, and SLN6PH, experienced significant size increases, potentially due to particle aggregation driven by weak van der Waals forces or lipid matrix rearrangement [25]. Besides, SLNPH formulations suggest a potential for aggregation or growth due to the recrystallization of the lipid matrix, indicating a level of instability in the SLNPH formulations throughout the storage period [27].

Additionally, the moisture absorption of SLNPH formulations, exceeding 40% as evidenced in Section 3.3, could also contribute to particle swelling. On the other hand, LLCPH formulations, including LLC4PH, LLC5PH, and LLC6PH, exhibited a similar trend of increasing particle size, with significant *p*-values indicating instability. NLCPH formulations, comprising NLC4PH, NLC5PH, and NLC6PH, also displayed significant size changes, possibly due to Ostwald ripening and structural reorganization induced by liquid lipids [28].

Analysis of zeta potential in **Figure 5 (B)** revealed a decrease in absolute values across all formulations, indicating a decline in stability. LLCPH formulations exhibited the lowest absolute surface charge, attributed to oleic acid's minimal ionization at physiological pH [29]. Moreover, the decline in the negative surface charge in LLCPH and NLCPH formulations could be due to Ostwald ripening effect, which could change the overall particle size distribution and subsequently reduce the magnitude of the zeta potential [28]. SLNPH formulations exhibited a decline in their positive surface charge, which might be resulting from particle aggregation over time. This aggregation can cause a decrease in the density of the surface charge, ultimately leading to a lowered negative zeta potential

[30].These findings align with moisture sorption data, indicating SLNPH and LLCPH formulations absorb moisture more effectively than NLCPH formulations, affecting ion interactions and surface charge distribution. Increased humidity promotes particle aggregation, altering zeta potential values.
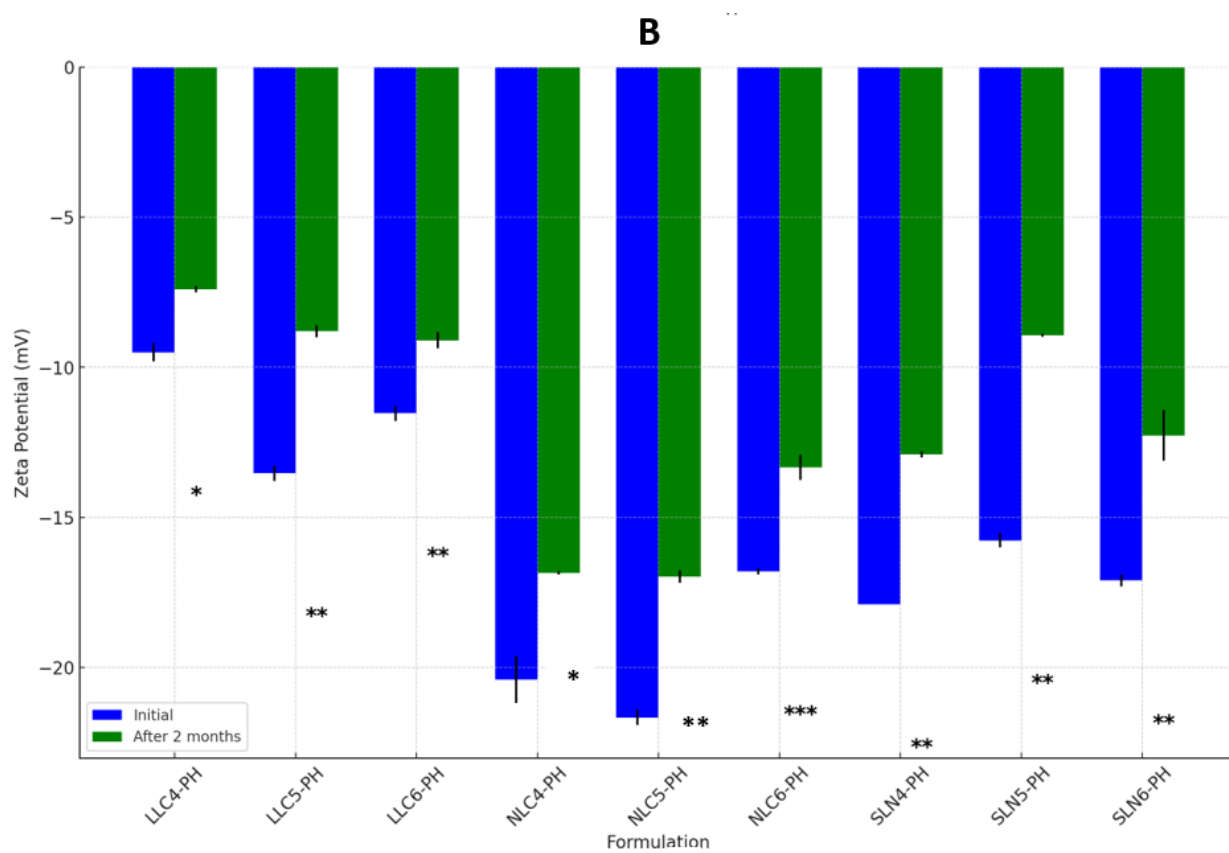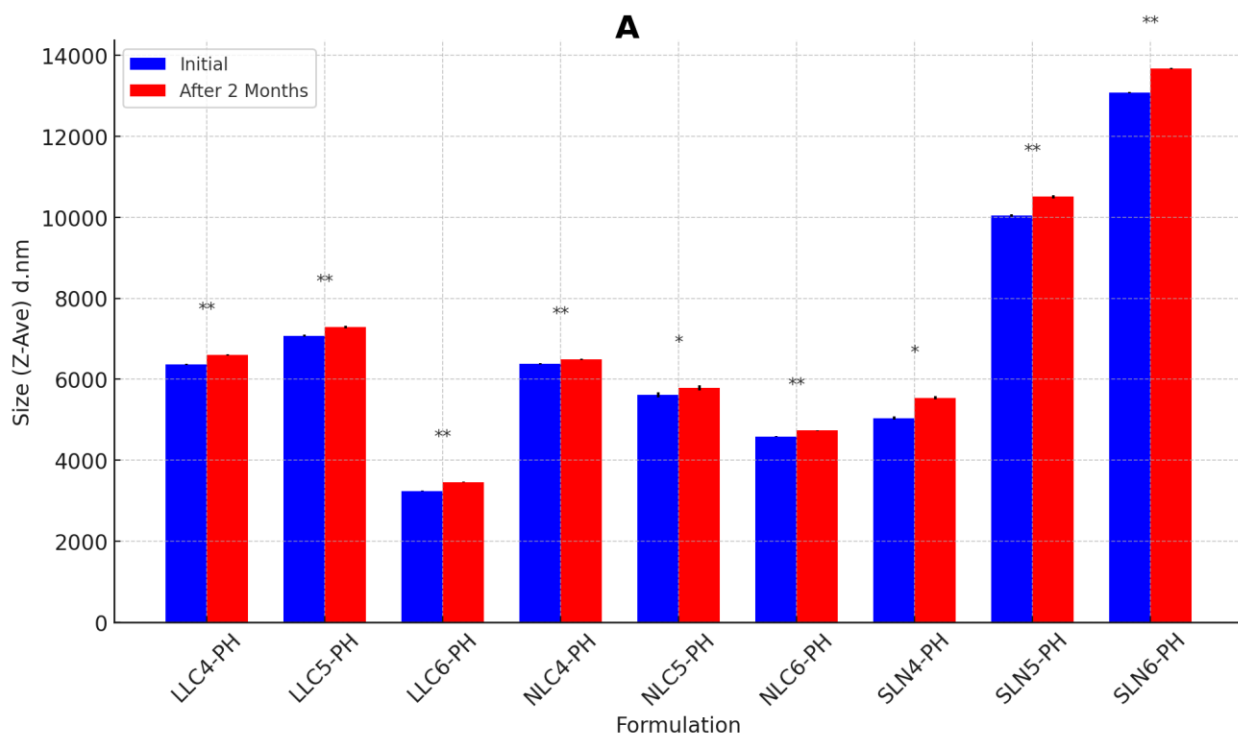
Figure 5. Comparative data on the stability of different spray-dried PMZ-HQ- loaded LNP powders over a period of two months, with **(A)** Particle size and **(B)** Zeta potential serving as indicators of stability. Both charts include the respective significance levels (*p*-values).

5.3.3 Analysis of moisture sorption using Dynamic Vapour Sorption (DVS)

Analysis of relative humidity sorption behavior was conducted for the formulation with the highest EE% among each LNP group, specifically (SLN4PH, NLC5PH, and LLC5PH), revealing distinct sorption and desorption profiles. LLC4PH and SLN4PH formulations demonstrated greater moisture absorption capacities, with maximum sorption exceeding 40%, while NLC5PH exhibited restrained interaction with moisture, with maximum sorption less than 30%.

The SLN4PH formulation shown in **Figure 6 (A)** exhibited dynamic sorption/desorption behavior, with asymmetric profiles at 80% RH and a lag in desorption during the second cycle, indicating potential hydration-induced structural changes. In contrast, the NLC5PH formulation in **Figure 6 (B)** showed consistent patterns between cycles, suggesting higher stability in moisture interaction. While LLC4PH indicated in **Figure 6 (C)** displayed signs of recrystallization, particularly at 80% RH, with pronounced water uptake in the first cycle and slower equilibrium attainment during desorption, possibly indicating the presence of water of crystallization affecting moisture interaction.
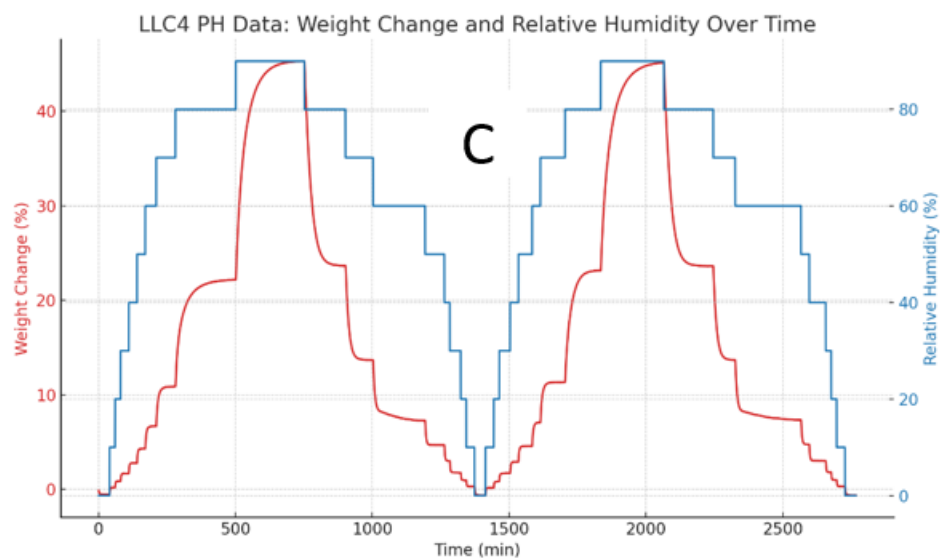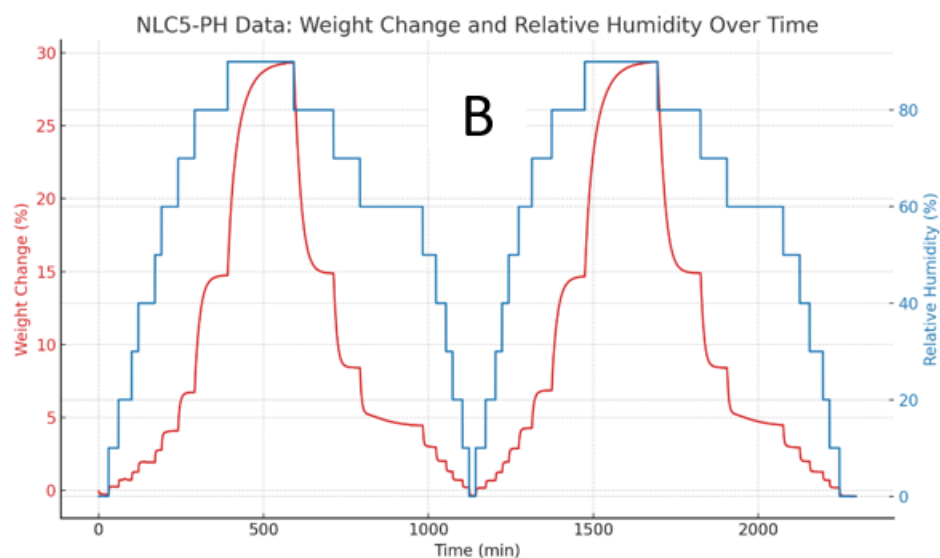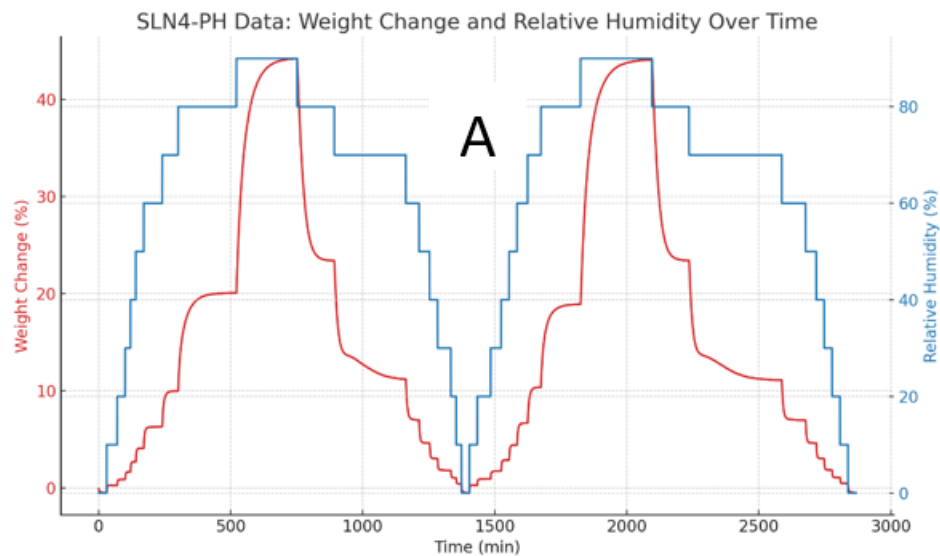
Figure 6. Dynamic Vapor Sorption profiles of various spray-dried PMZ- HQ-loaded LNP formulations, displaying characteristic moisture uptake and release over time for **(A)** SLN4PH, **(B)** NLC5PH, **and (C)** LLC4PH. The red line represents weight change percentage, and the blue line indicates relative humidity percentage over time.

5.3.4   Fourier Transform Infrared Spectroscopy (FTIR)

The FTIR spectroscopic analysis was conducted to identify changes in chemical bonds and to verify the encapsulation of PMZ and HQ within the spray-dried LNP formulations. The results revealed distinct and characteristic peaks for each compound studied. For PMZ, a sharp C=O stretching peak at 1697 cm^{-1} and aromatic ring vibrations between 1200 and 800 cm^{-1} was observed [31]. For HQ, the spectrum featured C=O stretching at 1650-1750 cm^{-1}, alongside C-N stretching at 1200-1350 cm^{-1} and S=O stretching around 1000-1300 cm^{-1} [32]. Stearic acid's notable C=O stretch at 1695 cm^{-1} paired with C-H stretching signals at 2915 and 2848 cm^{-1} [33]. Oleic acid's spectrum was marked by a sharp C=O stretch near 1705 cm^{-1} and C-H stretching between 2850-2950 cm^{-1} [34]. Finally, HPMC-E5 was identified by a characteristic C-O stretch at approximately 1052 cm^{-1}[35].

In the FTIR analysis presented in **Figure 7**, the SLNPH, NLCPH, and LLCPH formulations showed broadened bands above 3000 cm-1 (marked in rectangle shapes), and notable shifts in key vibrational frequencies, signaling molecular interactions within the lipid matrices. Specifically, diminished intensities in PMZ's aromatic C=C stretching (1450-1520 cm^{-1}) and C-H bending (1100-1400 cm^{-1}), alongside a reduced sharpness in the carbonyl (C=O) stretch peak at around 1695 cm^{-1}, suggested alterations in molecular orientation and bonding. Hydroxychloroquine's C-N stretching (1200-1350 cm^{-1}) and S=O stretching (1000-1300 cm^{-1}), as well as stearic acid's characteristic C=O stretch at 1695 cm^{-1} and C-H stretching at 2915 and 2848 cm^{-1}, also exhibited broadening, pointing to changes in their chemical environments. Oleic acid and HPMC-E5's spectral modifications further illustrated these complex interactions, with peak shifts to the right to a lower frequency indicating hydrogen bonding and miscibility within the formulations [36]. Overall,

the spectral data underscored the structural compatibility and integrity of the components, reflecting on the encapsulation efficiency and potential influence on the physical stability and performance of the LNP formulations.
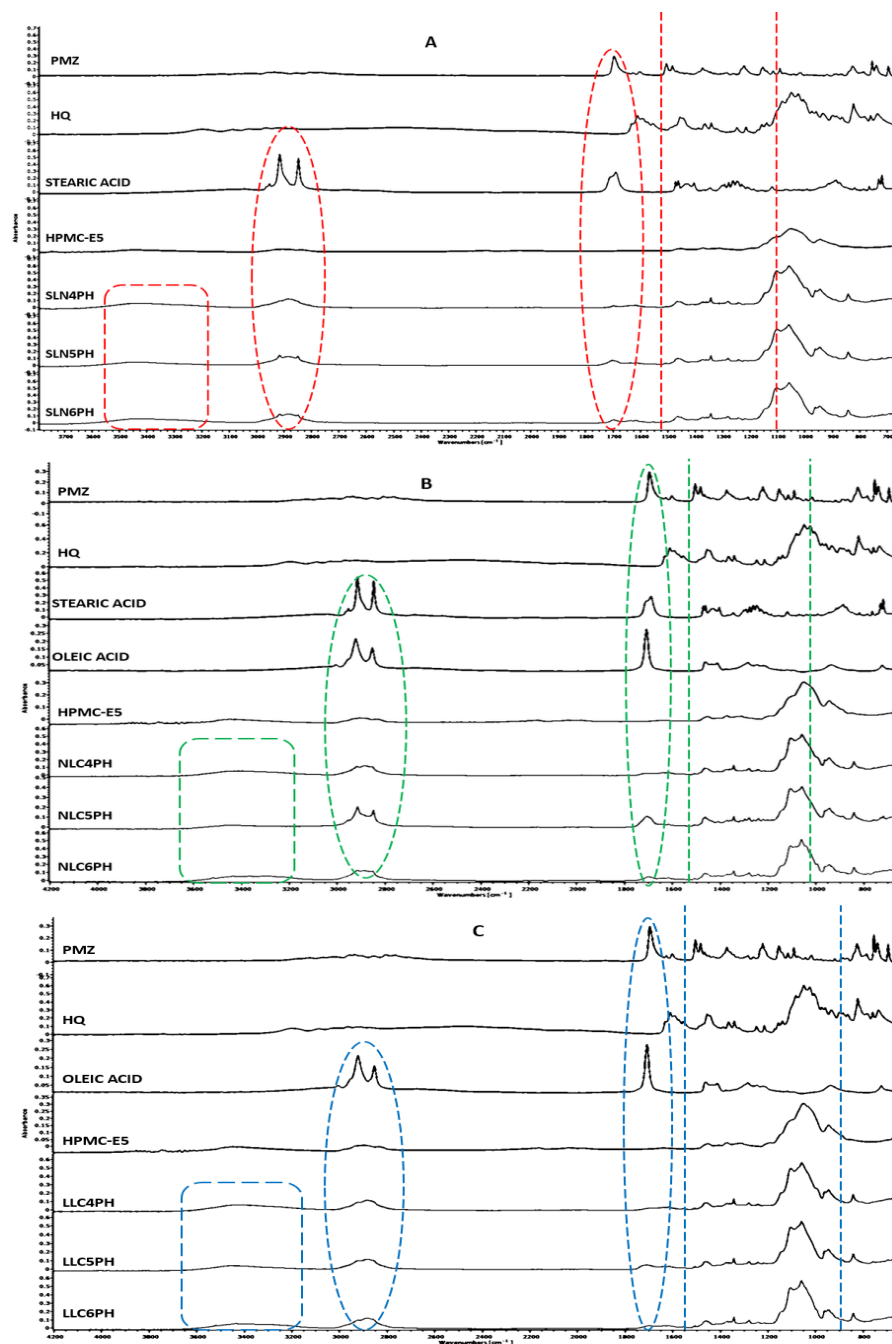

Figure 7. Shows a comparison using FTIR among three sets; **(A)** SLN4PH, SLN5PH, SLN6PH **(B)** NLC4PH, NLC5PH, NLC6PH and **(C)** LLC4PH, LLC5PH, LLC6PH. It also

details their components such, as pimozide (PMZ) hydroxychloroquine (HQ) HPMC E5 and stearic and oleic acids. The chart uses circles and lines to represent differences and frequencies in bands. The SLNPH spectra are highlighted in red NLCPH spectra in LLCPH spectra, in blue.

5.3.5 X-ray powder diffraction (XRPD)

The study revealed how the crystalline structures of spray- dried PMZ- HQ- loaded LNP formulations are influenced by their interactions with various lipids and excipients, impacting drug encapsulation and release strategies. XRPD patterns provided evidence of the crystalline nature of PMZ and HQ, with sharp peaks observed for PMZ at 2θ values of 5.211° (intensity: 196), 5.295° (intensity: 185), and 5.379° (intensity: 195), indicating its structured form [37]. Similarly, HQ's crystallinity was confirmed by significant peaks at 2θ = 5.232° (intensity: 167), 5.295° (intensity: 172), and 5.337° (intensity: 173) [38].

SLNPH formulations, particularly SLN4PH and SLN5PH in **Figure 8 (A)**, showed crystalline XRPD patterns with trehalose and OraRez respectively, while SLN6PH indicated changes in peak intensities due to isomalt, revealing excipients' influence on crystal behavior. NLCPH formulations in **Figure 8 (B)**, depicted shifts in crystalline structure due to the hybrid lipid matrix, with NLC4PH and NLC5PH demonstrating peak movements indicative of changes in PMZ and HQ encapsulation, and NLC6PH revealing distinctive crystalline modifications.

LLCPH analysis in **Figure 8 (C)**, showed structural changes across formulations involving oleic acid, PMZ, HQ, poloxamer 407, HPMC-E5, with LLC4PH, LLC5PH, and LLC6PH exhibiting peak shifts and intensity changes, suggesting new crystalline phases or the alteration of existing ones.
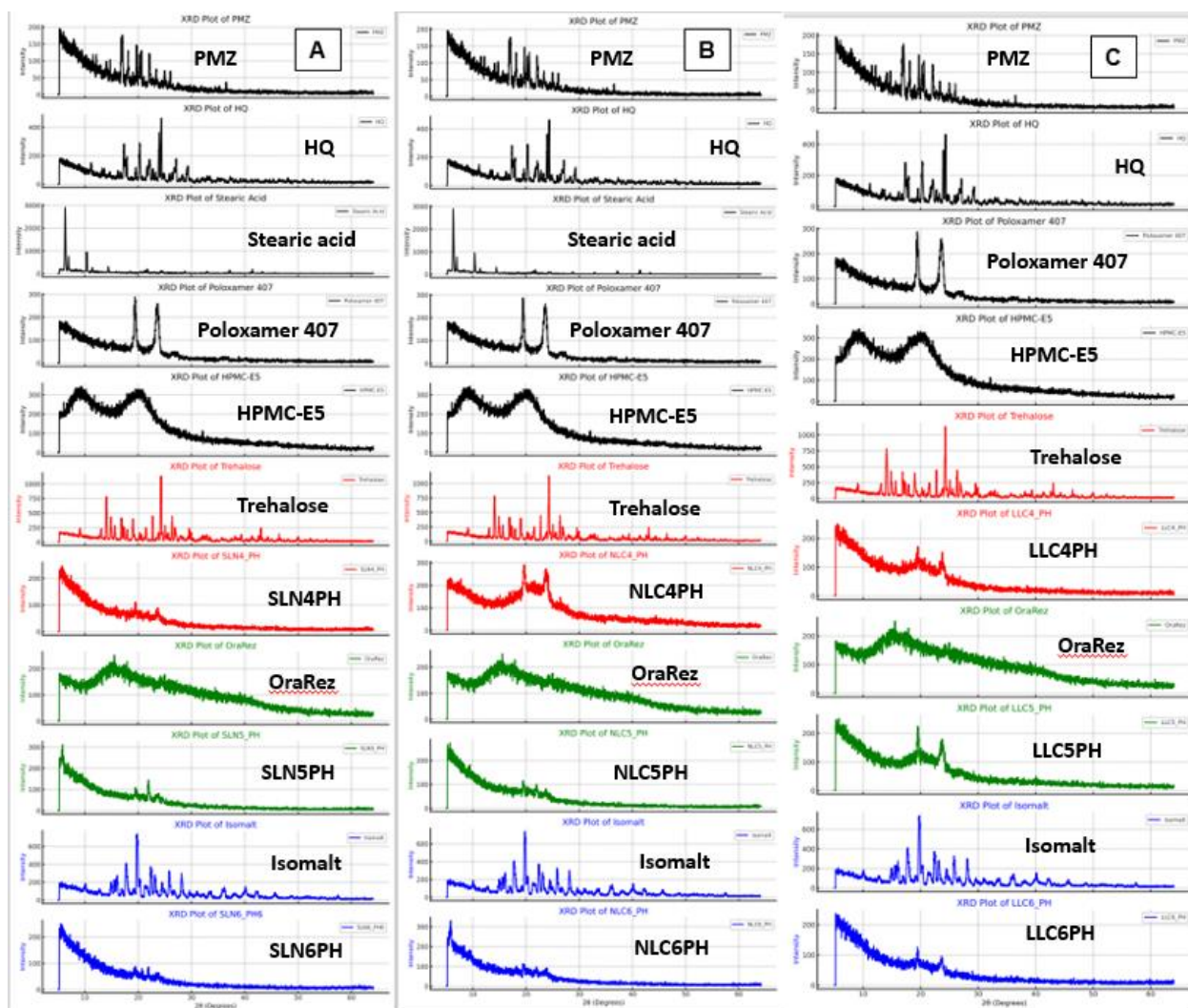
Figure 8. Displays XRPD patterns for the spray-dried LNP powders and their respective constituents. **(A)** SLNPH, **(B)** NLCPH, and **(C)** LLCPH.

5.3.6 Surface morphology

A critical observation made from the SEM images, as illustrated in **Figure 9 (A, B,** and **C)**, is that all formulations showed a size increase post-spray drying, transitioning them from nanoparticles to microparticles. This size augmentation could be attributed to the aggregation or fusion of nanoparticles during the spray drying process [20].

Figure 9 (A) displayed particles that exhibited a relatively smoother exterior, yet with slight depressions [39, 40]. Although there was evidence of some particle clustering, the

particles' loose configuration indicated a possibility for smooth dispersion when subjected to the shear forces of inhalation. Remarkably, the smoother surface of SLN4, in comparison to that of NLC5 and LLC4, coupled with the occurrence of micro-wrinkles, might reduce the tendency of particles to stick together, thereby enhancing their dispersibility.

In **Figure 9 (B)**, NLC5PH particles were characterized by a combination of extensive, flake-like structures and smaller, spherical particles exhibiting varied sizes and partially collapsed edges, typical of spray-dried particles [41]. The flake-like particles showed a layered, sheet-like form with uneven surfaces, whereas the spherical particles appeared more globular. This diversity in form, that is suggested to be arising from the interaction between stearic and oleic acids during the spray-drying process, could influence both flowability and aerodynamic properties. The increased surface area of the flake-like particles could pose a challenge to flowability but may offer aerodynamic benefits if adequately dispersed. However, the incorporation of the excipient is expected to improve particle dispersibility, thereby preserving flowability. The observed surface roughness might reduce particle cohesiveness, improve dispersion, and enhance flowability [42], thus facilitating deeper lung penetration and consistent dosing.

The SEM image of LLC4PH in **Figure 9 (C)** showed particles that exhibited smooth, powdered surfaces featuring grooves, aligning with findings from prior studies [43, 44].
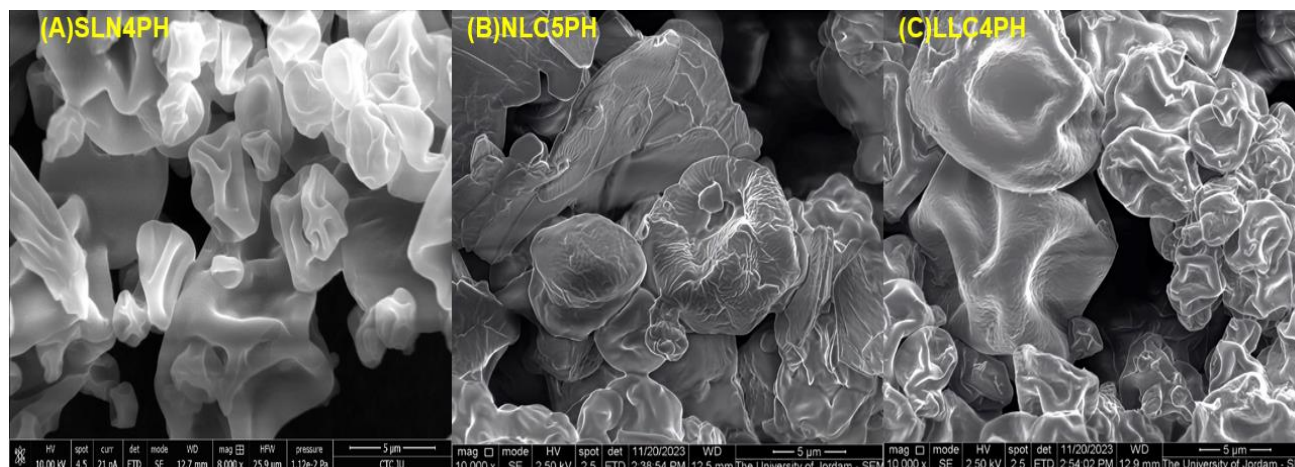
Figure 9. SEM images of **(A)**SLN4PH, **(B)**NLC5PH, and **(C)**LLC4PH spray-dried PMZ-HQ-loaded lipid formulations.

5.3.7 Evaluating the anti-proliferative activity of pimozide- hydroxychloroquine loaded lipid microparticles against A549 cells

Before investigating the combined anti-proliferative effects of spray-dried lipid microparticle formulations loaded with PMZ and HQ, and understanding the nature of their interaction, we first established a baseline by examining the effects of PMZ and HQ individually against A549 lung cancer cells. As shown in **Figure 10**, the results revealed that, after a 72-hour treatment period, PMZ exhibited an average IC_{50} of 13.27 μM which is consistent with previous literature results on the same cell line [45, 46]. On the other hand, HQ showed an average IC_{50} of 20.13 μM. These preliminary results set the stage for a more detailed analysis aimed at determining the type of interaction, whether synergistic, additive, or antagonistic—between PMZ and HQ in an *in vitro* setting.
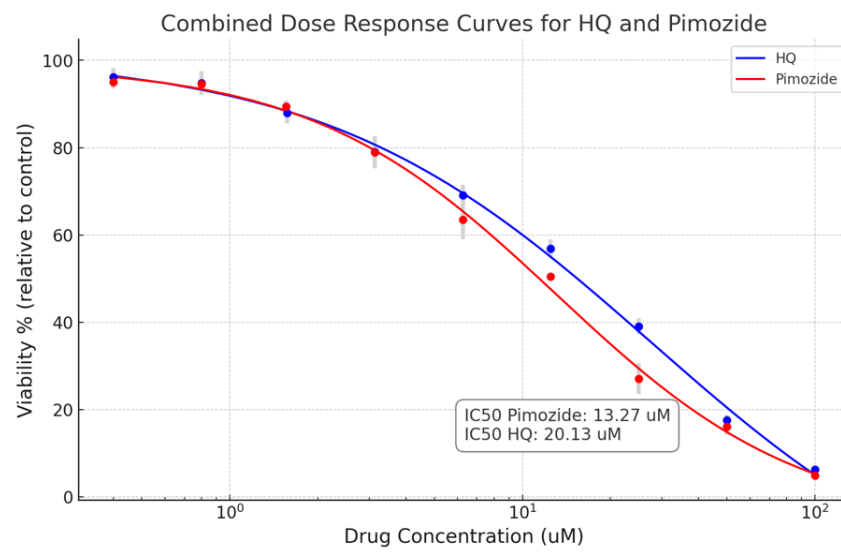
Figure 10. Anti-proliferative effect of free PMZ and HQ. A549 cells were treated with various concentrations of PMZ or HQ as free drugs for 72 hours prior to cell viability assessment using MTT assay. Graphs are presented as percentage viability relative to the untreated control. Data represent the mean ± S.D.

In our study, on the combined effects we looked at spray dried lipid formulations loaded with PMZ-HQ. Found three specific formulations, NLC4PH, NLC5PH and LLC5PH that showed significant anti proliferative effects on A549 lung cancer cells. Interestingly, all three formulations notably decreased the viability of A549 cells (**Figure 11 A- C**) and demonstrated an effect with combination index (CI) values below 1 (**Figure 11 E**). The CI values for NLC4PH, NLC5PH and LLC5PH were measured at 0.535, 0.627 and 0.718 respectively. To confirm that the observed anti proliferative impact was directly linked to the ingredients in the formulations (PMZ and HQ), we conducted tests using the excipients (**Figure 11 D**). These control experiments revealed that the excipients alone did not significantly affect cell viability compared to the control untreated group thus validating that the substantial reduction in cell viability was indeed a result of the interaction, between PMZ and HQ.

The observed enhancement of anti-proliferative action against A549 cell lines, accomplished by combining HQ with PMZ within the formulations, confirms findings from prior investigations. Since previous studies have documented HQ's ability to strengthen the anti-cancer effects of several chemotherapeutic agents such as epirubicin [47], doxorubicin [48], and bevacizumab [49] in a variety of cancer cells. While the precise processes are not entirely clear, HQ displays a range of effects, at the molecular level greatly improving the effectiveness of cancer treatments by closely integrating with key cellular functions like survival, growth and cell death. A key aspect of HQs role, in fighting cancer is its ability to block autophagy [50]. HQ targets this process by disrupting the fusion between autophagosomes and lysosomes, leading to the accumulation of cellular debris [51]. This action shifts the cellular balance towards stress and induction of apoptosis. This mechanism is further supported by the involvement of membrane Na+/H+ exchangers (NHE), which facilitate the uptake of HQ along with sodium ions in exchange for protons. This exchange contributes to the accumulation of these drugs within endosomes/lysosomes, further interfering with autophagic flux [52].

Parallel to its role in autophagy inhibition, HQ exerts a profound influence on apoptosis by modulating the expression and activity of key proteins involved in the apoptotic pathways, such as downregulating anti-apoptotic proteins like Bcl-2 and activating caspases [53]. Importantly, the anticancer effect of HQ significantly amplified through its interaction with the STAT3 signaling pathway [54] . STAT3, a key player in oncogenic processes, promotes tumor growth. By targeting and inactivating the STAT3 pathway, HQ exhibits a parallel mechanism to PMZ which also targets STAT3 pathway [55]. This inhibition leads to a cascade of intracellular events resulting in enhanced caspase activation, a crucial step in the execution phase of apoptosis.

Moreover, beyond targeting the cancer cells directly, HQ modifies the immune landscape within the tumour microenvironment. At the heart of this immunomodulatory effect, the inhibition of Toll-like receptors stands out. This inhibition ultimately leads to a reduction in the secretion and production of pro-inflammatory cytokines by various immune cells. The cytokines affected include interleukins (IL-6, IL-1), interferons (IFN-γ/α), and tumour

necrosis factor-alpha (TNF-α), along with the expression of TNF receptors on macrophages, T cells, and B lymphocytes. This immunomodulatory effect can paradoxically enhance the anti-tumour immune response, making the tumour microenvironment less conducive to cancer growth and more favourable to destruction by immune cells [56-58].
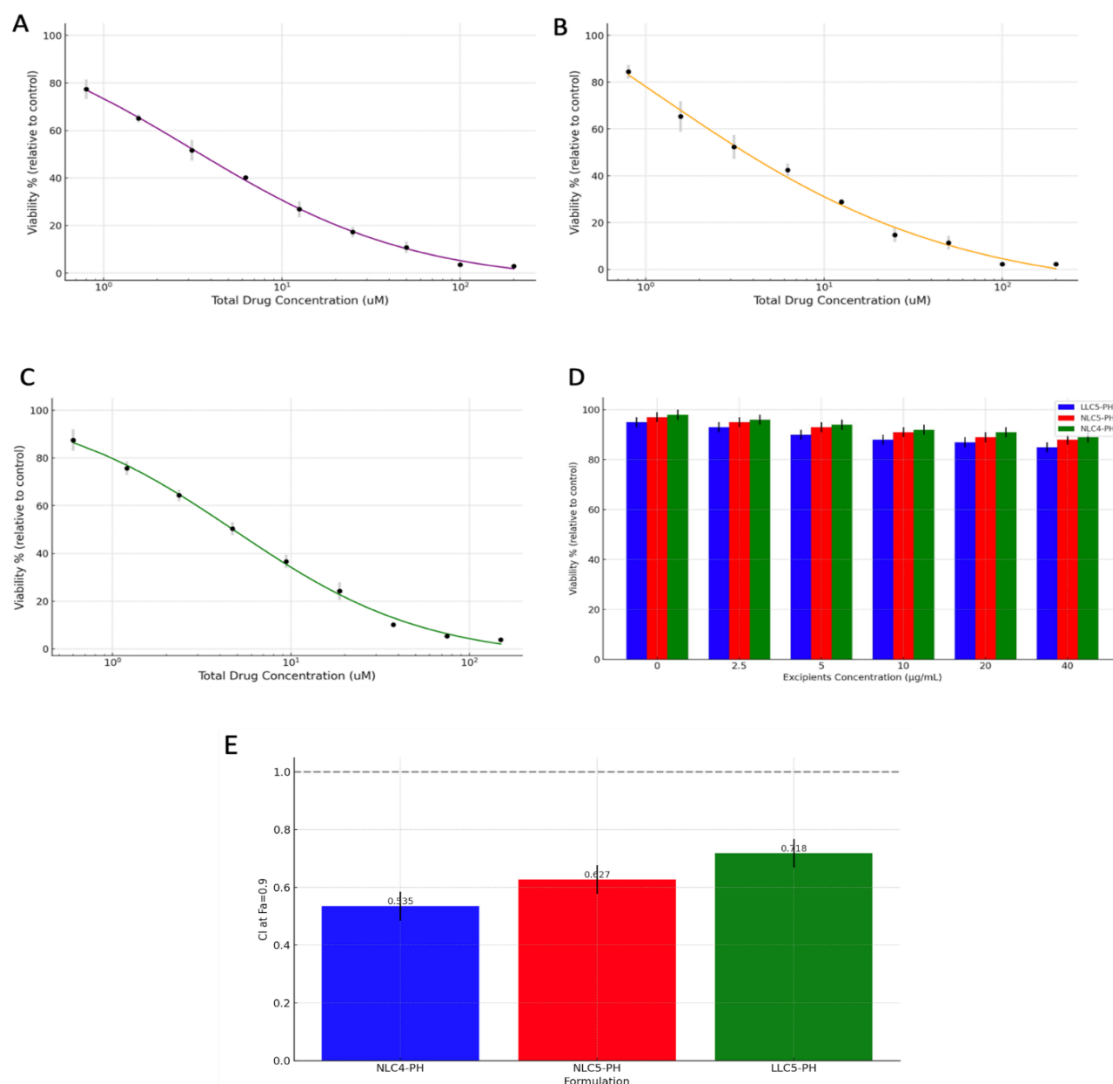

Figure 11. Synergistic anti-Proliferative effects of PMZ and HQ in spray-dried lipid formulations. A549 cells were treated with various concentrations of (A) NLC4PH, (B) NLC5PH, and (C) LLC5PH or (D) empty vehicle excipients for 72 hours prior to cell viability assessment using MTT assay. (E) CI values for each formulation at Fa=0.9 (90% inhibition

of cell viability), highlighting their synergistic effects. The horizontal blue line in (E) represents the cut-off point for the additive effect (CI = 1). Values below this line indicate a synergistic effect, values at this line indicate an additive effect, and values above this line indicate an antagonistic effect. The fitting model was logistic fitting

5.3.8 Evaluating the anti-inflammatory effect of spray- dried pimozide hydroxychloroquine loaded lipid formulations

After identifying three spray-dried PMZ-HQ loaded lipid formulations (NLC4PH, NLC5PH, and LLC5PH) that exhibited anti-proliferative activity against A549 lung cancer cells, the subsequent step involved evaluating their impact on the expression of various pro-inflammatory cytokines, compared to untreated control samples. The analyzed cytokines included IL-1β, IL-6, IL-8, and TNF-α. The results revealed a significant downregulation of all pro-inflammatory cytokines expression across all treated groups when compared to the untreated control (p<0.001) as shown in **Figure 12**. This anti-inflammatory effect of all formulations was largely attributed to the HQ component (**Supplementary figure 1**). HQ is known for its potent anti-inflammatory properties, which are mediated through several molecular mechanisms.

Firstly, the ability of HQ to interfere with lysosomal activity leads to a reduced processing and presentation of antigens, thereby diminishing the immune system's activation and response [59]. This mechanism plays a crucial role in the observed downregulation of cytokines like IL-1β and TNF-α, which are pivotal in the initiation of the inflammatory cascade. Secondly, the inhibition of Toll-like receptor (TLR) signaling by HQ contributes to the decrease in IL-6 and IL-8 levels, cytokines closely associated with the innate immune response and the recruitment of immune cells to sites of inflammation [60]. Additionally, by inhibiting autophagy and stabilizing cellular membranes, HQ further reduces the cellular capabilities to propagate inflammatory signals, aiding in the overall suppression of pro-inflammatory cytokine production [61]. Moreover, the effect of HQ on cytokine production can be linked to its direct and indirect suppression of NF-κB pathway

resulting in decreased transcription of pro-inflammatory genes, including those coding for IL-1β, IL-6, TNF-α, and IL-8 [62].
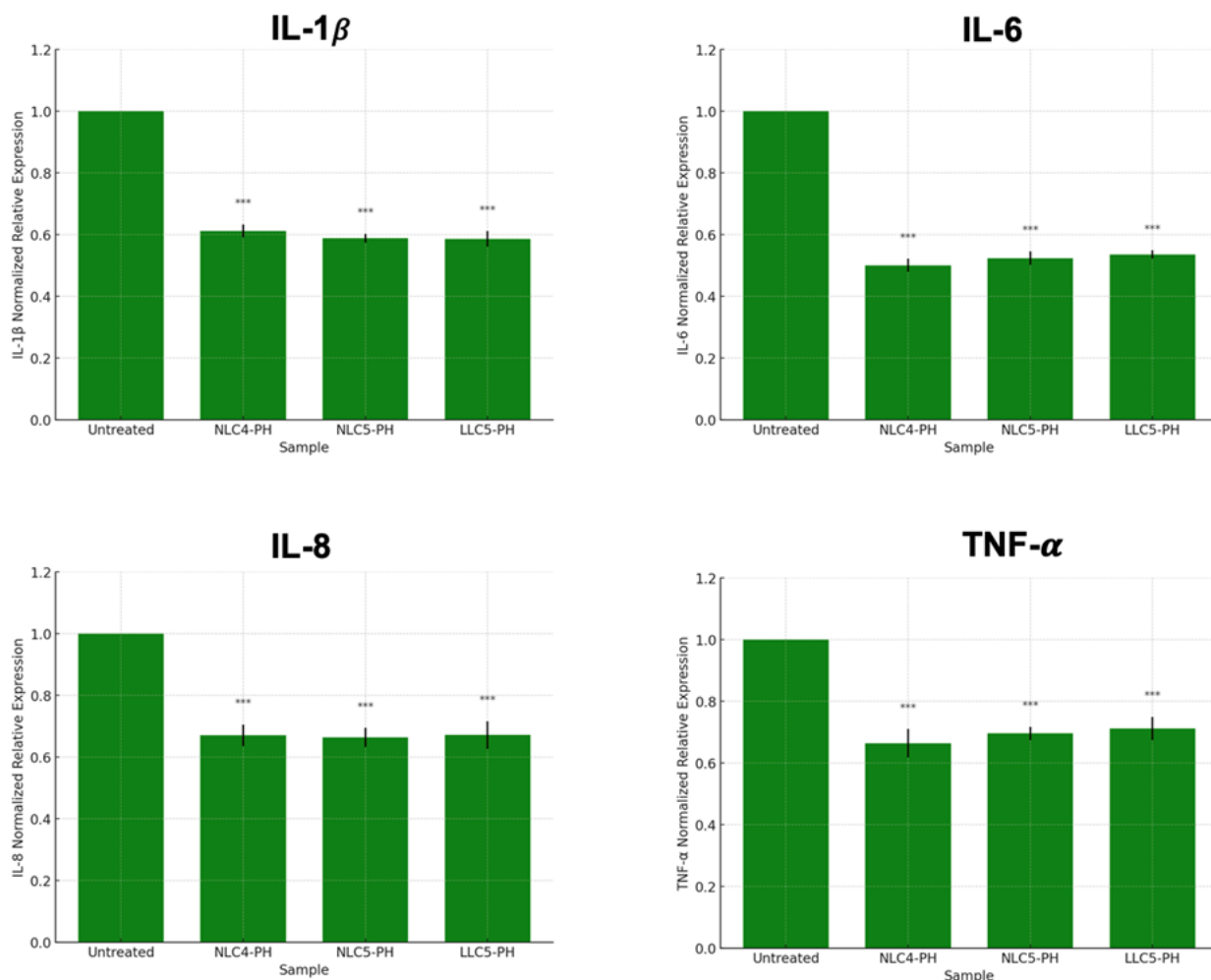
Figure 12. The anti-inflammatory effect of NLC4-PH, NLC5-PH, and LLC5-PH. Relative RNA expression of -1β, IL-6, IL-8, and TNF-α gene on THP-1 macrophages cell line. RNA was isolated and quantified using QPCR technique and the expression of the indicated genes was normalized against untreated cells.

5.3.9 Drug release studies

The release kinetic of PMZ and HQ from NLC4PH, NLC5PH, and LLC5PH formulations was monitored over a period of 72 hour. In the context of PMZ, all formulations showed a

biphasic release profile with an initial burst release during the first 4 hours followed by a sustained release kinetic where NLC4PH and NLC5PH had an average release of 23.17% and 29% respectively at the 4 hours timepoint. Interestingly, while the LLC5PH followed the same biphasic release patterns, the initial burst release was higher compared to the NLCPH formulations with 45.33% of PMZ was released during the first 4 hours **(Figure 13 A)**.

The case of HQ was not different from PMZ release where all formulations exhibited a biphasic release pattern with the LLC5PH formulation revealed the fastest initial burst release **(Figure 13 B)**. The distinct release profile observed in the LLC5PH formulation could be due to the physical properties of its lipids. Specifically, the liquid state of the lipid components which makes the formula less crystalline, resulting in a less ordered lipid matrix. This structure is likely responsible for the high initial burst release observed [13].
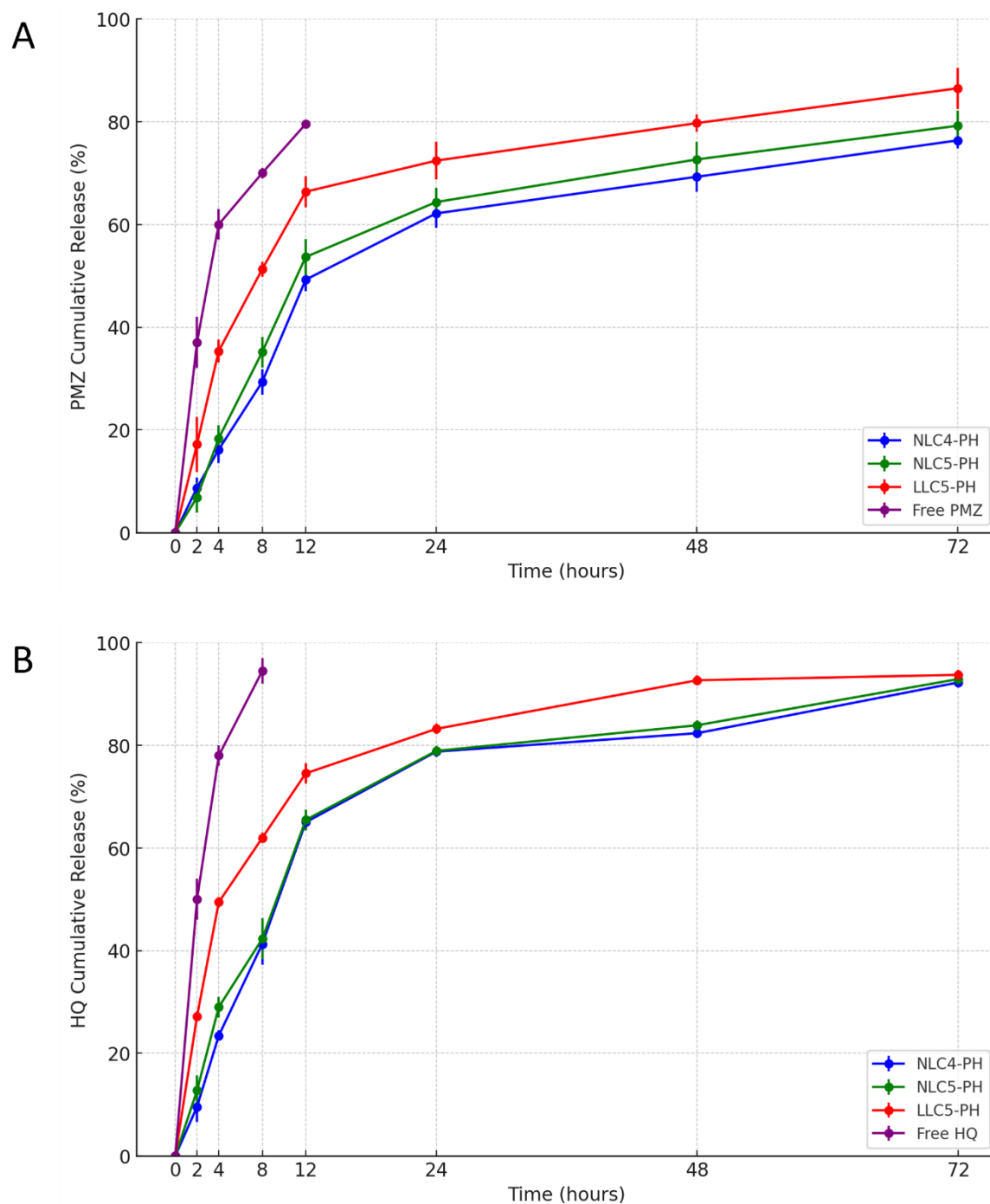
Figure 13. The release kinetic of **(A)** PMZ and **(B)** HQ from NLC4-PH, NLC5-PH, and LLC5-PH formulations. Free drugs were used as control. Values are means ± SD.

5.4 Conclusions

This study's investigation into spray-dried PMZ- HQ- loaded LNP formulations for non-small cell lung cancer (NSCLC) treatment highlights the potential of nanostructured lipid carriers (NLCPH) as superior vehicles for delivering pimozide (PMZ) and hydroxychloroquine (HQ). Demonstrating high encapsulation efficiencies, optimal particle sizes for pulmonary delivery, and favorable physical stability, NLCPH formulations emerged as particularly effective. Key findings from SEM, DVS, FTIR, and XRPD analyses provided deep insights into the physicochemical properties and structural integrity of the drug-loaded LNPs, affirming their effective encapsulation and stability.

Furthermore, biological evaluations revealed significant anti-proliferative effects and synergistic action between PMZ and HQ, alongside a notable reduction in pro-inflammatory cytokines, underscoring the added value of HQ's anti-inflammatory properties. The comprehensive study not only underscores the importance of formulation strategy in LNP-based drug delivery but also sets a foundation for advancing NSCLC therapy, offering a promising outlook for future cancer treatment advancements.

References:

[1]   A. C. Society., "American Cancer Society Facts and Figures," 1988.

[2]   R. Karuppasamy, S. Veerappapillai, S. Maiti, W.-H. Shin, and D. Kihara, "Current progress and future perspectives of polypharmacology: From the view of non-small cell lung cancer," in *Seminars in cancer biology*, 2021, vol. 68: Elsevier, pp. 84-91.

[3]   Z.-N. Lei *et al.*, "Chloroquine and hydroxychloroquine in the treatment of malaria and repurposing in treating COVID-19," *Pharmacology & Therapeutics,* vol. 216, p. 107672, 2020.

[4]   E. L. Nirk, F. Reggiori, and M. Mauthe, "Hydroxychloroquine in rheumatic autoimmune disorders and beyond," *EMBO molecular medicine,* vol. 12, no. 8, p. e12476, 2020.

[5]   Y. Li *et al.*, "Hydroxychloroquine induced lung cancer suppression by enhancing chemo-sensitization and promoting the transition of M2-TAMs to M1-like macrophages," *Journal of Experimental & Clinical Cancer Research,* vol. 37, pp. 1-16, 2018.

[6]   A. Olszewska *et al.*, "Escape from cisplatin-induced senescence of hypoxic lung cancer cells can be overcome by hydroxychloroquine," *Frontiers in Oncology,* vol. 11, p. 738385, 2022.

[7]   A. Duffy, J. Le, E. Sausville, and A. Emadi, "Autophagy modulation: a target for cancer treatment development," *Cancer chemotherapy and pharmacology,* vol. 75, pp. 439-447, 2015.

[8]   V. R. Salvi and P. Pawar, "Nanostructured lipid carriers (NLC) system: A novel drug targeting carrier," *Journal of Drug Delivery Science and Technology,* vol. 51, pp. 255-267, 2019.

[9]   B. Subramaniam, Z. H. Siddik, and N. H. Nagoor, "Optimization of nanostructured lipid carriers: Understanding the types, designs, and parameters in the process of formulations," *Journal of nanoparticle research,* vol. 22, pp. 1-29, 2020.

[10]   W.-H. Lee, C.-Y. Loo, M. Ghadiri, C.-R. Leong, P. M. Young, and D. Traini, "The potential to treat lung cancer via inhalation of repurposed drugs," *Advanced drug delivery reviews,* vol. 133, pp. 107-130, 2018.

[11]   S. Javed, B. Mangla, Y. Almoshari, M. H. Sultan, and W. Ahsan, "Nanostructured lipid carrier system: A compendium of their formulation development approaches, optimization strategies by quality by design, and recent applications in drug delivery," *Nanotechnology Reviews,* vol. 11, no. 1, pp. 1744-1777, 2022.

[12]   A.-K. Tuderman, C. J. Strachan, and A. M. Juppo, "Isomalt and its diastereomer mixtures as stabilizing excipients with freeze-dried lactate dehydrogenase," *International Journal of Pharmaceutics,* vol. 538, no. 1-2, pp. 287-295, 2018.

[13]   N. Aditya *et al.*, "Development and evaluation of lipid nanocarriers for quercetin delivery: A comparative study of solid lipid nanoparticles (SLN), nanostructured lipid carriers (NLC), and lipid nanoemulsions (LNE)," *LWT-Food Science and Technology,* vol. 59, no. 1, pp. 115-121, 2014.

[14]   P. Kaur, V. Mishra, T. Shunmugaperumal, A. K. Goyal, G. Ghosh, and G. Rath, "Inhalable spray dried lipidnanoparticles for the co-delivery of paclitaxel and doxorubicin in lung cancer," *Journal of Drug Delivery Science and Technology,* vol. 56, p. 101502, 2020.

[15]   S. Das and A. Chaudhury, "Recent advances in lipid nanoparticle formulations with solid matrix for oral drug delivery," *Aaps Pharmscitech,* vol. 12, pp. 62-76, 2011.

[16]   P. Mura, F. Maestrelli, M. D'Ambrosio, C. Luceri, and M. Cirri, "Evaluation and comparison of solid lipid nanoparticles (SLNs) and nanostructured lipid carriers (NLCs) as vectors to develop hydrochlorothiazide effective and safe pediatric oral liquid formulations," *Pharmaceutics,* vol. 13, no. 4, p. 437, 2021.

[17]   H. Nsairat *et al.*, "Lipid nanostructures for targeting brain cancer," *Heliyon,* vol. 7, no. 9, 2021.

[18]   C. Yue-Xing *et al.*, "The effect of l-leucine on the stabilization and inhalability of spray-dried solid lipid nanoparticles for pulmonary drug delivery," *Journal of Drug Delivery Science and Technology,* vol. 46, pp. 474-481, 2018.

[19]   P. Tewa-Tagne, S. Briançon, and H. Fessi, "Preparation of redispersible dry nanocapsules by means of spray-drying: development and characterisation," *European Journal of Pharmaceutical Sciences,* vol. 30, no. 2, pp. 124-135, 2007.

[20]   B. Siekmann and K. Westesen, "Thermoanalysis of the recrystallization process of melt-homogenized glyceride nanoparticles," *Colloids and surfaces B: Biointerfaces,* vol. 3, no. 3, pp. 159-175, 1994.

[21]   A. M. Lammert, S. J. Schmidt, and G. A. Day, "Water activity and solubility of trehalose," *Food Chemistry,* vol. 61, no. 1-2, pp. 139-144, 1998.

[22]   T. Lipiäinen, M. Peltoniemi, H. Räikkönen, and A. Juppo, "Spray-dried amorphous isomalt and melibiose, two potential protein-stabilizing excipients," *International Journal of Pharmaceutics,* vol. 510, no. 1, pp. 311-322, 2016.

[23]   C. Pardeshi *et al.*, "Solid lipid based nanocarriers: An overview/Nanonosači na bazi čvrstih lipida: Pregled," *Acta pharmaceutica,* vol. 62, no. 4, pp. 433-472, 2012.

[24]   A. Gordillo-Galeano and C. E. Mora-Huertas, "Solid lipid nanoparticles and nanostructured lipid carriers: A review emphasizing on particle structure and drug release," *European Journal of Pharmaceutics and Biopharmaceutics,* vol. 133, pp. 285-308, 2018.

[25]   K. Westesen, H. Bunjes, and M. Koch, "Physicochemical characterization of lipid nanoparticles and evaluation of their drug loading capacity and sustained release potential," *Journal of controlled release,* vol. 48, no. 2-3, pp. 223-236, 1997.

[26]   C. Freitas and R. H. Müller, "Spray-drying of solid lipid nanoparticles (SLNTM)," *European Journal of Pharmaceutics and Biopharmaceutics,* vol. 46, no. 2, pp. 145-151, 1998.

[27]   C. Freitas and R. H. Müller, "Correlation between long-term stability of solid lipid nanoparticles (SLN™) and crystallinity of the lipid phase," *European Journal of Pharmaceutics and Biopharmaceutics,* vol. 47, no. 2, pp. 125-132, 1999/03/01/ 1999, doi: https://doi.org/10.1016/S0939-6411(98)00074-5.

[28]   T. Delmas *et al.*, "How to prepare and stabilize very small nanoemulsions," *Langmuir,* vol. 27, no. 5, pp. 1683-1692, 2011.

[29]   D. P. Cistola, *Physicochemical Studies of Fatty Acids in Model Biological Systems (albumin, lipid bilayers, X-ray diffraction, non-esterified, nuclear magnetic resonance, NMR)*. Boston University, 1985.

[30]   Y.-C. Kuo and I.-C. Chen, "Evaluation of surface charge density and surface potential by electrophoretic mobility for solid lipid nanoparticles and human brain– microvascular endothelial cells," *The Journal of Physical Chemistry B,* vol. 111, no. 38, pp. 11228-11236, 2007.

[31]   H. Bera *et al.*, "Novel pimozide-β-cyclodextrin-polyvinylpyrrolidone inclusion complexes for Tourette syndrome treatment," *Journal of Molecular Liquids,* vol. 215, pp. 135-143, 2016/03/01/ 2016, doi: https://doi.org/10.1016/j.molliq.2015.12.054.

[32]   F. Faísca, V. Correia, Ž. Petrovski, L. C. Branco, H. Rebelo-de-Andrade, and M. M. Santos, "Enhanced In Vitro Antiviral Activity of Hydroxychloroquine Ionic Liquids against SARS-CoV-2," *Pharmaceutics,* vol. 14, no. 4, p. 877, 2022. [Online]. Available: https://www.mdpi.com/1999-4923/14/4/877.

[33]   P. Sawunyama, L. Jiang, A. Fujishima, and K. Hashimoto, "Photodecomposition of a Langmuir–Blodgett film of stearic acid on TiO2 film observed by in situ atomic force microscopy and FT-IR," *The Journal of Physical Chemistry B,* vol. 101, no. 51, pp. 11000-11003, 1997.

[34]   J. Ibarra *et al.*, "Synthesis and characterization of magnetite/PLGA/chitosan nanoparticles," *Materials Research Express,* vol. 2, pp. 1-17, 09/11 2015, doi: 10.1088/2053-1591/2/9/095010.

[35]   Z. Song *et al.*, "Improving Breviscapine Oral Bioavailability by Preparing Nanosuspensions, Liposomes and Phospholipid Complexes," *Pharmaceutics,* vol. 13, p. 132, 01/20 2021, doi: 10.3390/pharmaceutics13020132.

[36]   A. Bhanderi, F. Bari, and H. Al-Obaidi, "Evaluation of the impact of surfactants on miscibility of griseofulvin in spray dried amorphous solid dispersions," *Journal of Drug Delivery Science and Technology,* vol. 64, p. 102606, 2021.

[37]   N. Wyttenbach, A. Niederquell, P. Ectors, and M. Kuentz, "Study and Computational Modeling of Fatty Acid Effects on Drug Solubility in Lipid-Based Systems," *Journal of Pharmaceutical Sciences,* vol. 111, no. 6, pp. 1728-1738, 2022/06/01/ 2022, doi: https://doi.org/10.1016/j.xphs.2021.11.023.

[38]   A. N. F. Moraes *et al.*, "Compatibility study of hydroxychloroquine sulfate with pharmaceutical excipients using thermal and nonthermal techniques for the development of hard capsules," *Journal of Thermal Analysis and Calorimetry,* vol. 140, no. 5, pp. 2283-2292, 2020/06/01 2020, doi: 10.1007/s10973-019-08953-8.

[39]   V. Paramita, K. Iida, H. Yoshii, and T. Furuta, "Effect of additives on the morphology of spray-dried powder," *Drying Technology,* vol. 28, no. 3, pp. 323-329, 2010.

[40]   R. V. Tonon, C. R. Grosso, and M. D. Hubinger, "Influence of emulsion composition and inlet air temperature on the microencapsulation of flaxseed oil by spray drying," *Food research international,* vol. 44, no. 1, pp. 282-289, 2011.

[41]   H. Xi *et al.*, "Characterization of spray dried particles through microstructural imaging," *Journal of Pharmaceutical Sciences,* vol. 109, no. 11, pp. 3404-3412, 2020.

[42]   A. Baldelli and R. Vehring, "Analysis of cohesion forces between monodisperse microparticles with rough surfaces," *Colloids and Surfaces A: Physicochemical and Engineering Aspects,* vol. 506, pp. 179-189, 2016.

[43]   D. Li, L. Li, N. Xiao, M. Li, and X. Xie, "Physical properties of oil-in-water nanoemulsions stabilized by OSA-modified starch for the encapsulation of lycopene," *Colloids and Surfaces A: Physicochemical and Engineering Aspects,* vol. 552, pp. 59-66, 2018/09/05/ 2018, doi: https://doi.org/10.1016/j.colsurfa.2018.04.055.

[44]   A. Soottitantawat, F. Bigeard, H. Yoshii, T. Furuta, M. Ohkawara, and P. Linko, "Influence of emulsion and powder size on the stability of encapsulated D-limonene by spray drying," *Innovative Food Science & Emerging Technologies,* vol. 6, no. 1, pp. 107-114, 2005.

[45]   E.-H. Dakir *et al.*, "The anti-psychotic drug pimozide is a novel chemotherapeutic for breast cancer," *Oncotarget,* vol. 9, no. 79, p. 34889, 2018.

[46]   E. D. Wiklund *et al.*, "Cytotoxic effects of antipsychotic drugs implicate cholesterol homeostasis as a novel chemotherapeutic target," *International journal of cancer,* vol. 126, no. 1, pp. 28-40, 2010.

[47]   A. L. Liang *et al.*, "Chloroquine increases the anti-cancer activity of epirubicin in A549 lung cancer cells," *Oncology Letters,* vol. 20, no. 1, pp. 53-60, 2020.

[48]   S. Brezgin *et al.*, "Hydroxychloroquine Enhances Cytotoxic Properties of Extracellular Vesicles and Extracellular Vesicle–Mimetic Nanovesicles Loaded with Chemotherapeutics," *Pharmaceutics,* vol. 15, no. 2, p. 534, 2023.

[49]   L.-q. Liu *et al.*, "Hydroxychloroquine potentiates the anti-cancer effect of bevacizumab on glioblastoma via the inhibition of autophagy," *Biomedicine & Pharmacotherapy,* vol. 118, p. 109339, 2019.

[50]   P. M. P. Ferreira, R. W. R. de Sousa, J. R. de Oliveira Ferreira, G. C. G. Militão, and D. P. Bezerra, "Chloroquine and hydroxychloroquine in antitumor therapies based on autophagy-related mechanisms," *Pharmacological research,* vol. 168, p. 105582, 2021.

[51]   N. Sinha and G. Balayla, "Hydroxychloroquine and COVID-19," *Postgraduate medical journal,* vol. 96, no. 1139, pp. 550-555, 2020.

[52]   S. Wünsch, C. P. Sanchez, M. Gekle, L. Große-Wortmann, J. Wiesner, and M. Lanzer, "Differential stimulation of the Na+/H+ exchanger determines chloroquine uptake in Plasmodium falciparum," *The Journal of cell biology,* vol. 140, no. 2, pp. 335-345, 1998.

[53]   M. M. Hoque, Y. Iida, H. Kotani, I. D. Kartika, and M. Harada, "Hydroxychloroquine Promotes Bcl-xL Inhibition-induced Apoptosis in BxPC-3 Human Pancreatic Cancer Cells," (in eng), *Anticancer Res,* vol. 42, no. 7, pp. 3495-3506, Jul 2022, doi: 10.21873/anticanres.15836.

[54]   X. Lyu *et al.*, "Hydroxychloroquine suppresses lung tumorigenesis via inducing FoxO3a nuclear translocation through STAT3 inactivation," (in eng), *Life Sci,* vol. 246, p. 117366, Apr 1 2020, doi: 10.1016/j.lfs.2020.117366.

[55]   A. Ranjan, I. Kaushik, and S. K. Srivastava, "Pimozide Suppresses the Growth of Brain Tumors by Targeting STAT3-Mediated Autophagy," (in eng), *Cells,* vol. 9, no. 9, Sep 22 2020, doi: 10.3390/cells9092141.

[56]   S. S. Diebold, T. Kaisho, H. Hemmi, S. Akira, and C. Reis e Sousa, "Innate antiviral responses by means of TLR7-mediated recognition of single-stranded RNA," *Science,* vol. 303, no. 5663, pp. 1529-1531, 2004.

[57]   J. A. Ratikan, J. W. Sayre, and D. Schaue, "Chloroquine engages the immune system to eradicate irradiated breast tumors in mice," *International Journal of Radiation Oncology* Biology* Physics,* vol. 87, no. 4, pp. 761-768, 2013.

[58]   R. Thomé, S. C. P. Lopes, F. T. M. Costa, and L. Verinaud, "Chloroquine: Modes of action of an undervalued drug," *Immunology Letters,* vol. 153, no. 1, pp. 50-57, 2013/06/01/ 2013, doi: https://doi.org/10.1016/j.imlet.2013.07.004.

[59]   I. R. Rao *et al.*, "Hydroxychloroquine in nephrology: Current status and future directions," *Journal of Nephrology,* vol. 36, no. 8, pp. 2191-2208, 2023.

[60]   A. E. in 't Veld, M. A. Jansen, L. C. Ciere, and M. Moerland, "Hydroxychloroquine effects on TLR signalling: underexposed but unneglectable in COVID-19," *Journal of Immunology Research,* vol. 2021, pp. 1-7, 2021.

[61]   R. Xu, Z. Ji, C. Xu, and J. Zhu, "The clinical value of using chloroquine or hydroxychloroquine as autophagy inhibitors in the treatment of cancers: A systematic review and meta-analysis," *Medicine,* vol. 97, no. 46, p. e12912, 2018.

[62]   Y. R. Fauzi *et al.*, "Antitumor effects of chloroquine/hydroxychloroquine mediated by inhibition of the NF-κB signaling pathway through abrogation of autophagic p47 degradation in adult T-cell leukemia/lymphoma cells," *PloS one,* vol. 16, no. 8, p. e0256320, 2021.
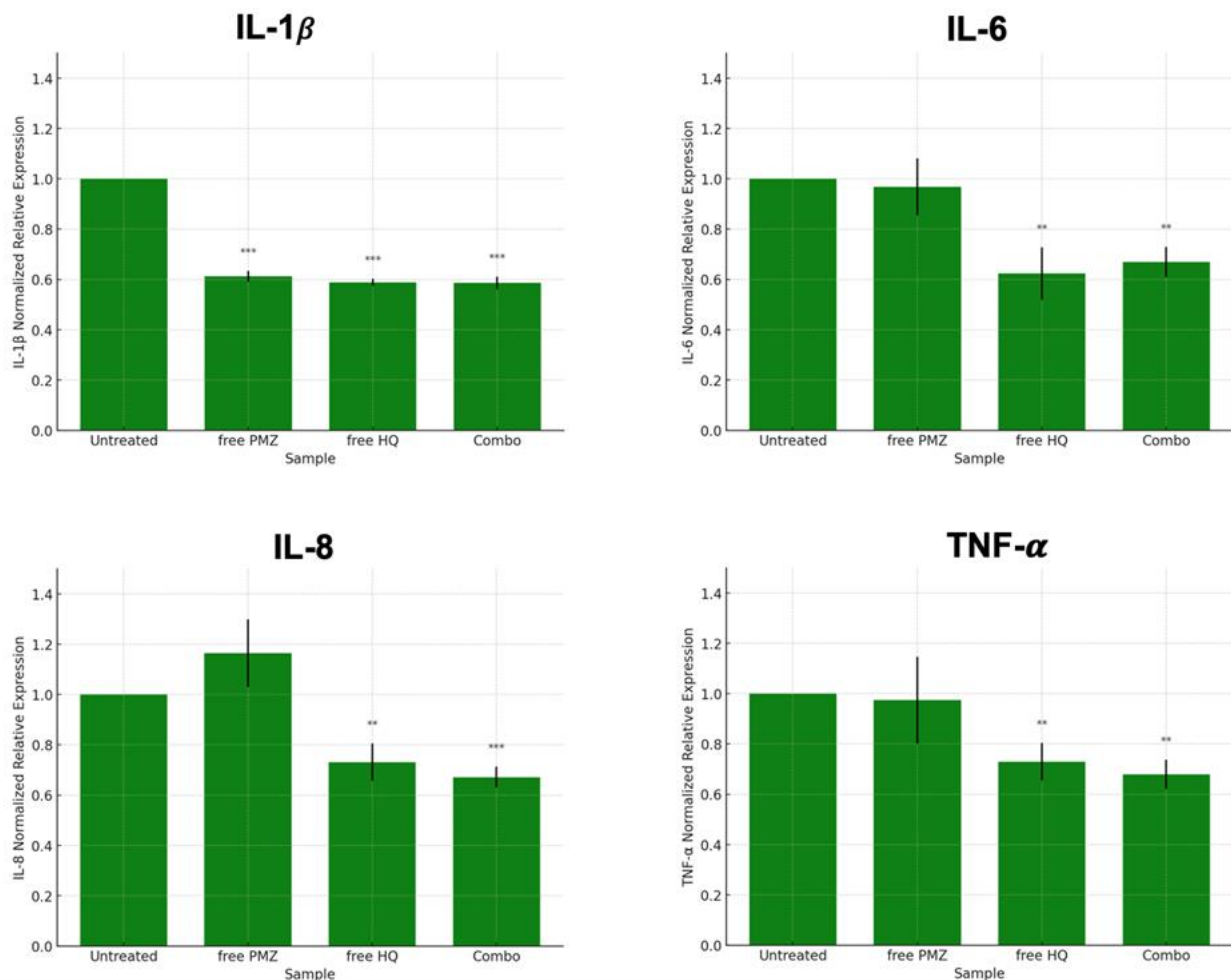
Supplementary figure 1. The anti-inflammatory effect of PMZ, HQ, and their combination as free agents. THP1 macrophages were treated with 10 μM HQ, 5 μM of PMZ, or their combination prior to QPCR analysis of the expression of the IL-1β, IL-6, IL-8, and TNF-α genes. Data was normalized against untreated cells.

Chapter 6

Comparison of the Therapeutic Potential of Pimozide and Hydroxychloroquine Combination Using Advanced Spray Drying Techniques

Arwa Omar Al Khatib[a,b], Mohamed El-Tanani[b], Hisham Al-Obaidi[a]*

[a] School of Pharmacy, University of Reading, Reading RG6 6AD, UK

[b] Faculty of Pharmacy, Al Ahliyya Amman University, Amman 19111, Jordan

Chapter Summary:

In this chapter, the study presents the development of microparticles for the co-delivery of pimozide (PMZ) and hydroxychloroquine (HQ) using the three-fluid nozzle (3FN) spray drying method. Additionally, it prepares the same formulations using the two-fluid nozzle (2FN) method to compare the impact of specific nozzle configurations and excipients on the recovery percentages, particle size, drug release kinetics, and therapeutic efficacy of the resulting powders. The 3FN method demonstrated higher recovery% for PMZ and produced larger particles. Drug release kinetics indicated that the 3FN spray drying method offered greater versatility over the 2FN method by providing a tailored release profile of the encapsulated bio-actives as intended. Formulations prepared by both methods exhibited synergistic antiproliferative effects against A549 cells and significant reductions in pro-inflammatory cytokines. However, antimicrobial tests showed no significant activity.

6.1 Introduction

Spray drying is a sophisticated technique used to create fine, dry powders from a liquid solution by rapidly drying with a hot gas. This method is particularly valuable in pharmaceutical applications for its ability to efficiently encapsulate drugs, leading to improved stability and solubility [1]. The advancements in this technology are evident through the implementation of the 2FN and 3FN configurations. These advanced spray drying strategies have significantly improved the engineering of particle properties for specialized pharmaceutical applications. They have become increasingly important for encapsulating and releasing substances in a targeted manner.

The 2FN process is regarded as the conventional method of spray drying, as it involves combining a liquid mixture of the drug and excipients with compressed gas. This setup allows the gas to shear the liquid into fine droplets, which quickly dry in the heated air of the drying chamber. The primary advantage of the 2FN is its simple design and ability to generate small particles with precise control over their size and distribution, making it useful for creating particles suitable for specific administration routes like inhalation [2]. With the 2FN technique one channel is dedicated to the feed while another handles the atomizing gas ensuring the creation of precise particle sizes crucial, for effective drug delivery [2]. Conversely, the 3FN enhances flexibility by incorporating an additional feed solution into the atomization process [3]. This extra fluid enables the creation of particle structures such as core-shell configurations, with the core holding the medication and the shell acting as a barrier to regulate release timing. This capability can be used to create multilayered or coated particles, enhancing the drug's protective properties and controlled release profiles [3].

This research specifically investigates the co-delivery of PMZ and HQ, two compounds that show promising benefits not only in their traditional uses but also as repurposed medications, for innovative therapies. Pimozide, which is typically used to treat

antipsychotic conditions has displayed encouraging results, in laboratory studies as a treatment for Non-Small Cell Lung Cancer (NSCLC) a prevalent and serious type of cancer [4]. By influencing pathways involved in tumor development and spread, PMZ has shown the ability to hinder the growth of cancer cells and prompt programmed cell death in cells [5, 6]. Similarly, HQ, a recognized medication for malaria and inflammation has been investigated for its potential to block autophagy processes in cancer cells enhancing the effectiveness of chemotherapy for NSCLC [7-9]. Its anti-inflammatory characteristics also suggest a range of applications that could be beneficial, in reducing inflammation linked to cancer and improving overall treatment results [10].

Given that cancer progression from inflammation can be influenced by inflammatory cells and various mediators, including cytokines [11], HQ has shown potential in suppressing these pro-inflammatory mediators alongside its promising anticancer activity [7-10]. Therefore, this study utilizes a combination therapy of PMZ and HQ, employing a unique design which involves two different methods of spray drying, 3FN and 2FN. Each method uses a combination of specific excipients, with one polymer (either PVP or HPMC-E5) and one excipient (either trehalose, OraRez, or isomalt). HPMC-E5 prevents aggregation, improves viscosity for controlled release, boosts mucoadhesive properties, and acts as a stabilizer and protective agent during spray drying [12-14]. It was selected for these formulations due to its effectiveness in developing spray-dried products. Commonly used in oral formulations, this polymer prolongs drug release and improves the aerosolization of inhaled formulations. It is non-toxic and inert when inhaled, and also enhances the bioavailability of spray-dried drugs by improving dissolution rates, inhibiting crystallization, stabilizing the drug, providing controlled release, and enhancing muco-adhesion and solubility [15-17].

PVP stabilizes APIs, enhances solubility, facilitates rapid lung absorption, and allows for controlled release formulations [18-21]. National regulatory bodies have deemed PVP safe as a pharmaceutical excipient, and extensive toxicity research has confirmed its biological inertness. It is non-toxic, non-irritant, and non-sensitizing, making it safe for oral, topical, and ocular applications [22]. On the other hand, trehalose stabilizes sensitive

molecules, improves powder flow and dispersibility, and controls hygroscopicity, serving as a bulking and taste-masking agent [23-25]. OraRez, a free acid of the co-polymer of methyl vinyl ether and maleic anhydride, forms protective films around APIs, enhancing stability, optimizing particle characteristics, and improving mucoadhesive properties [26, 27]. Isomalt ensures consistent particle formation, protects heat-sensitive APIs, prevents clumping, and improves patient compliance with its mildly sweet taste [28-31].

The 3FN method uses separate feeds for the inner and outer nozzles, while the 2FN method employs a single feed solution. In the 3FN method, PMZ is delivered through the inner nozzle and forms the core of the microparticle, whereas HQ is introduced via the outer nozzle alongside the polymer and excipient, forming the shell of the multi-layered particle. This research aims to develop a co-delivery system of PMZ and HQ intended for inhalation by utilizing 3FN spray drying method. Additionally, it aims to prepare the same formulations using 2FN and compare the impact of specific nozzle configurations and excipients on the stability, biological activity, and release kinetics of both encapsulated drugs. The release kinetics, influenced by the spray drying method, is essential for enhanced therapeutic activity and potential synergy. The hypothesis is to design a system that can provide a rapid burst release of HQ to address cancer-related inflammation and a sustained release of PMZ for targeted anticancer effects.

6.2 Materials and methods:

6.2.1 Materials

Pimozide, hydroxychloroquine, and trehalose were acquired from Sigma-Aldrich, US. DuPont in the Netherlands supplied the methocel E5 (HPMC E5). Polyvinylpyrrolidone (PVP) was purchased from Fluka Analytical, UK. Isomalt was bought from BENEO GmbH, Germany, and OraRez PVM/MA copolymer, an alternating copolymer of methyl vinyl ether and maleic anhydride was obtained from HARKE Pharma GmbH, Germany. The MTT reagent was purchased from ThermoFisher Scientific, US, and the dimethyl sulfoxide (DMSO) was obtained from Fisher Bioreagents, US.

6.2.2 Preparation of microparticles encapsulating PMZ and HQ by two and three fluid nozzle spray drying systems

In this study, HPMC or PVP were selected to encapsulate PMZ and HQ within a multilayer microcapsule or microsphere using the 3FN, and 2FN spray drying methods respectively, utilizing a Büchi mini spray dryer B-290 (Büchi Labortechnik AG, Falwil, Switzerland). In the 3FN method, utilized in formulations F1 through F5, 100 mg HQ, 150 mg of the polymer, and 60 mg excipient (trehalose, OraRez, or isomalt) were dissolved in 50 mL deionized water and stirred for 1 hour to ensure uniform dissolution. This solution was then fed through the outer nozzle at a constant flow rate for shell formation. Simultaneously, 100 mg PMZ was dissolved in 50 mL absolute ethanol and fed through the inner nozzle as the core bioactive material. In the conventional 2FN method, utilized in formulations F6 through F10, 100 mg PMZ and 100 mg HQ were mixed with 150 mg of the selected polymer and 60 mg excipient in 100 mL aqueous ethanol (50:50 v/v), and fed through the same nozzle, and encapsulated as microspheres. The spray drying parameters were uniformly applied across both methods, with a nitrogen gas flow rate of 50 mL/min, an inlet temperature of 140 °C (± 2 °C), an outlet temperature of 81 °C (± 2 °C), a feed flow rate of 2.4 mL/min, and the aspirator blower operating at full capacity. For the three-fluid nozzle application, the solutions were pumped simultaneously to ensure synchronized feed rates.

As shown in **Table 1**, a Design of Experiment (DoE) represented by a structured factorial design was employed to assess the influence of various variables, such as the method of spray drying and excipients, on drug stability, recovery%, release kinetics, and biological activities. The primary distinction between the formulations was the method of introducing the drugs into the system: formulations F1-F5 used a 3FN system, with PMZ fed through the inner nozzle and HQ, the polymer, and excipient sprayed through the outer nozzle, whereas formulations F6-F10 employed a 2FN system where all constituents were fed through a single nozzle. The second distinction was the specific excipients utilized: F1 and F6 used PVP and trehalose, F2 and F7 used PVP and isomalt, F3 and F8 used HPMC and trehalose, F4 and F9 used HPMC and OraRez, and F5 and F10 used HPMC and isomalt.

Table 1. DoE of formulations F1 through F10

Formulation	Spray drying method	Polymer	Excipient
F1	3FN	PVP	Trehalose
F6	2FN		
F2	3FN	PVP	Isomalt
F7	2FN		
F3	3FN	HPMC	Trehalose
F8	2FN		
F4	3FN	HPMC	OraRez
F9	2FN		
F5	3FN	HPMC	Isomalt
F10	2FN		

6.2.3 Recovery analysis

Each formulation, containing exactly 5 mg of PMZ, was dispersed in 2 mL of aqueous ethanol (3:1, v/v) and vortexed for 10 minutes. Similarly, each formulation with exactly 5 mg of HQ was dispersed in 2 mL of aqueous ethanol (3:1, v/v) and vortexed for 10 minutes. This process dissolved the bio actives and the polymer matrix, yielding a final drug concentration of 2.5 mg/mL for each drug. Following that, the actual concentrations of both drugs in the solution were quantified using HPLC. Based on the Area Under the Curve (AUC) from the HPLC results, the recovery% was calculated using the specific formula [32].

$$Recovery\ \%\ (w/w) = \frac{Actual\ Amount\ of\ Drug\ in\ Spray\text{-}dried\ particles}{Theoretical\ Drug\ Content} \times 100$$

(Equation 4)

6.2.4 High Performance Liquid Chromatography (HPLC) analysis

High Performance Liquid Chromatography (HPLC) analysis was performed using an Agilent 1100 Series instrument from the USA. The setup included a 15 cm C18 column and a detection wavelength of 270 nm. The HPLC's mobile phase consisted of 45% acetonitrile and 55% water, with the pH adjusted to 2.5 (±0.5) using 0.1% v/v phosphoric acid. An isocratic elution approach was used, with a flow rate of 1mL/min, injection volume of 20 µL, and run time of 10 minutes, measurements were conducted in triplicate.

6.2.5 Particle size analysis

In this study, the average particle size of the spray-dried PMZ-HQ powders were assessed using dynamic light scattering (DLS) with a Zetasizer Nano ZS from Malvern Instruments, UK. Each formulation was initially re-dispersed by mixing 5 mg with 5 mL of distilled water. Then, 10 µL of this dispersion was diluted further into a final volume of 1000 µL using distilled water. These samples were transferred into glass cuvettes and measured under controlled conditions: the temperature was maintained at 25 °C, the refractive index was set at 1.33, and the duration of measurement was 60 seconds. Measurements of average particle size were conducted in triplicate.

6.2.6 Fourier transform infrared spectroscopy (FTIR)

Fourier-transform infrared (FTIR) spectroscopy using a Perkin-Elmer Spectrum 100 spectrophotometer (Waltham, MA, USA) was employed to check for the interactions between the loaded APIs and the wall material. The measurements spanned a spectral range of 650 to 4200 cm^{-1}, with an average of 16 scans integrated for each spectrum.

6.2.7 X-ray powder diffraction (XRPD)

X-ray powder diffraction analysis was carried out using Bruker D8 Advance flat plate powder diffractometer (Bruker AXS GmbH, Germany). The samples were irradiated with

copper source radiation (1.54A° angstroms). The data collection was carried from 5.0° to 90° 2theta, 0.2° step size at 1.2 seconds per step.

6.2.8 Drug release studies

The release kinetics of PMZ and HQ from various formulations were studied using dialysis bags and analyzed with HPLC. Each formulation weighing 10 mg was dispersed in 5 mL of a simulated lung fluid (SLF) containing mixtures of salts; 100 mM NaCl, 5 mM KCl, 2 mM $CaCl_2$, 25 mM $NaHCO_3$, 5 mM Na_2HPO_4, 1 mM NaH_2PO_4, and 1 mM $MgCl_2$ hexahydrate, adjusted to a pH of 7.4 and vortexed for 3 minutes. The resulting mixture was then placed inside a dialysis bag to allow for controlled diffusion. The release of drugs was performed under sink conditions in 20 ml of release medium (SLF) to mimic lung conditions closely as possible at 37°C, with agitation using BioCote hotplate stirrer at 100 rpm.

At predetermined time intervals, 1 mL samples were withdrawn from the SLF, and immediately replaced with fresh SLF to maintain constant volume. This method ensured that the drug concentrations stayed below saturation levels, promoting continual diffusion of the drugs from the formulations. The samples collected were subsequently analyzed with HPLC. The data obtained from this analysis was used to determine the cumulative drug release percentages, thereby generating a kinetic profile of PMZ and HQ release from the various formulations under simulated lung conditions.

6.2.9 Antiproliferative effect against A549 cells

The antiproliferative effects of PMZ, HQ and various formulations (F1- F10) were assessed using an MTT assay by (Biorad). A549 human lung cancer cells were grown in RPMI 1640 medium with 2 mM L glutamine, 100 mg/mL penicillin/streptomycin, from (Gibco) and 10% bovine serum from (Euroclone). The cells were seeded in a 96 well plate, from (SPL Korea) at a density of 5×10^3 cells per well. Left to attach. The next day the cells

were treated with distinct concentrations of free PMZ, free HQ or one of the formulations (F1- F10) at doses ranging from 0.8 to 100 µM. Following a 72-hour treatment period cell viability was assessed using the MTT assay. This process involved adding 0.5 mg/mL MTT to each well and allowing a 3 -hour incubation for crystals to form. The formazan was then dissolved by adding 100 µL of DMSO to each well. Absorbance readings were taken at 570 nm using a BioTek Cytation 5 multi -mode plate reader, from the USA.

The results of cell viability were expressed as percentages relative to the untreated control group. The drug interactions were analyzed by calculating the combination index (CI) using the Chou and Talalay method [33], with CompuSyn software. A CI value below 1 indicated a synergistic effect, a value of 1 signified an additive effect, and a value above 1 suggested an antagonistic effect.

6.2.10 Quantification of pro-Inflammatory cytokine RNA expression in THP-1 cells using qPCR

The THP- 1 human monocytic cell line was grown in RPMI 1640 medium (Euroclone) with added 2 mM L glutamine, 100 mg/mL penicillin/streptomycin (Gibco), 4.5 g/L D glucose (Sigma), and 20% fetal bovine serum (Euroclone). To prompt the transformation, into macrophages the THP 1 cells were cultured at a density of 2×10^5 cells per mL, in RPMI medium supplemented with 100 nM Phorbol 12 myristate 13 acetate (PMA) in a 24 well plate allowing them to adhere for a day (SPL, Korea). After discarding adherent cells, the remaining macrophages were sustained in RPMI medium before being exposed to 5 µg/mL lipopolysaccharide (LPS) for an additional day. Following stimulation, the cells were treated with the formulations at concentrations equivalent to 10 µM of HQ for 48 hours. To measure RNA expression of IL-1β, IL6, IL-8, and TNF-α, approximately 1×10^6 cells were harvested, and RNA was extracted. The RNA concentration was quantified using a NanoDrop device (Thermo Fisher Scientific). A total of 0.5 µg of RNA was reverse transcribed to cDNA using the PrimeScript RT Master Mix (Takara, China) in a T100 Thermal Cycler (Biorad).

The qPCR reaction mixture included 2 µL of cDNA, 0.4 µL each of forward and reverse primers, 7.2 µL of nuclease-free water, and 10 µL of SYBR Premix Ex Taq (TliPlus) (Takara Bio). The PCR cycles were performed on a CFX96 C1000 Touch thermal cycler (Biorad) with an initial denaturation at 95°C for 3 minutes, followed by 40 cycles of denaturation at 95°C for 5 seconds and annealing at 61°C for 30 seconds. 18S-rRNA was used as the reference gene, and all samples were analysed in triplicate. Data analysis was conducted using the $2^{-\Delta\Delta CT}$ method through CFX Maestro Software (Biorad).

6.2.11 Antimicrobial activity measurements

The bacterial strains, including *Acinetobacter baumannii, Klebsiella pneumoniae and Pseudomonas aeruginosa* were sourced from the King Hussein Cancer Center (KHCC), in Amman, Jordan. Initially each compound was prepared with 200 µg per disc using buffer saline. In a follow up experiment the compounds in formulations F1, to F5 were diluted with 10% DMSO. Blank discs, infused with 200 µg of each formulation, were used in the disc diffusion assay and placed on Mueller Hinton agar (MHA) plates previously streaked with a fresh 0.5 McFarland standard inoculum of each bacterium. Imipenem, ertapenem, and minocycline were used as positive controls for *A. baumannii, K. pneumoniae, and P. aeruginosa*, respectively.

6.2.12 Statistical analysis

To compare the variations between formulations, a one-way analysis of variance (ANOVA) with Pythons SciPy library was used. All the statistical analyses were carried out with a significance level set at α=0.05. Any *p*-values, below this threshold indicated significant difference.

6.3 Results and discussion

6.3.1   Recovery analysis

Performing recovery analysis studies in our research is crucial due to the fact that most studies do not investigate the loss of drug during the spray drying process. To accurately assess the antiproliferative effects against A549 cells and quantify pro-inflammatory cytokine RNA expression, it is essential to normalize all experiments based on the actual amounts of drugs produced post-spray drying. This normalization ensures that the biological assay results are standardized according to the actual amounts of drugs present in the microparticles. Most studies fail to consider drug loss, despite its common occurrence in spray drying. Importantly, we ruled out drug loss due to chemical degradation, as confirmed by FTIR results showing no significant shifts or new peaks, indicating that the drug and excipients remained intact. Thus, our stability study further supports this finding. This innovative approach assesses the efficacy of spray drying using 2FN and 3FN methods to produce uniform microparticles, providing a more accurate evaluation of all biological assays' effectiveness based on such recovery percentage results.

The recovery percentages of both drugs, as shown in **Figure 1**, indicated a higher average recovery percentage for PMZ in 3FN (66% ± 0.9%) compared to 2FN (59.1% ± 1.90%). Similarly, for HQ, the recovery percentage in 3FN (53.1% ± 1.80%) was higher than in 2FN (49.8% ± 0.70%). This trend was observed across all spray-dried formulations, with PMZ consistently having higher recovery percentages than HQ. The recovery percentages of PMZ and HQ highlight the significant impact of solvent systems, nozzle configurations, and the properties of the drugs and excipients used. In formulations F1 through F5, where PMZ was dissolved in ethanol and fed through the inner nozzle as the core fluid, the use of the 3FN method played a crucial role. This method, characterized by a high Peclet number, promotes faster ethanol evaporation compared to the solute diffusivity, resulting in earlier shell formation. This early shell formation effectively controls the diffusion of PMZ to the surface, concentrating it at the core and achieving higher recovery percentages [34-36].

Conversely, HQ was dissolved in water and sprayed through the outer nozzle, suggesting its encapsulation into the shell layer. This trend was consistent across all formulations prepared using the 3FN method (F1 through F5). The distinct mixing of components in the 3FN system, with PMZ in ethanol and HQ, polymer, and excipient in deionized water, results in two fluids with different viscosities. This viscosity difference improves the core-to-wall ratio, boosting PMZ recovery while reducing HQ recovery [37-39]. These findings align with previous research, such as the study by Leena et al. (2022) on the co-encapsulation of curcumin and resveratrol, which reported improved recovery percentages using a 3FN spray drying system [38].

The 2FN system used in formulations F6 through F10, which atomizes a single feed solution with a high-speed gas stream, resulted in lower recovery percentages which could be attributed to the solubility properties of PMZ and HQ. PMZ, soluble in ethanol but insoluble in water, achieved optimal solubility and higher recovery in the 3FN system where it was dissolved in absolute ethanol. In contrast, the 2FN system fed PMZ through a single nozzle with HQ in a 50:50 v/v aqueous ethanol solution, significantly reducing its solubility and recovery. For HQ, which is soluble in water but sparingly soluble in the 50:50 v/v solution, the recovery decrease in the 2FN system was expected but less significant, as some HQ remains solubilized in the aqueous ethanol feed solution. This lower recovery% in 2FN highlights the challenges of mixed solvent systems. These challenges affect solubility and solution homogeneity, leading to non-uniform droplet formation during atomization, varied drying rates, and evaporation kinetics. Consequently, this is likely to result in non-uniform solidification and pockets of varying drug concentration, leading to lower recovery percentage [40, 41].

Expanding on the effects of the excipients, variations in PMZ recovery% in formulations F1-F5 using the 3FN method could be attributed to the different thicknesses of the polymer shell, using PVP or HPMC-E5, impacting drug encapsulation within the core [42]. The differential diffusion of fluids with different viscosities significantly improves PMZ recovery% while reducing HQ recovery%, consistent with findings by Pabari et al. (2012) and França et al. (2018) [39, 43]. PMZ's highest recovery% was observed in formulations

F4 and F9, which included HPMC-E5 and OraRez. The robust film-forming properties of HPMC-E5 and the cohesive properties of OraRez led to the smallest particle sizes, as shown in the particle size analysis in **Section 3.2**. This implies that the increased surface area to volume ratio and shorter diffusion pathways likely improved interactions and uniform solvent removal, leading to better recovery% [44, 45]. This finding is consistent with prior work on HPMC shells improving solubility and sustained release of hydrophobic drugs [46, 47]. For HQ, the highest recovery% was observed in formulations F5 and F10 using HPMC-E5 and isomalt. HPMC-E5 enhances HQ's solubility and provides thermal stability, while isomalt maintains capsule integrity with its low hygroscopicity and suitable Tg (60°C) [31, 48].
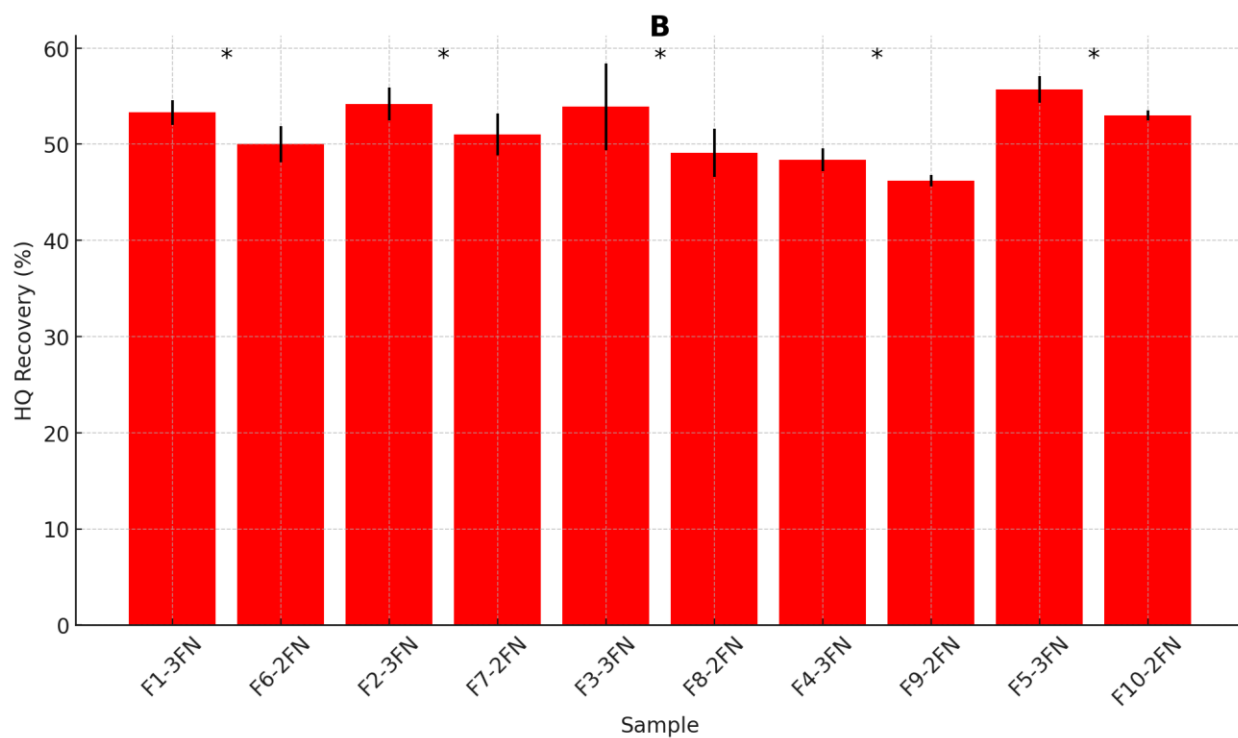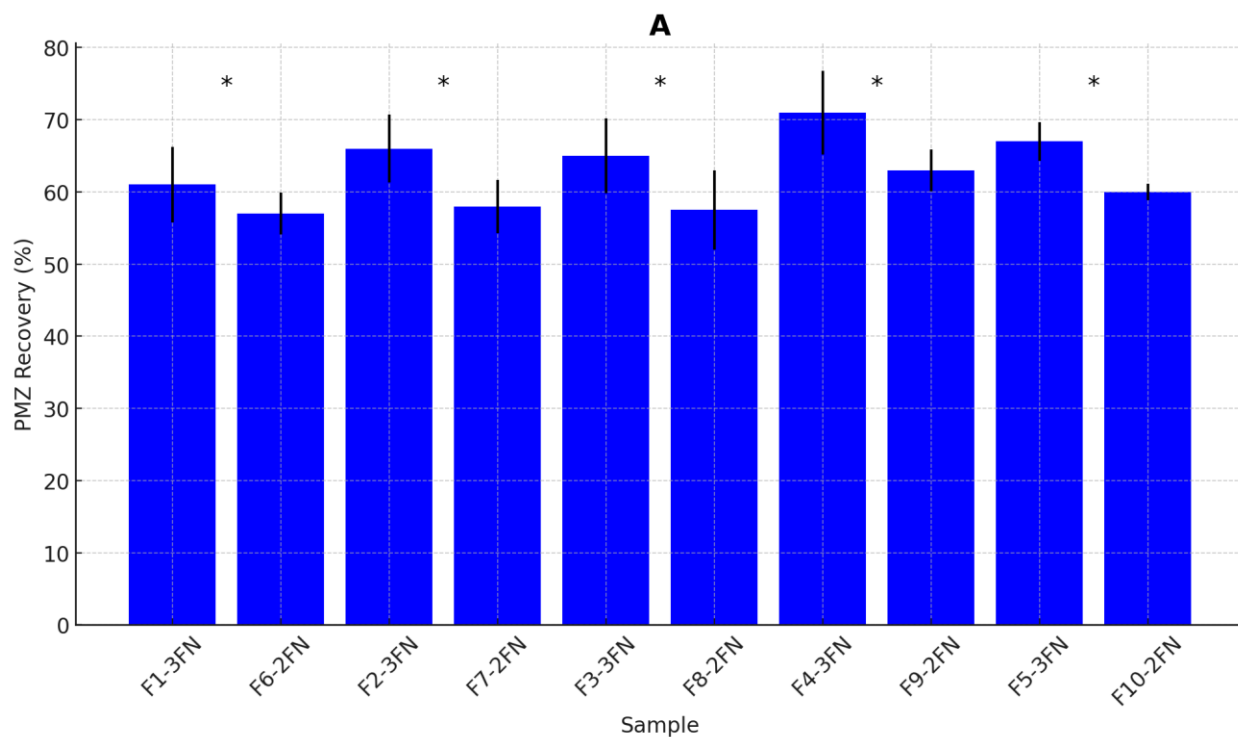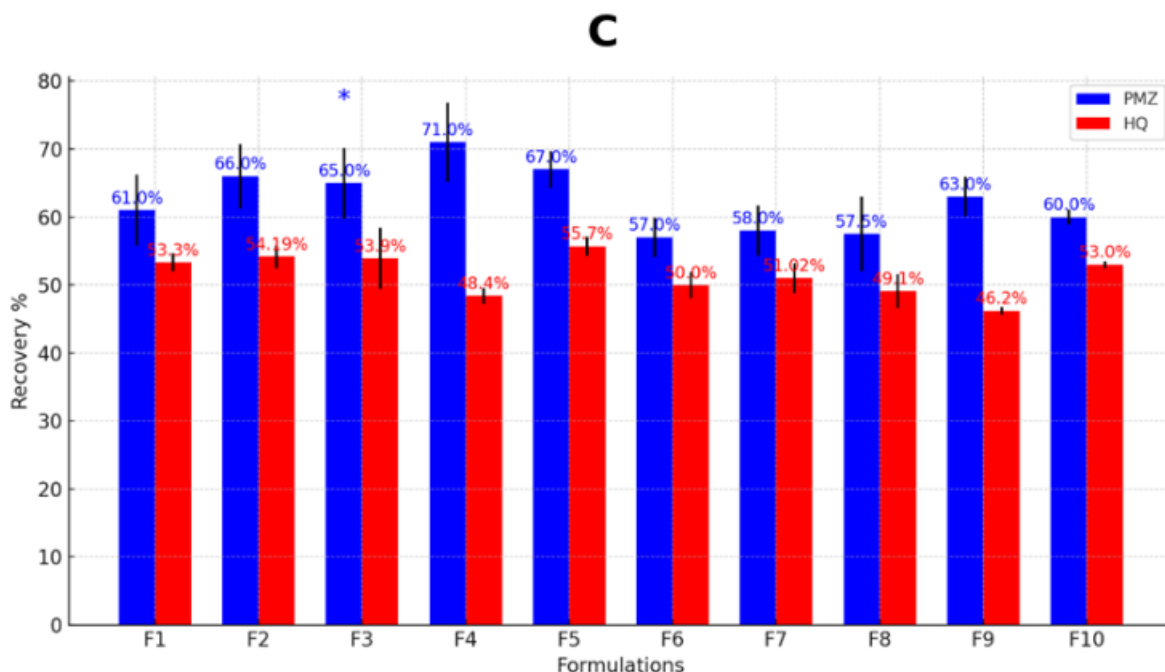
Figure 1. (A) Recovery% for PMZ in all spray dried formulations, with the respective significance levels (*p*-values) between 2FN and 3FN using the same formulations. **(B)** Recovery% for HQ in all spray dried formulations, with the respective significance levels (*p*-values) between 2FN and 3FN using the same formulations. **(C)** Recovery% for PMZ and HQ in all spray dried formulations with the significance levels (*p*-values) of each drug among all formulations.

6.3.2 Particle size analysis

The impact of nozzle configurations and solvent systems on the particle size distributions of ten PMZ- HQ spray-dried formulations were studied, revealing consistent trends across the experiments as shown in **Figure 2**. Notably, formulations utilizing a 2FN system (F6-F10) consistently resulted in smaller particle sizes compared to 3FN system counterparts. This observation is in line with previous studies, as one that reported nitrofurantoin powders spray-dried with a 2FN system had significantly smaller particle sizes than those using a 3FN system [49]. Smaller particles with higher surface area to volume ratios generally release drugs faster as evidenced in the in vitro release profiles in **Section 3.5**.

This observed trend towards larger particle sizes in formulations F1-F5 prepared by 3FN and smaller particle sizes in formulations F6-F10 prepared by 2FN method, can be attributed to the effect of the hydrophilic polymers (HPMC or PVP) in the 3FN configuration since they are located on the outer shell layer of the particles, this could cause these particles to retain water and dry more slowly, limiting the amount of shrinkage during spray drying. On the other hand, the 2FN method's uniform dispersion of the feed decreases water retention, enabling the particles to dry faster and consequently resulting in smaller particles [49]. Moreover, given that the particle size of spray-dried microcapsules is heavily influenced by the droplet size formed after atomization, with smaller droplet sizes producing smaller microcapsules. The high shear mixing and homogenization process in the 2FN method significantly reduces the emulsion droplet size, resulting in a smaller average diameter compared to the formulations prepared by the 3FN method. This reduction in droplet size is due to the intensity of mixing, where high shear forces create a turbulent environment that breaks larger droplets into much smaller ones. The energy input in the 2FN method is greater, providing more energy to disrupt the liquid phases into smaller droplets. Additionally, the 2FN method generates higher turbulence and shear forces, focusing energy directly on the fluid mixture and enhancing the emulsification process. High shear conditions in the 2FN method also reduce the likelihood of droplet coalescence, as the rapid formation of small droplets and their immediate stabilization prevent merging back into larger droplets. Furthermore, the specific design of the 2FN nozzle and its mixing mechanism make it more efficient in creating small droplets, ensuring a larger number of smaller droplets compared to the 3FN method [50].

Further elucidation on the vital roles of polymer and excipient choices in influencing particle size revealed that formulations employing PVP demonstrated notable differences in particle sizes based on the excipient used. F1, with PVP and trehalose, yielded particles measuring 3412 nm ± 203.0 nm, benefiting from trehalose's ability to stabilize and compact the matrix effectively. In contrast, F2 using PVP with isomalt, resulted in significantly larger particles sized at 6027 nm ± 280.0 nm. This increase can be attributed to the dual effect of PVP's viscosity [51, 52], which facilitates larger droplet formation, and

isomalt's bulking properties, which add volume, contributing to a looser and larger matrix formation [31, 53].

Shifting to formulations with HPMC-E5 which indicated a trend towards smaller particle sizes, optimized by the specific excipient used [54]. Particularly, F3 combining HPMC-E5 with trehalose, achieved particles sized at 2200 nm ± 175.0 nm. The hydrating properties of trehalose likely enhanced the density of the matrix without increasing bulk, leading to smaller, denser particles [55]. F4 presented the smallest particles in the series, measuring 1351 nm ± 56.00 nm, due to the effects of HPMC-E5's excellent film-forming ability and OraRez's adhesive properties, which facilitated tightly encapsulated, well-stabilized particles [56]. Conversely, F5 with HPMC-E5 and isomalt generated larger particles sized at 2723 nm ± 104.0 nm, mirroring the effect seen in F2, suggesting that isomalt's crystalline nature has contributed to increased volume and less compact matrix formation.
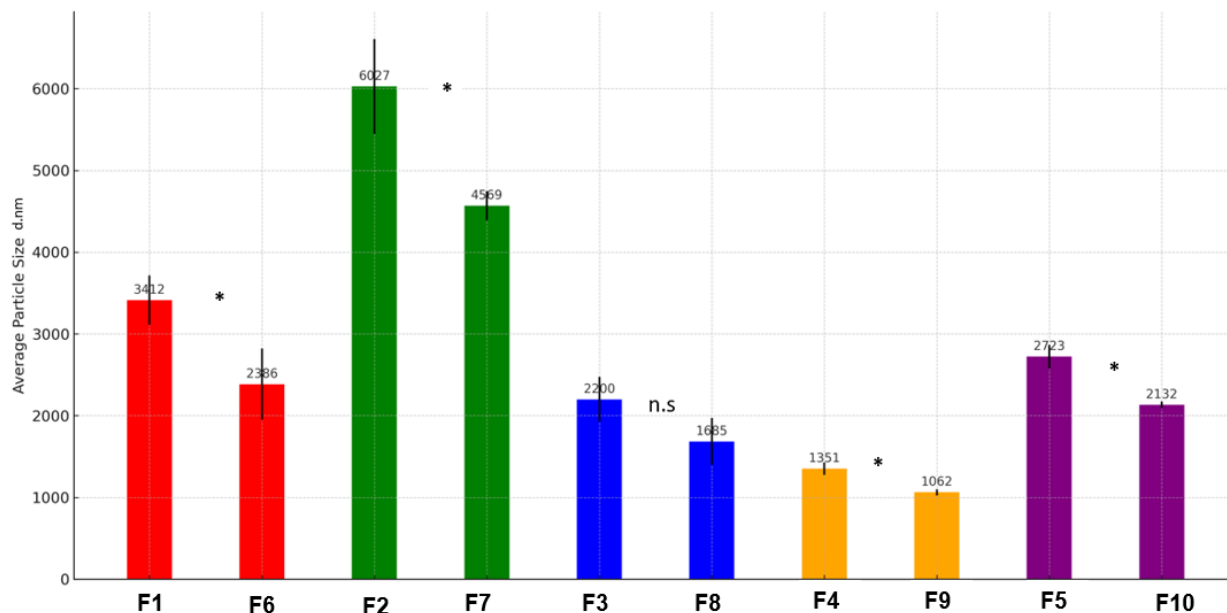

Figure 2. Comparison of the average particle size in 10 spray-dried formulations, each colour represents formulations having the same excipients: Group 1 (F1, F6) Group 2 (F2, F7) Group 3 (F3, F8) Group 4 (F4, F9) and Group 5 (F5, F10). The values indicate the mean, with standard deviation. * $p < 0.05$, calculated using one-way ANOVA.

6.3.3 Fourier transform infrared spectroscopy (FTIR)

FTIR spectral analysis was conducted to evaluate the molecular interactions between PMZ and HQ and the excipients during the formation of microparticles prepared by 2FN and 3FN methods. The spectra of PMZ-HQ spray-dried formulations were compared with their individual components, and revealed distinct characteristic peaks for each constituent, reflecting the diverse chemical functionalities present. The spectrum of PMZ revealed several characteristic fingerprint peaks, which correspond to specific functional groups within the molecule. Peaks around 1504 cm^{-1} are attributed to C=C stretching vibrations in the aromatic rings, while C-H stretching in these rings appeared near 3000 cm^{-1}. The presence of fluorine substituents contributes to peaks in the range of 1400-1200 cm^{-1} due to C-F stretching vibrations. The amide group in PMZ showed characteristic peaks with C=O stretching around 1695 cm^{-1} and N-H stretching between 3500-3200 cm^{-1}. Additionally, C-N stretching vibrations were observed around 1350-1000 cm^{-1}, and C-C stretching vibrations occurred between 1300-800 cm^{-1} [57]. HQ was distinguished by a prominent peak at 1049 cm^{-1}, indicating the symmetric stretching vibration of the sulfate group (SO_4^{2-}). Additional notable peaks were found around 1600 cm^{-1} for C=C and C=N stretching vibrations in the aromatic ring, and in the 1400-1500 cm^{-1} region for CH2 bending [58]. PVP has an amide carbonyl group in its structure, which showed a characteristic sharp peak C=O stretching at 1646 cm^{-1} [59, 60]. The stabilizers, trehalose and isomalt, exhibited O-H stretching at 3273 cm^{-1}, typical of hydroxyl groups, accompanied by other peaks for C-H and C-O stretching [61]. HPMC-E5 displayed peaks associated with C-H stretching at 2903 cm^{-1} and strong C-O stretching vibrations, suggestive of its polymeric nature, it has free OH groups, which resulted in a peak at 3455 cm^{-1} [60, 62]. Lastly, OraRez showed C=O stretching at 1750 cm^{-1}, pointing to the presence of ester linkage.

 To investigate the interactions between the drugs and polymers, the spectra of all spray-dried formulations were compared to the those of pure PMZ and pure HQ as well as the spectra of the respective excipients, using them as references to analyze the solid

dispersions. All investigated samples showed a broad peak above 3100 cm^{-1}, indicating hydrogen bonding interactions within the formulations. In F1, F2, F6, and F7 prepared with PVP, the NH group of PMZ forms hydrogen bonds with the carbonyl oxygen of PVP [63], while HQ forms similar bonds through its OH group and NH side chains. In HPMC-based formulations including F3, F4, F5, F8, F9, and F10, both PMZ and HQ establish hydrogen bonds with the OH groups in HPMC. Particularly, PMZ through its NH and carbonyl groups, and HQ through its OH and NH groups. These interactions stabilize the drug-polymer complexes, potentially enhancing the solubility of PMZ and HQ and promoting a controlled release profile.

As shown in **Figure 3**, the prepared formulations exhibited a peak within the range of 1400-1200 cm^{-1}, indicative of C-F stretching vibrations, confirming the presence of PMZ in the encapsulates. Additionally, each tested powder displayed a prominent peak at 1049 cm^{-1}, corresponding to the symmetric stretching vibration of the sulfate group (SO_4^{2-}) in hydroxychloroquine sulfate, which verifies that HQ is present in the spectra of all spray-dried formulations. The representative FTIR spectra of formulations prepared using the 3FN method (designated as F1) and those prepared using the 2FN method (designated as F6) in **Figure 3** showed similar broadening of some peaks, indicating hydrogen bonding between the drugs and excipients. These interactions help stabilize the amorphous forms of the drugs, as evidenced by the XRPD analysis in **Section 3.4**, enhance solubility, and improve controlled release, that is further determined by the in vitro release data in **Section 3.5**, thereby potentially increasing bioavailability [64].
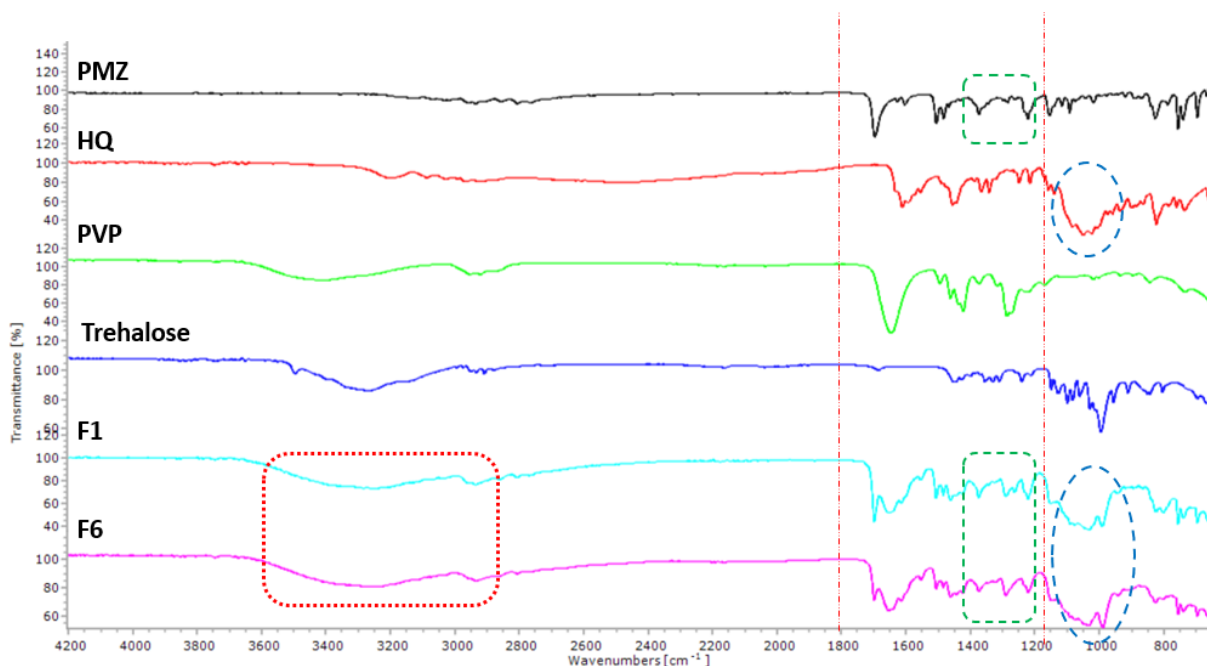
Figure 3. A representative comparative analysis using Fourier-transform infrared spectroscopy (FTIR) for two formulations F1- prepared by 3FN, and F6- by 2FN with their respective individual components including PMZ, HQ, polymer, and excipient. The graph uses circles and lines to indicate the broadening of peaks above 3000 cm^{-1} and the presence of fingerprint zones of both drugs within the formulation spectra.

6.3.4 Physical state of bioactive compounds in microparticles

The impact of microencapsulation on the crystallinity of PMZ and HQ was assessed using XRPD analysis. All individual components as well as spray-dried formulations were evaluated. Results shown in **Figure 4** provided evidence of the crystalline nature of PMZ and HQ, with sharp peaks observed for PMZ at 2θ values of 17.2° (intensity: 196), 18.2° (intensity: 185), and 19.7° (intensity: 192), indicating its crystalline structured form [65]. Similarly, HQ showed significant peaks at 24.358° with an intensity of 465, as well as other peaks at 24°, 20°, and 17° with intensities of 363, 292, and 284 respectively [66]. The amorphous state of PVP and OraRez was confirmed by the absence of sharp peaks in their diffractograms [59]. While HPMC exhibited two broad humps within the range of 5°-25°, indicating its amorphous state [67]. Trehalose and isomalt crystalline content was

evidenced with sharp peaks at 24.3° and 19.8°, respectively, suggesting distinct crystallographic features [68, 69].

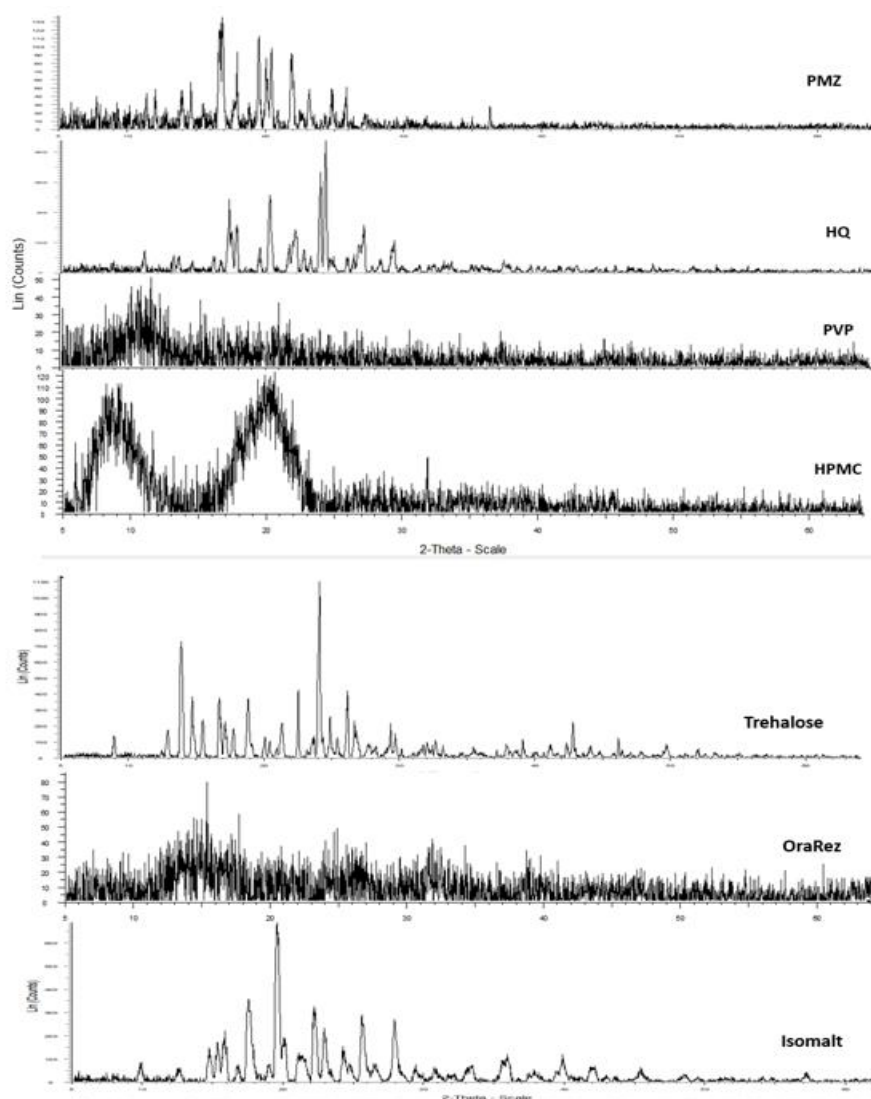**Figure 4.** XRPD patterns for PMZ, HQ, PVP, HPMC, trehalose, OraRez, and isomalt

As illustrated in **Figure 5**, none of the intense sharp peaks of PMZ or HQ are visible in any of the solid dispersions prepared using 2FN and 3FN. This suggests that in both methods, the drugs have been successfully transformed into an amorphous or molecularly dispersed state [70-72]. This finding aligns with a prior study which confirmed that

encapsulation alters the crystallinity of resveratrol and curcumin, converting them into an amorphous form [38]. With its greater free energy levels than the crystalline forms, the amorphous form is probably more soluble at saturation [73]. Encapsulation also enhances the effective surface area of drugs dispersed in microparticles, leading to rapid dissolution of the water-soluble matrix and thereby increasing the dissolution rate and absorption of the encapsulated molecules [74]. As a result, the amorphous state of these drugs improves their dissolution rates and solubility profiles, thereby boosting their bioavailability [75].
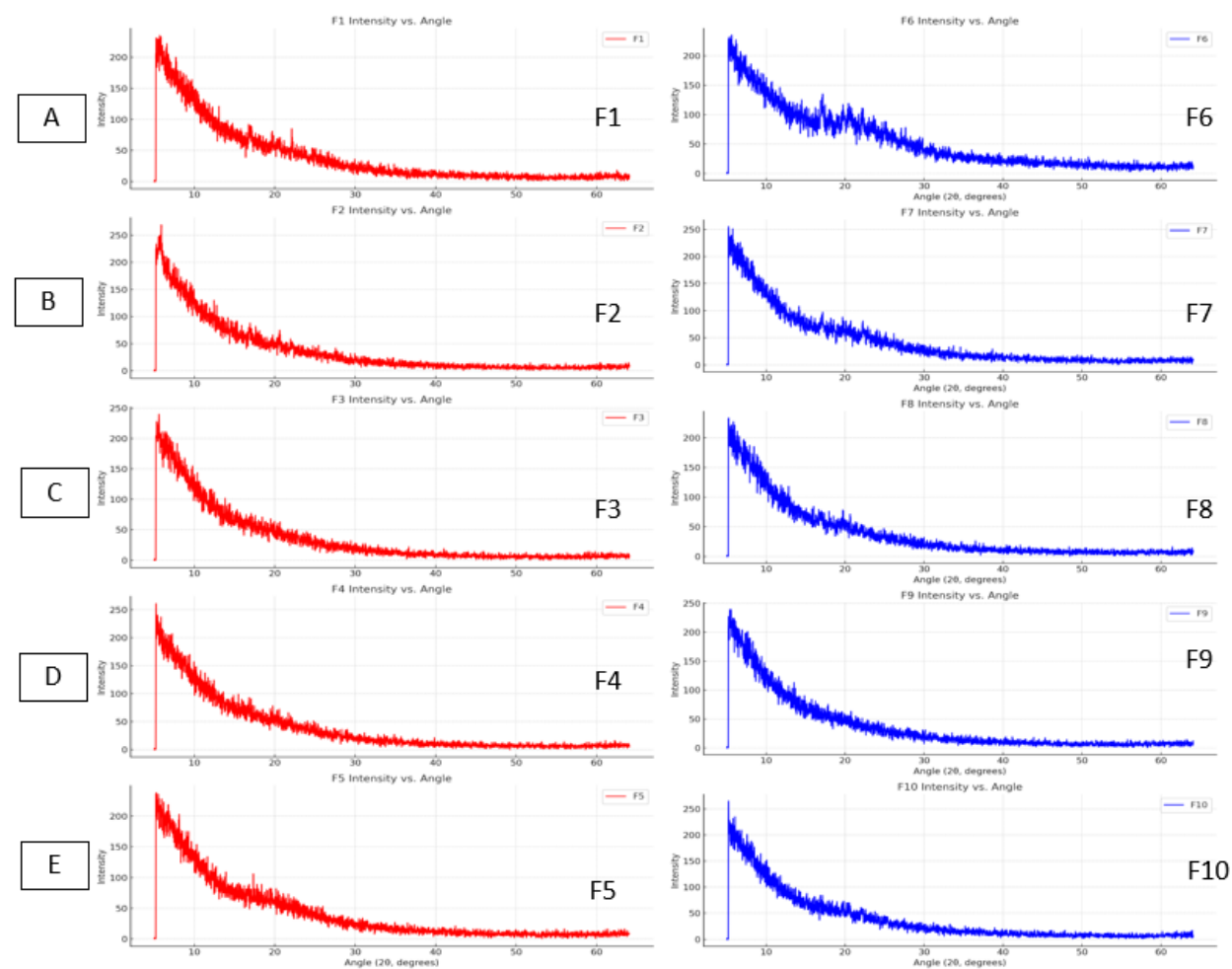

Figure 5. XRPD patterns for the spray-dried PMZ- HQ powders by 2FN and 3FN, **(A)** F1, and F6 **(B)** F2, and F7 **(C)** F3, and F8 **(D)** F4, and F9 **(E)** F5, and F10. Formulations where PMZ is fed via the inner nozzle and the combination of HQ, polymer, and excipient through

the outer nozzle in 3FN system (F1, F2, F3, F4, and F5) are shown in red. The formulations administered through a single nozzle in a 2FN system (F6, F7, F8, F9, and F10) are demonstrated in blue.

6.3.5 In vitro drug release

In vitro release studies are crucial for understanding how encapsulates behave under simulated lung conditions. **Figure 6** presents the release profiles of PMZ and HQ using SLF. The results reveal distinct differences in the release kinetics of PMZ and HQ across various formulations (F1-F10), influenced mainly by the spray drying method, polymer type, and particle size. The core-shell encapsulates produced by the 3FN spray drying method (formulations F1-F5) exhibited a slower release of PMZ (**Figure 6A**) compared to the traditional 2FN approach (formulations F6-F10) (**Figure 6C**). Initially, a rapid release was observed in all the core-shell spray-dried encapsulates prepared using the 3FN method, likely due to the presence of core droplets on the surface of the encapsulates [76]. This initial burst was then followed by a slower release. This could be attributed to the sustained release properties of the polymer forming the shell of the microcapsule, which swells under simulated lung conditions, gradually releasing the core contents [77].

Besides, PMZ, with a pKa of 8.6, will be mostly in its non-ionized form at pH 7.4, reducing its solubility in SLF. It has a poor water solubility (0.01 mg/mL at 25°C) and is relatively non-polar, leading to a slow dissolution rate in SLF. Additionally, its high partition coefficient (Log P of 6.3) suggests a preference for non-aqueous environments, further supporting its low solubility and slower dissolution rate compared to HQ. The recovery% results in **Section 3.1** supports this finding, showing that PMZ had a higher recovery%. Suggesting that when a larger proportion of the drug is encapsulated within the microparticles, the release tends to be more controlled and sustained. This is likely because the encapsulating material acts as a barrier, slowing the diffusion of the drug into the surrounding environment.

For HQ, which was fed through the outer nozzle in the 3FN method, the release was quicker due to its proximity to the particle surface (**Figure 6B**). Additionally, HQ is expected to dissolve faster and have higher solubility in SLF. With pKa values of 8.3 and 9.7, HQ will be largely ionized at SLF's pH of 7.4, enhancing its water solubility. Its high solubility and fast dissolution rate in SLF are further supported by its polar nature and very high solubility in water. As shown in the recovery% results in **Section 3.1**, HQ exhibited a lower recovery%, indicating that a larger fraction of the drug may be free or loosely associated with the microparticles. This results in a faster release, as the drug is more readily available to diffuse out.

Conversely, the 2FN method (formulations F6-F10), where both PMZ and HQ were fed through the same nozzle and distributed throughout the particle matrix, resulted in release kinetics for both drugs with less pronounced variations, highlighting the impact of the spray drying method **Figure 6 (C, D)**. Referring to the PMZ release profile prepared using 2FN in **Figure 6C**, it is evident that the release rate is faster compared to the profile using 3FN in **Figure 6A**. This difference can be attributed to the smaller particle sizes of F6-F10 prepared with 2FN, which offer larger contact surface areas to the SLF release medium [78]. Consequently, this leads to a faster release rate than the larger particles prepared by 3FN [79], as noted in the particle size analysis in **Section 3.2**. But when the drug was fed through the 3FN system's outer nozzle, as in HQ release profiles shown in **Figure 6B**, this observation was less pronounced, suggesting that in this case, the influence of nozzle configuration outweighs that of particle size.

Expanding on the impact of polymer on the release rate, it is interesting to note that the release of PMZ and HQ was slower in formulations (F1, F2) compared to (F3, F4, F5), and in (F6, F7) compared to (F8, F9, F10) as shown in Figures 6 (A, B, C, D). This variation could be mainly due to the structure and nature of the polymer [37]. Formulations (F1, F2, F6, F7) use PVP, while formulations (F3, F4, F5, F8, F9, F10) employ HPMC. HPMC, being highly hydrophilic, swells quickly and forms gels with lower viscosity, facilitating faster drug release [80]. In contrast, PVP forms thicker gels with higher viscosity, hindering drug movement and resulting in slower release [44, 81, 82] . This result is in line with a

prior study that found metformin release was prolonged more effectively using higher viscosity grade ethyl cellulose [83]. Additionally, HPMC's higher porosity is likely to enhance drug diffusion, accelerating release [84], whereas PVP's tighter polymer network reduces porosity and is expected to slow diffusion [85]. The particle size analysis in **Section 3.2**, which demonstrated that PVP-based particles had larger particle sizes compared to those generated using HPMC, supports these conclusions. Because the path of the encapsulated drug from the core to the surface is longer for larger particles, they often have a smaller surface area to volume ratio, which indicates a slower rate of dissolution. [86]. Furthermore, larger particles might take longer to hydrate and establish diffusion channels, which would further delay the release of the encapsulated drug [87].
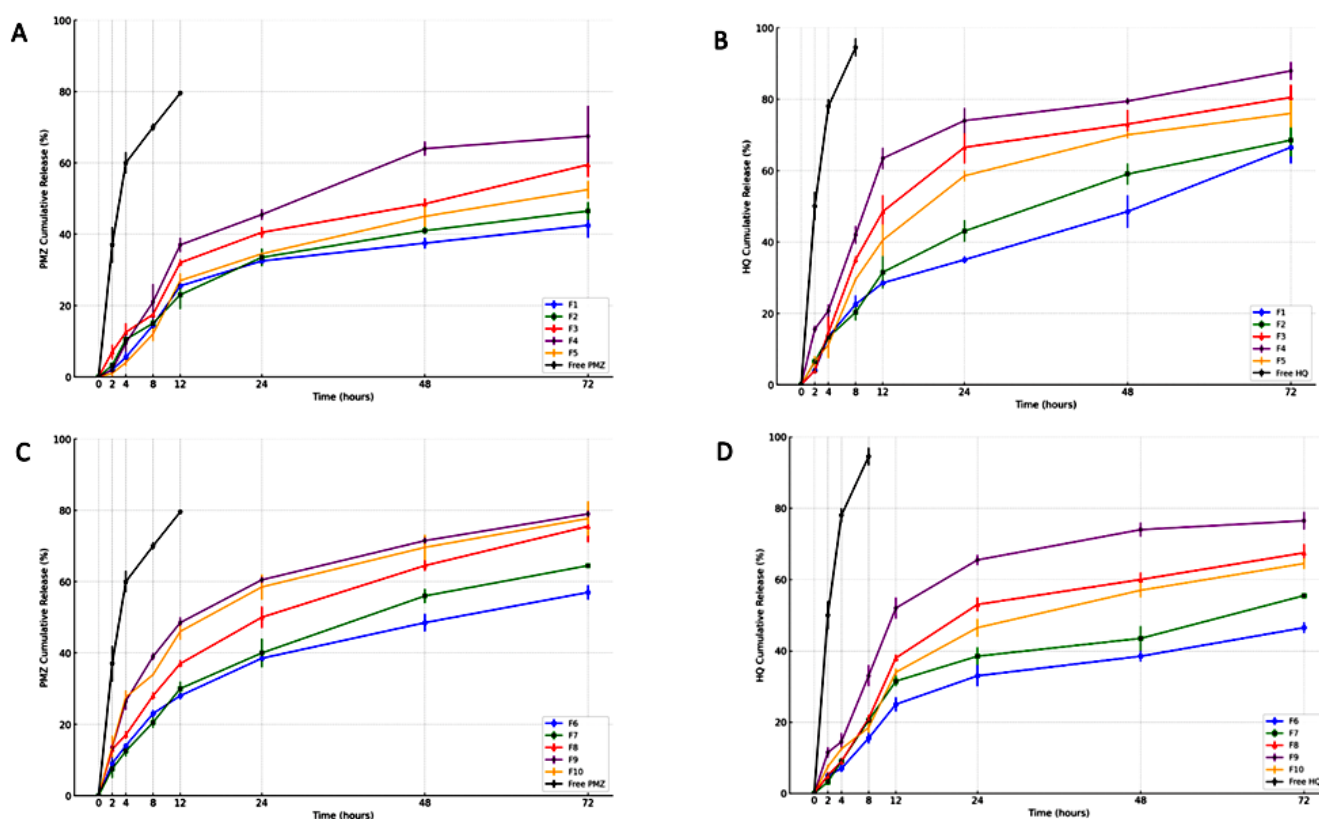

Figure 6. Comparison of release kinetics of HQ and PMZ from different formulation groups **(A)** Shows the release kinetics of PMZ (3FN) in F1-F5 formulations. **(B)** Shows the release kinetics of HQ (3FN) in F1-F5 formulations. **(C)** Shows the release kinetics of PMZ (2FN) in F6-F10 formulations. **(D)** Shows the release kinetics of HQ (2FN) in F6-F10 formulations

6.3.6   Antiproliferative effect against A549 cells

Before investigating the antiproliferative effect of the formulations on A549 cells, it was crucial to understand the antiproliferative effect of PMZ and HQ as single agents on A549 cells. The MTT assay is a colorimetric method used to assess cell metabolic activity by measuring the reduction of MTT, a yellow tetrazole, to purple formazan by mitochondrial enzymes in living cells, thereby reflecting the number of viable cells. In our study, this assay was employed to evaluate the cytotoxic effects of PMZ and HQ on the A549 cell line over 72 hours. The primary metric obtained from this assay is the IC50 value, which indicates the concentration of a compound needed to inhibit cell viability by 50%. The lower IC50 of PMZ (13.27 µM) compared to HQ (20.13 µM) suggests that PMZ is more effective at inducing cytotoxic effects at lower concentrations, implying a higher therapeutic potential or greater efficacy. However, these cytotoxicity data, particularly the IC50 values, are essential for determining safe dosage ranges for therapeutic applications. Lower IC50 values necessitate careful dosage optimization to prevent adverse effects, making controlled release of PMZ preferable to avoid potential toxicity **(Figure 7)**.
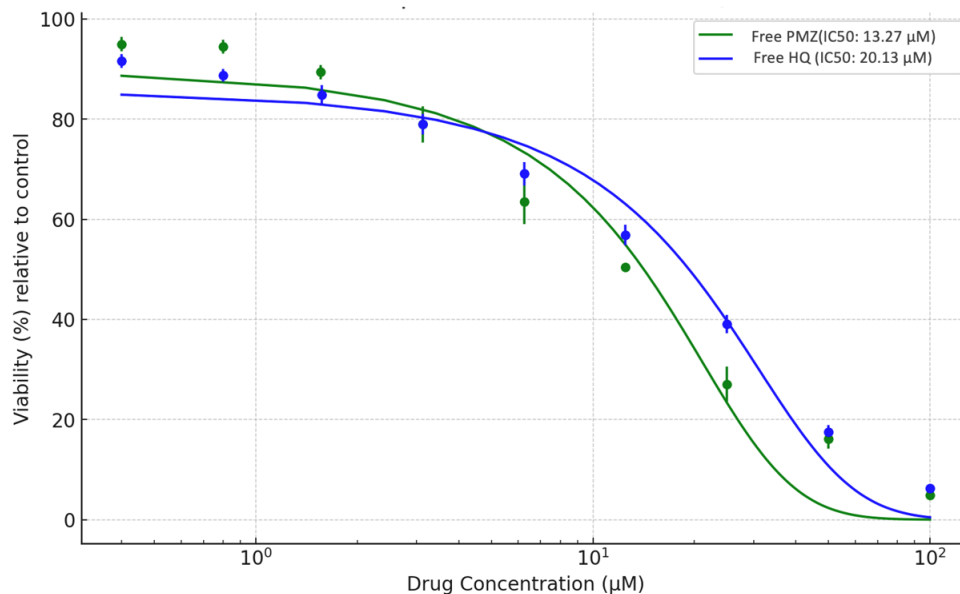
Figure 7. Anti-proliferative effect of free PMZ and HQ. A549 cells were treated with various concentrations of PMZ or HQ as free drugs for 72 hours prior to cell viability assessment using MTT assay. Graphs are presented as percentage viability relative to the untreated control. Data represent the mean ± S.D.

To further investigate the antiproliferative effects, the combined impacts of HQ and PMZ both as free drugs (in a 1:1 molar ratio, mirroring their utilized ratio in the formulations) and within the formulation on A549 cells were assessed. the combination index (CI) at a fraction of affected cells (Fa) of 0.9 for each formulation and for the free drug combination was calculated to determine the interaction between HQ and PMZ against A549 cells. The free combination control had an average value of 0.49 (± 0.04) Formulations F1 to F5 showed varying degrees of combination index. Formulation F1 exhibited the highest CI in this group with an average value of 1.17 (±0.09). Formulation F2 also showed a high CI with an average of 1.13 (±0.03). Formulations F3, F4, and F5 had lower CI values of 0.73 (±0.06), 0.65 (±0.03), and 0.77 (±0.04) respectively. The second group, formulations F6 to F10, generally exhibited higher CI values. Formulation F7 showed the highest CI with an average value of 1.23 (±0.06). Formulations F6 and F8 had CI values of 1.13 (±0.24) and 0.78 (±0.06) respectively. Formulations F9 and F10 showed CI values of 0.83 (±0.09) and 0.86 (±0.03) respectively.

In **Figure 8(A, B)** the combination of drugs showed the powerful synergistic effect, with a CI value of 0.49 indicating strong synergy. Most of the formulations also demonstrated CI values below 1 pointing to effects. However, formulations F1 and F2 displayed a contrasting trend, with CI values exceeding 1; specifically, F1 and F2 had CI values of 1.13 and 1.10 respectively indicating antagonistic interactions. The antagonistic effect observed in formulations F1 and F2 might not necessarily reflect true antagonism but could be related to their unique drug release profiles, as previously discussed. These formulations, with their larger particle sizes, demonstrated slower drug release rates compared to others, resulting in more prolonged release. The larger particle size could have also impeded their cellular uptake in A549 cells, thus preventing the drugs from

reaching effective concentrations within the cells. This slow release could lead to suboptimal drug concentrations, insufficient to effectively inhibit A549 cell proliferation, presenting as an apparent antagonistic interaction.

To confirm that the antiproliferative impacts were truly caused by the components of the formulations (HQ and PMZ), the effects of the excipients alone were also evaluated. The tests showed that these inactive substances had no impact, on cell viability in comparison to the control group without treatment, aligning with a previous study which demonstrated that PVP and HPMC-based solid dispersions did not exhibit any additional inhibitory effect on the Caco-2 cell line compared to the pure drug. [88]. This validates that the decrease, in cell viability was indeed a result of the combined effect of PMZ and HQ as shown in (**Figure 8C).**
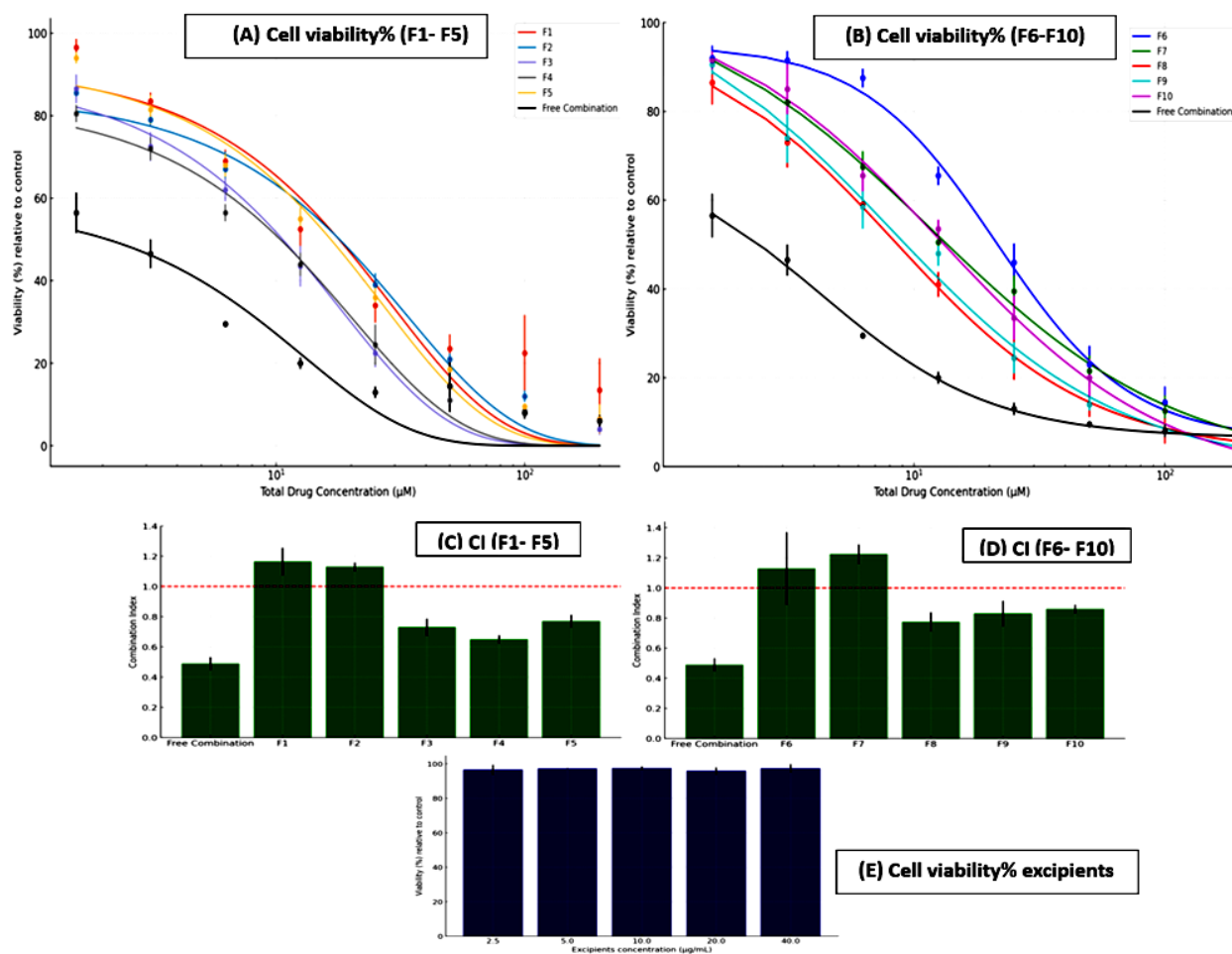
Figure 8. (A) Anti-proliferative effects of PMZ and HQ in F1-F5 **(B)** Anti-proliferative effects of PMZ and HQ in F6-F10 **(C)** Combination index of PMZ and HQ in F1-F5 formulations **(D)** Combination index of PMZ and HQ in F6-F10 formulations **(E)** Cell viability% of empty vehicles consisting of the same ratios of excipients in the formulations but without the drugs. CI was calculated for each formulation at Fa=0.9 (90% inhibition of cell viability).

PMZ promotes anti-proliferative action through a variety of ways. One of the key strategies by which PMZ exerts its anticancer activity is prevention of the STAT3 signalling pathway, a crucial transcription factor that is abnormally activated in a variety of malignancies and is critical for increasing cell survival, proliferation, angiogenesis, and immune evasion [89]. Additionally, PMZ disrupts calcium pathways that are needed for cell movement and division. By blocking calcium flow into cells PMZ stops cancer cells from using this process to grow and spread [90]. Another important aspect of PMZs function is its promotion of autophagy. While some cancer treatments aim to block autophagy to stop cancer cells from surviving PMZ actually triggers autophagy causing the build-up of vesicles and breaking down cellular elements ultimately leading to cell death through autophagy [91]. Moreover, PMZ interacts with pathways and mechanisms to combat cancer effectively. For example, it influences the Wnt/β pathway, which is recognized for its function, in controlling cell growth and development [92].

In the context of HQ, the enhanced anti-proliferative effect against A549 cell lines achieved by combining HQ with PMZ corroborates evidence from previous research. Prior studies have shown HQ's potential to augment the anti-cancer efficacy of various chemotherapeutic agents [93-95]. HQ acts via engaging in various molecular activities that notably enhance the effectiveness of cancer treatments. These actions are closely tied to processes like survival, growth and cell death. A key aspect of HQs role in treating cancer is its ability to block autophagy. HQ hinders the merging of autophagosomes with lysosomes causing a buildup of waste that tilts the balance towards stress and triggers cell death. This action is aided by membrane Na+/H+ exchangers (NHE) which help transport HQ into cells alongside sodium ions while protons, leading to an increased

accumulation of these substances, within endosomes/lysosomes and disrupting the flow of autophagy [96].

Additionally, HQ impacts apoptosis by influencing the expression and activity of crucial proteins in apoptotic pathways. It downregulates anti-apoptotic proteins such as Bcl-2 and activates caspases, pivotal in the execution phase of apoptosis [97]. HQ also significantly affects the STAT3 signalling pathway, a critical element in oncogenesis that promotes tumour growth. By inhibiting the STAT3 pathway, similar to PMZ's action [89], HQ facilitates a series of intracellular events that lead to increased caspase activation, intensifying the apoptotic response [98].

The effects of HQ go beyond targeting cancer cells; it also alters the environment within the tumour area. One significant aspect of this immune modifying impact is the suppression of Toll-like receptors, which leads to a decrease, in the release of cytokines by immune cells such as interleukins (IL 6, IL 1) interferons (IFN γ/α) and tumour necrosis factor alpha (TNF α). Additionally, it reduces the presence of TNF receptors on macrophages T cells and B lymphocytes [99-101]. This adjustment, in response surprisingly boosts the body's ability to fight against tumours resulting in a tumour environment that hinders cancer growth and aids in its destruction by cells.

6.3.7 Anti-inflammatory activity

After evaluating the ability of all formulations to inhibit the growth of A549 cells, the subsequent step was to investigate how these formulations could mitigate inflammation. The impact of the formulations (F1-F10) on the levels of pro-inflammatory cytokines was examined, in comparison to cells that were not treated. The investigated cytokines were IL 1β, IL 6, IL 8 and TNF α. The findings revealed a decrease in the expression of all inflammatory cytokines, in most treated groups when compared to the untreated group ($p<0.05$) (Refer to **Figure 9**).
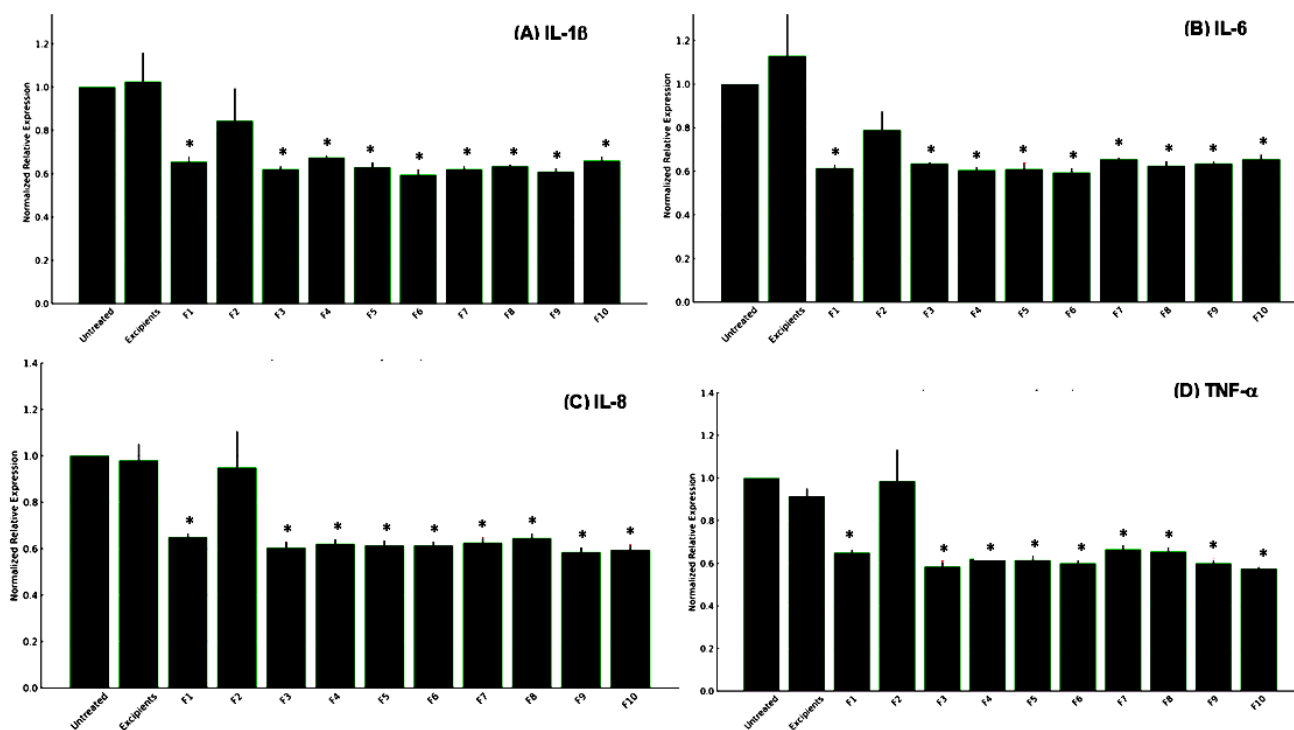
Figure 9. The anti-inflammatory effect of F-formulations. Relative RNA expression of (**A**) IL-1β, (**B**) IL-6, (**C**) IL-8, and (**D**) TNF-α gene on THP-1 macrophages cell line. RNA was isolated and quantified using QPCR technique and the expression of the indicated genes was normalized against untreated cells. The values indicate the mean, with standard deviation. * $p < 0.05$, calculated using one-way ANOVA.

For IL-1B, formulations F1 to F5 showed average reductions of 31%-39% (± 2.30%-17.6%), with notable reductions in F3 (38.0%, ± 2.30%) and F2 (15.5%, ± 17.6%). Formulations F6 to F10 had greater suppression, with decreases of 34%-41% (± 2.3%-5.9%). For IL-6, F1 to F5 reduced expression by 37%-39% (± 3.3%-10.7%), with significant reduction in F2 (21.0%, ± 10.7%). F6 to F10 resulted in 34.5%-40.5% reductions (± 1.10%-5.90%), with F7 showing the highest consistency (34.5%, ± 1.10%). For IL-8, F1 to F5 showed reductions of 35%-40% (± 3.4%-7.0%), with significant decreases in F2 (5.0%, ± 16%) and F3 (39.5%, ± 5.80%). F6 to F10 had reductions of 36%-43% (± 3.3%-5.8%). For TNF-α, F1 to F5 resulted in reductions of 34%-43% (± 2.2%-

15%), with significant reductions in F2 (1.50%, ± 15.1%) and F5 (38.5%, ± 10.3%). F6 to F10 exhibited decreases of 34%-43% (± 1.2%-3.4%).

Notably, the F2 formulation showed no significant change in cytokine levels, likely due to its larger particle size. The larger size did not suppress cytokine RNA expression levels, possibly because the reduced surface area to volume ratio of larger particles leads to a slower dissolution rate [102], thereby limiting the release of the active ingredient. Another reason could be the less efficient uptake by cells for larger particles [103], which reduces the effective concentration of the active ingredient reaching the cells. Studies, both in vivo and in vitro, have demonstrated that alveolar macrophages efficiently uptake particles in the 1–5 µm range [104]. Furthermore, larger particles tend to aggregate and settle, which further could reduce their availability and interaction with the cells.

The anti-inflammatory effects observed across all formulations were primarily attributed to HQ. By analysing the free drugs, it was found that PMZ had no significant effect on the levels of pro-inflammatory cytokines. In contrast, HQ and the combination of HQ and PMZ significantly reduced the expression of these cytokines, as demonstrated in **Supplementary figure 1**. HQ is well known for its inflammatory effects, which are achieved through various molecular mechanisms. HQ is famous, for its inflammatory properties, which work through multiple molecular pathways. Firstly, HQ interferes with lysosomal activity, leading to reduced processing and presentation of antigens. This reduction diminishes the activation and response of the immune system, which is crucial for the observed downregulation of cytokines such as IL-1β and TNF-α, both pivotal in initiating the inflammatory cascade [105]. Secondly, HQ suppresses the signalling of Toll receptors (TLR) leading to lower levels of IL 6 and IL 8. These cytokines play a role, in the body's immune response and the migration of immune cells, to areas of inflammation [106]. Additionally, HQ inhibits autophagy and stabilizes cellular membranes, further reducing the capacity of cells to propagate inflammatory signals, thereby aiding in the overall suppression of pro-inflammatory cytokine production [107]. Furthermore, the impact of HQ, on cytokine production is associated with its ability to directly and indirectly inhibit the NF κB pathway. This leads to a reduction in the transcription of genes that

promote inflammation, such as those, for IL 1β, IL 6 TNF α and IL 8. This broad anti-inflammatory effect highlights the promise of formulations containing HQ in controlling inflammatory reactions [108].

6.3.8 Antimicrobial activity

The spray-dried formulations were designed for inhalation delivery, intended to directly interact with microbial agents present in the respiratory mucosa. In this part of the study, the antimicrobial efficacy of these formulations, which contain PMZ, and HQ was tested. The microorganism *Acinetobacter baumannii, Klebsiella pneumoniae, Pseudomonas aeruginosa* were chosen for this evaluation due their role in causing severe respiratory infections [109]. The results of the disk diffusion method showed that none of the tested spray-dried PMZ- HQ formulations produced an inhibition zone as illustrated in **Figure 10**.

These negative results could likely be attributed to strain-specific resistance, given prior evidence of PMZ's effectiveness against different bacterial strains. For instance, studies have shown that PMZ can reduce the internalization of *S. enterica serovar Typhimurium and E. coli* by phagocytic cells in vitro [110, 111]. Additionally, PMZ has been effective in decreasing both the uptake and vacuolar escape of *Listeria monocytogenes* in bone marrow-derived macrophages [112], and it has also hindered the bacterial invasion and cell-to-cell spread in infections of non-phagocytic cells [113]. Furthermore, PMZ has been noted to block the AcrAB-TolC efflux pump in *Escherichia coli* [110]. The ineffectiveness observed in the test indicates that the antibacterial properties of PMZ could vary based on the bacteria strains present underscoring the importance of conducting more extensive studies to ascertain the range of PMZs antimicrobial efficacy.

1. *Acinetobacter baumannii*

1)PVP + Isomalt
2) PVP + Trehalose
3)PVP+Orarez
*) Minocycline (as a positive control)

2. *Klebsiella pneumonia*

1)PVP + Isomalt
2) PVP + Trehalose
3)PVP+Orarez
*) Imipenem (as a positive control)

3. *Pseudomonas aeruginosa*

1)PVP + Isomalt
2) PVP + Trehalose
3)PVP+Orarez
*) Ertapenem (as a positive control)
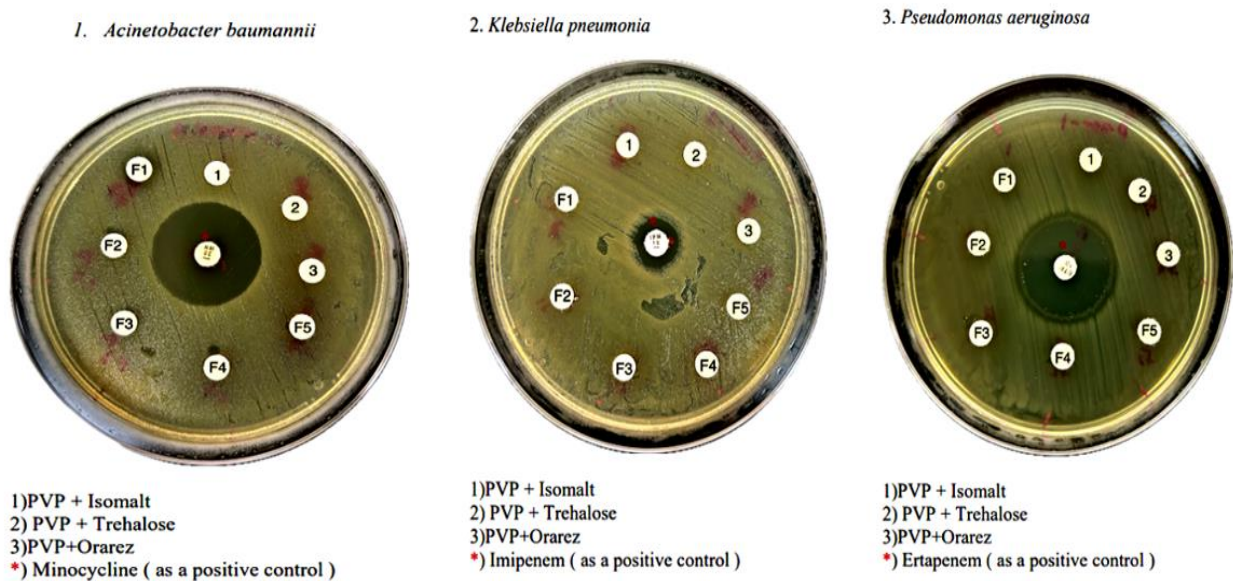
A

Isolate	F1	F2	F3	F4	F5
A.baumannii	0 mm	0 mm	0 mm	0 mm	0 mm
K.pneumoniae	0 mm	0 mm	0 mm	0 mm	0 mm
P.aeruginosa	0 mm	0 mm	0 mm	0 mm	0 mm

Solvent = <10% DMSO
Diluent = Phosphate buffer saline
Concentration : 200 µg
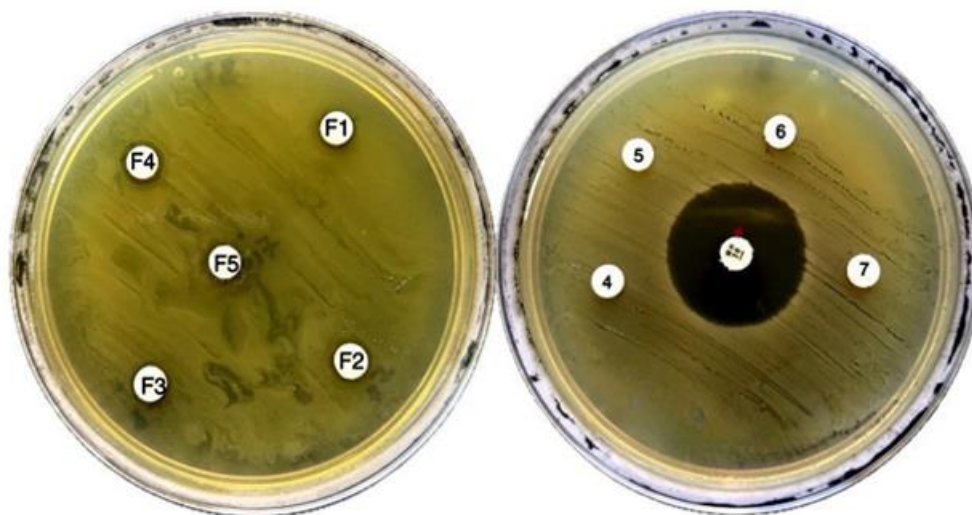
4) HPMC-E5 + Trehalose
5) HPMC-E5 + Isomalt
6) HPMC-E5 + Orarez
7) Buffer (as a negative control)
*) Minocyline (as a positive control)

B

Isolate	F1	F2	F3	F4	F5
A.baumannii	0 mm	0 mm	0 mm	0 mm	0 mm

Figure 10. Disc diffusion method result. **(A)** Mueller-Hinton Agar (MHA) plate streaked with**:** 1. *Acinetobacter baumannii, 2. Klebsiella pneumoniae, 3. Pseudomonas aeruginosa* tested against discs containing spray-dried F1-F5 formulations **(B)** MHA plate streaked with respective individual excipients.

6.4 Conclusions

Advanced spray drying techniques present a promising strategy to enhance the therapeutic efficacy of PMZ and HQ combinations. This study investigated the

comparative effectiveness of two such techniques: the 2FN and 3FN methods. The results demonstrated that the 3FN method achieved a higher recovery%, especially for PMZ. Particle size analysis revealed that the 3FN method produced larger particles compared to 2FN. FTIR results confirmed hydrogen bonding between the PMZ, HQ, and excipients in both methods, stabilizing the amorphous form. XRPD analysis confirmed the transformation to an amorphous state in both methods. Drug release kinetics showed that the 3FN spray drying method offered greater versatility over the 2FN method by providing a tailored release profile for the encapsulated bio actives. The multilayer encapsulates prepared by 3FN exhibited customized release profiles, with a prolonged sustained release for PMZ encapsulated in the core and a faster burst release for HQ encapsulated in the shell. Most formulations demonstrated synergistic antiproliferative effects against A549 cells and significantly reduced pro-inflammatory cytokines. Overall, the findings indicate that the 3FN spray drying method is superior to the 2FN method in enhancing the therapeutic potential of PMZ and HQ co-delivery for targeting inflammation and cancer cells. However, future work should include in vivo studies to evaluate the safety, bioavailability, and therapeutic efficacy of these spray-dried formulations in animal models, followed by clinical trials to confirm these findings in human subjects and assess the potential for widespread clinical use.

References:

[1]   C. Arpargaus, D. Rütti, and M. Meuri, "Enhanced solubility of poorly soluble drugs via spray drying," *Drug Delivery Strategies for Poorly Water-Soluble Drugs,* pp. 551-585, 2013.

[2]   N. Marasini *et al.*, "Development of excipients free inhalable co-spray-dried tobramycin and diclofenac formulations for cystic fibrosis using two and three fluid nozzles," *International Journal of Pharmaceutics,* vol. 624, p. 121989, 2022.

[3]   X. Wang *et al.*, "Advances in controlled-release fertilizer encapsulated by organic-inorganic composite membranes," *Particuology,* 2023.

[4]   B. Li *et al.*, "A novel drug repurposing approach for non-small cell lung cancer using deep learning," *PLoS One,* vol. 15, no. 6, p. e0233112, 2020.

[5]   I. Elmaci and M. A. Altinoz, "Targeting the cellular schizophrenia. Likely employment of the antipsychotic agent pimozide in treatment of refractory cancers and glioblastoma," *Critical Reviews in Oncology/Hematology,* vol. 128, pp. 96-109, 2018.

[6]   J. M. Gonçalves, C. A. B. Silva, E. R. C. Rivero, and M. M. R. Cordeiro, "Inhibition of cancer stem cells promoted by Pimozide," *Clinical and Experimental Pharmacology and Physiology,* vol. 46, no. 2, pp. 116-125, 2019.

[7]   Y. Song and E. Fields, "Pharmacological advances of chloroquine and hydroxychloroquine: from antimalarials to investigative therapies in covid-19," *Natural Product Communications,* vol. 15, no. 9, p. 1934578X20953648, 2020.

[8]   M. A. A. Al-Bari, "Chloroquine analogues in drug discovery: new directions of uses, mechanisms of actions and toxic manifestations from malaria to multifarious diseases," *Journal of Antimicrobial Chemotherapy,* vol. 70, no. 6, pp. 1608-1621, 2015.

[9]   W. Fong and K. K. To, "Repurposing chloroquine analogs as an adjuvant cancer therapy," *Recent Patents on Anti-Cancer Drug Discovery,* vol. 16, no. 2, pp. 204-221, 2021.

[10]   E. Schrezenmeier and T. Dörner, "Mechanisms of action of hydroxychloroquine and chloroquine: implications for rheumatology," *Nature Reviews Rheumatology,* vol. 16, no. 3, pp. 155-166, 2020.

[11]   H. Lu, W. Ouyang, and C. Huang, "Inflammation, a key event in cancer development," *Molecular cancer research,* vol. 4, no. 4, pp. 221-233, 2006.

[12]   E. Ilan *et al.*, "Improved oral delivery of desmopressin via a novel vehicle: mucoadhesive submicron emulsion," *Pharmaceutical research,* vol. 13, pp. 1083-1087, 1996.

[13]   M. B. Schulz and R. Daniels, "Hydroxypropylmethylcellulose (HPMC) as emulsifier for submicron emulsions: influence of molecular weight and substitution type on the droplet size after high-

pressure homogenization," *European Journal of Pharmaceutics and Biopharmaceutics,* vol. 49, no. 3, pp. 231-236, 2000.

[14]   J. Zheng, B. Wang, J. Xiang, and Z. Yu, "Controlled release of curcumin from HPMC (hydroxypropyl methyl cellulose) co-spray-dried materials," *Bioinorganic chemistry and applications,* vol. 2021, 2021.

[15]   T. A. Popov *et al.*, "Methyl-cellulose powder for prevention and management of nasal symptoms," *Expert Review of Respiratory Medicine,* vol. 11, no. 11, pp. 885-892, 2017.

[16]   Y. Kawashima, T. Serigano, T. Hino, H. Yamamoto, and H. Takeuchi, "A new powder design method to improve inhalation efficiency of pranlukast hydrate dry powder aerosols by surface modification with hydroxypropylmethylcellulose phthalate nanospheres," *Pharmaceutical research,* vol. 15, pp. 1748-1752, 1998.

[17]   G. A. Burdock, "Safety assessment of hydroxypropyl methylcellulose as a food ingredient," *Food and Chemical Toxicology,* vol. 45, no. 12, pp. 2341-2351, 2007.

[18]   N. Al-Zoubi, G. Al-Obaidi, B. Tashtoush, and S. Malamataris, "Sustained release of diltiazem HCl tableted after co-spray drying and physical mixing with PVAc and PVP," *Drug development and industrial pharmacy,* vol. 42, no. 2, pp. 270-279, 2016.

[19]   J. H. Lee *et al.*, "Enhanced dissolution rate of celecoxib using PVP and/or HPMC-based solid dispersions prepared by spray drying method," *Journal of Pharmaceutical Investigation,* vol. 43, pp. 205-213, 2013.

[20]   T. Sou, M. P. McIntosh, L. M. Kaminskas, R. J. Prankerd, and D. A. Morton, "Designing a multicomponent spray-dried formulation platform for pulmonary delivery of biomacromolecules: the effect of polymers on the formation of an amorphous matrix for glassy state stabilization of biomacromolecules," *Drying technology,* vol. 31, no. 13-14, pp. 1451-1458, 2013.

[21]   F. Tewes, L. Tajber, O. I. Corrigan, C. Ehrhardt, and A.-M. Healy, "Development and characterisation of soluble polymeric particles for pulmonary peptide delivery," *European Journal of Pharmaceutical Sciences,* vol. 41, no. 2, pp. 337-352, 2010.

[22]   O. Zachar, "Respiratory Infections Early-Stage Medication: Inhalation Formulation & Dosage of PVP Iodine," 2021.

[23]   M. A. Haque, J. Chen, P. Aldred, and B. Adhikari, "Denaturation and physical characteristics of spray-dried whey protein isolate powders produced in the presence and absence of lactose, trehalose, and polysorbate-80," *Drying technology,* vol. 33, no. 10, pp. 1243-1254, 2015.

[24]   S. Ohtake and Y. J. Wang, "Trehalose: Current Use and Future Applications," *Journal of Pharmaceutical Sciences,* vol. 100, no. 6, pp. 2020-2053, 2011/06/01/ 2011, doi: https://doi.org/10.1002/jps.22458.

[25]   A. Teo, Y. Lam, S. J. Lee, and K. K. Goh, "Spray drying of whey protein stabilized nanoemulsions containing different wall materials–maltodextrin or trehalose," *LWT,* vol. 136, p. 110344, 2021.

[26]   O. Ivaniuk, T. Yarnykh, and I. Kovalevska, "Determination of the bioadhesion indicators of vaginal gel with resveratrol and hyaluronic acid," 2019.

[27]   Y. S. Maslii, O. Ruban, Y. V. Levachkova, and T. Y. Kolisnyk, "Choice of mucosal adhesive in the composition of a new dental gel," 2020.

[28]   M. Auerbach and A. k. Dedman, "Bulking Agents–Multi-Functional Ingredients," *Sweeteners and sugar alternatives in food technology,* pp. 433-470, 2012.

[29]   A.-K. Koskinen *et al.*, "Physical stability of freeze-dried isomalt diastereomer mixtures," *Pharmaceutical Research,* vol. 33, pp. 1752-1768, 2016.

[30]   E. Matta, M. J. Tavera-Quiroz, and N. Bertola, "Isomalt-plasticized methylcellulose-based films as carriers of ascorbic acid," *Food and Bioprocess Technology,* vol. 13, pp. 2186-2199, 2020.

[31]   A. Sentko and I. Willibald-Ettle, "Isomalt," *Sweeteners and sugar alternatives in food technology,* pp. 243-274, 2012.

[32]   J. A. Bhushani, N. K. Kurrey, and C. Anandharamakrishnan, "Nanoencapsulation of green tea catechins by electrospraying technique and its effect on controlled release and in-vitro permeability," *Journal of Food Engineering,* vol. 199, pp. 82-92, 2017.

[33]   T.-C. Chou, "Drug combination studies and their synergy quantification using the Chou-Talalay method," *Cancer research,* vol. 70, no. 2, pp. 440-446, 2010.

[34]   M. A. Boraey, S. Hoe, H. Sharif, D. P. Miller, D. Lechuga-Ballesteros, and R. Vehring, "Improvement of the dispersibility of spray-dried budesonide powders using leucine in an ethanol–water cosolvent system," *Powder technology,* vol. 236, pp. 171-178, 2013.

[35]   R. Vehring, "Pharmaceutical particle engineering via spray drying," *Pharmaceutical research,* vol. 25, no. 5, pp. 999-1022, 2008.

[36]   R. Vehring, W. R. Foss, and D. Lechuga-Ballesteros, "Particle formation in spray drying," *Journal of aerosol science,* vol. 38, no. 7, pp. 728-746, 2007.

[37]   S. Nimbkar, M. M. Leena, J. A. Moses, and C. Anandharamakrishnan, "A modified 3-fluid nozzle spray drying approach for co-encapsulation of iron and folic acid," *Chemical Papers,* vol. 77, no. 7, pp. 4019-4032, 2023.

[38]   M. M. Leena, M. G. Antoniraj, J. Moses, and C. Anandharamakrishnan, "Three fluid nozzle spray drying for co-encapsulation and controlled release of curcumin and resveratrol," *Journal of Drug Delivery Science and Technology,* vol. 57, p. 101678, 2020.

[39]   D. França, Â. F. Medina, L. L. Messa, C. F. Souza, and R. Faez, "Chitosan spray-dried microcapsule and microsphere as fertilizer host for swellable– controlled release materials," *Carbohydrate polymers,* vol. 196, pp. 47-55, 2018.

[40]   J. W. Ivey, P. Bhambri, T. K. Church, D. A. Lewis, and R. Vehring, "Experimental investigations of particle formation from propellant and solvent droplets using a monodisperse spray dryer," *Aerosol Science and Technology,* vol. 52, no. 6, pp. 702-716, 2018.

[41]   T. T. Nguyen, T. Hirano, R. N. Chamida, E. L. Septiani, N. T. Nguyen, and T. Ogi, "Porous pectin particle formation utilizing spray drying with a three-fluid nozzle," *Powder Technology,* vol. 440, p. 119782, 2024.

[42]   S. Nimbkar, M. M. Leena, J. Moses, and C. Anandharamakrishnan, "Development of iron-vitamin multilayer encapsulates using 3 fluid nozzle spray drying," *Food Chemistry,* vol. 406, p. 135035, 2023.

[43]   P. Saralkar and A. K. Dash, "Alginate nanoparticles containing curcumin and resveratrol: preparation, characterization, and in vitro evaluation against DU145 prostate cancer cell line," *AAPS pharmscitech,* vol. 18, pp. 2814-2823, 2017.

[44]   C. Jin *et al.*, "Updates on applications of low-viscosity grade Hydroxypropyl methylcellulose in coprocessing for improvement of physical properties of pharmaceutical powders," *Carbohydrate Polymers,* vol. 311, p. 120731, 2023/07/01/ 2023, doi: https://doi.org/10.1016/j.carbpol.2023.120731.

[45]   T. Peng *et al.*, "Influence of polymers on the physical and chemical stability of spray-dried amorphous solid dispersion: dipyridamole degradation induced by enteric polymers," *Aaps Pharmscitech,* vol. 19, pp. 2620-2628, 2018.

[46]   B.-J. Lee, S.-G. Ryu, and J.-H. Cui, "Formulation and release characteristics of hydroxypropyl methylcellulose matrix tablet containing melatonin," *Drug development and industrial pharmacy,* vol. 25, no. 4, pp. 493-501, 1999.

[47]   K. Tahara, K. Yamamoto, and T. Nishihata, "Overall mechanism behind matrix sustained release (SR) tablets prepared with hydroxypropyl methylcellulose 2910," *Journal of controlled release,* vol. 35, no. 1, pp. 59-66, 1995.

[48]   T. Kshirsagar, N. Jaiswal, G. Chavan, K. Zambre, S. Ramkrushna, and D. Dinesh, "Formulation & evaluation of fast dissolving oral film," *World J. Pharm. Res,* vol. 10, no. 9, pp. 503-561, 2021.

[49]   M. N. Leslie, N. Marasini, Z. Sheikh, P. M. Young, D. Traini, and H. X. Ong, "Development of inhalable spray dried nitrofurantoin formulations for the treatment of emphysema," *Pharmaceutics,* vol. 15, no. 1, p. 146, 2022.

[50]   J. Cai, R. Lopez, and Y. Lee, "Effect of Feed Material Properties on Microencapsulation by Spray Drying with a Three-Fluid Nozzle: Soybean Oil Encapsulated in Maltodextrin and Sugar Beet Pectin," *Journal of Food Processing and Preservation,* vol. 2023, 2023.

[51]   D. Bolten and M. Türk, "Experimental study on the surface tension, density, and viscosity of aqueous poly (vinylpyrrolidone) solutions," *Journal of Chemical & Engineering Data,* vol. 56, no. 3, pp. 582-588, 2011.

[52]   Z. Mingzheng, X. Guodong, L. Jian, C. Lei, and Z. Lijun, "Analysis of factors influencing thermal conductivity and viscosity in different kinds of surfactant solutions," *Experimental Thermal and Fluid Science,* vol. 36, pp. 22-29, 2012.

[53]   H. Gurditta, A. A. Patel, and S. Arora, "Optimisation of sweetener and bulking agent levels for the preparation of functional Chhana-murki," *International journal of dairy technology,* vol. 68, no. 2, pp. 190-197, 2015.

[54]   V. Nagathan and K. Hallikeri, "Formulation and Evaluation of Topical Film Forming Systems Comprising of Non-Steroidal Anti-Inflammatory Drug," *Indian Journal of Pharmaceutical Sciences,* vol. 85, no. 5, 2023.

[55]   H. Kawai, M. Sakurai, Y. Inoue, R. Chujo, and S. Kobayashi, "Hydration of oligosaccharides: anomalous hydration ability of trehalose," *Cryobiology,* vol. 29, no. 5, pp. 599-606, 1992.

[56]   J. S. Masliy and O. Ruban, "The study of biopharmaceutical and adhesive characteristics of a dental gel," *Вісник фармації,* no. 1, pp. 28-32, 2018.

[57]   H. Bera *et al.*, "Novel pimozide-β-cyclodextrin-polyvinylpyrrolidone inclusion complexes for Tourette syndrome treatment," *Journal of Molecular Liquids,* vol. 215, pp. 135-143, 2016/03/01/ 2016, doi: https://doi.org/10.1016/j.molliq.2015.12.054.

[58]   F. Faísca, V. Correia, Ž. Petrovski, L. C. Branco, H. Rebelo-de-Andrade, and M. M. Santos, "Enhanced in vitro antiviral activity of hydroxychloroquine ionic liquids against SARS-CoV-2," *Pharmaceutics,* vol. 14, no. 4, p. 877, 2022.

[59]   J. Zhang, B. Yuan, and H. Ren, "Synthesis and Characterization of PVP/Tb 4/3 L•7H 2 O Luminescent Complex," *IOP Conference Series: Earth and Environmental Science,* vol. 170, p. 032043, 07/01 2018, doi: 10.1088/1755-1315/170/3/032043.

[60]   H. Somashekarappa, Y. Prakash, K. Hemalatha, T. Demappa, and R. Somashekar, "Preparation and characterization of HPMC/PVP blend films plasticized with sorbitol," *Indian Journal of Materials Science,* vol. 2013, 2013.

[61]   H. Kawashima and H. Goto, "Preparation and Properties of Polyaniline in the Presence of Trehalose," *Soft Nanoscience Letters,* vol. 01, 01/01 2011, doi: 10.4236/snl.2011.13013.

[62]   M. Ishtiaq, S. Asghar, I. ullah khan, M. Iqbal, and S. Khalid, "Development of the Amorphous Solid Dispersion of Curcumin: A Rational Selection of Polymers for Enhanced Solubility and Dissolution," *Crystals,* vol. 12, p. 1606, 11/10 2022, doi: 10.3390/cryst12111606.

[63]   G. Papageorgiou, A. Docoslis, M. Georgarakis, and D. Bikiaris, "The effect of physical state on the drug dissolution rate: miscibility studies of nimodipine with PVP," *Journal of thermal analysis and calorimetry,* vol. 95, no. 3, pp. 903-915, 2009.

[64]   K. A. Chan and S. G. Kazarian, "FTIR spectroscopic imaging of dissolution of a solid dispersion of nifedipine in poly (ethylene glycol)," *Molecular Pharmaceutics,* vol. 1, no. 4, pp. 331-335, 2004.

[65]   N. Wyttenbach, A. Niederquell, P. Ectors, and M. Kuentz, "Study and Computational Modeling of Fatty Acid Effects on Drug Solubility in Lipid-Based Systems," *Journal of Pharmaceutical Sciences,* vol. 111, no. 6, pp. 1728-1738, 2022/06/01/ 2022, doi: https://doi.org/10.1016/j.xphs.2021.11.023.

[66]   A. N. F. Moraes *et al.*, "Compatibility study of hydroxychloroquine sulfate with pharmaceutical excipients using thermal and nonthermal techniques for the development of hard capsules," *Journal of Thermal Analysis and Calorimetry,* vol. 140, pp. 2283-2292, 2020.

[67]   L. Nohemann, M. P. d. Almeida, and P. C. Ferrari, "Floating ability and drug release evaluation of gastroretentive microparticles system containing metronidazole obtained by spray drying," *Brazilian Journal of Pharmaceutical Sciences,* vol. 53, 2017.

[68]   K. Roe and T. Labuza, "Glass Transition and Crystallization of Amorphous Trehalose-sucrose Mixtures," *International Journal of Food Properties - INT J FOOD PROP,* vol. 8, pp. 559-574, 09/01 2005, doi: 10.1080/10942910500269824.

[69]   E. Khodaverdi, N. Khalili, F. Zangiabadi, and A. Homayouni, "Preparation, Characterization and Stability Studies of Glassy Solid Dispersions of Indomethacin using PVP and Isomalt as carriers," *Iranian journal of basic medical sciences,* vol. 15, pp. 820-832, 04/01 2012.

[70]   S. Kim, W. K. Ng, Y. Dong, S. Das, and R. B. Tan, "Preparation and physicochemical characterization of trans-resveratrol nanoparticles by temperature-controlled antisolvent precipitation," *Journal of Food Engineering,* vol. 108, no. 1, pp. 37-42, 2012.

[71]   Y.-H. Phillip Lee *et al.*, "Gefitinib–cyclodextrin inclusion complexes: physico-chemical characterization and dissolution studies," *Drug development and industrial pharmacy,* vol. 35, no. 9, pp. 1113-1120, 2009.

[72]   W. Liu, X. D. Chen, Z. Cheng, and C. Selomulya, "On enhancing the solubility of curcumin by microencapsulation in whey protein isolate via spray drying," *Journal of food engineering,* vol. 169, pp. 189-195, 2016.

[73]   D. E. Alonzo, G. G. Zhang, D. Zhou, Y. Gao, and L. S. Taylor, "Understanding the behavior of amorphous pharmaceutical systems during dissolution," *Pharmaceutical research,* vol. 27, pp. 608-618, 2010.

[74]   T. Mizoe, S. Beppu, T. Ozeki, and H. Okada, "One-step preparation of drug-containing microparticles to enhance the dissolution and absorption of poorly water-soluble drugs using a 4-fluid nozzle spray drier," *Journal of controlled release,* vol. 120, no. 3, pp. 205-210, 2007.

[75]   G. H. Shin, J. Li, J. H. Cho, J. T. Kim, and H. J. Park, "Enhancement of curcumin solubility by phase change from crystalline to amorphous in CUR-TPGS nanosuspension," *Journal of Food Science,* vol. 81, no. 2, pp. N494-N501, 2016.

[76]   S. Tan, C. Zhong, and T. Langrish, "Microencapsulation of pepsin in the spray-dried WPI (whey protein isolates) matrices for controlled release," *Journal of food engineering,* vol. 263, pp. 147-154, 2019.

[77]   K. Wasilewska and K. Winnicka, "Ethylcellulose–a pharmaceutical excipient with multidirectional application in drug dosage forms development," *Materials,* vol. 12, no. 20, p. 3386, 2019.

[78]   C. Berkland, M. King, A. Cox, K. K. Kim, and D. W. Pack, "Precise control of PLG microsphere size provides enhanced control of drug release rate," *Journal of controlled release,* vol. 82, no. 1, pp. 137-147, 2002.

[79]   S. Freiberg and X. Zhu, "Polymer microspheres for controlled drug release," *International journal of pharmaceutics,* vol. 282, no. 1-2, pp. 1-18, 2004.

[80]   C. G. Chiaregato, O. D. Bernardinelli, A. Shavandi, E. Sabadini, and D. F. S. Petri, "The effect of the molecular structure of hydroxypropyl methylcellulose on the states of water, wettability, and swelling properties of cryogels prepared with and without CaO2," *Carbohydrate polymers,* vol. 316, p. 121029, 2023.

[81]   A. Viridén, B. Wittgren, and A. Larsson, "The consequence of the chemical composition of HPMC in matrix tablets on the release behaviour of model drug substances having different solubility," *European journal of pharmaceutics and biopharmaceutics,* vol. 77, no. 1, pp. 99-110, 2011.

[82]   P. Franco and I. De Marco, "The Use of Poly (N-vinyl pyrrolidone) in the Delivery of Drugs: A Review," *Polymers,* vol. 12, no. 5, p. 1114, 2020.

[83]   A. B. Lokhande, S. Mishra, R. D. Kulkarni, and J. B. Naik, "Influence of different viscosity grade ethylcellulose polymers on encapsulation and in vitro release study of drug loaded nanoparticles," *Journal of pharmacy research,* vol. 7, no. 5, pp. 414-420, 2013.

[84]   L. Ma, T. Shi, Z. Zhang, X. Liu, and H. Wang, "Wettability of HPMC/PEG/CS Thermosensitive Porous Hydrogels," *Gels,* vol. 9, no. 8, p. 667, 2023.

[85]   M. Namasivayam, M. R. Andersson, and J. G. Shapter, "A comparative study on the role of polyvinylpyrrolidone molecular weight on the functionalization of various carbon nanotubes and their composites," *Polymers,* vol. 13, no. 15, p. 2447, 2021.

[86]   R. Singh and J. W. Lillard Jr, "Nanoparticle-based targeted drug delivery," *Experimental and molecular pathology,* vol. 86, no. 3, pp. 215-223, 2009.

[87]   M. Muhaimin, A. Y. Chaerunisaa, and R. Bodmeier, "Impact of dispersion time interval and particle size on release profiles of propranolol HCl and carbamazepines from microparticle blends system," *Scientific reports,* vol. 12, no. 1, p. 10360, 2022.

[88]   W. W. Mustafa, J. Fletcher, M. Khoder, and R. G. Alany, "Solid dispersions of gefitinib prepared by spray drying with improved mucoadhesive and drug dissolution properties," *AAPS PharmSciTech,* vol. 23, no. 1, p. 48, 2022.

[89]   A. Ranjan, I. Kaushik, and S. K. Srivastava, "Pimozide suppresses the growth of brain tumors by targeting STAT3-mediated autophagy," *Cells,* vol. 9, no. 9, p. 2141, 2020.

[90]   T. Immanuel, J. Li, T. N. Green, A. Bogdanova, and M. L. Kalev-Zylinska, "Deregulated calcium signaling in blood cancer: Underlying mechanisms and therapeutic potential," *Frontiers in oncology,* vol. 12, p. 1010506, 2022.

[91]   S. Zielke *et al.*, "Loperamide, pimozide, and STF-62247 trigger autophagy-dependent cell death in glioblastoma cells," *Cell death & disease,* vol. 9, no. 10, p. 994, 2018.

[92]   Y. Ren, J. Tao, Z. Jiang, D. Guo, and J. Tang, "Pimozide suppresses colorectal cancer via inhibition of Wnt/β-catenin signaling pathway," *Life sciences,* vol. 209, pp. 267-273, 2018.

[93]   A. L. Liang *et al.*, "Chloroquine increases the anti-cancer activity of epirubicin in A549 lung cancer cells," *Oncology Letters,* vol. 20, no. 1, pp. 53-60, 2020.

[94]   S. Brezgin *et al.*, "Hydroxychloroquine Enhances Cytotoxic Properties of Extracellular Vesicles and Extracellular Vesicle–Mimetic Nanovesicles Loaded with Chemotherapeutics," *Pharmaceutics,* vol. 15, no. 2, p. 534, 2023.

[95]   L.-q. Liu *et al.*, "Hydroxychloroquine potentiates the anti-cancer effect of bevacizumab on glioblastoma via the inhibition of autophagy," *Biomedicine & Pharmacotherapy,* vol. 118, p. 109339, 2019.

[96]   P. M. P. Ferreira, R. W. R. de Sousa, J. R. de Oliveira Ferreira, G. C. G. Militão, and D. P. Bezerra, "Chloroquine and hydroxychloroquine in antitumor therapies based on autophagy-related mechanisms," *Pharmacological research,* vol. 168, p. 105582, 2021.

[97]   M. M. Hoque, Y. Iida, H. Kotani, I. D. Kartika, and M. Harada, "Hydroxychloroquine Promotes Bcl-xL Inhibition-induced Apoptosis in BxPC-3 Human Pancreatic Cancer Cells," *Anticancer Research,* vol. 42, no. 7, pp. 3495-3506, 2022.

[98]   X. Lyu *et al.*, "Hydroxychloroquine suppresses lung tumorigenesis via inducing FoxO3a nuclear translocation through STAT3 inactivation," *Life sciences,* vol. 246, p. 117366, 2020.

[99]   A. E. in 't Veld, M. A. Jansen, L. C. Ciere, and M. Moerland, "Hydroxychloroquine effects on TLR signalling: underexposed but unneglectable in COVID-19," *Journal of Immunology Research,* vol. 2021, pp. 1-7, 2021.

[100]   W. Zhou, H. Wang, Y. Yang, Z.-S. Chen, C. Zou, and J. Zhang, "Chloroquine against malaria, cancers and viral diseases," *Drug Discovery Today,* vol. 25, no. 11, pp. 2012-2022, 2020.

[101]   J. A. Ratikan, J. W. Sayre, and D. Schaue, "Chloroquine engages the immune system to eradicate irradiated breast tumors in mice," *International Journal of Radiation Oncology* Biology* Physics,* vol. 87, no. 4, pp. 761-768, 2013.

[102]   D. Heng, D. J. Cutler, H.-K. Chan, J. Yun, and J. A. Raper, "What is a suitable dissolution method for drug nanoparticles?," *Pharmaceutical research,* vol. 25, pp. 1696-1701, 2008.

[103]   V. Kanchan and A. K. Panda, "Interactions of antigen-loaded polylactide particles with macrophages and their correlation with the immune response," *Biomaterials,* vol. 28, no. 35, pp. 5344-5357, 2007.

[104]   M. V. Baranov, M. Kumar, S. Sacanna, S. Thutupalli, and G. van den Bogaart, "Modulation of Immune Responses by Particle Size and Shape," (in eng), *Front Immunol,* vol. 11, p. 607945, 2020, doi: 10.3389/fimmu.2020.607945.

[105]   I. R. Rao *et al.*, "Hydroxychloroquine in nephrology: current status and future directions," *Journal of Nephrology,* vol. 36, no. 8, pp. 2191-2208, 2023/11/01 2023, doi: 10.1007/s40620-023-01733-6.

[106]   A. E. In 't Veld, M. A. A. Jansen, L. C. A. Ciere, and M. Moerland, "Hydroxychloroquine Effects on TLR Signalling: Underexposed but Unneglectable in COVID-19," (in eng), *J Immunol Res,* vol. 2021, p. 6659410, 2021, doi: 10.1155/2021/6659410.

[107]   R. Xu, Z. Ji, C. Xu, and J. Zhu, "The clinical value of using chloroquine or hydroxychloroquine as autophagy inhibitors in the treatment of cancers: A systematic review and meta-analysis," (in eng), *Medicine (Baltimore),* vol. 97, no. 46, p. e12912, Nov 2018, doi: 10.1097/md.0000000000012912.

[108]   Y. R. Fauzi *et al.*, "Antitumor effects of chloroquine/hydroxychloroquine mediated by inhibition of the NF-κB signaling pathway through abrogation of autophagic p47 degradation in adult T-cell leukemia/lymphoma cells," (in eng), *PLoS One,* vol. 16, no. 8, p. e0256320, 2021, doi: 10.1371/journal.pone.0256320.

[109]   S. M. S. Lim, A. Z. Abidin, S. Liew, J. Roberts, and F. Sime, "The global prevalence of multidrug-resistance among Acinetobacter baumannii causing hospital-acquired and ventilator-associated pneumonia and its associated mortality: A systematic review and meta-analysis," *Journal of infection,* vol. 79, no. 6, pp. 593-600, 2019.

[110]   J. A. Bohnert, S. Schuster, and W. V. Kern, "Suppl 1: Pimozide inhibits the AcrAB-TolC efflux pump in Escherichia coli," *The open microbiology journal,* vol. 7, p. 83, 2013.

[111]   A. Miró-Canturri, R. Ayerbe-Algaba, and Y. Smani, "Drug repurposing for the treatment of bacterial and fungal infections," *Frontiers in microbiology,* vol. 10, p. 428651, 2019.

[112]   L. A. Lieberman and D. E. Higgins, "A small-molecule screen identifies the antipsychotic drug pimozide as an inhibitor of Listeria monocytogenes infection," *Antimicrobial agents and chemotherapy,* vol. 53, no. 2, pp. 756-764, 2009.

[113]   J. Jampilek, "Drug repurposing to overcome microbial resistance," *Drug Discovery Today,* vol. 27, no. 7, pp. 2028-2041, 2022.
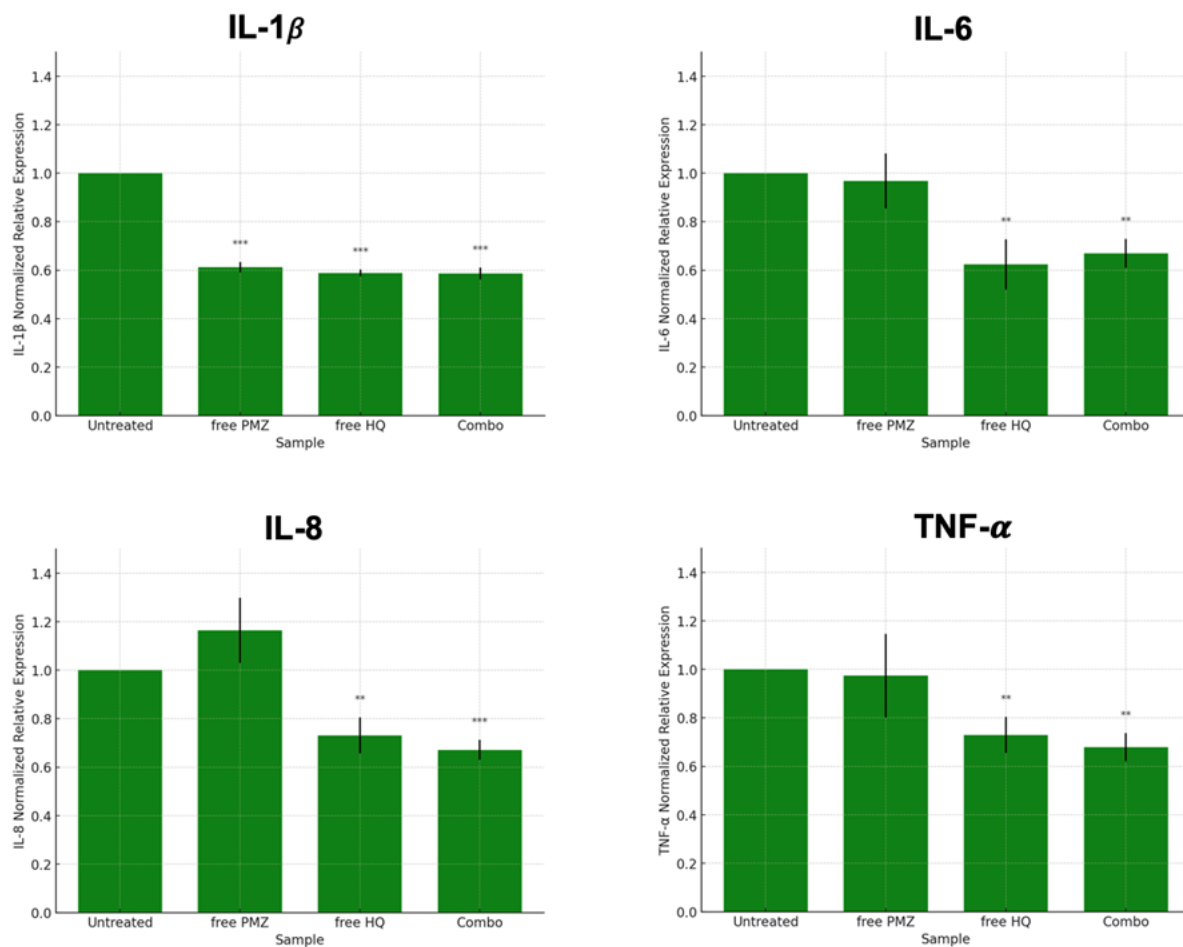
Supplementary figure 1. The anti-inflammatory effect of PMZ, HQ, and their combination as free agents. THP1 macrophages were treated with 10 μM HQ, 5 μM of PMZ, or their combination prior to QPCR analysis of the expression of the IL-1β, IL-6, IL-8, and TNF-α genes. Data was normalized against untreated cells.

Chapter 7

Use of Advanced Spray Drying Techniques by Employing a Combination Therapy for NSCLC and Respiratory Infections

Arwa Omar Al Khatib[a,b], Mohamed El-Tanani[b], Hisham Al-Obaidi[a*]

[a] School of Pharmacy, University of Reading, Reading RG6 6AD, UK

[b] Faculty of Pharmacy, Al Ahliyya Amman University, Amman 19111, Jordan

Chapter Summary:

Given the lack of significant antimicrobial activity observed with PMZ-HQ spray-dried formulations in the previous chapter, the idea of replacing PMZ with rifaximin (RFX), a drug known for its antimicrobial properties, was considered. In this chapter, the study explores the development of a co-delivery system for RFX and HQ to target bacterial infections and antitumor activity in NSCLC using advanced spray drying techniques. The three-fluid nozzle (3FN) method was tested with RFX in the inner nozzle and HQ in the outer nozzle, and vice versa, alongside the two-fluid nozzle (2FN) method. The comparison of these configurations evaluated their drug recovery efficiency, particle size, crystallinity, drug release kinetics, and therapeutic efficacy. The 3FN system showed higher recovery percentages and produced larger particles. Multilayer encapsulates from the 3FN method demonstrated enhanced sustained release when drugs were encapsulated in the core and faster burst release when encapsulated in the shell. Both methods' formulations exhibited synergistic antiproliferative effects against A549 cells, significant reductions in pro-inflammatory cytokines, and effective inhibition of *Acinetobacter baumannii*.

7.1 Introduction

Non-small cell lung cancer (NSCLC), which accounts for 85% of all lung cancer cases, leads to over 1.6 million deaths annually and presents significant treatment challenges due to its complexity and resistance to standard therapies [1, 2]. Despite advancements in diagnosing and treating NSCLC, early detection remains difficult due to the absence of symptoms. Pulmonary infections complicate lung cancer in 50-70% of cases, with patients frequently experiencing infections that not only hinder the effectiveness of oncological treatments but also affect overall survival [3-5]. Therapeutic resistance, tumor relapse, and metastasis further reduce survival rates [6, 7]. Respiratory infections, a global health concern, particularly affect the elderly, individuals with weakened immune systems, and those managing chronic respiratory conditions such as asthma and cystic fibrosis. Despite improvements in treatment, mortality rates related to lung diseases have seen minimal progress over the past half-century [8]. Consequently, NSCLC and respiratory infections require urgent attention for the development of more effective therapeutic approaches.

Spray drying is an advanced method used to produce fine, dry powders from a liquid solution through rapid drying with hot gas, particularly beneficial in pharmaceuticals for encapsulating drugs to enhance stability and solubility. It transforms a liquid or slurry into a dry powder using a hot gas, rapidly drying the material while forming it into powder. The process achieves this by atomizing the liquid into small droplets, increasing the surface area to volume ratio and enhancing heat and mass transfer for quick moisture evaporation [9]. Technological advancements, such as the two-fluid nozzle (2FN) and the three-fluid nozzle (3FN) configurations, have significantly improved particle engineering for specialized pharmaceutical applications.

The 2FN design combines a liquid containing the drug and excipients with compressed gas, allowing precise control over particle size and distribution, making it suitable for specific administration routes like inhalation. Conversely, the 3FN configuration adds an extra feed solution, facilitating the creation of complex particle structures like core-shell configurations, which improve drug protection and controlled release [10-12]. With the 2FN

strategy, the solution is fed through a single nozzle to produce droplets that are dried by gas. While the 2FN system is simple to operate and maintain, it may sometimes restrict control over particle size and distribution due to its atomization process [13]. The 3FN system enhances traditional spray drying by incorporating an extra channel that improves the atomization process, providing finer control over particle size and distribution [14].

The sophisticated design of the 3FN setup not only facilitates the drying and route of the droplets but also allows for the engineering of more complex particle morphologies, such as core-shell structures [15]. In a 3FN system, the inner and outer nozzles play distinct roles. The inner nozzle typically delivers the core material, which could be the active pharmaceutical ingredient, while the outer nozzles dispense a coating or shell material. This arrangement is critical for creating multi-layered particles, where the core is shielded by the shell, protecting the core material from degradation [16]. Additionally, the ability to control the feed from each nozzle independently allows for precise tuning of the particle characteristics, ensuring that each layer can be optimized for specific functions, such as controlled release rates or targeted delivery to particular sites within the body [16, 17]. This level of control is essential for the intended targeting of the inhaled anti lung cancer and antimicrobial therapies.

Repurposing of approved or failed pharmaceutical drugs has been gaining popularity since it involves early development steps such as preclinical and safety pharmacology, lead optimization, and candidate selection. With a rapidly increasing understanding of the pathogenesis of various diseases, it has been observed that sometimes a failed or approved drug may prove to be an effective treatment for a different condition [18, 19]. This study specifically investigates the combined delivery of rifaximin (RFX) and hydroxychloroquine (HQ), two compounds that not only demonstrate significant benefits in their conventional applications but also hold potential as repurposed drugs for novel treatments. Rifaximin, an antibiotic that has been in clinical use for more than 25 years. It is commonly prescribed for conditions, like encephalopathy traveler's diarrhea, irritable bowel syndrome and inflammatory bowel disease. Although rifaximin hasn't been traditionally explored for cancer treatment a recent investigation indicates that both

racemic rifaximin and one of its stereoisomers could impede the growth of cancer cell types by disrupting function [20].

HQ commonly known for its ability to suppress the immune system and reduce inflammation making it a valuable treatment option for managing symptoms of irritable bowel disease by blocking toll-like receptor signaling [21]. Beyond its primary uses, HQ also targets lysosomes, using its alkaline properties to reduce toxic oxygen production in leukocytes [22]. Furthermore, HQ has shown to be successful, in boosting the survival rates of mice with infections by much, as six times. This advantage comes from its ability to stop the growth of bacteria that depends on pH macrophages shielding them from harm and improving their capability to eliminate pathogens within cells [23]. Apart from its traditional applications, HQs involvement in cancer therapy is evident through its impact on autophagy, a mechanism that breaks down and reuses cellular parts during stressful situations. By blocking the merging of autophagosomes, with lysosomes HQ interferes with this process, which is usually heightened in cancer cells to aid their survival under stress and counteract chemotherapy [24].

RFX has been used as an antibiotic for years. Therefore, this study explores the co-delivery of RFX and HQ, employing a unique design which involves two different methods of spray drying, 3FN and 2FN. Each method uses a combination of specific excipients, with one polymer (either PVP or HPMC-E5) and one excipient (from trehalose, OraRez, or isomalt). HPMC-E5 prevents aggregation, improves viscosity for controlled release, boosts mucoadhesive properties, and acts as a stabilizer and protective agent during spray drying [25-27]. It was selected for these formulations due to its effectiveness in developing spray-dried products. Commonly used in oral formulations, this polymer prolongs drug release and improves the aerosolization of inhaled formulations. It is non-toxic and inert when inhaled, and also enhances the bioavailability of spray-dried drugs by improving dissolution rates, inhibiting crystallization, stabilizing the drug, providing controlled release, and enhancing muco-adhesion and solubility [28-30].

PVP stabilizes APIs, enhances solubility, facilitates rapid lung absorption, and allows for controlled release formulations [31-34]. National regulatory bodies have deemed PVP safe as a pharmaceutical excipient, and extensive toxicity research has confirmed its biological inertness. It is non-toxic, non-irritant, and non-sensitizing, making it safe for oral, topical, and ocular applications [35]. On the other hand, trehalose stabilizes sensitive molecules, improves powder flow and dispersibility, and controls hygroscopicity, serving as a bulking and taste-masking agent [36-38]. OraRez, a free acid of the co-polymer of methyl vinyl ether and maleic anhydride, forms protective films around APIs, enhancing stability, optimizing particle characteristics, and improving mucoadhesive properties [39, 40]. Isomalt ensures consistent particle formation, protects heat-sensitive APIs, prevents clumping, and improves patient compliance with its mildly sweet taste [41-44].

In the 3FN method, the process is performed twice for all formulations by simply reversing the feed solutions: first, RFX is fed through the inner nozzle to create the microparticle core while HQ, along with the polymer and excipient, is fed through the outer nozzle to form the shell. In the second instance, HQ combined with the polymer and excipient is fed through the inner nozzle to form the core, while RFX is fed through the outer nozzle to form the shell. In contrast, the 2FN method uses a single feed solution that contains both APIs and excipients. The objective of this study is to develop a co-delivery system for RFX and HQ to target NSCLC, incorporating additional antimicrobial and anti-inflammatory properties to manage cancer-related infections and inflammation.

7.2 Materials and methods:

7.2.1 Chemicals and reagents

Rifaximin was obtained from KEMPROTEC Limited, UK. Hydroxychloroquine, and trehalose were acquired from Sigma-Aldrich, US. DuPont in the Netherlands supplied the methocel E5 (HPMC E5). Polyvinylpyrrolidone (PVP) was purchased from Fluka Analytical, UK. Isomalt was bought from BENEO GmbH, Germany, and OraRez PVM/MA copolymer, an alternating copolymer of methyl vinyl ether and maleic anhydride was

obtained from HARKE Pharma GmbH, Germany. The MTT reagent was purchased from ThermoFisher Scientific, US, and the dimethyl sulfoxide (DMSO) was obtained from Fisher Bioreagents, US.

7.2.2 Preparation of particles encapsulating RFX and HQ by two and three fluid nozzle spray drying systems

In this study, HPMC or PVP were selected to encapsulate RFX and HQ within a multilayer microcapsule or microsphere using the 3FN, and 2FN spray drying methods respectively, utilizing a Büchi mini spray dryer B-290 (Büchi Labortechnik AG, Falwil, Switzerland). In the first setting of the 3FN method used in (R1 through R5), 100 mg RFX was dissolved in 50 mL absolute ethanol, and fed through the inner nozzle to represent the core bio active material. While 100 mg HQ, along with 150 mg of a polymer (PVP or HPMC) and 60 mg of an excipient (trehalose, OraRez, or isomalt) are dissolved in 50 mL deionized water and stirred for 1 hour to ensure uniform dissolution. This solution was simultaneously fed through the outer nozzle at a constant flow rate for shell formation. In the second setting used in (R6 through R10), 100 mg HQ combined with 150 mg of the polymer and 60 mg of the excipient were dissolved in 50 mL deionized water fed through the inner nozzle to form the core, while 100 mg RFX dissolved in 50 mL absolute ethanol was fed through the outer nozzle to form the shell. In the conventional 2FN method used in (R11 through R15), 100 mg of each drug were mixed with 150 mg of the selected polymer and 60 mg of the excipient in 100 mL aqueous ethanol (50:50 v/v), and fed through the same nozzle.

The spray drying parameters were uniformly applied across both methods, with a nitrogen gas flow rate of 50 mL/min, an inlet temperature of 140 °C (± 2 °C), an outlet temperature of 81 °C (± 2 °C), a feed flow rate of 2.4 mL/min, and the aspirator blower operating at full capacity. For the three-fluid nozzle application, the solutions were pumped simultaneously to ensure synchronized feed rates. As shown in **Table 1**, a Design of Experiment (DoE) represented by a structured factorial design was employed to assess the influence of various variables, such as the method of spray drying and excipients, on drug stability, recovery%, release kinetics, and biological activities. The primary distinction between the

formulations was the method of introducing the drugs into the system: formulations R1-R5 used a 3FN system (setting 1), with RFX fed through the inner nozzle and HQ, the polymer, and excipient sprayed through the outer nozzle, whereas formulations R6-R10 employed 3FN system (setting 2), with HQ, the polymer, and excipient fed through the inner nozzle and RFX, sprayed through the outer nozzle. In formulations R10-R15, a 2FN system was employed, where all constituents were fed through a single nozzle. Another distinction was the specific excipients utilized: R1, R6 and R11 used PVP and trehalose, R2, R7 and R12 used PVP and isomalt, R3, R8 and R13 used HPMC and trehalose, R4, R9 and R14 used HPMC and OraRez, and R5, R10 and R15 used HPMC and isomalt.

Table 1. DoE of formulations R1 through R15

Formulation	Spray drying method	RFX	HQ	Polymer	Excipient
R1	3FN	Inner nozzle	Outer nozzle	PVP	Trehalose
R6	3FN	Outer nozzle	Inner nozzle		
R11	2FN	Same nozzle			
R2	3FN	Inner nozzle	Outer nozzle	PVP	Isomalt
R6	3FN	Outer nozzle	Inner nozzle		
R12	2FN	Same nozzle			
R3	3FN	Inner nozzle	Outer nozzle	HPMC	Trehalose
R8	3FN	Outer nozzle	Inner nozzle		
R13	2FN	Same nozzle			
R4	3FN	Inner nozzle	Outer nozzle	HPMC	OraRez
R9	3FN	Outer nozzle	Inner nozzle		
R14	2FN	Same nozzle			
R5	3FN	Inner nozzle	Outer nozzle	HPMC	Isomalt
R10	3FN	Outer nozzle	Inner nozzle		
R15	2FN	Same nozzle			

7.2.3 Recovery analysis

Each formulation, containing exactly 5 mg of RFX, was dispersed in 2 mL of aqueous ethanol (1:1, v/v) and vortexed for 10 minutes. Similarly, each formulation with exactly 5 mg of HQ was dispersed in 2 mL of aqueous ethanol (1:1, v/v) and also vortexed for 10 minutes. This process dissolved the bio actives and the polymer matrix, yielding a final drug concentration of 2.5 mg/mL for each drug. Following that, the actual concentrations of both drugs in the solution were quantified using HPLC. Based on the Area Under the Curve (AUC) from the HPLC results, the recovery% was calculated using the specific formula [45]:

$$\text{Recovery \% (w/w)} = \frac{\textit{Actual Amount of Drug in Spray-dried particles}}{\textit{Theoretical Drug Content}} \times 100$$

(Equation 4)

7.2.4 High Performance Liquid Chromatography (HPLC) analysis

High Performance Liquid Chromatography (HPLC) analysis was performed using an Agilent 1100 Series instrument from the USA. The setup included a 15 cm C18 column and a detection wavelength of 270 nm. The HPLC's mobile phase consisted of 45% acetonitrile and 55% water, with the pH adjusted to 2.5 (±0.5) using 0.1% v/v phosphoric acid. An isocratic elution approach was used, with a flow rate of 1mL/min, injection volume of 20 µL, and run time of 10 minutes, measurements were conducted in triplicate.

7.2.5 Particle size analysis

In this study, the average particle size of all spray-dried RFX- HQ microparticles were determined using the dynamic light scattering (DLS) (a Zetasizer Nano ZS, (Malvern Instruments, UK). Briefly, 5 mg of each spray-dried powder was first re-dispersed in 5 mL of distilled water. A 10 µL sample from this dispersion was then further diluted to a final

volume of 1000 μL with distilled water. The resulting dispersions were then placed into a glass cuvette and subjected to measurements under controlled conditions, which included a temperature set at 25 °C, a refractive index fixed at 1.33, and a measurement duration of 60 seconds. Average particle size, and zeta potential were performed in triplicate.

7.2.6 Fourier transform infrared spectroscopy (FTIR)

The interactions between the encapsulated APIs and the wall material were analyzed using a Perkin-Elmer Spectrum 100 spectrophotometer (Waltham, MA, USA). Each component, including all individual core and wall materials and the encapsulates created using both 2FN and 3FN spray drying techniques, was examined. These analyses covered a spectral range from 650 to 4200 cm^{-1}, with each spectrum averaging 16 scans.

7.2.7 X-ray powder diffraction (XRPD)

X-ray powder diffraction analysis was carried out using Bruker D8 Advance flat plate powder diffractometer (Bruker AXS GmbH, Germany). The samples were irradiated with copper source radiation (1.54A° angstroms). The data collection was carried from 5.0° to 90° 2theta, 0.2° step size at 1.2 seconds per step.

7.2.8 Drug release studies

The release kinetics of RFX and HQ from various formulations were studied using dialysis bags and analyzed with HPLC. Each formulation weighing 10 mg was dispersed in 5 mL of a simulated lung fluid (SLF) containing mixtures of salts; 100 mM NaCl, 5 mM KCl, 2 mM $CaCl_2$, 25 mM $NaHCO_3$, 5 mM Na_2HPO_4, 1 mM NaH_2PO_4, and 1 mM $MgCl_2$ hexahydrate, adjusted to a pH of 7.4 and vortexed for 3 minutes. The resulting mixture was then placed inside a dialysis bag to allow for controlled diffusion. The release of drugs was performed under sink conditions in 20 ml of release medium (SLF) to mimic lung conditions closely as possible at 37°C, with agitation using BioCote hotplate stirrer at 100 rpm. At predetermined time intervals, 1 mL samples were withdrawn from the SLF, and immediately replaced with fresh SLF to maintain constant volume. This method ensured

that the drug concentrations stayed below saturation levels, promoting continual diffusion of the drugs from the formulations. The samples collected were subsequently analyzed with HPLC. The data obtained from this analysis was used to determine the cumulative drug release percentages, thereby generating a kinetic profile of RFX and HQ release from the various formulations under simulated lung conditions.

7.2.9   Antiproliferative effect of R-formulations against A549 cells

The antiproliferative effects of RFX, HQ and various formulations (R1- R15) were assessed using an MTT assay by (Biorad). A549 human lung cancer cells were grown in RPMI 1640 medium with 2 mM L glutamine, 100 mg/mL penicillin/streptomycin, from (Gibco) and 10% bovine serum from (Euroclone). The cells were seeded in a 96 well plate, from (SPL Korea) at a density of $5×10^3$ cells per well. Left to attach. The next day the cells were treated with distinct concentrations of free RFX, free HQ or one of the formulations (R1- R15) at doses ranging from 0.8 to 100 μM. Following a 72-hour treatment period cell viability was assessed using the MTT assay. This process involved adding 0.5 mg/mL MTT to each well and allowing a 3 -hour incubation for crystals to form. The formazan was then dissolved by adding 100 μL of DMSO to each well. Absorbance readings were taken at 570 nm using a BioTek Cytation 5 multi -mode plate reader, from the USA. The results of cell viability were expressed as percentages relative to the untreated control group. The drug interactions were analyzed by calculating the combination index (CI) using the Chou and Talalay method [46], with CompuSyn software. A CI value below 1 indicated a synergistic effect, a value of 1 signified an additive effect, and a value above 1 suggested an antagonistic effect.

7.2.10 Quantification of pro-Inflammatory cytokine RNA expression in THP-1 cells using qPCR

The THP- 1 human monocytic cell line was grown in RPMI 1640 medium (Euroclone) with added 2 mM L glutamine, 100 mg/mL penicillin/streptomycin (Gibco), 4.5 g/L D glucose (Sigma), and 20% fetal bovine serum (Euroclone). To prompt the transformation, into

macrophages the THP 1 cells were cultured at a density of 2×10^5 cells per mL, in RPMI medium supplemented with 100 nM Phorbol 12 myristate 13 acetate (PMA) in a 24 well plate allowing them to adhere for a day (SPL, Korea). After discarding adherent cells, the remaining macrophages were sustained in RPMI medium before being exposed to 5 µg/mL lipopolysaccharide (LPS) for an additional day. Following stimulation, the cells were treated with the formulations at concentrations equivalent to 10 µM of HQ for 48 hours. To measure RNA expression of IL-1β, IL6, IL-8, and TNF-α, approximately 1×10^6 cells were harvested, and RNA was extracted. The RNA concentration was quantified using a NanoDrop device (Thermo Fisher Scientific). A total of 0.5 µg of RNA was reverse transcribed to cDNA using the PrimeScript RT Master Mix (Takara, China) in a T100 Thermal Cycler (Biorad).

The qPCR reaction mixture included 2 µL of cDNA, 0.4 µL each of forward and reverse primers, 7.2 µL of nuclease-free water, and 10 µL of SYBR Premix Ex Taq (TliPlus) (Takara Bio). The PCR cycles were performed on a CFX96 C1000 Touch thermal cycler (Biorad) with an initial denaturation at 95°C for 3 minutes, followed by 40 cycles of denaturation at 95°C for 5 seconds and annealing at 61°C for 30 seconds. 18S-rRNA was used as the reference gene, and all samples were analyzed in triplicate. Data analysis was conducted using the $2-\Delta\Delta CT$ method through CFX Maestro Software (Biorad).

7.2.11 Antimicrobial activity measurements

7.2.11.1 Disc diffusion method

All *Acinetobacter baumannii* (*A. baumannii*) strains were clinical isolates obtained from Department of microbiology lab at King Hussien Cancer Center (KHCC), Amman, Jordan. All strains were sub cultured onto nutrient broth to obtain fresh colonies for either glycerol stock preparation or 0.5 McFarland standard preparation for antimicrobial assay. All procedures performed and drugs' preparations were done according to CLSI guidelines (CLSI M100, 2023). The disc diffusion method was performed by placing blank discs loaded with 200µg of each formula on Mulier Hinton agar (MHA) plates streaked with fresh

0.5 McFarland standard inoculum of each bacterial isolate individually. Plates were incubated overnight at 37 ◦C at ambient air condition and the diameter of the inhibition zone was measured in mm and noted down. The individual components of the formulas and the buffers used for preparation were also loaded on blank discs individually and tested as controls.

7.2.11.2   MIC Minimum Inhibitory Concentration

For each clinical isolates, 100 µl broth of 0.5 McFarland adjusted turbidity were placed on twofold serially diluted drug formula starting at 2000µg/ml.   All microtiter plates were placed in the incubator at 37°C for 12-18 hours. Results of the MIC were recorded as the last well that showed no visible growth with the lowest possible antibiotic concentration. The individual components of the formulas along with negative (media only) and positive (bacteria without drugs) controls were also tested.

7.2.12   Statistical analysis

To compare the variations between formulations, a one-way analysis of variance (ANOVA) with Pythons SciPy library was employed. All the statistical analyses were carried out with a significance level set at α=0.05. Any *p*-values, below this threshold indicated significant difference.

7.3   Results and discussion

7.3.1   Recovery analysis

It is essential to normalize all tests to the actual amounts of drugs produced after spray drying in order to precisely assess the antiproliferative effects on A549 cells and detect pro-inflammatory cytokine RNA expression. By using this normalization, it is made sure

that the biological assay results are consistent with the actual drug concentrations in the microparticles. Although drug loss during spray drying is a typical occurrence and is mostly related to wall deposition and low cyclone separation [11, 47], most studies fail to take this into account. FTIR measurements, which showed no significant shifts or new peaks, confirm that the drug and excipients remained intact, providing crucial evidence that drug loss due to chemical degradation has been ruled out. Accordingly, stability studies further support this finding. Based on such recovery % results, this novel approach evaluates the success of spray drying using 2FN and 3FN methods to generate homogenous microparticles, offering a more precise assessment of the efficacy of all biological experiments.

The recovery percentages of both drugs, as shown in **Figure 1**, indicated that the highest recovery% for both drugs was achieved when the drug was fed through the inner nozzle of 3FN, followed by the outer nozzle of 3FN, and the lowest recovery% was observed with the 2FN method. For HQ, the recovery% was 83.9% ± 3.20% (inner nozzle of 3FN), 81.1% ± 3.70% (outer nozzle of 3FN), and 78% ± 3.5% (2FN method). For RFX, the recovery% was 70.7% ± 3.90% (inner nozzle of 3FN), 67.9% ± 4.30% (outer nozzle of 3FN), and 64% ± 3.9% (2FN method). This trend was observed across all spray-dried formulations, with a higher average recovery percentage for HQ (81% ± 3.9%) compared to RFX (68% ± 4.3%). The recovery percentages of RFX and HQ highlight the significant impact of solvent systems, nozzle configurations, and the properties of the drugs and excipients used.

The 3FN method introduces three separate fluids into the drying chamber: one for the first drug, one for the second drug with excipients, and one for the atomizing gas, allowing better control over composition and distribution [47, 48]. By managing flow rates and concentrations separately, 3FN reduces non-uniform distribution and segregation seen in 2FN, leading to higher recovery percentages and more consistent drug content by minimizing drying rate differences and reducing wall deposition.

For RFX's recovery in formulations R1-R5 (3FN with RFX fed through the inner nozzle), the high Peclet number in the 3FN method promotes faster ethanol evaporation, leading to earlier shell formation and concentrating RFX at the core. This results in higher recovery compared to RFX's recovery in the shell of 3FN formulations (R6-R10) and in 2FN formulations (R11-R15). Conversely, HQ's recovery in formulations R6-R10 (3FN with HQ fed through the inner nozzle) was higher, indicating that HQ in water with polymer and excipient forms a more viscous and stable encapsulating layer, enhancing its recovery [49-51]. The distinct mixing of components with different viscosities improves recovery due to a better core-to-wall ratio, boosting HQ recovery in the core while reducing RFX recovery in the shell [16, 52, 53]. This aligns with previous research, such as Leena et al. (2022), which reported improved recovery using a 3FN spray drying system [52].

The 2FN system used in formulations R11 through R15, which atomizes a single feed solution with a high-speed gas stream, resulted in lower recovery percentages due to the solubility properties of RFX and HQ. RFX, soluble in ethanol but insoluble in water, had higher recovery in the 3FN system where it was dissolved in absolute ethanol. In the 2FN system, RFX was fed with HQ in a 50:50 v/v aqueous ethanol solution, reducing its solubility and recovery. HQ, soluble in water but sparingly in the 50:50 v/v solution, also showed reduced recovery, though less significantly. This lower recovery percentage in 2FN highlights the challenges of mixed solvent systems, which affect solubility and solution homogeneity. These challenges lead to non-uniform droplet formation during atomization, causing variations in droplet sizes. Smaller droplets dry faster and can trap more excipients or solvent inside, while larger droplets allow more time for components to redistribute. This can cause the drug and excipients to migrate within the droplets due to differences in diffusion rates and evaporation kinetics, resulting in non-uniform solidification and pockets of varying drug concentration, ultimately leading to lower recovery percentages [54, 55]. Furthermore, the low recovery percentage of the 2FN methods might also be attributed to the smaller particle sizes produced, as indicated in **Section 3.2** of the particle size analysis. This section revealed that 2FN produced the smallest particle sizes, and the low recovery percentage is likely due to product loss on the walls of the drying chamber and the cyclone's low capacity to separate fine particles (<2 μm) [56].

Excipients significantly impact drug solubility, particle size, and density, affecting particle collection efficiency in spray drying. Variations in excipients can lead to non-uniform drug distribution and recovery due to differences in solubility, viscosity, surface tension, and interactions between components. For HQ, the highest recovery (84.8% ± 1.40%) was observed in formulations (R3, R8, R13) containing HPMC and trehalose. HPMC's robust film-forming properties and trehalose's ability to replace water, reduce particle sticking, and allow finer atomization resulted in smaller particle sizes and improved recovery[57-59]. This is consistent with findings that HPMC shells enhance solubility and sustained release of hydrophobic drugs [60, 61]. The combination of HPMC and trehalose improved solubility, created more uniform particles, and facilitated better collection efficiency.

 In formulations R1 through R5 and R6 through R10 using the 3FN method, variations in recovery were attributed to the different thicknesses of the polymer shell with PVP or HPMC-E5. The differential diffusion of fluids with different viscosities improved the core drug's recovery but reduced the recovery of the drug in the shell [53, 62] PVP, with its lower density and better solubility enhancement properties, led to higher recovery percentages for RFX. Specifically, RFX's highest recovery (72.7% ± 3.01%) was observed in formulations (R1, R6, R11) using PVP and trehalose [63]. PVP's efficient encapsulation and protection of RFX particles during drying, combined with trehalose's high glass transition temperature and protective properties, significantly improved recovery compared to other stabilizers [64-66].

Statistical differences observed in **Figure 2** further support the impact of spray drying methods on the recovery percentage. Formulations with identical components but prepared using three different spray drying methods showed significant differences in their recovery.
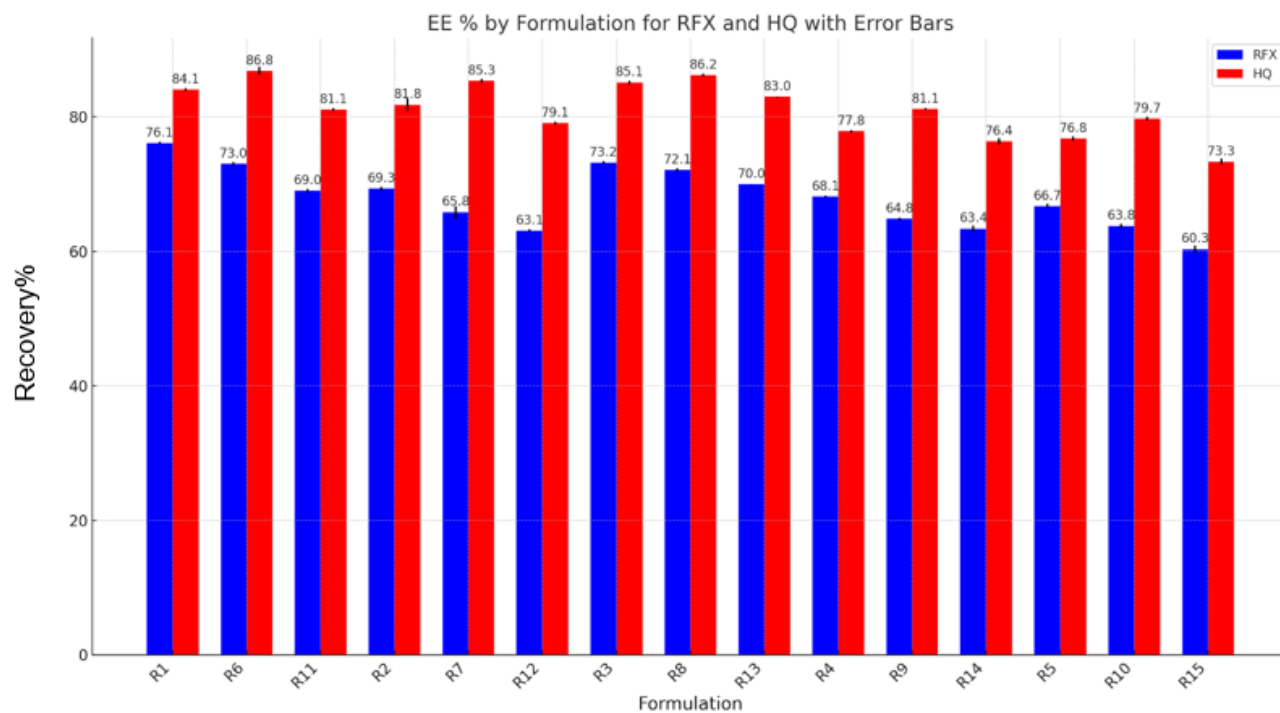
Figure 1. Recovery% of RFX and HQ in all spray-dried formulations. In these comparisons, HQ % is depicted in red, while RFX % in blue. Values mean ± standard deviation.
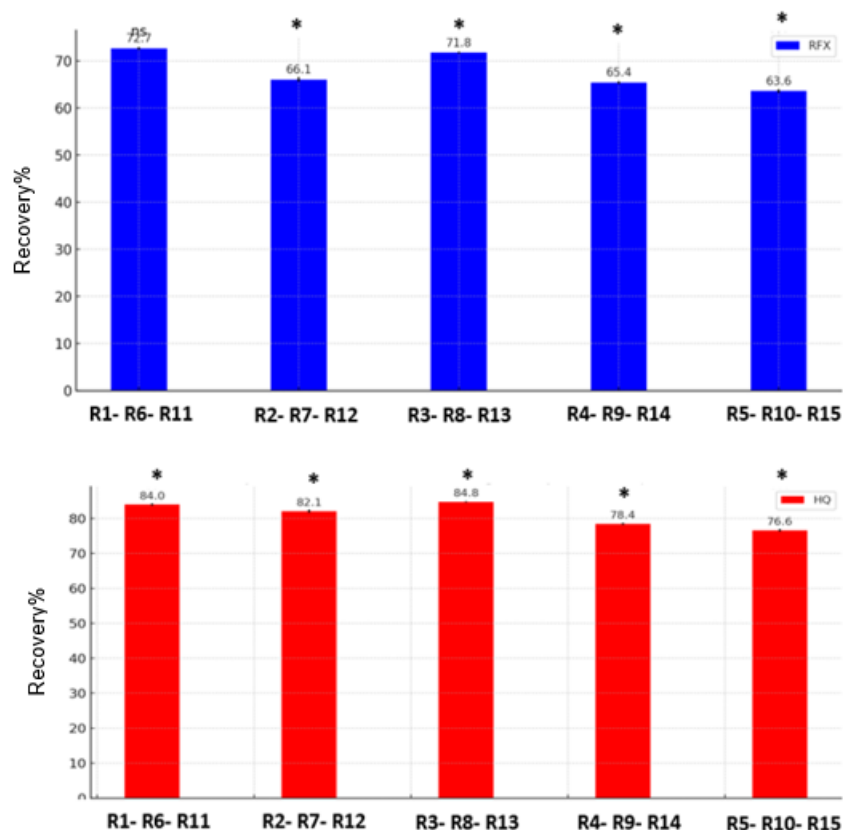
Figure 2. Bar graph representing comparisons in the recovery% across formulations having the same excipients utilizing three different method settings, Group 1 (R1, R6, R11), Group 2(R2, R7, R12), Group 3(R3, R8, R13), Group 4 (R4, R9, R14), and Group 5(R5, R10, R15). In these comparisons, HQ % is depicted in red, while RFX % in blue. Values are presented as mean ± standard deviation. * Indicates $p < 0.05$, determined using one-way ANOVA. Comparisons were made between formulations with identical components but prepared using three different spray drying methods. Groups marked with * show a significant difference, while those marked with n.s indicate no significant difference.

7.3.2 Particle size analysis

This research explored the effects of spray drying methods and excipients on the particle size distributions of fifteen RFX-HQ spray-dried formulations. The observed trend of particle sizes in formulations R1 through R15 as illustrated in **Figure 3** is influenced by the nozzle configuration and the feeding method of hydrophilic polymers (HPMC or PVP).

Formulations R1 through R5, prepared by 3FN with the polymer and excipient fed through the outer nozzle, resulted in larger particles followed by formulations R6 through R10, also prepared by 3FN but with the polymer and excipient fed through the inner nozzle. The smallest particles were found in formulations R10 through R15, prepared using the 2FN method.

This observed trend towards larger particle sizes in formulations R1-F5 prepared by 3FN and smaller particle sizes in formulations R11-R15 prepared by 2FN method, can be attributed to the effect of the hydrophilic polymers (HPMC or PVP) in the 3FN configuration since they are located on the outer shell layer of the particles, this could cause these particles to retain water and dry more slowly, limiting the amount of shrinkage during spray drying. On the other hand, the 2FN method's dispersion of the feed decreases water retention, enabling the particles to dry faster and consequently resulting in smaller particles [67]. Moreover, given that the particle size of spray-dried microcapsules is heavily influenced by the droplet size formed after atomization, with smaller droplet sizes producing smaller microcapsules. The high shear mixing in the 2FN method is suggested to significantly reduce the emulsion droplet size, and consequently leading to a smaller average diameter compared to the formulations prepared by 3FN method [48]. This finding aligns with a previous study that reported nitrofurantoin powders spray-dried with a 2FN system had significantly smaller particle sizes than those processed with a 3FN system [67]. Smaller particles with higher surface area to volume ratios generally release drugs faster as evidenced in the in vitro release profiles in Section 3.5.

Further elucidation on the vital roles of polymer and excipient in influencing particle size, revealed that formulations (R2, R7, and R12) using PVP with isomalt, resulted in significantly larger particles sized at 7068 nm ±195.0 nm, 1883 nm ±115.0 nm, and 527 nm ±88.0 nm respectively. This increase can be attributed to the dual effect of PVP's viscosity [68, 69], which facilitates larger droplet formation, and isomalt's bulking properties, which add volume, contributing to a looser and larger matrix formation [44, 70]. Shifting to formulations utilizing HPMC-E5 which indicated a trend towards smaller particle sizes, optimized by the specific excipients used [71]. Particularly, formulations (R4, R9, and R14) presented the smallest particles in the series, measuring 457 nm ±29.0 nm, 371

nm ±22.0 nm, and 303 nm ±3.0 nm respectively due to the effects of HPMC-E5's excellent film-forming ability and OraRez's adhesive properties, which facilitated tightly encapsulated, well-stabilized particles [72].
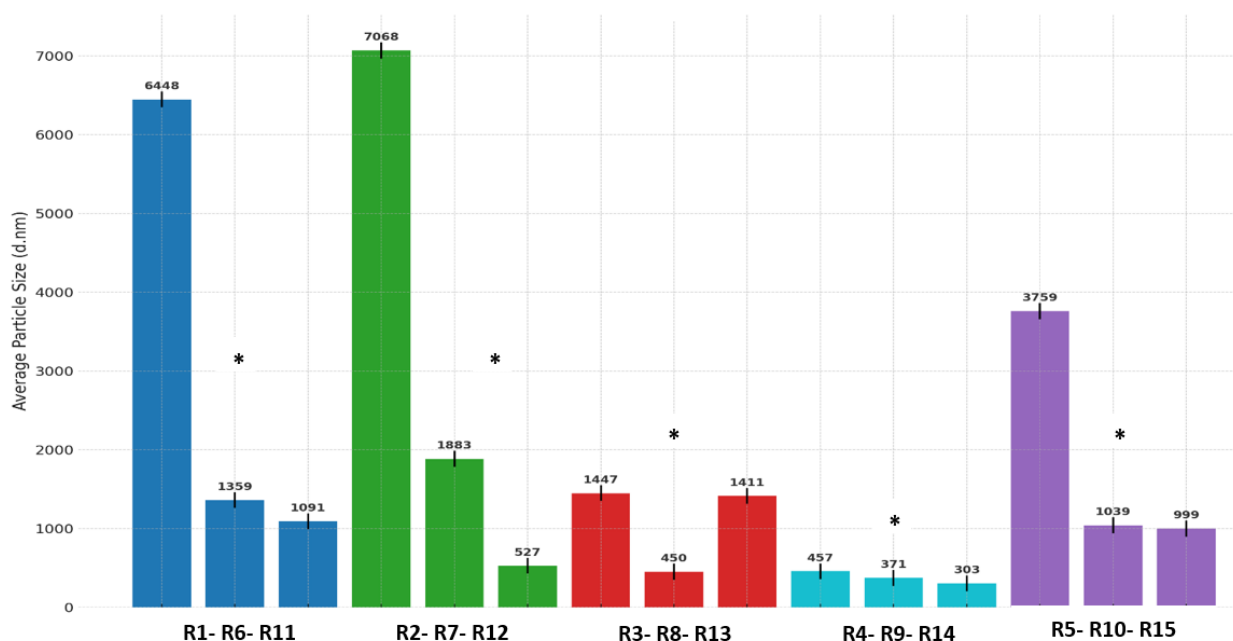

Figure 3. Bar graph comparing average particle sizes of formulations by constituents: Group 1 in blue (R1, R6, R11) with PVP and trehalose; Group 2 in green (R2, R7, R12) with PVP and isomalt; Group 3 in red (R3, R8, R13) with HPMC and trehalose; Group 4 in light blue (R4, R9, R14) with HPMC and OraRez; Group 5 in purple (R5, R10, R15) with HPMC and isomalt. Values are mean ± standard deviation. * $p < 0.05$, calculated using one-way ANOVA. Comparisons were made between formulations (within each group) that had identical components but were prepared using three different spray drying methods. All groups showed significant difference in their average particle sizes as annotated by *

7.3.3 Fourier transform infrared spectroscopy (FTIR)

FTIR spectral analysis was conducted to evaluate the molecular interactions between RFX and HQ and the excipients during the formation of microparticles prepared by 2FN and 3FN methods. The spectra of RFX-HQ spray-dried formulations were compared with

their individual components, and revealed distinct characteristic peaks for each constituent, reflecting the diverse chemical functionalities present. The spectrum of RFX revealed several characteristic fingerprint peaks, which correspond to specific functional groups within the molecule. Peaks around 1700 cm^{-1}, attributed to the C=O stretching vibration in carbonyl compounds, around 1600 cm^{-1}, corresponding to C=C stretching vibrations in aromatic rings, reflecting the presence of aromatic structures in the molecule; and around 1500 cm^{-1}, associated with various bending vibrations involving C-H bonds. Peaks between 1317 cm^{-1} and 1370 cm^{-1} are indicative of C-H bending vibrations from methyl groups attached to the complex polycyclic structure, with possible contributions from bending vibrations involving -OH groups attached to aromatic rings. Additionally, multiple peaks in the 1200-1000 cm^{-1} range are associated with C-O stretching vibrations and various bending modes involving O-H groups, highlighting the presence of hydroxyl and ether functionalities [73].

HQ was distinguished by a prominent peak at 1049 cm^{-1}, indicating the symmetric stretching vibration of the sulfate group (SO_4^{2-}). Additional notable peaks were found around 1600 cm^{-1} for C=C and C=N stretching vibrations in the aromatic ring, and in the 1400-1500 cm^{-1} region for CH2 bending [74]. PVP has an amide carbonyl group in its structure, which showed a characteristic sharp peak C=O stretching at 1646 cm^{-1} [75, 76]. The stabilizers, trehalose and isomalt, exhibited O-H stretching at 3273 cm^{-1}, typical of hydroxyl groups, accompanied by other peaks for C-H and C-O stretching [77]. HPMC-E5 displayed peaks associated with C-H stretching at 2903 cm^{-1} and strong C-O stretching vibrations, suggestive of its polymeric nature, it has free OH groups, which resulted in a peak at 3455 cm^{-1} [76, 78]. Lastly, OraRez showed C=O stretching at 1750 cm^{-1}, pointing to the presence of ester linkage.

To investigate the interactions between the drugs and polymers, the spectra of all spray-dried formulations were compared to the those of pure RFX and pure HQ as well as the spectra of the respective excipients, using them as references to analyze the solid dispersions. All investigated samples showed a broad peak above 3100 cm^{-1}, indicating hydrogen bonding interactions within the formulations. Particularly, the spectra reveal

hydrogen bonding interactions between RFX, PVP, and HPMC. The hydroxyl (-OH) stretching vibration of RFX, typically observed around 3200-3600 cm^{-1}, shows a minor shift, indicating hydrogen bonding with the carbonyl groups of PVP and HPMC. Specifically, in the RFX-PVP interaction, the carbonyl (C=O) stretching vibration of PVP shifts from 1651 cm^{-1} to 1646 cm^{-1}, while in the RFX-HPMC interaction, the carbonyl (C=O) stretching vibration of HPMC shifts from 1639 cm^{-1} to 1633 cm^{-1}. Similarly, hydrogen bonding interactions are observed between HQ, PVP, and HPMC. In the HQ-PVP interaction, both the hydroxyl (-OH) and amine (NH) stretching vibrations of HQ show a slight shift, and the carbonyl (C=O) stretching vibration of PVP shifts to 1646 cm^{-1}. In the HQ-HPMC interaction, the carbonyl (C=O) stretching vibration of HPMC shifts to 1633 cm^{-1}. These minor red shifts confirm the formation of hydrogen bonds and the interactions between the drugs and the polymers which could correspond to efficient encapsulation.

As shown in **Figure 4**, the prepared formulations exhibited a peak around 1500 cm^{-1}, indicative of the polycyclic structure, and peaks between 1317 cm^{-1} and 1370 cm^{-1} are indicative of C-H bending vibrations from methyl groups attached to the complex polycyclic structure confirming the presence of RFX in the encapsulates. Additionally, each tested powder displayed a prominent peak at 1049 cm^{-1}, corresponding to the symmetric stretching vibration of the sulfate group (SO$_4^{2-}$) in hydroxychloroquine sulfate, which verifies that HQ is present in the spectra of all spray-dried formulations. The representative FTIR spectra of formulations prepared using three distinct nozzle settings: R1- 3FN with RFX via the inner nozzle and HQ via the outer nozzle, R6- 3FN with HQ via the inner nozzle and RFX via the outer nozzle, and R11- using the 2FN method, as shown in **Figure 4** exhibited similar shifts in some peaks, indicating hydrogen bonding between the drugs and excipients. These interactions help stabilize the amorphous forms of the drugs, as evidenced by the XRPD analysis in **Section 3.4**, enhance solubility, and improve controlled release, that is further determined by the in vitro release data in **Section 3.5**, thereby potentially increasing bioavailability [79].
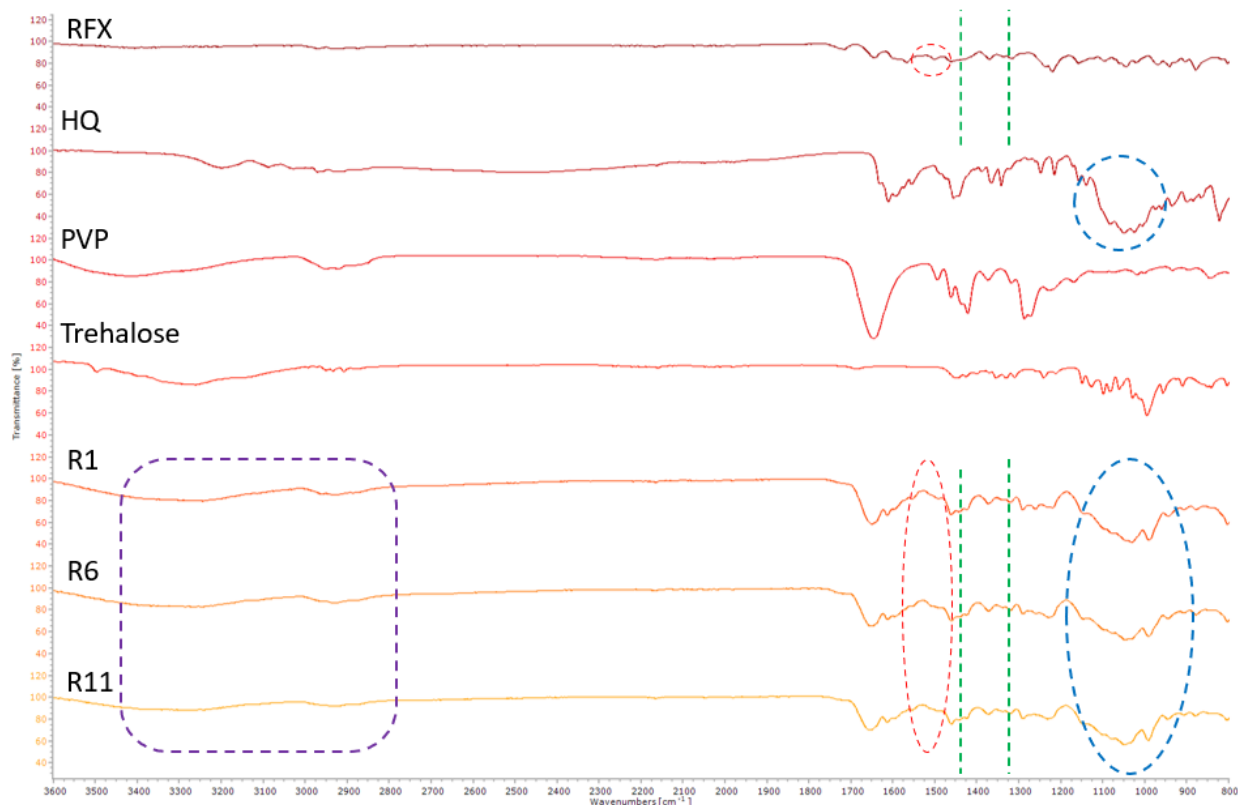
Figure 4. A representative comparative analysis using Fourier-transform infrared spectroscopy (FTIR) for three formulations R1- prepared by 3FN (RFX-inner, HQ-outer), and R6- by prepared by 3FN (HQ-inner, RFX-outer), and R11- prepared by 2FN with their respective individual components including RFX, HQ, polymer, and excipient. The graph uses circles and lines to indicate the broadening of peaks above 3000 cm^{-1} and the presence of fingerprint zones of both drugs within the formulation spectra.

7.3.4 Physical state of bioactive compounds in microparticles

The impact of microencapsulation on the crystallinity of RFX and HQ was assessed using XRPD analysis. All individual components as well as spray-dried formulations were evaluated. Results shown in **Figure 5** provided evidence of the crystalline nature of RFX and HQ, with sharp peaks observed for RFX at angles such as 5.65° and 18.86°, with the highest intensity recorded at 337, indicating its characteristic crystalline structured form [80]. Similarly, HQ showed significant peaks at 24.358° with an intensity of 465, as well as

other peaks at 24°, 20°, and 17° with intensities of 363, 292, and 284 respectively [81]. The amorphous state of PVP and OraRez was confirmed by the absence of sharp peaks in their diffractograms [75]. While HPMC exhibited two broad humps within the range of 5˚-25˚, indicating its amorphous state [82]. Trehalose and isomalt crystalline content was evidenced with sharp peaks at 24.3° and 19.8°, respectively, suggesting distinct crystallographic features [83, 84].
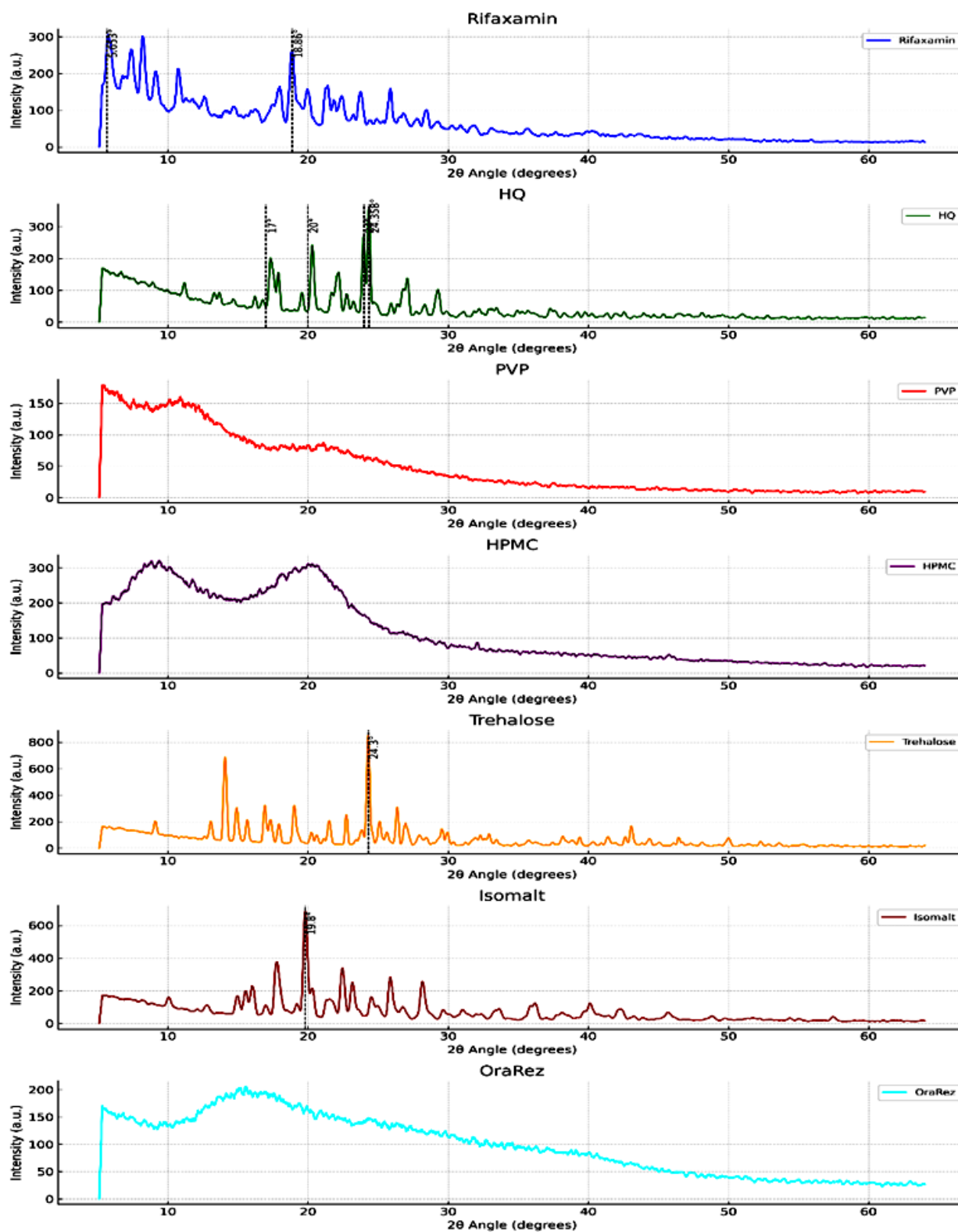
Figure 5. XRPD patterns for RFX, HQ, PVP, HPMC, trehalose, isomalt, and OraRez

As illustrated in **Figure 6**, none of the intense sharp peaks of RFX or HQ are visible in any of the solid dispersions prepared using 2FN and 3FN. This suggests that in both methods, the drugs have been successfully transformed into an amorphous or molecularly dispersed state [85-87]. This finding aligns with a prior study which confirmed that encapsulation alters the crystallinity of resveratrol and curcumin, converting them into an amorphous form [52]. With its greater free energy levels than the crystalline forms, the amorphous form is probably more soluble at saturation [88]. Encapsulation also enhances the effective surface area of drugs dispersed in microparticles, leading to rapid dissolution of the water-soluble matrix and thereby increasing the dissolution rate and absorption of the encapsulated molecules [89]. As a result, the amorphous state of these drugs improves their dissolution rates and solubility profiles, thereby boosting their bioavailability [90].
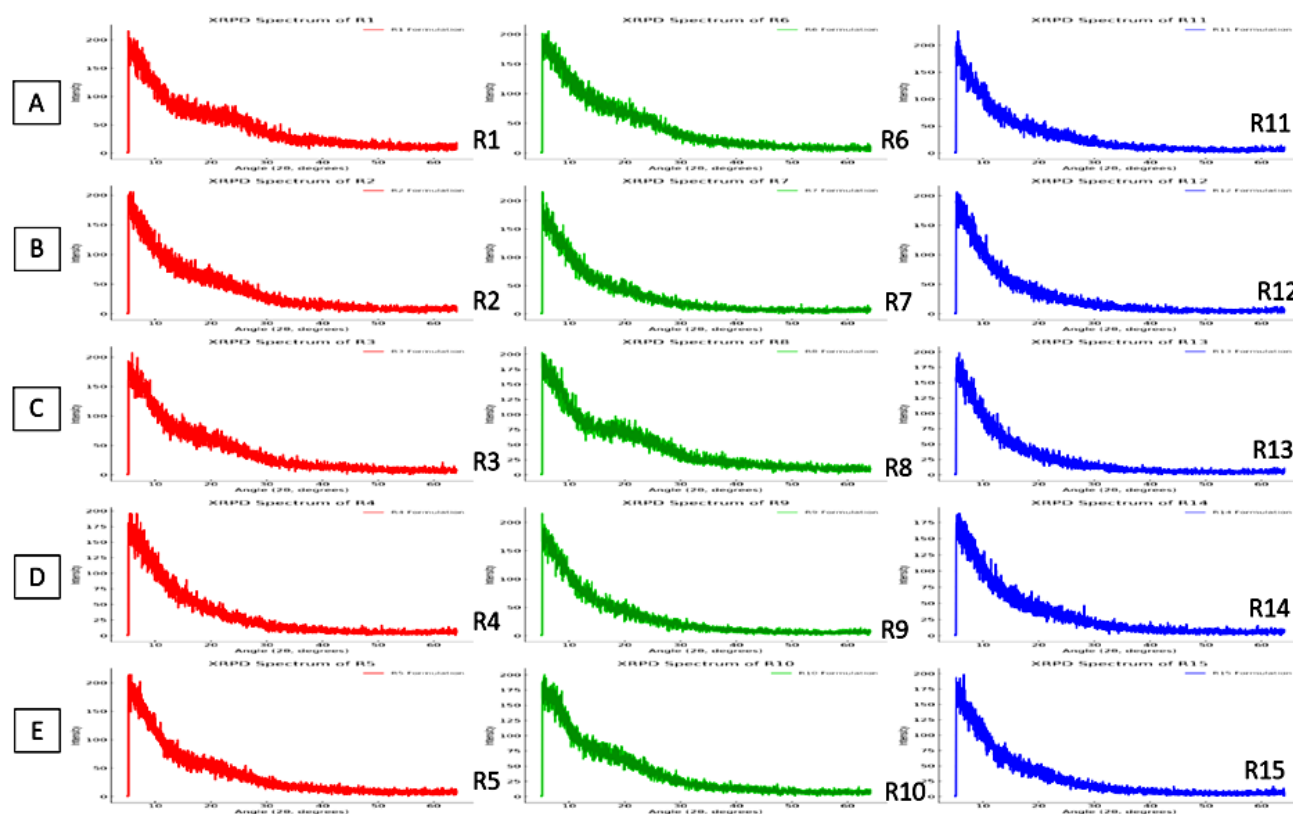
Figure 6. XRPD patterns for the spray-dried RFX- HQ powders, **(A)** R1, R6, and R11, **(B)** R2, R7, and R12 **(C)** R3, R8, and R13 **(D)** R4, R9, and R14 **(E)** R5, R10, and R15. Formulations where RFX is fed via the inner nozzle and the combination of HQ, polymer, and excipient through the outer nozzle in 3FN system are illustrated in red. The formulations spray-dried in an inversed approach of 3FN method, are represented in green. Lastly, formulations administered through a single nozzle in a 2FN system are shown in blue.

7.3.5   In vitro drug release

In vitro release studies are crucial for understanding how encapsulates behave under simulated lung conditions. **Figure 7** presents the release profiles of RFX and HQ using SLF. The results revealed distinct differences in the release kinetics of RFX and HQ across various formulations (R1-R15), influenced mainly by the spray drying method, polymer type, and particle size. The core-shell encapsulates produced by the 3FN spray drying method (formulations R1-R10) exhibited a slower release of the drug encapsulated in the core: RFX **Figure 7B** in (formulations R1-R5) and HQ **Figure 7C** in (formulations R6-R10) compared to their release in the traditional 2FN approach (formulations F11-F15) **Figure 7 (E, F)**. Initially, a rapid release was observed in all the core-shell spray-dried encapsulates prepared using the 3FN method, likely due to the presence of core droplets on the surface of the encapsulates [91]. This initial burst was then followed by a slower release of the drug encapsulated in the core. This could be attributed to the sustained release properties of the polymer forming the shell of the microcapsule, which swells under simulated lung conditions, gradually releasing the core contents [92].

In formulations (R1-R5) where RFX is fed through the inner nozzle and HQ through the outer nozzle in **Figure 7 (A, B)**, RFX with a pKa of 7.9, will be partially ionized at pH 7.4, which provides some increase in solubility but not as much as the full ionization of HQ. RFX is slightly soluble in water (0.2 mg/mL), and while it is polar, its larger molecular weight (785.94 g/mol) and partial ionization result in a moderate solubility and dissolution rate in SLF, supporting its low solubility and slower dissolution rate compared to HQ. On

the other hand, HQ release profiles in the same set of formulations R1-R5 exhibited faster release, due to its proximity to the particle surface. Additionally, HQ is expected to have higher solubility than RFX and dissolve faster in SLF. It has pKa values of 8.3 and 9.7, meaning it will be largely ionized at the SLF's pH of 7.4, which enhances its water solubility. Besides, it is very soluble in water and has a polar nature, leading to a fast dissolution rate in SLF.

In formulations (R6-R10) indicated in **Figure 7(C, D)** where HQ is fed through the inner nozzle and RFX through the outer nozzle, the release profiles showed slower release of HQ encapsulated into the core. However, this finding is further supported by the recovery% results in **Section 3.1** which indicated that HQ had a higher recovery%. Suggesting that when a larger proportion of the drug is encapsulated within the microparticles, the release tends to be more controlled and sustained. This is likely because the encapsulating material acts as a barrier, slowing the diffusion of the drug into the surrounding environment. In contrast, RFX being encapsulated within the shell of the microparticle with a closer proximity to the particle surface, showed a faster release in this set of formulations. However, the recovery% results in **Section 3.1** further support this faster release of RFX. RFX showed a lower recovery%, suggesting that a larger portion of the drug may be free or loosely associated with the microparticles. Because the drug can disperse out more easily as a result, the release happens faster.

Conversely, the 2FN method (formulations R11-R15) demonstrated in **Figure 7 (E, F)**, where both RFX and HQ were fed through the same nozzle and distributed throughout the particle matrix, resulted in release kinetics for both drugs with less pronounced variations, highlighting the impact of the spray drying method. It was evident that RFX's and HQ's release rates were faster compared to their respective release profiles when being fed through the inner nozzle of 3FN in **Figure 7B** and **Figure 7C** respectively. This difference could be attributed to the smaller particle sizes of R11-R15 prepared by 2FN, which offered larger contact surface areas to the SLF release medium [93]. Consequently, leading to a faster release rate than the larger particles prepared by 3FN [94], as noted in the particle size analysis in **Section 3.2**. Larger particles typically have a smaller surface

area to volume ratio resulting in less exposed surface area for drug release. This results in a slower dissolution rate because the distance the drug must travel from the core to the surface is greater [95]. Additionally, larger particles may require a longer hydration time to form channels that allow drug diffusion, further delaying drug release [96]. However, this observation was not very noticeable when compared with the release of drugs fed through the outer nozzle of 3FN system such as in **Figure 7 (A, D)** suggesting that the impact of nozzle configuration surpasses the effect of particle size in this context.

Expanding on the impact of polymer on the release rate, it is interesting to note that the release of RFX and HQ was slower in formulations (R1, R2) compared to (R3, R4, R5), and in (R6, R7) compared to (R8, R9, R10) and in (R11, R12) compared to (R13, R14, R15) as shown in **Figures 7 (A, B, C, D, E, and F)**. This variation is likely due to differences in the structure and nature of the polymer [16]. Formulations (R1, R2, R6, R7, R11, R12) used PVP, while formulations (R3, R4, R5, R8, R9, R10, R13, R14, R15) employed HPMC. HPMC, being highly hydrophilic, swells quickly and forms gels with lower viscosity, facilitating faster drug release [97]. In contrast, PVP forms thicker gels with higher viscosity, hindering drug movement and resulting in slower release [58, 98, 99] . This result is in line with a prior study that found metformin release was prolonged more effectively using higher viscosity grade ethyl cellulose [100]. Additionally, HPMC's higher porosity is likely to enhance drug diffusion, accelerating release [101], whereas PVP's tighter polymer network reduces porosity and is expected to slow diffusion [102]. These findings are supported by the particle size analysis in **Section 3.2**, which demonstrated that the PVP-based particles exhibited larger particle sizes than the particles prepared with HPMC.
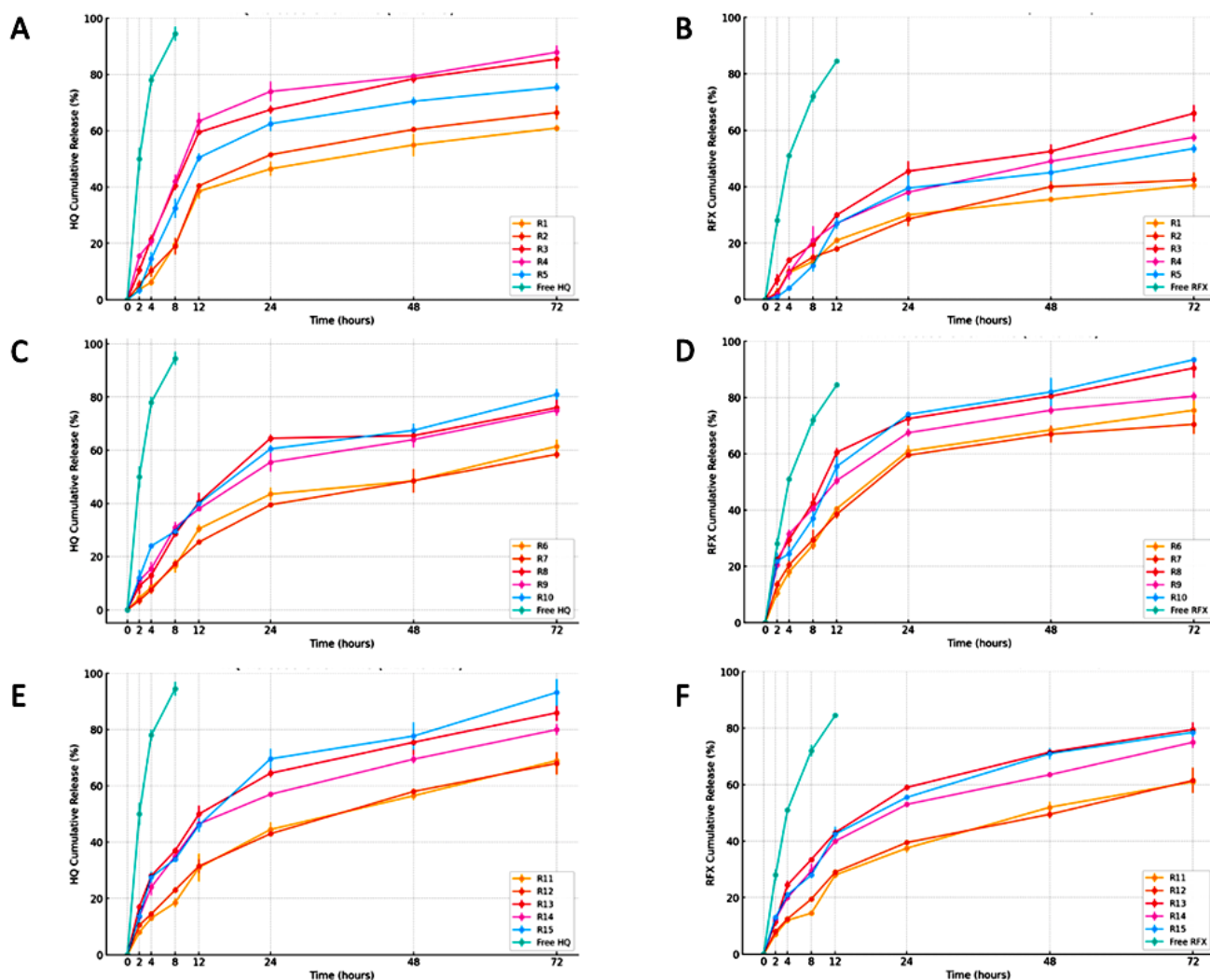
Figure 7. Comparison of release kinetics of HQ and RFX from different formulation groups **(A)** Release kinetics of HQ in R1-R5 formulations, 3FN (RFX inner-HQ outer nozzle) **(B)** Release kinetics of RFX in R1-R5 formulations, 3FN (RFX inner-HQ outer nozzle) **(C)** Release kinetics of HQ in R6-R10, 3FN (HQ inner-RFX outer nozzle) **(D)** Release kinetics of RFX in R6-R10, 3FN (HQ inner-RFX outer nozzle) **(E)** Release kinetics of HQ in R11-R15, 2FN **(F)** Release kinetics of RFX in R11-R15, 2FN. Free drugs were used as control. Values are means ± SD.

7.3.6 Antiproliferative effect against A549 cells

Before investigating the antiproliferative effect of the formulations on A549 cells, it was crucial to understand the antiproliferative effect of RFX and HQ as single agents on A549 cells. The MTT assay is a colorimetric method used to assess cell metabolic activity by measuring the reduction of MTT, a yellow tetrazole, to purple formazan by mitochondrial enzymes in living cells, thereby reflecting the number of viable cells. In our study, this assay was employed to evaluate the cytotoxic effects of RFX and HQ on the A549 cell line over 72 hours. The primary metric obtained from this assay is the IC50 value, which indicates the concentration of a compound needed to inhibit cell viability by 50%. The lower IC50 of HQ (20.13 µM) compared to RFX (25.32 µM) suggests that HQ is more effective at inducing cytotoxic effects at lower concentrations, implying a higher therapeutic potential or greater efficacy. However, these cytotoxicity data, particularly the IC50 values, are essential for determining safe dosage ranges for therapeutic applications. Lower IC50 values necessitate careful dosage optimization to prevent adverse effects, making controlled release of HQ preferable to avoid potential toxicity. (**Figure 8**).
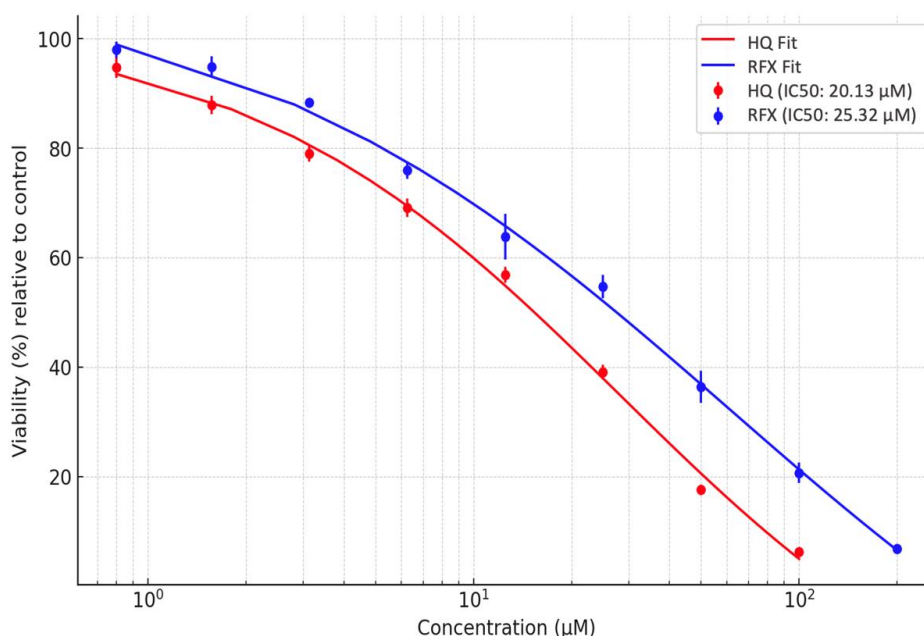

Figure 8. Anti-proliferative effect of free RFX and HQ. A549 cells were treated with various concentrations of RFX or HQ as free drugs for 72 hours prior to cell viability assessment

using MTT assay. Graphs are presented as percentage viability relative to the untreated control. Data represent the mean ± S.D.

To further explore the antiproliferative effects, the combined effects of HQ and RFX both as free drugs (at a molar ratio of 1:2.5, reflecting the utilized ratio of both agents in the formulations) and in the formulations on A549 cells were evaluated. The combination index (CI) for each formulation and for the free drug combination was calculated to understand the nature of the interaction between HQ and RFX against A549 cells.

In **Figure 9**, it is shown that the combination of drugs had a synergistic effect, with a low CI value of 0.545. Most of the formulations also displayed effects as their average CI values were below 1. The first group, R1 to R5, showed a combination index indicating varying degrees of synergy and antagonism. Formulations R1, R2, and R5 had CI values greater than 1, indicating antagonistic effects. Specifically, R1 had an average CI of 1.504 (±0.058), R2 had an average CI of 1.396 (±0.102), and R5 had an average CI of 1.543 (±0.132). On the other hand, formulations R3 and R4 demonstrated synergy with CI values less than 1. R3 had an average CI of 0.808 (±0.129), indicating a synergistic effect, and R4 had an average CI of 0.674 (±0.104), also showing synergy. The second group, R6 to R10, exhibited combination index values that mostly indicated synergy. Individual formulation averages in this group ranged from 0.488 (±0.130) for R6 to 0.821 (±0.131) for R10. Formulation R6 had a significantly low CI, indicating a strong synergistic effect, while R7 and R8 also showed synergy with average CIs of 0.747 (±0.090) and 0.738 (±0.015), respectively. R9 and R10 had CIs close to 1, with average values of 0.661 (±0.073) and 0.821 (±0.131), suggesting moderate to low synergy. The third group, R11 to R15, demonstrated combination index values predominantly indicating synergy. Individual formulation averages ranged from 0.514 (±0.104) for R12 to 0.688 (±0.057) for R13. Formulation R11 had an average CI of 0.579 (±0.075), indicating a synergistic effect, while R12 and R13 also showed synergy with average CIs of 0.514 (±0.104) and 0.688 (±0.057), respectively. R14 and R15 exhibited moderate synergy with average CIs of 0.617 (±0.045) and 0.614 (±0.033), respectively. Interestingly, the apparent antagonistic effect observed in formulations R1, R2, and R5 may not truly indicate antagonism. Instead,

this could be attributed to the unique drug release profiles of these formulations, as previously discussed. These formulations exhibited slower drug release compared to the others, likely due to their larger particle size, which resulted in more prolonged release. Besides, the larger particle size may have also hindered their accumulation in A549 cells, preventing the effective concentration of the drugs within the cells. Consequently, the slow release may have led to insufficient drug concentrations to effectively suppress A549 cell proliferation, reflecting an apparent antagonistic interaction.

In order to verify that the decrease, in cell proliferation was specifically caused by the drugs within the formulations (HQ and RFX), the effects of the excipients were also examined. These preliminary tests indicated that the excipients did not have an impact on cell survival when compared to the control group supporting the conclusion that the significant decrease, in cell viability was a result of the combined effects of RFX and HQ (as shown in **Figure 9D**).
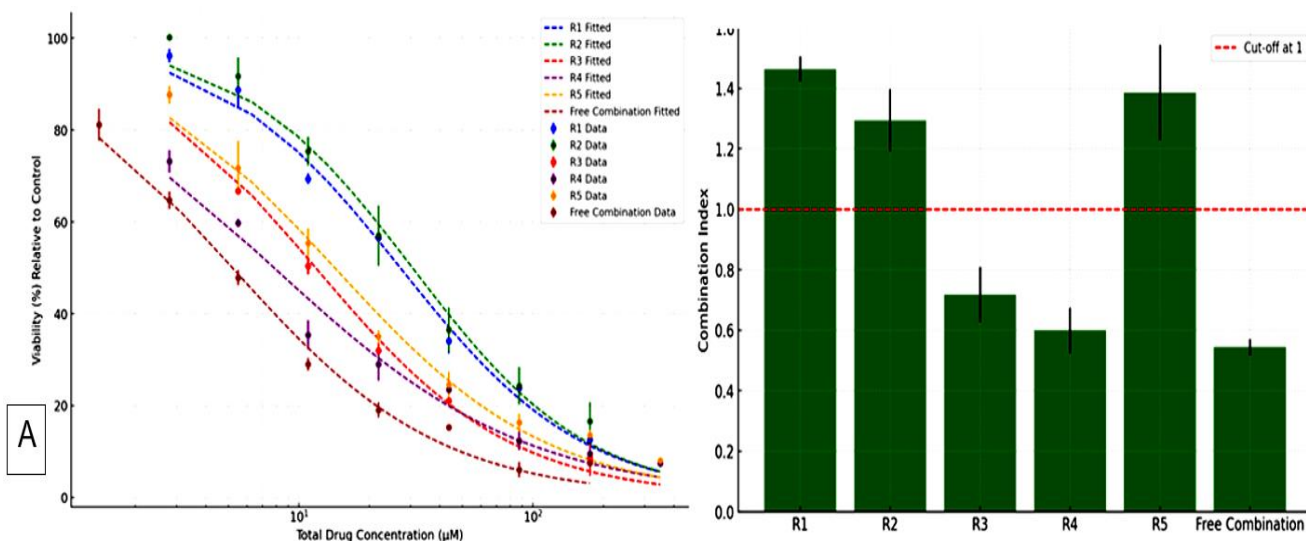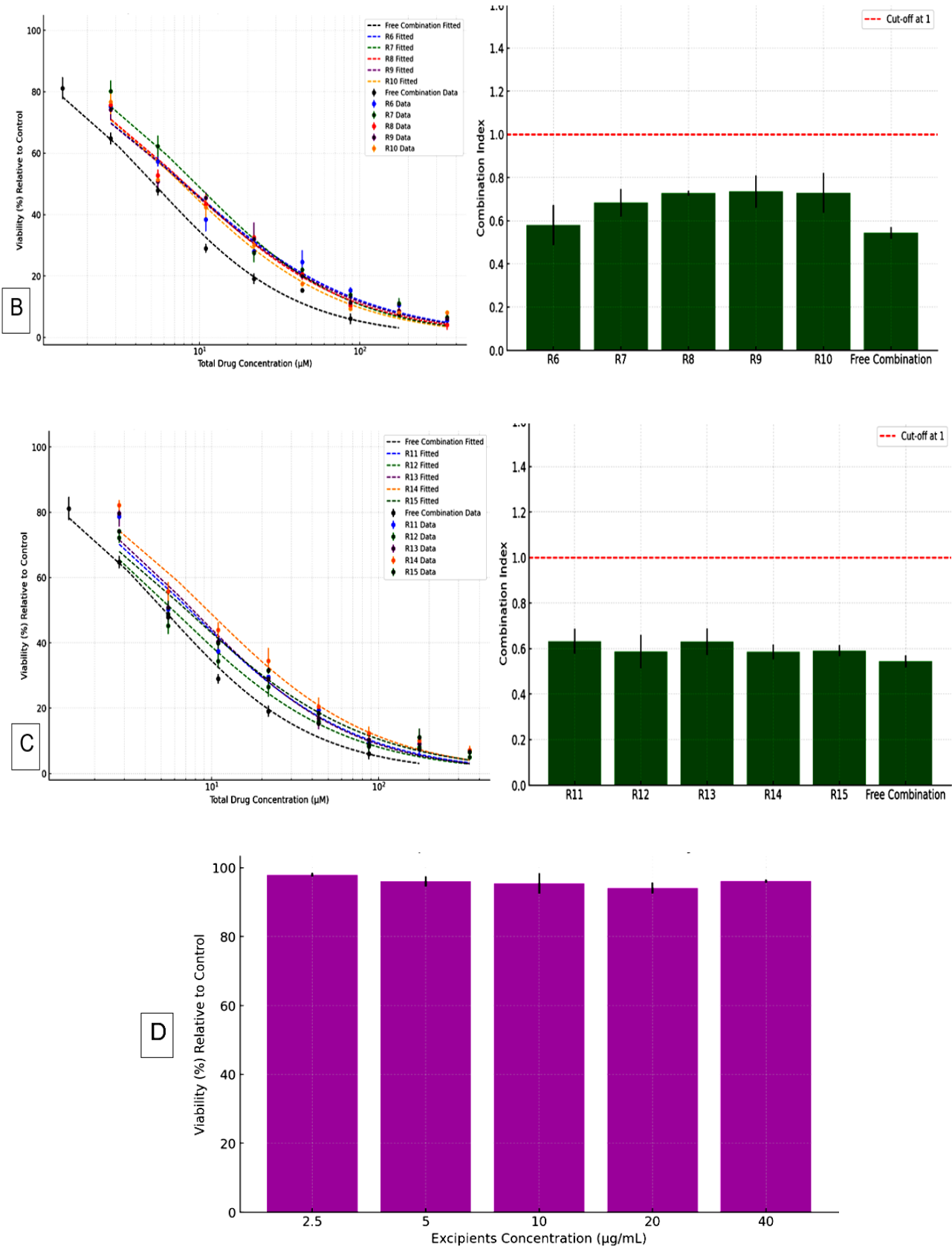
Figure 9. (A) Anti-proliferative effects and combination index (CI) of RFX and HQ in R1-R5 **(B)** Anti-proliferative effects and CI of RFX and HQ in R6-F10 **(C)** Anti-proliferative effects and combination index (CI) of RFX and HQ in R11-R15 **(D)** Cell viability% of empty vehicles consisting of the same ratios of excipients in the formulations but without the drugs. CI was calculated for each formulation at Fa=0.9 (90% inhibition of cell viability). Values are mean ± standard deviation. The horizontal red line represents the cut-off point for the additive effect (CI = 1). Values below this line indicate a synergistic effect, values at this line indicate an additive effect, and values above this line indicate an antagonistic effect. The fitting model was logistic fitting.

The antiproliferative impacts of RFX and HQ are diverse involving pathways that collectively produce strong anticancer effects. Esposito et al. conducted a study examining the proliferative effects of RFX, on Caco 2 cells in a laboratory setting. The research demonstrated that treating Caco 2 cells with RFX led to a decrease in their viability. Looking deeper into how RFX exerts its influence, the study emphasized a decrease, in the expression of proliferating cell nuclear antigen (PCNA) in Caco 2 cells treated with varying concentrations of RFX compared to untreated samples [103]. Additionally, the treatment, with RFX resulted in a decrease in the secretion of VEGF, release of NO, expression of VEGFR 2 and levels of matrix metalloproteinases MMP 2 and MMP 9 when compared to cells that were not treated. RFX also caused a reduction in the phosphorylation levels of Akt, mTOR and p38MAPK, in a concentration manner. Furthermore, it inhibited hypoxia inducible factor 1 α (HIF 1α), p70S6K, and NF κB [103]. These molecular changes collectively disrupt signalling pathways crucial for cell survival, proliferation, and angiogenesis, effectively reducing the cancer cell's viability.

On the other hand, it has been demonstrated that HQ can improve the cancer properties of different chemotherapy drugs in various types of cancer cells [24, 104, 105]. HQ aids in boosting the effectiveness of anticancer treatments by interacting with cellular processes like survival, growth and cell death. One of the main ways it fights cancer is, by blocking autophagy. HQ disrupts the fusion of autophagosomes and lysosomes causing

waste to build up and triggering cell death. This process is supported by proteins that help HQ accumulate in endosomes and lysosomes inhibiting autophagic flux [106].

In addition to inhibiting autophagy, HQ impacts apoptosis by modulating the expression and activity of key apoptotic proteins. It downregulates anti-apoptotic proteins like Bcl-2 and activates caspases, which are essential in the execution phase of apoptosis [107]. Notably, HQ also significantly influences the STAT3 signalling pathway, a crucial driver of oncogenesis. By targeting and inactivating the STAT3 pathway, HQ hampers tumour growth and enhances caspase activation [108].

Furthermore, HQ also alters the environment, in the tumour area. It hinders toll- like receptors (TLR) which leads to a decrease in the release of cytokines like IL 6, IL 1, IFN γ/α, and TNF α. This suppression results in reduced levels of TNF receptors, on macrophages, T cells, and B lymphocytes [109-111]. The modulation of the immune landscape paradoxically enhances the anti-tumour immune response, creating a microenvironment less conducive to cancer growth and more susceptible to immune cell-mediated destruction.

7.3.7 Anti-inflammatory activity

Prior to exploring how the formulations affect inflammation, the effects of HQ and RFX were first assessed individually and in combination. It was observed that both HQ and RFX alone resulted in a decrease, in the levels of inflammatory cytokines including IL 1 β, IL 6, IL 8 and TNF α when compared to the untreated control group. Interestingly, when HQ and RFX were combined there was a pronounced reduction in the expression of these cytokines than when each compound was used independently. This suggests a synergistic effect not with regard to their anti-proliferative properties but also, in terms of their ability to combat inflammation **(Figure 10)**.

Figure 10. The anti-inflammatory effect of HQ, RFX, and their combination. Relative RNA expression of **(A)** IL-1β, **(B)** IL-6, **(C)** IL-8, and **(D)** TNF-α gene on THP-1 macrophages cell line. RNA was isolated and quantified using qPCR technique and the expression of the indicated genes was normalized against untreated cells. Values are mean ± standard deviation. * $p < 0.05$, calculated using one-way ANOVA compared to the untreated control.

After evaluating the results of free drugs and their combination, we explored the anti-inflammatory effects of all the fifteen formulations (R1-R15). The analysis of gene expression showed that most of the formulations resulted in a decrease, in the levels of pro-inflammatory cytokines such, as IL 1β, IL 6, IL 8 and TNF α (refer to **Figure 11**). However, formulations R1 and R2 exhibited a non-significant change in cytokine levels, which can be attributed to their size limitation. The larger size did not suppress cytokine RNA expression levels, possibly because the reduced surface area to volume ratio of larger particles leads to a slower dissolution rate [112], thereby limiting the release of the

active ingredient. Another reason could be the less efficient uptake by cells for larger particles [113], which reduces the effective concentration of the active ingredient reaching the cells. Studies, both in vivo and in vitro, have demonstrated that alveolar macrophages efficiently uptake particles in the 1–5 μm range [114]. Furthermore, larger particles tend to aggregate and settle, which further could reduce their availability and interaction with the cells.

The 3FN method exhibited the most pronounced suppression of IL-1β. Particularly, the formulations with HQ fed through the inner nozzle and RFX through the outer nozzle showed decreases reaching up to 51% (± 2.9%). For IL-6, the formulations prepared using the same nozzle configuration resulted in reductions of up to 50% (± 4.9%). In the case of IL-8, formulations prepared by the 3FN method but with RFX fed through the inner nozzle and HQ through the outer nozzle showed reductions of up to 45% (± 7.3%). Similarly, for TNF-α expression, the formulations prepared by the same nozzle configuration achieved the highest reductions, reaching up to 46.5% (± 3.90%).

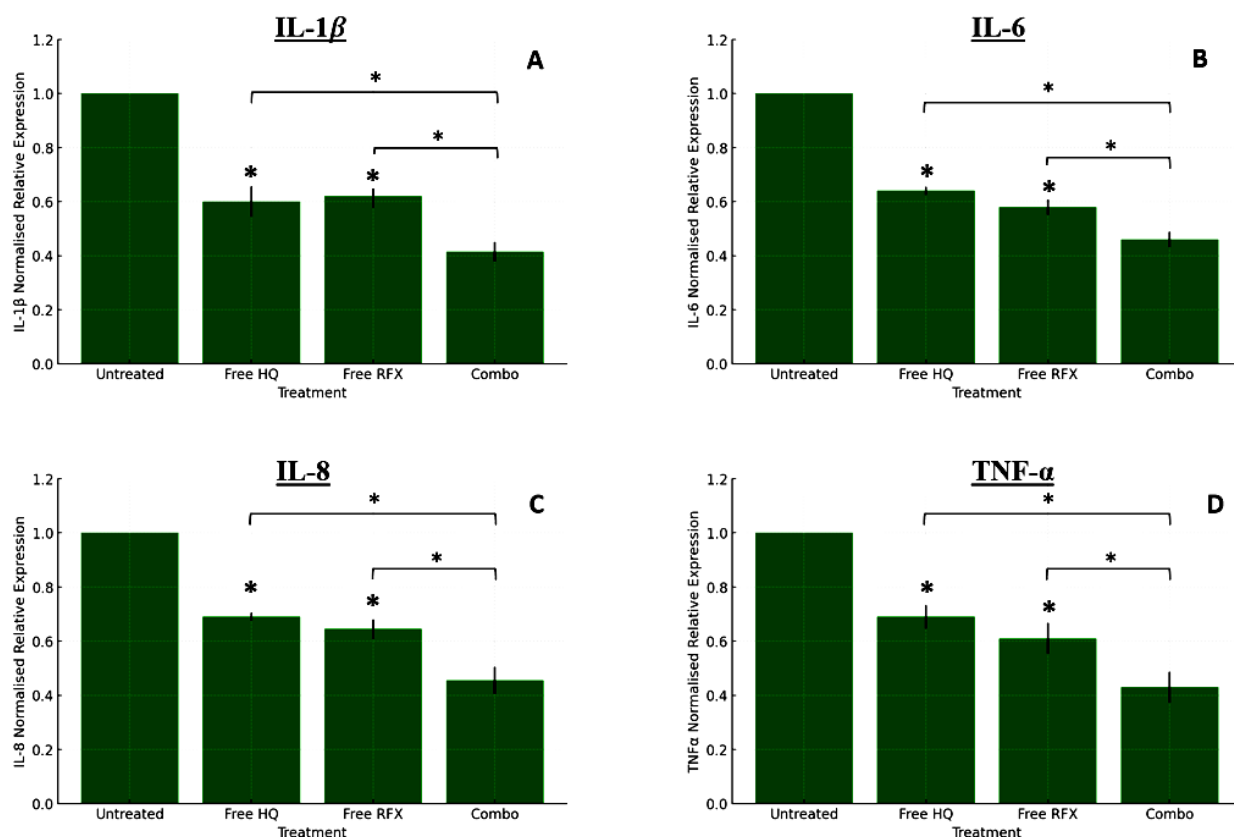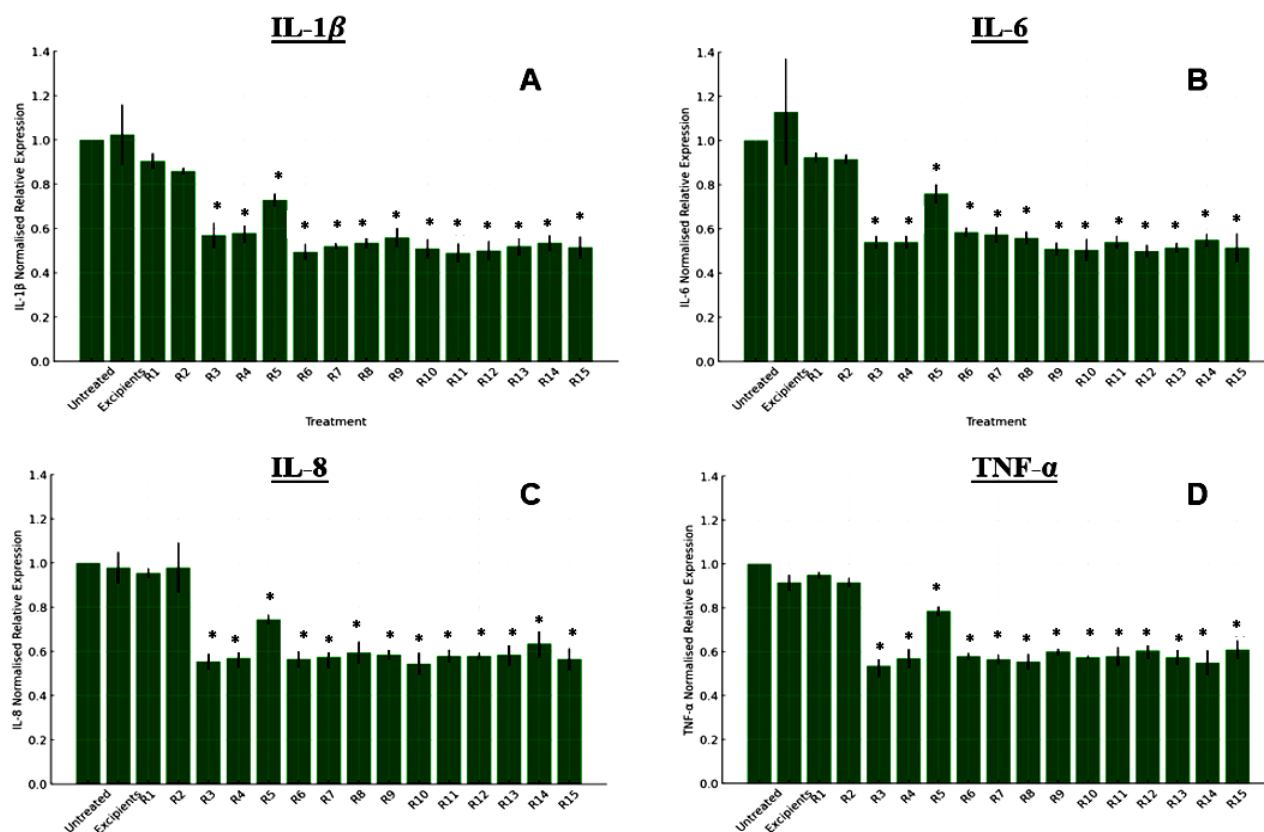**Figure 11.** The anti-inflammatory effect of R-formulations. Relative RNA expression of **(A)** IL-1β, **(B)** IL-6, **(C)** IL-8, and **(D)** TNF-α gene on THP-1 macrophages cell line. RNA was isolated and quantified using qPCR technique and the expression of the indicated genes was normalized against untreated cells. Values are mean ± standard deviation. * $p < 0.05$, calculated using one-way ANOVA compared to the untreated control.

HQ and RFX are recognized for their anti-inflammatory characteristics achieved through different but complementary molecular processes. HQ exerts its anti-inflammatory properties via various molecular routes. Initially, HQ disrupts lysosomal functions decreasing the processing and presentation of antigens. This decrease lowers the immune system's activation and response resulting in a decrease, in cytokines, like IL 1β and TNF α which play a role in starting the inflammatory process [115]. Secondly, HQ suppresses the signalling of TLR leading to lower levels of IL 6 and IL 8. These cytokines play a role, in the body's immune response and the migration of immune cells, to areas of inflammation [116]. Moreover, HQ inhibits autophagy and stabilizes cellular membranes, further reducing the capacity of cells to propagate inflammatory signals, thereby aiding in the overall suppression of pro-inflammatory cytokine production [117]. HQ's effect on cytokine production is also linked to its suppression of the NF-κB pathway, resulting in decreased transcription of pro-inflammatory genes, including IL-1β, IL-6, TNF-α, and IL-8 [118].

On the other hand, RFX has been extensively researched for its anti-inflammatory properties. One study revealed that RFX therapy had an impact, on the balance of gut bacteria and lowered the levels of cytokines like IL 1β, IL 6, and TNF α in individuals, with Parkinson's disease. This led to protecting the integrity of the blood brain barrier and enhancing both motor skills and cognitive abilities. Furthermore, RFX modulates microglial function and increases the release of anti-inflammatory factors in chronic unpredictable mild stress (CUMS)-induced depression models in rats, indicating its neuroprotective effects through gut microbiota regulation [119]. Supporting this, a study

conducted by Kang et al. (2016) found that treatment with RFX significantly reduced the levels of IL-1β and IL-6 in the small and large intestine in vivo [120].

At the molecular level, RFX slows down the movement of endotoxins and pro-inflammatory cytokines into the bloodstream. This decrease, in inflammation is partially influenced by the creation of chain fatty acids such as butyrate. These fatty acids boost anti-inflammatory cytokines like IL 10 and IL 1ra while also decreasing pro-inflammatory ones such, as TNF α and IL 1β [121]. Together, the combined use of HQ and RFX in this study elucidates their complementary anti-inflammatory mechanisms. HQ's broad inhibition of key inflammatory pathways, coupled with rifaximin's modulation of systemic inflammation through gut microbiota, highlights their potential synergistic effect. This synergy is evident in the enhanced reduction of pro-inflammatory cytokines observed in the experiments, supporting the efficacy of HQ-containing formulations in effectively managing inflammatory responses.

7.3.8 Antimicrobial activity

RFX, a non-absorbable, broad-spectrum antibiotic, is commonly used for treating traveler's diarrhea as it requires direct contact with the pathogens present [122]. The formulations created through spray-drying were developed for inhalation delivery, aiming to make direct contact with microbial agents on the respiratory mucosa. In this section of the research, the antimicrobial effectiveness of these spray-dried formulations containing RFX was evaluated. The microorganism *A. baumannii* was selected for testing due to its significance in causing pneumonia and its association with multidrug resistance (MDR) mechanisms [123]. *A. baumannii* has emerged as a critical bacterium needing effective treatment strategies because of the scarce therapeutic alternatives available [124]. The phenotype known as extensive drug resistance (XDR) is defined by its resistance to several antibiotics, leaving only colistin or tetracyclines as viable treatment options [125].

The results from the disc diffusion method showed that all the tested spray-dried formulations produced an inhibition zone measuring approximately 14 mm (**Figure 12** and **Table 2**). The size of the inhibition zones for rifaximin alone was comparable to those produced by the spray-dried formulations. Conversely, the individual excipients used in the formulations did not produce any detectable inhibition zones, suggesting that the antibacterial effect was attributable solely to the drug RFX. Furthermore, these components did not affect the size of the inhibition zones measured. These results highlight the potential of these formulations in providing effective antimicrobial activity with controlled release for targeted pulmonary delivery to treat cancer-related lung infections.
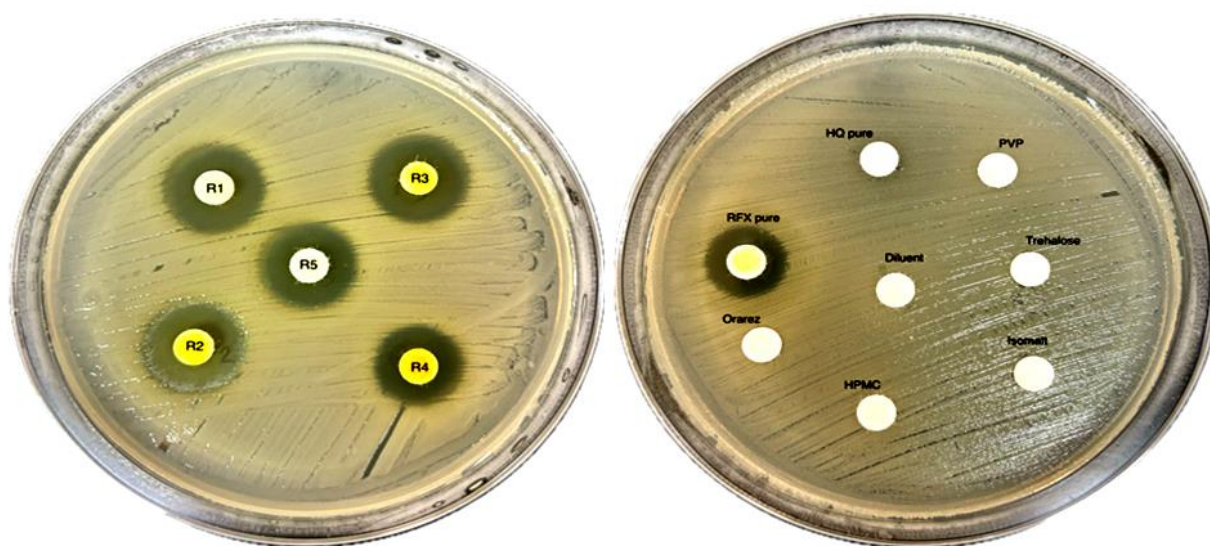

Figure 12. Disc diffusion method result. The figure shows a Mueller-Hinton Agar (MHA) plate streaked with Extensively Drug-Resistant (XDR) *A. baumannii* isolate tested against discs containing spray-dried R1-R5 formulations and their respective individual components.

Table 2. Disc diffusion method inhibition zone measurements of the tested isolates

Isolate#	Phenotype	R1	R2	R3	R4	R5	RFX pure	HQ pure
1	MDR	13 mm	16 mm	15 mm	14 mm	14 mm	15 mm	0 mm
2	XDR	16 mm	16 mm	16 mm	14 mm	15 mm	15 mm	0 mm
3	XDR	14 mm	15 mm	15 mm	13 mm	14 mm	13 mm	0 mm
4	XDR	14 mm	15 mm	11 mm	11 mm	12 mm	12 mm	0 mm
5	XDR	14 mm	15 mm	11 mm	11 mm	12 mm	12 mm	0 mm
Mean		14.2 mm	15.4 mm	12.6 mm	12 mm	13 mm	13.4 mm	0 mm

The MIC minimum inhibitory concentration data confirmed the disc diffusion results and indicated that the mean of MIC was 250 µg/ml (**Table 3, and Supplementary Figure 13 (A)**). The effect was due to the drug RFX as none of the excipients exhibited antibacterial effect as shown in (**Table 4, and Supplementary Figure 13 (B)**).

Table 3. Minimum inhibitory concentration (MIC) results for formulations (R1-R5)

#	Phenotype	R1	R2	R3	R4	R5	RFX pure	HQ pure
1	Sensitive	250 µg/ml	250 µg/ml	250 µg/ml	250 µg/ml	250 µg/ml	250 µg/ml	>= 2000 µg/ml

2	XDR	125 µg/ml	62.5 µg/ml	125 µg/ml	125 µg/ml	125 µg/ml	250 µg/ml	>= 1000 µg/ml
3	XDR	500 µg/ml	250 µg/ml	250 µg/ml	250 µg/ml	500 µg/ml	250 µg/ml	>= 2000 µg/ml
4	XDR	250 µg/ml	125 µg/ml	250 µg/ml	125 µg/ml	250 µg/ml	250 µg/ml	>= 2000 µg/ml
5	XDR	250 µg/ml	250 µg/ml	250 µg/ml	250 µg/ml	250 µg/ml	250 µg/ml	>= 2000 µg/ml
Mean		275 µg/ml	187 µg/ml	225 µg/ml	175 µg/ml	275 µg/ml	250 µg/ml	>= 1400 µg/ml

Table 4. Minimal inhibitory concentration (MIC) results for excipients

#	Phenotype	PVP	Trehalose	Isomalt	OraRez	HPMC-E5
1	Sensitive	>= 2000 µg/ml	>= 2000 µg/ml	>= 2000 µg/ml	>= 2000 µg/ml	>= 2000 µg/ml
2	XDR	>= 2000 µg/ml	>= 2000 µg/ml	>= 2000 µg/ml	>= 2000 µg/ml	>= 2000 µg/ml
3	XDR	>= 2000 µg/ml	>= 2000 µg/ml	>= 2000 µg/ml	>= 2000 µg/ml	>= 2000 µg/ml
4	XDR	>= 2000 µg/ml	>= 2000 µg/ml	>= 2000 µg/ml	>= 2000 µg/ml	>= 2000 µg/ml

5	XDR	>= 2000 µg/ml	>= 2000 µg/ml	>= 2000 µg/ml	>= 2000 µg/ml	>= 2000 µg/ml
Mean		>= 2000 µg/ml	>= 2000 µg/ml	>= 2000 µg/ml	>= 2000 µg/ml	>= 2000 µg/ml

7.4 Conclusions

Considering that pulmonary infections often worsen lung cancer and that lung cancer patients frequently suffer from these infections, which diminish both their overall survival and the effectiveness of anticancer treatments. A novel co-delivery system using RFX and HQ for targeting bacterial infections and antitumor activity in NSCLC was successfully developed using the 3FN spray drying method. Specifically, optimal results were achieved with HQ fed through the inner nozzle and RFX through the outer nozzle, as some formulations with the reversed setup showed no significant change in cytokine levels. The physicochemical properties of the resulting powders showed recovery% of 83.9% ± 3.20% for HQ and 67.9% ± 4.30% for RFX. Particle size analysis revealed that the 3FN system produced larger particles compared to the 2FN system. FTIR results confirmed hydrogen bonding between RFX, HQ, and excipients in both methods, stabilizing the amorphous form, which was also confirmed by XRPD.

The 3FN method provided advanced customized release profiles, facilitating a rapid release of RFX to combat respiratory infections and a controlled, prolonged release of HQ for targeted anticancer effects. In vitro efficacy demonstrated synergistic antiproliferative effects against A549 cells and revealed complementary anti-inflammatory mechanisms. HQ broadly inhibited key inflammatory pathways, while RFX modulated systemic inflammation, underscoring the potential synergistic effect of these formulations in addressing cancer-related inflammation. Moreover, this newly developed co-delivery system effectively inhibited *Acinetobacter baumannii*, highlighting its potential for treating resistant infections. Overall, the 3FN spray drying method excelled in developing an RFX-HQ co-delivery system with substantial therapeutic activity for targeting NSCLC and associated infections or inflammations. The best results were achieved with HQ

encapsulated in the core, exhibiting a sustained release profile to target antitumor activity in NSCLC while minimizing toxicity, particularly since HQ has a lower IC50 than RFX. Conversely, RFX encapsulated in the shell exhibited a faster initial release to manage cancer-related infections and enhance overall cytotoxicity. It would be interesting to investigate other drug combinations, particularly those with narrow therapeutic windows, and examine the impact of different excipients on controlled release kinetics.

References:

[1]   M. B. Schabath and M. L. Cote, "Cancer progress and priorities: lung cancer," *Cancer epidemiology, biomarkers & prevention,* vol. 28, no. 10, pp. 1563-1579, 2019.

[2]   D. Das, J. Wang, and J. Hong, "Next-Generation Kinase Inhibitors Targeting Specific Biomarkers in Non-Small Cell Lung Cancer (NSCLC): A Recent Overview," *ChemMedChem,* vol. 16, no. 16, pp. 2459-2479, 2021.

[3]   E. Perlin *et al.*, "The impact of pulmonary infections on the survival of lung cancer patients," *Cancer,* vol. 66, no. 3, pp. 593-596, 1990.

[4]   S. Kohno *et al.*, "The pattern of respiratory infection in patients with lung cancer," *The Tohoku Journal of Experimental Medicine,* vol. 173, no. 4, pp. 405-411, 1994.

[5]   K. Akinosoglou, K. Karkoulias, and M. Marangos, "Infectious complications in patients with lung cancer," *European Review for Medical & Pharmacological Sciences,* vol. 17, no. 1, 2013.

[6]   A. Chang, "Chemotherapy, chemoresistance and the changing treatment landscape for NSCLC," *Lung Cancer,* vol. 71, no. 1, pp. 3-10, Jan 2011, doi: 10.1016/j.lungcan.2010.08.022.

[7]   P. Seve and C. Dumontet, "Chemoresistance in non-small cell lung cancer," *Curr Med Chem Anticancer Agents,* vol. 5, no. 1, pp. 73-88, Jan 2005, doi: 10.2174/1568011053352604.

[8]   J. Soler-Cataluña, M. A. Martinez-Garcia, P. R. Sánchez, E. Salcedo, M. Navarro, and R. Ochando, "Severe acute exacerbations and mortality in patients with chronic obstructive pulmonary disease," *Thorax,* vol. 60, no. 11, pp. 925-931, 2005.

[9]   R. Deshmukh, P. Wagh, and J. Naik, "Solvent evaporation and spray drying technique for micro-and nanospheres/particles preparation: A review," *Drying technology,* vol. 34, no. 15, pp. 1758-1772, 2016.

[10]   C. Arpargaus, D. Rütti, and M. Meuri, "Enhanced solubility of poorly soluble drugs via spray drying," *Drug Delivery Strategies for Poorly Water-Soluble Drugs,* pp. 551-585, 2013.

[11]   N. Marasini *et al.*, "Development of excipients free inhalable co-spray-dried tobramycin and diclofenac formulations for cystic fibrosis using two and three fluid nozzles," *International Journal of Pharmaceutics,* vol. 624, p. 121989, 2022.

[12]   X. Wang *et al.*, "Advances in controlled-release fertilizer encapsulated by organic-inorganic composite membranes," *Particuology,* 2023.

[13]   L. G. Luna Alanis, "Design and evaluation of novel spray drying atomization methods for in-line mixing and particle size control," University of Illinois at Urbana-Champaign, 2023.

[14]   J. Cai, "Evaluation of the microencapsulation performance by spray drying with a three-fluid nozzle," University of Illinois at Urbana-Champaign, 2021.

[15]   F. B. Villa, C. G. Chiaregato, and R. Faez, "Novel core-shell microcapsules incorporating macro/micronutrients in PVA/starch matrix," *Materials Today Communications,* vol. 38, p. 108017, 2024.

[16]   S. Nimbkar, M. M. Leena, J. A. Moses, and C. Anandharamakrishnan, "A modified 3-fluid nozzle spray drying approach for co-encapsulation of iron and folic acid," *Chemical Papers,* vol. 77, no. 7, pp. 4019-4032, 2023/07/01 2023, doi: 10.1007/s11696-023-02761-z.

[17]   M. G. Antoniraj, M. M. Leena, J. Moses, and C. Anandharamakrishnan, "Cross-linked chitosan microparticles preparation by modified three fluid nozzle spray drying approach," *International journal of biological macromolecules,* vol. 147, pp. 1268-1277, 2020.

[18]   N. Krishnamurthy, A. A. Grimshaw, S. A. Axson, S. H. Choe, and J. E. Miller, "Drug repurposing: a systematic review on root causes, barriers and facilitators," *BMC health services research,* vol. 22, no. 1, p. 970, 2022.

[19]   M. Rudrapal, S. J. Khairnar, and A. G. Jadhav, "Drug repurposing (DR): an emerging approach in drug discovery," *Drug repurposing-hypothesis, molecular aspects and therapeutic applications,* vol. 1, no. 1, 2020.

[20]   A. Radadiya and A. Shah, "Bioactive benzofuran derivatives: An insight on lead developments, radioligands and advances of the last decade," *European journal of medicinal chemistry,* vol. 97, pp. 356-376, 2015.

[21]   J. Vitte *et al.*, "Immune modulation as a therapeutic option during the SARS-CoV-2 outbreak: The case for antimalarial aminoquinolines," *Frontiers in Immunology,* vol. 11, p. 2159, 2020.

[22]   J. Clark *et al.*, "Inhibiting the Systemic Autophagic Syndrome-A Phase II Study of Hydroxychloroquine and Aldesleukin in Renal Cell Carcinoma Patients (RCC). A Cytokine Working Group (CWG) Study Prometheus protocol#: IIT11PLK01."

[23]   L. Senerovic, D. Opsenica, I. Moric, I. Aleksic, M. Spasić, and B. Vasiljevic, "Quinolines and quinolones as antibacterial, antifungal, anti-virulence, antiviral and anti-parasitic agents," *Advances in Microbiology, Infectious Diseases and Public Health: Volume 14,* pp. 37-69, 2020.

[24]   L.-q. Liu *et al.*, "Hydroxychloroquine potentiates the anti-cancer effect of bevacizumab on glioblastoma via the inhibition of autophagy," *Biomedicine & Pharmacotherapy,* vol. 118, p. 109339, 2019.

[25]   E. Ilan *et al.*, "Improved oral delivery of desmopressin via a novel vehicle: mucoadhesive submicron emulsion," *Pharmaceutical research,* vol. 13, pp. 1083-1087, 1996.

[26]   M. B. Schulz and R. Daniels, "Hydroxypropylmethylcellulose (HPMC) as emulsifier for submicron emulsions: influence of molecular weight and substitution type on the droplet size after high-pressure homogenization," *European Journal of Pharmaceutics and Biopharmaceutics,* vol. 49, no. 3, pp. 231-236, 2000.

[27]   J. Zheng, B. Wang, J. Xiang, and Z. Yu, "Controlled release of curcumin from HPMC (hydroxypropyl methyl cellulose) co-spray-dried materials," *Bioinorganic chemistry and applications,* vol. 2021, 2021.

[28]   T. A. Popov *et al.*, "Methyl-cellulose powder for prevention and management of nasal symptoms," *Expert Review of Respiratory Medicine,* vol. 11, no. 11, pp. 885-892, 2017.

[29]   Y. Kawashima, T. Serigano, T. Hino, H. Yamamoto, and H. Takeuchi, "A new powder design method to improve inhalation efficiency of pranlukast hydrate dry powder aerosols by surface modification with hydroxypropylmethylcellulose phthalate nanospheres," *Pharmaceutical research,* vol. 15, pp. 1748-1752, 1998.

[30]   G. A. Burdock, "Safety assessment of hydroxypropyl methylcellulose as a food ingredient," *Food and Chemical Toxicology,* vol. 45, no. 12, pp. 2341-2351, 2007.

[31]   N. Al-Zoubi, G. Al-Obaidi, B. Tashtoush, and S. Malamataris, "Sustained release of diltiazem HCl tableted after co-spray drying and physical mixing with PVAc and PVP," *Drug development and industrial pharmacy,* vol. 42, no. 2, pp. 270-279, 2016.

[32]   J. H. Lee *et al.*, "Enhanced dissolution rate of celecoxib using PVP and/or HPMC-based solid dispersions prepared by spray drying method," *Journal of Pharmaceutical Investigation,* vol. 43, pp. 205-213, 2013.

[33]   T. Sou, M. P. McIntosh, L. M. Kaminskas, R. J. Prankerd, and D. A. Morton, "Designing a multicomponent spray-dried formulation platform for pulmonary delivery of biomacromolecules: the effect of polymers on the formation of an amorphous matrix for glassy state stabilization of biomacromolecules," *Drying technology,* vol. 31, no. 13-14, pp. 1451-1458, 2013.

[34]   F. Tewes, L. Tajber, O. I. Corrigan, C. Ehrhardt, and A.-M. Healy, "Development and characterisation of soluble polymeric particles for pulmonary peptide delivery," *European Journal of Pharmaceutical Sciences,* vol. 41, no. 2, pp. 337-352, 2010.

[35]   O. Zachar, "Respiratory Infections Early-Stage Medication: Inhalation Formulation & Dosage of PVP Iodine," 2021.

[36]   M. A. Haque, J. Chen, P. Aldred, and B. Adhikari, "Denaturation and physical characteristics of spray-dried whey protein isolate powders produced in the presence and absence of lactose, trehalose, and polysorbate-80," *Drying technology,* vol. 33, no. 10, pp. 1243-1254, 2015.

[37] S. Ohtake and Y. J. Wang, "Trehalose: Current Use and Future Applications," *Journal of Pharmaceutical Sciences,* vol. 100, no. 6, pp. 2020-2053, 2011/06/01/ 2011, doi: https://doi.org/10.1002/jps.22458.

[38] A. Teo, Y. Lam, S. J. Lee, and K. K. Goh, "Spray drying of whey protein stabilized nanoemulsions containing different wall materials–maltodextrin or trehalose," *LWT,* vol. 136, p. 110344, 2021.

[39] O. Ivaniuk, T. Yarnykh, and I. Kovalevska, "Determination of the bioadhesion indicators of vaginal gel with resveratrol and hyaluronic acid," 2019.

[40] Y. S. Maslii, O. Ruban, Y. V. Levachkova, and T. Y. Kolisnyk, "Choice of mucosal adhesive in the composition of a new dental gel," 2020.

[41] M. Auerbach and A. k. Dedman, "Bulking Agents–Multi-Functional Ingredients," *Sweeteners and sugar alternatives in food technology,* pp. 433-470, 2012.

[42] A.-K. Koskinen *et al.*, "Physical stability of freeze-dried isomalt diastereomer mixtures," *Pharmaceutical Research,* vol. 33, pp. 1752-1768, 2016.

[43] E. Matta, M. J. Tavera-Quiroz, and N. Bertola, "Isomalt-plasticized methylcellulose-based films as carriers of ascorbic acid," *Food and Bioprocess Technology,* vol. 13, pp. 2186-2199, 2020.

[44] A. Sentko and I. Willibald-Ettle, "Isomalt," *Sweeteners and sugar alternatives in food technology,* pp. 243-274, 2012.

[45] J. A. Bhushani, N. K. Kurrey, and C. Anandharamakrishnan, "Nanoencapsulation of green tea catechins by electrospraying technique and its effect on controlled release and in-vitro permeability," *Journal of Food Engineering,* vol. 199, pp. 82-92, 2017.

[46] T.-C. Chou, "Drug combination studies and their synergy quantification using the Chou-Talalay method," *Cancer research,* vol. 70, no. 2, pp. 440-446, 2010.

[47] D. Leng, K. Thanki, C. Foged, and M. Yang, "Formulating inhalable dry powders using two-fluid and three-fluid nozzle spray drying," *Pharmaceutical research,* vol. 35, pp. 1-11, 2018.

[48] J. Cai, R. Lopez, and Y. Lee, "Effect of Feed Material Properties on Microencapsulation by Spray Drying with a Three-Fluid Nozzle: Soybean Oil Encapsulated in Maltodextrin and Sugar Beet Pectin," *Journal of Food Processing and Preservation,* vol. 2023, 2023.

[49] M. A. Boraey, S. Hoe, H. Sharif, D. P. Miller, D. Lechuga-Ballesteros, and R. Vehring, "Improvement of the dispersibility of spray-dried budesonide powders using leucine in an ethanol–water cosolvent system," *Powder technology,* vol. 236, pp. 171-178, 2013.

[50] R. Vehring, "Pharmaceutical particle engineering via spray drying," *Pharmaceutical research,* vol. 25, no. 5, pp. 999-1022, 2008.

[51] R. Vehring, W. R. Foss, and D. Lechuga-Ballesteros, "Particle formation in spray drying," *Journal of aerosol science,* vol. 38, no. 7, pp. 728-746, 2007.

[52] M. M. Leena, M. G. Antoniraj, J. Moses, and C. Anandharamakrishnan, "Three fluid nozzle spray drying for co-encapsulation and controlled release of curcumin and resveratrol," *Journal of Drug Delivery Science and Technology,* vol. 57, p. 101678, 2020.

[53] D. França, Â. F. Medina, L. L. Messa, C. F. Souza, and R. Faez, "Chitosan spray-dried microcapsule and microsphere as fertilizer host for swellable– controlled release materials," *Carbohydrate polymers,* vol. 196, pp. 47-55, 2018.

[54] J. W. Ivey, P. Bhambri, T. K. Church, D. A. Lewis, and R. Vehring, "Experimental investigations of particle formation from propellant and solvent droplets using a monodisperse spray dryer," *Aerosol Science and Technology,* vol. 52, no. 6, pp. 702-716, 2018.

[55] T. T. Nguyen, T. Hirano, R. N. Chamida, E. L. Septiani, N. T. Nguyen, and T. Ogi, "Porous pectin particle formation utilizing spray drying with a three-fluid nozzle," *Powder Technology,* vol. 440, p. 119782, 2024.

[56] A. Sosnik and K. P. Seremeta, "Advantages and challenges of the spray-drying technology for the production of pure drug particles and drug-loaded polymeric carriers," *Advances in colloid and interface science,* vol. 223, pp. 40-54, 2015.

[57] T. Kshirsagar, N. Jaiswal, G. Chavan, K. Zambre, S. Ramkrushna, and D. Dinesh, "Formulation & evaluation of fast dissolving oral film," *World J. Pharm. Res,* vol. 10, no. 9, pp. 503-561, 2021.

[58] C. Jin *et al.*, "Updates on applications of low-viscosity grade Hydroxypropyl methylcellulose in coprocessing for improvement of physical properties of pharmaceutical powders," *Carbohydrate Polymers,* vol. 311, p. 120731, 2023/07/01/ 2023, doi: https://doi.org/10.1016/j.carbpol.2023.120731.

[59] T. Peng *et al.*, "Influence of polymers on the physical and chemical stability of spray-dried amorphous solid dispersion: dipyridamole degradation induced by enteric polymers," *Aaps Pharmscitech,* vol. 19, pp. 2620-2628, 2018.

[60] B.-J. Lee, S.-G. Ryu, and J.-H. Cui, "Formulation and release characteristics of hydroxypropyl methylcellulose matrix tablet containing melatonin," *Drug development and industrial pharmacy,* vol. 25, no. 4, pp. 493-501, 1999.

[61] K. Tahara, K. Yamamoto, and T. Nishihata, "Overall mechanism behind matrix sustained release (SR) tablets prepared with hydroxypropyl methylcellulose 2910," *Journal of controlled release,* vol. 35, no. 1, pp. 59-66, 1995.

[62] P. Saralkar and A. K. Dash, "Alginate nanoparticles containing curcumin and resveratrol: preparation, characterization, and in vitro evaluation against DU145 prostate cancer cell line," *AAPS pharmscitech,* vol. 18, pp. 2814-2823, 2017.

[63] A. H. Khasraghi and L. M. Thomas, "Preparation and evaluation of lornoxicam film-forming gel," *Drug Invention Today,* vol. 11, no. 8, pp. 1906-1913, 2019.

[64] C. Olsson, H. Jansson, and J. Swenson, "The role of trehalose for the stabilization of proteins," *The Journal of Physical Chemistry B,* vol. 120, no. 20, pp. 4723-4731, 2016.

[65] Y. Mizunoe *et al.*, "Trehalose protects against oxidative stress by regulating the Keap1–Nrf2 and autophagy pathways," *Redox biology,* vol. 15, pp. 115-124, 2018.

[66] J. K. Kaushik and R. Bhat, "Why Is Trehalose an Exceptional Protein Stabilizer?: An analysis of the thermal stability of proteins in the presence of the compatible osmolyte trehalose," *Journal of Biological Chemistry,* vol. 278, no. 29, pp. 26458-26465, 2003.

[67] M. N. Leslie, N. Marasini, Z. Sheikh, P. M. Young, D. Traini, and H. X. Ong, "Development of inhalable spray dried nitrofurantoin formulations for the treatment of emphysema," *Pharmaceutics,* vol. 15, no. 1, p. 146, 2022.

[68] D. Bolten and M. Türk, "Experimental study on the surface tension, density, and viscosity of aqueous poly (vinylpyrrolidone) solutions," *Journal of Chemical & Engineering Data,* vol. 56, no. 3, pp. 582-588, 2011.

[69] Z. Mingzheng, X. Guodong, L. Jian, C. Lei, and Z. Lijun, "Analysis of factors influencing thermal conductivity and viscosity in different kinds of surfactant solutions," *Experimental Thermal and Fluid Science,* vol. 36, pp. 22-29, 2012.

[70] H. Gurditta, A. A. Patel, and S. Arora, "Optimisation of sweetener and bulking agent levels for the preparation of functional Chhana-murki," *International journal of dairy technology,* vol. 68, no. 2, pp. 190-197, 2015.

[71] V. Nagathan and K. Hallikeri, "Formulation and Evaluation of Topical Film Forming Systems Comprising of Non-Steroidal Anti-Inflammatory Drug," *Indian Journal of Pharmaceutical Sciences,* vol. 85, no. 5, 2023.

[72] J. S. Masliy and O. Ruban, "The study of biopharmaceutical and adhesive characteristics of a dental gel," *Вісник фармації,* no. 1, pp. 28-32, 2018.

[73] S. Riccardo, D. Nava, M. Nebuloni, B. Pastura, and E. Pini, "Structural elucidation of the Rifaximin Ph. Eur. Impurity H," *Journal of pharmaceutical and biomedical analysis,* vol. 51, pp. 858-65, 10/01 2009, doi: 10.1016/j.jpba.2009.10.012.

[74] F. Faísca, V. Correia, Ž. Petrovski, L. C. Branco, H. Rebelo-de-Andrade, and M. M. Santos, "Enhanced in vitro antiviral activity of hydroxychloroquine ionic liquids against SARS-CoV-2," *Pharmaceutics,* vol. 14, no. 4, p. 877, 2022.

[75]   J. Zhang, B. Yuan, and H. Ren, "Synthesis and Characterization of PVP/Tb 4/3 L•7H 2 O Luminescent Complex," *IOP Conference Series: Earth and Environmental Science,* vol. 170, p. 032043, 07/01 2018, doi: 10.1088/1755-1315/170/3/032043.

[76]   H. Somashekarappa, Y. Prakash, K. Hemalatha, T. Demappa, and R. Somashekar, "Preparation and characterization of HPMC/PVP blend films plasticized with sorbitol," *Indian Journal of Materials Science,* vol. 2013, 2013.

[77]   H. Kawashima and H. Goto, "Preparation and Properties of Polyaniline in the Presence of Trehalose," *Soft Nanoscience Letters,* vol. 01, 01/01 2011, doi: 10.4236/snl.2011.13013.

[78]   M. Ishtiaq, S. Asghar, I. ullah khan, M. Iqbal, and S. Khalid, "Development of the Amorphous Solid Dispersion of Curcumin: A Rational Selection of Polymers for Enhanced Solubility and Dissolution," *Crystals,* vol. 12, p. 1606, 11/10 2022, doi: 10.3390/cryst12111606.

[79]   K. A. Chan and S. G. Kazarian, "FTIR spectroscopic imaging of dissolution of a solid dispersion of nifedipine in poly (ethylene glycol)," *Molecular Pharmaceutics,* vol. 1, no. 4, pp. 331-335, 2004.

[80]   G. Viscomi *et al.*, "Crystal forms of rifaximin and their effect on pharmaceutical properties," *Crystengcomm,* vol. 10, 07/23 2008, doi: 10.1039/b717887e.

[81]   A. N. F. Moraes *et al.*, "Compatibility study of hydroxychloroquine sulfate with pharmaceutical excipients using thermal and nonthermal techniques for the development of hard capsules," *Journal of Thermal Analysis and Calorimetry,* vol. 140, pp. 2283-2292, 2020.

[82]   L. Nohemann, M. P. d. Almeida, and P. C. Ferrari, "Floating ability and drug release evaluation of gastroretentive microparticles system containing metronidazole obtained by spray drying," *Brazilian Journal of Pharmaceutical Sciences,* vol. 53, 2017.

[83]   K. Roe and T. Labuza, "Glass Transition and Crystallization of Amorphous Trehalose-sucrose Mixtures," *International Journal of Food Properties - INT J FOOD PROP,* vol. 8, pp. 559-574, 09/01 2005, doi: 10.1080/10942910500269824.

[84]   E. Khodaverdi, N. Khalili, F. Zangiabadi, and A. Homayouni, "Preparation, Characterization and Stability Studies of Glassy Solid Dispersions of Indomethacin using PVP and Isomalt as carriers," *Iranian journal of basic medical sciences,* vol. 15, pp. 820-832, 04/01 2012.

[85]   S. Kim, W. K. Ng, Y. Dong, S. Das, and R. B. Tan, "Preparation and physicochemical characterization of trans-resveratrol nanoparticles by temperature-controlled antisolvent precipitation," *Journal of Food Engineering,* vol. 108, no. 1, pp. 37-42, 2012.

[86]   Y.-H. Phillip Lee *et al.*, "Gefitinib–cyclodextrin inclusion complexes: physico-chemical characterization and dissolution studies," *Drug development and industrial pharmacy,* vol. 35, no. 9, pp. 1113-1120, 2009.

[87]   W. Liu, X. D. Chen, Z. Cheng, and C. Selomulya, "On enhancing the solubility of curcumin by microencapsulation in whey protein isolate via spray drying," *Journal of food engineering,* vol. 169, pp. 189-195, 2016.

[88]   D. E. Alonzo, G. G. Zhang, D. Zhou, Y. Gao, and L. S. Taylor, "Understanding the behavior of amorphous pharmaceutical systems during dissolution," *Pharmaceutical research,* vol. 27, pp. 608-618, 2010.

[89]   T. Mizoe, S. Beppu, T. Ozeki, and H. Okada, "One-step preparation of drug-containing microparticles to enhance the dissolution and absorption of poorly water-soluble drugs using a 4-fluid nozzle spray drier," *Journal of controlled release,* vol. 120, no. 3, pp. 205-210, 2007.

[90]   G. H. Shin, J. Li, J. H. Cho, J. T. Kim, and H. J. Park, "Enhancement of curcumin solubility by phase change from crystalline to amorphous in CUR-TPGS nanosuspension," *Journal of Food Science,* vol. 81, no. 2, pp. N494-N501, 2016.

[91]   S. Tan, C. Zhong, and T. Langrish, "Microencapsulation of pepsin in the spray-dried WPI (whey protein isolates) matrices for controlled release," *Journal of food engineering,* vol. 263, pp. 147-154, 2019.

[92]   K. Wasilewska and K. Winnicka, "Ethylcellulose–a pharmaceutical excipient with multidirectional application in drug dosage forms development," *Materials,* vol. 12, no. 20, p. 3386, 2019.

[93]   C. Berkland, M. King, A. Cox, K. K. Kim, and D. W. Pack, "Precise control of PLG microsphere size provides enhanced control of drug release rate," *Journal of controlled release,* vol. 82, no. 1, pp. 137-147, 2002.

[94]   S. Freiberg and X. Zhu, "Polymer microspheres for controlled drug release," *International journal of pharmaceutics,* vol. 282, no. 1-2, pp. 1-18, 2004.

[95]   R. Singh and J. W. Lillard Jr, "Nanoparticle-based targeted drug delivery," *Experimental and molecular pathology,* vol. 86, no. 3, pp. 215-223, 2009.

[96]   M. Muhaimin, A. Y. Chaerunisaa, and R. Bodmeier, "Impact of dispersion time interval and particle size on release profiles of propranolol HCl and carbamazepines from microparticle blends system," *Scientific reports,* vol. 12, no. 1, p. 10360, 2022.

[97]   C. G. Chiaregato, O. D. Bernardinelli, A. Shavandi, E. Sabadini, and D. F. S. Petri, "The effect of the molecular structure of hydroxypropyl methylcellulose on the states of water, wettability, and swelling properties of cryogels prepared with and without CaO2," *Carbohydrate polymers,* vol. 316, p. 121029, 2023.

[98]   A. Viridén, B. Wittgren, and A. Larsson, "The consequence of the chemical composition of HPMC in matrix tablets on the release behaviour of model drug substances having different solubility," *European journal of pharmaceutics and biopharmaceutics,* vol. 77, no. 1, pp. 99-110, 2011.

[99]   P. Franco and I. De Marco, "The Use of Poly (N-vinyl pyrrolidone) in the Delivery of Drugs: A Review," *Polymers,* vol. 12, no. 5, p. 1114, 2020.

[100]   A. B. Lokhande, S. Mishra, R. D. Kulkarni, and J. B. Naik, "Influence of different viscosity grade ethylcellulose polymers on encapsulation and in vitro release study of drug loaded nanoparticles," *Journal of pharmacy research,* vol. 7, no. 5, pp. 414-420, 2013.

[101]   L. Ma, T. Shi, Z. Zhang, X. Liu, and H. Wang, "Wettability of HPMC/PEG/CS Thermosensitive Porous Hydrogels," *Gels,* vol. 9, no. 8, p. 667, 2023.

[102]   M. Namasivayam, M. R. Andersson, and J. G. Shapter, "A comparative study on the role of polyvinylpyrrolidone molecular weight on the functionalization of various carbon nanotubes and their composites," *Polymers,* vol. 13, no. 15, p. 2447, 2021.

[103]   G. Esposito *et al.*, "Rifaximin, a non-absorbable antibiotic, inhibits the release of pro-angiogenic mediators in colon cancer cells through a pregnane X receptor-dependent pathway," *International Journal of Oncology,* vol. 49, no. 2, pp. 639-645, 2016.

[104]   A. L. Liang *et al.*, "Chloroquine increases the anti-cancer activity of epirubicin in A549 lung cancer cells," *Oncology Letters,* vol. 20, no. 1, pp. 53-60, 2020.

[105]   S. Brezgin *et al.*, "Hydroxychloroquine Enhances Cytotoxic Properties of Extracellular Vesicles and Extracellular Vesicle–Mimetic Nanovesicles Loaded with Chemotherapeutics," *Pharmaceutics,* vol. 15, no. 2, p. 534, 2023.

[106]   P. M. P. Ferreira, R. W. R. de Sousa, J. R. de Oliveira Ferreira, G. C. G. Militão, and D. P. Bezerra, "Chloroquine and hydroxychloroquine in antitumor therapies based on autophagy-related mechanisms," *Pharmacological research,* vol. 168, p. 105582, 2021.

[107]   M. M. Hoque, Y. Iida, H. Kotani, I. D. Kartika, and M. Harada, "Hydroxychloroquine Promotes Bcl-xL Inhibition-induced Apoptosis in BxPC-3 Human Pancreatic Cancer Cells," *Anticancer Research,* vol. 42, no. 7, pp. 3495-3506, 2022.

[108]   X. Lyu *et al.*, "Hydroxychloroquine suppresses lung tumorigenesis via inducing FoxO3a nuclear translocation through STAT3 inactivation," *Life sciences,* vol. 246, p. 117366, 2020.

[109]   A. E. in 't Veld, M. A. Jansen, L. C. Ciere, and M. Moerland, "Hydroxychloroquine effects on TLR signalling: underexposed but unneglectable in COVID-19," *Journal of Immunology Research,* vol. 2021, pp. 1-7, 2021.

[110]   W. Zhou, H. Wang, Y. Yang, Z.-S. Chen, C. Zou, and J. Zhang, "Chloroquine against malaria, cancers and viral diseases," *Drug Discovery Today,* vol. 25, no. 11, pp. 2012-2022, 2020.

[111] J. A. Ratikan, J. W. Sayre, and D. Schaue, "Chloroquine engages the immune system to eradicate irradiated breast tumors in mice," *International Journal of Radiation Oncology* Biology* Physics,* vol. 87, no. 4, pp. 761-768, 2013.

[112] D. Heng, D. J. Cutler, H.-K. Chan, J. Yun, and J. A. Raper, "What is a suitable dissolution method for drug nanoparticles?," *Pharmaceutical research,* vol. 25, pp. 1696-1701, 2008.

[113] V. Kanchan and A. K. Panda, "Interactions of antigen-loaded polylactide particles with macrophages and their correlation with the immune response," *Biomaterials,* vol. 28, no. 35, pp. 5344-5357, 2007.

[114] M. V. Baranov, M. Kumar, S. Sacanna, S. Thutupalli, and G. van den Bogaart, "Modulation of Immune Responses by Particle Size and Shape," (in eng), *Front Immunol,* vol. 11, p. 607945, 2020, doi: 10.3389/fimmu.2020.607945.

[115] I. R. Rao *et al.*, "Hydroxychloroquine in nephrology: current status and future directions," *Journal of Nephrology,* vol. 36, no. 8, pp. 2191-2208, 2023/11/01 2023, doi: 10.1007/s40620-023-01733-6.

[116] A. E. In 't Veld, M. A. A. Jansen, L. C. A. Ciere, and M. Moerland, "Hydroxychloroquine Effects on TLR Signalling: Underexposed but Unneglectable in COVID-19," (in eng), *J Immunol Res,* vol. 2021, p. 6659410, 2021, doi: 10.1155/2021/6659410.

[117] R. Xu, Z. Ji, C. Xu, and J. Zhu, "The clinical value of using chloroquine or hydroxychloroquine as autophagy inhibitors in the treatment of cancers: A systematic review and meta-analysis," (in eng), *Medicine (Baltimore),* vol. 97, no. 46, p. e12912, Nov 2018, doi: 10.1097/md.0000000000012912.

[118] Y. R. Fauzi *et al.*, "Antitumor effects of chloroquine/hydroxychloroquine mediated by inhibition of the NF-κB signaling pathway through abrogation of autophagic p47 degradation in adult T-cell leukemia/lymphoma cells," (in eng), *PLoS One,* vol. 16, no. 8, p. e0256320, 2021, doi: 10.1371/journal.pone.0256320.

[119] H. Li *et al.*, "Rifaximin-mediated gut microbiota regulation modulates the function of microglia and protects against CUMS-induced depression-like behaviors in adolescent rat," *Journal of Neuroinflammation,* vol. 18, no. 1, p. 254, 2021/11/04 2021, doi: 10.1186/s12974-021-02303-y.

[120] D. J. Kang *et al.*, "Rifaximin Exerts Beneficial Effects Independent of its Ability to Alter Microbiota Composition," (in eng), *Clin Transl Gastroenterol,* vol. 7, no. 8, p. e187, Aug 25 2016, doi: 10.1038/ctg.2016.44.

[121] H. Li *et al.*, "Rifaximin-mediated gut microbiota regulation modulates the function of microglia and protects against CUMS-induced depression-like behaviors in adolescent rat," (in eng), *J Neuroinflammation,* vol. 18, no. 1, p. 254, Nov 4 2021, doi: 10.1186/s12974-021-02303-y.

[122] M. A. E. Hamd *et al.*, "Ziziphus spina-christi leaf-derived carbon dots as a fluorescence nanosensor to evaluate rifaximin antibacterial via inner filter effect: greenness and whiteness studies," *Chemosensors,* vol. 11, no. 5, p. 275, 2023.

[123] S. M. S. Lim, A. Z. Abidin, S. Liew, J. Roberts, and F. Sime, "The global prevalence of multidrug-resistance among Acinetobacter baumannii causing hospital-acquired and ventilator-associated pneumonia and its associated mortality: A systematic review and meta-analysis," *Journal of infection,* vol. 79, no. 6, pp. 593-600, 2019.

[124] M. Bassetti, L. Labate, C. Russo, A. Vena, and D. R. Giacobbe, "Therapeutic options for difficult-to-treat A cinetobacter baumannii infections: a 2020 perspective," *Expert Opinion on Pharmacotherapy,* vol. 22, no. 2, pp. 167-177, 2021.

[125] I. Karaiskos, S. Lagou, K. Pontikis, V. Rapti, and G. Poulakou, "The "old" and the "new" antibiotics for MDR gram-negative pathogens: for whom, when, and how," *Frontiers in public health,* vol. 7, p. 460782, 2019.
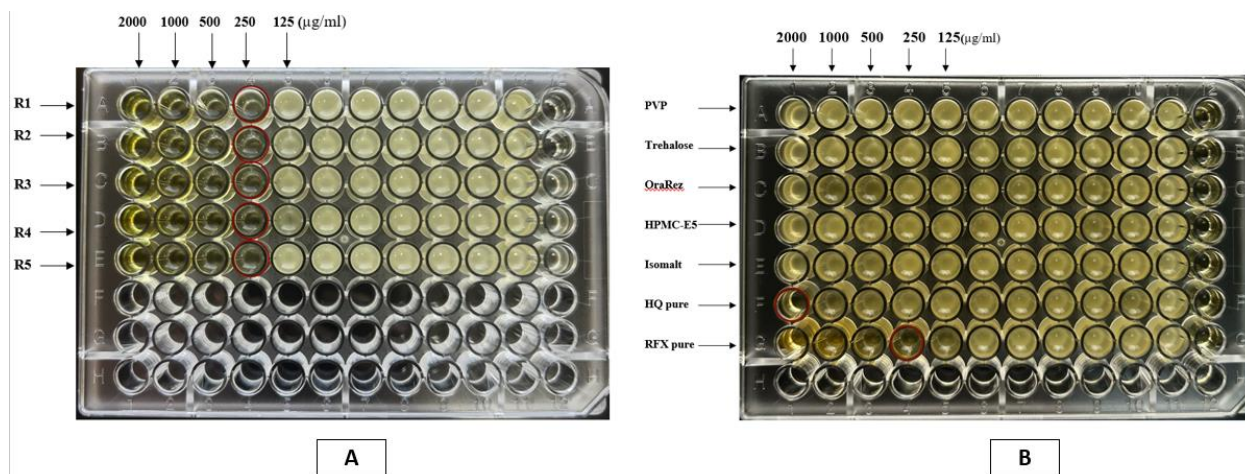
Supplementary Figure 13. (A) Minimum inhibitory concentration (MIC) results for formulations (R1-R5), **(B)** Minimum inhibitory concentration (MIC) results for free dugs and excipients.

Chapter 8

General Discussion and Conclusion

Chapter Summary:

This chapter provides a summary and discussion of the key findings of this work. It includes a critical assessment of the results and the methodologies employed, along with recommendations for future research within the broader context of the field.

8.1 Introduction

Non-small cell lung cancer (NSCLC) constitutes 85% of all lung cancer cases, presenting significant treatment challenges due to its complexity and resistance to conventional therapies. Despite progress in diagnosis and treatment, NSCLC continues to be a major health issue, causing over 1.6 million deaths worldwide annually [1]. The disease often remains undetected in its early stages due to a lack of visible symptoms. Additionally, therapeutic resistance, tumor relapse, and metastatic spread further hinder effective treatment and reduce survival rates. Pulmonary infections complicate lung cancer in 50-70% of cases, and lung cancer patients often experience frequent infections which not only hinder the effectiveness of oncological treatments but also impact overall survival [2-4]. Respiratory infections, those caused by bacteria that is resistant to multiple drugs make treating lung conditions like NSCLC more challenging. These bacteria, such, as *Acinetobacter baumannii* pose a problem in hospitals due to their resistance to antibiotics complicating treatment efforts [5-7]. This becomes particularly risky for individuals with compromised immune systems. Moreover, a history of lung infections may result in chronic health issues such as inflammation and cellular damage. These factors can elevate the risk of developing lung cancer by impacting lung function and reducing defenses [8].

Advanced drug delivery systems, including nanoparticle carriers and inhaled therapies, offer promising solutions by directly delivering therapeutic agents to tumor sites. These methods enhance treatment efficacy, minimize side effects, and bypass the body's defense mechanisms [9]. In pulmonary drug delivery, these systems are crucial for effectively targeting and treating infections, reducing resistance, and improving patient outcomes. Particle engineering is a transformative approach in the formulation of Active Pharmaceutical Ingredients (APIs), using advanced techniques to modify particle size, shape, surface properties, and crystallinity. These modifications enhance bioavailability, solubility, and stability, addressing key pharmaceutical challenges. By intersecting with advanced drug delivery systems like solid dispersions, and nanoparticles, particle engineering improves the effectiveness, delivery, and controlled release of medications, leading to better patient adherence and therapeutic outcomes.

There are some recent examples in the literature detailing the promising advancements in inhalable nanoparticle-based drug delivery systems for lung cancer. The use of spray drying techniques to produce dry powder formulations of lipid nanoparticles (LNPs), solid lipid nanocarriers (SLNs), and nanostructured lipid carriers (NLCs) for the delivery of chemotherapeutics, siRNA, and targeted therapies showed the potential for improved efficacy, reduced side effects, and enhanced patient compliance in lung cancer treatment [10-12]. However, there is often limited discussion about spray drying of liquid lipid carriers (LLCs), and utilizing combination therapies of repurposed drugs in this context. Furthermore, there is not much debate regarding how the parameters of the spray drying process affect the type of solid dispersion that is created, particularly when it comes to using the 3-fluid nozzle (3-FN) spray drying method to prepare dual drug-loaded spray-dried solid dispersions.

This thesis aimed to improve the efficacy of drug delivery systems for non-small cell lung cancer (NSCLC) and respiratory infections. This was accomplished through particle engineering, specifically by combining lipid nanoparticles with solid dispersions to create new spray-dried LNPs loaded with one or two repurposed drugs. Additionally, the thesis developed new spray-dried solid dispersions using two repurposed drugs with a three-fluid nozzle (3FN) system, allowing control over one drug's fast burst release and the other's sustained release.

This section provides a quick assessment of the work, including an overview of the earlier chapters (8.2), a review of the experimental findings, and recommendations for next research (8.3).

8.2   Summary of Key Findings

8.2.1 Inhaled Medicines for Targeting Non-Small Cell Lung Cancer (Chapter 2)

This chapter provided an overview of the advantages and challenges of inhaled drug delivery for non-small cell lung cancer (NSCLC). Inhaled delivery enhances drug precision, reduces systemic side effects, and bypasses first-pass metabolism, resulting in higher bioavailability and faster action. Challenges include the complex respiratory tract structure and mucociliary clearance affecting drug deposition. Various inhalation devices (PMDIs, DPIs, nebulizers) offer distinct benefits. Accurate drug deposition assessment is crucial, using lung imaging, pharmacokinetic analysis, and in silico models. Preferred particle size for chemotherapy is 1-5 μm. Carrier-free nanodrugs show promise for improved outcomes, synthesized through nanoprecipitation and spray-drying. Targeting strategies include active targeting with ligands/antibodies and passive targeting using the enhanced permeability and retention (EPR) effect. Emerging systems, like nanoparticles, liposomes, and pH-sensitive systems, enhance targeted delivery. Investigated drugs include azacitidine, bevacizumab, doxorubicin, curcumin, and paclitaxel. Key benefits of inhaled therapies are reduced side effects, targeted delivery, and improved patient compliance.

8.2.2 Spray-Dried Nano lipid Powders for Pulmonary Drug Delivery (Chapter 3)

This chapter highlights significant advancements in using spray-dried nano lipid powders for treating lung diseases, including infections. Pulmonary drug delivery offers benefits like a non-invasive route, localized lung delivery, reduced enzymatic activity, low drug degradation, high patient compliance, and bypassing first-pass metabolism. Lipid nanoparticles (SLNs and NLCs) are effective due to their biocompatibility, biodegradability, deep lung deposition, controlled drug release, and good muco-adhesion. The spray drying technique, being scalable and commercially viable, produces stable particles with enhanced drug encapsulation and bioavailability. Dry powder inhalers (DPIs) efficiently deliver medication directly to the lungs with high stability and increased bioavailability. SLNs and NLCs are particularly promising for treating lung cancer and lung infections as tuberculosis (TB), as they allow targeted drug delivery, improving efficacy and reducing systemic toxicity.

8.2.3 Development of Pimozide Spray- dried Lipid Nanoparticles with Enhanced Targeting of Non-small cell Lung Cancer (Chapter 4)

This chapter reported the development and evaluation of pimozide-loaded lipid nanoparticles (LNPs) for targeted treatment of non-small cell lung cancer (NSCLC). Using the microemulsion technique, three types of LNPs including SLNs, NLCs, and LLCs were synthesized and optimized into fine powders via spray drying. NLC formulations achieved the highest encapsulation efficiency (EE%), attributed to the inclusion of oleic acid which disrupted the lipid matrix's crystalline structure, enhancing drug encapsulation. In contrast, SLN formulations had the lowest EE% due to their solid lipid content, which limits the ability to encapsulate the drug effectively. Spray drying increased particle sizes and slightly reduced EE% across all LNP types. Dynamic vapor sorption analyses (DVS) revealed diverse moisture sorption trends, with LLCs showing the highest capacity due to their porous structure. FTIR and Raman spectroscopy confirmed successful drug encapsulation and uniform distribution within the LNPs, while X-ray powder diffraction indicated varying degrees of crystallinity, with LLCs being the most amorphous. SEM analysis revealed changes in surface morphology post spray drying.

With regards to the antiproliferative tests against A549 lung cancer cells, certain NLC and LLC formulations were particularly effective, with lower IC50 values compared to free pimozide, indicating improved therapeutic potential. Drug release studies showed a biphasic release pattern, ensuring sustained drug availability. Given that this study underscored the potential of pimozide-loaded LNPs as a promising strategy for treating NSCLC, evaluating the combination effect with another repurposed drug to achieve enhanced antiproliferative with additional anti-inflammatory effects was considered, thereby enhancing the overall impact. This consideration prompted us to continue with the work discussed in section 8.2.4. (Chapter 5).

8.2.4 Enhancing NSCLC Treatment: Advanced Lipid Nanoparticle Formulations and Spray Drying Techniques with Repurposed Pimozide and Hydroxychloroquine (Chapter 5)

This chapter aimed to enhance the treatment of non-small cell lung cancer (NSCLC) by developing and evaluating lipid nanoparticle (LNP) formulations loaded with pimozide (PMZ) and hydroxychloroquine (HQ). Three types of PMZ-HQ loaded LNPs including, solid lipid nanoparticles (SLNPH), nanostructured lipid carriers (NLCPH), and liquid lipid carriers (LLCPH) were prepared and optimized using spray-drying technique. Among these, NLCPH formulations were the most promising, demonstrating superior EE% for PMZ and HQ due to their flexible structure, which allows better drug accommodation. In contrast, SLNPH showed lower EE%, likely due to the crystalline nature of the solid lipid matrix, while LLCPH had intermediate values, highlighting the role of lipid fluidity in drug encapsulation. Post-spray drying, all formulations exhibited a shift from nano to micro-scale particle sizes, with SLNPH showing the largest increase, indicating higher aggregation susceptibility.

NLCPH and LLCPH maintained more controlled particle sizes, with NLCPH also demonstrating enhanced colloidal stability through uniform size distribution and higher negative zeta potential values. Over two months of storage, NLCPH formulations showed better stability compared to SLNPH and LLCPH. DVS analysis indicated higher moisture absorption for LLCPH and SLNPH compared to NLCPH. FTIR analysis confirmed the encapsulation of PMZ and HQ, revealing changes in the molecular environment within the formulations. XRPD analysis indicated that NLCPH formulations underwent significant modifications in crystalline structure, potentially enhancing drug solubility and stability. SEM images showed that spray drying transformed nanoparticles into microparticles, with variations in surface morphology across formulations. Biological evaluations demonstrated significant anti-proliferative activity against A549 lung cancer cells, highlighting the synergistic effect of PMZ and HQ in NLCPH and LLCPH formulations, which significantly reduced cell viability. These formulations also exhibited notable anti-inflammatory effects by downregulating pro-inflammatory cytokines. Release kinetics

showed a biphasic release profile, with NLCPH offering sustained release, while LLCPH had a higher initial burst release due to its liquid lipid matrix.

8.2.5 Comparison of the Therapeutic Potential of Pimozide and Hydroxychloroquine Combination Using Advanced Spray Drying Techniques (Chapter 6)

Building on the potential anti-proliferative activity against A549 lung cancer cells of the PMZ- HQ combination from the previous section, this subsequent chapter reported the preparation and characterization of a novel co-delivery system for PMZ and HQ using advanced spray drying techniques. This system is aimed at targeted anticancer activity and the management of cancer-related inflammation and infection in NSCLC. Particles were prepared using both conventional two-fluid nozzle (2FN) and three-fluid nozzle (3FN) methods to compare the impact of specific nozzle configurations and excipients on the recovery%, particle size, drug release kinetics, and therapeutic efficacy of the resulting formulations.

Results showed higher recovery% for both PMZ and HQ in 3FN compared to 2FN. For PMZ, the recovery was 66% ± 0.9% in 3FN and 59.1% ± 1.9% in 2FN. For HQ, the recovery was 53.1% ± 1.8% in 3FN and 49.8% ± 0.7% in 2FN. Particle size analysis indicated that the 3FN system favored larger particles, while the 2FN system generated smaller particles. FTIR results confirmed hydrogen bonding between the PMZ, HQ, and excipients in both methods, stabilizing the amorphous form. XRPD confirmed the transition to an amorphous state for both methods. The antiproliferative assays showed lower IC50 of PMZ (13.27 µM) compared to HQ (20.13 µM) suggesting that PMZ is more effective at inducing cytotoxic effects at lower concentrations. Lower IC50 values necessitate careful dosage optimization to prevent adverse effects, making controlled release of PMZ preferable to avoid potential toxicity. The multilayer encapsulates prepared by 3FN exhibited customized release profiles, with prolonged sustained release for PMZ in the core and a faster burst release of HQ in the shell. Most formulations demonstrated synergistic antiproliferative effects against A549 cells (CI < 1) and significantly reduced pro-inflammatory cytokines. Overall, the 3FN spray drying method proved superior to the

2FN method in enhancing the therapeutic potential of the PMZ and HQ combination. However, no significant antimicrobial activity was observed, suggesting further investigation is needed.

8.2.6 Use of Advanced Spray Drying Techniques by Employing a Combination Therapy for NSCLC and Respiratory Infections (Chapter 7)

Given the lack of significant antimicrobial activity observed with PMZ-HQ spray-dried formulations in the previous section, the idea of replacing PMZ with rifaximin (RFX), a drug known for its antimicrobial properties, was considered. This chapter detailed the development of an innovative co-delivery system for RFX and HQ to target both bacterial infections and antitumor activity in NSCLC using advanced spray drying techniques. To further expand and deepen the study, this section focused on the 3FN spray drying strategy, introducing two configurations (RFX in the inner nozzle and HQ in the outer, and vice versa). This approach was evaluated alongside the 2FN method to determine the impact of nozzle configuration on recovery%, particle size, drug release kinetics, and therapeutic efficacy.

Results showed the highest recovery% with the 3FN system. Specifically, feeding RFX through the inner nozzle and HQ through the outer nozzle resulted in the highest recovery% for HQ (84% ± 3.0%) and RFX (71% ± 3.5%). Reversing this setup slightly lowered the recovery%. The lowest recovery% was observed with the 2FN system (78% ± 3.5% for HQ and 64% ± 3.9% for RFX). Particle size analysis revealed that the 3FN system produced larger particles compared to 2FN. The antiproliferative assays showed lower IC50 of HQ (20.13 µM) compared to RFX (25.32 µM) suggesting that HQ is more effective at inducing cytotoxic effects at lower concentrations. Lower IC50 values necessitate careful dosage optimization to prevent adverse effects, making controlled release of HQ preferable to avoid potential toxicity. The 3FN method provided advanced tailored release profiles and demonstrated synergistic antiproliferative effects against A549 cells while significantly reducing pro-inflammatory cytokines through complementary anti-inflammatory mechanisms. HQ broadly inhibited key inflammatory

pathways, and RFX modulated systemic inflammation, highlighting the potential synergistic effect of these formulations in addressing cancer-related inflammation. Additionally, the method effectively inhibited *Acinetobacter baumannii*. Overall, the 3FN spray drying method excelled in developing an RFX-HQ co-delivery system with substantial therapeutic activity for targeting NSCLC and associated infections or inflammations. The best results were achieved with HQ encapsulated in the core, exhibiting a sustained release profile to target antitumor activity in NSCLC while minimizing toxicity, particularly since HQ has a lower IC50 than RFX. Conversely, RFX encapsulated in the shell exhibited a faster initial release to manage cancer-related infections and enhance overall cytotoxicity.

8.3 Evaluation of Experimental Content and Suggestions for Future Work

8.3.1 Overview and Impact of Particle Engineering

The experimental chapters of this thesis (Chapters 4, 5, 6, and 7) collectively highlight the transformative potential of particle engineering, particularly in the context of LNPs and spray drying techniques, to improve the treatment of NSCLC and related infections and inflammations. The focus on advanced spray drying strategies, especially the 3FN method, and the detailed examination of release kinetics underscore the significant advances made towards achieving targeted and effective drug delivery systems.

In Chapter 4, the development of PMZ-loaded LNPs was explored using SLNs, NLCs, and LLCs. Advanced particle engineering techniques led to high encapsulation efficiency and stability, particularly for NLCs, due to their flexible lipid structure that enhanced drug encapsulation. The stability and uniform distribution of the drug within the nanoparticles were confirmed through various characterization techniques. Additionally, the spray-dried NLC and LLC formulations exhibited significant antiproliferative effects against A549 lung cancer cells, with improved therapeutic potential indicated by lower IC50 values compared to free pimozide. The biphasic release pattern observed ensured sustained drug availability, enhancing the overall treatment efficacy.

Building on the success of single-drug formulations, Chapter 5 advanced the treatment of NSCLC by developing LNP formulations loaded with PMZ and HQ. The use of spray drying technique complemented the co-delivery system, with NLCPH formulations showing superior EE% for both PMZ and HQ due to the flexible lipid structure allowing better drug accommodation. After spray drying produced, the formulations exhibited biphasic release profiles, indicated in a faster initial release followed by a sustained release. These formulations exhibited significant antiproliferative and anti-inflammatory effects, synergistically reducing cell viability and pro-inflammatory cytokines, thereby demonstrating enhanced therapeutic potential.

Chapter 6 further investigated the impact of innovative spray drying techniques by comparing the conventional 2FN and advanced 3FN methods for the co-delivery of PMZ and HQ. The findings emphasized the importance of nozzle configuration on therapeutic outcomes. The 3FN method resulted in higher recovery% and tailored release profiles, with the ability to customize drug release kinetics. The multilayer encapsulation achieved through 3FN enabled prolonged sustained release for PMZ and faster burst release for HQ. The 3FN formulations demonstrated superior antiproliferative effects against A549 cells and significant anti-inflammatory activity, highlighting the potential for targeted cancer therapy.

Chapter 7 expanded the therapeutic scope by developing a co-delivery system for RFX and HQ, targeting both bacterial infections and antitumor activity in NSCLC. The advanced 3FN spray drying technique proved to be particularly effective in optimizing drug recovery% and stability. The 3FN system achieved the highest recovery% for both drugs, with the optimal configuration being RFX in the inner nozzle and HQ in the outer nozzle. The tailored release profiles facilitated by the 3FN method allowed for synergistic antiproliferative effects and significant reduction in pro-inflammatory cytokines. Additionally, the formulations effectively inhibited *Acinetobacter baumannii*, addressing both cancer and respiratory infections.

8.3.2 Impact and Future Directions

The work presented in these chapters underscores the significant impact of particle engineering in enhancing drug delivery systems for NSCLC. The advanced 3FN spray drying technique, in particular, has shown remarkable potential in optimizing drug recovery%, stability, and tailored release kinetics. These advancements translate into improved therapeutic outcomes, with targeted and sustained drug delivery reducing side effects and improving patient compliance. Future research should focus on optimizing formulations, and conducting comprehensive in vivo studies to validate the promising in vitro results and assess systemic toxicity and long-term stability of the formulations which are critical for clinical translation. Besides, it would be interesting to explore the co-encapsulation of different drug combinations, especially those with narrow therapeutic windows to develop controlled release formulations using 2FN and 3FN systems.

References:

[1]   D. Das, J. Wang, and J. Hong, "Next-Generation Kinase Inhibitors Targeting Specific Biomarkers in Non-Small Cell Lung Cancer (NSCLC): A Recent Overview," *ChemMedChem,* vol. 16, no. 16, pp. 2459-2479, 2021.

[2]   E. Perlin *et al.*, "The impact of pulmonary infections on the survival of lung cancer patients," *Cancer,* vol. 66, no. 3, pp. 593-596, 1990.

[3]   S. Kohno *et al.*, "The pattern of respiratory infection in patients with lung cancer," *The Tohoku Journal of Experimental Medicine,* vol. 173, no. 4, pp. 405-411, 1994.

[4]   K. Akinosoglou, K. Karkoulias, and M. Marangos, "Infectious complications in patients with lung cancer," *European Review for Medical & Pharmacological Sciences,* vol. 17, no. 1, 2013.

[5]   R. M. Martin *et al.*, "Identification of pathogenicity-associated loci in Klebsiella pneumoniae from hospitalized patients," *Msystems,* vol. 3, no. 3, pp. 10.1128/msystems. 00015-18, 2018.

[6]   A. Y. Peleg, H. Seifert, and D. L. Paterson, "Acinetobacter baumannii: emergence of a successful pathogen," *Clinical microbiology reviews,* vol. 21, no. 3, pp. 538-582, 2008.

[7]   P. D. Lister, D. J. Wolter, and N. D. Hanson, "Antibacterial-resistant Pseudomonas aeruginosa: clinical impact and complex regulation of chromosomally encoded resistance mechanisms," *Clinical microbiology reviews,* vol. 22, no. 4, pp. 582-610, 2009.

[8]   E. A. Engels, "Inflammation in the development of lung cancer: epidemiological evidence," *Expert review of anticancer therapy,* vol. 8, no. 4, pp. 605-615, 2008.

[9]   A. Florczak, I. Grzechowiak, T. Deptuch, K. Kucharczyk, A. Kaminska, and H. Dams-Kozlowska, "Silk particles as carriers of therapeutic molecules for cancer treatment," *Materials,* vol. 13, no. 21, p. 4946, 2020.

[10]   P. Kaur, V. Mishra, T. Shunmugaperumal, A. K. Goyal, G. Ghosh, and G. Rath, "Inhalable spray dried lipidnanoparticles for the co-delivery of paclitaxel and doxorubicin in lung cancer," *Journal of Drug Delivery Science and Technology,* vol. 56, p. 101502, 2020.

[11]   C. M. Zimmermann *et al.*, "Spray drying siRNA-lipid nanoparticles for dry powder pulmonary delivery," *Journal of Controlled Release,* vol. 351, pp. 137-150, 2022.

[12]   Z. Bakhtiary *et al.*, "Microparticles containing erlotinib-loaded solid lipid nanoparticles for treatment of non-small cell lung cancer," *Drug development and industrial pharmacy,* vol. 43, no. 8, pp. 1244-1253, 2017.